

**THE MEASUREMENT AND CORRECTION  
OF  
SACRAL OBLIQUITY**

John Dulhunty D.C., MACC

A thesis submitted in partial fulfilment of the requirements for the degree  
of

**Doctor of Philosophy**

Department of Chiropractic  
Faculty of Science and Engineering  
Macquarie University  
Sydney

March 2015

## DECLARATION

I certify that the work in this thesis entitled “The Measurement and Correction of Sacral Obliquity” has not previously been submitted for a degree, nor has it been submitted as part of requirements for a degree to any other university or institution other than Macquarie University.

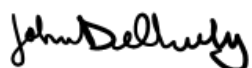
I also certify that the thesis is an original piece of research and has been written by me. Any help and assistance that I have received in my research work and the preparation of the thesis itself have been appropriately acknowledged.

In addition I certify that all information sources and literature are indicated in the thesis. All figures represent my own work unless otherwise indicated.

The research presented in this thesis was approved by the Macquarie ethics Review Committee, reference number:

Human Ethics Approval:

HE26 MAY2006-DO4706



John Dulhunty  
2015

## ACKNOWLEDGEMENTS

- My father  
Who inspired me to never set limits on what can be accomplished, and for helping me appreciate the value of pursuing knowledge and rational thought.
- My wife and family  
Their contribution goes beyond support. It encompasses the encouragement and sharing needed to realise dreams, accepting the reality of everyday participation and the very real sacrifices needed.

I would like to acknowledge and thank those who provided help with specific aspects of this thesis.

- My supervisors  
Assoc Prof Subra Vemulpad  
Dr Peter Bull (retired)  
Dr Ray Hayak (retired)
- Macquarie Engineering & Technical Services (METS), for their help in the design and fabrication of the radiographic phantom and in particular:  
Walther Adendorff  
Brian Hayes
- Help and advice on the statistical analysis of data.  
The late Associate Professor Julian Leslie
- Providing 50 sets of anonymised pelvic CT data from a private radiographic practice.  
Dr Peter Kitchener
- Radiographic imaging of the pelvic phantom.  
Dr Bruce Liebowitz (Queensland Radiology, Mackay). Provided five data sets of the pelvic phantom with different pre-set sacral obliquity angles.  
  
Caroline Falconi (Radiography, Sonography, Chiropractic Program head CQU university). Provided five AP and Lateral CT scan views of the pelvic phantom with different pre-set sacral obliquity angles.
- For making available sacral specimens used in the study.  
The Anatomy Department of Sydney University
- Help and advice on the statistical analysis of data.  
Ken Beath, Lecturer, Statistics Department, Macquarie University

## **ABSTRACT**

The primary objective of the study involved the identification and quantification of systematic errors associated with the measurement of sacral obliquity on radiographic images. A secondary objective was to provide an estimate of true sacral obliquity derived from measurements made on radiographic images of the spine that could be used in a clinical setting to correct or reduce frontal plane obliquity.

Methods used in the study included graphical, radiographic and mathematical models. They were used to evaluate the measurement of dihedral angles such as structural asymmetry of the sacral base and vertebral endplates in the frontal plane. A radiographic phantom was imaged using plain film, CT, and slot scan (scout) views. The variation of measurements using different views was compared to the known sacral obliquity value of the phantom.

Results obtained from the studies demonstrate that different radiographic and analytical methods produced significant differences in the measurements of sacral obliquity for each of the imaging modalities and analytical methods.

The study developed, tested and validated algorithms to calculate true dihedral angles from angles measured on radiographic images. The algorithms were designed to be employed when the protocols developed to ensure reliable measurement of angular relationships were not met or were unable to be adhered to. The measurement of sacral obliquity on radiographic images was used in the development of algorithms to calculate the amount of correction needed to level the sacral base in upright standing and sitting postures.

Trigonometric techniques were developed and applied to measurements of sacral obliquity obtained from radiographic images of the erect spine to provide accurate dimensions of ischial or foot orthotics that would be required to level the sacral base in sitting or standing posture respectively.



<b>TABLE OF CONTENTS</b> .....	<b>Page Number</b>
Declaration.....	i
Acknowledgements .....	ii
Abstract.....	iii
Table of contents.....	iv
Preface .....	vii
<b>Chapter 1</b>	
Sacral Obliquity: An Introduction .....	1
1.1 Introduction .....	2
1.2 Morphology of lumbopelvic segments .....	17
1.3 Clinical implications of skeletal asymmetry .....	27
1.4 Functional and structural pelvic obliquity .....	32
1.5 Research outline .....	47
1.6 Ethics considerations .....	48
<b>Chapter 2</b>	
Measuring Sacral Obliquity on Radiographic Images: An Overview .....	50
2.1 Measuring sacral obliquity on radiographic images .....	51
2.2 Measuring dihedral angles on radiographic images.....	65
2.3 Radiographic modalities and methods.....	78
2.4 Radiographic projection factors .....	91
2.5 Summary and conclusion .....	109
<b>Chapter 3</b>	
Sacral Obliquity Measured on Radiographic Images of 16 Dry Bone Specimens .....	112
3.1 Dry bone sacral specimens .....	113
3.2 Radiographic setup for plain film imaging .....	129
3.3 Plain film radiographic analysis .....	131
3.4 Results .....	137
3.5 Summary and conclusion .....	142

## **Chapter 4**

Sacral Obliquity Measured on Radiographic Images of a Pelvic Phantom .....	147
4.1 Introduction .....	148
4.2 Plain film radiographic positioning .....	153
4.3 Radiographic image analysis.....	158
4.4 Summary and conclusion .....	163

## **Chapter 5**

Sacral Obliquity Measured on CT Images of a Pelvic Radiographic Phantom .....	165
5.1 Computed tomography (CT) .....	166
5.2 Multiplanar reconstruction of image data .....	169
5.3 Three-dimensional volume rendering of spinal CT data.....	179
5.4 Slot scan (scout view) of pelvic radiographic phantom.....	186
5.5 Summary and conclusion .....	189

## **Chapter 6**

Sacral Obliquity Measured on Graphic Models of the Pelvis .....	191
6.1 Graphic models .....	192
6.2 Perspective projection .....	198
6.3 Data analysis.....	205
6.4 Summary and conclusion .....	206

## **Chapter 7**

Sacral Obliquity Measured on Computed Tomography Studies of the <i>in vivo</i> Pelvis .....	207
7.1 Computed tomography of fifty <i>in vivo</i> lumbopelvic spines.....	208
7.2 <i>In vivo</i> studies of the pelvis using MPR and volume rendering .....	213
7.3 Summary and conclusion .....	216

## **Chapter 8**

Correcting Sacral Obliquity in Sitting and Standing Postures.....	217
8.1 Correcting sacral obliquity .....	218
8.2 Calculating orthotic size .....	224
8.3 Mathematical and graphical models .....	276
8.4 Results.....	290
8.5 Mathematical and graphical analysis.....	304
8.6 Discussion.....	307
8.7 Summary and conclusion .....	309

## **Chapter 9**

Summary and Conclusions,.....	310
9.1 Introduction .....	311
9.2 Limitations of study .....	312
9.3 Clinical implications of the study.....	313
9.4 Future research related to the measurement of sacral obliquity .....	322
9.5 Conclusion .....	323

<b>References</b> .....	326
-------------------------	-----

## **Appendix 1**

Corrective Algorithms To Determine True Sacral Obliquity .....	369
--	-----

## **Appendix 2**

Glossary and Abbreviations.....	385
---------------------------------	-----

## **Appendix 3**

Final Ethics Approval Letter.....	413
-----------------------------------	-----

**PREFACE**

The clinically based analysis of radiographic images to assess positional and structural relationships as well as the functional integrity of the spine and pelvis necessitates the interpretation of two dimensional graphical representations of three dimensional objects. An aspect of this task requires an understanding of projection principles and the identification of inherent errors associated with the projection and viewing of three dimensional objects as two dimensional images. As the basis of this study is the interpretation of such images and is ultimately based on the graphical analysis of acquired radiographic images, the presentation of the material in this study is heavily dependent on graphical imagery. The format for the presentation of this study is therefore influenced by the graphical nature of the material and research methods.

As it was not within the scope of the study to verify the true angle of the sacral base *in vivo*, alternate methods employing a pelvic model with known degrees of sacral obliquity and an idealised graphical model with specified degrees of sacral obliquity and sacral base angulation were developed and used in the study. While these models contained some error as an intrinsic feature of their construction and manipulation, their general accuracy and standardised analysis methods meant they could be used as a reference standard against which radiographic analysis and corrective algorithms could be compared.



## **SACRAL OBLIQUITY: AN INTRODUCTION**

## CHAPTER 1

*“All’s oblique;  
There’s nothing level in our cursed natures”*

William Shakespeare

### 1.1 INTRODUCTION

The spine is a major component of the axial skeleton of the human body. It is bilaterally symmetrical around the mid-sagittal plane of the body in order to efficiently transmit forces from the skull to the lower limbs as one of its functions. It is generally comprised of thirty three individual segments. These are divided into seven cervical vertebra, twelve thoracic, five lumbar, five sacral and four coccygeal segments. The sacral segments will generally start to fuse to form one bone around age sixteen and by mid-thirties will usually be completely fused into a single bone (1).

The sacrum is the ‘sacred bone’ of the body. The name *os sacrum*, given by the Romans and *hieron ostoun* by the Greeks to the heavy bone that forms the mechanical base of the spine is derived from the Latin *sacer*, ‘holy or consecrated’ (2). The sacrum has the shape of an inverted pyramid with the base angled upward and anterior in upright posture.

Obliquity relates to the state of an object or plane being inclined or slanted. Sacral obliquity is the tilting or slanting of the sacral bone when viewed from the front. A level base has been generally considered the ideal mechanical orientation for the foundation of the spine (3). A loss of frontal plane symmetry is considered to have clinical significance, health related implications (4) and to even influence the perception of attractiveness (5).

The graphical analysis of conventional plain film radiographs (PF) and computed tomography (CT) images is considered by many clinicians and researchers to be the ‘gold standard’ or ‘yardstick’ for scoliosis screening and for determining the positional relationship of spinal segments (6). Radiographic imaging is routinely used by clinicians from various

disciplines to quantify the positional relationship of structures within the axial skeleton (7-10). Analysis of radiographic images often includes the assessment of absolute and relative position of spinal segments and individual bones of the spine and pelvis (11-15). In this respect, radiographic imaging has been used to assess and quantify leg length imbalance (LLI), scoliosis, pelvic obliquity, and the shape and magnitude of lateral spinal curves (scoliosis). Many practitioners from various health care professions rely on the information from such studies to make clinical decisions regarding treatment strategies for individual patients, to monitor the therapeutic response to such treatments and quantify changes that have occurred over time. The reliable measurement of sacral obliquity has implications for research into spinal pathomechanics as well as the assessment and treatment of spinal pain syndromes (16), ergonomic advice and design (17) and establishing individual performance and postural criteria for athletes (18, 19) and workers (3).

Most of the angular measurements made on spinal radiographic images such as Cobb angles involve measuring the angle between lines that represent hypothetical global planes (horizontal and vertical), planes of the body or planes representing structural surfaces within the body. A line drawn or constructed on a radiographic image is idealised as a one-dimensional line segment joining two end points that represent the edge of a plane or two points on a plane. The third point defining the plane, if not specified, is assumed to be a point lying perpendicular to any point on the line.

Obliquity can be described technically as the deviation of a plane, or line representing the plane, from another plane or line. This description includes deviation of a line representing a plane from a line representing the vertical and horizontal planes. The degree of obliquity is measured as the angle of such a deviation. Medical references to *obliquity* in relation to the spine most often relate to the degree of angulation of points on a specified surface relative to the horizontal plane.

A dihedral angle is formed between two planes that are not parallel and therefore meet at a common line of intersection (20, 21). A plane is any flat, two-dimensional surface that exists in its own right as either a real or hypothetical surface or as a subspace of a three-dimensional structure. A plane can be defined as a surface resting on any three points or a single point in the plane and a normal vector that starts at the point.

The normalized cross product of any two non-collinear vectors lying in a plane yields the normal unit vector to the plane. A normal vector to the plane is any vector that starts at a point in the plane and has a direction that is orthogonal (perpendicular) to the surface of the plane. Thus, the size of a dihedral angle can be defined as the angle formed by two intersecting lines, one in each plane, that are both perpendicular to the straight edge along which the two planes intersect, or the acute angle formed between the normal unit vectors representing the planes (22).

Planes of particular interest in the present study are those that are commonly used to define the orientation of the sacrum and vertebral segments of the spine in the frontal plane as measured on radiographic images. Two angles of particular interest are *sacral obliquity* for the pelvis and *Cobb angles* used to measure the relative lateral tilting of individual vertebral segments of the spine on radiographic images (23).

The particular interest in the validity of Cobb angles as an angle measurement relates to the reliance on the Cobb method as the standard and most commonly used clinical method for quantifying and classifying scoliotic curves of the spine by clinicians (24-26). Sacral obliquity was selected as the primary entity investigated in this study for the opposite reason, that is, it is not a well-established or well investigated clinical entity. While sacral obliquity has been investigated as a specific entity (27, 28) there is a general lack of agreement by clinicians and investigators as to the clinical significance, the optimal method



for quantifying sacral obliquity and its relationship to other structural and functional parameters such as scoliosis and anisomelia. There have been no reports in the relevant literature on the validity of measurements of sacral obliquity made on spinal radiographic images.

The commonality between sacral obliquity angles that are of interest for this study and Cobb angles is that both involve the measurement of dihedral angles on anteroposterior radiographic images of the spine and/or pelvis. Angulation of the sacral base in the frontal plane was chosen as the primary focus as it involves the measurement of complex three-dimensional rotations on specific two-dimensional images of the spinal structures involved. This process inherently produces systematic errors that can influence the validity of the measurements of both sacral obliquity and Cobb angles obtained directly from radiographic images (15, 29).

#### *1.1.1 Pelvic and Sacral Obliquity*

The pelvis as a unit transmits forces from the trunk to the lower limbs through the junction with the spine at the sacral base and through the legs at the acetabulum. The sacrum is the bone situated at the base of the spine in the vertical midline of the body when viewed in the frontal plane. Its primary mechanical role is to transmit forces to and from the spine above and the pelvic girdle and hips below (30-32). The most mechanically efficient orientation of the sacral base in performing this task in upright posture (sitting or standing), when viewed from the front, is perpendicular to the force of gravity (32-36). Mechanical efficiency of the pelvis is optimal with reflective symmetry in the frontal plane around the gravitational weight-line of the body (Figure 1).

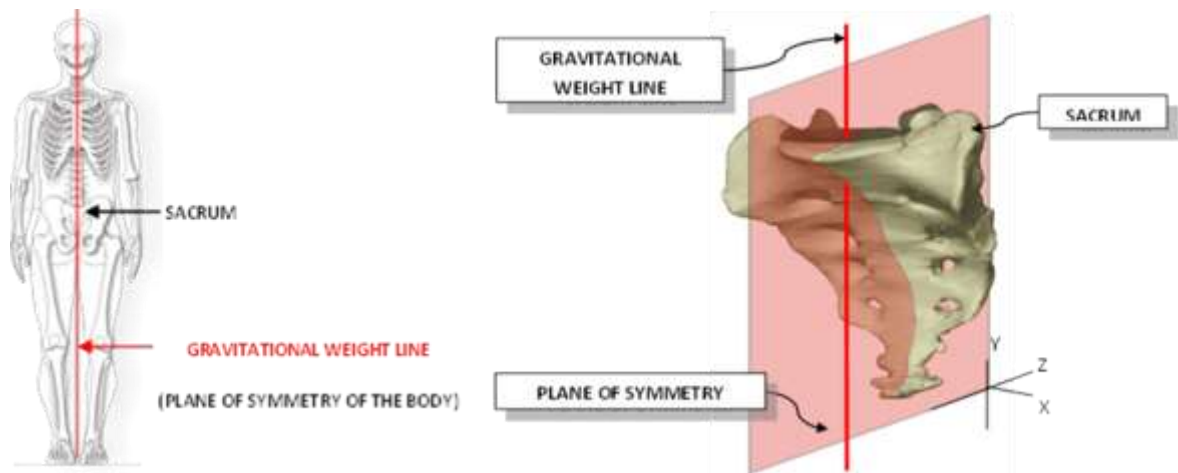
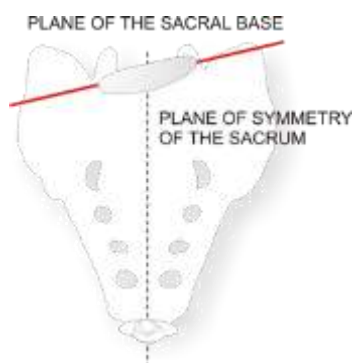


Figure 1. Reflective symmetry in the frontal plane around the gravitational weight-line of the body (left) and reflective symmetry of the sacrum (right)

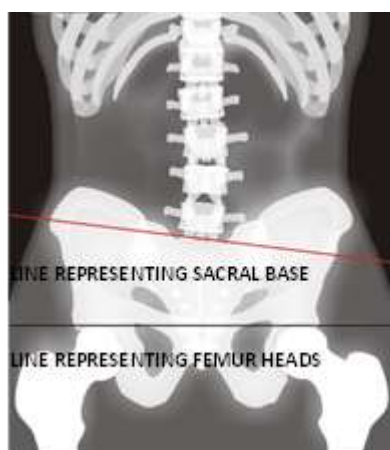
As the pelvis forms the primary supportive link between the trunk or axial skeleton and lower limbs or appendicular skeleton (37), its orientation relative to gravity is crucial in the efficient transmission of forces between these elements of the musculoskeletal system (38, 39). Obliquity of the pelvis in the frontal plane, and by inference the sacrum, has direct mechanical and functional implications for the spine above and weight bearing structures below (3, 40-42). The force of gravity is ubiquitous and influences both the structure and function of the human spine in upright posture (30, 43-45). The magnitude and direction of this force remains unchanged throughout life (34). The orientation of skeletal structures to gravity directly influences the internal loads within the structures of the pelvis and the behaviour of associated structures (46-48).

A lack of reflective structural symmetry of the sacral base relative to the body of the sacrum in the frontal plane can result in an angulation of the sacral base or '*sacral obliquity*' (Figure 2).



**Figure 2. Plane of reflective symmetry of the sacrum with structural asymmetry of the sacral base resulting in sacral obliquity**

Sacral obliquity as a clinical entity distinct from pelvic obliquity has been defined as “an angular deviation of the sacrum from the line drawn parallel to a line across the femoral heads on a supine anteroposterior (A-P) view of the sacrum” (49) (Figure 3). A direct inference from this definition is that the sacral base, as a structural part of the pelvis, has a different degree of obliquity to that of the pelvis as a unit. However, the term *pelvic obliquity* is generally used when referring to the pelvis as a unit without reference to the functional or structural symmetry of the pelvis itself (Figure 3).



**Figure 3. Radiographic representation of pelvis and femur heads demonstrating sacral obliquity relative to the femur heads**

A more encompassing definition of sacral obliquity includes pelvic obliquity and covers any angular deviation of the sacral base in the frontal plane from the horizontal plane in erect posture (28, 33, 50, 51). Based on these definitions, angulations of the sacral base in the

frontal (coronal) plane can be divided into 'relative' or 'absolute' sacral obliquity respectively. Relative sacral obliquity describes angulation of the sacral base in the frontal plane in relation to other structures, primarily the ilia, femur heads or lumbar spine and generally represents internal pelvic or sacral asymmetry. This relationship would remain unchanged with various orientations of the structures to gravity e.g. standing, sitting or lying down.

Absolute sacral obliquity refers to the angulation of the sacral base in the frontal plane for a specified orientation of the body in a global reference frame or in relation to gravity for a specific posture such as standing or sitting. Relative and absolute sacral obliquity may or may not be equivalent, depending on the symmetry of other structures and functional status of other components of the framework of the body. Absolute sacral obliquity is closely associated with, and is implied in another commonly used concept relating to functional asymmetry of the spine and pelvis. The concept involves *leg-length imbalance* (LLI) or *leg-length deficiency* (LLD). One of the clinical implications for detecting and quantifying differences in leg length (anisomelia) is the influence that leg-length imbalance or deficiency has on the frontal plane angulation of the sacral base (52) (Figure 4).

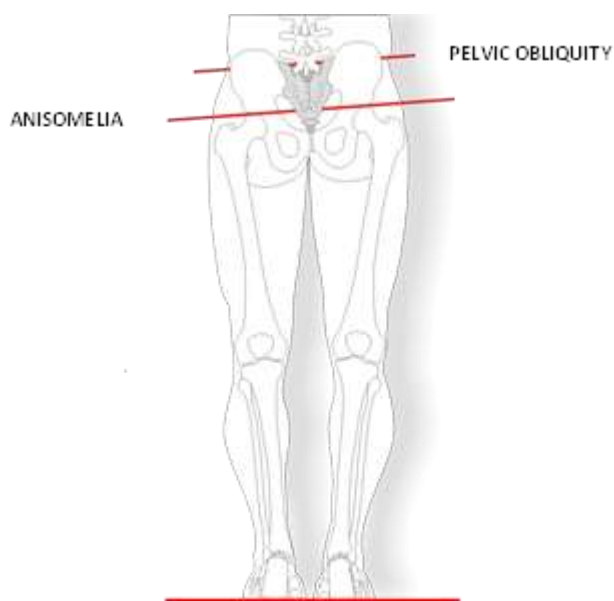


Figure 4. Implied relationship between sacral obliquity and anisomelia

Structural and functional asymmetry of the skeletal system has been implicated as a factor in pain syndromes (4, 52-62), degenerative and structural changes (17, 40, 63-66) and musculoskeletal function (67-71). However, based on studies that either showed a weak link or failed to show any link between the two, a number of investigators have questioned the relationship of pelvic obliquity and leg length imbalance with functional spinal problems and pain syndromes (72-76). Fann (59) reported that the majority of patients treated using heel lifts reported an improvement in their pain symptoms. Her studies indicated that the extent of pelvic obliquity is similar in subjects with and without chronic low back pain. Her conclusion was that there must be other factors to account for the benefit of correcting the pelvic obliquity.

It is relatively common for musculoskeletal clinicians and researchers to assess the positional and functional integrity of the pelvis, and by implication the sacrum, in relation to structural changes and functional spinal patterns (11, 17, 28, 33, 40, 50, 54-56, 63-70, 77-79) and spinal pain syndromes (3, 4, 31, 34, 35, 50, 57-62, 67, 71-77, 79). In a review of procedures used to assess the positional and functional integrity of the lumbopelvic spine by chiropractors and other manual therapists, Hestbæk and Leboeuf-Yde (80) found that none of the tests studied had been sufficiently evaluated in relation to their reliability and validity.

Manual evaluation of the iliac crests is a clinical method commonly used to assess pelvic obliquity. In a study designed to investigate the occurrence of pelvic asymmetry Timgren and Soinila (50) used manually assessed iliac crest levels to determine difference in height from left to right in neurologic patients with symptoms not explained by their neurologic diagnosis. They found in the patients who had also been examined using radiographs, that asymmetry of the pelvis was consistently correlated with two to four degrees of obliquity of the sacrum. However, they gave no indication of the reliability or validity of these measurements.

A measuring frame was used by Al-Eisa *et al* (42) to quantify pelvic asymmetry in the frontal plane. Their study indicated that altered mechanics in the lumbar spine in the form of asymmetric lateral flexion was highly associated with subtle anatomic abnormalities (asymmetry) in the pelvis. Again, in this study there was no indication of the validity of the method used to quantify lateral pelvic tilt (obliquity) and actual sacral base level. Piva *et al* (81) also assessed the reliability of a measuring device comprising an inclinometer used to measure iliac crest level. The objective was to determine the reliability of the device in measuring iliac crest height in the sitting and standing positions with the plan to investigate if a change in the iliac crest height was associated with pain or lower back and pelvic dysfunction. While this study demonstrated generally good reliability for the device to measure the degree of tilt of the iliac crests in standing posture and moderate reliability in sitting posture, there was no assessment of the validity of the measurement in relation to the orientation or alignment of the sacral base in either position.

There has not been a generally accepted 'gold standard' developed to validate the methods used in quantifying sacral obliquity *in vivo*. This has meant that clinicians have not had access to a validated method for assessing the orientation of the base of the spine in the frontal plane for a particular individual or for gathering generalised epidemiological data. The result is a general lack of demonstrably reliable and valid information about the incidence, distribution and magnitude of sacral obliquity and its relationship to musculoskeletal disorders (11, 80-85). This has allowed a wide range of opinions and assumptions amongst health care professionals in regard to the structural, positional and functional integrity of the sacrum. Their differing opinions relate to the cause, consequences and clinical significance of lumbopelvic alignment and the positional orientation of the sacrum (3, 17, 27, 31-36, 40-42, 52-56, 59-61, 63-67, 71, 73-76, 83, 84).

Extrapolating the findings of studies investigating leg length imbalance and pelvic obliquity, sacral obliquity could have specific implications for musculoskeletal clinicians (27, 53, 59, 63-65, 86-90), sports physicians (77, 91) and ergonomists (92-94). A fundamental part of the postural advice given by many of those who assess and treat musculoskeletal problems has long included instructions such as “stand up straight, sit up straight, keep the back straight when lifting etc.” (95, 96). This type of advice is generally based on the tacit assumption of structural symmetry of the components of the musculoskeletal system, and of frontal plane alignment of the spine in particular.

As the sacrum performs the role of the functional and structural base of the spine, it has a fundamental influence on the overall symmetry of the spine (37). Like any weight bearing structure the foundation is of prime importance to overall alignment and the mechanical relationship of structural components of the axial skeleton to gravity. This relationship has been suggested by Irvin (65), Zabjek *et al* (63) and Fann (54, 59) as well as other osteopaths (32, 83), chiropractors (78, 79) and medical specialists (97). They independently describe levelling the sacrum as the mechanism behind the reduction of specific types of scoliosis with the use of unilateral heel lifts to level the sacral base in the frontal plane.

The approach of various groups to the assessment of pelvic and sacral obliquity and its significance particularly as an entity relative to sitting and standing postures can be classified into generalised categories (98). These categories are helpful in illustrating prevailing attitudes and general concepts relating to pelvic alignment and sacral obliquity and their presumed influence on spinal alignment.

Within a group comprising such disciplines as manual therapy, ergonomics, occupational health and safety (manual handling) and sports physiology, normal or ideal posture is often based on straightness or symmetry of the spine and pelvis in the frontal plane (94, 95, 99-

105). This concept is predicated on a presumption of structural and functional symmetry of the spine as the optimal mechanical configuration with relatively small amounts of structural obliquity considered to be of little clinical significance (52, 102-105). Generally practitioners within this grouping tacitly endorse the concepts underlying ‘stand up straight, sit up straight and keep your back straight when lifting’ and advocate strategies aimed at maintaining a ‘normal’ and balanced posture as the ideal (95, 101, 102). Based on these concepts, postural symmetry underlies diagnosis and treatment strategies and advice given on optimal postures (31, 32, 44, 52, 65, 67, 74, 77-79). It is also reflected in ergonomic design (106-110), prescribed exercises and back care advice available to the public that is based on, or assumes structural, positional and functional symmetry of skeletal structures (102, 108-111). Advice and treatment strategies are often based on ideal or theoretical constructs and assumptions (105, 112) rather than firm data relating to structural or positional symmetry of the spine and pelvis in specific individuals (39-42, 82, 85, 113, 114).

As a second group, orthopaedic surgeons and allied therapists often treat obliquity of structures of the spine with associated back pain syndromes on a pragmatic basis without necessarily assigning or defining a specific cause. For example, Jacob and McKenzie (115) suggest that *a priori* knowledge ‘about common spinal disorders can blind clinicians to meaningful and individual phenomena.’ They advocate *a posteriori* empiric study of phenomena related to spinal loading, after which pathoanatomic explanations are proffered. In a review article Asher and Burton (116) state that adolescent idiopathic scoliosis is a condition of unknown cause and conclude that even though the natural history and long-term treatment effects remain somewhat incomplete, informed decisions can be made regarding management options.

Measurable loss of symmetry is frequently described or designated as ‘idiopathic’. Idiopathic scoliosis is defined by the Scoliosis Research Society (49) as a “structural spinal curvature for which the cause has not been established.” The diagnosis of idiopathic



scoliosis implies that there is no evidence of underlying physical or radiographic pathology (87). This form of scoliosis is the most common type, representing 80% of all scoliosis (33). Many practitioners treat obliquity of the spine without attributing, acknowledging or ascribing a specific cause (33, 115-120). Classification and treatment of functional or mechanical low back pain and scoliosis is often based on the assumption that it is of unknown origin (87, 117). Treatment can involve surgical and bracing correction for scoliosis (33, 121, 122), exercise programmes (33, 119, 123-127) and postural advice (33, 118, 119, 128). These treatments can be considered 'successful' in terms of pain relief and cosmetics without designating a specific cause (118-120, 125).

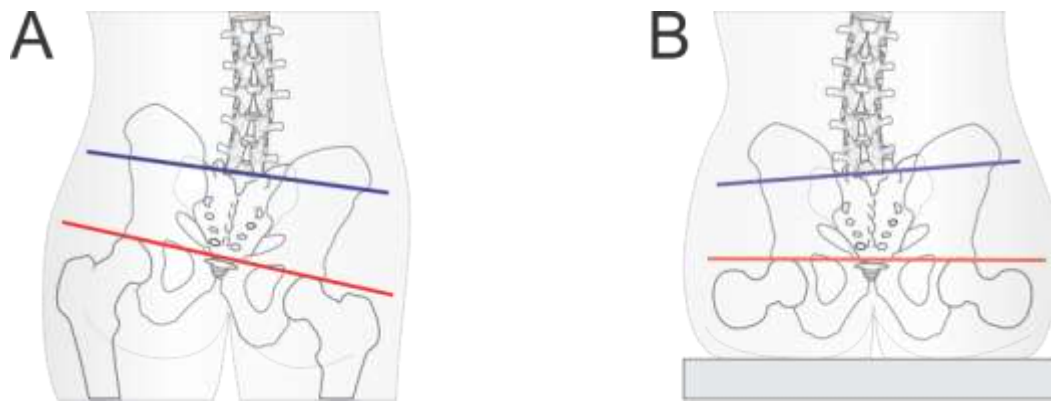
Another group of practitioners, including many chiropractors and osteopaths, treat musculoskeletal pain and functional disorders with acceptance of obliquity of structures comprising the spine and pelvis as an *a priori* fact. The cause of this asymmetry is generally attributed to joint misalignment as the underlying mechanism (12, 13, 31, 50, 78, 79, 90). This grouping also includes many podiatrists, physiotherapists and to a lesser extent some medical practitioners (77, 86, 129-131). The cause of the observed obliquity is commonly attributed by these practitioners to a variety of misalignments and functional changes in the musculoskeletal system. These practitioners generally employ techniques to assess, improve or restore positional and functional integrity to elements of the body's skeletal framework. In order to do so they often use procedures to assess pelvic alignment, functional leg length imbalances and spinal alignment as part of their treatment modalities. The presumed cause for this obliquity is commonly attributed to correctable joint, soft tissue and functional factors. Widely advocated chiropractic and osteopathic techniques are used to assess, interpret and correct pathomechanics of the lumbopelvic spine (132-134). These techniques often involve the use of radiographic and other clinical tests to analyse and quantify positional dyskinesia. Others use observational tests such as assessing functional leg length imbalance (69, 72, 90, 135, 136), palpation (137, 138) and the relative position of the iliac crests (81) as diagnostic or assessment tools. However, there is little evidence

validating these procedures or the assumptions they are based on (80, 84, 86, 135-140). Drerup and Hierholzer (141) used rasterstereography and curvature analysis to localise the lumbar dimples which were used in their study to indicate pelvic movement. They noted a systematic lag in displacement of the dimples relative to the pelvis from tilting of the pelvis. They assumed that either soft tissue effect or torsion of the pelvis was responsible for the observed behaviour of the lumbar dimples. However, they concluded that the dimples could not be taken as exact indicators for orientation and movement of the pelvis and assumed pelvic torsion could only be determined to exist based on independent measurement.

A relatively small number of health care professionals and researchers, along with some researchers from non-health care disciplines suggest that the sacrum and other segments of the spine may exhibit a significant degree of structural asymmetry (17, 27, 28, 39, 40, 65, 78, 79, 83, 85, 98) (Figure 2). This approach, while accepting the presence of frontal plane asymmetry, is distinct from the more widely held view that leg length imbalance and joint misalignments are the underlying causes of the observed angulations of the sacral base and superimposed scoliotic spinal curves. The inherent assumption in the concept that equates pelvic obliquity and absolute sacral obliquity is that the degree of tilt of the pelvis in the frontal plane is assumed to be equal to the degree of sacral tilt. Opposing these views, clinicians such as Brown *et al* (27) and Liebensohn (79) suggest that sacral obliquity represents a distinct and separate entity with its own clinical significance and not just a consequence of pelvic obliquity. A number of clinical and radiographic procedures are based on the assumption that sacroiliac joint misalignment resulting in relative sacral obliquity is a quantifiable and significant entity (13, 27, 40, 41, 65, 78, 79, 83). However there are no studies in the available literature that unequivocally validate this assumption (142).

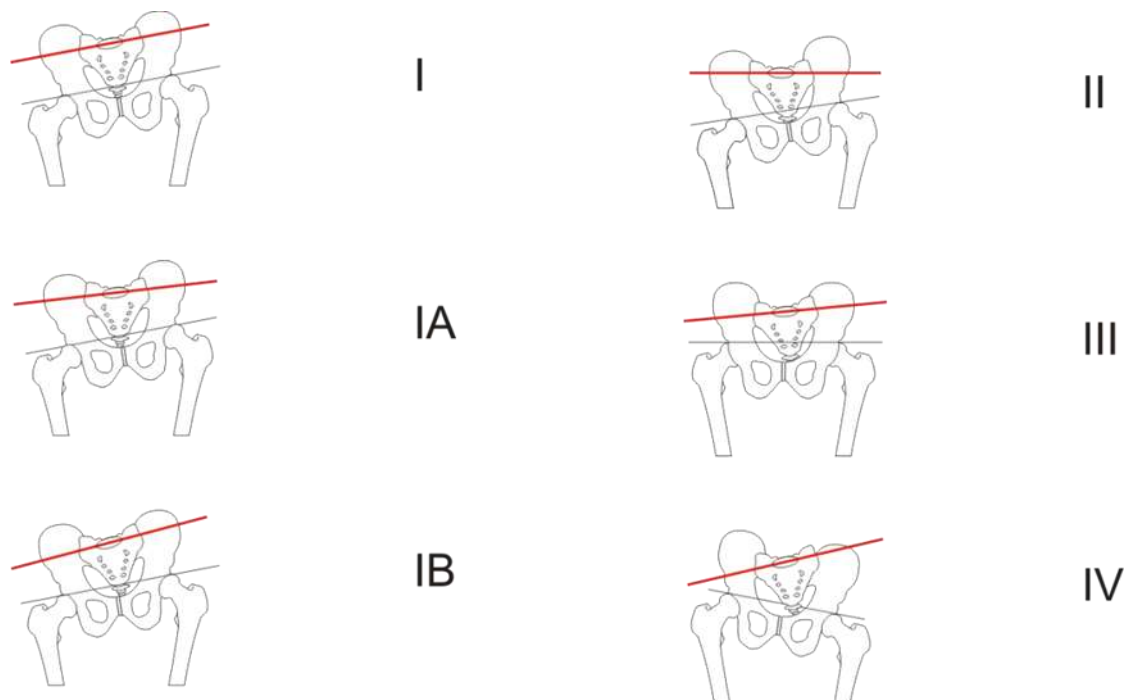
The differentiation of sacral obliquity, pelvic obliquity and leg length imbalance has two major implications for clinicians. The first is that the assumption of equivalency of sacral obliquity and pelvic obliquity could lead to a misdiagnosis or seemingly conflicting information regarding the patient's structural alignment or lack of it. Dott *et al* (86) for example suggest that treatment based on palpatory examinations of the iliac crest presupposes a direct and consistent relationship between the pelvic bones (innominates) and the sacral base. They conclude that in cases of mild to moderate short leg syndromes, the iliac crest height is an unreliable predictor of the direction or degree of sacral base levelness. Fann (11) suggests that '*unelucidated*' factors, other than leg length discrepancy, must contribute to the development of chronic pain and degenerative changes in the lumbar spine. Fann also goes on to state that measuring solely the femoral heads instead of the sacral base ignores the complexity of the mechanics between the lumbar spine and pelvis. In support of this view, a review by Papaioannou *et al* (66) of the records and physical findings of twenty three young adults that had significant untreated leg length inequality revealed no relationship between the underlying cause of the anisomelia or its duration and the severity of the spinal abnormality.

Another implication in assuming equivalency of absolute sacral and pelvic obliquity manifests itself when changing from sitting to standing posture. If the orientation of the sacral base involves both pelvic obliquity due to leg length imbalance and relative sacral obliquity due to internal pelvic asymmetry, the level of the sacral base in the frontal plane can be measurably different when changing from sitting to standing posture (Figure 5).



**Figure 5.** Change in the orientation of the sacral base from standing posture (A) to sitting posture (B) with the internal architecture of the pelvis remaining constant. The blue line represents the plane of the sacral base and the red line represents the plane of the femur heads

Juhl *et al* (83) using lumbar radiographic studies examined the prevalence of six types of postural asymmetry involving leg length imbalance, sacral obliquity and scoliosis. The study describes differences between anisomelia or leg length imbalance and absolute sacral obliquity that result from internal pelvic asymmetry. They suggest that an angulation of the sacral base relative to the femur heads coupled with an actual leg length difference produces six distinct postural patterns (Figure 6).



**Figure 6.** The six combinations of sacral obliquity and leg length imbalance used by Juhl *et al* and other osteopathic clinicians

### *1.1.2 Scoliosis (Vertebral Endplate Obliquity)*

A scoliosis is a lateral curvature of the spine involving obliquity of vertebra in the frontal plane (49). Cobb angles are commonly used to measure vertebral obliquity on anteroposterior or posteroanterior plain radiographs of the spine as a method of quantifying and classifying scoliotic curves (143). In order to measure a scoliotic curve the end or transitional vertebra are identified as the segments common to the reference curve and the curves above and below. The end vertebra are the most superior and inferior vertebra which are least displaced and rotated and has the maximally tilted (oblique) end plate. Obliquity is measured using a line drawn along the superior end plate of the superior end vertebra and another line drawn along the inferior end plate of the inferior end vertebra. If the end plates are indistinct the line may be drawn through the pedicles. The angle between these two lines (or lines drawn perpendicular to them) is measured as the Cobb angle.

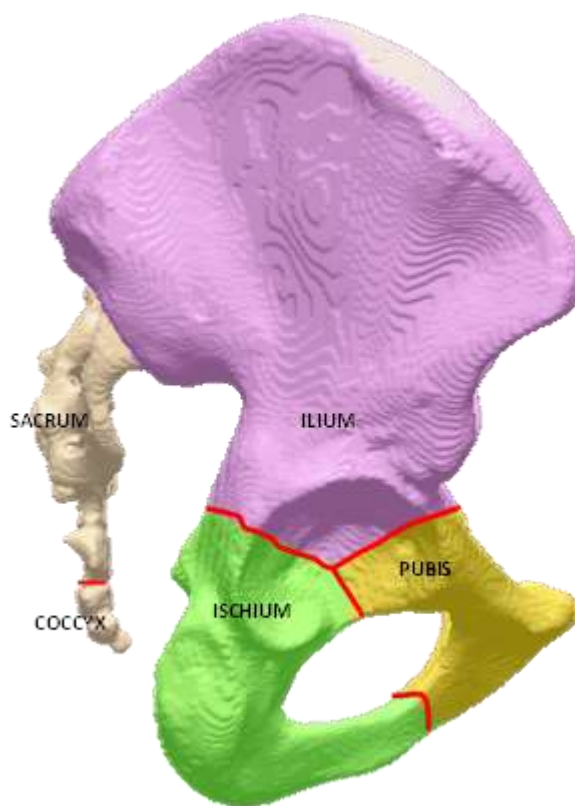
Chiropractic radiographic analysis of the spine is used to produce a 'listing' of a vertebra and is commonly used to indicate structural '*dysrelationships*' of spinal segments (12). The loss of positional integrity of pelvic and spinal segments is traditionally referred to as a subluxation. According to Gonstead (12, 13), lines constructed parallel to the adjacent vertebral endplates will converge if a lateral flexion malposition is present and will be parallel if no such subluxation exists.

## **1.2 MORPHOLOGY OF LUMBOPELVIC SEGMENTS**

Specific aspects of anatomy, morphology and functioning of the joints of the pelvis and spine are relevant to an understanding of obliquity angles. A number of authors (30, 37, 44, 100, 142, 144, 145) have previously outlined the clinically significant anatomy, morphology and function of the lumbopelvic region.

### *1.2.1 Bones of the pelvis*

The average adult pelvis is comprised of eleven individual bones (37). These are the five sacral segments, fused in the adult spine, four coccygeal segments, sometimes fused to form two or three moveable segments, and two innominate bones. The innominate bones are in turn made up of three separate bones that are fused in the adult pelvis with a point of commonality at the centre of the acetabulum. They are the ilium, ischium, and pubis bones (Figure 7). The morphology of the osteological pelvis as a whole has been considered to exhibit reflective symmetry around the mid sagittal plane (82).



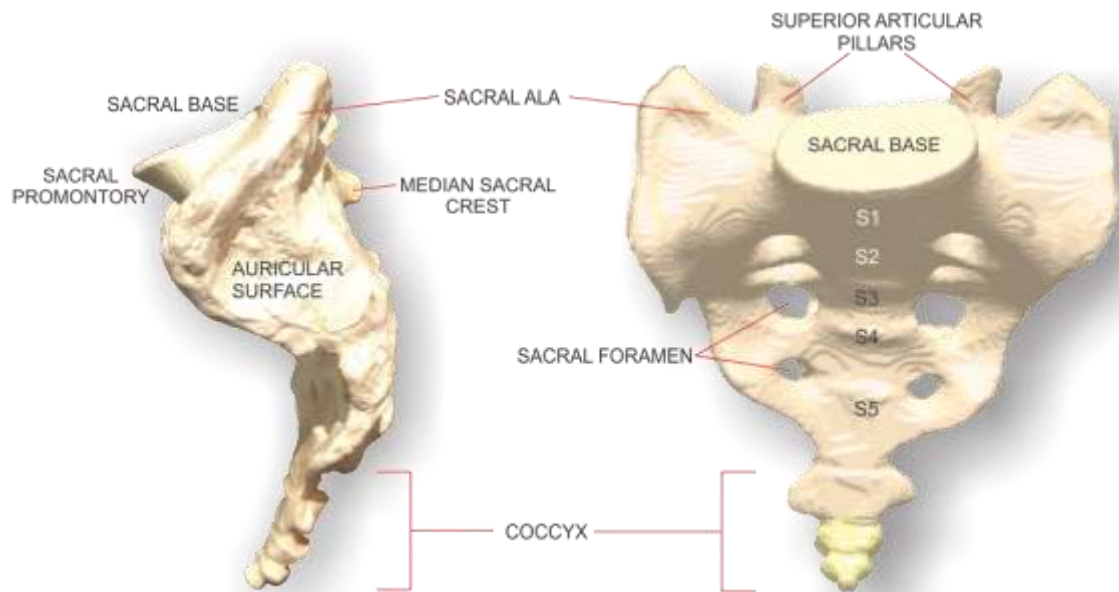
**Figure 7. The individual bones that make up the adult pelvis**

The sacrum has been described in the context of surgically relevant anatomy by Cheng and Song (37). They describe the human sacrum as generally being made up of the five sacral segments that fuse by involution of the intervening discs to form a large triangular shaped bone that forms the posterosuperior wall of the pelvis. The triangle is inverted with its apex pointing to the caudal end of the body or inferiorly in upright posture. It is aligned and centred on the mid-sagittal plane of the body. The five sacral segments have a similar

structure to a typical lumbar vertebra in that they are comprised of the body, which is equivalent to the body of a typical lumbar vertebra, the vertebral arch and a costal element. Early in life, ossification of the lateral aspect of each segment, made up of the lateral aspect (transverse process) of the vertebral arch and the costal element join together to form the sacral ala (145). The ala on each side of the five individual segments eventually fuse to form one bone with the lateral aspect of the first three forming the irregular flattened articular surface of the sacroiliac joints.

The sacral base is the superior articulating surface of the sacrum and represents the equivalent of the vertebral endplate. It articulates with the 5<sup>th</sup> lumbar vertebra above at the lumbosacral junction. Lee and Hodges (145) describe the cranial aspect of the first sacral vertebra as consisting of the vertebral body inferiorly (the sacral base) with the anterior projecting edge known as the sacral promontory.

The coccyx is usually made up of four rudimentary vertebral segments that combine into two or three segments in adulthood. The first coccygeal segment articulates with the last (5<sup>th</sup>) sacral segment above at the sacrococcygeal symphysis. In most instances this joint has only limited movement (Figure 8).

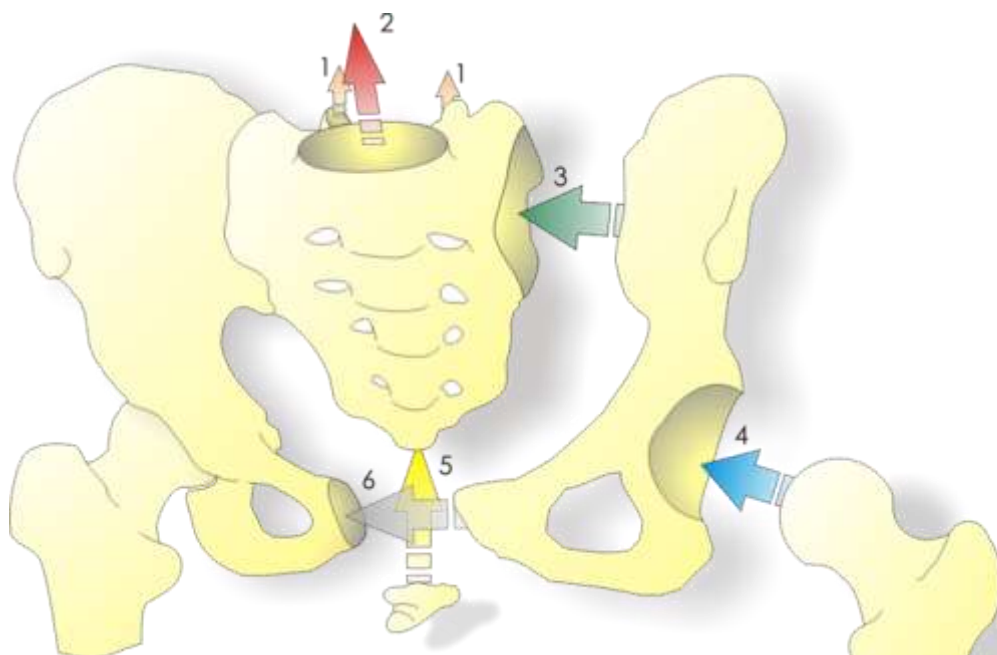


**Figure 8. Side and front view of the sacrum with anatomical features identified**

### 1.2.2 Joints of the pelvis

There are nine articulations associated directly with the bony pelvis (Figure 9). Each innominate bone articulates with the sacrum at the diarthrodial sacroiliac joints. These are strong, weight bearing synovial joints with irregular elevations and depressions and strong intrinsic and extrinsic ligaments that produce and maintain interlocking of the two bones with weight bearing and small amounts of movement. Each innominate bone articulates with the opposite innominate at the symphysis pubis, an amphiarthrotic joint, and with a femur head at the acetabulofemoral joint. The sacrum articulates with the lumbar vertebra above and the coccyx below. The sacral base articulates with the intervertebral disc of the vertebra above (usually the 5<sup>th</sup> lumbar) at the lumbosacral junction and a pair of facet joints articulates directly with the inferior articular facets of the same vertebra. The coccyx articulates with the sacrum at the sacrococcygeal joint.



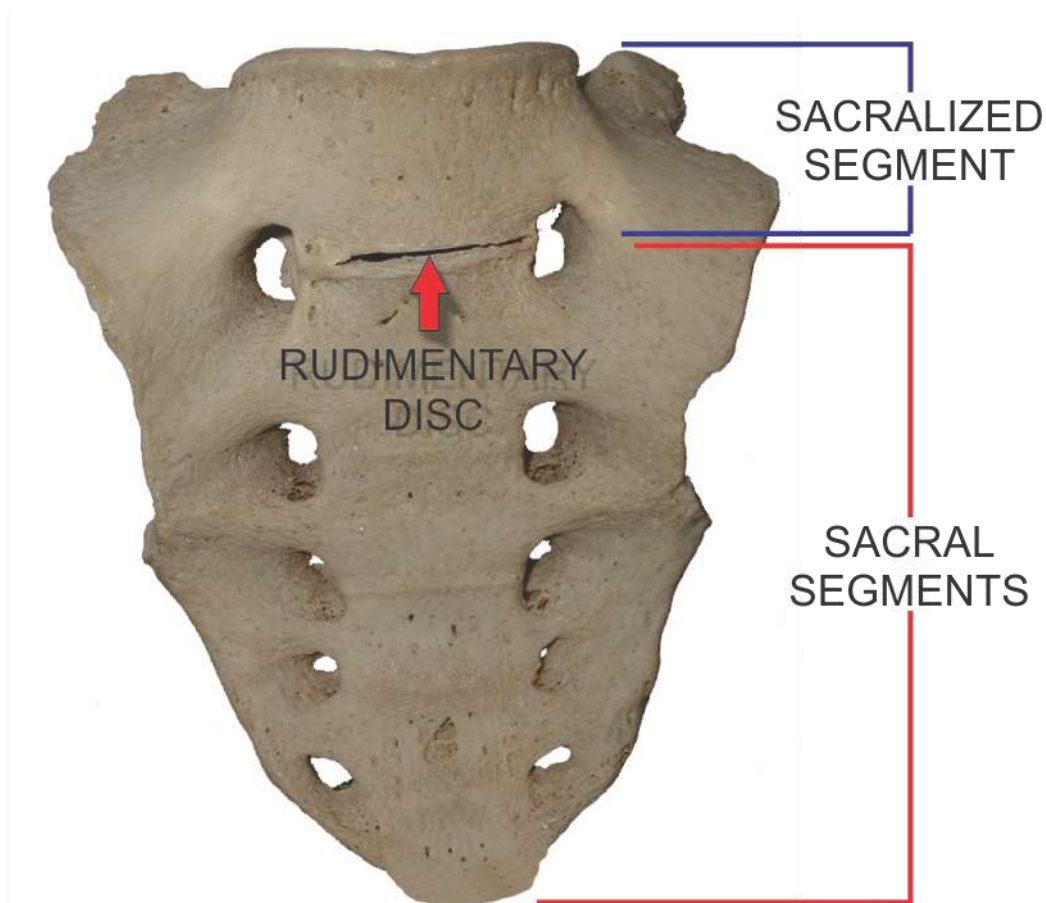


**Figure 9. The nine major articulations of the pelvis. 1. Two facet joints 2. Lumbosacral disc 3. Two sacroiliac joints 4. Two acetabulofemoral joints 5. Sacrococcygeal joint 6. Pubic symphysis**

The sacrum has six articulations, although this can vary with congenital variations at the lumbosacral junction and sacroiliac joints. Commonly there are the two sacroiliac joints laterally, the lumbosacral articulation and two facet joints at the lumbosacral junction and sacrococcygeal symphysis between the sacrum and coccyx. The innominate bones form the outer part of the sacroiliac joints on either side of the sacrum and articulate with each other at the symphysis pubis to form the pelvic girdle. The innominate bones articulate on either side of the pelvis with the femur heads at the acetabulofemoral joints.

A variation found at the lumbosacral junction that can influence the number of joints in the region and make identification and classification of the sacral base difficult involves a transitional segment where the last lumbar vertebral (what would normally be L5) or the first sacral segment (what would normally be S1) can have characteristics of the sacrum or lumbar segment respectively. In a study of 300 consecutive patients with lumbar spine related pain syndromes Delport *et al* (146) reported that 30% had a transitional lumbosacral segment that was not always visible on advanced imaging. They classified the type of transitional segment into one of four groups comprising complete or incomplete bony union

and bilateral or unilateral articulation of the transverse processes. In a review article of the classification, imaging findings and clinical relevance of transitional lumbosacral segments Konin and Walz (147) concluded that transitional vertebra involving the sacral base are common anomalies of the spine that need accurate identification and numbering of the affected segment. They suggest from their review that while it has been long contested, there is fairly convincing evidence of an association of low back pain with transitional segments. They further state that knowledge of the biomechanical alterations within the spine caused by transitional segments at the lumbosacral junction could help radiologists and clinicians understand and recognise the imaging findings seen in patients with low back pain and a transitional segment (Figure 10).



**Figure 10. A sacrum comprised of six individual segments due to the addition of a transitional lumbosacral segment**

### 1.2.3 Movement within the pelvic girdle

Movement has been shown to occur within the pelvic girdle at the sacroiliac joints and the symphysis pubis (142, 145). The most significant movement demonstrated is nutation and counter-nutation of the sacrum around a transverse axis (100, 148) (Figure 11).

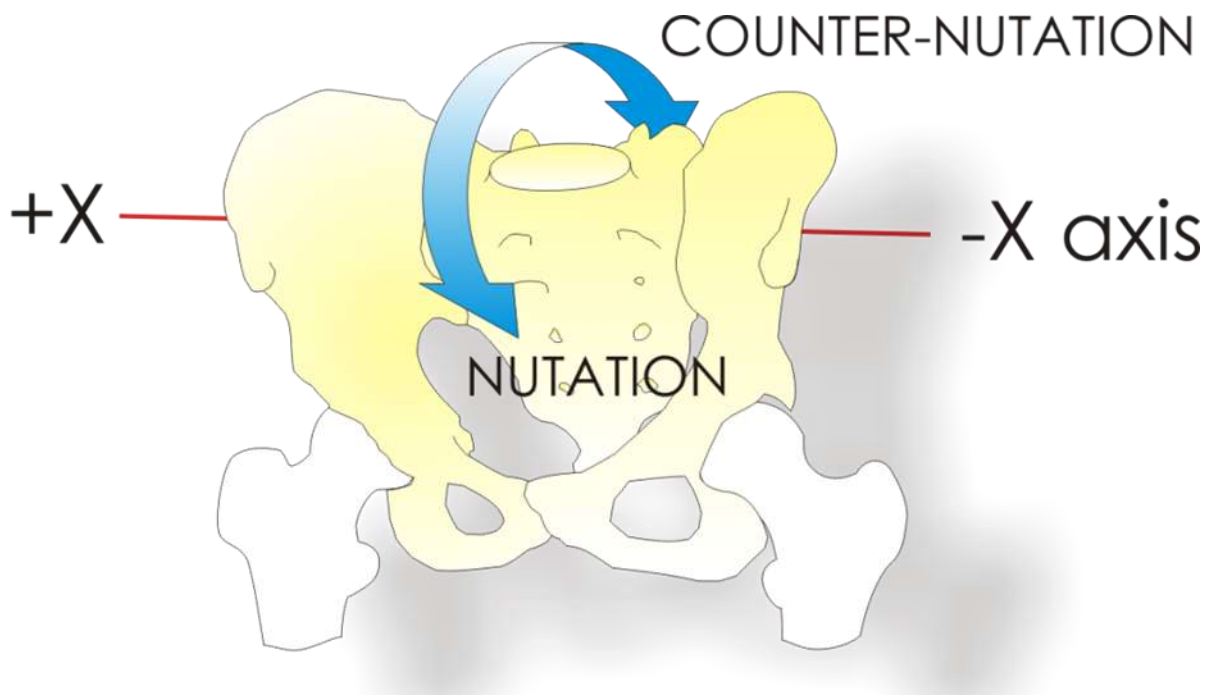


Figure 11. Rotation of the sacrum around the x-axis described as nutation (+x) and counter-nutation (-x)

Movement of the SI joints has been interpreted as being clinically significant in low back pain syndromes (44, 77, 149-152) functional patterns of the spine (31, 32, 34, 41, 77) and sacroiliac joint pain (149, 153). The sacrum under physiological loading conditions has been shown to have only very small movement around the Z-axis (148, 152, 154, 155) (Figure 12). Hu *et al* (148) found that it is in the range of 0.5 degrees for axial rotation in adult cadaveric spines.

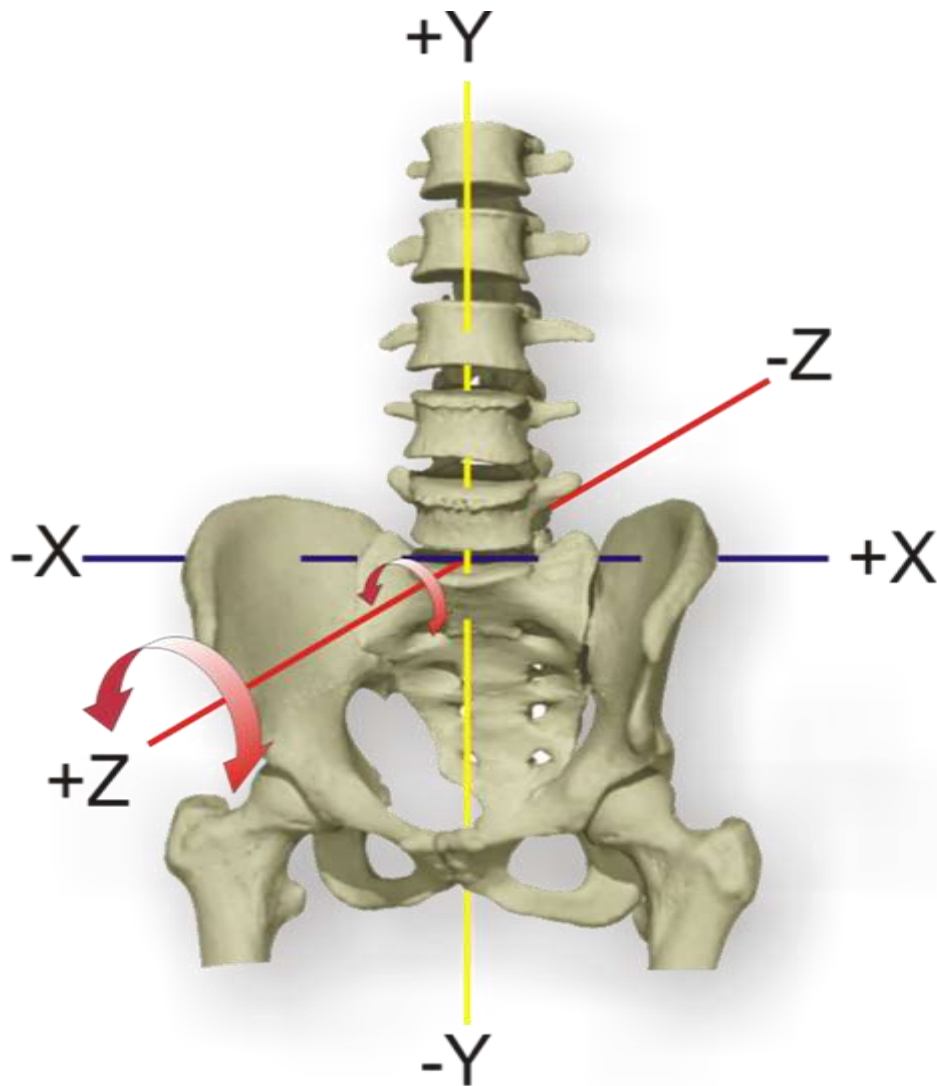


Figure 12. Lateral tilt of the sacrum around the Z-axis

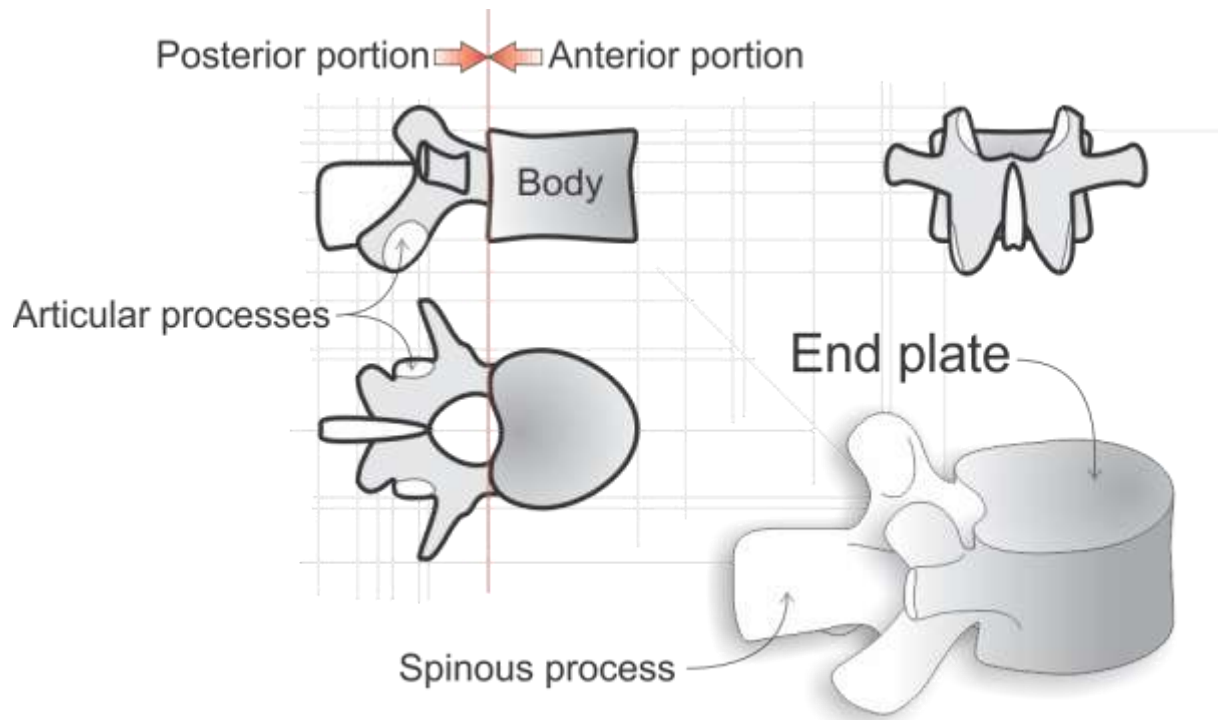
Rotation of the ilia, either unilaterally or as counter rotation of the opposite ilia, has been suggested as another mechanism that results in relative obliquity of the sacral base (12, 13, 77). However, clinical assessment of this movement has not been validated in the relevant literature.

There is general consensus from studies of movement involving the sacroiliac joints that there is an extremely small amount of linear and rotational movement of the sacrum relative to the ilia in the frontal plane. Based on a comprehensive systematic literature review of sacroiliac (SI) joint movement, Goode *et al* (151) concluded that motion at the sacroiliac

joint is limited to what they describe as “minute amounts” of rotation and translation with frontal plane rotation in the range of -0.5 to 0.8 degrees. Stureson *et al* (154-156) in three separate studies involving radiostereometric analysis of SI joint movement demonstrated Z-axis rotation of less than  $0.3^{\circ}$  with a standard error of measure of  $0.1^{\circ}$ . While some distortion of the pelvic ring may occur due to movement at the SI joints in various postures, the difference in position of the sacrum relative to the ilia accounts for only a minute change in the orientation of the sacral base relative to the innominate bones and hence the degree of relative sacral obliquity. Contraction of the transverse abdominis was found by Richardson *et al* (157) to decrease the laxity of the sacroiliac joint in their *in vivo* study of healthy subjects. The study was designed to demonstrate the biomechanical effect that contraction of the transverse abdominis has as an effective exercise in low back pain. Movement of the sacroiliac joints had been shown to be influenced not only by structural quality and integrity of the sacroiliac joints but also by active contraction of lumbopelvic muscles (158). This effect would be absent in *in vitro* studies that attempt to quantify sacroiliac joint movement.

#### 1.2.4 Vertebral morphology

There are 33 individual segments making up the human spine. The adult vertebral column usually consists of 24 moveable segments that are irregular bones consisting of two distinct morphological portions, both with general symmetry around the mid sagittal plane. The vertebral body is the large roughly cylindrical anterior part of each segment (except C1 the atlas) with almost flat top and bottom surfaces known as the end plates. These surfaces are integral with, and form the support for the intervertebral discs that lie above and below each segment, except for the axis (one disc below) and the atlas vertebra (no discs). The outer rim of each end plate is the fused ring apophysis and is slightly raised from the surface. It is a narrow portion of smoother, denser bone compared to the more porous centre region (Figure 13).



**Figure 13. Morphology of a typical vertebral segment**

The posterior portion comprises two pedicles attached to the vertebral body and a lamina on either side that form the posterior portion of the neural arch. There are transverse processes on both sides of the posterior element and one spinous process at the junction of the laminae in the mid line. A pair of superior and inferior articular processes provides the structural support for the zygapophysial joints except for C1 and superior joints of C2. The number of joints associated with each vertebra varies with the region of the spine involved.

#### *1.2.5 Vertebral movement*

The 24 freely moveable segments in the typical weight bearing human spine consists of seven cervical, twelve thoracic and five lumbar vertebrae. The degrees of freedom and ranges of movement vary with each segment and each region of the spine.

Each spinal segment can rotate through various degrees of rotation in the three planes X, Y and Z (Figure 12). These rotations are referred to in anatomical terms as flexion/extension, lateral flexion and rotation. There is minimum displacement between individual vertebrae

due to shear strain in the normal spine. A consideration in the evaluation, classification and quantification of spinal movement involves coupling patterns of individual spinal segments and spinal regions. Each region of the spine has gross coupling patterns that are influenced by the kyphotic or lordotic curve associated with the region and the architecture of the joints associated with the region of the spine involved.

### **1.3 CLINICAL IMPLICATIONS OF SKELETAL ASYMMETRY**

#### *1.3.1 Structural asymmetry of the spine*

Structural asymmetry of the skeletal framework has been identified as a clinically significant factor in a variety of anatomical areas (3, 4, 27, 39, 40, 42, 48, 55, 57, 59, 60, 66, 69, 70, 72-74, 76, 78, 79, 82, 83, 85, 90, 91, 97, 113, 114, 159). Structures of the musculoskeletal system that have been identified as exhibiting significant structural asymmetry include:

- Innominate bones (3, 42, 82, 160)
- Sacrum (27, 39, 40)
- Lower limbs (70, 72, 161-163)
- Vertebra including atlas and occipital condyles (114, 159, 164)
- Other skeletal structures (161, 162, 165, 166)

Assessment of structural asymmetries of the axial skeleton, with the possible exception of anisomelia, has not generally been incorporated into validated clinical diagnostic protocols and specific treatment procedures. Fann (11) emphasises this point by suggesting that most of the literature relating to skeletal asymmetry has addressed the role of leg length discrepancies (LLD) in relation to back pain. This view is supported by Al-Eisa *et al* (3) who suggest that patients with low back pain may have a distinct compensatory mechanism, secondary to pelvic asymmetry that puts the lumbar spine under greater stress. Opposing this view, Levangie (73) found that pelvic asymmetry determined from external pelvic

landmarks was not positively associated with low back pain in any way that seemed clinically meaningful.

Altered functional patterns and pain syndromes have been associated by a number of investigators with pelvic skeletal asymmetry (3, 4, 42, 59, 70, 92). The reliability and validity of physical examination procedures used to assess or measure skeletal asymmetry in a clinical setting has been critically reviewed. Levangie (73) concluded from her study of 144 cases and 138 control subjects that evaluation and treatment strategies based on the clinical assessment of pelvic asymmetry should be questioned. The reliability of procedures commonly used by osteopaths to assess asymmetry of landmarks presumed to indicate pelvic somatic dysfunction was investigated by Kmita and Lucas (167). They concluded that the reliability of the particular examination procedures was low and not clinically useful. Ross *et al* (114) came to a similar conclusion regarding the validity of palpation used in a clinical setting to assess the cervical spine. They found that asymmetric joint geometry is common in this region of the spine and this could mislead the clinician when assessing joint motion. In a review of the literature relating to the reliability and validity of tests to assess the positional integrity of the sacroiliac joints, Huijbregts (168) found that current research did not support a specific diagnosis in the sense of a sacroiliac joint positional fault or specific hypomobility as needed to guide manual medicine interventions of sacroiliac joint dysfunction. Bowman and Gribble (169) also found that for three common clinical tests used to assess apparent discrepancies in leg length or structural asymmetry of the lower limbs, agreement was no greater than would be expected by chance.

The clinical methods employed to assess structural and functional obliquity of the spine are frequently linked to the therapeutic and outcome objectives of the professions involved. McGill (36) suggests that each professional group attempts to identify the primary dysfunction according to its particular type of treatment. In this respect most of the clinical



methods employed to assess the positional integrity of the spine and the significance attached to the findings are, to a large extent, based on assumptions relating to the presumed cause of the clinical presentation. Commonly expressed assumptions include the presence of sacroiliac joint misalignments and dysfunction (hyper- and hypo-mobility) (77), functional leg length imbalance (90), muscular imbalances and manipulable lesions of the musculoskeletal system (34). A group comprised mainly of practitioners who specialise in musculoskeletal disorders or manipulative therapies, such as orthopaedists, chiropractors, physiotherapists and osteopaths, have developed a wide range of clinical practices and assessment methods aimed specifically to assess positional integrity and asymmetry of the spine and pelvis (80, 137-140, 162, 170-175). These orthopaedic and other clinical tests include functional and postural assessment of the musculoskeletal system, spinal imaging and specific clinical tests.

### *1.3.2 Functional assessment*

Functional assessment of musculoskeletal symmetry can involve quantifying ranges of motion (175, 176), specific muscle strength testing (16, 171) and palpation of joints for mobility and positional integrity (137, 172, 174, 177). Static palpation tests used to assess asymmetry and dysfunction of the pelvic region were evaluated by Holmgren *et al* (175). They concluded that for clinical practice, the tests used as methods for detecting pelvic asymmetry were of doubtful utility. Studies such as these suggest that asymmetrical spinal patterns are commonly assessed and attributed to joint dysfunction and positional changes between structural elements of the spine and pelvis without the tests and clinical methods having been subjected to rigorous validation. Pain provocation tests (149, 171) along with other specific clinical tests (171, 173, 178-181) have been developed and employed by clinicians to assess the integrity the sacroiliac joints and pelvic alignment. Global postural variations are considered to be indicative of asymmetry of specific structures or representing specific joint dysfunction (136, 170, 171, 181-183).

McGrath (149) concludes from a review of the relevant literature that sacroiliac joints (SIJ) motion has been shown to be 'minute, unpredictable and its measurement neither reliable nor valid'. Because of the lack of demonstrated inter and intra reliability he suggests that the belief held by many clinicians that SIJ motion is in fact manually palpable also remains open to question. Stovall and Kumar (177) in their review of the literature to establish the state of knowledge on the reliability of clinical assessment of asymmetry in the lumbar spine and pelvis conclude that assessment of bony anatomic landmark asymmetry has not been demonstrated to be a reliable method of palpatory assessment. They identified that one reason for their review was the wide range of palpatory approaches that have been used for detecting dysfunction in the spine and pelvis prior to manipulative intervention. In this context, bony anatomic landmark asymmetry is hypothesized mainly by chiropractors and osteopaths to give information on the relative positions of the structures in question. Maigne *et al* (184) found in their study to objectively evaluate specific sacroiliac pain provocation manoeuvres that no single clinical test is sufficiently sensitive to differentiate among multiple anatomic variations and the other surrounding tissues. They concluded that provocation tests in patients with negative response to blocks are not specific tests of sacroiliac joint pain.

### *1.3.3 Spinal imaging*

Plain film radiography is a commonly used clinical tool for assessing obliquity of the spine and pelvis (174, 179, 185, 186), particularly by professional groups such as chiropractors (12, 13, 41, 78, 79) and osteopaths (8, 171) as well as medical practitioners as in the case of scoliosis assessment (33, 52, 187). Based on a three-dimensional study of the pelvis, Boulay *et al* (160) suggest that asymmetry of the lower part of the pelvis, particularly at the acetabulum level, is not accessible in a clinical setting making evaluation difficult if not impossible. They also concluded that because of osseous superposition on plain film radiographs, it is very difficult to measure the asymmetry of the pelvis at the acetabulum level with commonly used radiographic views of the pelvis. Other investigators have

identified potential systematic errors associated with plain film radiography of the pelvis that could influence the validity of structural asymmetry measurements (8, 29, 187-191). Kuchera and Kuchera (8) commenting on the validity of postural radiographs make the observation that a lack of standardisation of osteopathic radiographic protocols has rendered many measurements meaningless for the purposes of positional diagnosis, patient follow-up, or research.

Computerised tomography (CT) and magnetic resonance imaging (MRI) have also been used as clinical methods to assess the positional integrity and symmetry of the pelvic region (7, 192-195). These methods have generally been shown to be valid and reliable for the clinical assessment of asymmetry of the spine and pelvis. Cargil *et al* (193) used three dimensional MRI studies to measure intervertebral movements between postures. Using three-dimensional reconstructions of MRI data they were able to measure individual postural patterns. They concluded that with improvements in imaging technology the method could have a wide variety of applications. However, advanced spinal imaging methods are not commonly utilised in a clinical setting mainly due to the high dose of potentially harmful ionising radiation in the case of CT imaging, and the cost involved and limited availability of advanced spinal imaging equipment particularly for imaging weight bearing postures (196-199).

#### *1.3.4 Specific clinical tests and assessment methods*

There are numerous other methods used to assess functional and positional patterns of the spine and pelvis that are utilised by practitioners in a clinical setting. Some of these methods include proprietary radiographic analytical methods employed by chiropractors using protocols such as the technique developed by Gonstead (12, 13). Other techniques include physiotherapy based McKenzie methods (200) and osteopathic techniques presented by Schiowitz *et al* (171), Dowling (181) as well as tests that involve functional

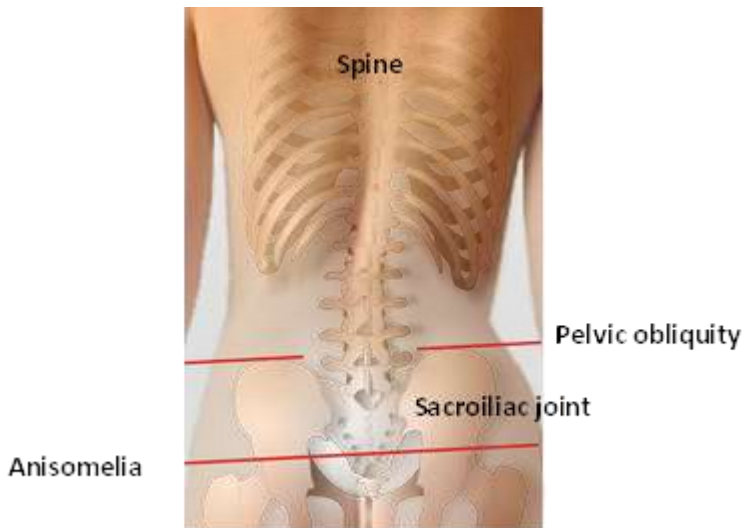
and postural assessment such as those used by Alexander technique practitioners (107, 118).

Medical, chiropractic and osteopathic practitioners such as Schamberger (77), Illi (41), Gonstead (12, 13), and Irvin (65) have attributed the functional patterns and pain syndromes to loss of joint integrity, particularly of the sacroiliac joints. However, despite these commonly held beliefs, a relatively small number of clinicians and researchers, including Brown *et al* (27), Barge (78), Juhl *et al* (83), Cartstens (40) and Liebenson (79) have suggested that the clinically observed patterns attributed to spinal and sacroiliac joint dysfunction are, at least in a significant number of cases, the result of structural asymmetry of the sacrum in the frontal plane. They independently suggest that structural asymmetry of the sacrum is a significant clinical factor either wrongly attributed to functional alignment asymmetry, or largely unobserved in clinical practice. Liebenson (79), states that the most frequent fallacy is for clinicians to associate disturbed body static alignment with pelvic obliquity and leg length differences rather than with the levelness of the sacral base.

#### **1.4 FUNCTIONAL AND STRUCTURAL PELVIC OBLIQUITY**

Pelvic obliquity is any deviation of the horizontal plane of the pelvis from level and is usually measured in an upright posture by comparing the relative height of the iliac crests to see if one side of the pelvis is higher than the other (201). Pelvic obliquity, lateral pelvic tilt and other terms representing the same or similar concepts have been used by researchers and clinicians with an assumption of inter-changeability with sacral obliquity in describing an angulation in the frontal plane of the base of the spine in erect posture (Figure 14). For example, studies have attempted to relate pelvic obliquity and leg length imbalance to lumbar spine scoliosis or back pain. Studies such as those by Giles (164), Giles and Taylor (55) and others (61, 62, 64, 66, 71) tacitly assume equivalency of pelvic and sacral obliquity. In a review of the literature relating to leg length inequality (LLI), Colloca (90) references numerous authors who equate scoliosis and postural changes directly to the

presence of leg length imbalance (or inequality). However others suggest that an oblique pelvis may or may not equate directly with obliquity of the sacrum (79, 83, 86, 171).

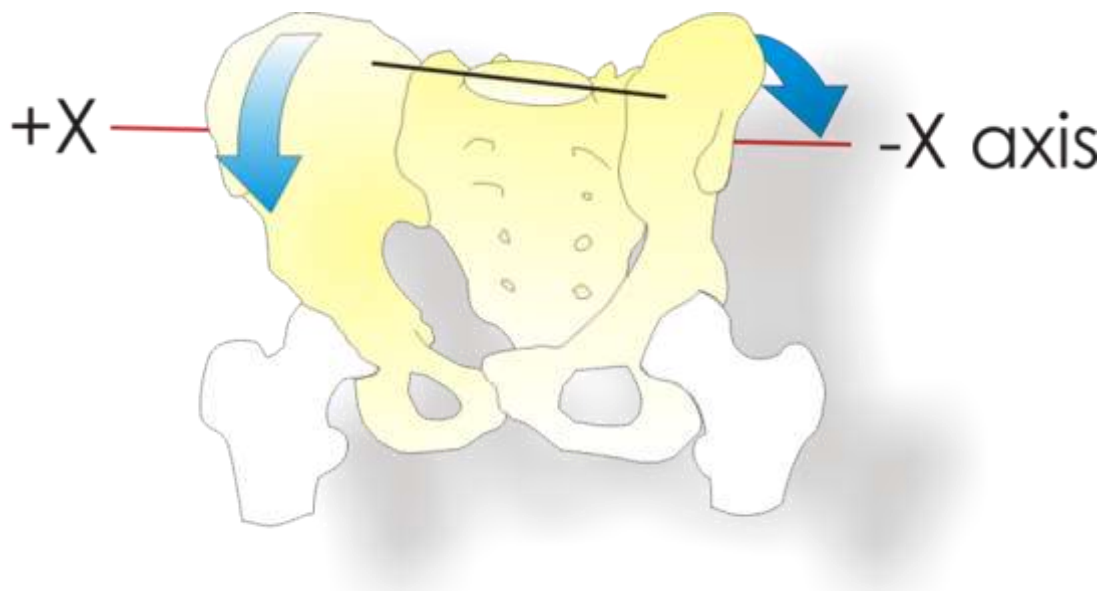


**Figure 14. The relationship between anisomelia, sacroiliac joints and pelvic obliquity with the spine above**

The concepts of sacral and pelvic obliquity, when used as descriptive terms for the orientation of two different structures i.e. the sacrum and ilia, cannot be assumed to be synonymous. A study by Hoikka *et al* (74) supports this differentiation by demonstrating a lack of correlation between the direction of lumbar scoliosis and leg-length inequality in their study of one hundred patients with chronic low-back pain.

Leg length imbalance (inequality) and sacroiliac joint misalignment or dysfunctions are two clinical presentations commonly associated with pelvic obliquity in the frontal plane (8) (Figure 14). These involve either structural or functional asymmetry of components of the musculoskeletal system. Functional asymmetry of the pelvis has been attributed to leg length imbalance and sacroiliac misalignments by chiropractors (13), medical practitioners (77) and osteopaths (177, 202). Leg length imbalance has in turn been attributed to both structural (anisomelia) and functional asymmetry of the lower limbs (13, 50, 72).

Sacroiliac joint dysfunction is considered by many clinicians as a form of functional asymmetry affecting the positional relationship of the sacrum and components of the pelvis under static or dynamic loading conditions (12, 13, 31, 34, 41, 116, 138, 150, 160, 171, 174, 181) (Figure 15). These two factors are considered the major contributing factors in observed pelvic obliquity even though the magnitude, distribution and clinical significance of both factors is considered controversial and unsubstantiated by many researchers and clinicians (80, 84, 142, 149, 151, 154, 155, 168-170, 175, 178, 186, 194, 203, 204) (Figure 15).



**Figure 15. Pelvic torsion due to counter rotation of the ilia proposed as a method that would result in a functional sacral obliquity**

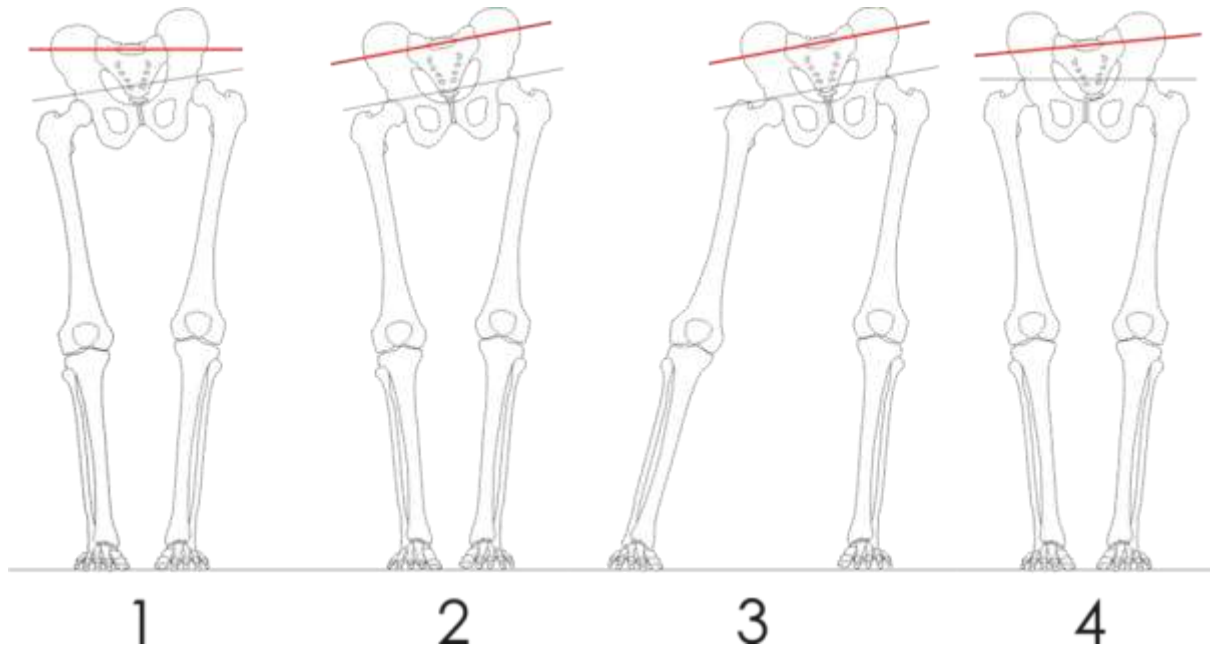
Structural pelvic asymmetry has been identified as another compounding factor that is difficult to quantify in a clinical setting (82, 85). Badii *et al* (85) found that innominate asymmetry greater than five millimetres only occurred in approximately 5% of their three hundred and twenty three study participants. Their study contrasts with the one reported by Ingelmark and Lindstrom (205) who studied the association between leg length inequality and pelvic asymmetry in two hundred and seventy patients. Ingelmark and Lindstrom defined pelvic asymmetry as measured on standing anteroposterior radiographs of the

pelvis as the difference in the measured distance from the iliac crest to the acetabulum on either side. They reported a difference of greater than five millimetres in fifty one per cent of patients participating in the study. Al-Eisa *et al* (4) in their study of fluctuating asymmetry and its relationship to lower back pain found that the low back pain group had a significantly higher mean pelvic asymmetry ratio compared to normal controls. A positive association between non-specific low back pain and pelvic asymmetry was also found in a study by Al-Eisa *et al* (3). This study also showed a link between pelvic asymmetry and altered trunk motion in sitting position. Plochocki (39) analysed asymmetry in the human sacrum in a sample of two hundred and thirty eight individuals. He found significant directional asymmetry in all three directions (frontal, coronal and sagittal) resulting in the sacrum having a highly variable morphology which he associated with handedness.

Fann (11) investigated the validity of using radiographs to measure pelvic obliquity. In this particular study Fann used a line representing the sacral base as previously described by Tilley (188), as the plane representing the relationship of the pelvis to the horizontal plane. A limitation of the study was that it measured absolute sacral (pelvic) obliquity induced by inserting a heel lift of a given size under one leg for the radiographic study. The investigation did not attempt to evaluate the validity of radiographic methods used to measure relative sacral obliquity, positional changes in the sacroiliac joints or pelvic symmetry.

The clinical significance of assessing pelvic obliquity and leg length imbalance is based on an implied assumption that the measured asymmetry represents an obliquity of the structural base of the spine (79). However, in most studies the validity and reliability of assessing pelvic obliquity has been documented without specific reference to the sacral base. The significance of the distinction between sacral and pelvic obliquity is that the sacral base acts as the structural foundation of the spine whereas the pelvis as a unit acts as the structural link between the lower limbs and the spine. The sacrum is an integral part

of the pelvis but the pelvis does not necessarily define its relative or absolute position (Figure 16).



**Figure 16. Anisomelia (1 – 2) and isomelia (no leg length discrepancy) (3 - 4) with different pelvic patterns and degrees of sacral obliquity**

Leg length imbalance, or anisomelia, is defined as a structural inequality of the lower limbs or lack of symmetry in the length of the paired bones of the lower limbs (69). Leg length imbalance has been extensively studied in patients with low back pain, functional spinal disorders and other musculoskeletal problems (57, 70, 72, 136, 206-209). The significance of leg length imbalance relative to sacral obliquity is related to its influence on, or relationship to pelvic obliquity as a causative factor (Figure 17). Functional leg length imbalance has been posited as due to postural and muscle changes or changes in the positional relationships within the pelvis (50, 136) (Figure 17).



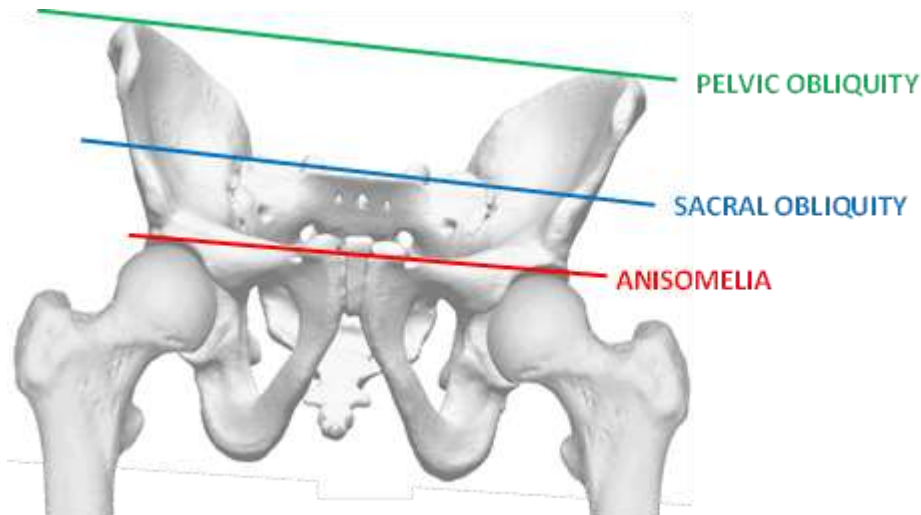


Figure 17. Anisomelia (red), absolute sacral obliquity (blue) and pelvic obliquity (green)

According to Knutsen (72) the clinical significance of leg length imbalance is a contentious issue for practitioners. He based this opinion on an extensive review of the relevant literature. There are a number of methods commonly used to quantify leg length inequality in a clinical setting involving the measurement of relative leg lengths in a prone or supine position, erect pelvic landmark evaluation and radiographic analysis (183). Of the commonly used methods, radiographic assessment is considered the 'gold standard' (90, 135).

There are varying opinions expressed in the literature on what can be considered a clinically significant amount of leg length inequality (69, 90, 135). Knutson (72), in a review and recommendation for clinical decision-making relating to the prevalence, magnitude, effects and clinical significance of leg-length inequality, suggests that for most people anatomic leg-length inequality does not appear to be clinically significant until the magnitude reaches twenty millimetres. This magnitude as a clinical 'breakpoint' is also proposed by Gurney (69) who believes that it may be much higher in young people. However, a study by Mahar *et al* (68) supported their hypothesis that a leg-length discrepancy of as little as one centimetre may be biomechanically important. The clinical significance of a one centimetre leg length difference is supported by Steen *et al* (210).

They state, based on their review of the relevant literature, that there is an association between a difference in leg length of more than one centimetre and low back pain.

In discussing heel lifts for postural correction, Fann (54) found that ninety three patients with low back pain had an average of eight millimetres of pelvic obliquity. Friberg (60) also found that correction of leg length inequality with the use of an adequate shoe lift resulted in an alleviation of symptoms in the majority of subjects studied ( $n = 798$ ). The symptoms showed highly significant correlation with leg length inequality of five to twenty five millimetres. Patients with an '*unlevelling*' of the sacral base of greater than two millimetres were used in a study by Hoffman and Hoffman (36) to assess the effect of levelling the sacral base using heel lifts. They found heel lifts provided a statistically significant relief from low-back pain. In a study of conservative correction of leg-length discrepancy of 10 mm or less in patients with chronic low back pain, Defrin *et al* (61) found that shoe inserts significantly reduced both pain intensity and disability. However, based on a study of two hundred and forty seven men and women aged 35 to 54 years, some with disabling back pain and others symptom free, Soukka *et al* (211) found that an association between mild leg-length inequality (mean SD, 5.3 +/- 4.0 mm) and lower back pain was questionable.

Patients with lumbar scoliosis with an accompanying '*unlevelness*' of the sacrum equivalent to two to seventeen millimetres were studied by Irvin (65) to determine the effect of heel lifts on the lumbar curve. He demonstrated a significant reduction of the curve from an average of  $7.5^{\circ}$  to an average of  $5.3^{\circ}$ . A similar study using heel lifts was carried out by Papaioannou *et al* (66). However, they found that the scoliosis was minor in patients with discrepancies of less than 2.2 cm. In contrast, Kuchera (34) states that patterns of imbalance recorded along the spine may be caused by as little as 1.5 mm difference in leg length and can be accompanied by clinical symptoms including back pain. For idiopathic scoliosis patients with a mean age of twelve years Zabjek *et al* (63) found that using

appropriate heel lifts ranging between 5mm and 15 mm resulted in acute postural adaptations with a decrease in the measured Cobb angle (Figure 18).

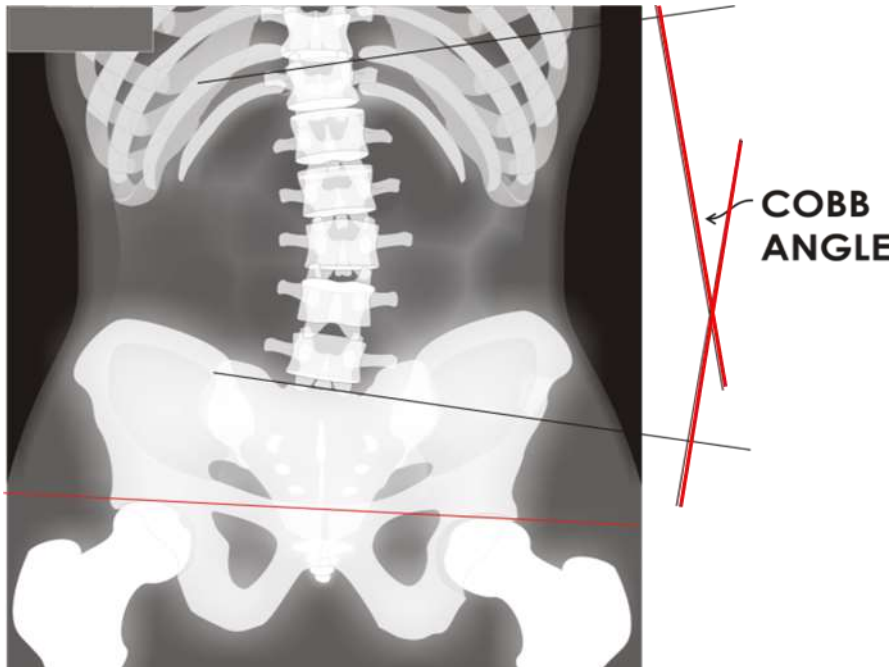


Figure 18. Cobb angle measured as a tangent to the end points of a lateral curve of the spine

Most of the studies and clinical procedures that assess functional leg length imbalance or anisomelia involve either direct measurement of leg lengths that commonly involves radiographic analysis or the use of a more indirect approach such as measuring iliac crest height in erect posture. Neither of these two methods inherently assesses the orientation of the sacral base that is implied in the relationship between leg length imbalance and associated degenerative changes in the spine, spinal pain syndromes, and spinal functional patterns. This problem is addressed by Schiowitz *et al* (171) and others such as Kuchera (34), Hoffman and Hoffman (53) and Kuchera and Kuchera (8). They independently recommend directly assessing the position or levelness of the sacral base. They, along with clinicians such as Juhl *et al* (83), Irvin (65), Tiley (189), Liebensohn (79), and Barge (78) explicitly differentiate therapy directed at restoring leg length balance as opposed to therapies directed to restoring levelness of the sacral base. Edelman (212) states that ‘the very aim in the treatment of leg length differences must be a horizontal position of the upper

edge of the sacrum.’ The osteopathic physician, according to Kuchera and Kuchera (8), is more interested in levelling the sacral base than equalising leg lengths. They state that levelling the sacral base is usually of more clinical significance than comparison of anatomical leg lengths.

Spinal asymmetry has been attributed to, or associated with, clinically observable or palpable sacroiliac joint misalignments, muscular imbalance, as well as other clinically assessed functional changes affecting the sacroiliac joints (8, 32, 34, 171, 172). These clinical diagnostic procedures generally involve assessment of the orientation and symmetry of the pelvis in lying, sitting or standing posture. Few of the tests and assessment methods used to identify or quantify the presumed cause of spinal pathomechanics and spinal pain syndromes have validated or assessed positional integrity against a generally accepted or quantifiable standard, particularly in relation to positional and functional integrity of the pelvis (80, 139, 153).

Clinical assessment of pelvic alignment can be divided into three basic categories. These are (1) static radiographs, (2) static and motion palpation of landmarks associated with sacroiliac joints and (3) functional and structural leg length imbalances. A factor commonly associated with pelvic obliquity by many clinicians is sacroiliac joint dysfunction or a positional change of one or both of the sacroiliac joints (12, 13, 41, 50, 67, 77, 150, 213). Schamberger (77), for example, believes that three types of pelvic misalignment involving the sacroiliac joints commonly cause some form of functional asymmetry.

Schamberger states that pelvic misalignment results in a ‘*malalignment syndrome*’ (Figure 15). The syndrome is characterised by distortion of the pelvic ring with changes in the alignment of the appendicular skeleton and compensatory changes in the soft tissue structures with occasional visceral involvement. Similar concepts have been expressed by Timgren and Soinila (50). Their findings, relating to a study involving one hundred and fifty

neurologic patients, suggest that an acquired postural asymmetry of the sacroiliac joint is a common although often neglected cause of various neurological and other pain related symptoms. They found from their study that these symptoms could be relieved by what they described as a simple and safe manual treatment. However, Tullberg *et al* (84), using roentgen stereophotogrammetric analysis of patients with sacroiliac joint dysfunction found that manipulation of the sacroiliac joints, while normalizing different types of clinical test results, was not accompanied by altered position of the sacroiliac joints. Because the pre and post clinical tests were normalised following manipulation they concluded that the tests used to assess positional integrity of the sacroiliac joints used as part of the study were not valid.

The movement generally considered to be normal for the sacroiliac joints in a clinical setting has been reported to range from  $0^{\circ}$  to  $2^{\circ}$  around various axes. Tests with symmetric forces on the sacrum carried out by Egund *et al* (214) showed that the sacrum rotated mainly about a transverse (X-) axis and at most by approximately two degrees. A systematic review of the literature relating to three-dimensional movements of the sacroiliac joints by Goode *et al* (151) concluded that motion of the sacroiliac joints is limited to minute amounts of rotation and translation. They described one form of movement of the sacroiliac joints as rotation around a sagittal (Z-) axis. The axis courses in an anterior-posterior direction between the joints. Rotation around this axis due to trunk movement associated with going from supine to standing ranged from  $0.1^{\circ}$  to  $-0.3^{\circ}$ .

Ranges of movement of the sacroiliac joints with similar rotation angles are supported by a study conducted by Jacob and Kissling (215). This study involved healthy volunteers between 20 and 50 years of age. They found the average value for total rotation of the sacrum around the X-axis was only  $1.7^{\circ}$ . Sturesson *et al* (154, 156) used radiostereometric analysis to measure sacroiliac joint movement in a standing hip flexion and reciprocal straddle position. The average rotation of the sacrum around the Z-axis did not exceed 1

degree for hip flexion with a mean of  $0.1^{\circ}$  on the right and  $0.2^{\circ}$  on the left. The same rotation of the sacrum between the extremes of the reciprocal straddle position averaged  $-0.5^{\circ}$  on the left and  $-0.4^{\circ}$  on the right with a range from  $0^{\circ}$  to  $-1.4^{\circ}$ .

A cadaveric study of elderly subjects has reported larger movement at the sacroiliac joints ranging from three up to seventeen degrees (216). This range of movement occurred particularly around the transverse (X-) axis, with Smidt *et al* (216) commenting that motion at the joints in the other two planes was small.

Adams *et al* (30) suggest that sacroiliac joint movements differ little in patients with symptomatic and pain free joints. The consensus from research in to sacroiliac joint movement is that *in vivo* rotation has rarely been found to exceed two degrees in any of the axes of movement with nutation and counter-nutation (X-axis rotation) considered normal and most variable movement for the sacroiliac joints in going from supine to standing. There is also general consensus that there is little or no rotation around the Z-axis (149, 151-156, 217, 218). Z-axis rotation of the sacrum due to movement within the sacroiliac joints would result, if present in an otherwise symmetrical pelvis, in relative obliquity of the sacral base (Figure 12).

A difficulty with assessing the sacrum as the functional and structural base of the spine in a clinical setting is the lack of external landmarks that are considered a valid representation of the orientation of the structure being assessed (167, 168, 219). The studies and reviews independently conducted by Kmita (167), Huijbregts (168) and Potter (219) suggest that most external landmarks that can be used in a clinical setting are not appropriate for quantifying the position of the sacral base due to a lack of demonstrated reliability and validity. Cattley *et al* (220) and Holmgren and Waling (175) also found that there is a lack of validity in tests used to quantify positional integrity of the pelvis and related structures. There is also a reported lack of specificity and sensitivity of the assessment methods with

many landmarks used because of their accessibility and clinical utility rather than a demonstrated mechanical or structural significance. As an example, palpation of the iliac crests in cases of mild to moderate leg length imbalance has been shown by Dott *et al* (86) to lack reliability as an indicator of sacral base levelness (absolute sacral obliquity).

Based on a similar investigation of standing assessment of leg length imbalance using palpation and observation, Gibbons *et al* (204) suggest that manual medicine practitioners cannot be sure that they are able to accurately and reliably detect leg length imbalance of one centimetre or less. The reliability and validity of clinical tests to assess the positional integrity of the sacroiliac joints, leg length imbalance and pelvic tilt have generally failed to reach an acceptable standard for clinical use (80, 84, 116, 137, 139, 152, 167-169, 172, 173, 175, 183, 204, 219-223). While some test procedures have been shown to be reliable for detecting, provoking or eliciting pain associated with these joints (224), they are generally unreliable when used to assess movement or positional integrity of the joints.

Many clinicians including orthopaedists, chiropractors, osteopaths and physiotherapists assess structural and functional asymmetry of the spine, pelvis and limbs based on advanced spinal imaging (CT and MRI) (196, 197, 225-229), and plain film radiography (11, 13, 14, 27, 41, 43, 65, 78, 79, 83, 230, 231). However, effective treatment outcomes based on changes in spinal alignment as assessed on spinal radiographic images are not always predicated on the identification of a specific cause or diagnosis based on these investigations. Examples are the many patients who are diagnosed and treated for 'idiopathic' scoliosis (33, 119). Other clinicians and researchers suggest that there is no generalised need to identify a specific cause using radiographic imaging in order to effectively treat acute spinal pain syndromes (115, 120, 232). Still other investigators such as Harrison *et al* (29), based on a mathematical review of distortion of spinal and pelvic projection images on full spine radiographs have concluded that anteroposterior plain films

cannot provide any realistic knowledge of spinal position and are therefore inappropriately used for this purpose.

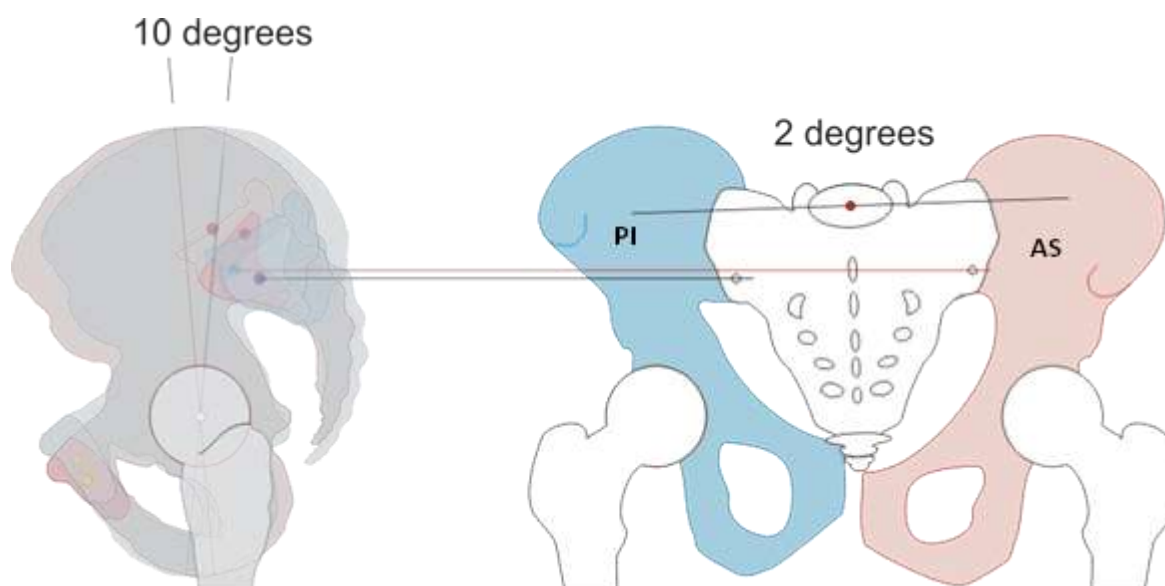
A relatively large number of clinicians employing manipulative therapy use radiographic imaging in order to identify what they consider the structural and functional cause of spinal pain syndromes. Radiographs are used in these circumstances to identify and quantify the positional relationships of spinal structures. Despite concerns expressed by some investigators (29, 189, 191, 233-238) regarding the validity of measuring sacroiliac joint dysfunction and positional changes on plain film radiographs, many practitioners particularly chiropractors and osteopaths, use analytical procedures that involve the interpretation of erect A-P lumbopelvic views (8, 12, 188). While Harrison (15, 239, 240) and others (11, 14, 143, 241-245) have demonstrated reproducibility, validity and reliability of specific radiographic analytical procedures, a review of methods for quantitative evaluation of spinal curvature by Vrtovec *et al* (228) conclude that evaluation of spinal curvature in three-dimensions remains a challenging task in the field of medical image processing, analysis and understanding.

Sacral obliquity is an angulation of the sacral base in the frontal plane and can be defined in structural (anatomical), absolute or relative terms. Structural (anatomical) sacral obliquity results from a lack of reflective symmetry of the sacrum or of the components of the bony skeleton in the frontal plane resulting in an angulation of the sacral plateau relative to the vertical line of symmetry of the body. While there is evidence that the sacrum exhibits a significant degree of structural asymmetry (39, 44, 145) particularly relating to the articular surfaces of the sacroiliac joints, there are no reliable studies quantifying the degree of asymmetry or angulation of the sacral base.

Relative sacral obliquity is the alignment of the sacral plateau relative to other structures of the pelvis. The pelvic reference plane is commonly the plane forming a tangent to the two



acetabula or both femur heads. Relative sacral obliquity could be due to structural asymmetry of the sacrum about its own vertical axis of symmetry or asymmetry of the innominate bones particularly in the relationship between the acetabula and the sacroiliac joints or asymmetrical movement within the sacroiliac joints (Figure 19). Gonstead (13) suggested that movement of one innominate bone relative to the other in an anterior superior (AS) or posterior inferior (PI) direction at the sacroiliac joints would result in one side of the sacrum moving up and the other down resulting in sacral obliquity as measured on A-P lumbopelvic radiographic images.



**Figure 19. A proposed functional change in the orientation of the ilia around the femur heads would result in sacral obliquity in the frontal plane. The Gonstead listings of PI and AS indicate direction of movement of the individual ilia**

Absolute sacral obliquity refers to the orientation of the sacral plateau to the horizontal plane in erect posture such as sitting or standing. The implication of differentiating sacral obliquity i.e. structural, relative and absolute, is that relative sacral obliquity remains unchanged with various orientations of the pelvis as a unit. Absolute sacral obliquity is related to the orientation of the pelvis in space or the global reference frame. Absolute sacral obliquity in erect posture can result from relative sacral obliquity in combination with functional and structural leg length imbalances. Absolute sacral obliquity in the sitting

position can involve structural sacral and ischial asymmetry, variation in supporting structures, seating properties and unequal weight distribution of the trunk (3, 92, 246-251) .

There are no reports in the literature of clinical methods used to directly assess sacral obliquity having been validated against an objective and quantifiable standard. Measurements have been made by practitioners in a clinical setting by analysing erect AP lumbopelvic radiographs using the sacral alae, the sacral grooves (sulci) and other structures used to represent the sacral plateau (11-14, 189). However the validity of most of these measurements has not been established. Brown *et al* (27), in their clinical role as orthopaedic surgeons, have observed that sacral obliquity is a discrete entity, requiring specific radiographic views to demonstrate it. Fann (11, 14) has published several articles differentiating pelvic obliquity from sacral obliquity and suggesting that the measurement of sacral obliquity on plain film radiographs is valid and reliable using measurement protocols previously advocated for use by osteopaths. Many developers of chiropractic clinical methods such as Illi (41), Barge (78) and Gonstead (12, 13) and osteopathic clinical methods as described by Hoffman and Hoffman (53) and Irvin (65), have suggested that levelness of the sacral base is of clinical significance and a significant factor in musculoskeletal pain syndromes and functional disorders. Many of these approaches use radiographs of the lumbopelvic spine to quantify the degree of tilt of the sacral base.

Very few studies have reported the extent and magnitude of structural or relative sacral obliquity as a specific and quantifiable entity. One of the larger studies was conducted by Juhl *et al* (83) who analysed over four hundred AP lumbopelvic plain film radiographs. They suggested that various patterns of sacral and pelvic obliquity were of clinical significance in relation to lumbar spine scoliosis. Their study found sacral obliquity equal to ten millimetres or more of leg length imbalance (LLI) in approximately 30% of those studied. While the method of radiographic analysis was based on an accepted osteopathic

technique, and similar to the technique validated by Fann (11), they gave no indication as to the validity of the measurements used in their study.

While both Fann (11) and Juhl *et al* (83) used similar methods of analysis, there were significant differences between the two studies that did not allow for the demonstrated validity found in one study to be transferred to, or imply validity of the other. The validity study conducted by Fann was based on incremental increases in leg length using a heel lift while Juhl *et al* used an absolute measure of sacral obliquity as seen on pelvic radiographs.

Barge (78) also suggested that a large percentage (40%) of female patients he examined in a clinical setting had a measurable sacral obliquity on AP lumbopelvic radiographs. He advocated a specific sacral base view as the best way to visualise the lateral tilt of the sacral base. Barge did not provide data validating his measurements or methods. Brown *et al* (27) reported finding only sixty-three cases of primary sacral obliquity over a 17 year period with a maximum sacral obliquity identified as 20°. Their study involved specific lumbopelvic radiographs inclined to the sacral base, resulting in a similar view to the one used by Barge, but taken in a supine position as opposed to erect posture. While they suggested that this particular view was the only way to demonstrate sacral obliquity they gave no supporting data for this opinion.

## **1.5 RESEARCH OUTLINE**

One aspect of the investigation was to evaluate the validity of sacral obliquity and other positional measurements made on radiographic images of the spine and pelvis. This was undertaken as various clinicians use these (or similar) measurements as a basis for their clinical assessment and treatment of patients with little or no indication of validity.

Another aspect of the study was to develop protocols to minimise, and algorithms to correct for systematic errors associated with the measurement of dihedral angles such as sacral obliquity and Cobb angles measured on radiographic images of the spine.

Investigations were pursued in three phases:

1. Assess the validity of measuring specific dihedral angles on plain film radiographs, CT and slot scan digital radiographic images. This was done by obtaining radiographic images of sacral specimens, *in vivo* CT studies, an idealised pelvic phantom and developing graphic and mathematical models for analysis (chapters 2 - 7).
2. Develop and apply protocols and algorithms to minimise or correct systematic errors associated with the measurement of dihedral angles on radiographic images of the spine (chapter 8). The algorithms were validated using a radiographic phantom, graphic models and trigonometric analysis.
3. Provide algorithms to facilitate clinical applications of the data obtained from radiographic images (chapter 9).

## **1.6 ETHICS CONSIDERATIONS RELATED TO THIS WORK**

Approval (Reference Number HE26 MAY2006-DO4706) was given by the Macquarie University Ethics Committee to obtain radiographic data sets in the form of computerised axial tomography (CT) scans from a specified radiographic private practice (City Radiology, BMA House 135 Macquarie St, SYDNEY NSW 2000). The managing partner of the specified radiographic practice was approached and agreed to provide the anonymised imaging data sets in accordance with the provisions of the Macquarie University Ethics Committee approval document. The data sets were obtained by the radiographic practice as part of examinations conducted on patients referred to this practice. The patients were

referred to the radiographic practice by general medical practitioners and medical specialists for diagnostic investigations of a variety of undisclosed complaints and medical conditions. The radiology studies involved diagnostic CT examinations of the lumbopelvic spine or abdomen.

The CT imaging was not done for research purposes. The views and protocols used for each study were part of the routine diagnostic procedures used by the radiology practice and were undertaken solely for diagnostic or therapeutic purposes. The image data sets were the property of the diagnostic practice and were subject to the Information Privacy Principles contained in the Privacy Act 1988 (Cth) (252).

Permission to examine and use the data sets for this study was granted by the Macquarie University Ethics Committee subsequent to, and independently of their clinical use. A condition for the acquisition of the data sets stipulated by the ethics committee was that the process of data retrieval ensured anonymity of patients and the removal of any personally identifying information from the data sets by the radiographic practice before making the data sets available. This involved the radiographic practice removing any personal or identifying information from the study data file before making it available for analysis. The only information relating to the individual patients of the radiological practice, apart from the image information itself, was the age and gender of the individuals involved. All other identifying information was removed before acquiring the data sets. The data sets were retrieved from the picture archiving system (PACS) used by the radiologist and stored on compact disc (CD) disks in Digital Imaging and Communications in Medicine (DICOM) file format for subsequent use in the study.



## **MEASURING SACRAL OBLIQUITY ON RADIOGRAPHIC IMAGES: AN OVERVIEW**

## CHAPTER 2

*“When you change the way you look at things,  
the things you look at change.”*

Wayne Dyer

### 2.1 MEASURING SACRAL OBLIQUITY ON RADIOGRAPHIC IMAGES

From a clinical perspective, the assessment of functional and mechanical integrity of the spine and other musculoskeletal structures requires reliable and valid measurements. These measurements are used to establish normal parameters for each individual and to measure deviations from normal alignment. Measurements are also used to document and quantify change in specified parameters in order for practitioners to make effective decisions regarding the need to treat, the nature of the therapeutic intervention and response to treatment. In this respect, practitioners from various disciplines who treat musculoskeletal disorders such as chiropractors, osteopaths, manual therapists and orthopaedic surgeons, commonly employ clinical and radiographic procedures to assess the orientation of the pelvis and spine in the frontal plane.

Lateral tilt of the pelvis is of clinical significance largely due to the mechanical relationship the pelvis has to other components of the axial skeleton. Mechanically, it acts as the structural foundation of the upright spine. The sacral plateau provides the base for the flexible spine above and also acts as the structural link between the trunk above and lower limbs below in upright posture. It has been suggested that in this role the orientation of the sacral base in the frontal plane has an impact on the mechanical, structural, functional aspects and defines the positional integrity of the lumbosacral area as well as the musculoskeletal system generally (17, 27, 31, 34, 40, 41, 50-55, 65, 77-79, 83, 86).

Tilt of the sacral base and Cobb angles represent the projection of dihedral angles onto radiographic images. They represent the measurement of the angle formed between two

non-parallel planes projected as a two-dimensional image (20, 21). One plane is the endplate of the segment involved (sacral or vertebral) and the other is either a plane representing another segment or the horizontal plane. Obliquity of the sacral base and Cobb angles can be measured with varying degrees of accuracy on anteroposterior (A-P) plain film radiographs, computed tomography (CT) images and digital slit scan views.

The visualisation and measurement of sacral obliquity on radiographic images has similarities and associated problems as the measurement of Cobb angles has for the quantification of scolioses. The sacral base represents the end plate of the first sacral segment and is used as the plane representing the angle of the sacral base in the frontal plane in the same way that the end plate of a vertebra does for Cobb angles. The projection of dihedral angles such as Cobb angles and sacral obliquity represent a potential source of systematic error in the measurement of sacral obliquity.

Random errors can generally be identified by statistical analysis of multiple repeats of the measurements as they tend to fluctuate around the mean representing the true measurements. Inherent systematic error of angles on radiographs, generally are not detected by repeating the process.

Systematic error can best be detected as a deviation against a known reference value. These errors can be corrected once they are detected by applying a corrective algorithm to the measurements or by modifying the measurement process and protocol.

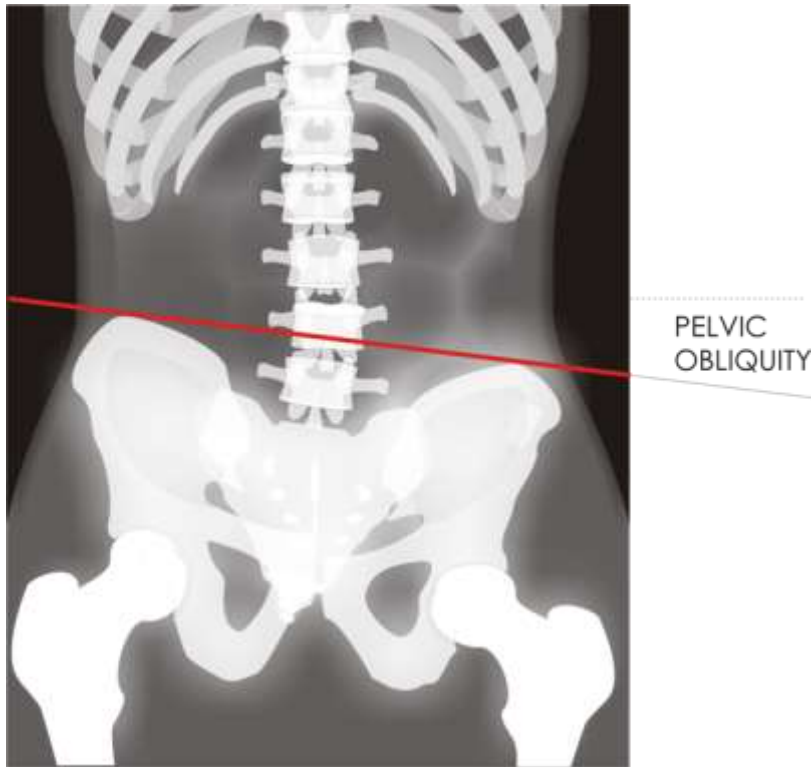
The shape and appearance of the sacral base on radiographic images resembles the endplate of other typical vertebral segments (excluding the atlas), particularly the lumbar vertebra. The shape and relationship of the sacral base to the image plane and viewing angle present the same or similar measuring issues as other segments of the spine (Figure 20).





Figure 20. The end plates of the lumbar vertebra and the sacral base (highlighted in red) have a similar appearance in the frontal view and represent the same anatomical structure

There are three similar and related concepts relevant to tilting of the sacral base in the frontal plane. These are pelvic obliquity, anisomelia or leg length imbalance and sacral obliquity. Any deviation of the pelvis as a unit from the horizontal plane in an erect posture is referred to as pelvic obliquity or pelvic 'unlevelling' (57). Pelvic obliquity has also been defined as a tilting of the pelvis in relation to the lumbar spine and trunk (59) (Figure 21).



**Figure 21. Pelvic obliquity with the crest of the ilia tilted in the frontal plane relative to the horizontal plane**

The cause of pelvic obliquity, with implied sacral obliquity, has been attributed to leg length imbalance (64), pelvic structural asymmetry (3) and positional changes affecting the sacroiliac joints (12). When assessing the impact of leg length imbalance or pelvic obliquity on other structures, such as the lumbar spine, or as a cause of musculoskeletal pain syndromes, there is a tacit or implied assumption that the leg length imbalance or pelvic obliquity is directly related to, and congruent with tilt of the sacral base (212) (Figure 22).

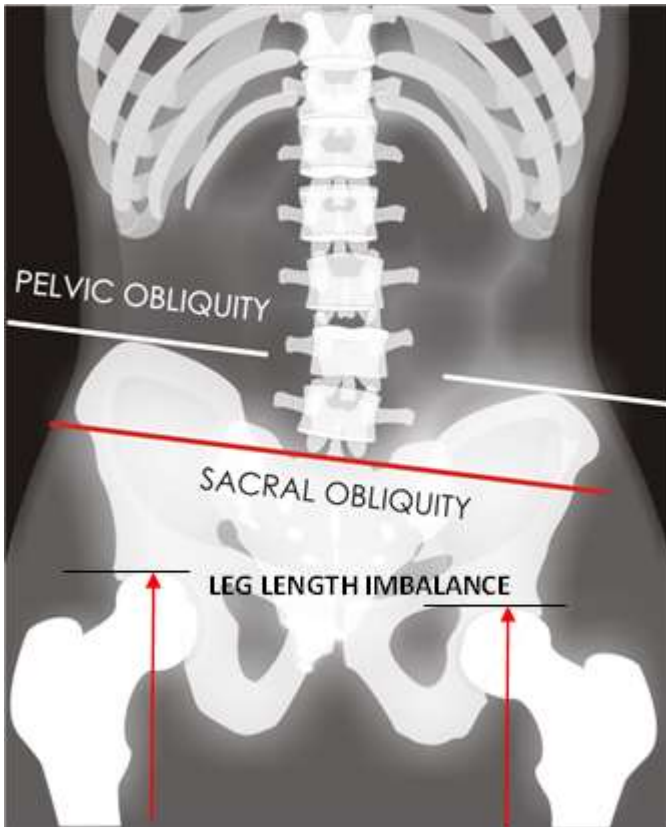


Figure 22. The implied relationship between pelvic obliquity, leg length imbalance and sacral obliquity

Obliquity of the sacral base in the frontal plane is usually considered as either an absolute tilt in upright posture in relation to the horizontal plane or as a relative tilt in relation to other lumbopelvic structures such as the femur heads (10-12, 83). Tilting or angulation of the sacral base is implied in the clinical assessment of pelvic obliquity and lower limb imbalance (8, 11, 34, 79, 86, 171, 212).

Non-radiographic clinical procedures developed to assess sacral obliquity in the frontal plane include the assessment of iliac crest height (81) and leg length measurement (80, 135). There are no standardised or universally accepted reference points for measuring pelvic obliquity in a clinical setting (51). Michaud *et al* (253) use a line joining the anterior superior iliac spine (ASIS) to calculate pelvic obliquity using the formula:

$$\theta = \frac{180}{\pi} * \arctan \frac{(Ys - Yp)}{\sqrt{(Xs - Xp)^2 + (Zs - Zp)^2}}$$

where  $(X_s, Y_s, Z_s)$  and  $(X_p, Y_p, Z_p)$  are the three-dimensional (3D) coordinates of the two sides of the pelvis and denote the anterior-posterior, vertical, and medial-lateral directions, respectively. The prosthetic side of the pelvis was designated  $p$  and the sound side designated  $s$ .

The reliability and validity of these non-radiographic methods is generally considered to be poor (80, 139). It is commonly accepted that radiographs have greater clinical significance and accuracy for the quantification of sacral obliquity over other clinical assessment methods (136, 139, 207).

The analysis of plain film radiographs and computed tomography images to quantify positional relationships of the spine and pelvis generally involves constructing lines to measure angles and distances on two-dimensional images. These lines and angles constructed on images representing surfaces of individual structures, or different structures, are compared to each other and are used to quantify the three dimensional positional relationships of the structures involved. The relationships represent the absolute or global position of structures in relation to gravity represented by a global reference frame, or the relative position within a local reference frame.

Measuring error is a problem inherent in the quantification of angles and distances on radiographic images used to evaluate the positional relationships of spinal structures. Several sources of error have been identified and documented in relation to the measurement of positional relationships of three-dimensional objects on two-dimensional images such as radiographic images. These errors are independent of errors that have been associated with projection factors (29, 191, 239, 241, 254-257) and include:

- Misinterpretation and poor identification of structures (14, 189, 258)
- Positioning / repositioning errors (174, 239, 255, 259)

- Errors associated with measurement accuracy (6, 240, 242, 260)

The measurement of sacral obliquity and Cobb angles on radiographic images are commonly subject to a combination of these measuring errors (29). The sum of these errors can be summarised using formulae that define the relationship between the true angle and the angle measured on the image:

Actual projected angle ( $X$ ) = measured angle ( $I_i$ )  $\pm$  measuring error ( $\varepsilon_i$ )

$$X = I_i \pm \varepsilon_i$$

The other form of error involves systematic error or bias that results in consistent underestimation or overestimation of a true value. Systematic error has been defined as the repetitive difference between a computed, estimated, or measured value and the true, specified, or theoretically correct value (261). The difference is caused by *non-random* fluctuations from an unknown source, which once identified, can usually be eliminated or compensated for (227, 228, 235, 262, 263). Some systematic errors related to the analysis of conventional radiographic and CT images have been identified. They include radiographic projection error that produces magnification and distortion of the object being measured as well as errors associated with the measurement of angles on two-dimensional planes (20, 105, 146, 241, 254). Lundh *et al* (257) suggest, in relation to radiographic pelvimetry, that each single radiographic measurement (SM) can be defined as the sum of the true value (TV) of the dimension plus a systematic error (se) of measurement, plus a random error (re) of measurement. They summarise this relationship using the formula:

$$SM = TV + se + re$$

All radiographic measuring uncertainty is therefore due to either random or systematic error (264). Fluctuations in the measured data (in either direction) from the true value due to precision limitations of the observation and measurement are considered *random measuring errors*. Random errors usually result from the observer's inability to make the same measurement in exactly the same way to get exactly the same value. As random errors generally have a Gaussian normal distribution around a mean or true value their

impact can be minimised by increasing the number of observations or repeated measurement and applying statistical analysis to the results.

As systematic errors are not random or unpredictable, if the sources can be identified, they can generally be addressed by either removing the cause or accommodating for the factors that are contributing to the error or bias. A major source of systematic error when interpreting radiographic images involves the measurement of positional relationships on two-dimensional images that represent the compound rotation of three-dimensional objects. These errors can occur when the measured positional relationships are interpreted as the actual distances and angles involved (51, 146, 191, 231, 234, 235). This type of error can be associated with the projection of compound angles onto a viewing plane from orientations or directions that are not perpendicular to the axis of rotation of the objects and the viewing plane (265). Exemplifying this type of error is a study by Baker (51) which showed that a pelvic model with an anterior tilt of -10 to -30 degrees and rotation of -20 to +20 degrees resulted in up to 10 degrees of pelvic obliquity despite the fact that the pelvis was perfectly level in the frontal plane.

A known source of systematic error associated with the measurement of angles on two-dimensional images is due to the interpretation of the projected angle formed between inclined or non-parallel planes (29, 266). Angles between non-parallel planes are known as dihedral angles (20). The measurement of a true dihedral angle is dependent on the viewing or projection angle relative to the line of intersection of the planes. For this reason, the true angles formed between planes are not always projected as a true dihedral angle on plain film radiographic images and CT slices (231, 256, 262, 267). A systematic error when quantifying dihedral angles can be present even when allowance has been made for random measurement error through statistical methods.

Mistakes are not generally considered a form of statistical error analysis (268). Mistakes, because they are often so far from the mean, can be considered outliers in statistical analysis. However it is important to distinguish between outliers that represent measurement or transcribing mistakes and those that indicate an error in the data collection method or in the relationship between what is theoretically being measured and what is actually being measured. Outliers are sometimes ignored for the purpose of statistical analysis of data to account for transcript or random errors (269). If the same measuring procedure, recording and transcribing methods were reapplied, the mistake would theoretically be revealed. However, if the value remains outside the established range of random error when the measurement is repeated, then the outlier can indicate the presence of a systematic error (270).

Such a systematic error could result from the inappropriate selection of reference points that are not directly representative of the factor being measured. The measurement of degree of tilt of the leaning tower of Pisa is an obvious example of the need for selecting appropriate reference points on which to base the measurement of structural lean or tilt relative to the horizontal plane. Viewed in a direction that is perpendicular to the plane of tilt, either side or the top of the tower can be used to construct a line and the angle relative to the horizontal can be measured. However, if the line is constructed on the top or either of the sides that are visible when viewed in the plane of the tilt, no angle will be apparent. The systematic error in this case would result in a type II or false negative error (270).

Type I and Type II errors are concepts which are related to hypothesis testing (271). Simply explained, for the tower example, a Type I error is the probability of measuring an angle when none is present due to inappropriate reference points or viewing angle. A Type II error in this example would be the probability of measuring an angle as perpendicular when in fact there was an angle of tilt present. In this case the angle could be disguised as normal, interpreted merely a measuring error or a measurement significantly different from

the mean and dismissed as an outlier in a statistical analysis of the data. In these cases a significant systematic measuring error could go undetected.

Often measuring points are chosen for convenience rather than their ability to directly represent the actual quality being assessed. This has the potential to introduce confounding factors into the measurement. As with the leaning tower example, it would be a mistaken assumption that in measuring the vertical alignment of a structure the surface chosen is irrelevant. The assumption may be true for most symmetrical buildings with random measuring error being verifiable using statistical methods, but would produce a statistical outlier or systematic error for any non-symmetrical structure.

Non-random measuring error that is due to a reproducible inaccuracy causing a consistent distortion of the measurement in the same direction is difficult to detect and cannot be analysed statistically as the data is biased in the same direction. Systematic errors, if the effect is identified as occurring according to a system can be expressed by a mathematical formulation or corrected using an algorithm (Appendix 1).

#### *2.1.1 Random error*

Random error is a constant companion of any measurement relating to the position or shape of an object. This type of error is caused by inherently unpredictable fluctuations in the readings of a measurement device, methods used or in the observer's interpretation of the measurement. Repeated sampling should reduce this effect by establishing a mean value with Gaussian distribution.

Random errors influence the reliability of x-ray analytical methods but not the validity of the measurements. The reliability of any measurement is the extent to which the measurements are free of random errors. Random errors associated with measuring dihedral angles and distances on radiographic images include:



- Subject positioning (272)
- Identification of reference points (6, 257)
- Measuring precision (273)

### *2.1.2 Subject positioning*

Random error in the measurement of obliquity on radiographic images can be present due to variability in the process of reproducible positioning of the subject relative to the image plane and radiation source. Positioning protocols have been employed to minimize this source of random error but their use is far from common or uniform (15, 174). It has been reported that inconsistent subject positioning prior to exposure can result in variation of up to 17° in the angle of scoliosis measured by Cobb method (59).

### *2.1.3 Identification of reference points*

The identification of anatomical landmarks on radiographic images for measurement purposes can produce random errors associated with the variations of the reference points themselves. The reference points used in the Cobb method are the lateral margins of the vertebral endplates as visualized on the AP plain film view of the spine. Reference points are often chosen because they are considered to be less affected by congenital abnormalities than other landmarks (61). All reference points associated with spinal structures can exhibit structural asymmetry and anomalies that may be the result of congenital variability, degenerative changes or the activation of the Hueter-Volkman principle or Wolff's Law (46, 47). These changes are often due to applied asymmetrical loading of the structures involved (55). The anatomical variations can make it difficult to reliably identify the reference points on specific views and repeated examinations.

### *2.1.4 Radiographic measuring precision*

Random error in measurements obtained from radiographic images is often created by the variability in precision by the individual responsible for identifying reference points, constructing lines and measuring angles. The errors can be created by an individual with repeated measurements (intra-examiner error) or between individuals making the same measurement (inter-examiner error). A number of factors have been suggested or shown to produce variability in measurements when made by the same examiner (intra-examiner reliability) or by different examiners (inter-examiner reliability):

- Image quality (274-276)
- Professional training and background of the examiner (274)
- Type of image (digital or radiographic film) (196, 277)
- Measuring device used (273)
- Thickness of the lines used (278)

The cumulative effect of these errors associated with the measurement of Cobb angles on radiographic images have been described as being as high as  $9.6^{\circ}$  for intra-examiner errors and as high as  $11.8^{\circ}$  for inter-examiner error (279). Greiner (230) suggests the standard measurement error for Cobb angles when the same end vertebrae are used for measurements is  $3^{\circ}$  to  $5^{\circ}$  for the same observer and  $5^{\circ}$  to  $7^{\circ}$  for different observers.

The magnitude of change in a Cobb angle that is necessary to be certain of significant anatomical change has been estimated to range from  $10^{\circ}$  (280) to as high as  $23^{\circ}$  (279). This lack of validity and reliability in the measurement of obliquity of spinal segments has implications for clinicians and therapists who assess and treat musculoskeletal conditions. With lack of accuracy and precision there is the potential for various treatment protocols to be mistakenly applied or withheld as well as the inability to identify or incorrect identification of the cause. However, the present study was not designed to test the diagnostic validity or clinical utility of the measurement of spinal segment obliquity. Neither was the sensitivity

and specificity of spinal segment obliquity as a clinical diagnostic method nor the relationship and the appropriateness of the methods used in relation to clinical outcomes examined or assessed in this study.

The magnitude of the Cobb angle describing a scoliotic spine is potentially greater than for sacral obliquity as the Cobb angle is the combination of the obliquity of both end vertebra of the curve being measured whereas the sacral obliquity angle can represent the inclination of only one segment related to the horizontal plane. Even if the degree of measuring error related to the selection of end vertebra as is found with the measurement of Cobb angles is accounted for, there is significant potential for measurement error in quantifying sacral obliquity on A-P erect radiographic images. Because of the reported range of sacral obliquity, this type of error could render the measurement of sacral obliquity unreliable as a clinical assessment. Gstoetter *et al* (281) looked at the reliability of assessing Cobb angles and concluded that one pitfall in Cobb (dihedral) angle measurement on radiographic images is involved with the method itself. Even with minimal measurement error the anteroposterior and lateral image measuring system is based on individual two-dimensional pictures which do not represent a proper three-dimensional measuring system. They suggest that for the Cobb angle measurement method the definition of end vertebrae introduces the main source of error. They believe that for this reason digital radiography does not improve the measurement accuracy for Cobb angles. This however, is not generally an issue with sacral obliquity measurement.

The error associated with measuring precision is the degree to which repeated measurements such as Cobb angles and sacral obliquity produce the same value when the same image is analyzed by one or multiple examiners. This is also called reproducibility or repeatability of the measurement. The quantification of measuring precision is related to the intra- and inter-observer reliability. Repeatability refers the variation in measurements when the same image is analyzed by the same observer using the same measuring

devices and methods, and repeated during a short time period. Reproducibility is the variation arising using the same measuring methods by different observers and over longer time periods.

#### *2.1.5 Systematic error associated with measurements made on radiographic images*

Systematic errors, not random errors, influence the *validity* of measurements such as those commonly made on radiographic images. Random error doesn't threaten the validity of the measurement but may keep the analysis from showing the effects being investigated. Systematic errors affect the accuracy of the measurements being made relative to their true value due to an inherent bias or skewing of the measurements. The shift in accuracy of measurements made on radiographic images can be due to multiple factors that include:

- Image resolution and exposure factors
- Magnification / Distortion
- Transformation of three-dimensional object into two-dimensional images

Systematic errors involve variation in the mean of many separate measurements that differ significantly from the actual or true value of the measured attribute. The methodology involved in the measurement of radiographs can result in errors that are predictable and constant or proportional to the true value.

If the cause of the systematic error can be identified, then it can usually be eliminated, accounted for or corrected mathematically. An example relevant to the present study would be the calculation of an object's height from the measurement of its shadow. Random error could be involved in the actual measurement of the shadow. The other source of error would be systematic error related to the position of the light source and or the image plane relative to the object. This could be corrected by applying a mathematical formula that contained variables such as position of the image plane and light source at the time the

measurement was made (Appendix 1). It could also be eliminated or minimised by applying a protocol that standardises the measurement process (268).

Kawchuk (279) has described various alternatives, patches and fixes that have been proposed for methods of plain film quantification of scoliosis. While he suggests some improvements do offer reduction of error, digitization of landmarks for example, he suggests that there is the additional concern that two dimensional (2D) radiographic imaging of spinal structures does not accurately portray the three dimensional (3D) relationships of those structures.

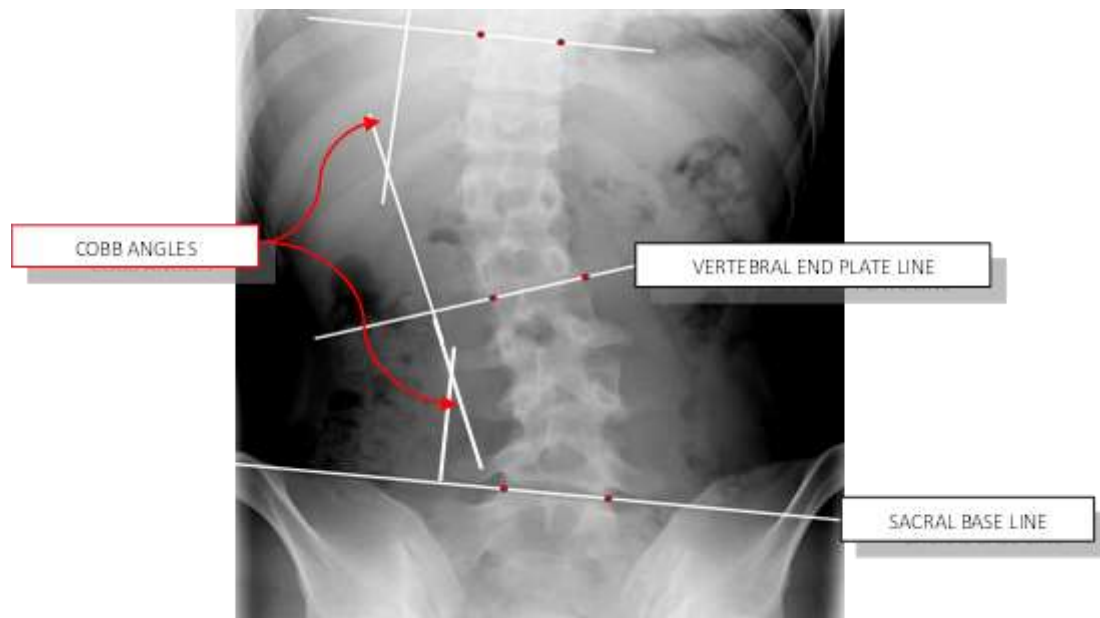
The difference between measured two dimensional relationships and actual three dimensional spatial relationships, as in the measurement of dihedral angles, can be described mathematically by the theorems of projective geometry (282) and geometric modeling (283). These theorems and models can be applied to the projection of structures appearing on a radiographic image to predict distortion and/or magnification of the structures involved. Inherent factors in various radiographic projection modalities and protocols such as the angle of the primary beam relative to the object and image plane along with source-object and object-film distances combine to result in a unique and specific amount of magnification and distortion of the objects visualized on each image. These changes in measured dimension and angular relationships may be of clinical significance with introduced error in the process of landmark identification, measurement of distances and quantification of angles.

## **2.2 MEASURING DIHEDRAL ANGLES ON RADIOGRAPHIC IMAGES**

A wide range of imaging modalities employing both ionising and non-ionising radiation methods have been used to assess positional relationships within the spine. The present study is primarily concerned with the validity of methods commonly used to quantify the spatial orientation of spinal structures such as the sacral base as they are seen on

radiographic images used in a clinical setting. While this study has been designed to test for systematic errors associated with the measurement of angles made on the radiographic images, it has not been designed to test the clinical validity or utility of those measurements.

Many of the lines used in the analysis of radiographic images represent planes. Examples are the lines drawn on conventional radiographs to obtain Cobb angles (185, 284) and measure the positional relationship of other skeletal structures (Figure 23).



**Figure 23.** Cobb angle measured on AP lumbopelvic radiograph. The Cobb angle is measured as the acute angle formed at the intersection of lines drawn perpendicular to the vertebral end plate lines. The vertebral end plate lines are constructed on the vertebra at either end of the curve. In this example the sacral base line is considered a vertebral end plate line for the construction of the lower Cobb angle

These lines represent the plane of the end plate of the involved vertebra (Figure 3.2). The lines used to measure Cobb angles (vertebral end plate), sacral obliquity (sacral base) and leg length imbalance (femur heads) are the X-axes of a local reference frame attached to a surface representing the structure involved (Figure 24).

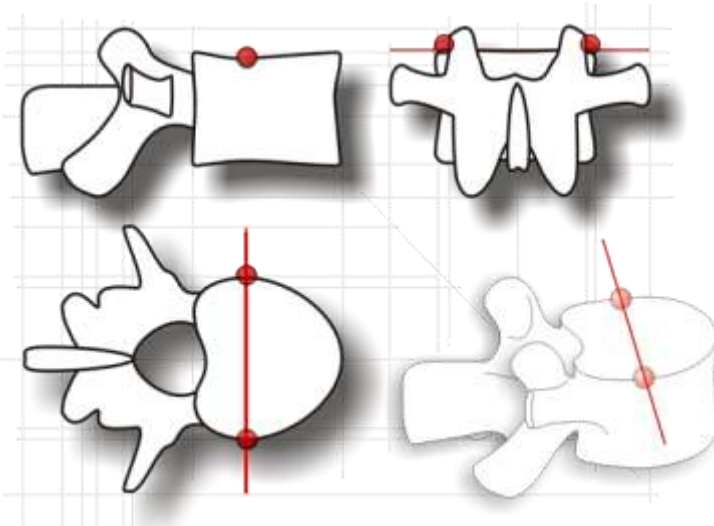


Figure 24. Four views (side, back, top and oblique) of the line representing the plane of the end plate of a vertebra (sacral base) and its relationship to the edge of the vertebral body (red dots)

In the same way, a line constructed on the lateral (sagittal) plain film view of the sacral base is used to quantify pelvic orientation to the horizontal plane and is known as sacral base angle (SBA) or Ferguson's base angle (FBA) (285, 286) (Figure 25).

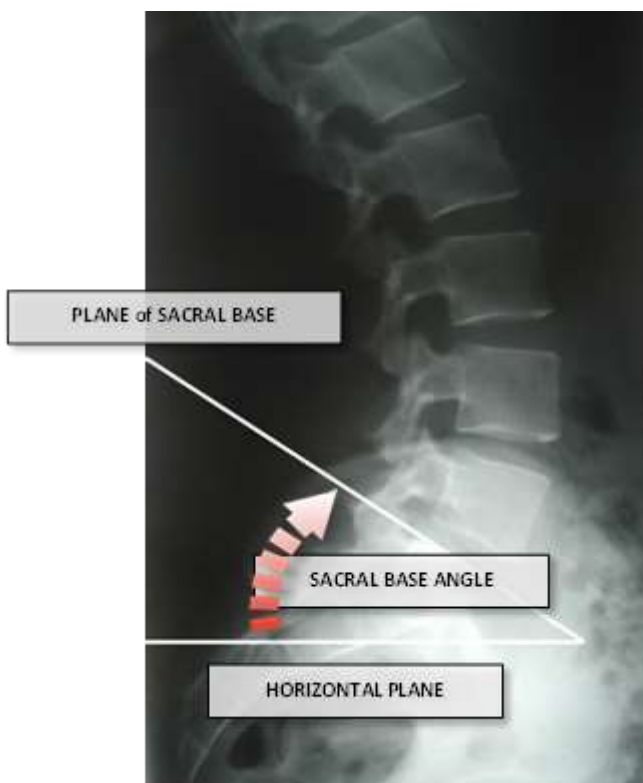
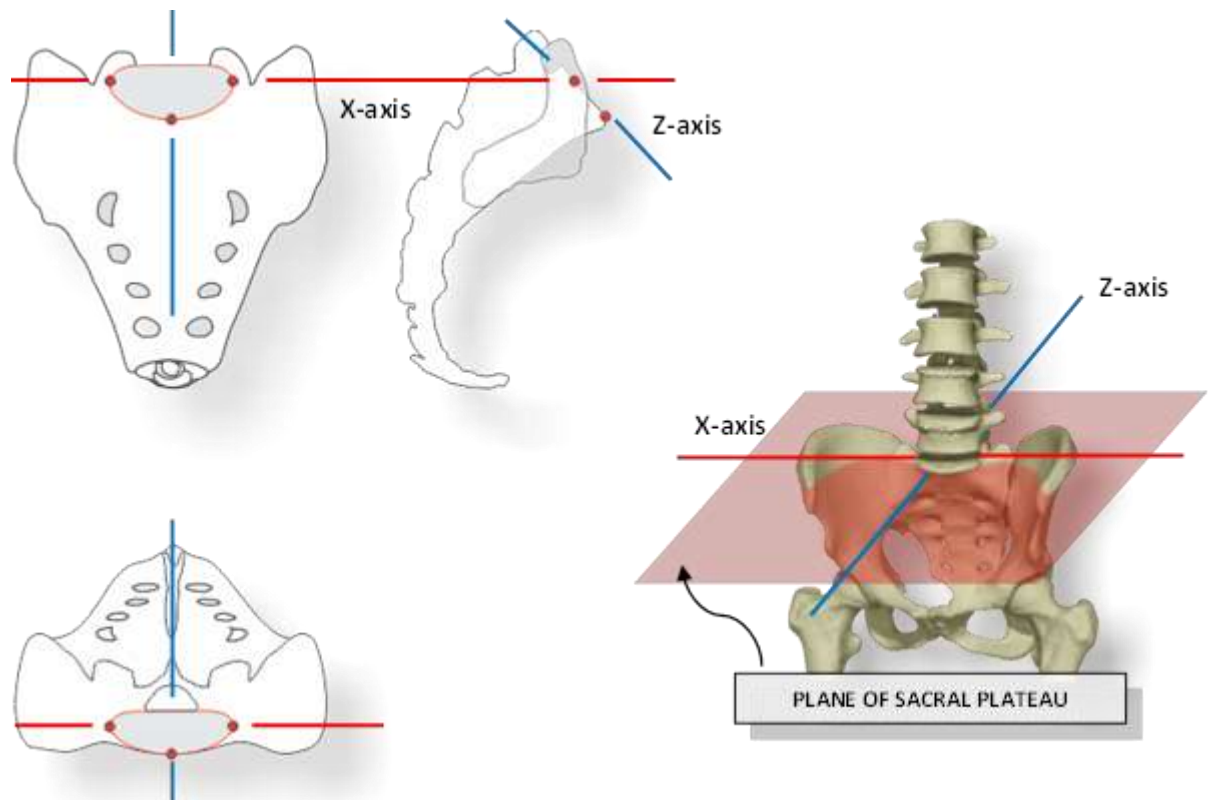


Figure 25. Lateral view of the lumbopelvic spine showing the sacral base angle. The sacral base angle is measured as the acute angle between the plane of the sacral plateau and the horizontal plane

The line constructed on the sacral base represents the plane of the sacral plateau viewed from the side. The lines in these examples represent the end view of a plane or Z-axis of a local reference plane (Figure 26). Sacral obliquity is another measurement of the plane of the sacral base and is measured as the tilt of the plane of the sacral base around the Z-axis (frontal plane) (Figure 26).



**Figure 26. Four views (front, side, top and oblique view) of the lumbopelvic spine illustrating the X and Z-axes of the sacral base**

The acute angle formed by the intersection of two planes or the vectors normal to the planes is by definition a dihedral angle (22) (Figure 27). Cobb angles, sacral base angle and sacral obliquity are all representations of dihedral angles measured on radiographic images.



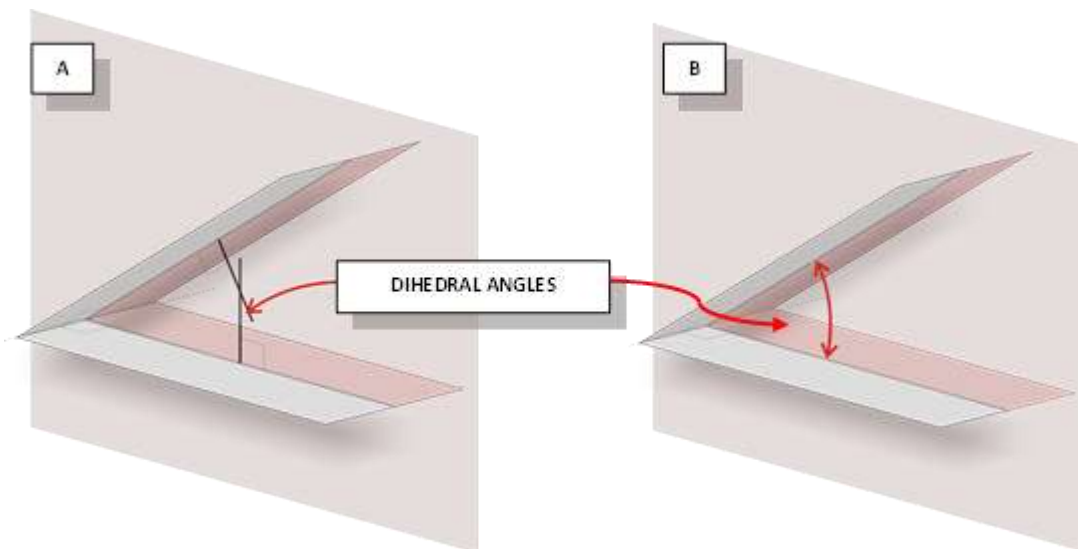


Figure 27. A dihedral angle is the angle formed between two non-parallel planes and can be measured as the acute angle between vectors perpendicular to the planes (A) or the acute angle formed between the planes measured perpendicular to the line of intersection of the planes (B)

The projection of the planes forming a dihedral angle onto a two-dimensional viewing plane can result in measured or apparent angles not being the same as the true or actual dihedral angles. The magnitude of the apparent dihedral angle can be influenced by rotations of the planes around axes other than the one formed at their junction relative to the viewing plane. This would occur if the plane of the sacral base were angled in both the frontal (X-Y) and sagittal (Y-Z) planes when projected or viewed on a radiographic image with a combination of sacral obliquity and sacral base angle (Figure 28).

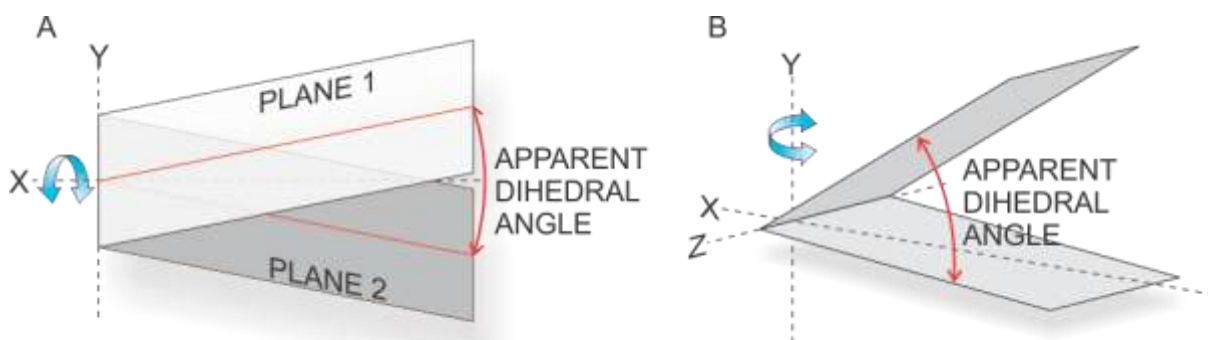


Figure 28. The apparent magnitude of the dihedral angle can be influenced by rotation of the planes around axes other than the one formed at their junction relative to the viewing plane. An apparent dihedral angle occurs if the plane of the sacral base is angled around the frontal X-axis (A) or sagittal Y-axis (B) when projected or viewed as it would be viewed on a radiographic image with a combination of sacral obliquity, pelvic rotation and/or sacral base angle

### 2.2.1 Quantifying True Dihedral Angles

There are several methods used to quantify a true dihedral angle (TDA). One involves measuring the acute angle formed between two lines constructed from a point on the line of intersection of two planes of interest so that one line lies in each plane and perpendicular to the line of intersection (261) (Figure 27). Another method involves measuring the acute angle formed between intersecting vectors that are perpendicular to their respective planes (261). The measurement of intersecting vectors forms the basis of the Cobb method for measuring spinal curves. To be considered a true dihedral angle, the angle of intersection between the vectors must be measured in a plane perpendicular to the line of intersection of the two planes of interest (Figure 27).

An apparent dihedral angle (ADA) is a form of systematic error that occurs on a two-dimensional image when the viewing or cutting plane is not perpendicular to the line created by the intersection of the two planes or the vectors perpendicular to the planes (Figure 28). An apparent dihedral angle can also be measured if the planes of interest are rotated around more than one axis relative to the image plane.

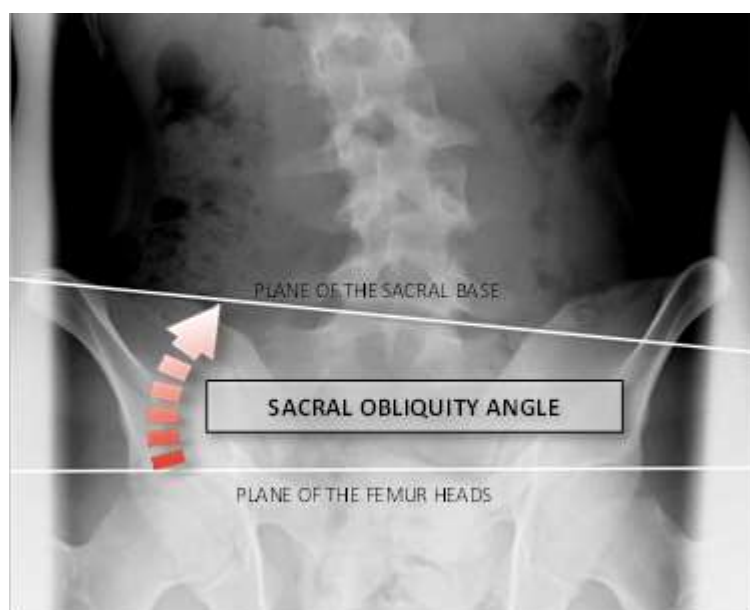
In order to make accurate measurements of a true dihedral angle (TDA) projected on a two-dimensional image or viewing plane, the following three basic conditions or requirements must be met (21).

- The edges of the planes of interest must be projected as lines
- The junction between two planes must be projected as a point
- The projection or viewing plane must be perpendicular to the line representing the junction of the two planes

These rules ensure the accurate and reliable measurement of angles formed between two planes with a common line of intersection that are rotated in one or more directions by

ensuring that the influence of rotations around other axes are eliminated or accounted for. However, these rules are not, or cannot be applied or adhered to in all situations when projecting or viewing images of three-dimensional objects on to a two-dimensional image plane as with skeletal radiography. The result creates the potential for systematic measuring errors to affect the quantification of true dihedral angles such as sacral obliquity.

The Scoliosis Research Society (SRS) defines sacral obliquity as “*an angular deviation of the sacrum from the line drawn parallel to a line across the femoral heads on a supine AP view of the sacrum*” (49) (Figure 29).

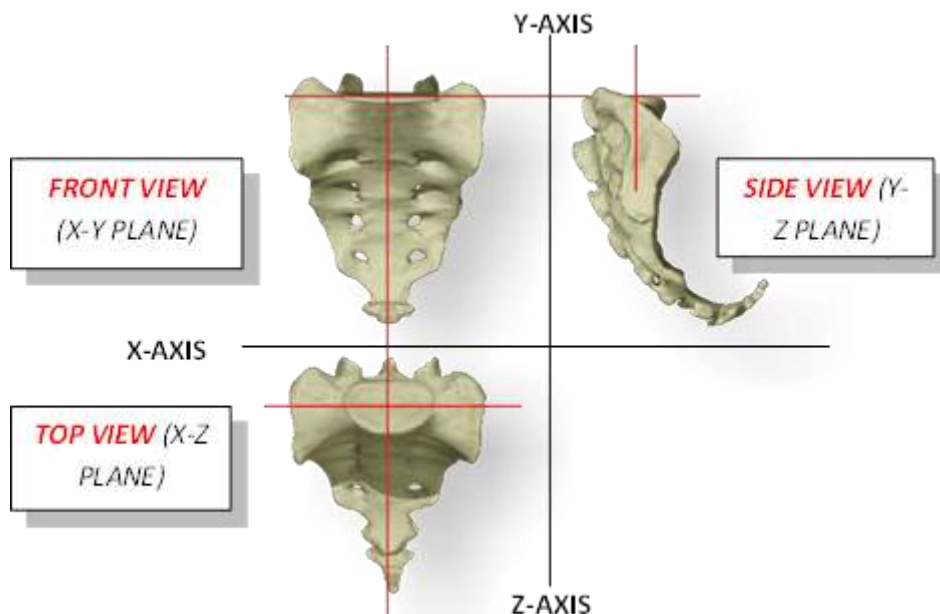


**Figure 29. Sacral obliquity angle is formed between the plane of the sacral base and the plane of the femur heads when the sacral base is viewed as a line in the frontal plane**

These two lines represent the plane of their respective structures as they appear on radiographic images. There is an inherent problem with the definition used by the SRS and similar definitions of sacral obliquity. The problem is associated with the measurement of dihedral angles on CT images and plain film radiographs (279). Measuring sacral obliquity involves the projection of the sacral base onto plain film radiographs or CT images. This introduces the variability of the angle of the sacral base in the sagittal plane e.g. Ferguson’s

base angle, as well as the possibility of pelvic rotation at the time the image was created. Both of these positional variables have the potential to introduce a systematic measuring error in the form of an apparent dihedral angle with the degree of sacral obliquity measured on the image interpreted as a true dihedral angle.

The most accurate measurement of the sacral base angle would be made when the sacral base (Ferguson's) angle is zero degrees relative to the projection beam, perpendicular to the image plane and the projection rays lie in the same plane as the sacral base (287) (Figure 30).



**Figure 30. Optimal viewing position of the sacral base relative to the viewing plane for the measurement of obliquity of the sacral base**

With the sagittal alignment of the sacral base at an angle other than perpendicular to the image plane and aligned with the projection beam, a given sacral obliquity angle could project as having a zero, a plus, or a minus angular deviation depending on the effective projection angle. This effect is similar to the variation documented by Slane and Bull (233) for femur head height measurement on plain films with different projection angles. The variation of the measured or projected angle is due to both projection distortion and the

inherent inaccuracy associated with measuring dihedral angles on a two dimensional image plane (Figure 31).

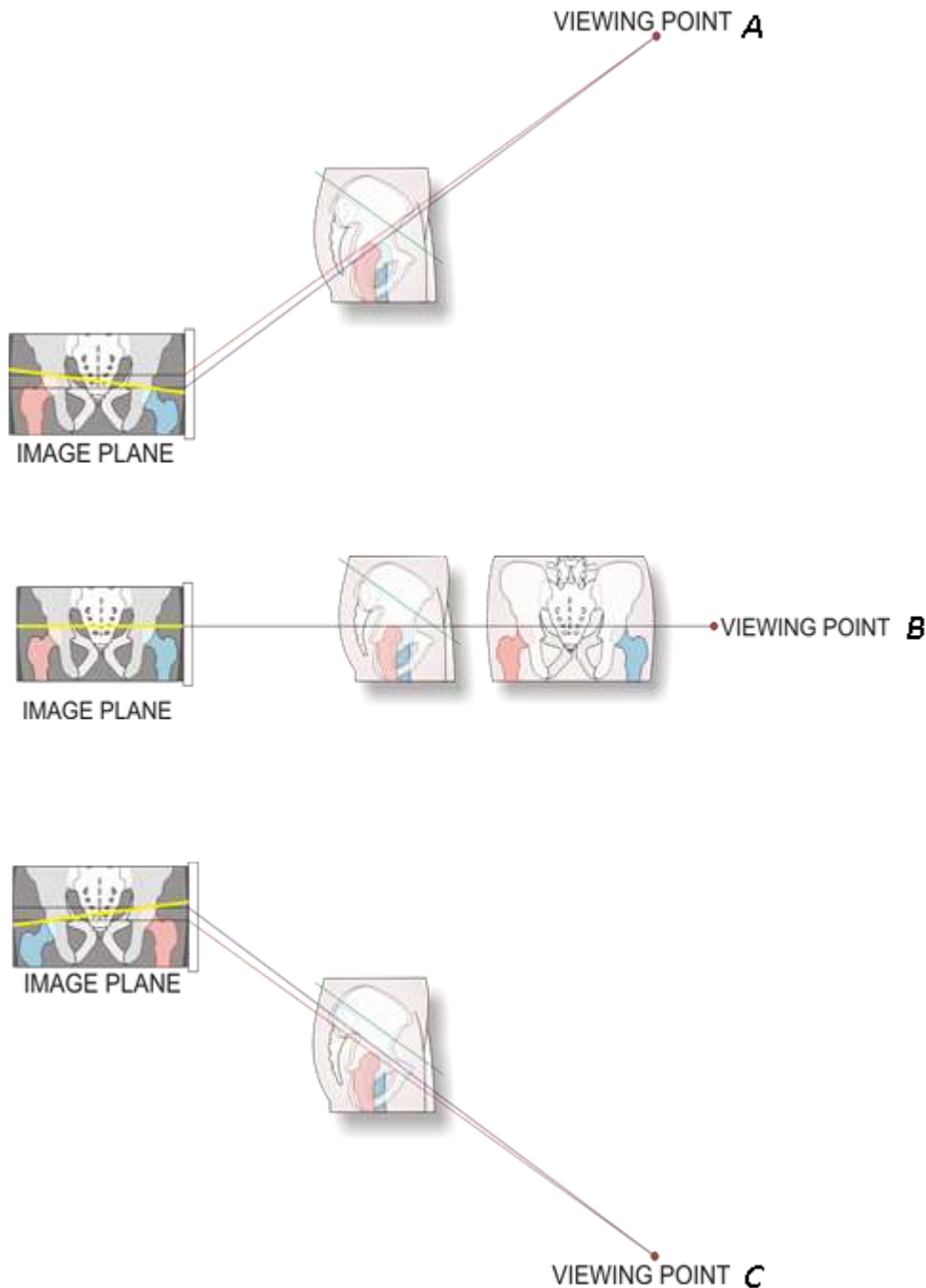
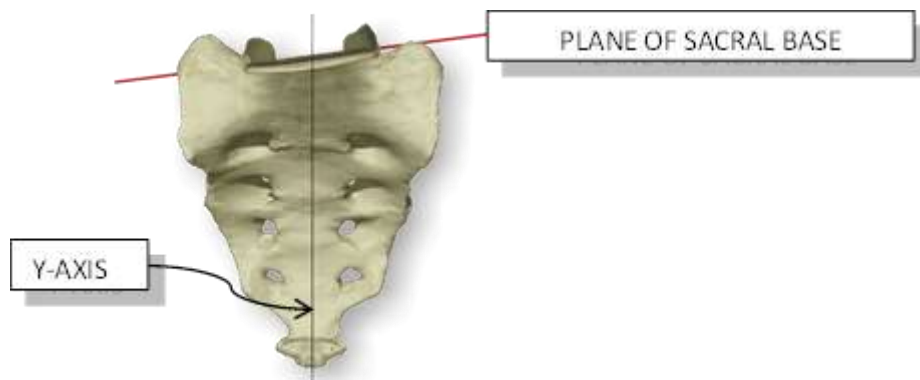


Figure 31. The effect of combined projection angle and rotation on the measured dihedral angle (anisomelia). With the x-ray tube in position (A), the left femur head projects higher than the right due to pelvic rotation even when there is no vertical height difference between femur heads. The same positioning of the pelvis produces the opposite effect (right higher than the left) with the x-ray tube in position (C). With the x-ray tube in position (B) the pelvic rotation would have no effect on the height of the projected femur heads if they are of equal height

### 2.2.2 Pelvic Obliquity

Pelvic obliquity is defined by the Scoliosis Research Society (SRS) (49) as “*angulation of the pelvis from the horizontal in the frontal plane, possibly secondary to a contraction below the pelvis, e.g. of the hip joint or angulation due to a leg length inequality.*” The definitions of sacral and pelvic obliquity proposed by the SRS differ not only with respect to the structures they relate to but also in the reference planes used to specify the degree of obliquity of the structures involved. Sacral obliquity is defined by the SRS in relation to the femur heads based on an internal (relative) reference frame. This can be due to a lack of reflective symmetry of the sacrum around the Y-axis (4, 39, 40, 79, 94) (Figure 32).



**Figure 32.** Obliquity of the sacral base resulting in a lack of reflective asymmetry of the sacrum around the Y-axis

Structural reflective asymmetry could be due to congenital factors, fluctuating asymmetry, or physiological processes reflected in Wolff’s law (288-290) and Hueter-Volkmann law (46) that relate mechanical loads to bone morphology. Sacral obliquity could also potentially result from structural asymmetry of the ilia (85) or a loss of positional and functional integrity involving the joints between the individual bones that form the pelvis (13, 31, 50, 77) (Figure 33).

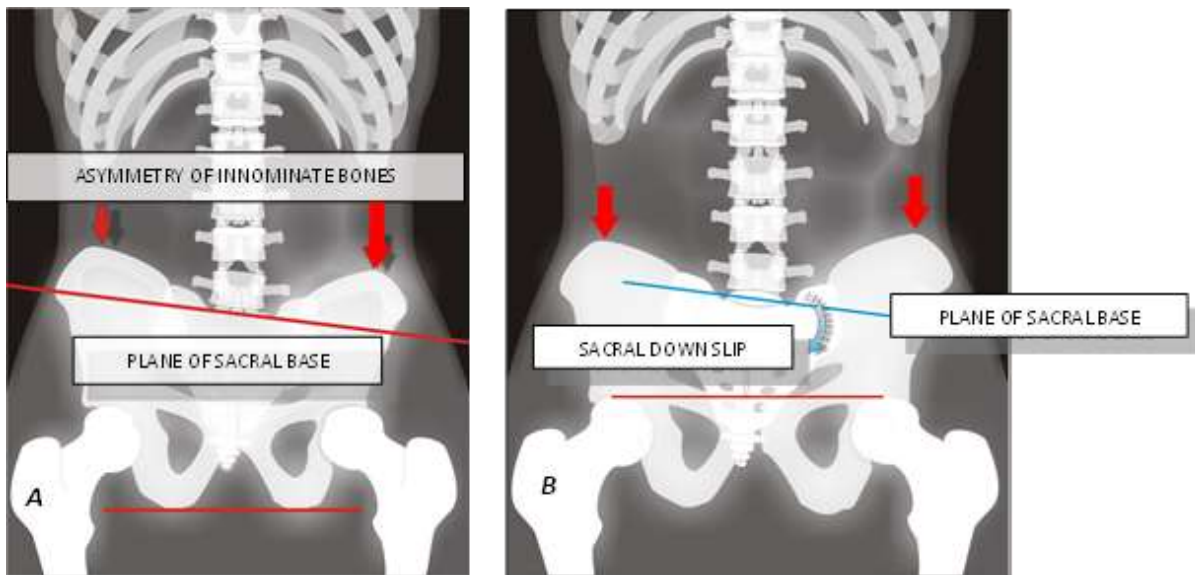


Figure 33. A. Structural asymmetry of the innominate bones resulting in tilt of the sacral base in the frontal plane. B. 'Down slip' or 'up slip' of the sacrum at either or both of the sacro-iliac joints resulting in relative sacral obliquity

The SRS define *pelvic obliquity* in relation to the global (absolute) reference frame. In this respect pelvic obliquity is often associated with functional or structural anisomelia (32, 34, 172, 203, 291) and functional or postural asymmetry (17, 56, 59, 60, 63-66) (Figure 34).

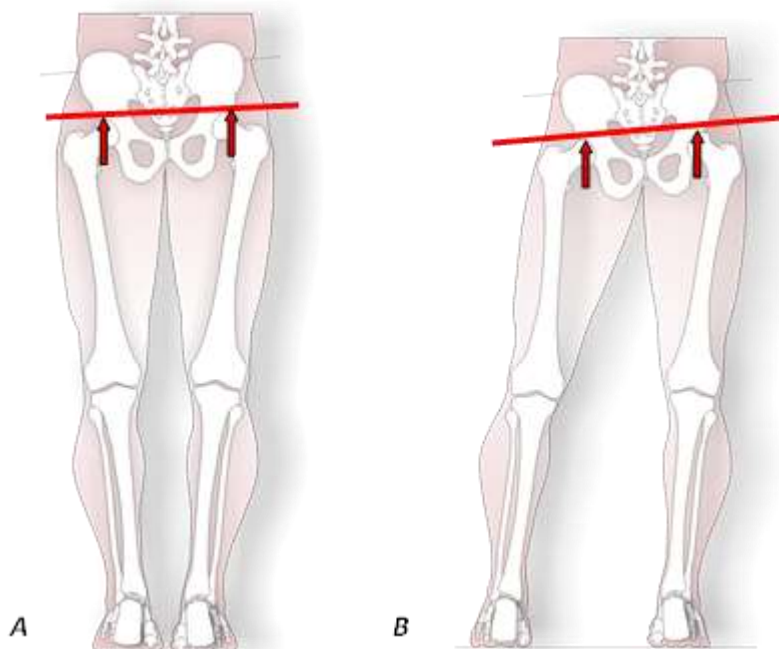
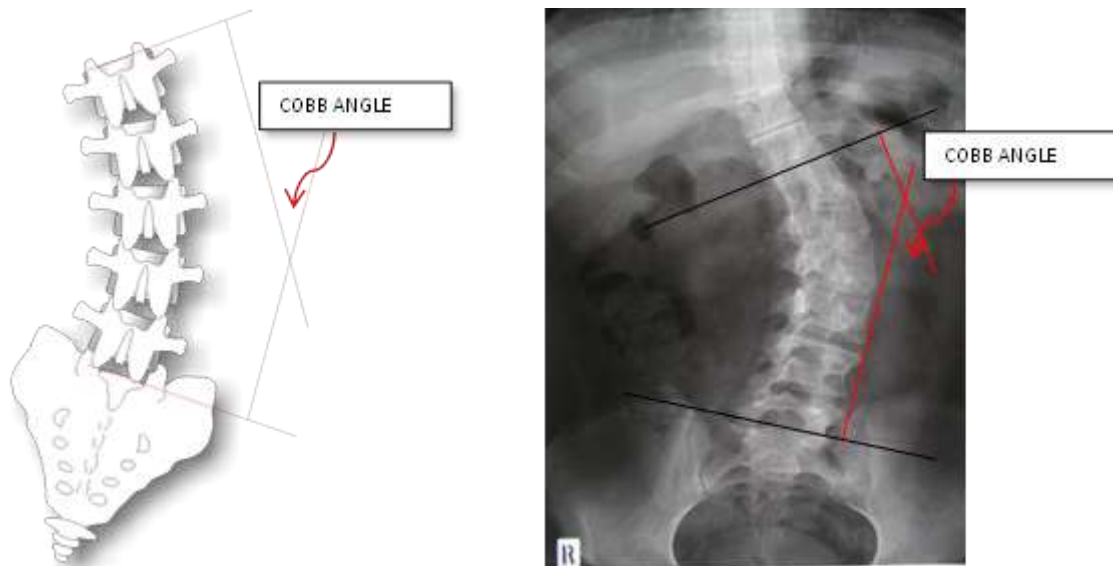


Figure 34. Structural anisomelia (A) and functional anisomelia (B) causing the pelvis to be lower on one side resulting in absolute sacral obliquity

Spinal frontal plane curvatures (scolioses) are commonly quantified using the Cobb method of radiographic analysis (187, 279, 292). The Cobb method involves identifying the vertebrae at the end-points of the curve or the transition point between two curves (292). A line is constructed that represents the plane of the end plate of the vertebra at the ends of the curve as projected on an anteroposterior (A-P) plain film radiographic view of the spine (279). The relative angle between the planes or vectors perpendicular to the planes forms the Cobb angle. This could theoretically involve any spinal segment including the sacral base. If the sacrum were the segment at the end of the scoliotic curve, the Cobb angle would involve the measurement of sacral obliquity in the frontal plane (Figure 35).



**Figure 35. Cobb angle formed between the sacral base and first lumbar vertebra**

The measurement of sacral obliquity, pelvic obliquity and Cobb angles on plane film radiographic images and computed tomography (CT) images, inherently involves the measurement of the relative and absolute position of three-dimensional structures as the intersection of planes forming dihedral angles, viewed on two-dimensional images (146, 190, 256, 292, 293).



Even though scoliosis and sacral obliquity are defined as a displacement of spinal segments in the frontal plane, there is a recognised coupling pattern directly associated with these displacements. The coupling effect associated with scolioses has been described and quantified by Kapandji (100), Harrison (294, 295) and others investigating spinal pathomechanics (296, 297). As the lateral displacement is invariably associated with, or superimposed on a lordotic or kyphotic curve along with rotation in the horizontal plane, the combination of rotations produces a compound angle of inclination in relation to an orthogonal reference plane or imaging plane. Lateral angular displacement of vertebra in a scoliotic spine can theoretically range through any number of degrees from zero degrees to one hundred and eighty degrees.

The clinical significance placed on the degree of displacement and rate of change of the displacement varies with different therapeutic and clinical objectives. The differences are often associated with different health care providers. Osteopaths, physiotherapists and chiropractors on a professional level are generally concerned with relatively small amounts of lateral displacement representing joint dysfunction and positional dis-relationships. These displacements have been traditionally associated with 'somatic dysfunction' by osteopaths, joint dysfunction by physiotherapists and 'subluxations' by chiropractors. Orthopaedic surgeons however, are generally concerned with scoliotic curves in excess of thirty to forty degrees and curves that are rapidly increasing in magnitude.

Each of these professional groups have investigated 'sacral obliquity' as the relationship of the sacral base to other bony structures (relative sacral obliquity) and the 'levelness' of the sacral base in sitting and standing postures (absolute sacral obliquity). The clinical objectives of chiropractors and osteopaths in identifying sacral obliquity are very similar in respect to treatment strategies. Both groups traditionally use manipulative techniques aimed at restoring positional and functional integrity to the spine. In this respect, the pelvis

in general and the sacrum in particular, has been identified as having an influence on the overall positional and functional integrity of the framework of the body.

Medical practitioners and allied health professionals such as physiotherapists have also investigated functional disorders and pain syndromes associated with asymmetry and structural variations of the spine and the musculoskeletal system. Pelvic obliquity has been of interest to orthopaedic specialists particularly in relation to the clinical management of scoliosis (33). Sacral obliquity (pelvic obliquity) has also been specifically studied in relationship to patients with paraplegia and in particular, those confined to wheelchairs (247, 298). These studies have been mainly in relation to the impact pelvic obliquity may have on weight distribution in sitting posture. Various other groups such as ergonomists, anatomists and sports biomechanists have specifically looked at structural asymmetry of the pelvis and the influence it has on mechanical loading of the spine and other structures of the body.

Two factors of particular interest in this study involved identifying the existence of systematic errors that may be inherent in the measurement of sacral obliquity in the frontal plane measured on plain film radiographs and CT images. Both of these measurements have been associated with functional disability of the musculoskeletal system and musculoskeletal pain syndromes. These specific measurements provide information that is an integral part of the clinical decision making process for various clinicians working with back and neck pain, joint dysfunction and other musculoskeletal complaints.

### **2.3 RADIOGRAPHIC MODALITIES AND METHODS**

To identify and quantify systematic errors associated with the measurement of dihedral angles a pelvic model was designed and constructed with five predetermined interchangeable sacral obliquity angles (Figure 36).

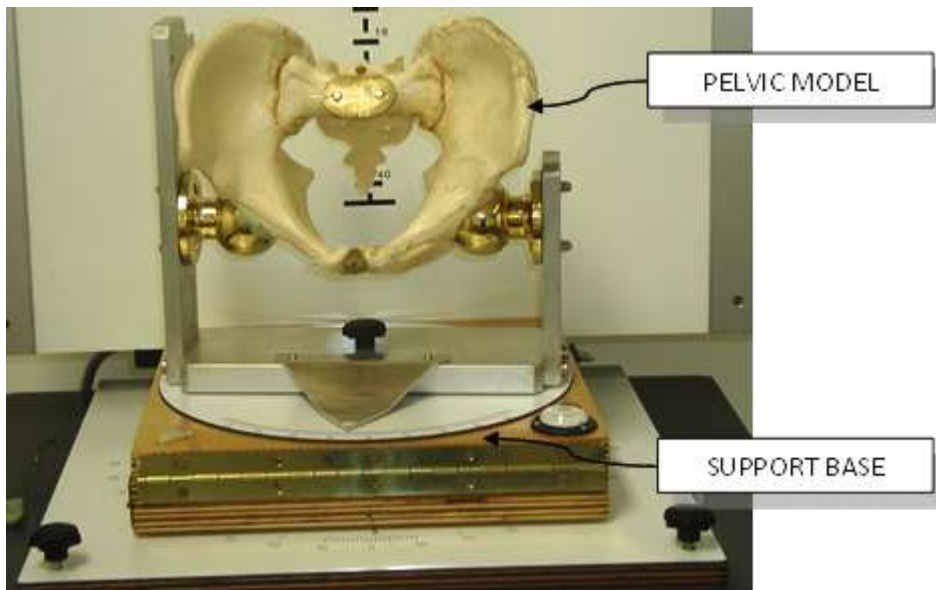


Figure 36. Pelvic model located in its supporting frame

The model was used as a radiographic phantom for both plain film and CT imaging. The pelvic model allowed simulation of specific degrees of sacral obliquity as it would be seen on plain film radiographs and imaged as computed tomography (CT) studies. Digital images of the phantom obtained using both radiographic methods were analysed to identify and quantify potential systematic errors. This was done by comparing the measured values on the images against the pre-set dihedral angles representing obliquity of the sacral base.

Algorithms were developed to calculate the true dihedral angles associated with the measurement of structural and functional alignment of the spine and pelvis on radiographic images. The algorithms were designed to be employed when the protocols developed to ensure reliable measurement of positional relationships were not met or were unable to be adhered to when the radiographs were taken or the data acquired.

In order to quantify and compare angles obtained from three different sources it was necessary to specify and define the reference frames, reference points, and lines being used and the specific angles being measured. The three methods were based on radiographic images using different imaging protocols, descriptive geometry and

trigonometry. The three methods used a common co-ordinate system that specified the origin and orientation of the structures and surfaces involved, the specific angles being measured on each view and other factors that required standardisation in order to remove ambiguity from the terms and facilitate meaningful comparisons of the measurements.

Spinal imaging methods used to quantify rotation or tilt of spinal segments in the coronal plane commonly involve plain film radiography, computed tomography imaging and slot scan digital radiography. Graphical analysis of an idealised sacrum with specified amounts of sacral obliquity was used as an additional method of imaging to control for the variables inherent in radiographing physical specimens.

Three different objects were used in the study to compare two radiographic projection and analytical methods. These were:

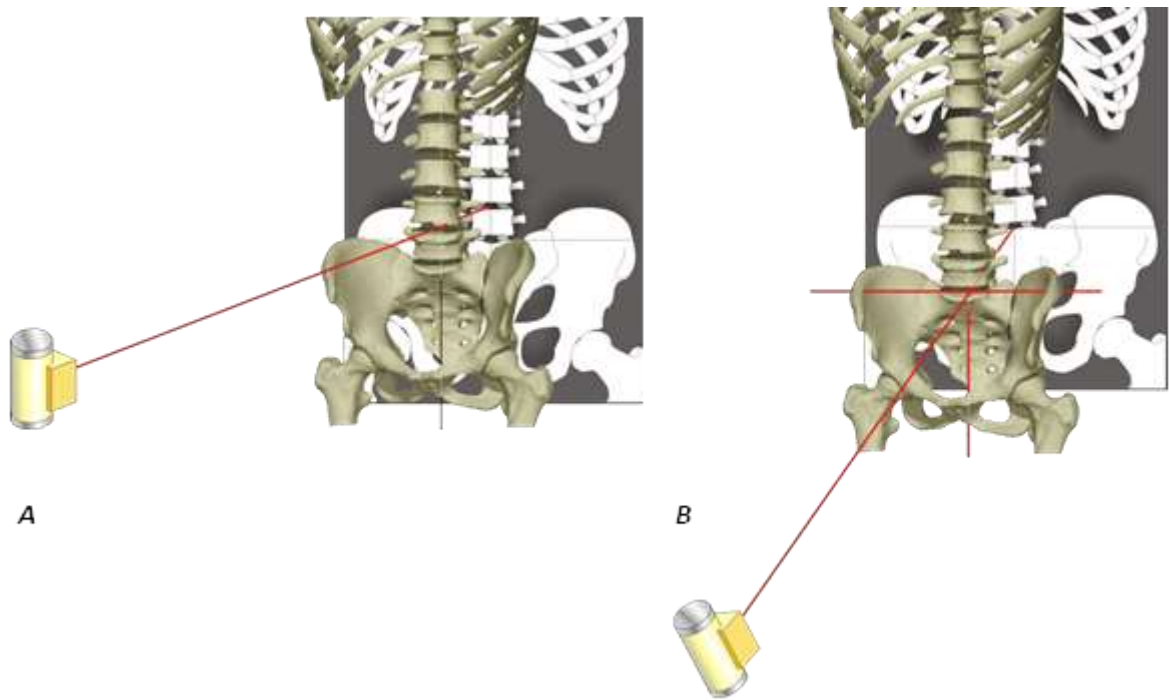
- 16 dry bone specimens
- A radiographic phantom with 5 interchangeable wedges representing pre-set degrees ( $0^{\circ}$ ,  $5^{\circ}$ ,  $10^{\circ}$ ,  $15^{\circ}$ ,  $20^{\circ}$ ) of sacral obliquity.
- An idealised graphical and mathematical model

### *2.3.1 Plain Film Radiography*

Erect lumbopelvic radiographs are utilised by clinicians from various disciplines such as chiropractic, osteopathy and musculoskeletal medicine in order to assess lumbopelvic alignment in the coronal plane and leg length imbalances. Reasons for the wide spread use of plain film radiography to image the spine involves the availability of facilities, relatively low cost, time involved for study and a lower exposure to ionising radiation than other forms of imaging involving ionising radiation such as CT imaging (7, 196, 299).

A significant number of chiropractors routinely use radiographs to assess the degree of tilt of the pelvis and sacrum in the frontal plane (9, 12, 242, 300). These procedures are similar to those employed by osteopathic physicians to assess spinal alignment (8) and for scoliosis screening by medical practitioners and orthopaedic specialists (33, 301). While the reliability of radiographic analysis used to assess positional integrity and overall alignment of the spine and pelvis has been demonstrated for specific techniques (14, 15, 174, 239, 240, 243), in general the validity of those radiographs and the associated analytical methods has been questioned (29, 191, 236, 238, 254). The sensitivity of the resulting measurements to changes in various radiographic parameters such as the relationship of the pelvis to the position of the x-ray tube (central ray) (29, 233, 241, 302), patient positioning (237, 303) and the choice of reference points for analysis (8, 228, 262, 304) have been documented.

The two plain film views used for comparison in this study have been advocated or widely used in clinical practice to evaluate the positional integrity of the pelvis and the sacrum in particular (9, 35, 61, 78, 104, 174, 265, 305). The anteroposterior (A-P) radiographic view is the standard technique used by most musculoskeletal clinicians for assessing pelvic alignment (8, 12, 79, 255, 306). However, a number of investigators and clinicians have suggested that an erect view with the central ray angled to match the lumbosacral angle as seen in the lateral view gives a more reliable measurement of true sacral obliquity (27, 41, 78, 188, 266, 284, 307) (Figure 37). A similar view of the lumbopelvic junction is referred to as Ferguson's view (308). The cephalic angled view of the pelvis, generally taken in supine posture, is recommended as a spot view to clearly visualise the sacroiliac joints and lumbosacral junction (255, 301, 306, 309). This spot view differs from the erect full lumbopelvic view proposed by other clinicians to measure sacral obliquity but is sometimes also referred to as a Ferguson view (147, 307).

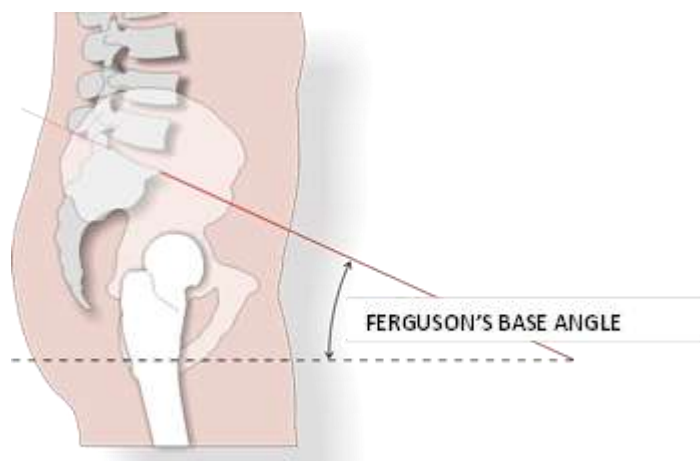


**Figure 37. (A) A-P lumbopelvic view with central ray perpendicular to film (B) Sacral base view with the central ray angle to match the sacral plateau in erect posture**

The A-P lumbopelvic view involves positioning of the patient in erect posture for a plain film radiographic image of the lumbopelvic spine with the x-ray tube angled so that the central ray is perpendicular to the film and centred on the cassette both horizontally and vertically (11, 12, 99, 255, 306). The concept of a '*central ray*' has been defined or used in a number of different ways. One definition describes the central ray as the one ray that emerges from the x-ray tube that is perpendicular to the film (310-312). However, this definition of a central ray does not necessarily apply to the cephalic angled view of the pelvis. Another definition of the central ray describes the relationship of the x-ray beam to the anatomical structures of interest and can vary depending on the positioning of the film and x-ray tube for a particular individual (313).

The angled sacral base view is also taken in erect posture with similar positioning to the A-P view but with the x-ray tube angled to approximate the slope of the sacral base as seen in the sagittal plane (Figure 37). This angle is known as Ferguson's base angle (254) (Figure 38). No studies could be found in the relevant literature that specifically investigated either

the individual validity of these methods or the relative performance of the two methods in quantifying sacral obliquity.



**Figure 38. Ferguson's base angle used to angle the central ray for the erect sacral base view of the lumbopelvic spine**

The specific purpose of this study was to identify the presence of any systematic error in either of two plain film radiographic views and their associated image analytical methods. Because systematic error can only be identified if the true value is known it is not generally possible or convenient to confirm the validity of a particular imaging method and its associated analytical protocols using *in vivo* studies. However, any systematic measuring error inherent in one or both of the methods studied could result in differences in the measured sacral obliquity angle obtained from the two different views of the same specimen.

A secondary part of this study was to investigate the effect that using different measuring points identified on images of the sacrum would have on the measurement of sacral obliquity and the intra- and inter-examiner reliability of these measurements. Any significant difference in the measurements for an individual sacrum or specified amount of sacral obliquity would suggest a lack of validity (sensitivity/specificity) in one or both of the radiographic protocols used and the possibility of systematic error affecting the measurements. A difference could theoretically occur from a systematic projection error

due to structural asymmetry affecting part of the specimen such as the sacral base or ala, variation in the placement of the specimen relative to the central-ray beam or from a problem in the specific analytical method and measuring points employed to measure sacral obliquity, or any combination of these factors.

The present study was specifically designed to identify and quantify any difference in what has been interpreted as the degree of sacral obliquity measured on the different radiographic views. While the sacral base view has been suggested as a better way of visualising the sacral base on radiographic images by a number of authors (27, 41, 78, 188, 284), there are no reliable or comprehensive studies to substantiate this claim. It is not known for instance if one view systematically underestimates the degree of obliquity or the other view overestimates the obliquity or if there is any difference at all between the views.

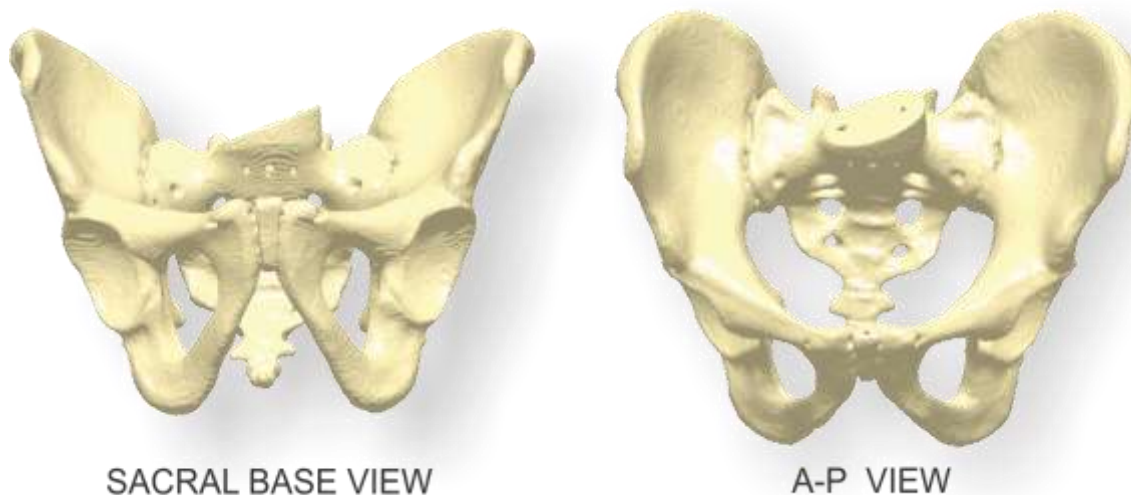
Quantifying sacral obliquity using these views was not designed to test the validity or reliability of obtaining the true degree of sacral obliquity against a '*gold standard*'. It was primarily designed to identify any quantifiable and significant difference between the two views for any particular specimen or for a particular degree of obliquity and identify any general trend in the measurements that would indicate a systematic error in one or both of the methods.

### 2.3.2 Computed Tomography

The use of computed tomography (CT) to image the bones and soft tissues of the axial skeleton has been shown to be an accurate and reliable method of measuring angular and linear relationships in the range needed to quantify sacral obliquity (314). An advantage of CT imaging to assess positional integrity of the spine and pelvis is that the structures can be manipulated post examination using multiplanar reconstructions (MPR) or three-dimensional volume rendering (198, 315) (Figure 39). These techniques remove or



minimise some of the geometric problems associated with measuring angles relating to three-dimensional structures on two-dimensional images.



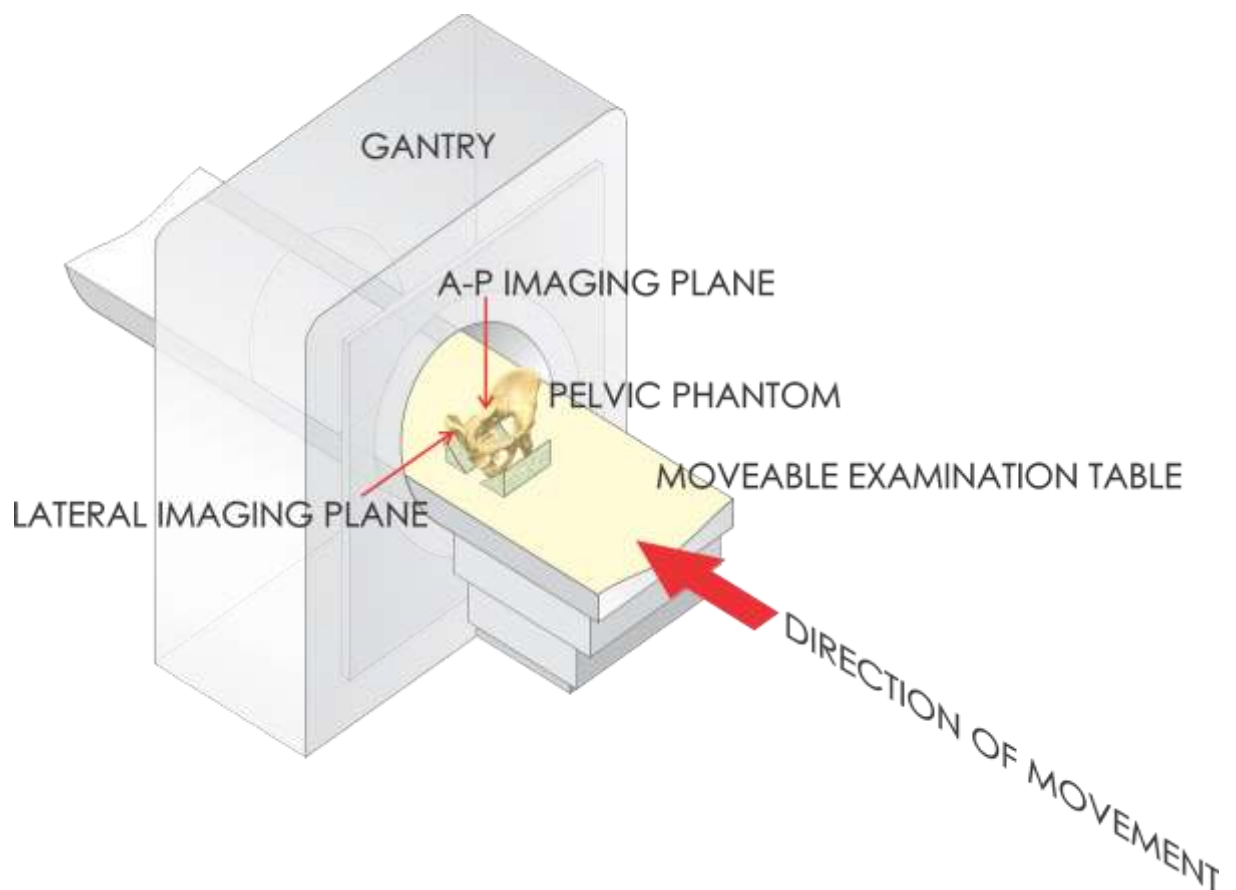
**Figure 39. A three-dimensional reconstruction of a pelvic model manipulated to produce two views from the same data set**

The angle formed between two non-parallel three-dimensional planes is known as a dihedral angle. The viewing angle and orientation of the object(s) incorporating the planes of interest influences the validity of the angle measured on a two dimensional image. The ability to manipulate the planes of interest after acquiring the image data facilitates the accurate measurement of dihedral angles such as sacral base obliquity and Cobb angles. A major disadvantage of CT scans of musculoskeletal system for many clinicians is that they are commonly taken in a non-erect and non-weight bearing posture, usually in the supine position (226, 316, 317). For most lumbopelvic or abdominal studies the relative position of the lower limbs is unknown.

### *2.3.3 Slot-Scan Digital Radiology (SSDR) and Scanned Projection Digital Radiography (SPDR)*

Slot-scan digital radiology (SSDR) has been a development of digital radiography that provides high-quality weight bearing spinal imaging with relatively low irradiation for the resultant image quality (318-321). This form of image acquisition (SSDR) is analogous to

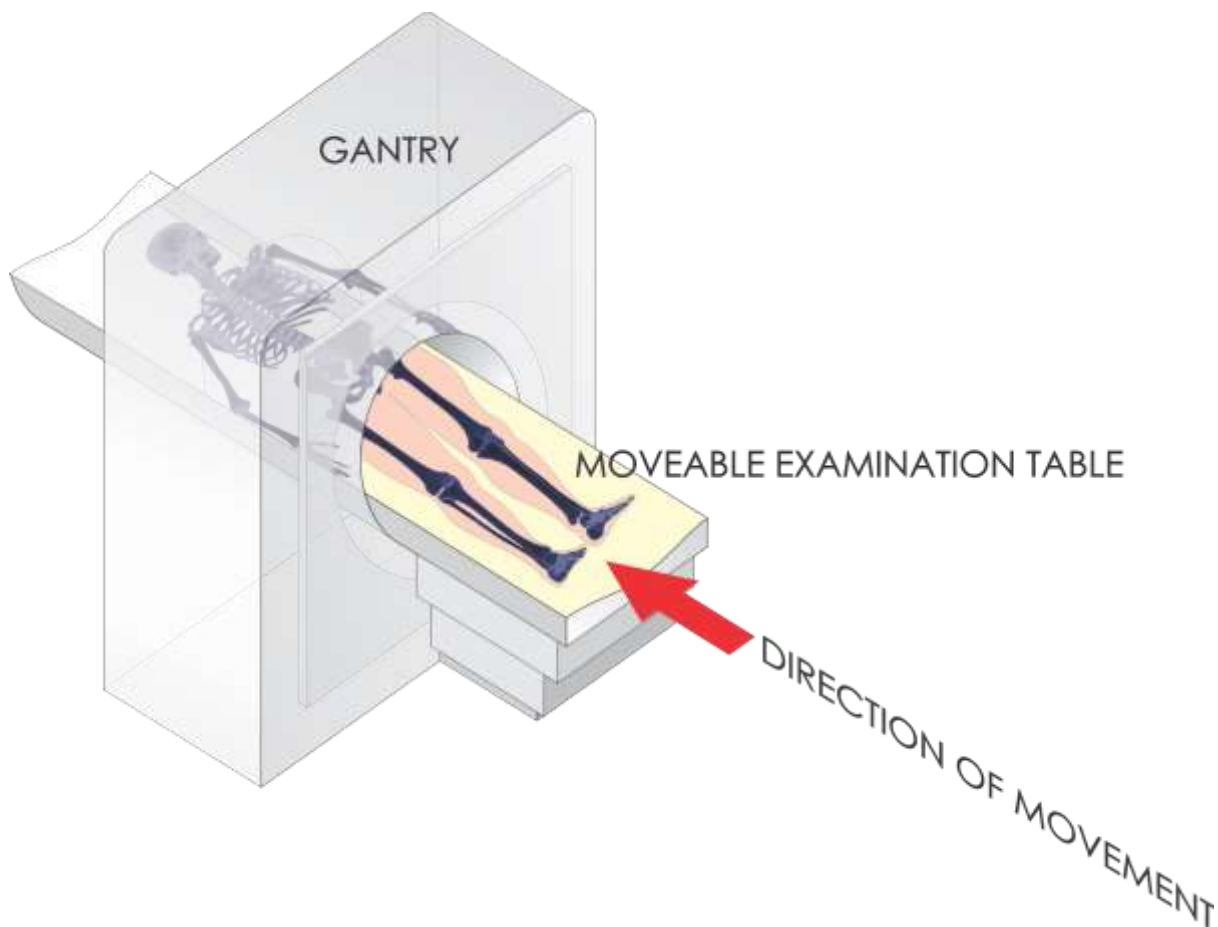
the Scanned Projection Digital Radiography image (SPDR), commonly referred to as a *scout view* or *scanogram* used in conjunction with Computed Tomography (CT) imaging (322, 323). To obtain a scanogram image the patient or object is translated through the CT gantry and through the plane of a fixed fan beam x-ray source (Figure 40). The resulting image generated from fixed receptors is similar in general appearance to a conventional projection radiography image. A major difference is that there is no geometric magnification in the direction to translation with the spatial resolution of the resulting image in the scanning direction determined by the fan beam thickness.



**Figure 40.** The pelvic phantom positioned on the moveable examination table in preparation for the scout views

Both SSDR and SPDR are collimated to use a thin x-ray beam rather than the cone shaped beam used in conventional radiography. Because SPDR views are performed with the tube fixed they are technically projection radiographs rather than CT scans even though they are

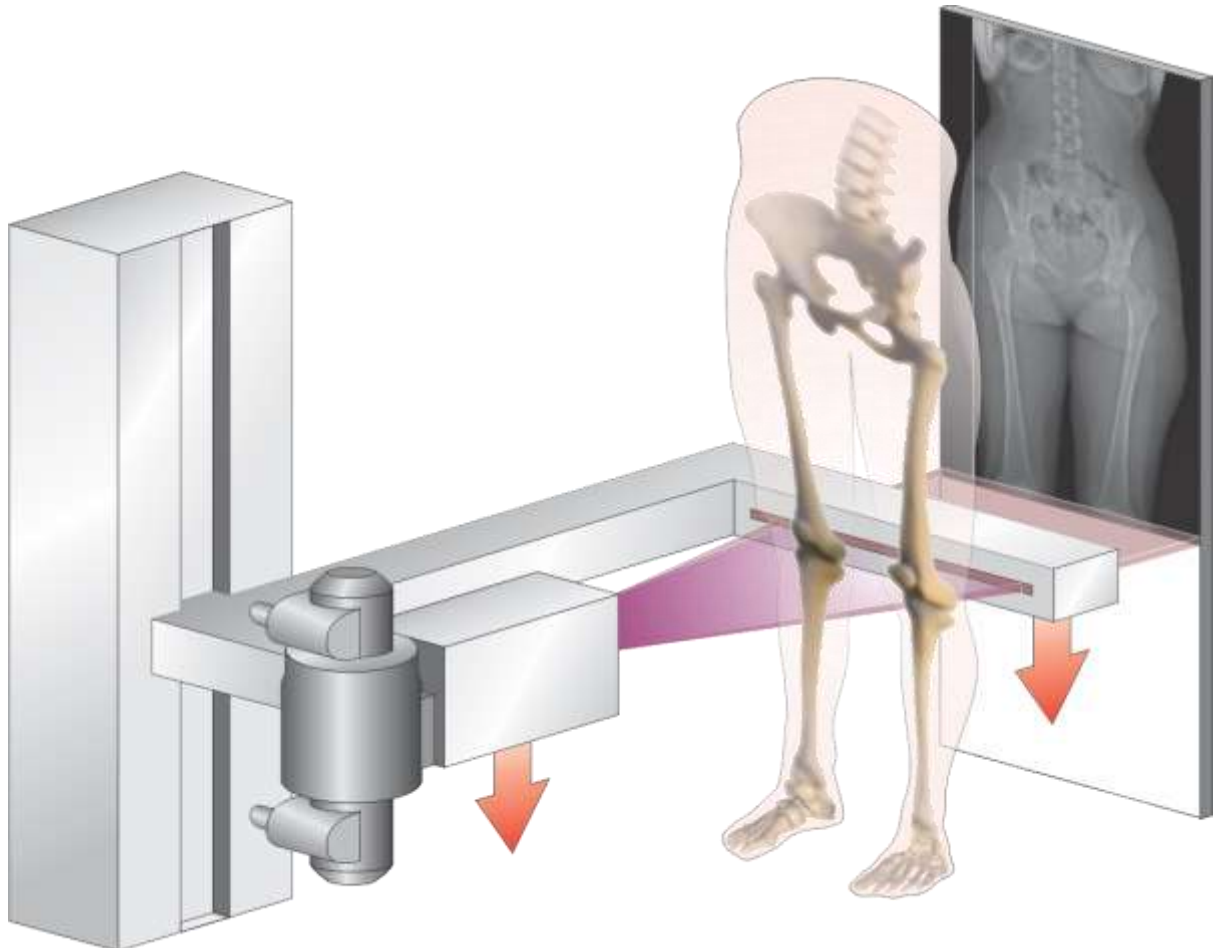
commonly used as part of a typical CT study. SPDR views commonly comprise an anteroposterior (A-P) and lateral projection of the area being scanned. The major difference between SSDR and SPDR generated images is that the table moves through the gantry along an axis perpendicular to the scanning plane in SPDR while the x-ray source and detectors move along (or down) the patient for SSDR (Figure 41).



**Figure 41. The movement of the table through the gantry of the CT machine to produce a Scanned Projection Digital Radiography image (SPDR)**

SSDR and SPDR produce images that have very similar geometrical properties. For both SSDR (and SPDR) the x-ray beam is collimated to produce a narrow horizontal fan-shaped beam that moves relative to the axial skeleton simultaneously with the detector. The image is acquired line by line by scanning the fan-shaped X-ray beam at a constant speed in a vertical direction for erect spinal views and horizontal direction for supine SPDR

lumbopelvic views. With both views the image is gradually built up over an extended time during scanning (321, 324) (Figure 42).



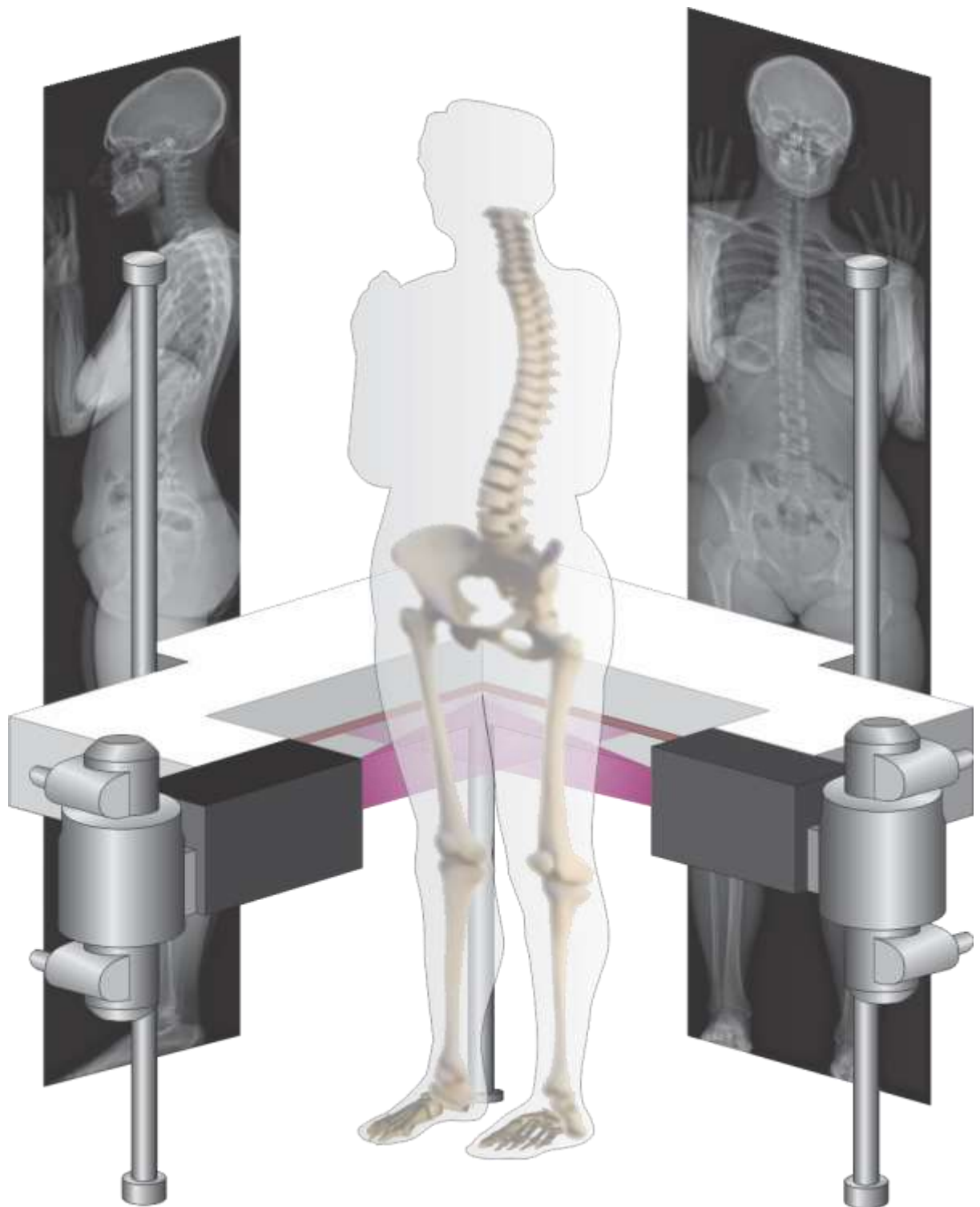
**Figure 42. SSDR use a thin x-ray beam to form the image as the tube moves downward rather than the cone shaped stationary beam used in conventional radiography**

Scanning systems have been developed based on x-rays transmitted with intensities that vary as they pass through the body to produce light that is collected by fibre optics and conveyed to arrays of charge-coupled devices (CCD). Other methods involve photon counting detectors, e.g. crystalline silicon x-ray detectors and multichannel gaseous ionisation chambers (321, 324, 325).

An advantage of many SSDR systems is that they detect each x-ray photon absorption event in the detector. This results in low levels of scatter radiation thus eliminating the need

to use an anti-scatter grid (324). While the purpose of an anti-scatter grid is to increase image contrast and detail by absorbing or minimising the scatter radiation emitted by body tissues before they reach the film or imaging device, it results in higher exposure factors and non-diagnostic (blank) areas on the image. SSDR systems have the potential to significantly lower exposure factors and the ionising radiation dose to the patient which makes them ideal for assessing positional relationships within or between spinal structures (326, 327). Other advantages provided by this form of digital radiography are an improved dynamic range, improved low-contrast resolution, fast access to the resultant images, and the opportunity for dedicated image processing (321).

While Computed Tomography (CT) is considered the gold standard for volume rendering 3D reconstructions of bone structures (328), CT scans are not well suited for accurate reconstructions of large bone structures, such as the spine. This is mainly due to the high doses of radiation that are necessary to image large areas at high resolution. Other factors that limit CT scanning for spinal use when they are compared to plain film radiography are their expense, lack of equipment portability, and they require patients to be lying down in non-weight bearing postures for the studies. Biplanar SSDR is an alternative to CT and plain film imaging in that it can produce 3D reconstructions of spinal structures that make accurate measurements of positional relationships possible with relatively low exposure of the patient to ionising radiation (329, 330) (Figure 43).



**Figure 43. Bidirectional slot scan with two x-ray tubes synchronised and moving in the same direction to produce an A-P and lateral image at the same time**

Magnetic resonance imaging (MRI) was not included in the study primarily because of the limited clinical application of this method of measuring Cobb angles. While open MRI systems have been introduced that facilitate erect postural studies of the spine, this type of

equipment remains relatively limited compared to the other forms of spinal imaging included in the study. Cobb angle measurements using this type of equipment have been shown to be as reliable as CT imaging and plain film analysis of scoliotic spines (331).

## **2.4 RADIOGRAPHIC PROJECTION FACTORS**

Conventional or plain film (PF) radiography, computed radiography (CR), digital radiography (DR) and computed tomography (CT) use photosensitive film or gas detectors to directly or indirectly capture ionising radiation that passes differentially through the body's tissues. The ionising radiation for each of these methods originates from a relatively small point source (focal spot), passes through structures within the body, and emerges with altered intensity depending on the tissue density that it has passed through e.g. gas, water, fat, mineral and metal. The exposure of the film by or detection by sensors of the emerging ionising radiation produces a two dimensional image that maps the relative densities of the structures and tissues through which the beam has passed (332, 333).

With computed tomography (CT) the images are two-dimensional axial slices that comprise a data set for each subject. For computed (CR) and digital radiography (DR) the resulting image is composed of two dimensional grey-scale pixels rendered on an imaging screen with each pixel representing the filtered digitised intensity of the beam at that point. The resolution of the image is proportional to the size of each pixel (Figure 44). Computed and digital radiography allows wide latitude in the image quality through the use of computerised adjustment of contrast and brightness of the image post-exposure. This post-processing flexibility of most digital systems enables a variety of optimization techniques to improve image quality for specific tissues (333).

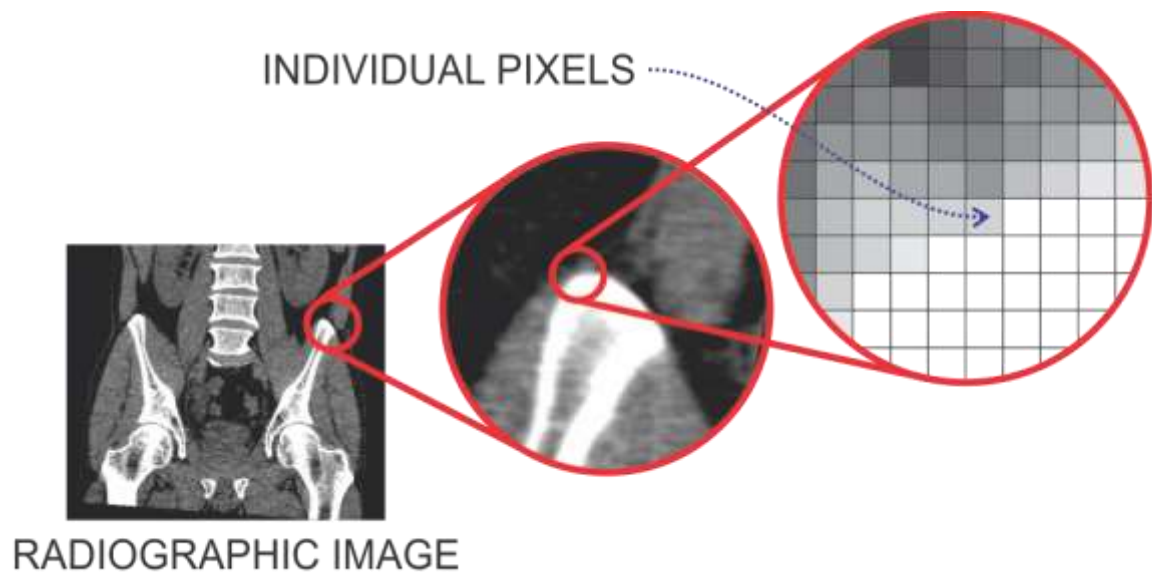


Figure 44. A pixel is the smallest discrete unit making up the image. Each pixel is comprised of a specific uniform grey scale colour. The number of pixels in each row and column determines the resolution of the image

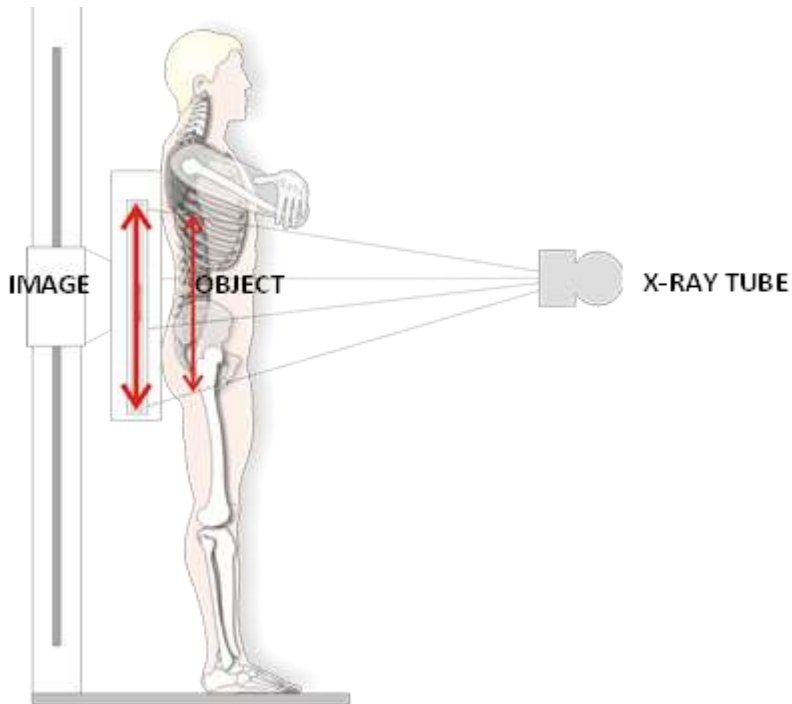
For plain film (PF) radiographic imaging, based on screen / film (conventional) systems, the image quality and resolution are dependent on grid ratios, the graininess and sensitivity of intensifying screens and characteristics of the photosensitive film (334). These factors are established prior to the exposure and are only modified post-exposure by variables in the processing method. The screens and film convert ionising radiation coming from the x-ray tube that has passed through the subject into visible light that in turn exposes a photosensitive film. This film is then chemically treated to produce a grey-scale image proportional to the beam intensity at each point on the film. The screen and film combination influences and sets the signal contrast, latitude of the dynamic range as well as sharpness and noise.

#### 2.4.1 Geometrical Properties

Apart from the resolution and quality of the radiographic image, there are geometrical properties of conventional, digital and computed radiography that involve the projection of a three-dimensional object onto a planar surface from a point source with inherent magnification and distortion of the resulting image (29, 287). Dimensions are always

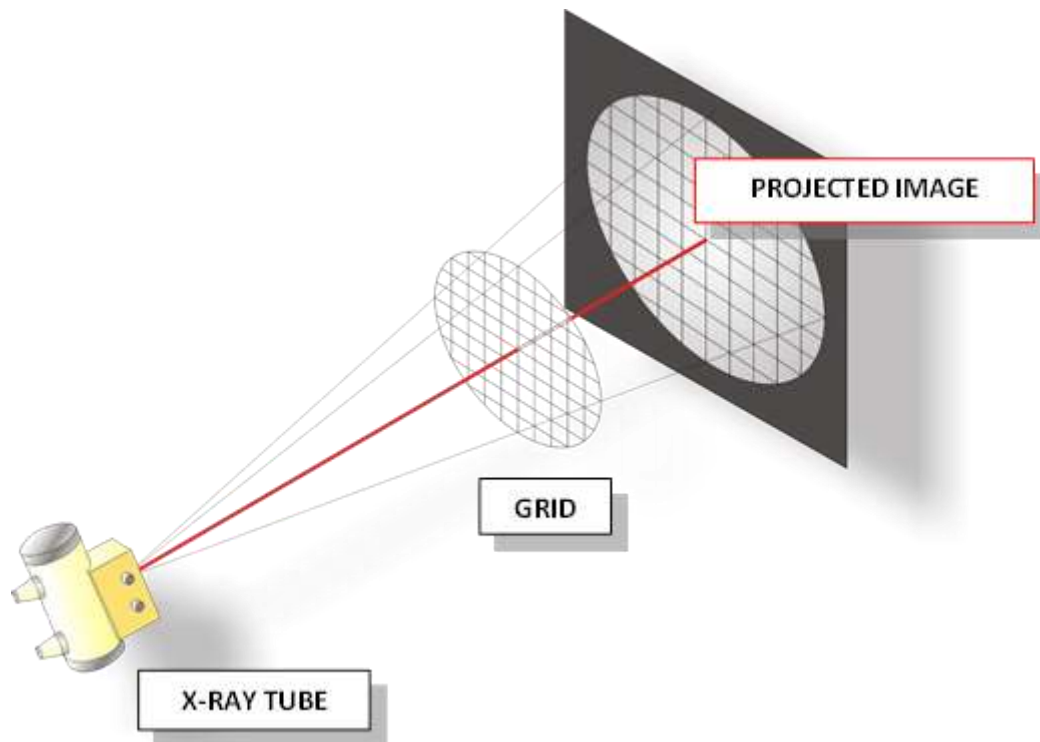


greater in at least one dimension on the projected image relative to the dimensions of the actual structure. This is also associated with a change in visualised angular relationships of structures and surfaces (29, 244) (Figure 45).



**Figure 45. Because the object is between the beam source and the image, the graphical representation of the object has larger dimensions than the object**

Changes in the projected image are due to the point source of the projection rays and to the fact that the object is always between the source of the rays (focal spot) and the viewing plane (film) (Figure 46).



**Figure 46. Inherent magnification creates greater dimensions on the projected image than the actual structure**

This creates a geometrical disadvantage for plain film and computerised radiography in that an individual two-dimensional image cannot be directly manipulated geometrically once the exposure has been made even though the image quality of digital images can be manipulated post-exposure. The viewing angle and the resulting positional relationships of the structures represented in the image are fixed at the time of exposure. CT and some digital biplanar images can be reconstructed using specific algorithms to produce manipulable volumetric (3D) representations of structures (325, 329, 330).

For an individual plain film (PF) or computerised radiographic (CR) image, the positional relationship and dimensions of the objects depicted is dependent on four basic interrelated geometrical factors (287):

- Position of the central ray of the x-ray beam relative to the object
- Angle of the image plane relative to the x-ray beam and object
- Source/image distance

- Object/image distance

#### 2.4.2 Central ray (CR) or Primary ray (PR)

The primary or central ray of an x-ray beam has three intrinsic properties related to the production of a measurable image of a three-dimensional object (313). The first is related to the intensity of the beam, the other two are related to the geometric or projection properties of the beam.

Beam intensity is not uniform but varies with the intrinsic characteristics of the x-ray tube producing what is called the heel effect. Due to internal geometrical characteristics of the x-ray tube the intensity of the x-ray beam is not uniform in the plane perpendicular to the focal spot of the anode. This variation in the intensity of the primary beam is referred to the heel effect. Electrons coming from the cathode bombard the anode producing ionising radiation in all directions. The greatest intensity of the resulting x-ray beam is to the cathode side of the x-ray tube (335). The intensity of the beam depends on the angle at which the x-rays are emitted from the focal spot. Factors that influence the architecture include the positional relationship and size of the anode and cathode, and the size, shape and angulation of the focal spot (335, 336). The intensity of the x-ray beam is greatest where the angle of incidence of the electron beam is equal to the angle of exit of the x-ray beam from the focal spot of the anode and decreases to zero in the plane of the focal spot. If the central ray is assigned a value of 100% the beam intensity on the anode side of the tube would approach 0% due to the heel effect and would be greater than 100% on the cathode side of the tube (335) (Figure 47).

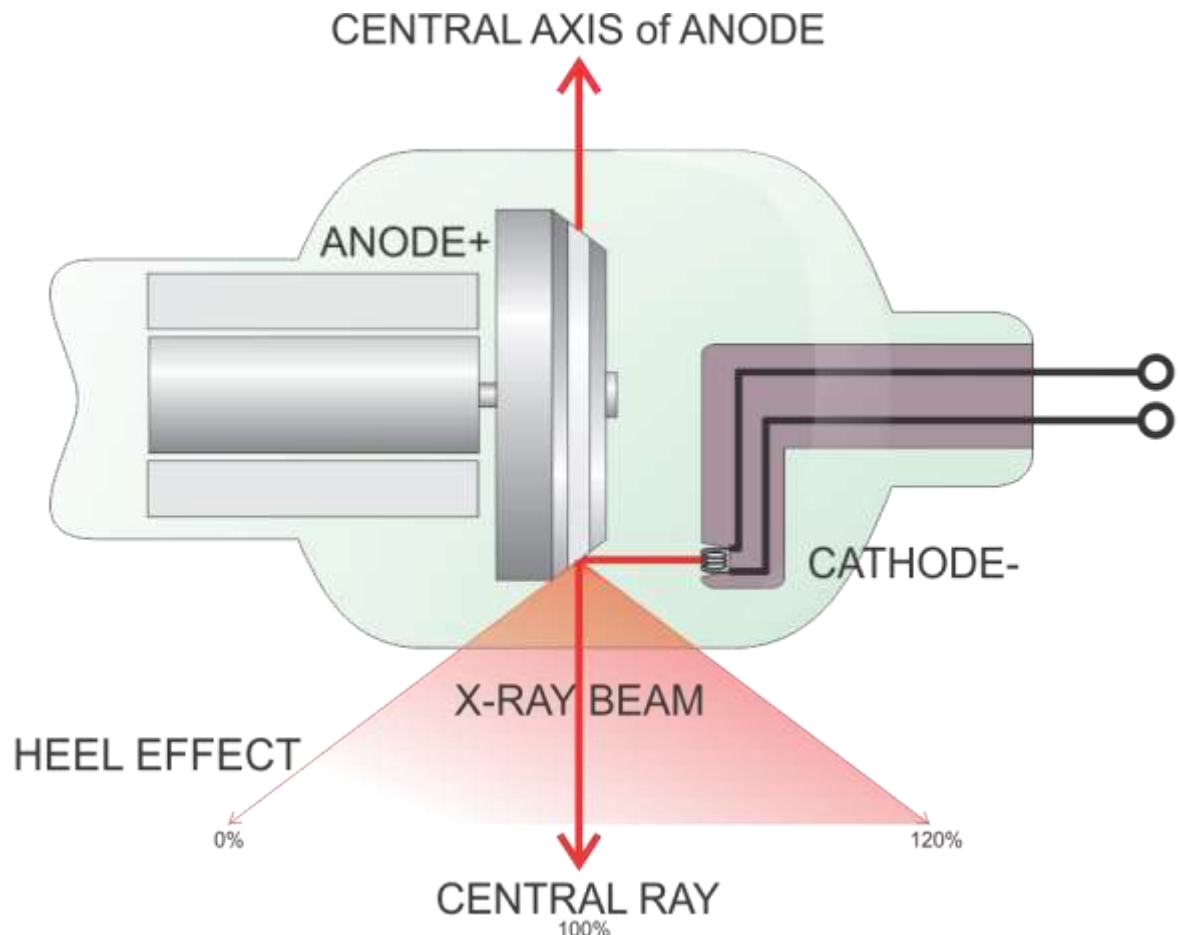


Figure 47. The heel effect influences the intensity of the resultant x-ray beam

The relationship between focal spot width and the size of the projected focal spot is determined by the anode angle (336). Anode angles generally range from about  $7^\circ$  to  $20^\circ$  (337). The steeper the anode angle the smaller the projected or effective focal spot (Figure 48). A smaller effective or projected focal spot provides better spatial resolution of the structure on the image plane. The size of the effective focal spot is geometrically related to the actual focal spot with the following relationship where  $\theta$  is the anode angle:

$$\text{Effective focal length} = \text{Actual focal length} \times \sin \theta$$

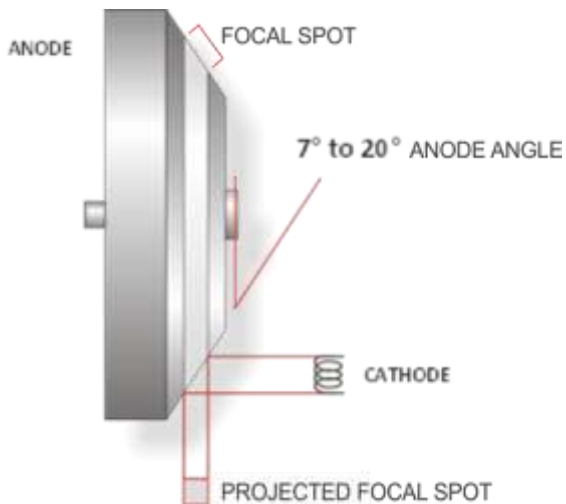


Figure 48. Relationship between focal spot width and the size of the projected focal spot. The anode angle (7-20 degrees) is the slope the focal spot forms relative to the vertical

X-ray intensity usually reduces significantly toward the anode end of the tube because of the heel effect. The heel effect is produced by the geometry of an angled anode target with lower intensity of the beam toward the anode (heel) end. The significance of the heel effect on the visualised structures forming the radiographic image is that it can alter what is perceived or viewed as the border or line of demarcation of a given structure (335) (Figure 49).

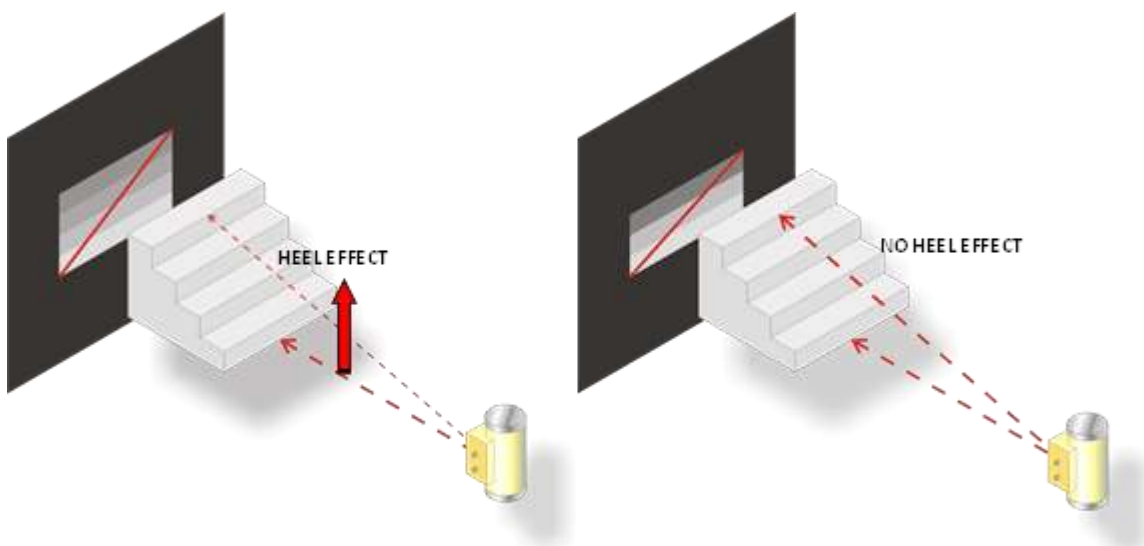
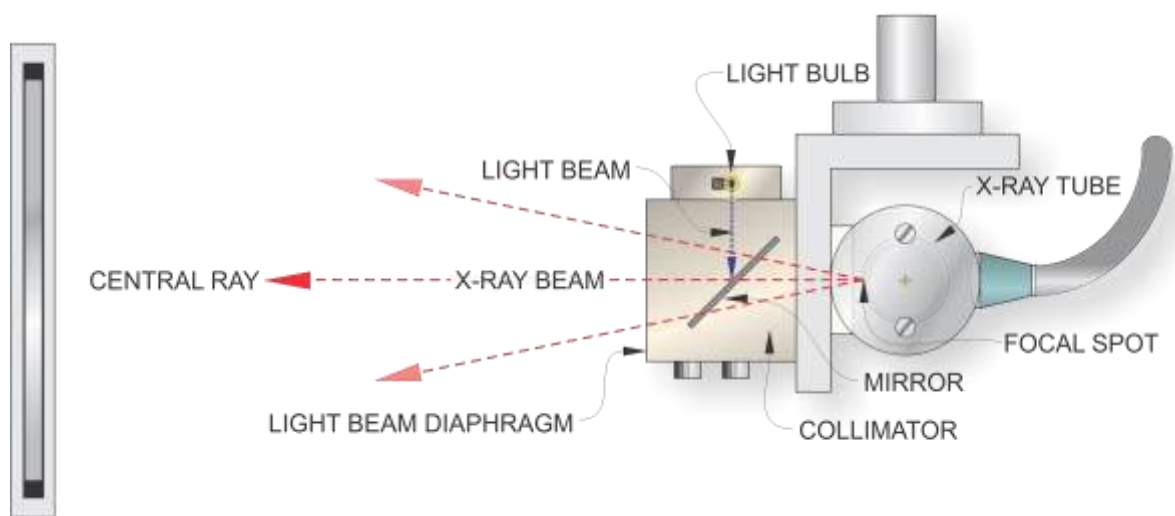


Figure 49. The heel effect causes a loss of beam intensity resulting in a variation in the projected image and visualized angles

### 2.4.3 Geometric or projection properties

The size of the focal spot coupled with the source to object distance and the object to image distance determine the majority of the image projection characteristics and image sharpness of a given study. The alignment of the x-ray beam, the object and the image plane can also influence projection geometry and the resulting two-dimensional image of a three-dimensional object. The x-ray beam emerging from the x-ray tube can be classified as a central ray and horizontal and vertical primary rays (Figure 50).



**Figure 50. The central ray can be defined as the individual ray that originates from the centre of the focal spot and emerges perpendicular to plane of the anode**

Fox (313) suggests that there is 'a common misconception that there exists only one possible "*central x-ray beam*" arising from the x-ray tube and that it is the one that somehow is oriented to the axis of the x-ray tube on its collimator.' He further emphasizes that there is an infinite number of x-ray beams emanating from the point source of radiation (the x-ray tube anode). He suggests any one of these rays could be defined as "the central x-ray beam." One definition of the central ray (CR) suggests it is the unique ray emanating from the focal spot of an x-ray tube that is perpendicular to the electron stream that flows from the cathode to the anode within the tube. Based on this definition of the central ray it is an internal property governed by the intrinsic architecture of the x-ray tube (338). Another definition suggests that being perpendicular to the image plane or film makes one

particular ray the unique central ray for any given position of the x-ray tube (339). Using this definition the central ray is located at the origin of the X and Y-axes and represents the Z-axis of orthogonal projection planes relative to the image plane or film and is often located at the geometric centre of the film (Figure 51).

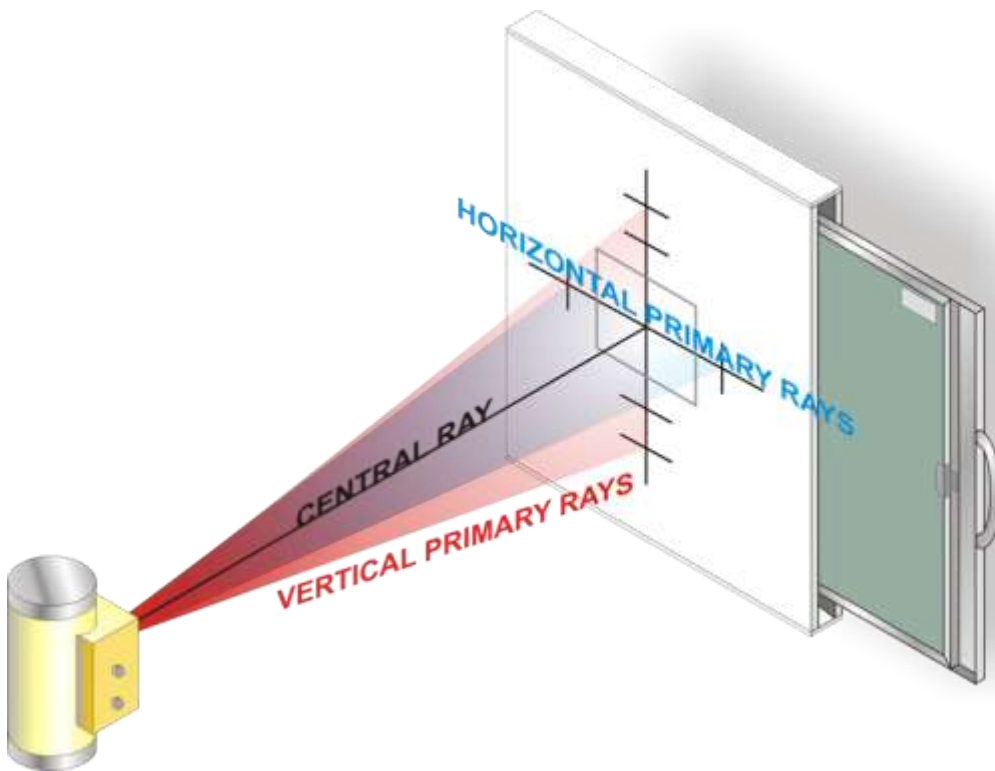


Figure 51. The central ray is the one ray common to both the horizontal and vertical rays and represents the origin of the X and Y-axes of the image

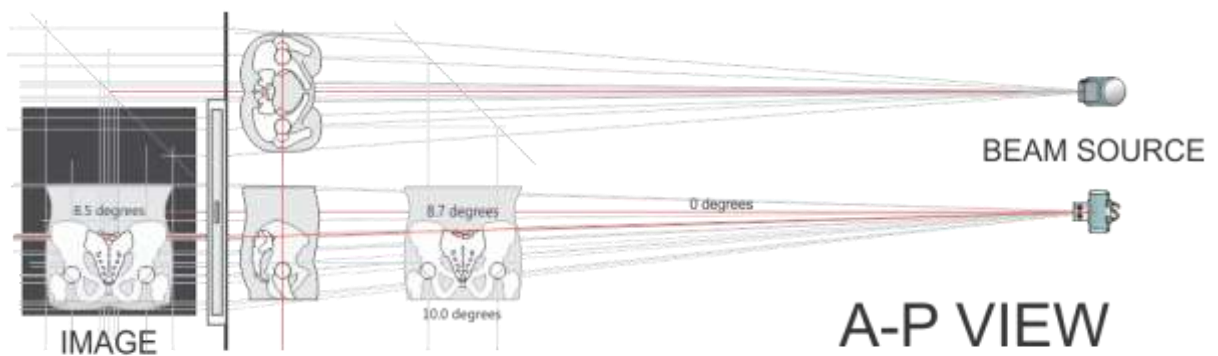
Fox (313) uses a definition that is particularly relevant for stereotaxis proposes. His definition of the central ray is any ray emitted from the tube that superimposes two selected points on the image plane. If a primary beam or central ray is considered the ray that would superimpose any two specified points when they are projected by that particular x-ray beam onto a film or an image plane then any individual ray emanating from the x-ray tube can fulfil this role.

The components of the x-ray beam that lie in a horizontal plane that passes through the central ray are considered the horizontal primary rays (HPR). The horizontal rays form the

X-axis of an orthogonal projection plane that contains the central ray (Figure 51). The portions of the x-ray beam that lie in a vertical plane that passes through the central ray are considered the vertical primary rays (VPR). The vertical rays form the Y-axis of an orthogonal projection plane that contains the central ray (Figure 51).

A plane constructed on or representing an object will have specific angular relationships to the rays emanating from the focal spot of the x-ray tube and to the image or projection plane. The measured angulation of a plane in a perspective projection and the measured positional relationships of objects vary with the position and orientation of a specified object and plane relative to the point source of the lines of projection and the orientation of the image plane.

Changing the angle of projection for the vertical alignment of the central ray relative to the plane of the sacral base can alter the projected view of the structure. Two views resulting from a change in the angle of the central ray are the conventional A-P lumbopelvic view of the pelvis (Figure 52).and the sacral base view.



**Figure 52. Projection of the pelvis in erect posture with the central ray perpendicular to the image plane**

In the sacral base view (Figure 53).the central ray is aligned and angled to the sacral base. Because of the divergence of the x-ray beam not all the disc spaces and surfaces are visualised optimally in the common A-P lumbopelvic projection. The divergence is



particularly pronounced at the L5-S1 level with the central ray at the level of the mid lumbar vertebra (Figure 52). The Ferguson or sacral base view can be employed to optimise the visualisation of the L5-S1 interspace (309).

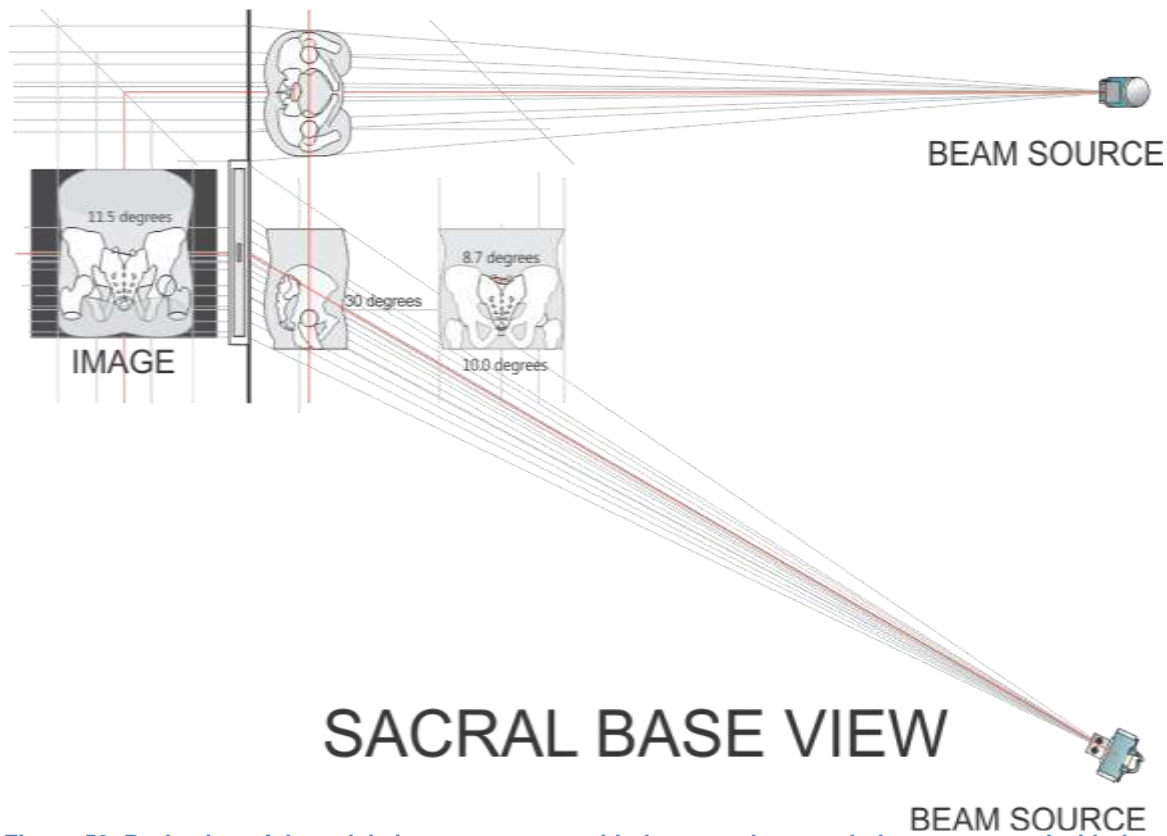


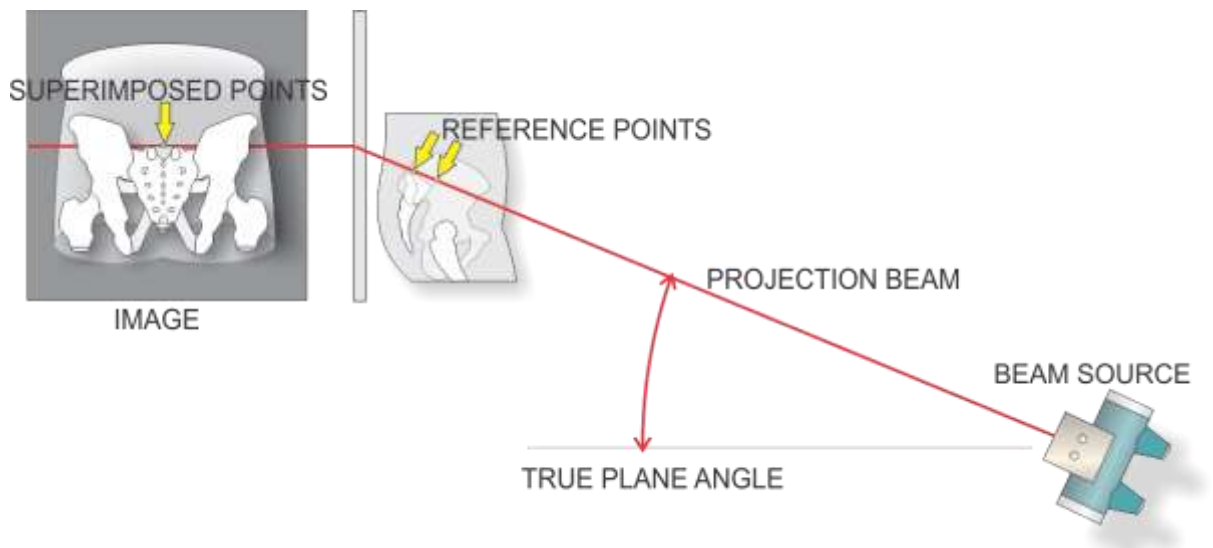
Figure 53. Projection of the pelvis in erect posture with the central ray angled to correspond with the slope of the sacral base

The sacral base view has been proposed by a number of clinicians such as Illi (41), Tilly (188), Brown *et al* (27), and Barge (78) as a way of better visualising the sacral plateau when it is being viewed from the front in erect posture. Illi believed that vertebral segments that appeared normal or perfect on a standard supine A-P view were revealed as having lesions or malformed using the sacral base view. He also believed from clinical observation that segments that were thought to be “badly misshaped, infiltrated, decalcified or even the focus of an osseous disease” were found to be perfectly normal on a sacral base view. Brown *et al* describe sacral obliquity as not easily discernible on an A-P or P-A scoliosis films. They suggest that to demonstrate sacral obliquity on a radiographic image requires a

Ferguson view to appreciate the abnormality. They further suggest that AP films of the lumbopelvic spine can show level hips while a sacral base view reveals sacral obliquity in the same individual.

To define the projected relationships of three-dimensional objects such as the sacral base as it is viewed on a two-dimensional image, the angular relationships of the projection rays were defined for this study as either a true plane angle (TPA) or an actual projection angle (APA) in relation to the point source (focal spot).

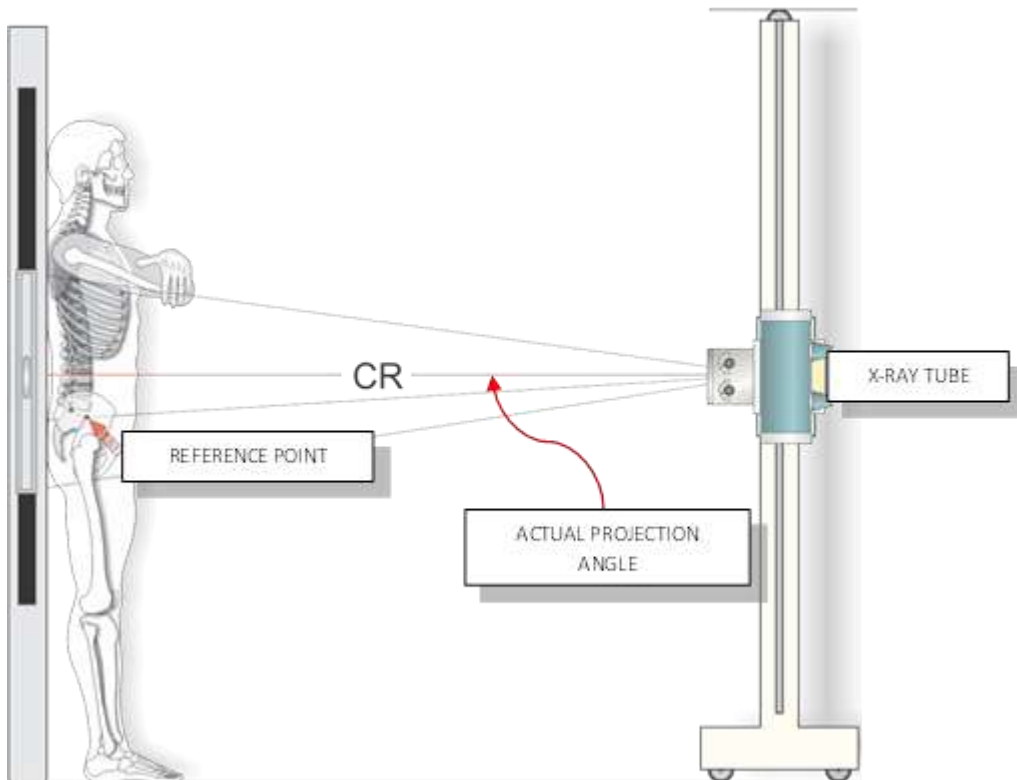
Any two points with Z-axis displacement that project with no vertical (Y-axis) or horizontal (X-axis) displacement in the viewing plane, form an angle relative to the viewing or projection plane. This angle is defined as the true plane angle (TPA) for the plane containing the points (Figure 54).



**Figure 54.** The true plane angle (TPA) is defined by any two points with horizontal displacement that would project with no vertical (Y-axis) displacement

The horizontal or vertical angle formed between the central ray (CR) and a ray from the focal spot passing through a specified point (Figure 55). The actual projection angle should be the same as the angle calculated from the projected image as the lateral projection

angle (LPA) or plan projection angle (PPA). The actual projection angle is not influenced by rotation of the x-ray tube.



**Figure 55.** The actual projection angle (APA) is formed between the central ray and any specific point on the object

With two specified points positioned so that they are perpendicular to the image plane and with the x-ray tube aligned and angled so that the ray representing 100% intensity of the beam is aligned with the specified points and perpendicular to the image plane, all three factors would coincide (Figure 56) (A). In other configurations, these three factors can be represented by three very different rays each with different geometric properties (Figure 56) (B).

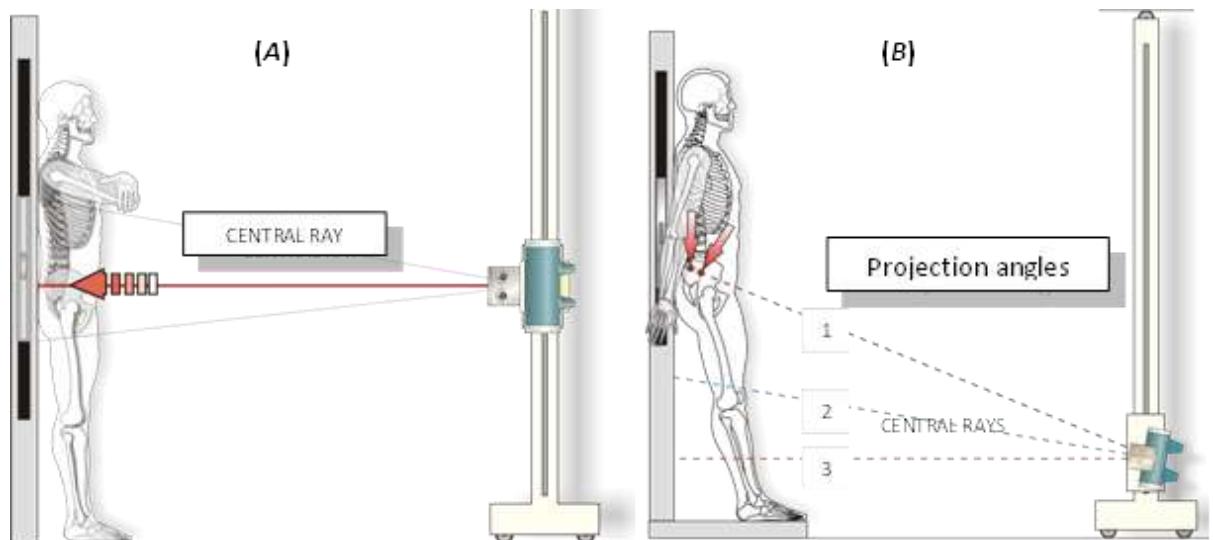


Figure 56. (A) The three concepts of the central ray coincide (B) The three different concepts of the central ray relative to: (1). object (2). x-ray tube (3). image plane

If the central ray is considered the one ray that emanates from the focal spot of the x-ray tube and travels perpendicular to the image plane (287), points equally spaced from this central ray will exhibit increasing degrees of magnification the further they are located from the central point (Figure 57).

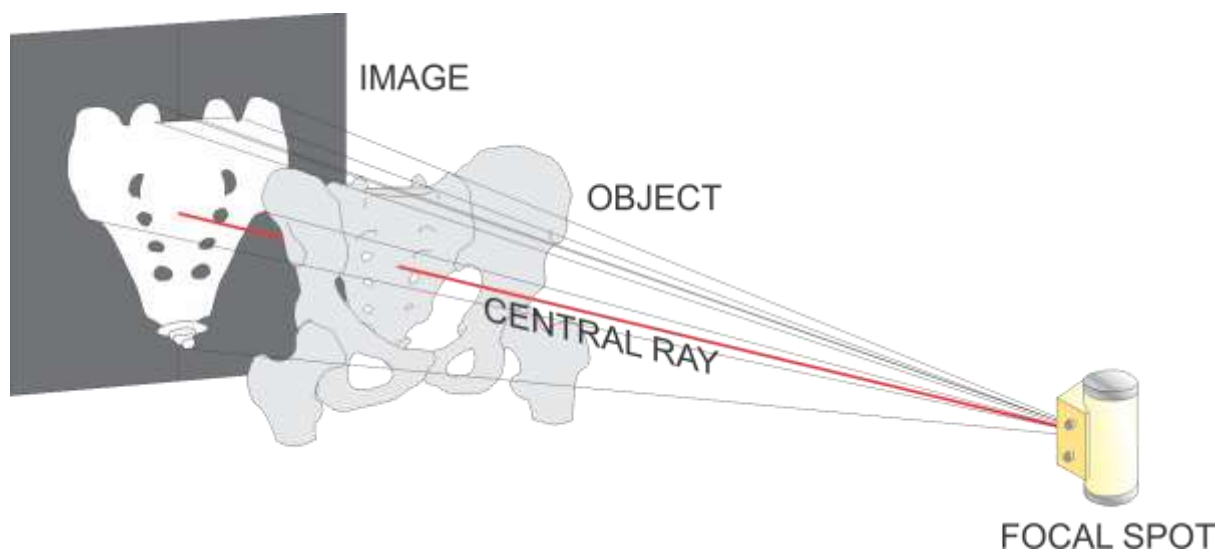


Figure 57. Points equally spaced from the central ray will exhibit increasing degrees of magnification the further from the centre they are located

Zengel and Davis (287) used trigonometry to calculate the degree of magnification of an object on chiropractic radiographs. The formula they use is based on the divergent

properties of the x-ray beam that results in the image size (I) being equal to the object size (O) multiplied by a magnification factor (MF):

$$I = O * MF$$

The magnification factor is equal to the source to image distance (SID) divided by the source to object distance (SOD) (Figure 58):

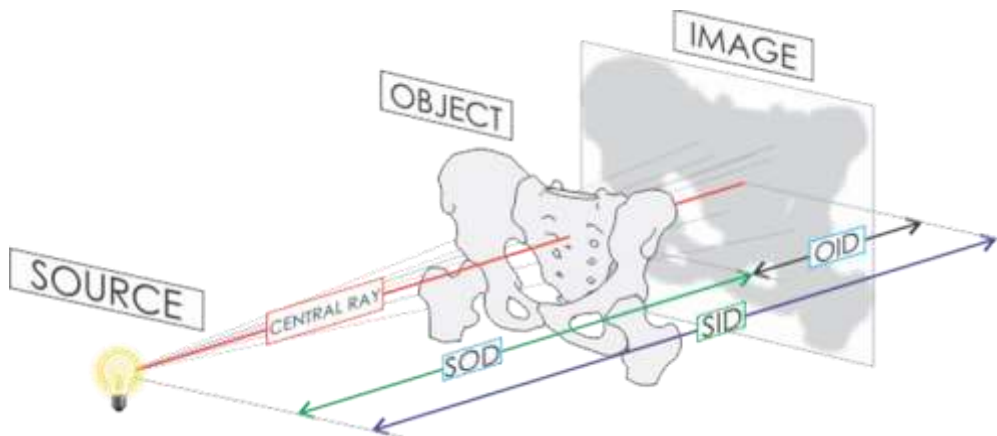
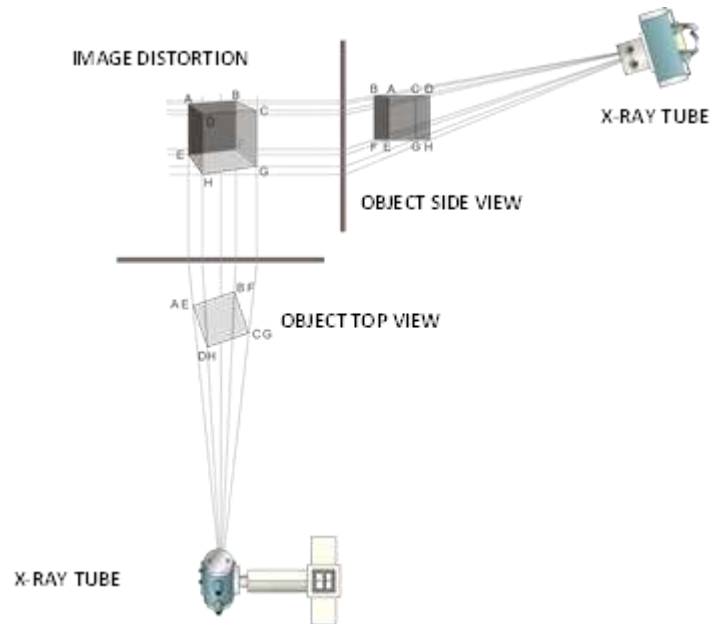


Figure 58. As the object is located between the source and image plane magnification will occur with greater amounts of magnification the further the object is from the central ray

$$I = O * SID/SOD$$

A common characteristic of radiographic projection is spatial distortion. All conventional x-ray images suffer from this effect. Projection distortion results in images that do not faithfully reproduce the three-dimensional surface relationships of an object or the spatial relationships between objects because of unequal magnification in different regions of the field of view or from one image to another (Figure 59).



**Figure 59. Projection of a cube demonstrating the effect of radiographic distortion with none of the angles projected as true right angles**

The effect can be illustrated using an image of a wire frame that has no depth, projected onto an image plane as it would be with an x-ray beam (Figure 60). The angles (but not distances) measured on the projected image (**A**) are the same as the angles formed by the object because the object (wire frame) is parallel to the image plane. Distortion can be measured in the angles **X** and **Y** formed by the sides of the projected grid in image (**B**). The distortion occurs because of the varying distances of the sides of the frame from the image plane. The projected angles will not be the same as the angles formed by the actual object. This is due to unequal magnification of the object by the x-ray beam.

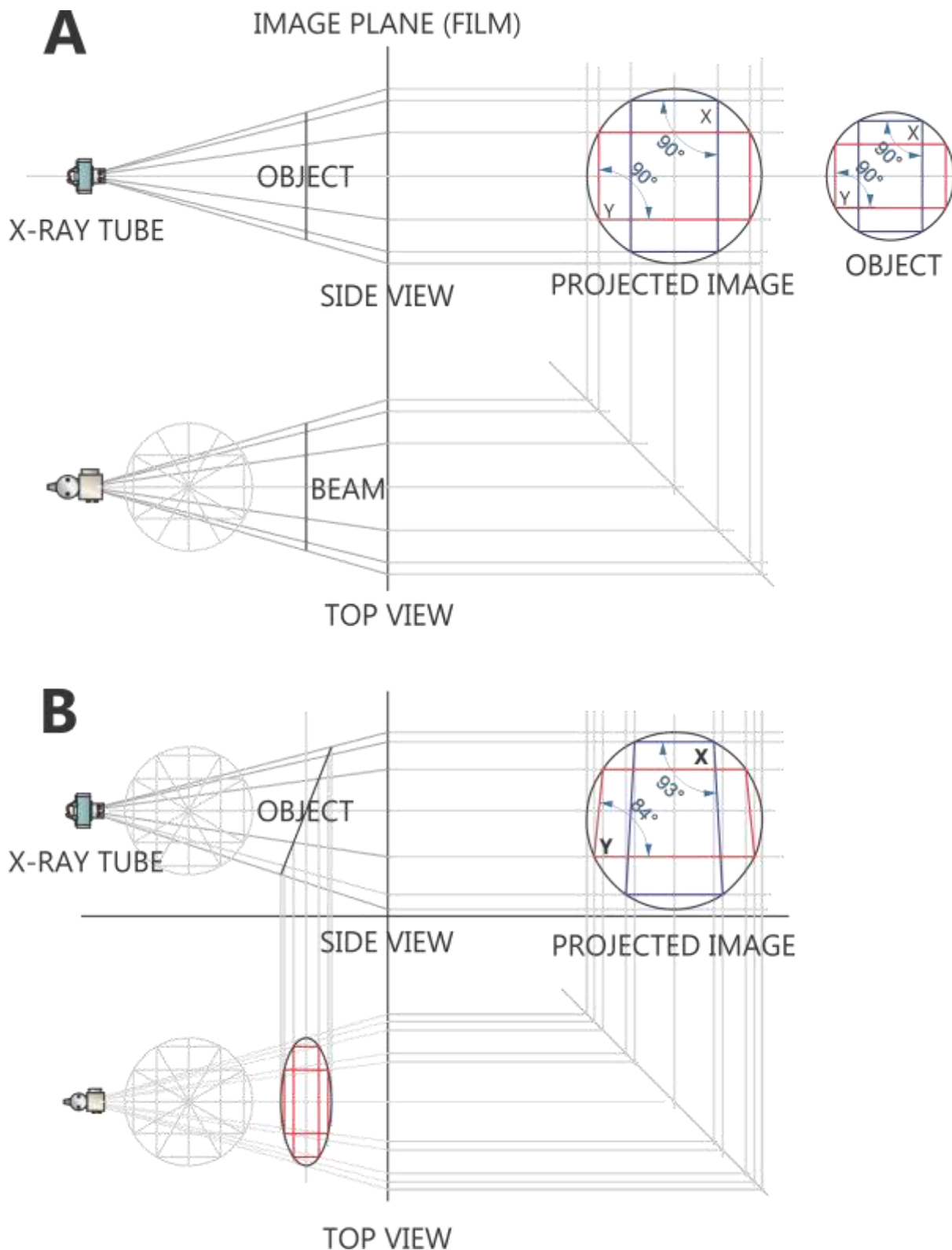


Figure 60. A graphical representation of the projection from a point source of a circular structure with an embedded reference frame. A. With the structure parallel to the image plane the true angles X and Y are projected onto the image. B. Projection of structure angled relative to the image plane result in distortion of the angles. Angle X projects larger and angle Y projects smaller than a true right angle

Angles formed on, or are part of surfaces are preserved on projected images if the plane containing the angles is parallel to the image plane. The size of components of the three-dimensional object will change with changes in the position and the distance from the image plane or the x-ray tube. Components nearer the x-ray tube (focal spot) and further from the image plane will be magnified to a greater extent than those with the opposite relationship to the focal spot and image plane.

The angles formed between corresponding reference points on two surfaces that are parallel to the image plane but with different object image distances (OID) will change due to the unequal magnification of the two surfaces. The true angles are preserved and not subject to projection distortion when they are contained on surfaces that are parallel to the image plane. The right angles formed at BAD, ADC, EHG and FEH project as true right angles whereas angles ABC, BCD, EFG and FGH do not project as true right angles (Figure 61).



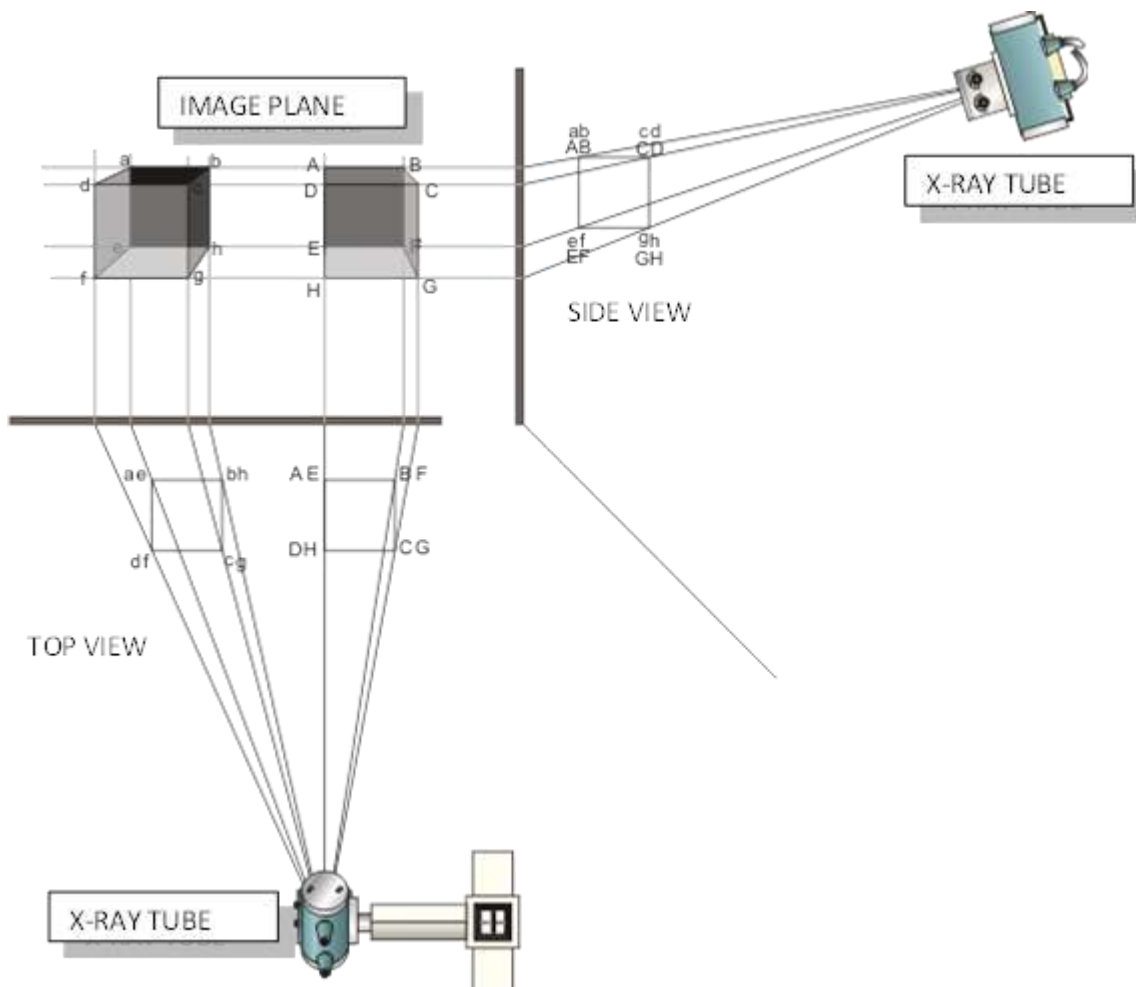


Figure 61. Graphical representation of the radiographic magnification of two cubes positioned with one face parallel to the image plane (film) but different relationships to the x-ray tube

## 2.5 SUMMARY AND CONCLUSION

A number of radiographic modalities and specific views of the lumbopelvic spine can be used to measure sacral obliquity with various degrees of accuracy. Two general types of errors that would be of concern to clinicians if present would involve random error and systematic error.

Random error can affect any individual patient or examination and is not restricted to measuring sacral obliquity on radiographs. Random error can be present in any measurement. For this reason the reliability of radiographic analysis was not an objective of this study.

The focus of this study was assessing the validity of radiographic methods and specifically involved the identification and quantification of systematic error in the use of radiographic images for measuring sacral obliquity. The validity of five different radiographic views that can be used to measure sacral obliquity were examined for the presence of systematic error. Generally if systematic errors are present they cannot be identified by repeating the radiographic study and applying statistical analysis. Systematic errors can be detected by comparison of results from one method of analysis with other independently obtained results using different methods or techniques or comparison of results with a known reference value.

Dry bone specimens and a radiographic phantom with pre-set degrees of sacral obliquity were used to identify the presence and magnitude of systematic errors. Two different imaging modalities were used to image the radiographic phantom and involved plain film (conventional) radiography as well as CT imaging. The measurements obtained were validated against a graphical model of the pelvis. Each of the modalities (plain film and CT images) involved multiple views of the sacrum. These are summarised as:

1. CR plain film imaging of 16 dry bone sacral specimens.
  - a) APV
  - b) SBV
2. CR plain film imaging of pelvic phantom with different degrees of sacral obliquity.
  - a) APV
  - b) PAV
  - c) SBV
  - d) ZAV
3. CT imaging of pelvic phantom with different degrees of sacral obliquity.
  - a) multiplanar reconstruction
    - APV
    - SBV

- b) 3D reconstruction
- 4. CT imaging study of fifty *in vivo* lumbopelvic spines
  - a) multiplanar reconstruction
    - APV
    - SBV
  - b) 3D reconstruction
- 5. CT scanned projection digital radiography (SPDR) of radiographic pelvic phantom with five different amounts of sacral obliquity.



**SACRAL OBLIQUITY MEASURED ON  
RADIOGRAPHIC IMAGES OF 16 DRY BONE  
SACRAL SPECIMENS**

## CHAPTER 3

*“I am inclined to believe that life as it is manifested to us must be a function of the asymmetry of the universe or of the consequence of this fact.”*

— Louis Pasteur

### 3.1 INTRODUCTION

The primary objective of this chapter was to identify the presence of systematic errors associated with the measurement of frontal plane sacral asymmetry measured on plane film radiographic images. The specific systematic error being evaluated relates to the projection of dihedral angles onto a two-dimensional image plane. Sacral obliquity is tilting of the sacral base in the frontal plane and represents a dihedral angle. Sacral obliquity is commonly associated with rotation around two or more axes of rotation. This is because in the normal anatomical orientation of the sacrum in upright posture the sacral plateau is inclined relative to two planes. The angles measured on a two dimensional radiographic image are Ferguson’s base angle and sacral tilt or obliquity. The projection of dihedral angles on a two dimensional image plane creates inherent systematic errors in measuring the true dihedral angle.

A true dihedral angle can only be measured if the viewing angle lies along one of the planes forming the angles and there is no rotation around other axes. If however the viewing angle is perpendicular to the plane no dihedral angle can be measured. Measurement of any given dihedral angle will fall somewhere within these extremes. Therefore the radiographic projection view used to measure sacral obliquity can result in a systematic error.

Two views of the sacrum that have been advocated for measuring sacral obliquity are the standard erect A-P lumbopelvic view and a sacral base view. A factor associated with

these two different views other than the viewing angle that can result in a systematic error when measuring sacral obliquity, is the visibility and identification of reference points and landmarks used to define the reference plane. On the standard A-P view the sacral base is superimposed over other structures obliterating or obscuring reference points making them difficult to identify. To overcome this, analytical protocols often incorporate reference points that can be easily identified on the radiographic images and used for convenience. However this can result in a systematic error in generating the line representing the plane being measured.

In order to identify either of these two types of systematic error sixteen dry bone specimens were radiographed using the two views (A-P view and sacral base view) with the objective of finding a significant difference in the measured sacral obliquity between the two views of the same sacrum.

Dry bones specimens were used because they represent the morphology of the sacrum on a radiographic image. While they don't contain soft tissue components they appear on a radiographic image in a very similar way to actual spinal structures with similar reference points. As the study was not meant to provide information on the validity and reliability of measurement of sacral obliquity but rather to identify systematic errors related to the measurement of dihedral angles, dry bone specimens fulfilled this role.

Random errors can generally be detected as a fluctuation by repeated measurement of sacral obliquity on the either views. To help differentiate outliers and major random errors from systematic errors all measurements were done three times. For this study the degree of error was not important. Due to the lack of reliable studies there was no way of knowing the distribution of sacral obliquity in a given data set or which of the two views generated a systematic error in any one of the 16 sacrum.

### 3.1.1 Dry Bone Sacral Specimens

A convenience sample of sixteen dry sacral bone specimens was selected from an osteological collection available to the Department Chiropractic at Macquarie University. No specific history or information was available relating to any of the specimens, such as age, gender or genetic background. Thirteen specimens in the study consisted of only the sacrum without either the coccyx or innominate bones.

The angle representing sacral obliquity was measured on films taken with the sacrum in a fixed position relative to the image plane and with the x-ray tube positioned so that the central ray was either perpendicular to the cassette or angled relative to the individual sacral base of each sacrum. The source image distance (SID) and exposure factors remained the same for both views.

The sixteen sacrums were positioned and radiographed in one of two orientations to the horizontal primary rays to represent a sacral base view with the central ray aligned to the sacral base for one view and as a standard A-P view of the pelvis for the other. Four of the sacrums were photographed in the two positions to illustrate normal anatomical features (sacrum 3) and anatomical or structural variations (sacrums 1, 2, 16).

Sacrum 1 (with right ilium attached) photographed as SBV and AP view (Figure 62)

Sacrum 1 (with ilium attached) plain film radiographs of SBV and AP view (Figure 63)

Sacrum 2 (with left ilium attached) photographed as SBV and AP view (Figure 64)

Sacrum 2 (with ilium attached) plain film radiographs of SBV and AP view (Figure 65)

Sacrum 3 (normal sacrum) photographed as SBV and AP view (Figure 66)

Sacrum 3 plain film radiographs of SBV and AP view (Figure 67)

Sacrum 4 plain film radiographs of SBV and AP view (Figure 68)

Sacrum 5 plain film radiographs of SBV and AP view (Figure 69)

Sacrum 6 plain film radiographs of SBV and AP view (Figure 70)

Sacrum 7 plain film radiographs of SBV and AP view (Figure 71)

Sacrum 8 plain film radiographs of SBV and AP view (Figure 72)

Sacrum 9 plain film radiographs of SBV and AP view (Figure 73)

Sacrum 10 plain film radiographs of SBV and AP view (Figure 74)

Sacrum 11 plain film radiographs of SBV and AP view (Figure 75)

Sacrum 12 plain film radiographs of SBV and AP view (Figure 76)

Sacrum 13 plain film radiographs of SBV and AP view (Figure 77)

Sacrum 14 plain film radiographs of SBV and AP view (Figure 78)

Sacrum 15 plain film radiographs of SBV and AP view (Figure 79)

Sacrum 16 photographed (with transitional segment) as SBV and AP view (Figure 80)

Sacrum 16 plain film radiographs of SBV and AP view (Figure 81).

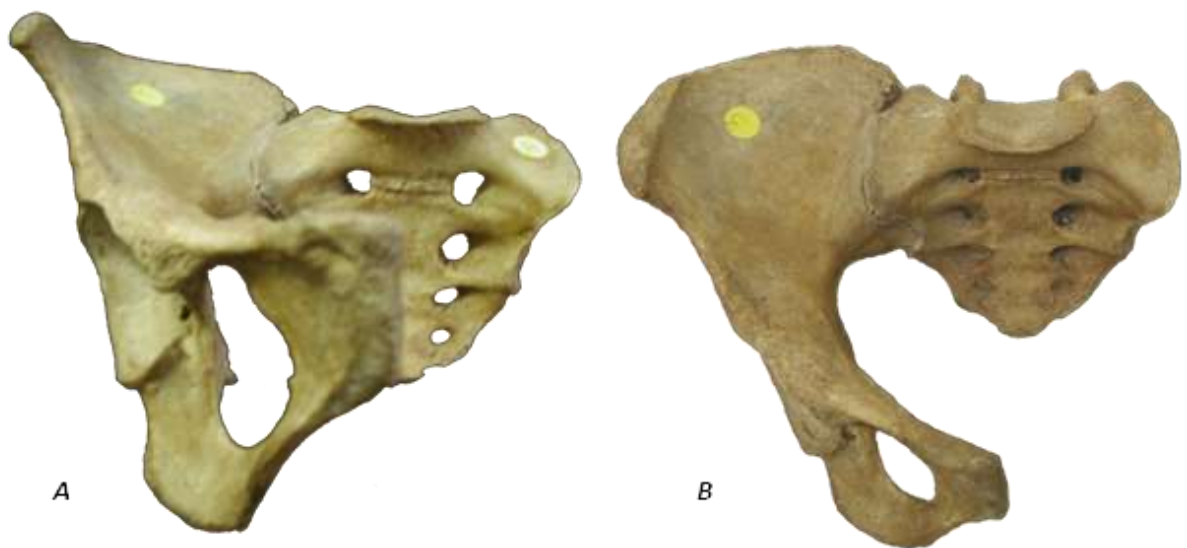


Figure 62. Sacrum 1 photographed in (A) sacral base view and (B) A-P view





Figure 63. Plain film radiographs of sacrum 1 (A) sacral base view (B) A-P view



Figure 64. Sacrum 2 photographed in the position for (A) the sacral base view and (B) A-P view



Figure 65. Plain film radiographs of sacrum 2 (A) sacral base view (B) A-P view

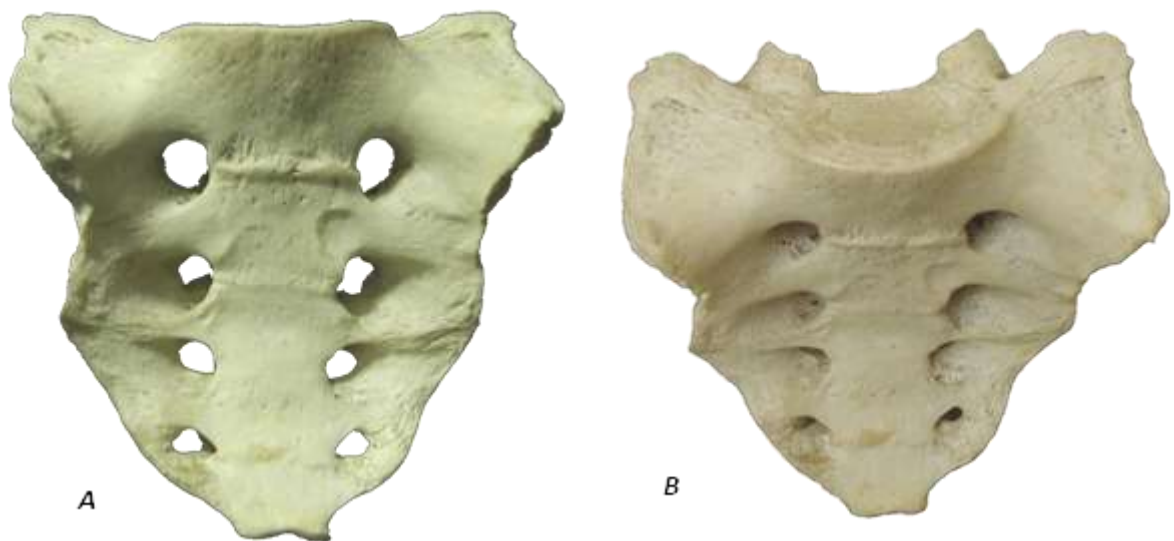


Figure 66. Sacrum 3 photographed in the position for (A) the sacral base view and (B) the A-P view

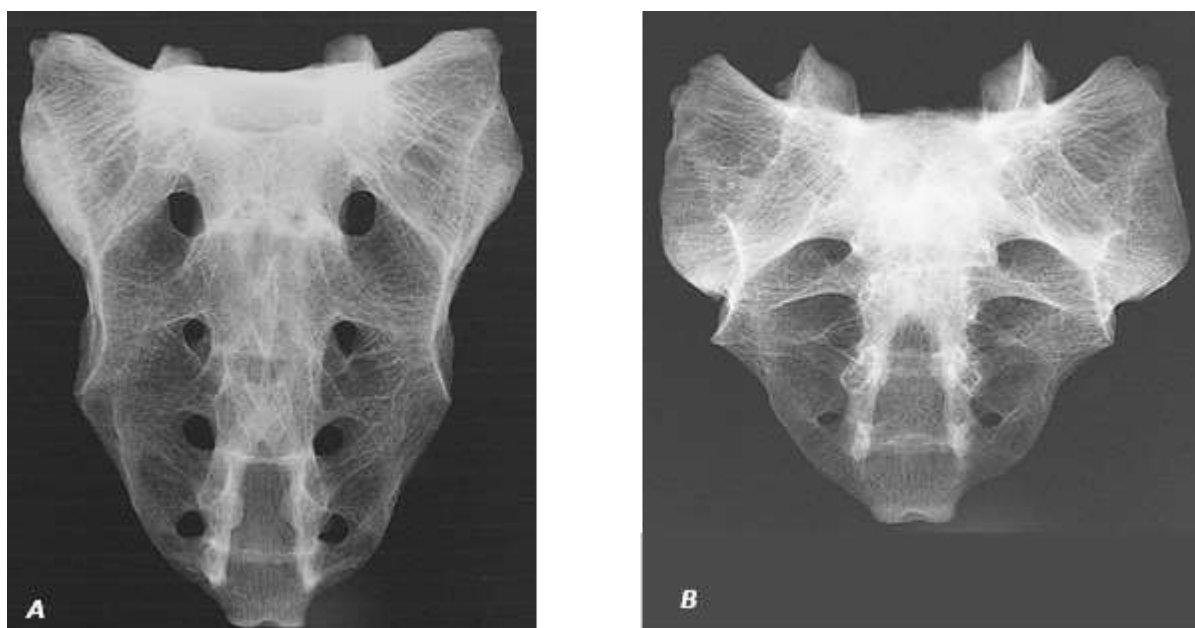


Figure 67. Plain film radiographs of sacrum 3 (A) sacral base view (B) A-P view

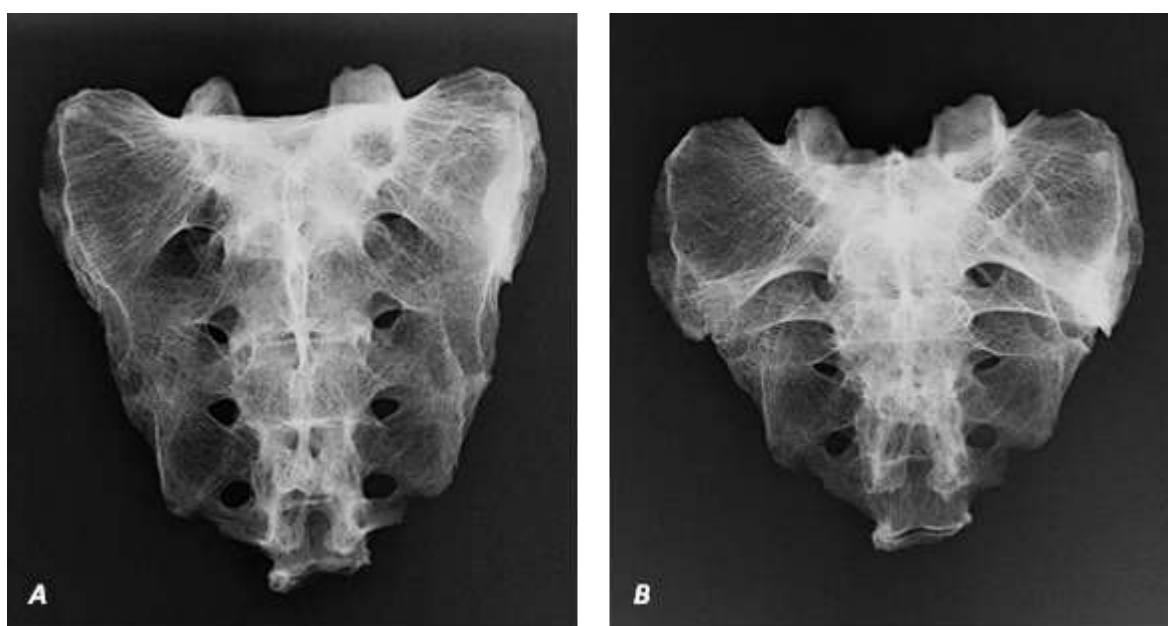


Figure 68. Plain film radiographs of sacrum 4 (A) sacral base view (B) A-P view

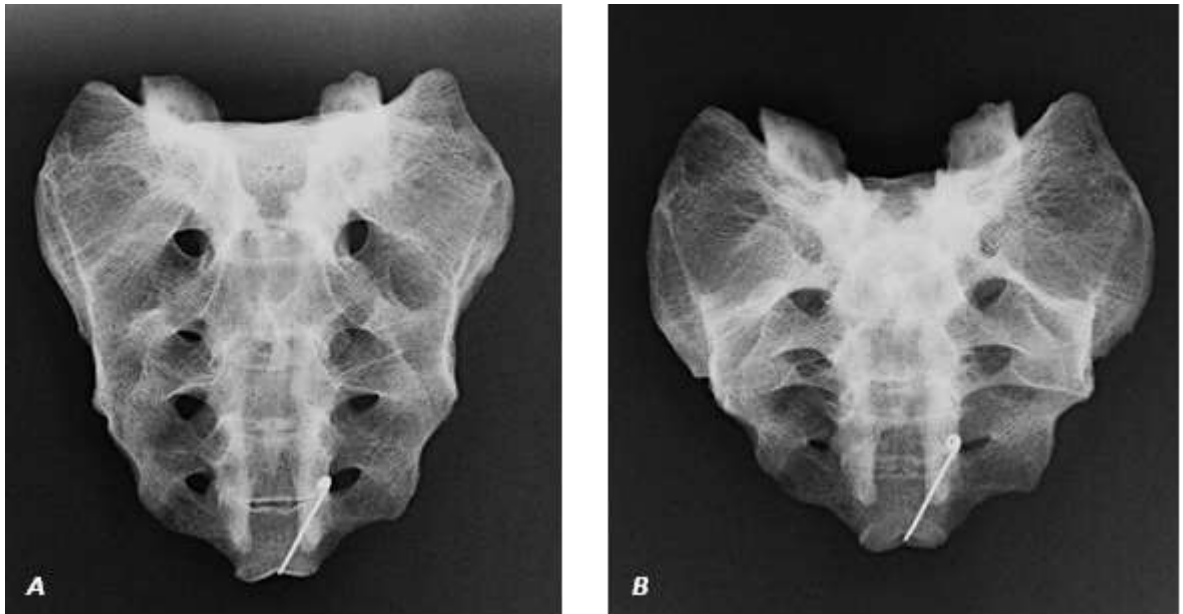


Figure 69. Plain film radiographs of sacrum 5 (A) sacral base view (B) A-P view



Figure 70. Plain film radiographs of sacrum 6 (A) sacral base view (B) A-P view

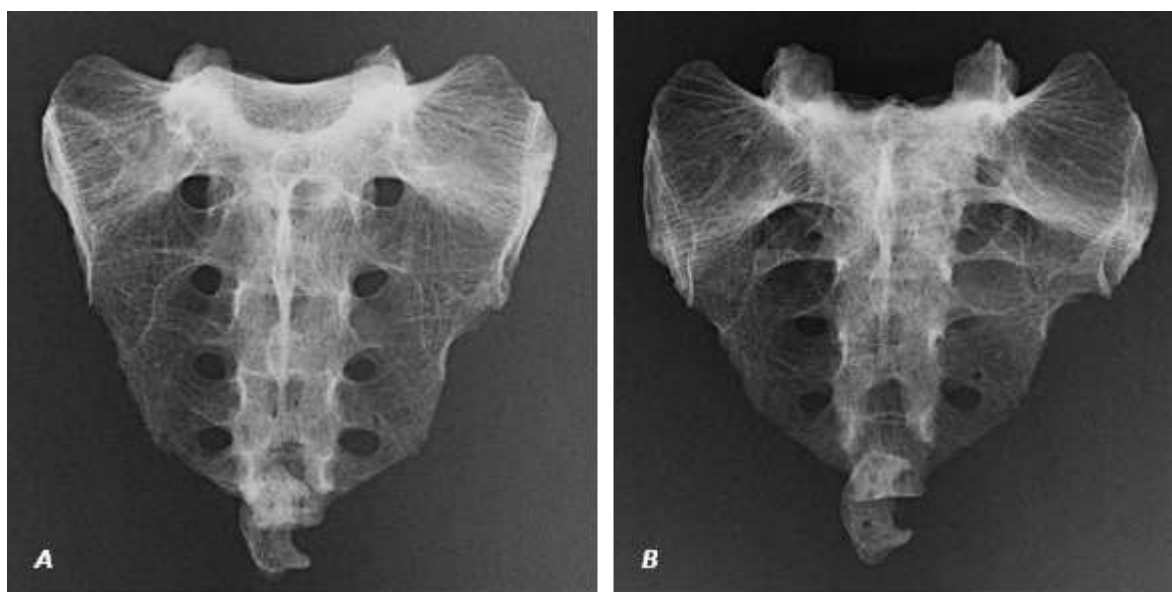


Figure 71. Plain film radiographs of sacrum 7 (A) sacral base view (B) A-P view

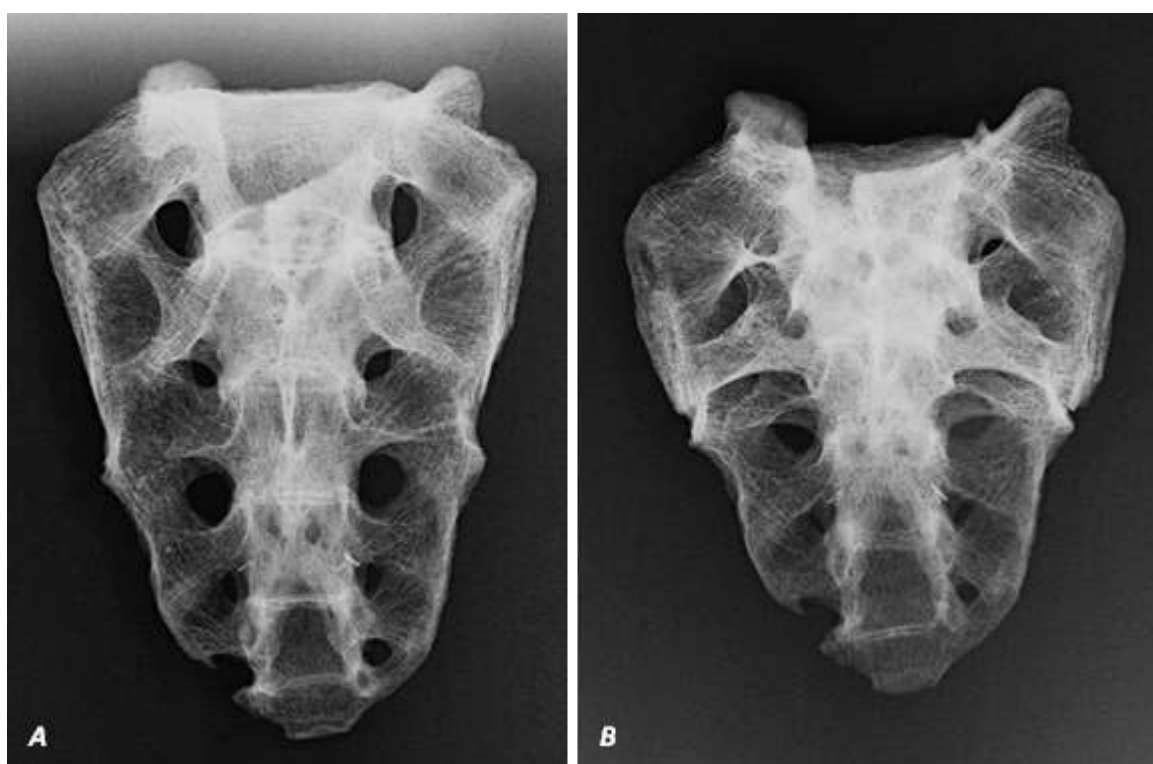


Figure 72. Plain film radiographs of sacrum 8 (A) sacral base view (B) A-P view



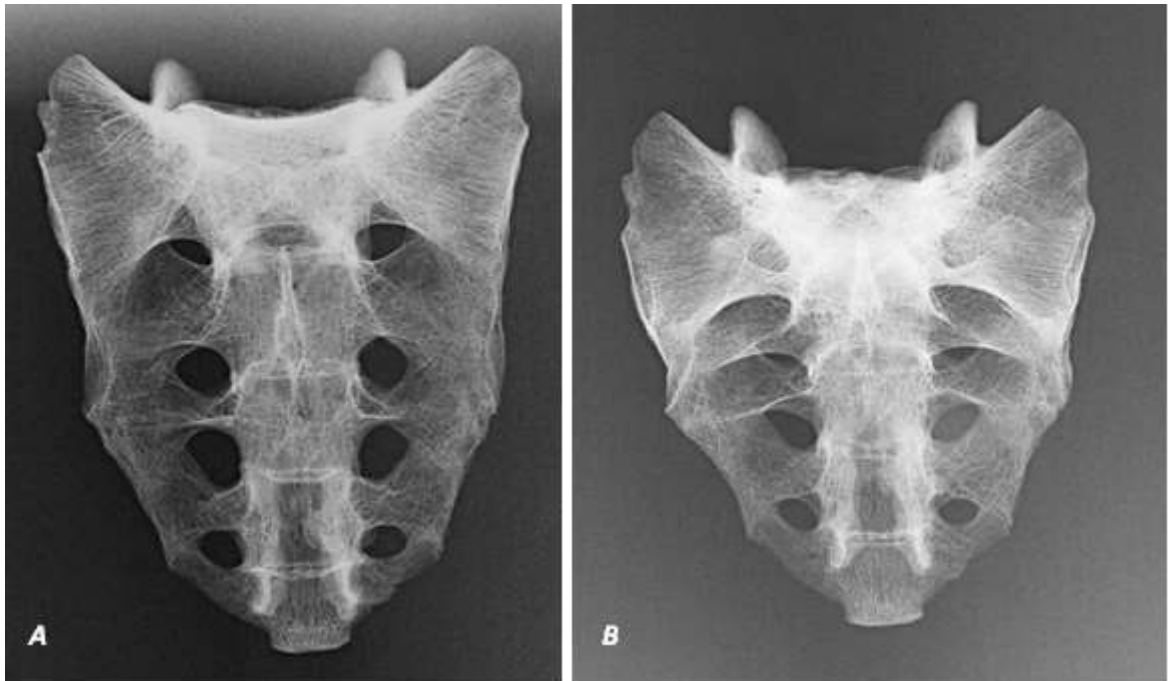


Figure 73. Plain film radiographs of sacrum 9 (A) sacral base view (B) A-P view

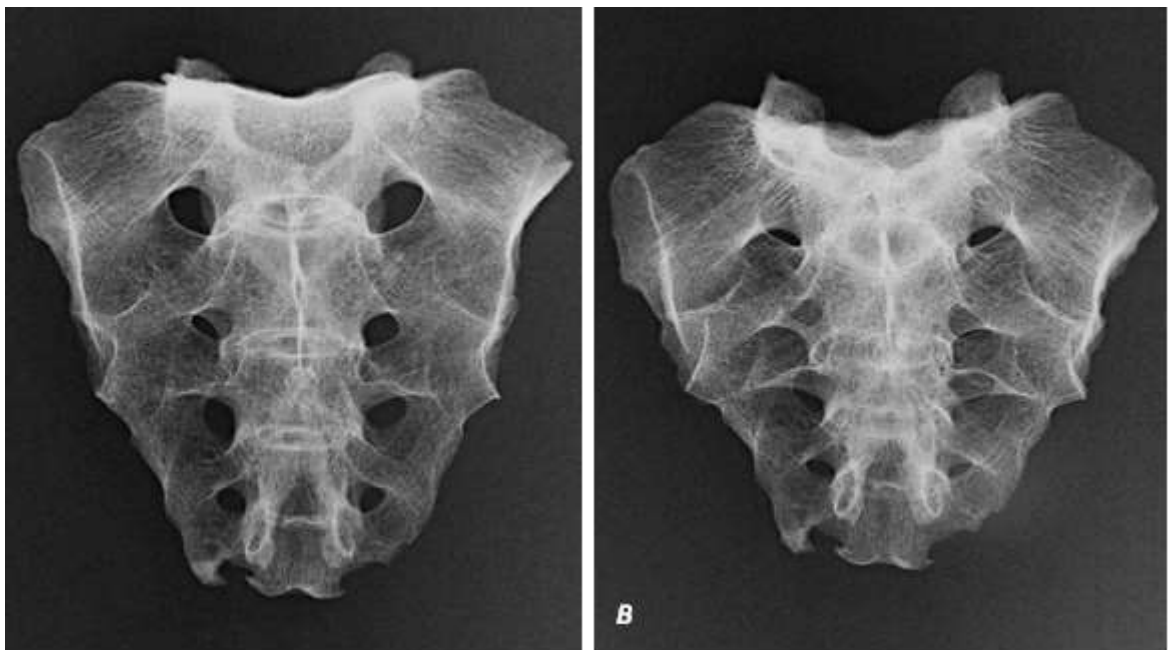


Figure 74. Plain film radiographs of sacrum 10 (A) sacral base view (B) A-P view

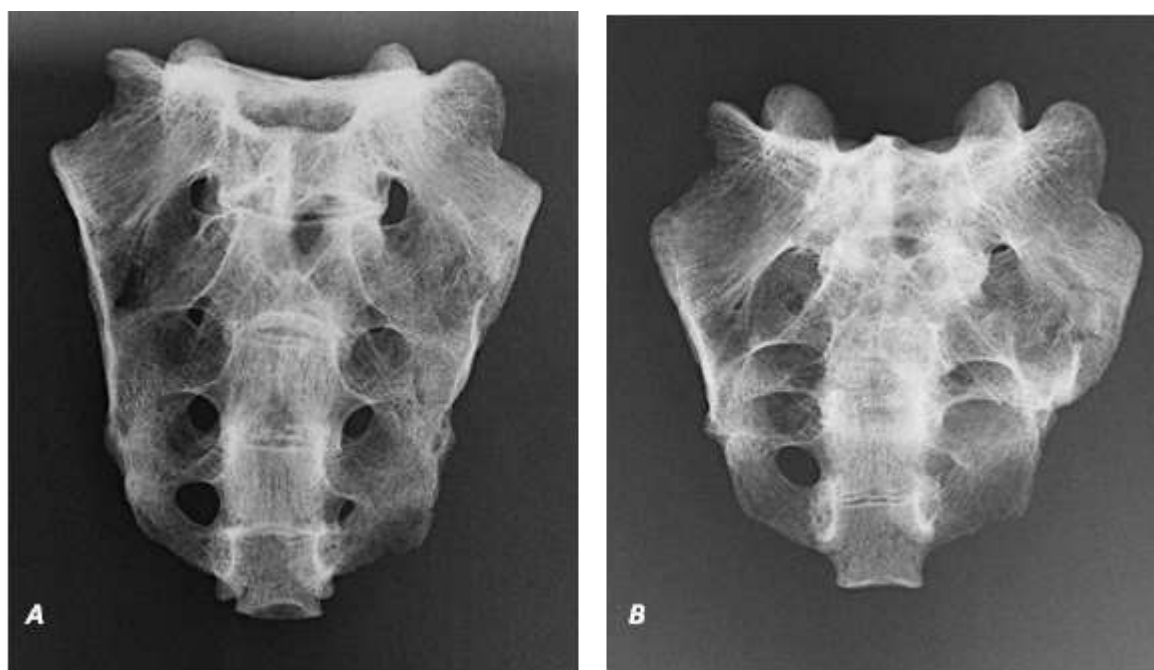


Figure 75. Plain film radiographs of sacrum 11 (A) sacral base view (B) A-P view



Figure 76. Plain film radiographs of sacrum 12 (A) sacral base view (B) A-P view

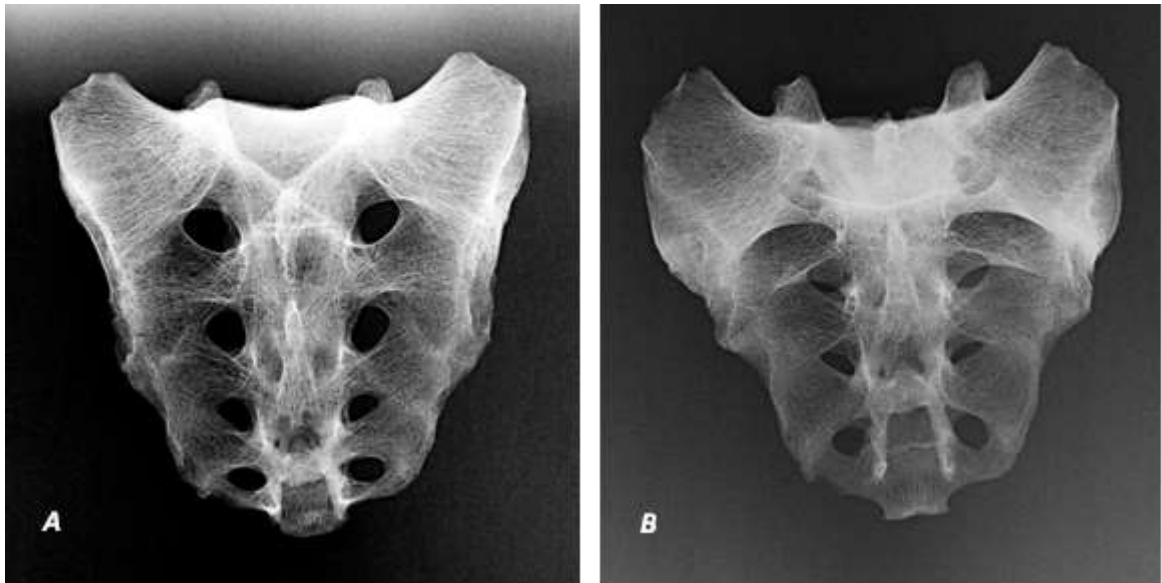


Figure 77. Plain film radiographs of sacrum 13 (A) sacral base view (B) A-P view

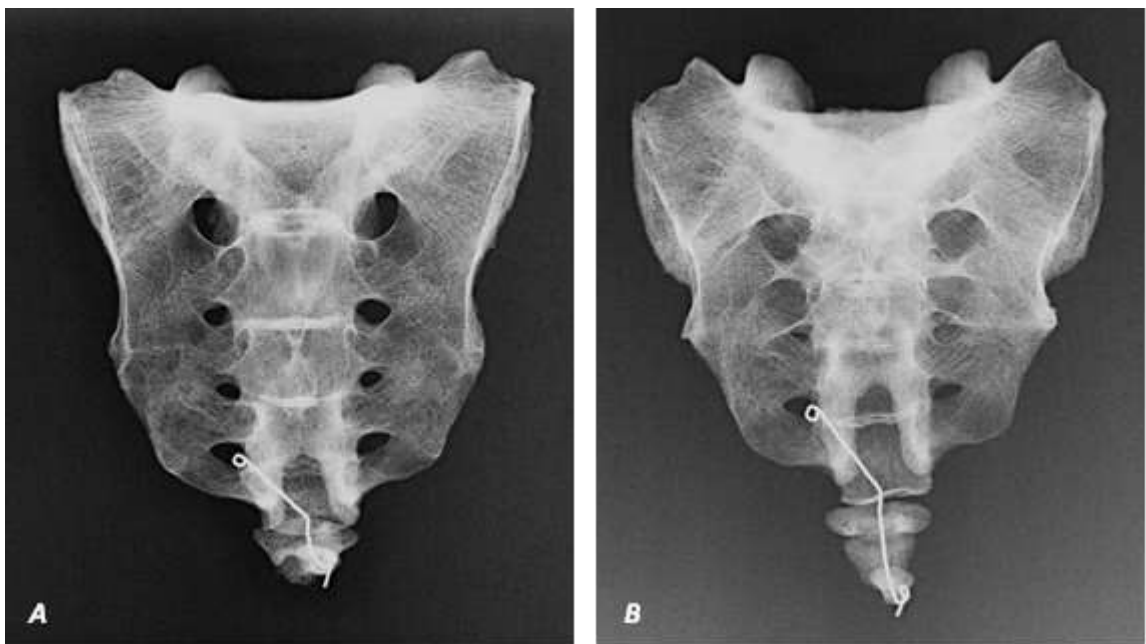


Figure 78. Plain film radiographs of sacrum 14 (A) sacral base view (B) A-P view



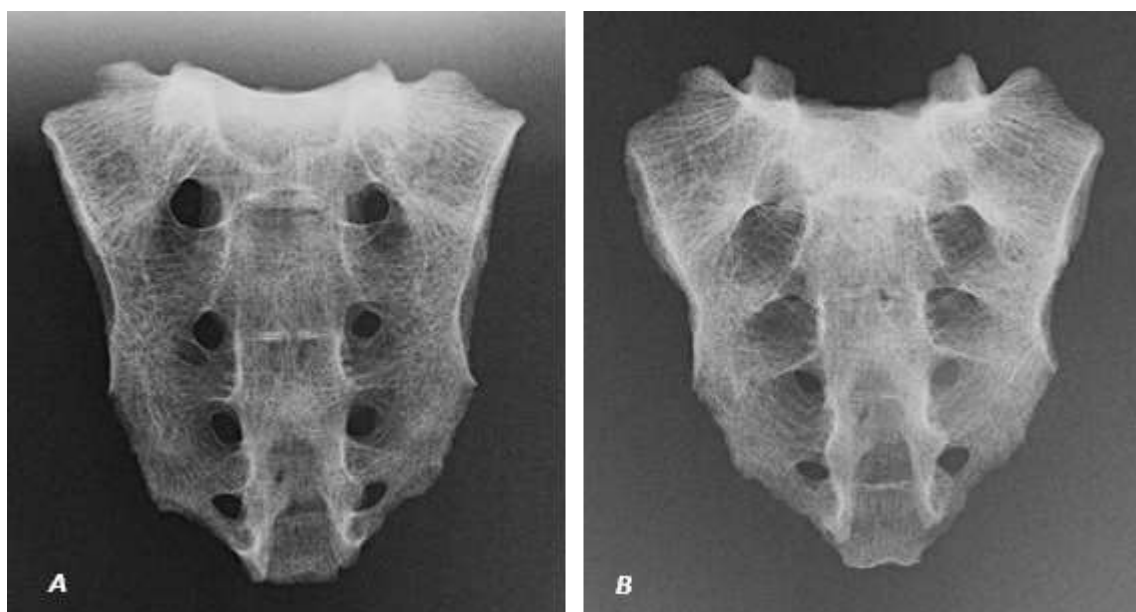


Figure 79. Plain film radiographs of sacrum 15 (A) sacral base view (B) A-P view

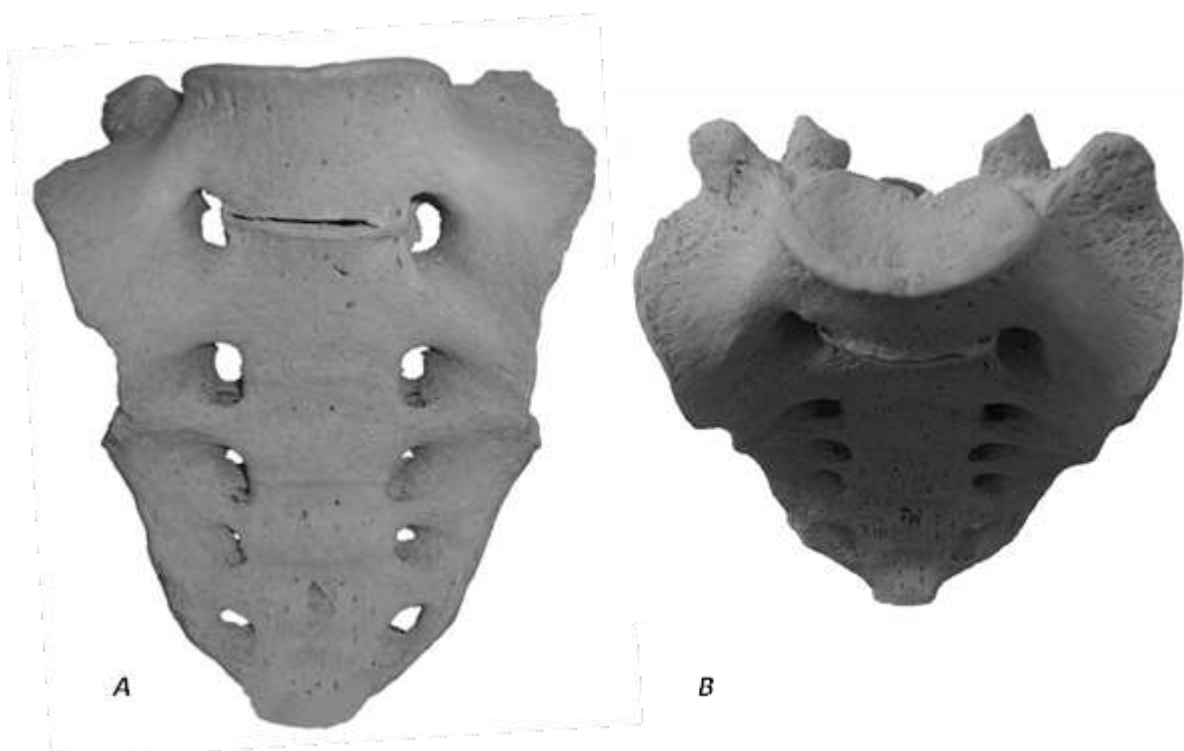


Figure 80. Sacrum 16 photographed in the position for (A) the sacral base view and (B) the A-P view

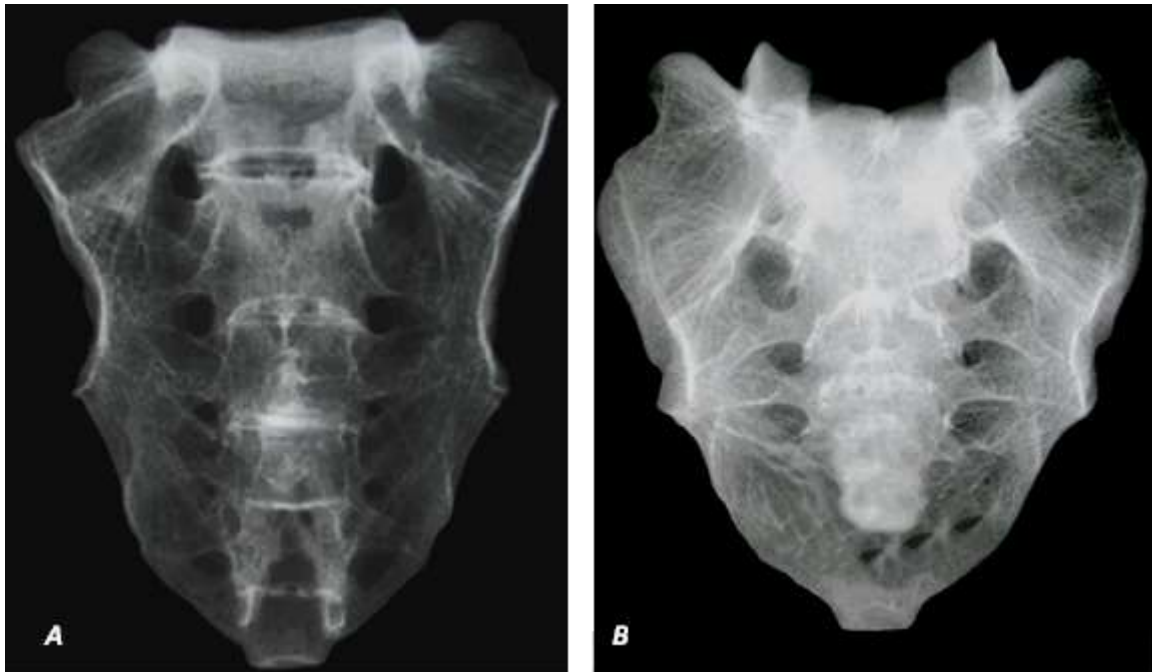


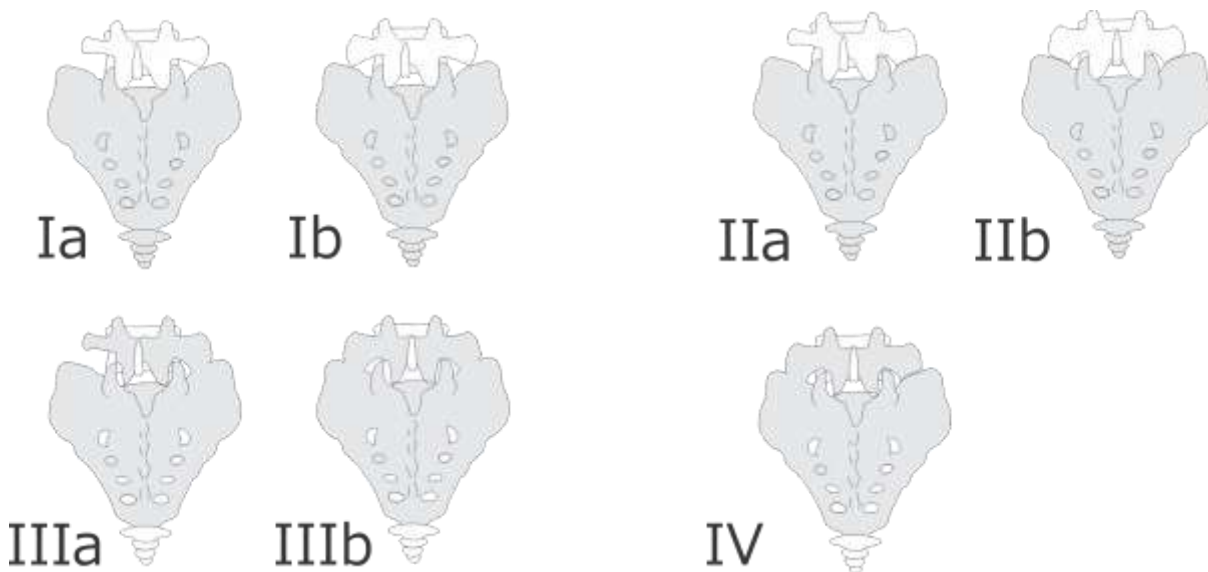
Figure 81. Plain film radiographs of sacrum 16 (A) sacral base view (B) A-P view

### 3.1.2 General morphology of the sacral specimens

Two of the sixteen sacral specimens, sacrum 1 (Figure 62) and sacrum 2 (Figure 64) used in this study had a fused sacroiliac joint obliterating the joint and locking the sacrum to the involved ilia. This condition is seen more frequently after the fifth decade in both sexes but more frequently in males (152). Even though an ankylosed sacroiliac joint could influence absolute sacral obliquity on an erect radiograph of the lumbosacral spine this was not a consideration when comparing the two views. The ankylosis of the sacroiliac joint had no direct influence on the projection or measurement of absolute sacral obliquity as measured on the two images of the sacrum as the sacrum remained in an arbitrary and fixed position for the two views.

Two specimens in the study group, sacrum 8 (Figure 72) and sacrum 16 (Figure 80), had what could be classified, or described as, a sacralised lumbar segment. This created atypical sacral bones with six fused sacral segments. In both cases the transitional lumbosacral segment resulted in a complete sacralisation of what would have been the fifth

lumbar vertebra resulting in a specimen made up of six fused segments. This type of transitional lumbosacral segment is described by Kricun (147, 301) as a type IIIB sacralisation (Figure 82). Hahn *et al* (340) found a prevalence of fifteen sacralised lumbar segments in two hundred patients (7.5%) using magnetic resonance imaging and quote a reported prevalence of 3% to 21% in the reviewed literature.



**Figure 82. Types of transitional lumbosacral segments involve four morphological characteristics. Type I involves unilateral (Ia) or bilateral (Ib) dysplastic transverse processes. Type II involves incomplete unilateral (IIa) or bilateral (IIb) lumbarisation or sacralisation. Type III involves complete osseous fusion of the transverse process. Type IV involves unilateral type II transition with a type III on the contralateral side**

The atypical specimens were included in the study even though Hsieh *et al* (341) suggest the prevalence of sacralisation of the fifth lumbar segment is generally low in chiropractic patients. However, they found that this type of anomaly is likely to be encountered by chiropractors taking routine radiographs of the lumbopelvic spine with one health centre studied reporting 6.5% of 786 patients having transitional lumbosacral segments. Delport *et al* (146) found that the percentage of patients with a transitional lumbosacral segment was higher than the percentage found in the general population. In their prospective observational study of three hundred consecutive patients with lower back pain, 30% had a transitional vertebra. They suggest that this high percentage may be due to the alteration in mechanics caused by a transitional vertebra contributing to pain generation. Asymmetrical

sacralisation could contribute to angulation of the sacral base in the frontal plane and asymmetry of the sacral alae.

While two of the specimens contained a transitional lumbosacral segment and were therefore atypical sacrum, this number as a percentage of the total number was within that found in a clinical setting. In cases of a transitional lumbopelvic segment the superior surface of what would have been the 5<sup>th</sup> lumbar vertebra is often considered the functional sacral base with these variations often associated with dimensional changes and morphological proportion of the sacrum (342).

Asymmetrical shape or dimensions of the sacrum as described by Plochocki (39), particularly those involving the ala and sacral base, would have an effect on the projected image of that structure on radiographic images. The selection of reference points is often determined by their visibility and distinctness on the resulting image rather than their fidelity in quantifying the relationship or orientation of the structure being measured (14, 189). As an example, points on the sacral ala are often used to reference the obliquity of the sacral base on A-P radiographic images (13, 14).

Some of the sixteen specimens exhibited structural asymmetry that had the potential to influence the validity of reference points used or suggested as a method to quantify sacral obliquity. The asymmetry had the appearance on the radiographs of congenital variations and adaptive changes that would be consistent with spinal changes that have been described as '*degenerative*' changes and structural anomalies (343). The non-congenital structural characteristics were consistent with calcification of soft tissues of the sacroiliac joints and osteophytic lipping of the sacral base. Visual inspection of the dry bone specimens and radiographic images showed evidence of structural asymmetry due to soft tissue changes affecting the sacral base and the sacral ala on particular specimens such as sacrum 2 and sacrum 10.

### 3.2 RADIOGRAPHIC SETUP FOR PLAIN FILM IMAGING

Triangular foam blocks were used as positioning wedges to place each specimen in front of the cassette holder to simulate the approximate position and orientation of the sacrum in erect posture. Each sacrum was centred horizontally to the mid-line of the film with rotation and tilt within tolerances that would generally be considered acceptable or normal on a plain film radiograph of the region (244, 245) (Figure 83).

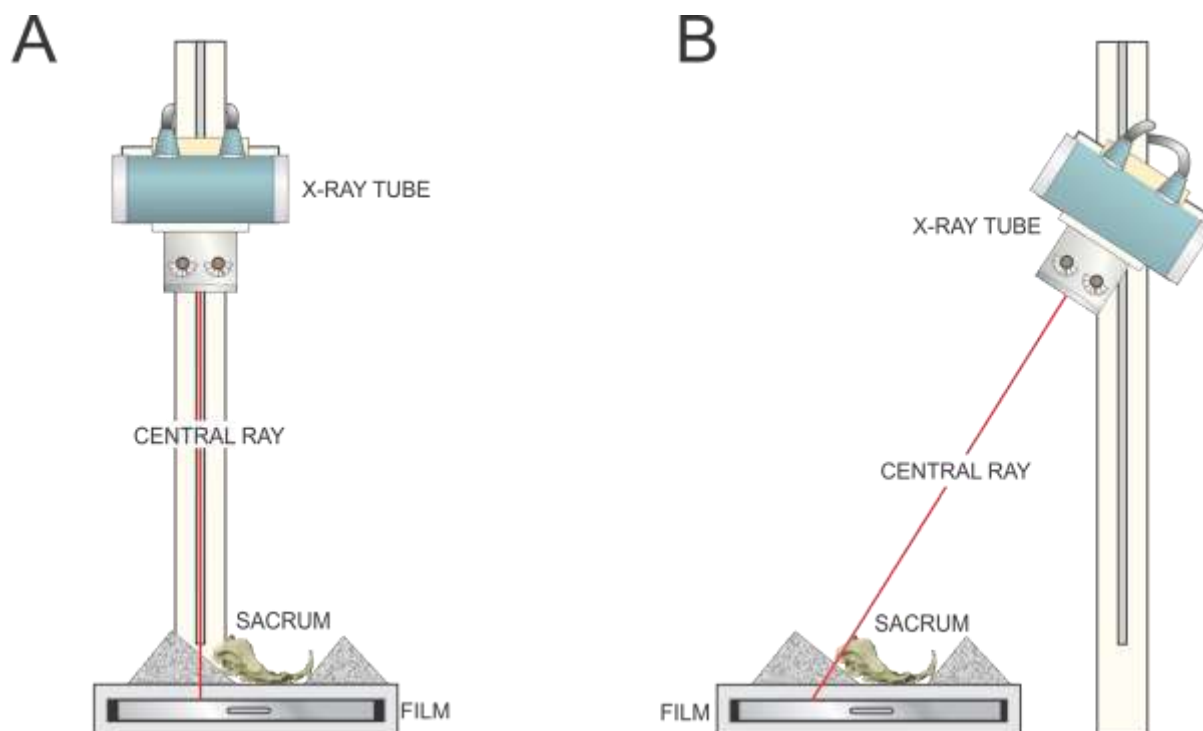
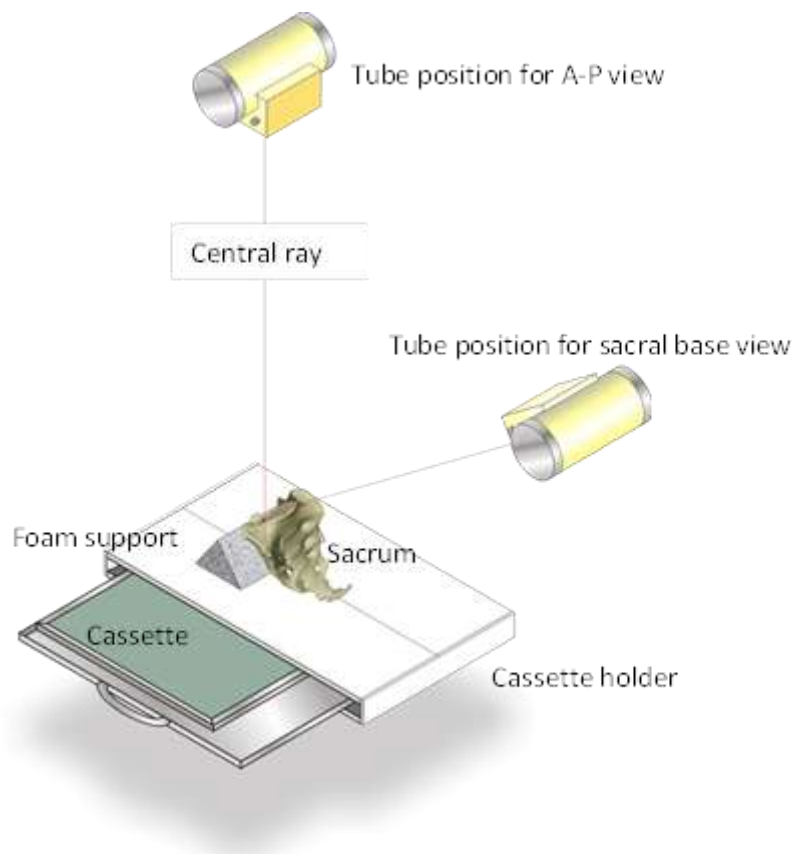


Figure 83. The x-ray tube was aligned and perpendicular to the cassette (A). X-ray tube angle relative to sacrum and cassette for the sacral base view (B)

The mid-sagittal plane of the sacral base was aligned to the vertical centre of the cassette containing the radiographic film. The crests of the ilia were considered to be approximately six centimetres above the sacral base for those specimens that only consisted of the sacral bone and no ilia. For the standard A-P view, the x-ray tube was aligned, and perpendicular to the crests of the ilia or aligned with a point six centimetres above the sacral base for the specimens that only consisted of the sacral bone (Figure 83) (A). A second exposure was made with the x-ray tube angled along the lumbosacral angle (Ferguson's base angle) and aligned with the upper surface of the sacral plateau (Figure 83) (B). This view has been

recommended by a number of clinicians as providing a superior visualisation of the sacral base (27, 41, 78, 188, 266, 284). The position of the specimen and cassette holder remained unchanged for the second exposure (Figure 84).



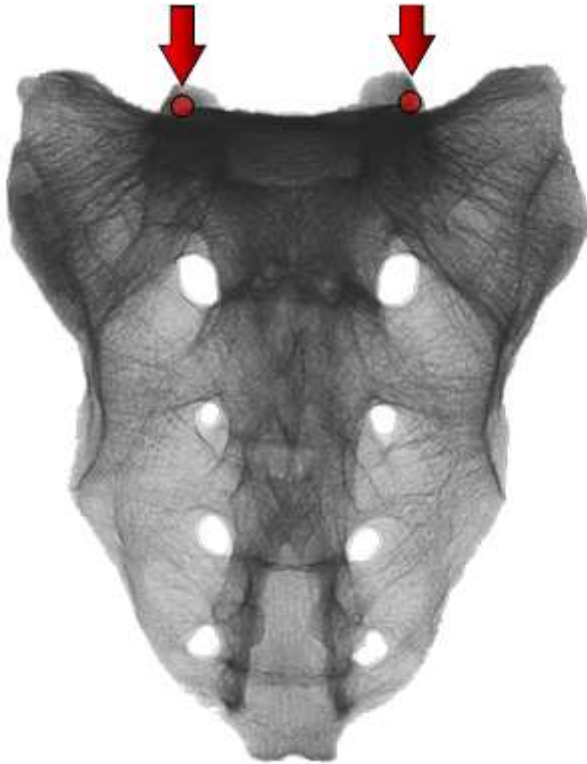
**Figure 84.** The relationship of the x-ray tube to the sacral base and cassette for the two views compared in the study

The source to image (film) distance (SID) was one hundred centimetres (forty inches) for each exposure. The exposure was made on a Sedecal – SHF310 North American Imaging x-ray machine with exposure factors of 40 kvp at 0.5 mas, using a fine focal spot. The image was recorded on a digital cassette and downloaded to a Toshiba workstation employing Fujifilm FCR V.2 imaging software. Using this software, the exposure factors were corrected and optimised for viewing bony structures such as the sacrum. The images were then sent via a local area network to a remote computer where they were saved in the Joint Photographic Experts Group (jpeg) standard format with minimal compression. This

format retained the aspect ratio (width divided by height) of the image but neither absolute size nor true linear dimensions.

### **3.3 PLAIN FILM RADIOGRAPHIC ANALYSIS**

The *jpeg* format allowed reliable angular but not linear measurements to be made. As the *jpeg* format preserves the aspect ratio of the image all angles measured were congruent with the angles on the original image to a degree equal to the tolerance interval of the measurement. The digital radiographic analysis software was used to measure the angles representing absolute sacral obliquity on the images. The two sets of images were read in random order on three separate occasions over a three month period. The standard view films were read as a group as were the sacral base views. This was done to minimise familiarisation or recall of specific features or details relating to the individual images. Absolute sacral obliquity was measured on the sixteen sacral base views (SBV) using a line constructed by locating the superolateral borders of the sacral plateau as described by Harrison (239), Barge (78) and Pettibon (284)(Figure 85).

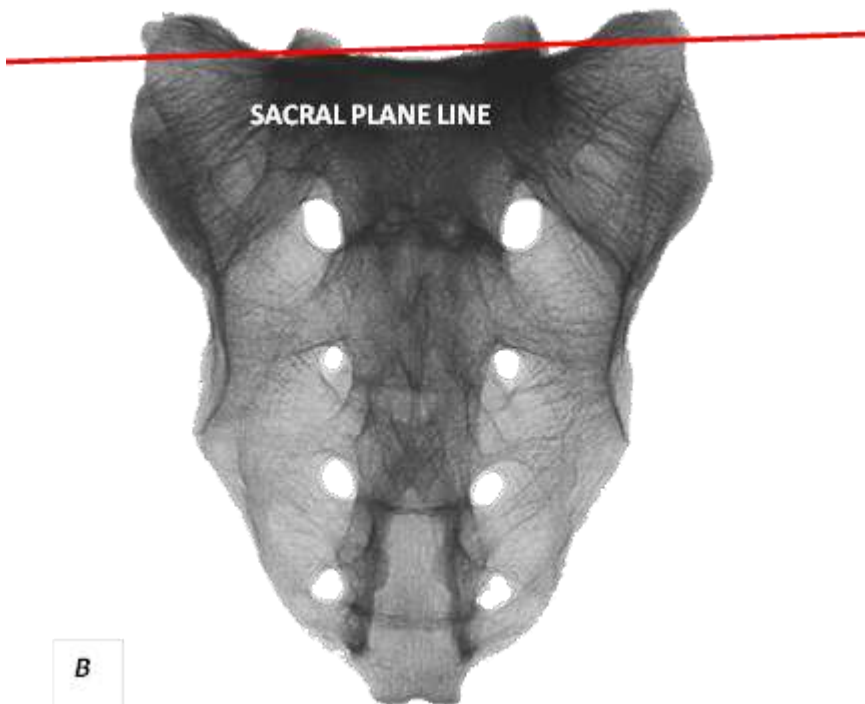


**Figure 85. Points (red dots) identified on a lumbopelvic radiograph as representing the superiolateral borders of the sacral base**

A computer generated line was constructed to pass through these points (Figure 86).

Harrison (266) refers to this line as the sacral plane line (SPL). For convenience this name was adopted for the present study.





**Figure 86. A line referred to as the sacral base line was constructed on radiographic image of the sacral base through points representing the superiolateral borders of the sacral base**

The inclination of the line was measured to three decimal places as a deviation angle from a line representing the horizontal plane. The angle was designated as positive if angled down on the right (+Z-axis rotation), negative if angled down on the left (-Z-axis rotation) and zero if horizontal. This angle was designated the sacral base angle (SBA) (Figure 87).

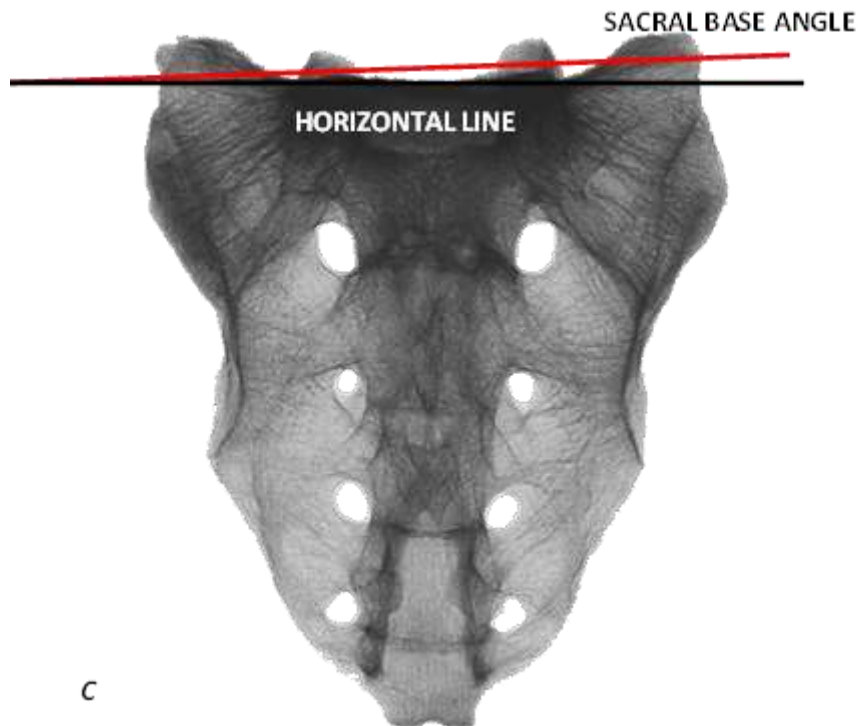


Figure 87. The angle between the sacral base line and the horizontal plane is referred to as the sacral base angle

On the standard view, because the lateral margins of the sacral plateau are neither generally visible nor easily defined, a line was drawn between points representing the junction of the sacral ala and the articular pillars on either side (Figure 88).

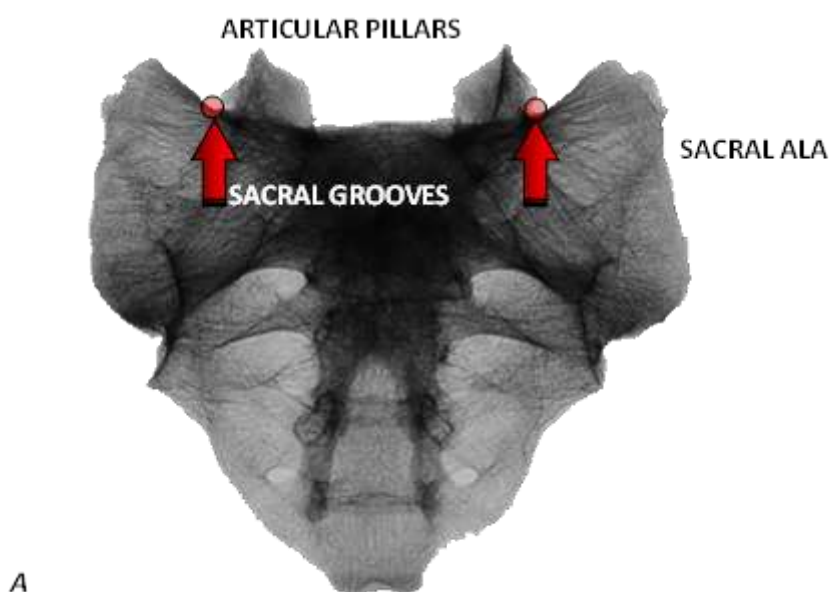


Figure 88. Points were placed on the A-P film to represent the 'sacral grooves' formed at the point where the sacral ala overshadow the respective articular processes

Gonstead (13) refers to these points as the 'sacral grooves' and the line as the 'horizontal plane line of the sacrum' (HPL). In their study investigating the reliability of measuring sacral obliquity on radiographs, Fann *et al* (14) refer to a line constructed using similar points as an 'intersulcate line'. This line was based on points previously described by Tilley (189) (Figure 89).

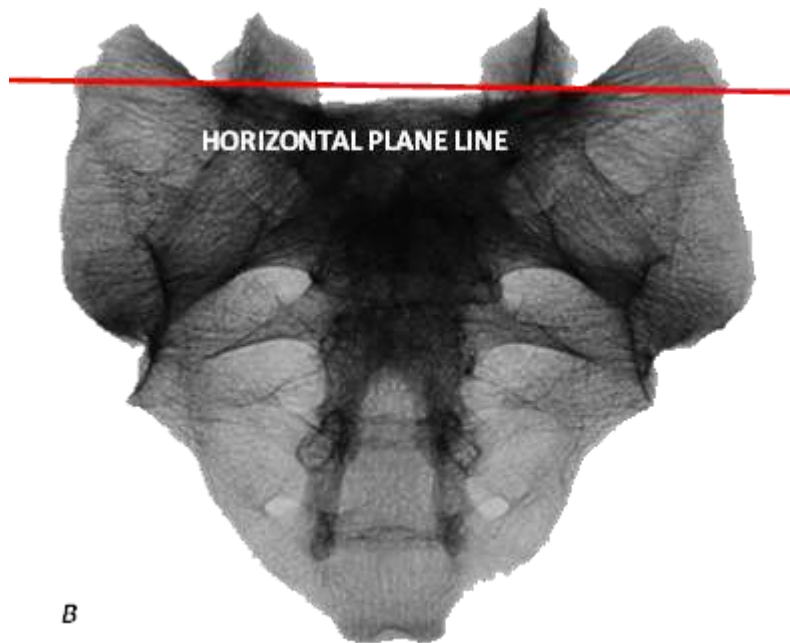


Figure 89. A line was drawn connecting the points representing the sacral grooves and is referred to as the horizontal plane line

The inclination of the line was measured to three decimal places as a deviation angle from a line representing the horizontal plane. The angle was designated in the same manner as the sacral base angle as positive if angled down on the right (+Z axis rotation), negative if angled down on the left (-Z axis rotation) and zero if horizontal. For this study, the angle was referred to as the A-P angle (Figure 90).

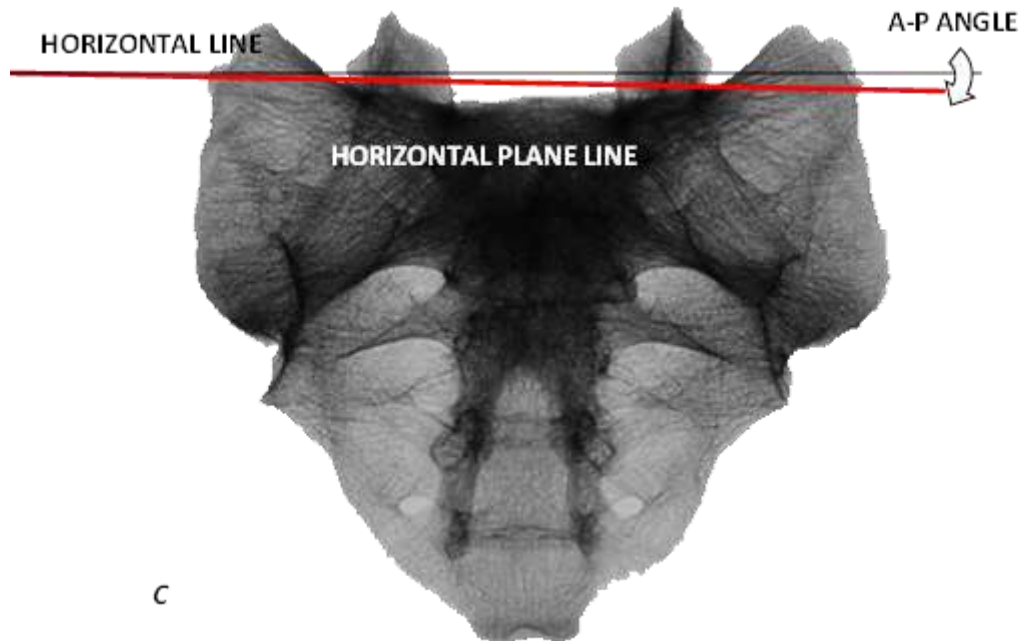


Figure 90. The angle between the horizontal plane line and a line representing the horizontal plane is referred to as the A-P angle

The angulation between the lines used in this study were measured and recorded in the same manner as for the sacral base view. As with the sacral base view, the line drawing, measuring and recording of angles for each film was carried out in randomised order on three separate occasions over a three month period to minimise familiarity with individual images. The result was ninety six sets of angular measurements representing three readings on both views for each of the sixteen specimens.

Because the sacral plateau is projected as an oval and not well visualised on most standard A-P lumbopelvic radiographs (29, 78, 266) the horizontal plane line (HPL) and the sacral plane line (SPL) line could not be constructed using the same methods and points for both films. The reference points and line drawing were therefore the ones applicable and commonly used for the specific view being analysed.

Statistical analysis of the data was performed to investigate the random measuring error involved in the study. Intra-observer reliability was calculated using appropriate statistical methods. The objective was to investigate whether there was any significant difference

between the sacral base angle (SBA) representing the degree of absolute sacral obliquity measured on the sacral base view (SBV) and A-P angle (APA) measured on the A-P view (APV) for any individual sacrum.

### **3.4 RESULTS**

The results of the measurement of sacral obliquity, repeated three times on two different views of each of the sixteen sacral specimens were recorded (Table 1). This resulted in three measurements for each image and six measurements for the two views of each sacrum with a total of 96 measurements for all sixteen sacral specimens.

Table 1. Repeated measurement of sacral obliquity on A-P and Sacral Base views of 16 dry bone sacral specimens

SACRUM	READING	SBA	APA
SACRUM 1	1st	3.0	1.7
	2nd	3.0	1.9
	3rd	3.0	1.6
SACRUM 2	1st	-12.4	1.4
	2nd	-12.5	1.6
	3rd	-12.5	1.5
SACRUM 3	1st	0.9	-0.4
	2nd	0.9	-0.4
	3rd	0.9	-0.6
SACRUM 4	1st	4.8	4.3
	2nd	4.9	3.8
	3rd	4.8	4.0
SACRUM 5	1st	4.4	1.5
	2nd	4.2	1.1
	3rd	4.4	1.5
SACRUM 6	1st	1.8	0.7
	2nd	1.5	0.2
	3rd	1.5	0.0
SACRUM 7	1st	0.3	0.7
	2nd	0.3	0.4
	3rd	0.3	0.6
SACRUM 8	1st	2.3	2.0
	2nd	2.3	1.3
	3rd	2.3	1.6
SACRUM 9	1st	1.2	1.8
	2nd	1.2	2.2
	3rd	1.2	2.1
SACRUM 10	1st	1.9	1.1
	2nd	1.9	0.9
	3rd	1.9	1.1
SACRUM 11	1st	-3.8	-0.2
	2nd	-3.6	-1.0
	3rd	-3.5	-1.2
SACRUM 12	1st	1.6	0.9
	2nd	1.6	0.9
	3rd	1.8	0.7
SACRUM 13	1st	0.5	4.3
	2nd	0.8	4.2
	3rd	0.8	4.2
SACRUM 14	1st	2.8	0.3
	2nd	2.8	0.3
	3rd	2.8	0.3
SACRUM 15	1st	-1.4	-1.2
	2nd	-1.7	-1.0
	3rd	-1.4	-1.2
SACRUM 16	1st	2.0	-0.5
	2nd	1.4	-0.4
	3rd	1.2	-0.3

The average of three repeated measures along with the variation of the individual measurements was calculated for each sacrum to indicate the repeatability of the measurements (and as a way of excluding random error in the measurements) (Table 2).

**Table 2. Average (Ave) and variation from the average of three measurements of sacral obliquity made on two different radiographic views of sixteen dry bone sacral specimens**

SACRUM	Average	Variation of Individual Measurements from Average		
	SBA (degrees)	Measurement 1	Measurement 2	Measurement 3
1	3.0	0	0	0
2	-12.4	0	0.1	0.1
3	0.9	0	0	0
4	4.8	0	0.1	0
5	4.3	0.1	-0.1	0.1
6	1.6	0.2	-0.1	-0.1
7	0.3	0	0	0
8	2.3	0	0	0
9	1.2	0	0	0
10	1.9	0	0	0
11	-3.6	0.2	0	-0.1
12	1.6	0	0	0.2
13	0.7	-0.2	0.1	0.1
14	2.8	0	0	0
15	-1.5	-0.1	0.2	-0.1
16	1.5	0.5	-0.1	-0.3

SACRUM	APA (degrees)	Measurement 1	Measurement 2	Measurement 3
1	1.7	0	0.2	-0.1
2	1.5	-0.1	0.1	0
3	-0.5	-0.1	-0.1	0.1
4	4.0	0.3	-0.2	0
5	1.4	0.1	-0.3	0.1
6	0.3	0.4	-0.1	-0.3
7	0.6	0.1	-0.2	0
8	1.6	0.4	-0.3	0
9	2.0	-0.2	0.2	0.1
10	1.0	0.1	-0.1	0.1
11	-0.8	-0.6	0.2	0.1
12	0.8	0.1	0.1	-0.1
13	4.2	0.1	0	0
14	0.3	0	0	0
15	-1.1	0.1	-0.1	0.1
16	-0.4	0.1	0	-0.1

The angulation of the SBA and APA measurements for sacrams 2, 3, and 16 were in opposite (+ $\theta$ Z, - $\theta$ Z) directions. The measurement of obliquity on one film indicated the sacral base was low on one side while the corresponding measurement on the other film indicated the sacral base was low on the contralateral side. For these three sacrams the side of the measured sacral obliquity was reversed on the two films. For each sacrum except for three (7, 9, 13) the average SBA measurement was generally greater than the APA measurement (Figure 91).

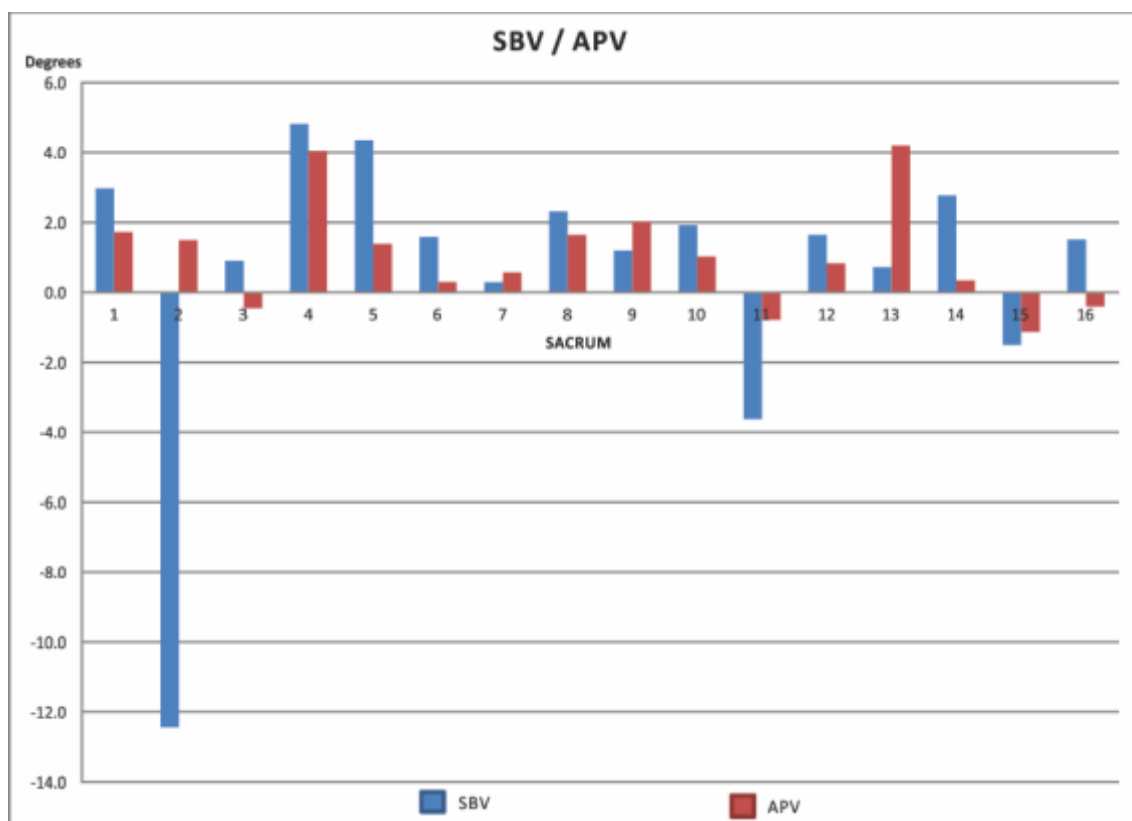


Figure 91. Average of three readings of sacral obliquity angle (SOA) on sacral base (SBV) and A-P (APV) views for each of the 16 sacra

The objective of the measurements was not to determine the incidence or magnitude of sacral obliquity in a selected sample of dry bone sacral segments. Instead, the primary objective was to identify differences in the measurements for any given specimen between the two views. A marked difference in the measurement of sacral obliquity between the two views for any one of the sacral specimens would indicate a possible systematic error



associated with the projection method, patient positioning protocols or the analytical method or a combination of these factors (Figure 92). The average difference between views for all sixteen specimens was 2.3 degrees and 1.5 degrees excluding specimen two. For sacrum two the difference between the two views was 13.9 degrees. This represents six times the average difference of the sixteen specimens. This magnitude of difference indicates that the measurement of sacral obliquity for this particular specimen was highly dependent on the radiographic view and analytical procedures used.

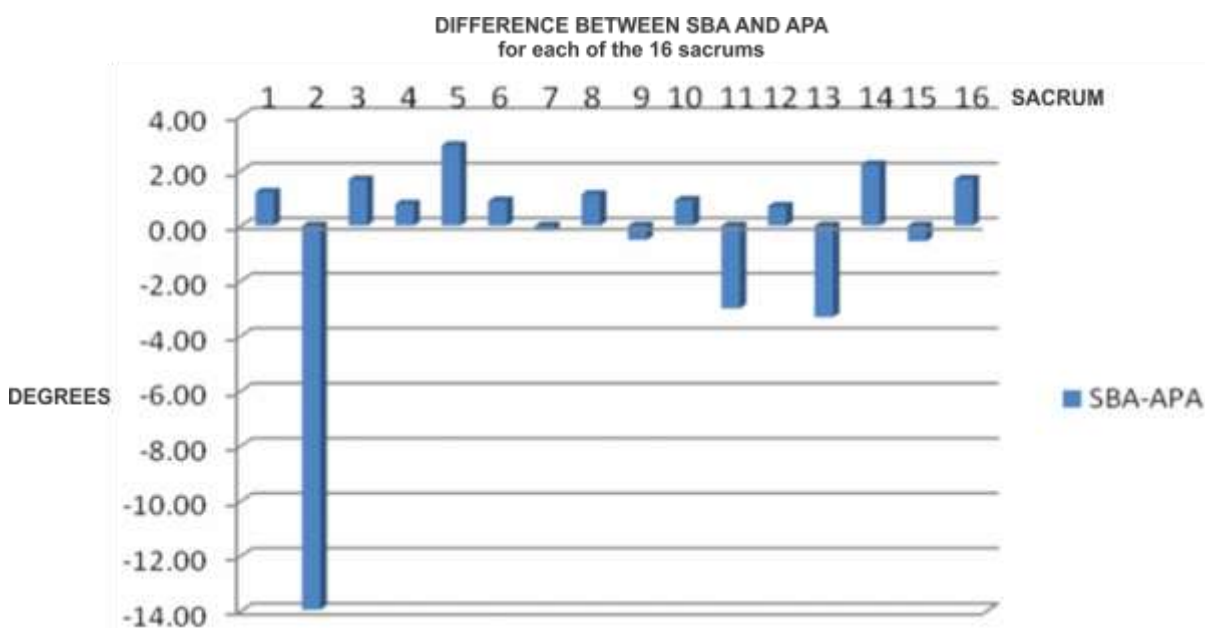


Figure 92. The difference between the sacral base angle (SBA) and the AP angle (APA) for each of the sixteen sacrums measured respectively on the two radiographic views (SBV and APV)

As each sacrum was placed only in a position with the sacral base approximately level in the frontal plane, the amount of structural sacral obliquity was not able to be measured for any of sixteen specimens. For this reason the degree of difference was the only significant measurement in relation to this study. Sacrum number two in these circumstances was considered an extreme outlier in statistical terms (344). This was calculated based on the definition of an outlier as any data point more than 1.5 interquartile ranges (IQRs) below the first quartile or above the third quartile (345). However in terms of the objective of this study this was a highly significant finding indicating that the particular view used and the

measurement protocols to quantify sacral obliquity can significantly influence the quantification of sacral obliquity indicative of systematic error.

### **3.5 SUMMARY and CONCLUSION**

The major objective of the study was to investigate the effect different x-ray tube positions, including standard (APV) and angled (SBV), and the associated line drawing methods had on the measurement of sacral obliquity as viewed on plain film radiographs and digital images. The study was designed to identify several possible outcomes relating to the validity of measurement of sacral obliquity measured on radiographic images.

There was an assumption, based on previous studies (15, 240), that measuring error would be random and would have an equal probability of being present in all measurements made. For this reason the results were not subjected to direct statistical analysis to check for, or correct, random errors in the analytical process. A previous study (240), using similar analytical and measuring techniques, had shown random measurement errors in the range of 1.1 degrees to 1.8 degrees for angles measured on A-P radiographs by different observers. Data obtained in a study by Morrissy *et al* (23) indicated that, for a careful examiner making manual measurements of scoliosis on plane films with no extrinsic (systematic) error, there is a ninety-five per cent chance that error in the measurement will be less than 3 degrees. However, Bould *et al* (257) showed that a digital image analysis system was up to twenty times more accurate than the human eye when measuring simple radiographic dimensions. They suggested that the improvement in accuracy could be due to the ability to magnify the image and manipulate the image quality factors of brightness and contrast to optimise structural definition. All measurements used in the present study were based on digital analysis of the radiographic data.

As a study outcome comparison of the radiographic protocols and associated analysis methods used could have produced a significant variation in the measurement of sacral obliquity for any individual sacrum studied.

A common source of this type of error, if it occurs, is the projection of three-dimensional structures as two-dimensional radiographic images (186, 241). One reason for this result is associated with the difficulty different observers have in the identification and selection of relevant measuring points on specific projection views for individual subjects (189).

The results were not used to confirm or demonstrate the validity of these measurements or procedures. As there was no 'gold standard' employed in the plain film dry bone study to measure absolute sacral obliquity, no method was available to determine or quantify 'true' sacral obliquity.

Agreement of measurements using the two different radiographic and analytical methods for each sacrum would have suggested that each sacrum was symmetrical and the reference points were interchangeable for measuring purposes. Even if this result had been achieved the two radiographic methods and their associated analytical procedures may have produced measurements that reflected a constant systematic error. Without a validated 'gold standard' this possibility could not, and was not tested as part of the study.

The results of the study revealed a significant variance in the angles derived from the two radiographic and analytical methods for five of the specimens and to a marked degree of variance for one sacrum in particular and was consistent for all three readings. This finding suggests that at least some of the sacral specimens studied, and one sacrum in particular, lacked structural symmetry. This lack of structural symmetry resulted in a significant difference in the projection and measurement of the sacral base in one of the views. The degree of asymmetry would appear to produce a non-uniform projection of the measuring

points associated with the two views. This lack of symmetry made the combination of projection angle, reference points and line marking potentially critical factors in the validity of the radiographic assessment of sacral obliquity. The two methods described failed to consistently measure the same angle of the sacral base relative to the horizontal plane in the frontal (coronal) view of the sacrum on plain film radiographs.

Had there been a consistent and predictable variation between the measured angles in much the same way that Cobb's and Ferguson's angles vary in measuring scoliosis (301, 346) the implication would be that they were measuring the same effect but with consistently different magnitudes resulting in a related or proportional systematic error. The quantifiable mathematical relationship between the tangent and cord of a specified arc, assuming the end points are the same, is reflected in the relationship between the Cobb's and Ferguson's methods of measuring a scoliosis (229, 256). However, some of the sacral specimens being studied were asymmetrical, with a resulting non-uniform variation in the measured sacral base angulation relative to the horizontal plane. Had the two analytical methods produced consistently different angles it could have been due to the different projection of compound angles with the object being inclined in two or three planes, or variation of the angle of observation and relationship of the object to the image plane (256, 347-349).

The outcome of this chapter involved a number of the sacral specimens showing little or no difference in measured obliquity in the different views while others showed significant to marked differences. This outcome was due to one, or a combination of two basic causes. From the result it could be concluded that structural symmetry was lacking in at least some of the specimens and one projection method and its associated analytical method failed to detect the anomaly (type II error) or the other method measured what appeared to be an anomaly that was non-existent (type I error). This outcome would suggest a lack of

specificity or sensitivity in either one or both of the methods in quantifying the true sacral obliquity angle.

Several factors have been identified as contributing to errors associated with the measurement of angles and distances on plain film radiographs (9, 15, 29, 174, 189, 237, 239). These include magnification and distortion inherent in plain film radiography, identification and consistency of reference points, errors with the measuring process and the two dimensional projection of objects rotated in three planes. The use of digital imaging generally reduces the random error from the measuring process (242) but does not eliminate systematic errors associated with identifying reference points and projection distortion (6, 190, 226, 228, 229, 231, 235, 350-353). Most of these recognised errors produce predictable systematic errors such as magnification and distortion of the resulting image.

Variable results can occur from structural asymmetry of the object being assessed. Adaptive changes can create difficulty and inconsistency in identifying and selecting the appropriate reference points on either of the two views studied. Structural asymmetry of the structures being studied can produce variation of projected alignment when measured on different views of the same structure. The magnitude of the measured angle is dependent on the reference points selected to represent the plane of interest. A detailed examination of sacrum two in the study sample, the sacrum exhibiting the greatest variation on the two views, suggests that the variation in measurement is due to intrinsic structural asymmetry of the sacral base relative to the ala. Structural asymmetry exists between the plane of the sacral plateau and the sacral ala resulting in marked variation in the alignment of the reference points as seen on the resulting radiograph depending on which set of points was chosen.

Once the presence of systematic error has been established one way to both identify and quantify the source of the systematic error in the measurement of sacral obliquity is to use a known reference value. Other than using in vivo studies where the true measurement could be established an alternative is to use a phantom in the form of a pelvic radiographic model with a known degree of sacral obliquity.



**SACRAL OBLIQUITY MEASURED ON PLAIN FILM  
RADIOGRAPHIC IMAGES OF A PELVIC PHANTOM**

## CHAPTER 4

*“What difference is there, do you think, between those in Plato's cave who can only marvel at the shadows and images of various objects, provided they are content and don't know what they miss, and the philosopher who has emerged from the cave and sees the real things?”*

- Desiderius Erasmus

### 4.1 INTRODUCTION

In order to not only establish the presence of systematic error in sacral obliquity but to also quantify the degree of error and also the possible source of the error a known reference value was needed. The parameters that are prone to error when measured on radiographic images in relation to sacral obliquity involve the position of the femur heads and the degree of asymmetry or tilt of the sacrum relative to the femur heads in the frontal plane or the relationship of the sacral base to the horizontal plane. One other indirect factor is the structural symmetry or positional alignment of the pelvis around a central vertical axis. To control or account for these factors a pelvic radiographic model was designed and constructed with interchangeable wedges representing five specified sacral obliquity angles.

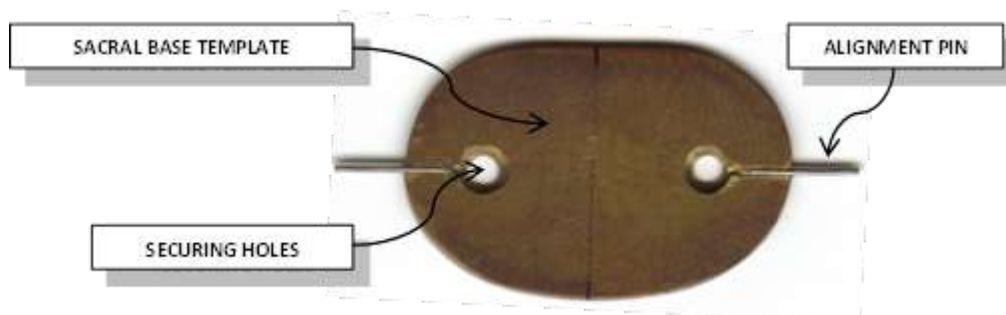
The purpose of the model was to act as a ‘gold standard’ to test the validity of measuring dihedral angles in the form of sacral obliquity and obliquity of the vertebral end plates on plain film radiographs and CT images. Four replaceable plastic wedges were constructed with various degrees of angulation in the frontal (X-Y) plane and shaped to match a template of the sacral plateau. The four wedges were machined with high precision to have a predetermined degree of angulation between the upper and lower surfaces. The sacral base of the phantom was machined to be flat and approximately level to the plain of the femur heads. The wedges were secured to the sacral base with two radiolucent locating screws. The wedges were used to replicate pre-set degrees sacral and vertebral obliquity with angles of 5, 10, 15 and 20 degrees (Figure 93).





**Figure 93. Four interchangeable wedges used to replicate 5, 10, 15, and 20 degrees of sacral base obliquity**

A brass plate with the same shape as the wedges and same securing points was constructed with two short pins extending outward in the line of the major axis of the sacral base. The plate was used in addition to the wedges for the plane film radiographs in order to visualise the X-axis of the sacral base on the resulting images. Without the plate, the reference points for the sacral base were not easily located, particularly on the AP views of the pelvis (Figure 94). This would have introduced the unwanted variable of possible inconsistent identification of the major axis of the sacral base on the radiographic images.



**Figure 94. Brass plate used as a template for the radiographic imaging of the sacral base and to visualise the plane of the sacral base on radiographs**

As the purpose of the study was to assess the validity rather than the reliability of the measurement, the pins allowed for a more convenient method of identifying the same points on the different views.

The pelvic model was constructed to represent the positional and anatomical relationship of the bony structures making up the pelvis. The model was used as a radiographic phantom to project the bony landmarks of the pelvis on plain film radiographs, scout views and helical CT studies. The pelvic model was constructed in such a way that it could be

positioned for plain film radiographs with predetermined rotations relative to the vertical and horizontal primary rays (Figure 95).

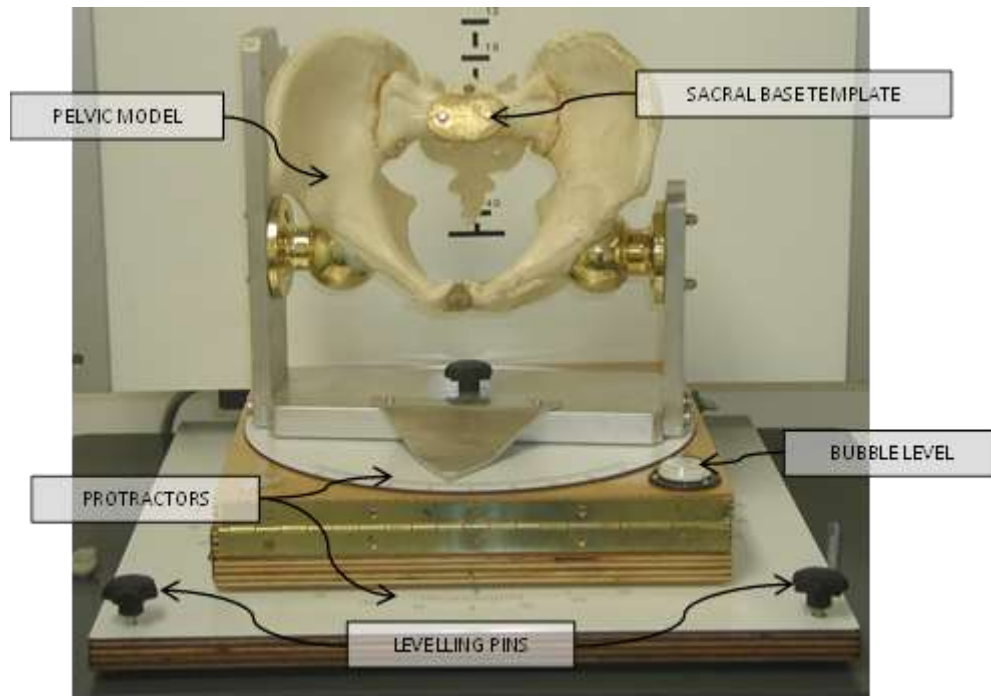


Figure 95. Pelvic model and supporting frame

For the computed tomography (CT) studies, the model was placed in a position relative to the table and gantry of the CT machine that replicated the anatomical position of an individual undergoing a pelvic or abdominal CT examination. The scout views were performed in two positions, one in the same or similar position as for the CT scans while the other scout view was performed in a similar position except that the plane of the sacral base was in the same plane as the x-ray beam.

The pelvic model was obtained from a full spine plastic model (Vertebral Column with Pelvis QS21-3, Mentone Education Centre, 215 Chesterville Road, Moorabbin, Victoria, 3189, Australia) being a replica of a natural spine. The bones included the sacrum, two ilia and a plastic piece representing the cartilage of the symphysis pubis. These bones were permanently fixed in their anatomical position. This involved gluing together the two sacroiliac joints and the symphysis pubis. No attempt was made to ensure reflective symmetry of

the model around the Y-axis. The model was moulded from actual bony structures with possible inherent bony irregularities creating potential alignment differences between the plane of the sacral base and the plane forming a tangent to the femur heads with the sacral base in the horizontal plane. For this reason the sacral base was machined to approximate the two planes when the sacral base was horizontal and to provide a smooth base for the attachment of the machined wedges representing specified degrees of sacral obliquity.

The radiographic phantom was designed and constructed with design features similar to those incorporated in radiographic holding devices used by Tannast *et al* (354) to analyse femoroacetabular impingement. A similar device was also used by Kakaty *et al* (355) to obtain pelvic radiographs used to assess the ischial spine sign on A-P pelvic radiographs.

The supporting frame for this study was constructed from two basic components, a pelvic support and a levelling base. The pelvic support could be moved around the Y-axis with its own reference protractor attached to the levelling base. The protractor was used for simulating the position of the pelvis with various relative Y-axis rotations (Figure 95). The protractor and a levelling bubble on the base were not specifically aligned to the reference frame inherent in the setup of the radiographic equipment. As a result, the initial orientation of the pelvis when the protractor and level indicated zero rotation of the pelvis around specific axes and horizontal orientation of the sacral base was only an approximation and only used for comparative reference. The actual pelvic rotation could only be confirmed on radiographic images retrospectively (Figure 96).

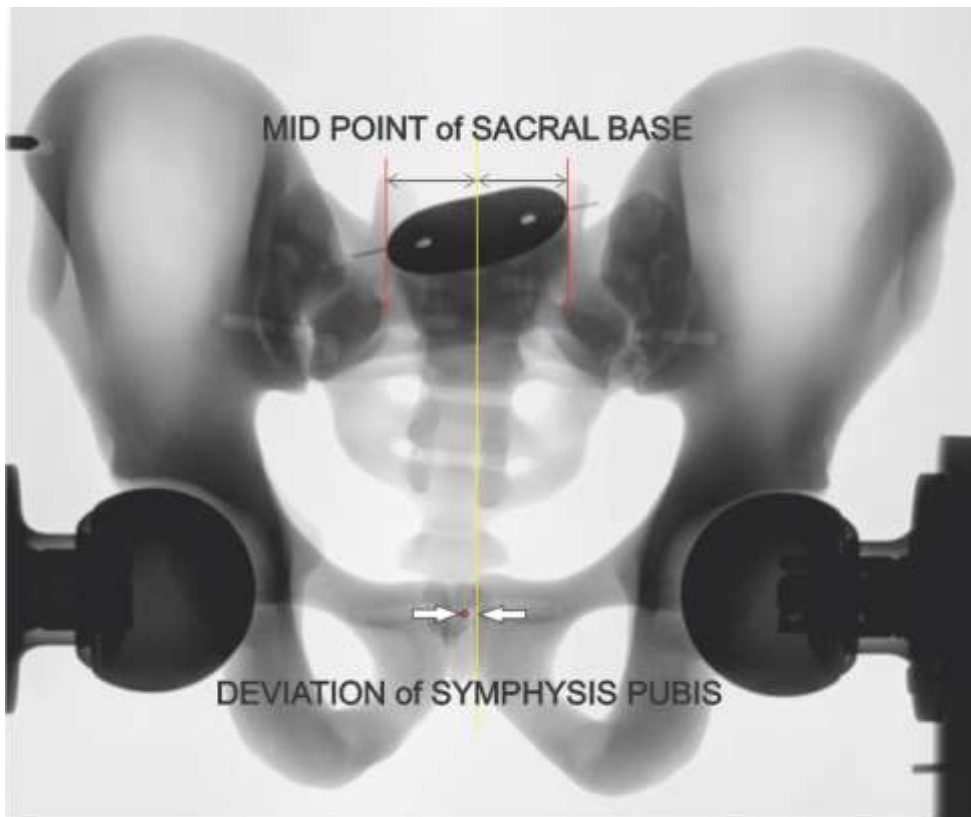


Figure 96. A-P radiograph of the pelvic phantom demonstrating the method used to measure rotation on the image

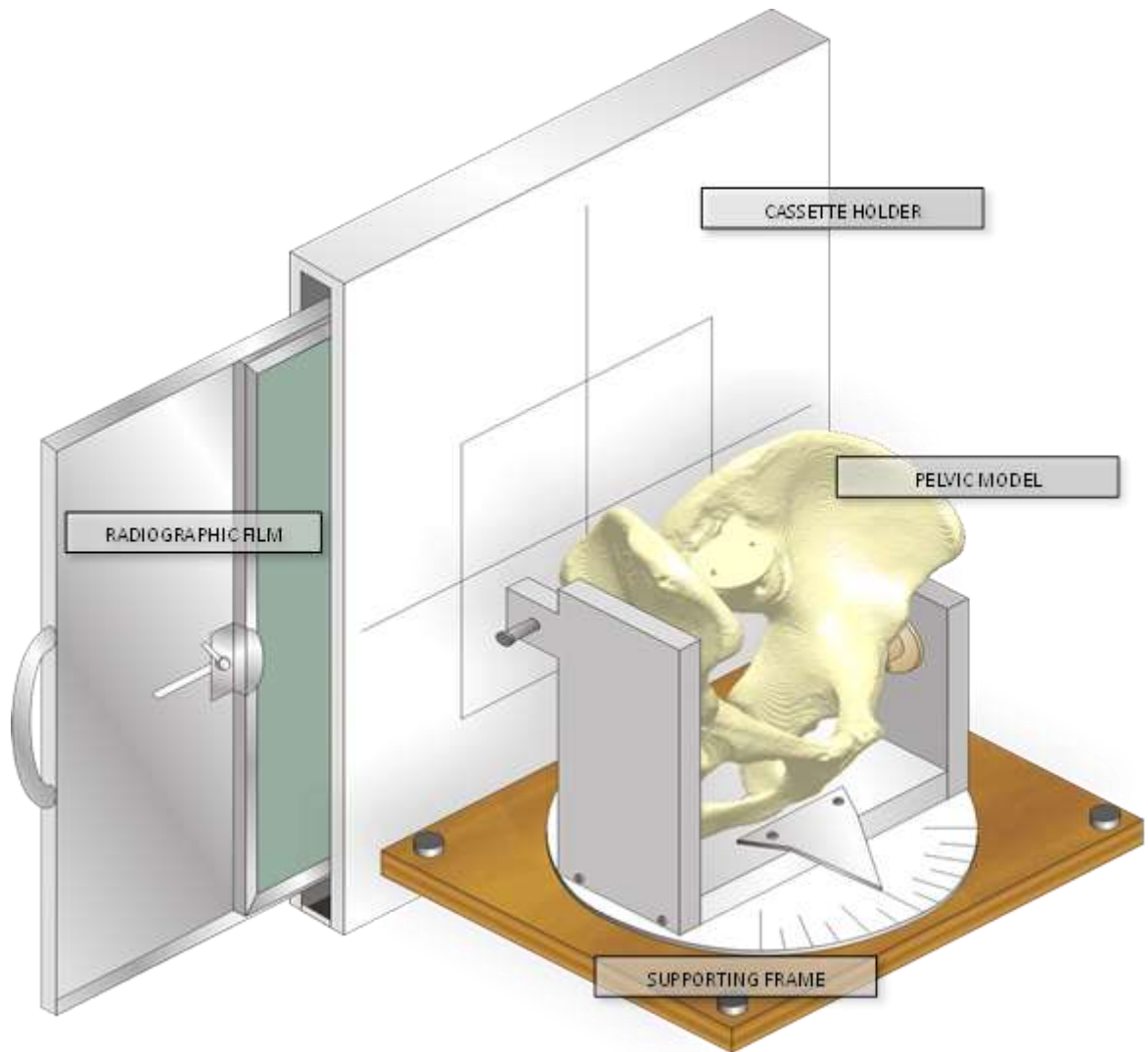
#### 4.1.1 Components of the supporting frame

- a. Pelvic support was made from three aluminium bars secured in the form of a 'U' shaped frame with an axis of rotation centred on the base of the frame to facilitate rotation around its own Y-axis. The pelvic support was secured to the levelling base through a central lockable pivot. The lateral supports incorporated two spherical structures slightly smaller than the acetabula of the pelvic model and attached on the inward facing surfaces at the same height from the base to simulate the position and function of the femur heads. A locating pin on one of the upright supports was used to position the pelvis around an X-axis that passed through the femur heads. There were three pre-set positions for the locating pin to be inserted in the support frame and a locating notch on the corresponding ilia.

- b. Levelling base with four adjusting screws located on each corner. A levelling bubble was attached to the base to indicate the orientation of the base relative to the horizontal plane. Horizontal alignment was achieved by adjusting the four independent adjustable alignment screws at each corner of the base to centralise the alignment bubble. A protractor was attached to the base with the line indicating  $0^{\circ}$  on the protractor aligned to the Z-axis and centred on the base (Figure 95).

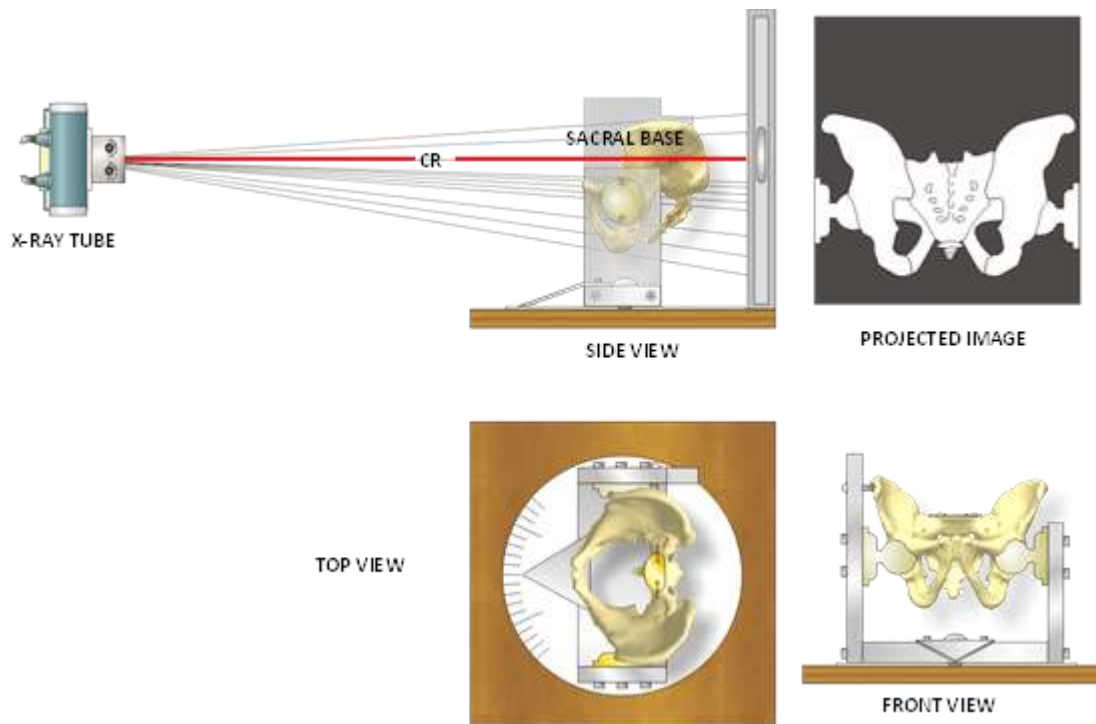
#### **4. 2 PLAIN FILM RADIOGRAPHIC POSITIONING**

The predetermined neutral position of the pelvis for the plain films represented approximate alignment of the X-axis and Z-axis of the pelvis with the global X-Z axes. The X-axis lies at the junction of the transverse and frontal planes. The Z-axis lies at the junction of the mid-sagittal and the transverse planes. The pelvis could be set to represent specified degrees of rotation around the Y-axis and X-axis. The Y-axis lies at the junction of the frontal and mid-sagittal planes. Once rotated around either the X-axis or Y-axis, or any combination of these axes, the model could be locked into a fixed position relative to the base. A relocatable locating pin on one side of the support frame, in conjunction with an indentation on the corresponding ilia, was used to fix the pelvis in one of three predetermined positions around the X-axis (Figure 97).



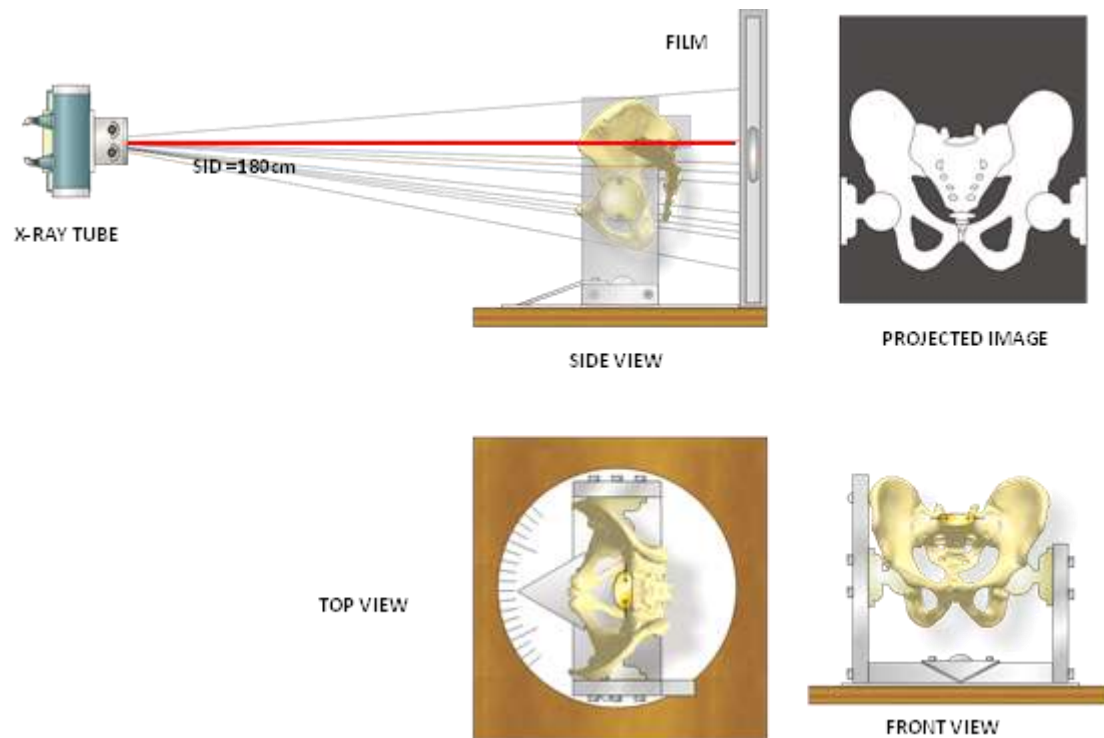
**Figure 97. Pelvic model (radiographic phantom) positioned in relation to the cassette holder and radiographic film**

The first location positioned the pelvis so that the plane of the sacral base was horizontal to the levelling base and perpendicular to the film cassette for the zero angle view (ZAV). This view represented a zero sacral base angle (Ferguson's base angle) within the global reference frame and relative to the cassette. In this position, the central ray of the x-ray tube was horizontal and aligned to the plane of the sacral base (Figure 98).



**Figure 98. View of the pelvis with the sacral base rotated to match the horizontal plane and the central ray projecting the plane of the sacral base as a line**

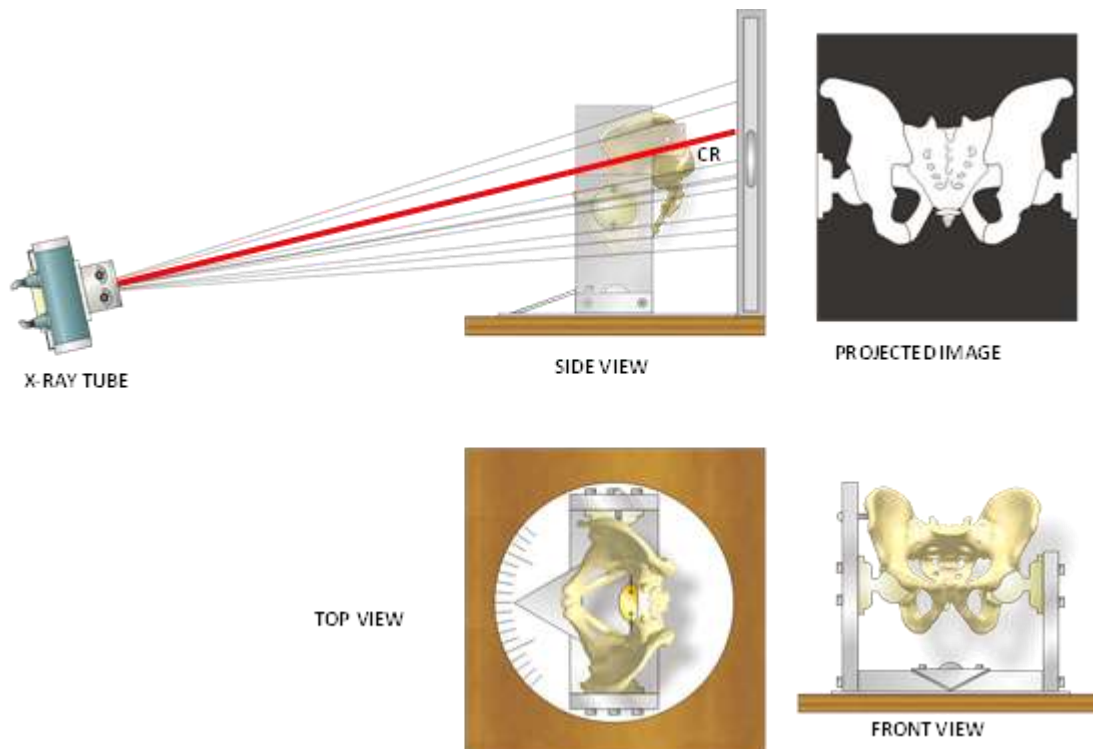
The second position of the pin represented the orientation of the pelvis in upright posture, as it would be for a standard erect AP view of the lumbopelvic spine. This resulted in an angle of the sacral base equivalent to a Ferguson's base angle of approximately  $37.5^\circ$ . The central ray of the x-ray tube remained in the same orientation and alignment as for the zero sacral base angle view (Figure 99).



**Figure 99. A-P view of the pelvis with a sacral base angle of approximately 37.5 degrees and the central ray horizontal and directed at the centre of the sacral base**

The third position of the pin represented an intermediate angulation of the sacral base, as it would be for a typical erect sacral base view with pelvis rotated slightly to the posterior from the erect position. The angle of the sacral base for this view was approximately 28.5 degrees. The x-ray tube was tilted so that the central ray was aligned and angled to match the slope of the sacral base. This resulted in the central ray being tilted relative to the cassette at angle equivalent to the sacral (Ferguson's) base angle ( $28.5^{\circ}$ ) (Figure 100).





**Figure 100. Sacral base view (SBV) of the pelvic model with the pelvis rotated posterior around the femur heads and the central ray aligned and angled to match the sacral base angle of approximately 28.5 degrees**

The lockable pivot in the centre of the support frame acted as the axis of rotation for the supporting frame and as a means of locking the pelvis in relation to rotation around the Y-axis of the levelling base. This position represented the neutral position of the pelvis or zero degrees of Y-axis rotation. The vertical centre of the model was aligned to the vertical centre of the cassette and to the vertical primary rays of the x-ray beam (Figure 101). This was done by using the collimator to align the horizontal and vertical primary rays of the x-ray tube with the horizontal and vertical axes of the cassette and the vertical axis of the model.

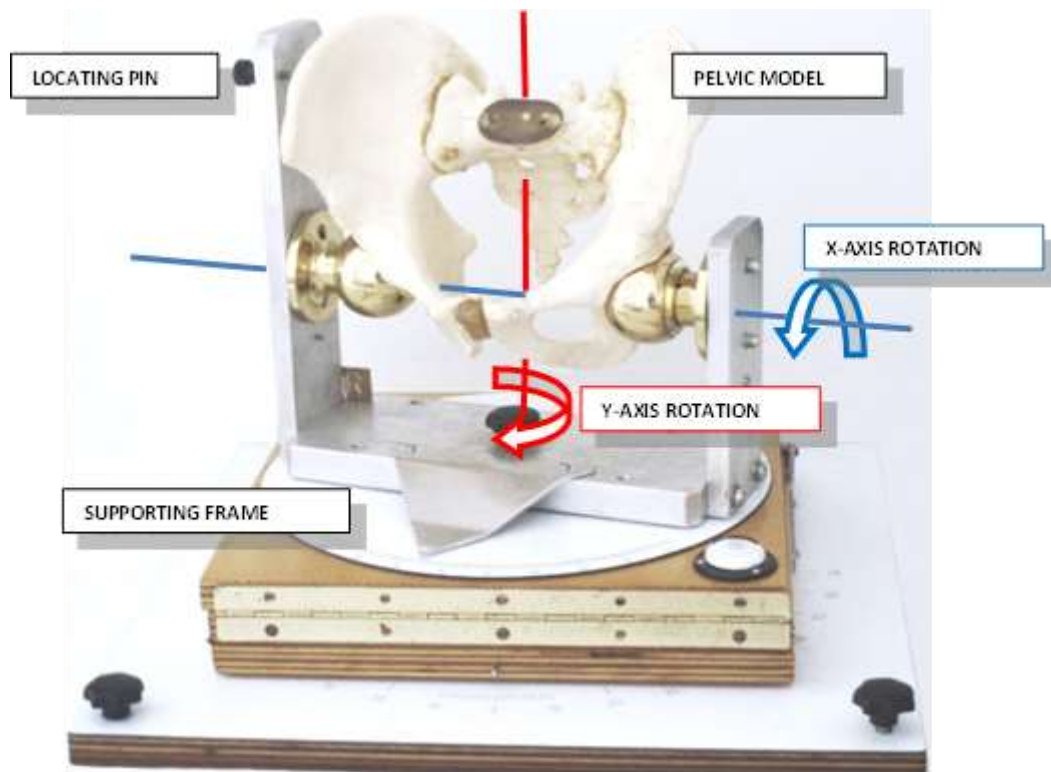


Figure 101. Axes of rotation of the pelvic model around the X and Y-axes. Sacral obliquity is rotation of the sacral base around the Z-axis

Each of the views was repeated with the same relative positioning for 0, 5, 10, 15 and 20 degrees of sacral obliquity using the sacral wedges. The source to image distance (SID) for each view was 180 cm (72 in). The exposures were made on a Sedecal – SHF310 North American Imaging x-ray machine with exposure factors of 40 kvp at 0.5 mas, using a fine focal spot. The image was recorded on a digital cassette and downloaded to a Toshiba workstation employing Fujifilm FCR V.2 imaging software (26-30, Nishiazabu 2-Chome, Minato-Ku, Tokyo 106-8620, Japan). The exposure factors were corrected and optimised for viewing bony structures such as the sacrum using the supplied software.

#### 4.3 RADIOGRAPHIC IMAGE ANALYSIS

A *Digital Imaging and Communications in Medicine* (DICOM) format viewer was provided with the data sets to view the medical digital imaging studies that were saved to CD disks in this format. DICOM format is recognized as an international standard used for the transfer and manipulation of medical imaging data such as CT and CR studies. The header

component of the DICOM files contains information about the digital imaging method, image dimensions, etc., as well as all of the image data containing the three dimensional pixel information. The DICOM viewer facilitates the analysis and display of images based on the DICOM standard. It does this in various display modes, at adjustable display distances (magnification) and provides variable windowing settings for individual images.

#### 4.3.1 Plain (conventional) Film Radiographs Analysis

The plain films were saved in their original DICOM format and exported and saved as JPEG images using Dicom LiteBox Version 3.02b, (Sorna Corporation, 2020 Silver Bell Road, Eagan, MN 55122 USA) (Figure 102). The exported bitmap images retained the original aspect ratio but not the linear dimensions of the DICOM image. This allowed angular but not linear measurements to be obtained from the JPEG images.

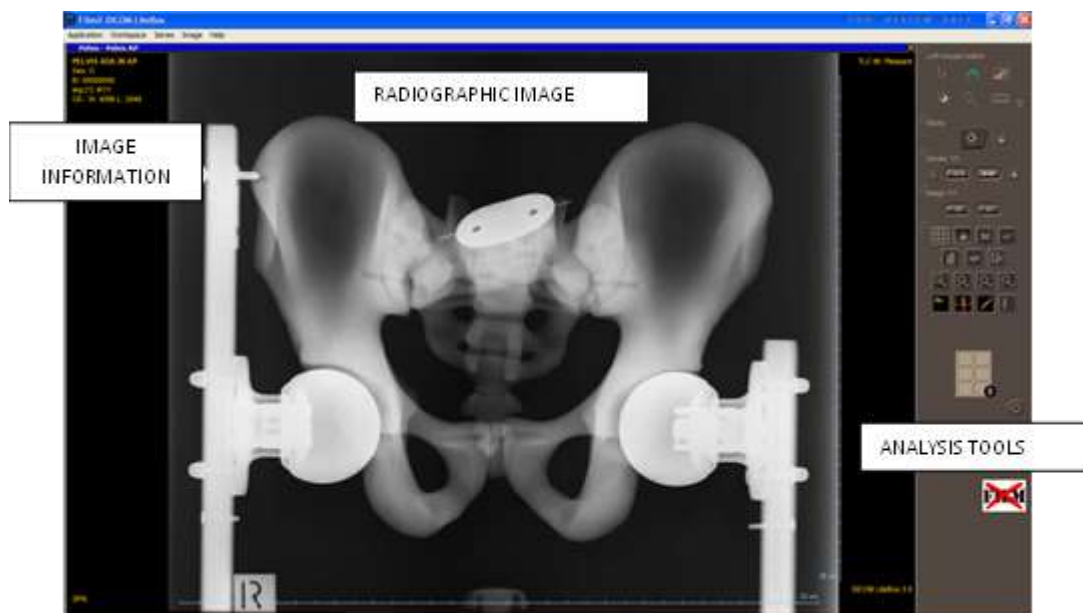


Figure 102. Dicom LiteBox analysis screen with radiographic image of the pelvic model

The images were transferred from the Dicom LiteBox program using the '**copy to clipboard**' function in the **IMAGE** dropdown menu and directly imported into CorelDRAW X4 software (Corel Corporation, 1600 Carling Avenue, Ottawa, Ontario, K1Z 8R7, Canada) using the '**paste**' function in the **EDIT** dropdown menu. The images were analysed using

line drawing and measuring tools incorporated in the program. This provided consistency and accuracy of the measuring methods to three decimal places for angles (Figure 103). The measurements were recorded and compiled using Microsoft Excel 2007 (Microsoft Corporation, One Microsoft Way, Redmond, WA 98052-6399).



**Figure 103. CorelDRAW image manipulation screen and drawing tools**

The relative sacral obliquity angle was measured for the five degrees of pre-set sacral obliquity for each of the three views. This resulted in fifteen individual images of the pelvic model. A line representing the plane of the femur heads was constructed as tangent to the upper surface of the structural support of the model that represented the size and position of the femur heads. A second line was constructed on the sacral base representing the major axis of the sacral base as seen in each of the views. The angle between these two lines was measured and recorded as the relative sacral obliquity angle (Figure 104).

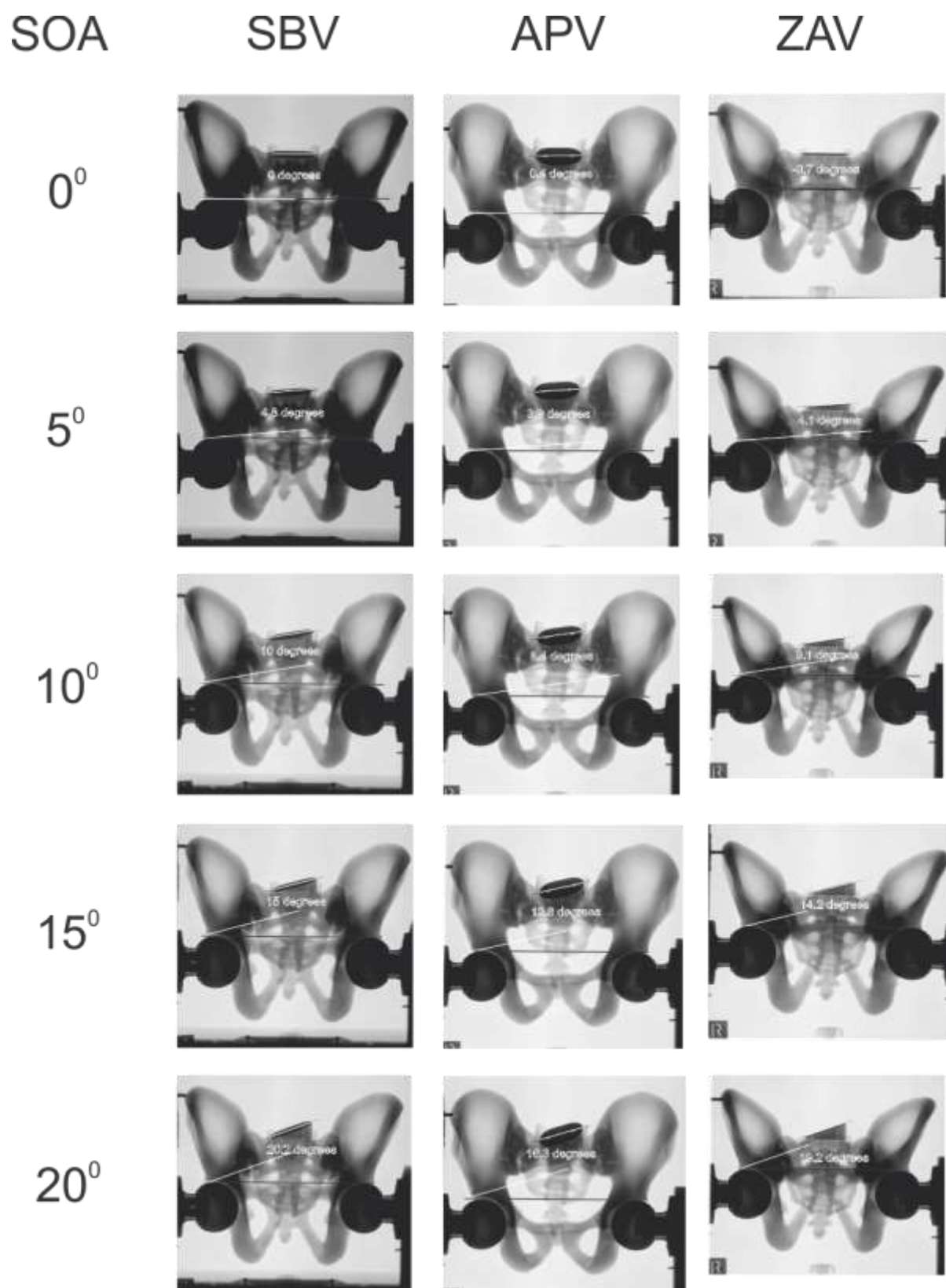


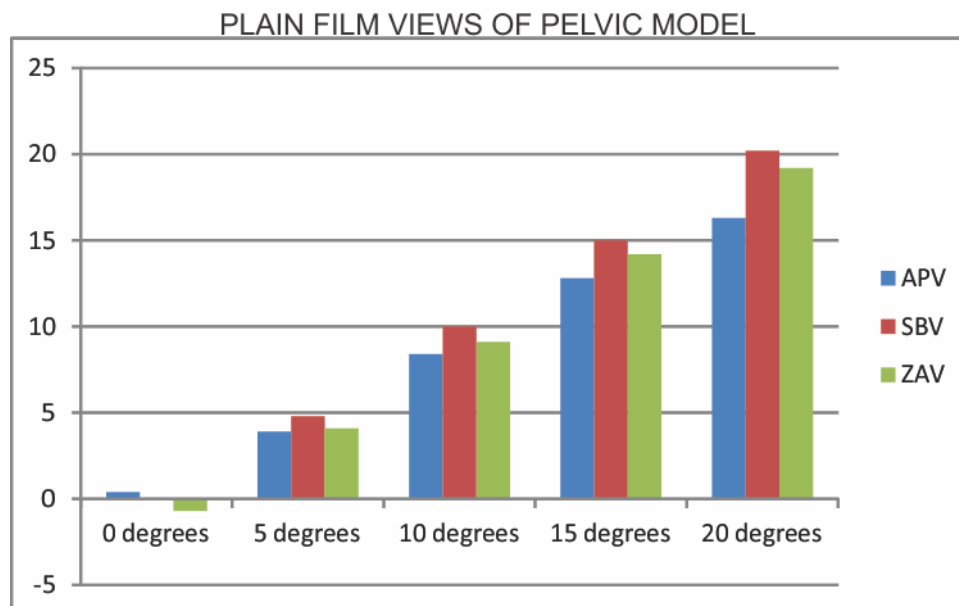
Figure 104. Plain film images of the radiographic phantom with 0, 5, 10, 15 and 20 degrees of sacral obliquity taken as a sacral base view (first column), A-P view (second column) and zero angle view (third column) perpendicular to the image plane (film)

#### 4.3.2 Data analysis Plain film (CR) of Pelvic Radiographic Phantom

The values obtained from the measurement of sacral obliquity on the three plain film views of the pelvis taken with five predetermined sacral wedge angles (0°, 5°, 10°, 15°, 20°) and using two different measuring methods are set out in (Table 3) and (Figure 105).

**Table 3. Sacral obliquity measured on the three plain film views of the pelvis taken with five predetermined sacral wedges**

SOA	APV	SBV	ZAV
0 degrees	0.4	0.0	-0.7
5 degrees	3.9	4.8	4.1
10 degrees	8.4	10.0	9.1
15 degrees	12.8	15.0	14.2
20 degrees	16.3	20.2	19.2



**Figure 105. Graphical representation of the SOA measured on three different views of the pelvic model with wedges representing 0, 5, 10, 15, and 20 degrees of sacral obliquity**

Linear regression models were fitted for each of the 3 measures with SOA as a predictor (Table 4).

**Table 4. Linear regression models were fitted for each of the three measures with SOA as a predictor.**

Outcome	Intercept Est (95% CI)	SOA Est (95% CI)
APV	0.22 (-0.63,1.08)	0.81 (0.74,0.88)
SBV	-0.12 (-0.42,0.18)	1.01 (0.99,1.03)
ZAV	-0.68 (-0.95,-0.41)	0.99 (0.97,1.01)

For APV there is a systematic reduction in observed APV with increasing SOA, as indicated by the slope of 0.81 (95% CI 0.74,0.88). The other two outcomes have a slope with 95% CI including 1.0, indicating no evidence that the slope is not 1.0.

For the intercept both APV and SBV have a confidence interval including zero, showing no evidence that at an SOA of zero these measures are not zero. However for ZAV the confidence interval does not include zero indicating a systematic bias where the measured values are consistently lower. This observation is most likely due to the fact that the plane of the sacral base of the radiographic phantom was only proximately aligned to the horizontal plane in the frontal view.

#### **4.4 SUMMARY and CONCLUSION**

The analysis of plain film radiographic images of a pelvic phantom with predetermined degrees of sacral base asymmetry (obliquity) were consistent with a predictable systematic error associated with the measurement of sacral obliquity using radiographic images. The measurement of sacral obliquity on the three views (SBV, APV, ZAV) varied proportionally

with two factors. These were the angle between the central ray and the angle of the sacral base (Ferguson's base angle) and the angulation of the central ray to the image plane with other factors being constant such as pelvic rotation. This suggests the systematic error is directly related to the orientation of the structure being measured relative to the x-ray beam and the orientation of the structure relative to the image plane.

The absolute degree of sacral obliquity was not a critical factor as the reflective symmetry of the phantom was not controlled for as part of the imaging process. As the sacral plateau was in a constant frontal plane orientation but not necessarily absolutely level for each view, the difference in the five degrees of sacral obliquity measured on the three different views of the same structure were considered the significant variable.





**SACRAL OBLIQUITY MEASURED ON  
COMPUTED TOMOGRAPHY IMAGES OF A  
PELVIC RADIOGRAPHIC PHANTOM**

**CHAPTER 5**

*“In order to understand true realities, men need to do mental blending.”*

— Toba Beta

**5.1 COMPUTED TOMOGRAPHY (CT)**

Computed tomography (CT) is a radiographic imaging method employing computerised digital geometry processing to generate a series of two-dimensional slices or a three-dimensional image of the internal structure of an object. Goldman (356) has documented the development of computerized tomography along with the general principles involved in using x-rays to generate images of the body, including bone. With conventional CT scanning the raw data is obtained from a large series of two-dimensional images taken around a single axis of rotation while helical scanning uses continuous data acquisition, during which the patient translates through the scanner while the x-ray tube rotates around the patient. Computerised reconstruction of the data from the x-ray sensors produces a volume of data in the form of ‘voxels’. A *voxel* is a volume element, representing a value on a regular grid in three-dimensional space. This is analogous to a pixel, which represents two dimensional image data. As with pixels, voxels themselves typically do not contain their position in space (their coordinates). Each voxel’s position is inferred based on its position relative to other voxels i.e. their position in the data structure that makes up a single volume image. A voxel represents the sub-volume box with constant scalar/vector value inside which is equal to scalar/vector value of the corresponding grid/pixel of the original discrete representation of the volumetric data (357).

A computer program can manipulate the data in order to illustrate the inherent property of various structures and tissues to block an ionising x-ray beam. Computer software allows this volume of data to be reformatted in various planes or even as volumetric (3D) representations of the structures involved. An x-ray beam passes through an object and is detected according to the density of the tissue encountered. Detectors sensitive to the

ionizing radiation of the x-ray beam are positioned around the circumference of the scanner or directly opposite the x-ray tube (the source ionizing radiation) to collect attenuation readings from multiple angles (Figure 106).

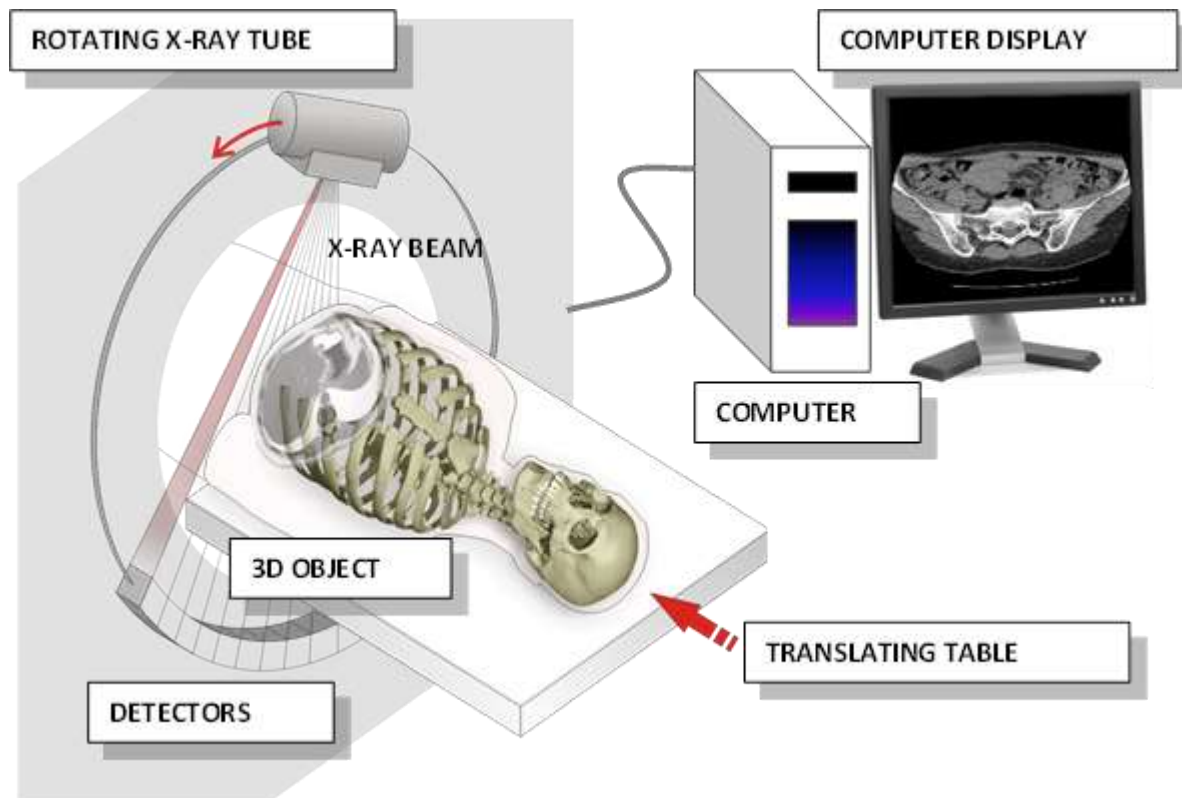
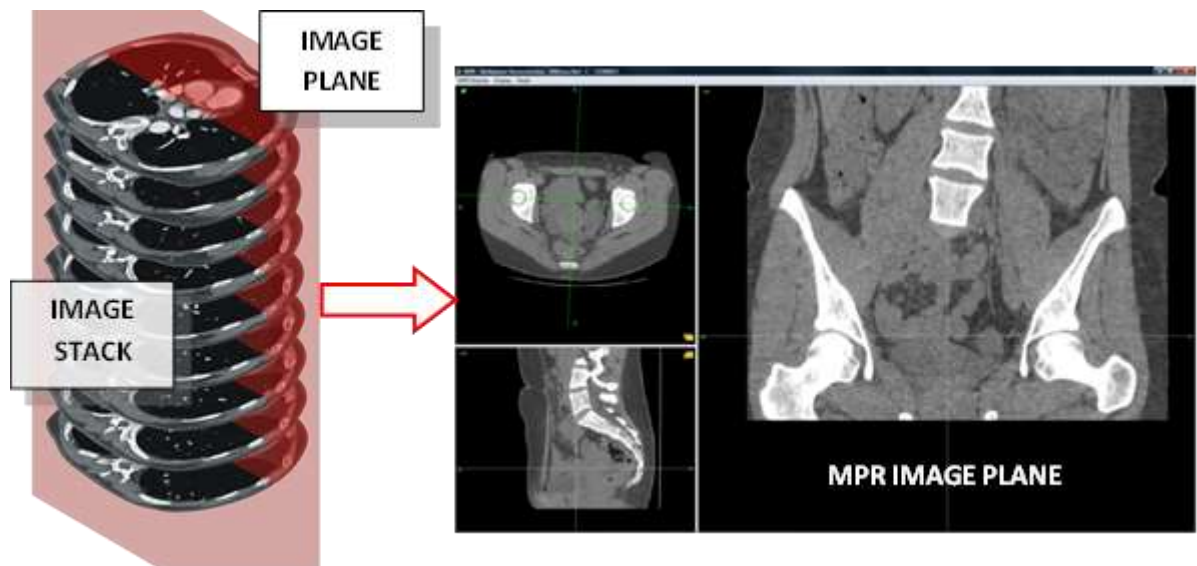


Figure 106. CT data acquisition and image production

These different views through the patient are combined using a computerised algorithm to reconstruct image slices, image planes through the data set producing multiplanar reconstructions (MPR), or a three-dimensional object (3D reconstruction).

In the CT scanner, the x-ray tube (source) rotates around the patient positioned on a table that moves horizontally relative to the x-ray beam. On the opposite side of the patient from the tube is an x-ray detector. The detector receives the portion of the beam that makes it through the patient. The beam is sampled via multiple channels. The signal received by each channel is digitized and sent to the reconstruction processor. Measurements are typically taken about 1000 times per second. Scan rotations can be 1 to 2 seconds long for

discrete slices or longer periods for helical scans. Each view/channel chunk of scan data is compared to calibration scan data of air, water and polyethylene, (soft plastic) previously acquired in the exact same relative location. The comparisons allow the image elements to have a known value for a particular substance in the body regardless of differences in patient size and exposure factors. The picture quality is improved by increasing the number of samples or views. The advantages of computerized tomography include non-invasive three-dimensional imaging of the spine and musculoskeletal system and the ability to reconstruct images in multiple viewing planes or as structures that can be manipulated in three-dimensional space (Figure 107).



**Figure 107. Multi-planar reconstruction from the primary CT data set**

The boundaries of a voxel are exactly in the middle between neighbouring grids. Voxel data sets have a limited resolution, as precise data is only available at the centre of each cell. Under the assumption that the voxel data is sampling a suitably band-limited signal, accurate reconstructions of data points in between the sampled voxels can be attained by low-pass filtering the data set. Visually acceptable approximations to this low pass filter can be attained by polynomial interpolation such as tri-linear or tri-cubic interpolation. The value of a voxel may represent various properties. In CT scans, the values are Hounsfield units, giving the opacity of material to X-rays (356).

Hounsfield scale is a quantitative linear scale for describing radio-density based on the transformation of the original linear attenuation coefficient measurement. It has been calculated using the radio-density of distilled water at standard temperature and pressure (STP) and a scale relating the density of distilled water to air at standard temperature and pressure (STP). Water is zero in Hounsfield units while air is minus one thousand Hounsfield units (-1000). Bone is approximately plus one thousand Hounsfield units (+1000) (358).

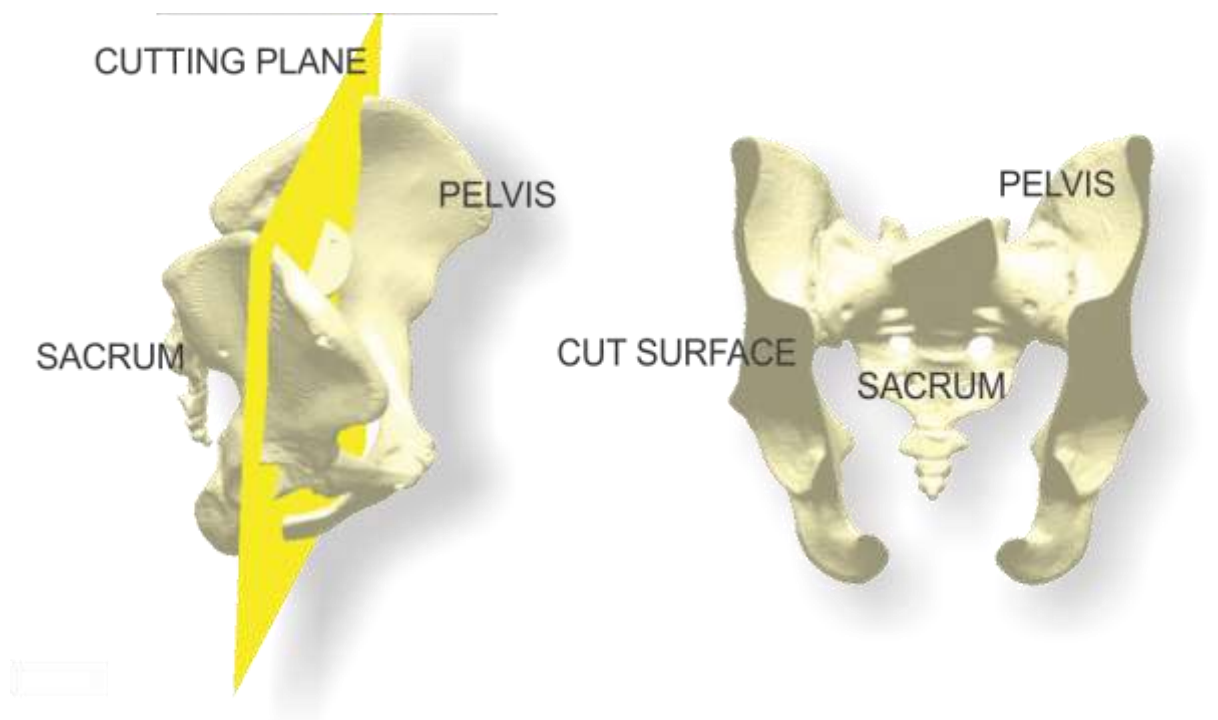
## **5.2 MULTIPLANAR RECONSTRUCTION OF IMAGING DATA**

Because the image plane or the three-dimensional image of the pelvis could be manipulated after acquiring the imaging data, it was not necessary to place the pelvic model in a fixed or predetermined position relative to the table or gantry of the CT machine. However, to minimise any potential distortion due to off-axis positioning of the phantom the sacral base was centred using the laser cross-hairs set up during instillation of the equipment to represent the optimal geometrical positioning of the target structure in the machine.

The reconstructed three-dimensional image or viewing planes could be manipulated around three primary axes for viewing after acquiring the imaging data. This was done using specific computer software. With multiplanar reconstruction (MPR) of the data, the imaging plane could be manipulated relative to the orientation of the pelvis in space to achieve a predetermined view of a plane through the structure of interest. For both three-dimensional images and MPR slices, this was achieved using specific proprietary computer software thus avoiding the need to locate the pelvis in a specific or absolute predefined position. A single CT data set was obtained for each pre-set sacral obliquity angle (0, 5, 10, 15, 20) totalling five sets of data.

### 5.2.1 CT data manipulation

Besides plain film radiology, the program used in this study also included the capacity for displaying CT data sets in the form of two-dimensional stacks and multiplanar reconstructions (MPR). For computerized tomographic image acquisitions this function was used to view structures in planes other than in their original orientation to the projection plane. MPR involves reformatting images with the viewing plane in any orientation and position within the volume made up of original slices i.e. image stack. The stacks could be viewed as a series of two-dimensional cross-sectional images with the plane of the images orientated perpendicular to the horizontal axis of the CT scanner (Figure 107). The computer program was used to interpret and display the large volume of data generated by the radiographic scanning processes to create two-dimensional cross-sectional images of the pelvis (Figure 108).



**Figure 108.** The cutting plane splits the pelvis into anterior and posterior portions through the major axis of the sacral base with the cut section view as a multiplanar reconstruction

These images were then displayed on a high-resolution computer monitor. This process formed the basis of data manipulation for the helical or spiral computed tomography. The

standard display format for CT imaging of the pelvis is comprised of a specific number of two-dimensional 'slices' that are stacked to form a sequence of images from superior to inferior through the pelvis (359).

Multipanar reconstruction (MPR) is a means of viewing organs, tissues and skeletal structures in planes other than original slice planes or the orientation of structures (360). This is achieved by the computerised manipulation of digital information obtained from computed tomography scans. It involves re-calculating the composition of images based on planes located in any orientation and position inside the volume making up the original data set (Figure 109).



Figure 109. AP multiplanar reconstruction (MPR) from CT data with the A-P image generated along the cutting plane (left). The cutting plane is visualised on the lateral view of the structures involved

The multiplanar reconstruction (MPR) is achieved by using a computer to manipulate which of the voxels that make up the imaging data from a CT scan are visualised in the two dimensional image planes as pixels. Each pixel density is proportional to the Hounsfield unit it represents with a proportional colouring or grey scale intensity. Dimensions are derived from the relative three-dimensional location of the voxel within the data set.

### 5.2.2 Measurement of multiplanar reconstruction (MPR) images

The CT data sets used for the MPR reconstructions were individually imported into DICOM LiteBox. The program was used to make measurements in pixels on multiplanar reconstructed images. The image stacks contained calibration information (pixel size) in the vertical and horizontal directions. All linear measurements were shown in millimeters after a conversion from pixels to millimeters and rotation angles were measured in degrees. The software company issues a disclaimer that states that the measurements are shown for information purposes with accuracy dependent on image thickness and the calibration accuracy. The disclaimer further states that the measurements cannot be considered as a real anatomical measurement. However several studies have validated measurements made on MPR images derived from CT data sets that conform to DICOM protocols (361, 362). Measurements made using the specific data acquisition source and analytical program were tested for calibration of angles and dimensions.

MPR reconstruction was performed on the image stack loaded in DICOM LiteBox from the original data set. By default there are three basic image views displayed on the computer screen in their own viewing window. The displayed views in each of the viewing windows are representative of the following cutting planes:

- Sagittal (Y-Z plane): is represented by the A, P, H and F markers.
- Axial (X-Z plane): is represented by the R, L, A and P markers.
- Coronal (X-Y plane): is represented by the R, L, H and F markers.

R – Right side. L – Left side. A – Front (Anterior). P – Back (Posterior). H – Top (Head). F – Bottom (Feet). X-axis (L-R), Y-axis (A-P), Z-axis (H-F) or (top-bottom)



Three mutually perpendicular axes representing viewing planes were displayed in each viewing window that could be either translated or rotated. This facilitated manipulation of the images seen in the other two viewing windows by either translation or rotation of the relative axis. The axes were designated A-P, L-R and H-F by the program. Manipulations of the relevant A-P, L-R or H-F axes as translations or rotations performed in the reference view resulted in two new reconstructed viewing planes through the stack. These planes were displayed concurrently in the other two viewing windows. Any one of the three views could be designated the reference view.

The nature of the studies undertaken, and the method of data collection, precluded the application of any standardised procedure for positioning the pelvis in relation to either the gantry or the table at the time the scans were made. Therefore the relationship of the reference planes of the pelvis to the default viewing plane generated by the computer software could not be specified. There was no fixed predetermined angular relationship between the slices generated by the radiographic equipment and the bony structures of the pelvis.

The multiplanar reconstruction (MPR) function facilitated the retrospective re-alignment of the structures of interest to the viewing plane. Three MPR A-P views were created from the data sets. For the sacral base view (SBV) the pelvis was aligned so that it was viewed with the acetabula parallel to the horizontal and viewing planes no pelvic rotation and the edge of the sacral base viewed as a line. The A-P view involved similar positioning except the sacral base angle was viewed in the same orientation as it was when the data was acquired (Figure 110).

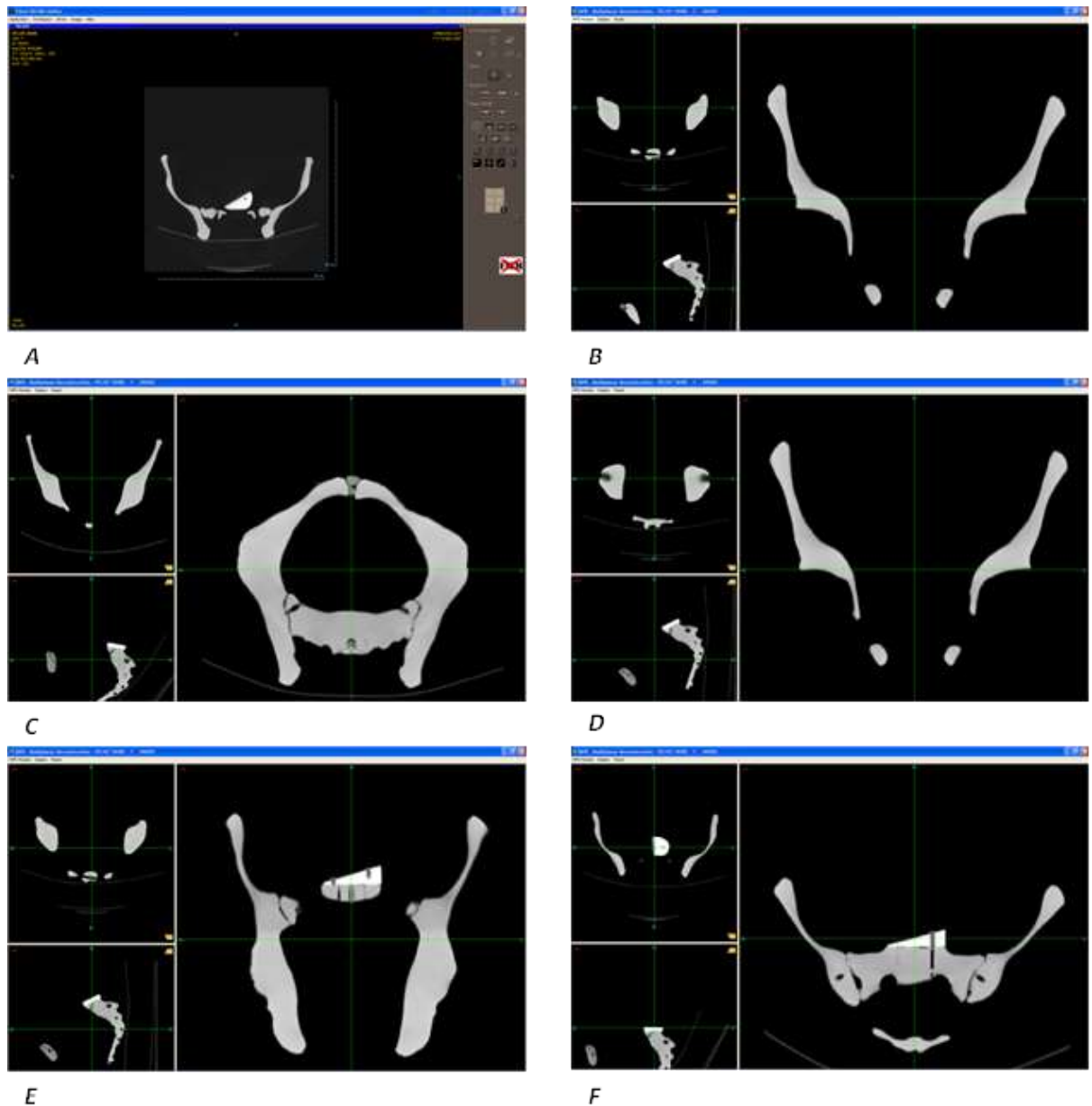


Figure 110. Steps used to orientate the pelvis or model after importing a CT study into the viewing program. A. Imported data set B. Multiplanar reconstruction of data set with default orientation of viewing planes C. Removing Y-axis rotation by aligning the symphysis pubis with the sacral tubercle (Z-axis) or femur heads (X-axis) D. Removing Z-axis rotation by aligning the superior margin of the acetabula E. A viewing plane was aligned with the major axis of the sacral base with the pelvis in the default position relative to the X-axis F. The viewing is centred on the sacral base and perpendicular to it

### 5.2.3 Y-axis orientation

The pelvis was reorientated first by ensuring that there was no rotation of the femur heads in the axial (X-Z) plane i.e. around the Y-axis. This was done by translating the L-R reference axis in the coronal view so that the femur heads were visible in the axial view.

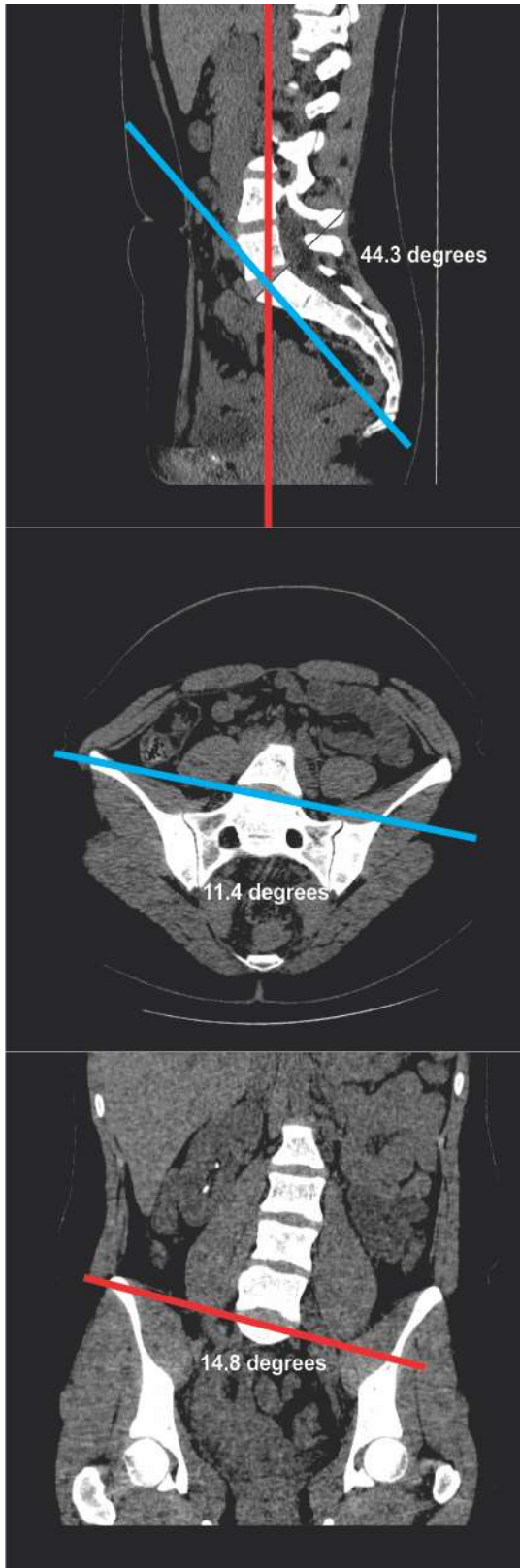
The reference axes were rotated and translated in the axial view so that the L-R axis was aligned with the centre of each femur head.

#### 5.2.4 Z-axis orientation

The reference axes were rotated in the coronal (X-Y) view so that the L-R reference axis formed a tangent to the top of the femur heads. The tangent points were verified in the axial view by ensuring that the L-R reference axis passed through the last visible point of each femur head as the L-R reference line was translated upward in the coronal view. The same process was also used to ensure that the tangent points on the femur heads appeared or disappeared simultaneously in the axial view as the L-R reference axis was raised or lowered respectively in the coronal view.

#### 5.2.5 X-axis orientation

Copies of two coronal (A-P) image planes with the pelvis aligned to the Y and Z-axes but in the default X-axis, orientation were made using Microsoft Windows clipboard. In the first image, the H-F viewing plane passed through the centre of the femur heads in the sagittal (Y-Z) plane. In the second image, the H-F viewing plane passed through the centre of the sacral base in the sagittal viewing window (Figure 111). These images were imported into Corel DRAW using the *Edit special paste* function. This displayed the image with the original aspect ratios and angular relationships but did not retain the original dimensions.



LATERAL MPR

SACRAL BASE VIEW MPR

A-P VIEW MPR

Figure 111. Lateral and two MPR views of the lumbopelvic spine reconstructed from data set. In the first view the plane is perpendicular to the sacral base (blue on lateral view) and in the second view the plane is parallel to the scanner bed (red line on lateral view)

To obtain the zero X-axis rotation (ZAV) or sacral base view (SBV), the orientation of the plane of the sacral base was manipulated by rotating the reference axes around the X-axis (L-R) so that the A-P axis was aligned to, and centred on the sacral base in both the axial and the sagittal viewing windows. The coronal (A-P) image was captured and transferred to CorelDRAW in the same manner as the image of the default A-P orientation.

Lines were constructed on the resulting images using the line tool function in CorelDRAW. Specified points were identified on the images with the aid of the magnification function. This helped in identifying borders and lines of demarcation. Two limitations involved the grey scale inherent in radiographic imaging and the '*pixelisation*' of the CT data. Another difficulty involved the structures themselves. In a number of the radiographic studies there were significant adaptive changes involving the margins of joints as well as irregularities on the surface of the bones being studied. Despite these limitations, the identification of points and landmarks on digital images has been shown to have a high degree of validity and reliability (363-365).

#### *5.2.6 Measuring angles*

The freely moveable guidelines in CorelDRAW were set in the horizontal and vertical planes of the drawing window. Guidelines are lines that can be placed anywhere in the drawing window to aid in object placement, orientation and measurement. Objects or the measuring tool can be 'snapped' to the guidelines and other objects, so that when an object is moved near a guideline or other object, it can be lined up with precision to the line or other object. This facilitates the accurate identification and precise placement of measuring points and placement of the various measuring tools. The horizontal guideline was used as a standardised horizontal plane for angular measurements. The imbedded angle tool was used to measure the acute angle between the lines and guidelines placed on the images being analysed. The measurements obtained from the image analysis were recorded and compiled using Microsoft Excel 2007 (Figure 112).

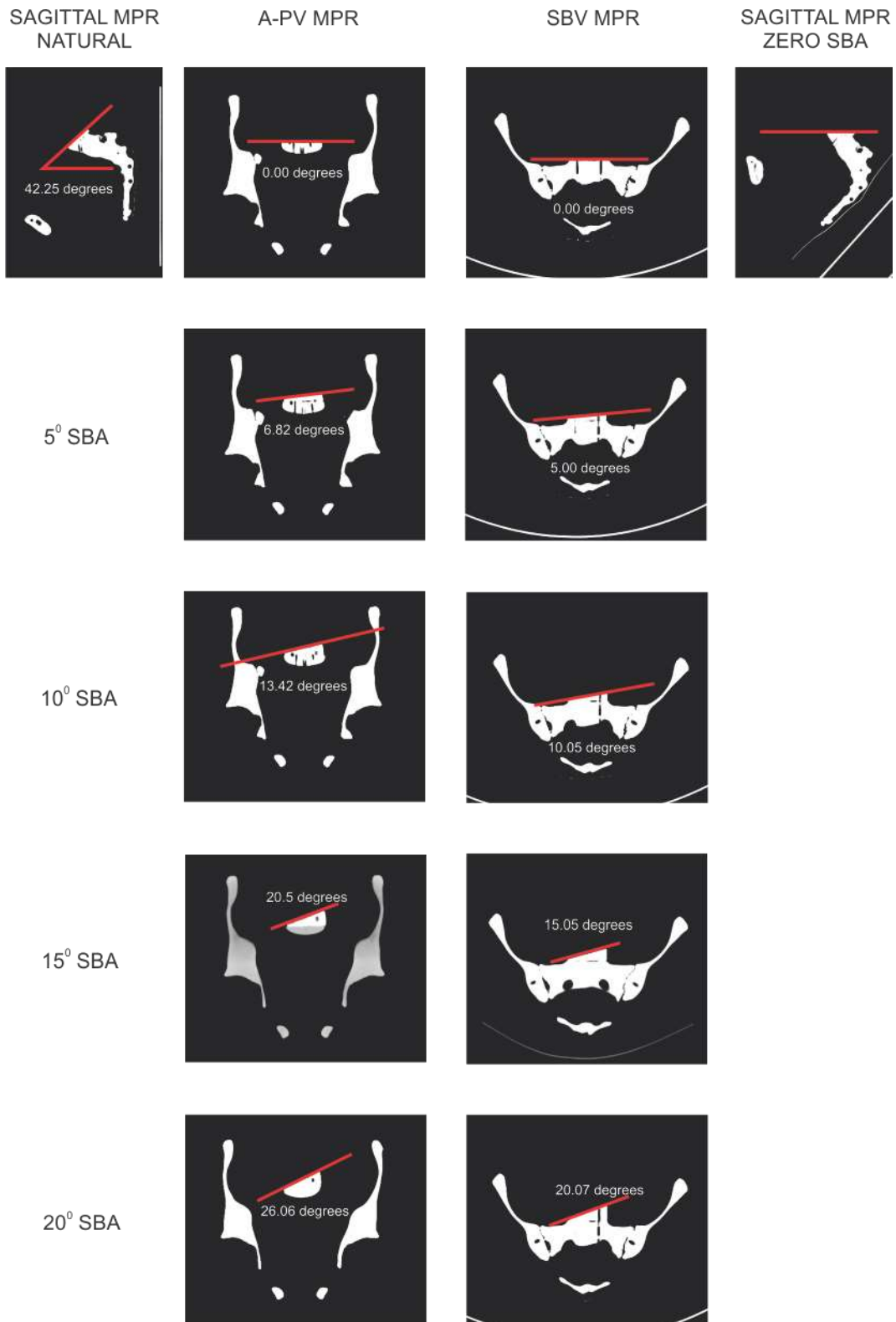
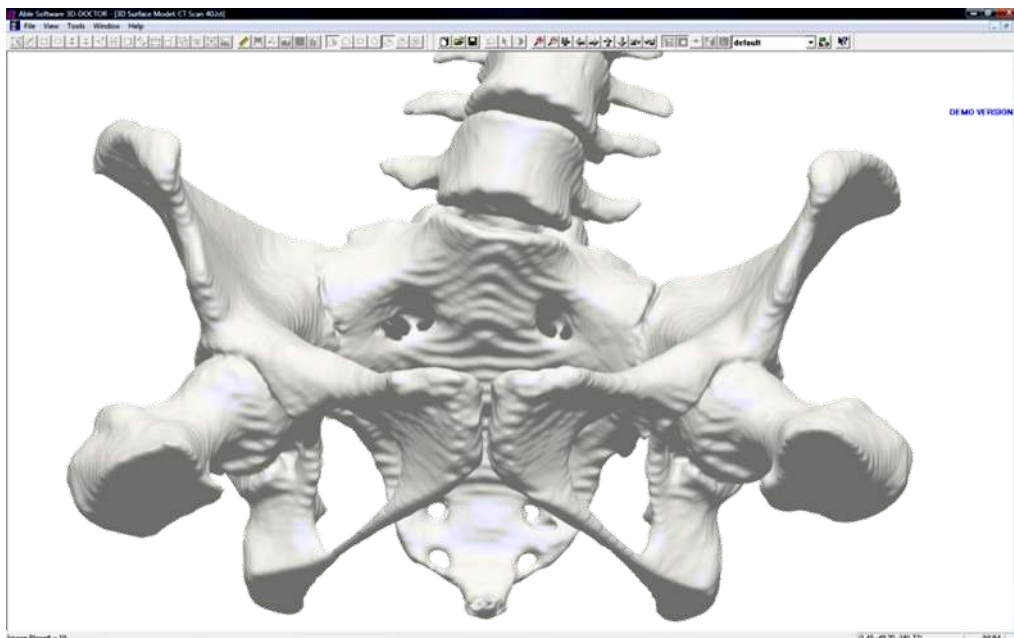


Figure 112. MPR reconstructions of CT pelvic radiographic phantom data sets. Each data set represents one of the five preset sacral obliquity angles 00, 50, 100, 150, 200. The reconstructions were centred on the sacral base with the model either positioned with pelvis orientated as it would be if the subject was in the supine position or with the plane of the MPR perpendicular and aligned to the transverse axis of the sacral base

### 5.3 THREE-DIMENSIONAL VOLUME RENDERING OF SPIRAL CT DATA

Three-dimensional (3D) reconstruction of computed tomography scans using proprietary software (3D-DOCTOR, Able Software Corp. 5 Appletree Lane Lexington, MA 02420-2406, USA) allows volume rendering of selected tissue (Figure 113). The three-dimensional object can be produced by specifying voxels of similar density ranges contained within the selected data set. With 3D reconstruction of computed tomography data, the resulting image can be viewed and manipulated in space as if it was a discrete three-dimensional object that can be positioned and viewed with any combination of rotations or translations about the three primary axes (X, Y, Z) (366).

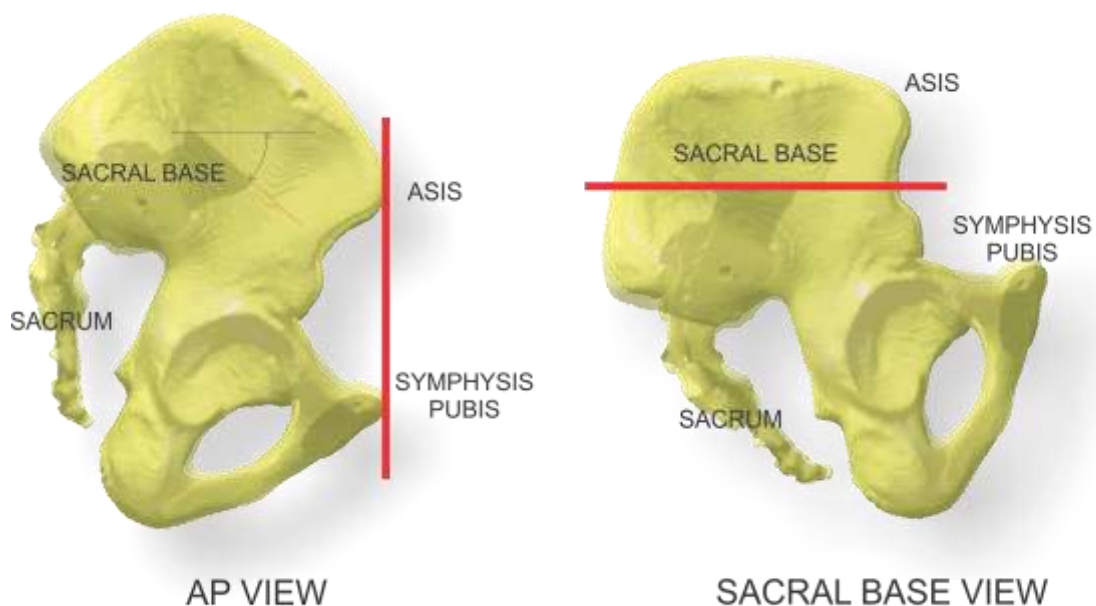


**Figure 113. Reconstructed 3D image generated from a CT data set**

Each data set, comprising a specific number of 2D slices was opened using 3D-Doctor software and saved as a 3D image stack. A region of interest was selected that included as much of the pelvis as was available in the data set. Object boundaries representing the bony structures of the pelvis were selected and volume rendering of the 3D surface was created using the appropriate tools.

The resulting image representing the bones of the pelvis could be manipulated in virtual space as a 3D object with rotation available around three mutually perpendicular axes. The pelvis was viewed in both orientations as an orthographic projection rather than perspective projection. The orthographic projection retained the dimensional and angular relationships of the objects as they were rotated.

Two images representing the pelvis in two different orientations to the viewing plane were created. In one image the pelvis was viewed from the front (coronal plane) as it would be in erect posture while the second image was viewed in the same plane with the pelvis rotated around the X-axis so the plane of the sacral base was aligned to the horizontal plane (Figure 114).



**Figure 114.** The pelvis was viewed from the front in two different orientations to the viewing plane. One represented the pelvis in the erect standing position and the other with the sacral base horizontal

For the A-P view the pelvis was orientated as it would typically be found in upright posture with the anterior superior iliac spine (ASIS) vertically over the symphysis pubis. The 3D model was rotated so there was no rotation around the Y-axis. Rotation around the Y-axis



was considered zeroed when the symphysis pubis was aligned vertically with the mid line of the sacrum (Figure 115).

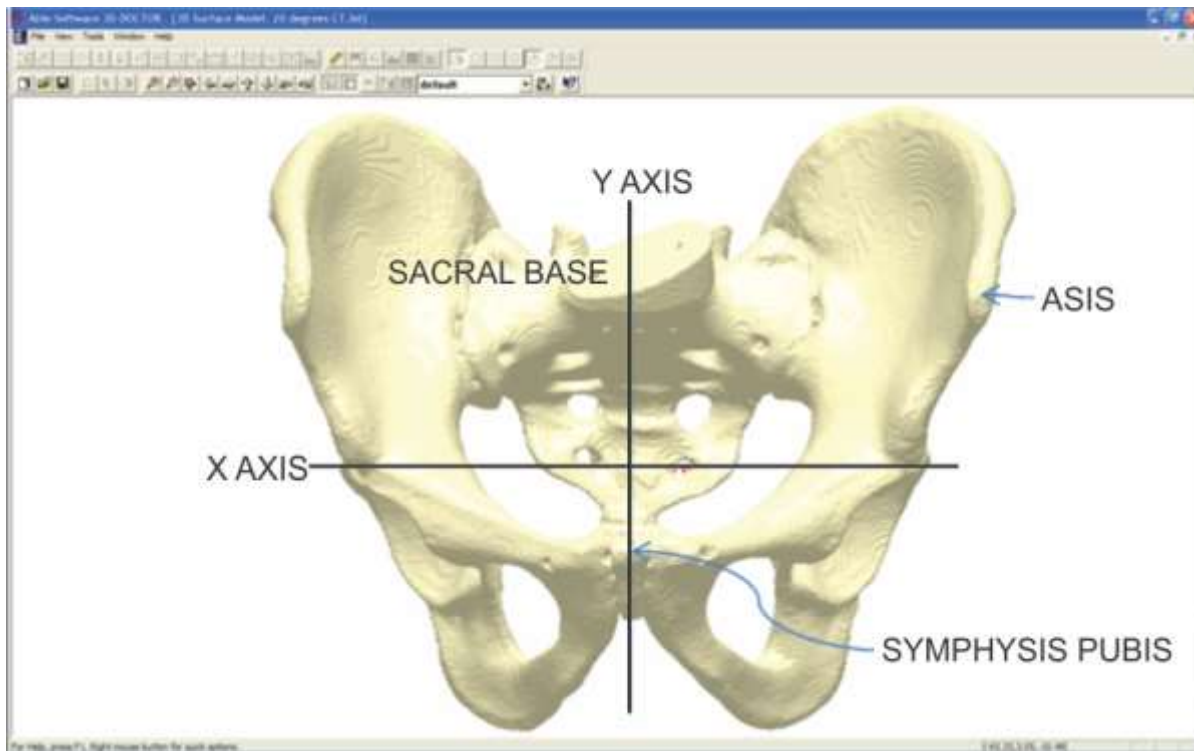
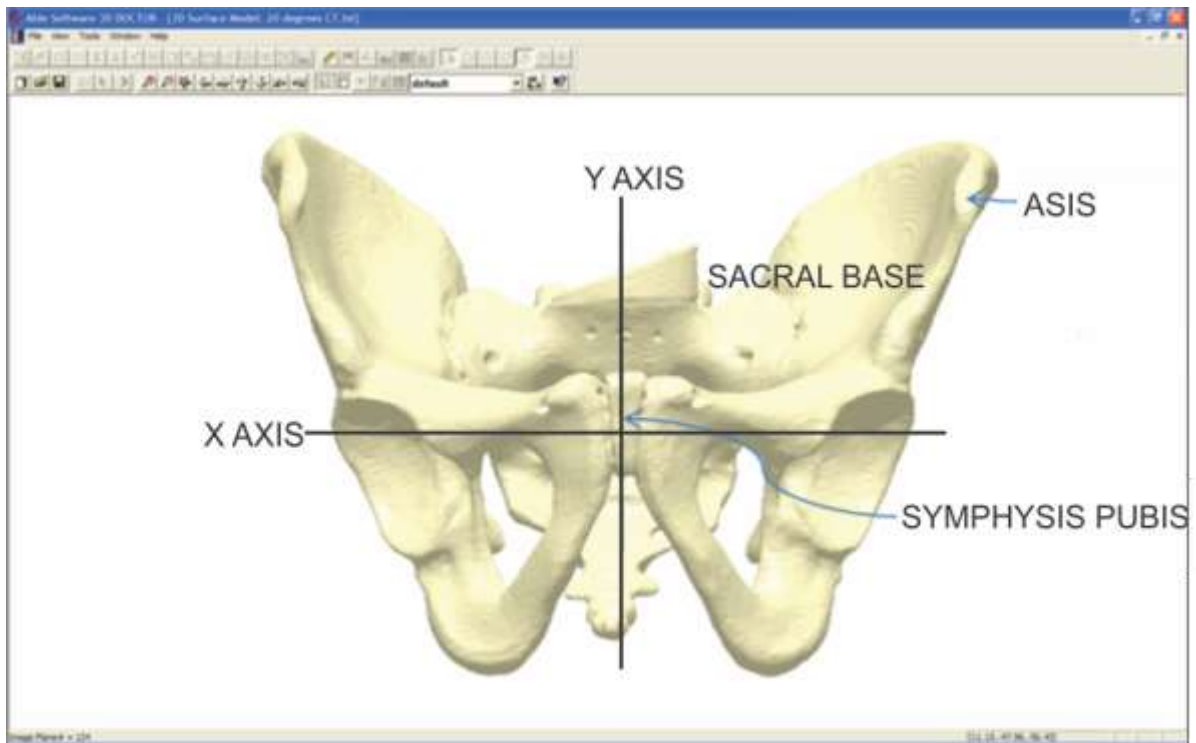


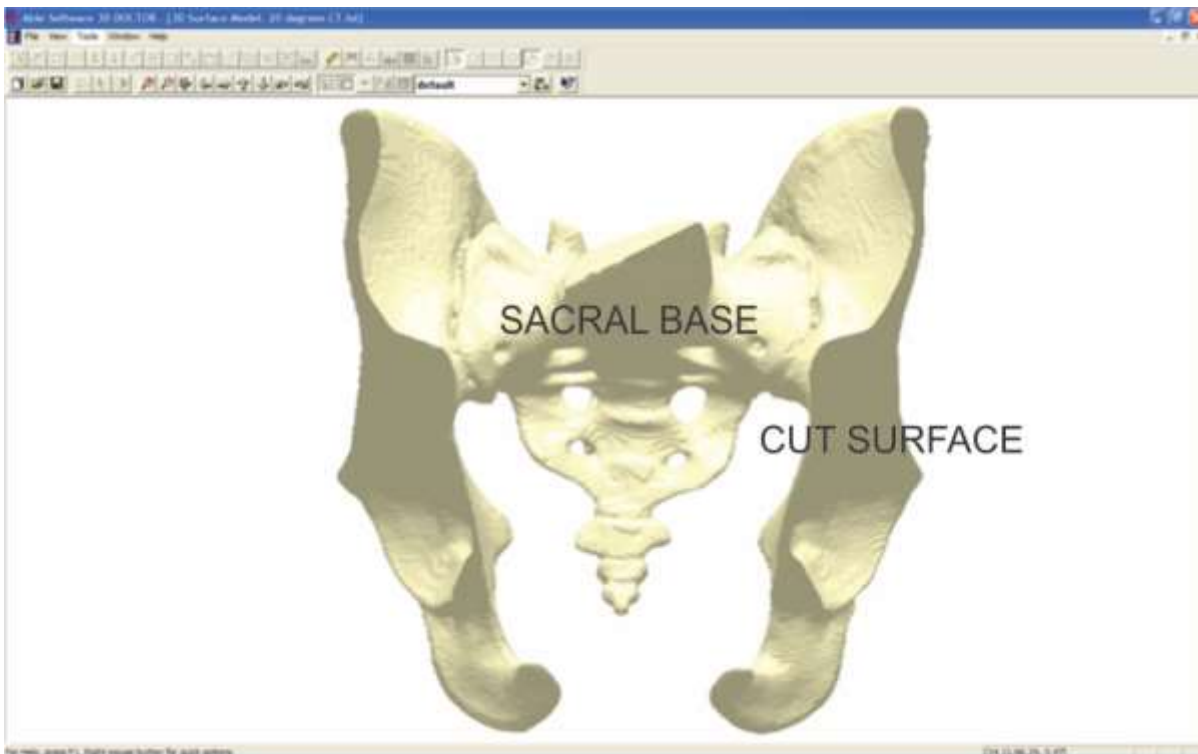
Figure 115. The pelvis was rotated around the Y-axis so that the symphysis pubis was aligned with the plane of symmetry of the sacrum

The second image (sacral base view) viewed the sacrum with no rotation around the Y-axis and the plane of the sacral base viewed as a line with the anterior and posterior edges of the sacral base superimposed. The sacral base in this view was aligned with the Z-axis of the viewing frame (Figure 116).



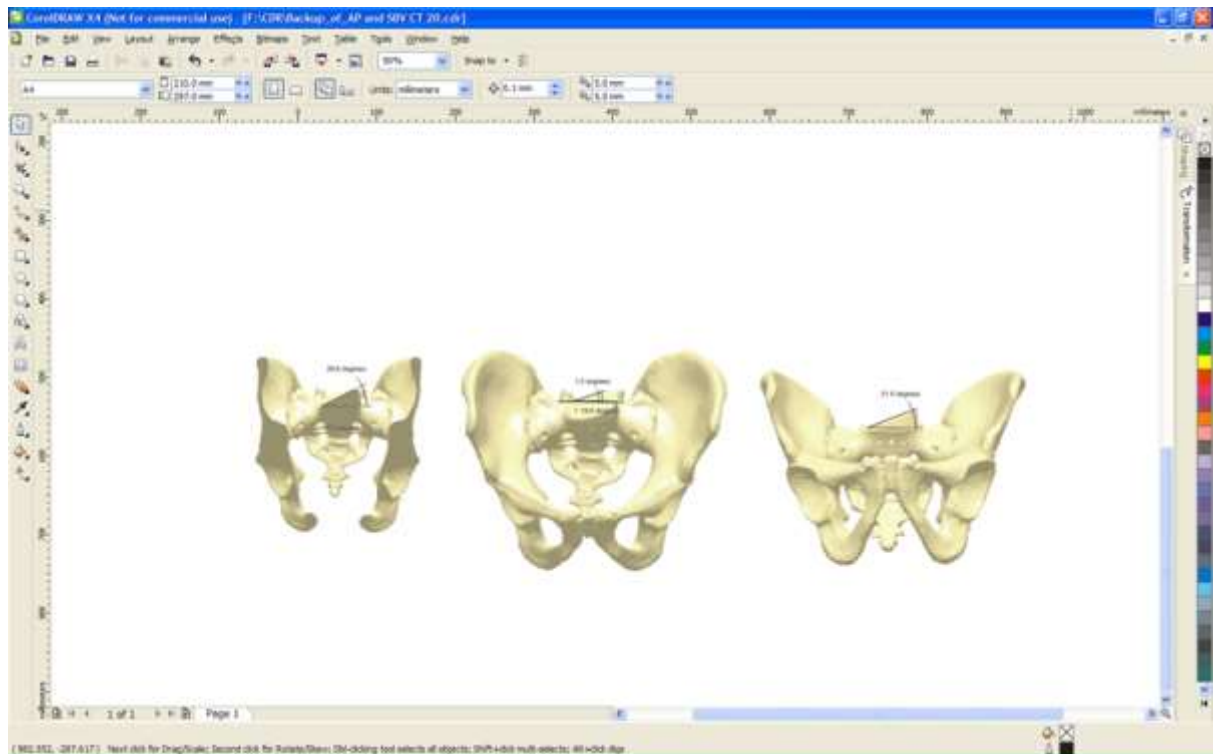
**Figure 116.** The pelvis was rotated around the X-axis until the plane of the sacral base was viewed as a line

A third view (cutting plane view) was produced by positioning a vertical coronal cutting plane to pass through the major axis of the sacral base with the pelvis in the upright position. The resulting images were copied and transferred to CorelDRAW. This process, using Windows clipboard to transfer the image, preserved the aspect ratio of the image but caused the linear dimensions to change. Using this method the angular measurements remained constant and scalable (Figure 117).



**Figure 117.** The cutting plane was used to split the object (pelvis) into anterior and posterior portions through the major axis of the sacral base

Using the tools incorporated in CorelDRAW a line was constructed to represent a tangent to the top of both iliac crests as seen on the three views of the pelvis (AP, SBV, Cutting plane). The angle formed between this line (intercristal line) and a horizontal guideline was measured using the CorelDraw angle dimension tool to an accuracy of one decimal place. The image was rotated so that the intercristal line (ICL) was aligned to the horizontal plane (Figure 118).



**Figure 118.** The angular measuring tool was used to measure the sacral base in the three different views derived from the 3D pelvic model

On the sacral base view a line was constructed representing the plane of the sacral plateau. This was done by joining points placed on the lateral superior aspects of the brim of the sacral base. The included angle formed at the junction of this line and the femur head line (FHL) was measured to an accuracy of one decimal place using the angular dimension tool in CorelDRAW. This angle represented the obliquity of the sacral base in the frontal plane.

The absolute sacral obliquity angle was measured on the sacral base views (SBV) using a similar method described independently by Harrison (239), Barge (78) and Pettibon (284). It involved placing a computer-generated line through points described by these authors. Harrison refers to this line as the sacral plane line (SPL). This name was adopted for the present study. The inclination of the line was considered positive if angled down on the right (+X-axis rotation), negative if angled down on the left (-X-axis rotation) and zero if horizontal. The measurements were recorded and compiled using Microsoft Excel 2007.

### 2.3.3 CT Pelvic Radiographic Phantom MPR + Three-Dimensional Volume Rendering

#### a) Data analysis of MPR based on two different views (APV and ZAV).

Multiplanar reconstructed images of the pelvic phantom with five different orientations of the sacral base in the frontal plane were constructed from CT data. The images were analysed and the measured degree of sacral obliquity recorded and compared in table form (Table 5).

**Table 5. Analysis of MPR CT images of the pelvic model in two different orientations to the viewing plane**

SOA	ZAV	APV	MPR angle
0 degrees	0.0	0.0	34.6
5 degrees	5.0	6.8	34.4
10 degrees	10.0	13.5	34.3
15 degrees	15.0	16.7	34.5
20 degrees	20.0	26.1	34.5

#### b) 3-D Volume rendered reconstruction

3-D Volume rendered images of the pelvic phantom with five different orientations of the sacral base in the frontal plane were constructed from CT data. The images were analysed and the measured degree of sacral obliquity recorded and compared in table form (Table 6).

Table 6. Analysis of CT 3D volume rendered pelvic model

SOA	SOA 3D (0°)	SOA 3D (AP)	MPR angle
0 degrees	0.0	0.0	42.0
5 degrees	5.0	3.9	39.6
10 degrees	10.1	8.7	40.7
15 degrees	15.1	13.4	41.1
20 degrees	20.0	16.3	41.1

#### 5.4 SLOT SCAN (SCOUT VIEW) OF PELVIC RADIOGRAPHIC PHANTOM

CT data sets were obtained that included scout views of the pelvic phantom. The same pelvic radiographic model used to obtain the plain film radiographic images was used to obtain five slot scan digital radiographic (SSDR) images of the model with five different predetermined sacral obliquity angles (0°, 5°, 10°, 15° and 20°) in two different orientations.

##### 5.4.1 Pelvic model positioning

For one of the orientations the pelvic phantom was aligned so that it replicated the supine position a patient would commonly be placed in for a lumbopelvic CT examination. The other orientation was with the sacral base parallel to the x-ray beam. This view was taken in order to measure sacral obliquity when the Y-axis of the sacral base was parallel to the x-ray beam.

The measurement of sacral obliquity on the projected images was not intended to assess the validity of CT imaging in quantifying sacral obliquity by directly comparing the measured value with the actual degree of obliquity present in the model. The primary objective was to quantify the relative difference in the measurement of sacral obliquity between the two orientations of the pelvis relative to the gantry (imaging plane) of the machine (Figure 119).

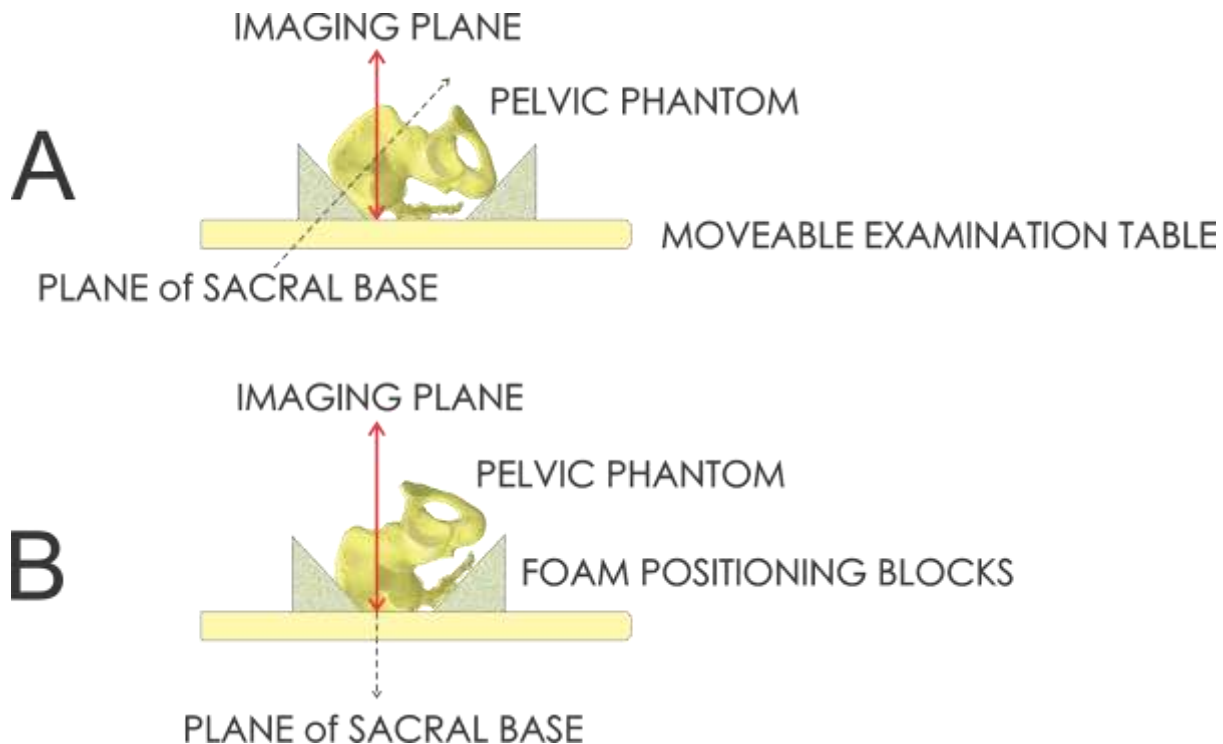


Figure 119. The positioning of the pelvic phantom relative to the plane of the x-ray beam for the two orientations of the sacral base A. Position replicating supine lumbopelvic CT examination B. Pelvic phantom positioned with sacral base parallel to the x-ray beam

The CT scout views taken in the two orientations of the pelvic phantom, involved both A-P and lateral views each with the five different pre-set sacral base wedge angles (Figure 120). A disadvantage of the SPDR generated images when compared with normal CT data acquisition is that the images could not be viewed in any plane other than the orientation the object was in at the time the image was recorded. In this respect the SPDR views are the same as plain film or CR imaging. This disadvantage has been overcome with the development of bi-planar plain film radiography (330) involving orthographic projections or multidirectional SSDR imaging where a three-dimensional computer generated reconstruction of the spine can be constructed from two images obtained simultaneously (325, 329). The measurements were recorded and compiled using Microsoft Excel 2007.

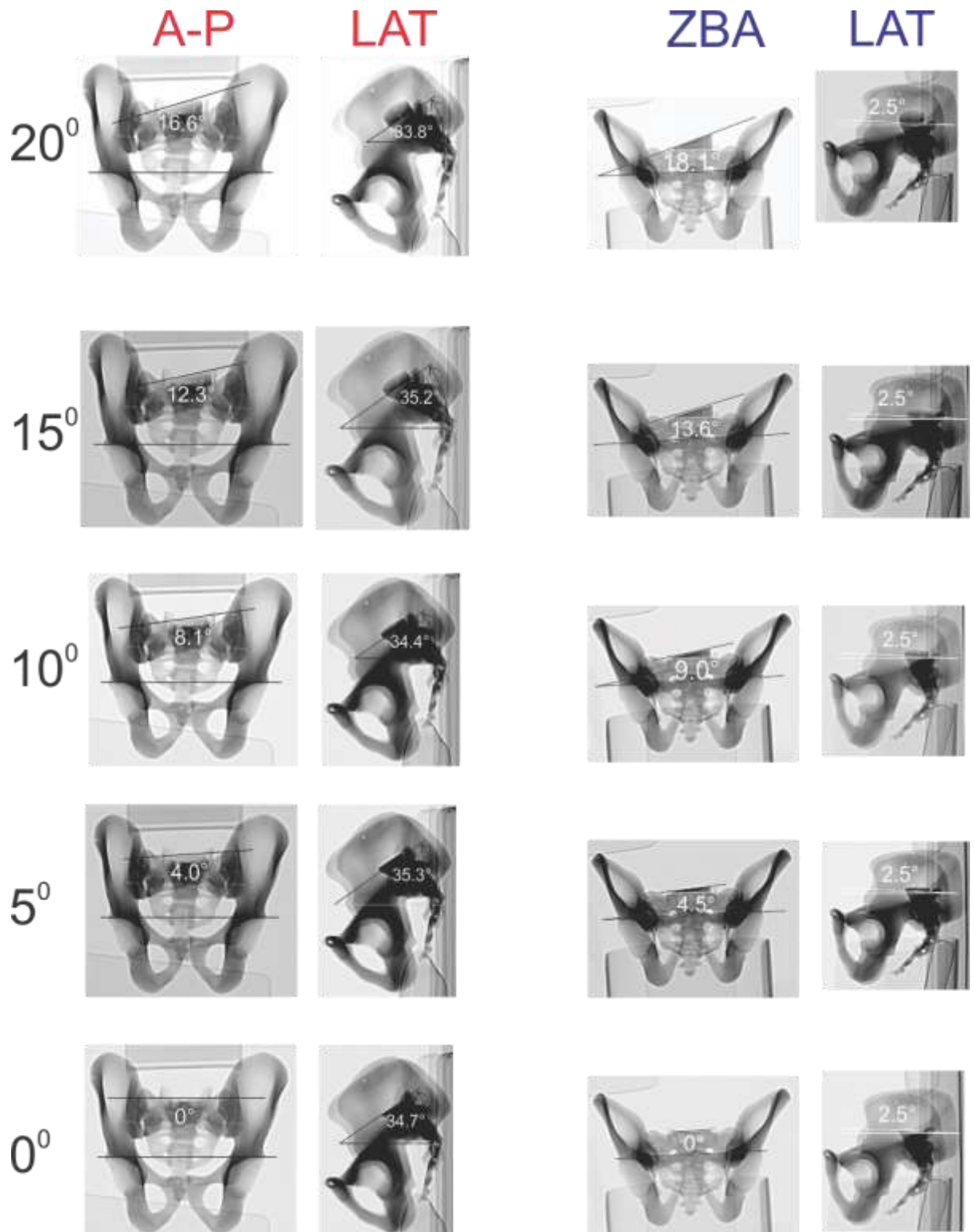


Figure 120. SPDR images of pelvic phantom in supine position with 20, 15, 10, 5 and 0 degree wedges (0 - 20 degrees of sacral obliquity). The four columns represent AP and lateral projections of the pelvis in a typical supine orientation relative to the viewing planes (AP, LAT) (left two columns) and with the pelvis orientated to approximate the sacral base parallel with the viewing plane (ZBA, LAT) (right two columns)



Tables 7 and 8 summarise the measurement of sacral obliquity on slot scan images with the pelvis oriented to approximate the angle the sacrum would be relative to the beam (Table 7) and oriented to represent the sacral base perpendicular to the beam (Table 8).

**Table 7. Slot Scan (SSDR) / CT Scout View of pelvic radiographic phantom in neutral position**

CT Slot Scan Neutral Orientation		
SOA	Measured SOA	Measured SBA
0	0	34.5
5	4.1	34.5
10	8.2	34.5
15	12.3	34.5
20	16.8	34.5

**Table 8. Slot Scan (SSDR) / CT Scout View with approximated zero sacral base angle**

CT Slot Scan Zero Sacral Base Orientation		
SOA	Measured SOA	Measured SBA
0	0	2.5
5	4.5	2.5
10	9.0	2.5
15	13.6	2.5
20	18.1	2.5

Both slot scan views resulted in measurements that were less than the actual degree of sacral obliquity except for zero sacral obliquity. This would be consistent with the projection principles involved in slot scan projections. Magnification occurs only in one plane (transverse) so measured angles are distorted rather than magnified even when parallel to the imaging plane. Inclination of the sacral base in two planes (sacral obliquity plus sacral base angle) increased the difference between the true sacral obliquity angle and the measured angle.

## 5.5 SUMMARY and CONCLUSION

Volume rendered 3D images and MPR reconstructed images of the pelvis offer reliable formats to measure sacral obliquity providing certain protocols are followed in generating

the images used for analysis of sacral obliquity. Slot Scan generated images give less valid measurements of dihedral angles such as sacral obliquity. This is particularly the case when the pelvis is in an orientation that approximates the normal anatomical position.



**SACRAL OBLIQUITY MEASURED ON A GRAPHIC  
MODEL OF THE PELVIS**

## CHAPTER 6

*“To learn to see - to accustom the eye to calmness, to patience, and to allow things to come up to it; to defer judgment, and to acquire the habit of approaching and grasping an individual case from all sides.”*

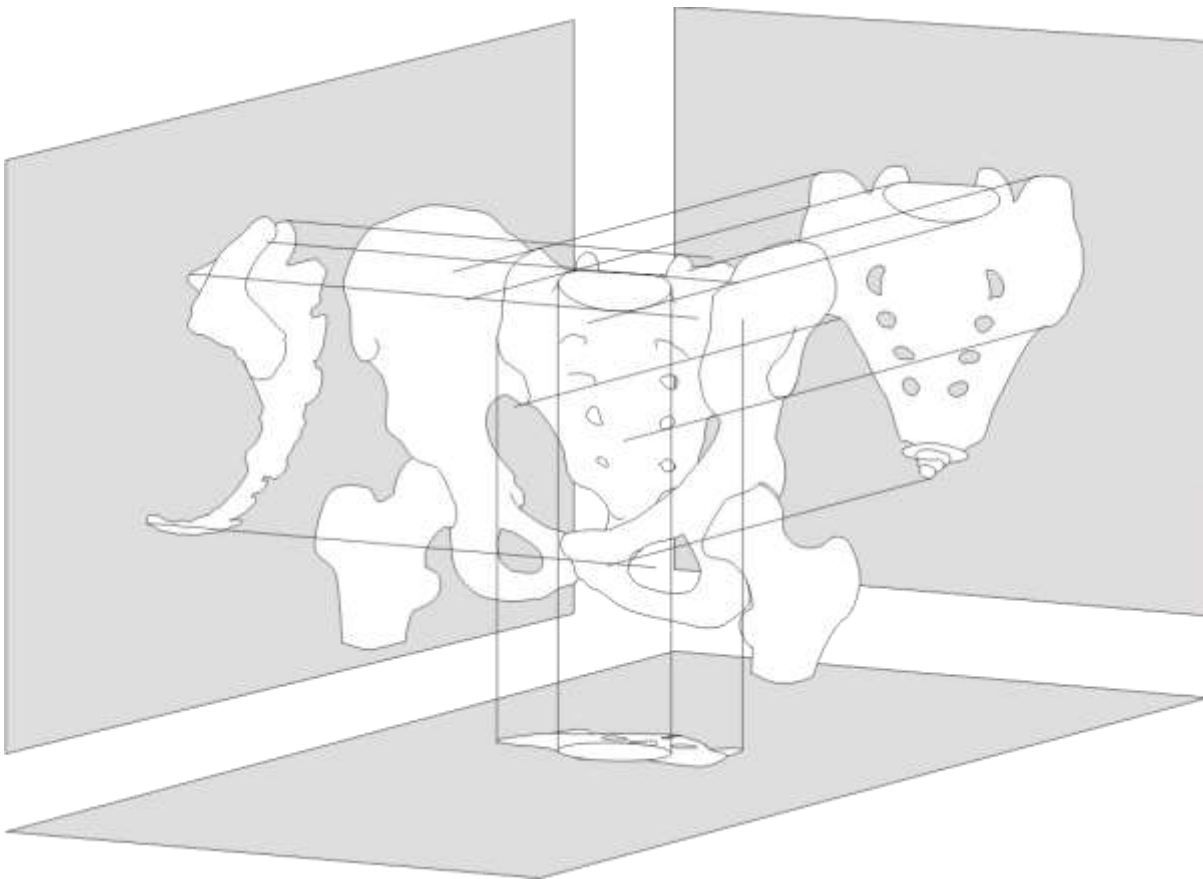
— Friedrich Nietzsche

### 6.1 GRAPHIC MODELS

Descriptive geometry involves the representation and solving of problems relating to the orientation and relationship of objects in three-dimensional space using the principles of orthogonal and projective geometry (20). Descriptive geometry can be used to construct and manipulate an idealised structure in order to measure apparent angles representing surfaces or planes on the structure as they would appear when viewed from various specified directions. The techniques and projection methods of descriptive geometry can be used to measure the spatial relationship between surfaces and objects such as spinal structures with a high degree of accuracy (367).

#### 6.1.1 Orthographic projection

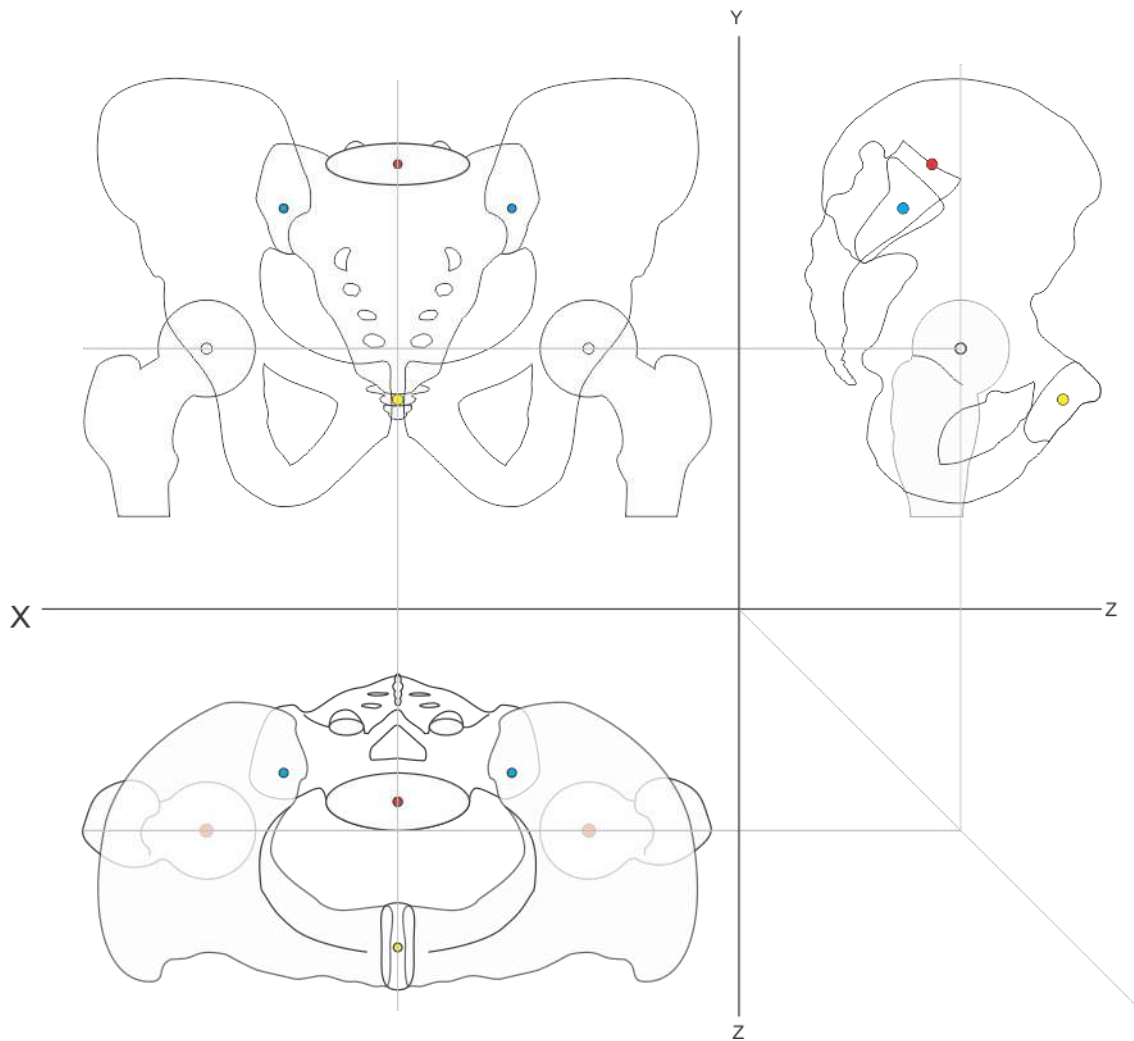
An orthographic projection is a method of representing a three-dimensional object as a line drawing that retains the specific relationships and orientation of the object so that the measurement of distances and angles can be made. The drawing is constructed using parallel projection lines that are perpendicular to the image plane from specific points on the object (Figure 121).



**Figure 121. Orthographic projection of a three-dimensional object onto three mutually perpendicular image planes using parallel projection lines that are perpendicular to the respective image planes**

A systematic arrangement of mutually perpendicular orthographic views of a specific structure or object can be employed to visualise the object with any two adjacent views lying on perpendicular planes of projection. Using these methods an idealised graphical model of the pelvis was constructed using CorelDraw, a computer based vector graphics editing program. The program facilitated the use of descriptive geometry protocols to create an orthographic projection of the three-dimensional pelvic structures and display them as two-dimensional images (20). Orthographic views usually involve a front, side and top view of an object all drawn to scale. Complex objects or specific problems may require auxiliary views to depict true measurements and angles related to the structure. Auxiliary views are obtained by projection of dimensions onto a plane that is perpendicular to one of the three principle planes of projection but is inclined to the other two.

The idealised graphical depiction of the pelvis was drawn with reflective symmetry around the Y-axis in the frontal plane. The graphical model was based on measurements obtained from the radiographic phantom. This basic model was then modified to incorporate specified degrees of sacral obliquity. The model was drawn in different orientations to the image plane to represent A-P and sacral base radiographic views (Figure 122).

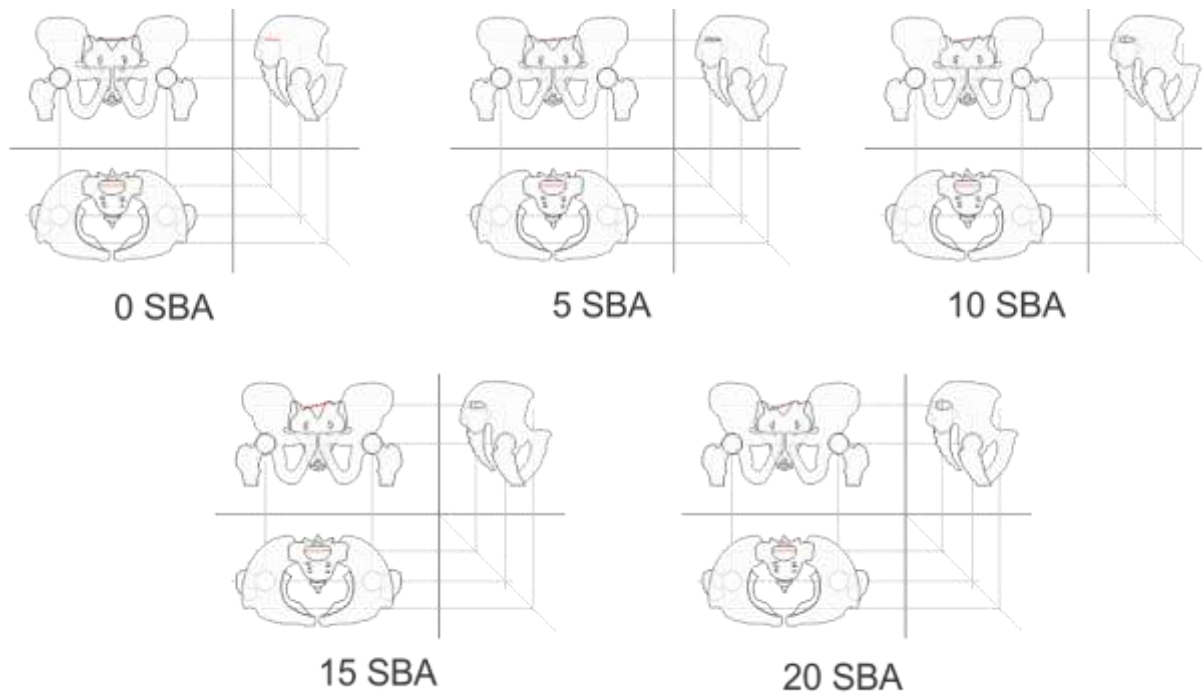


**Figure 122.** Orthographic drawing of an ideal pelvis with the front, top and side views represented by the XY, XZ and YZ planes

#### 6.1.2 Orthographic projection of sacral base

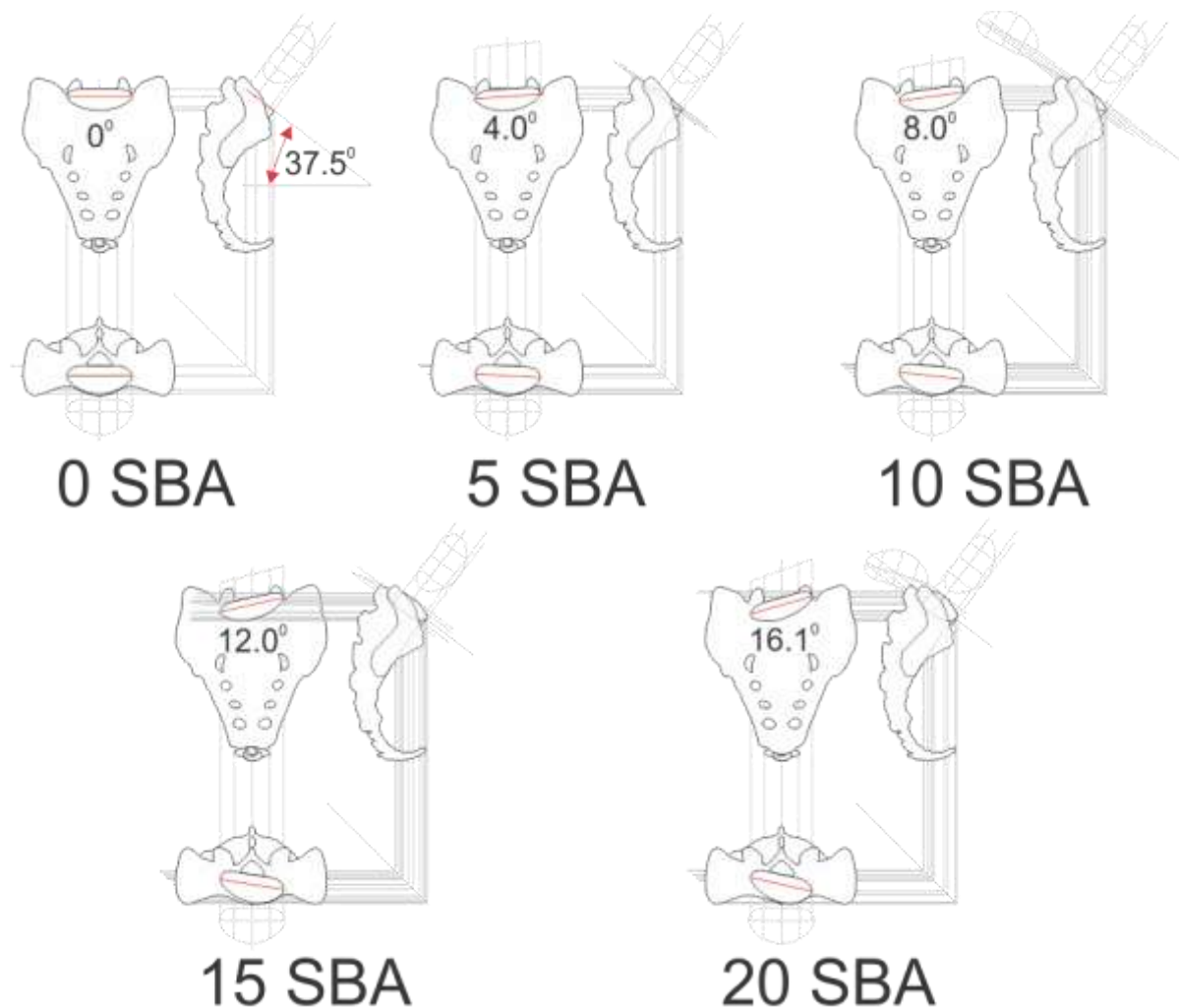
A graphical representation of an idealised sacrum was constructed to scale using approximate sizes obtained from the pelvic model used in the radiographic phantom studies. Two A-P views of the sacrum were constructed with 5 different degrees of sacral

obliquity ( $0^\circ$ ,  $5^\circ$ ,  $10^\circ$ ,  $15^\circ$ ,  $20^\circ$ ). One of the two views of each sacrum represented an orthographic projection of a standard erect front view of the pelvis with the sacral base horizontal (zero angle view) (Figure 123).



**Figure 123. Orthographic projection of the pelvis with the sacral base orientated to the horizontal plane**

The other orthographic view represented five individual sacrums with specified amounts of sacral obliquity ( $0^\circ$ ,  $5^\circ$ ,  $10^\circ$ ,  $15^\circ$ ,  $20^\circ$ ) with the sacral base angle tilted  $37.5^\circ$  to the horizontal (SBA or Ferguson's base angle). The angle of the sacral base was plotted in the front view for each sacrum (Figure 124).



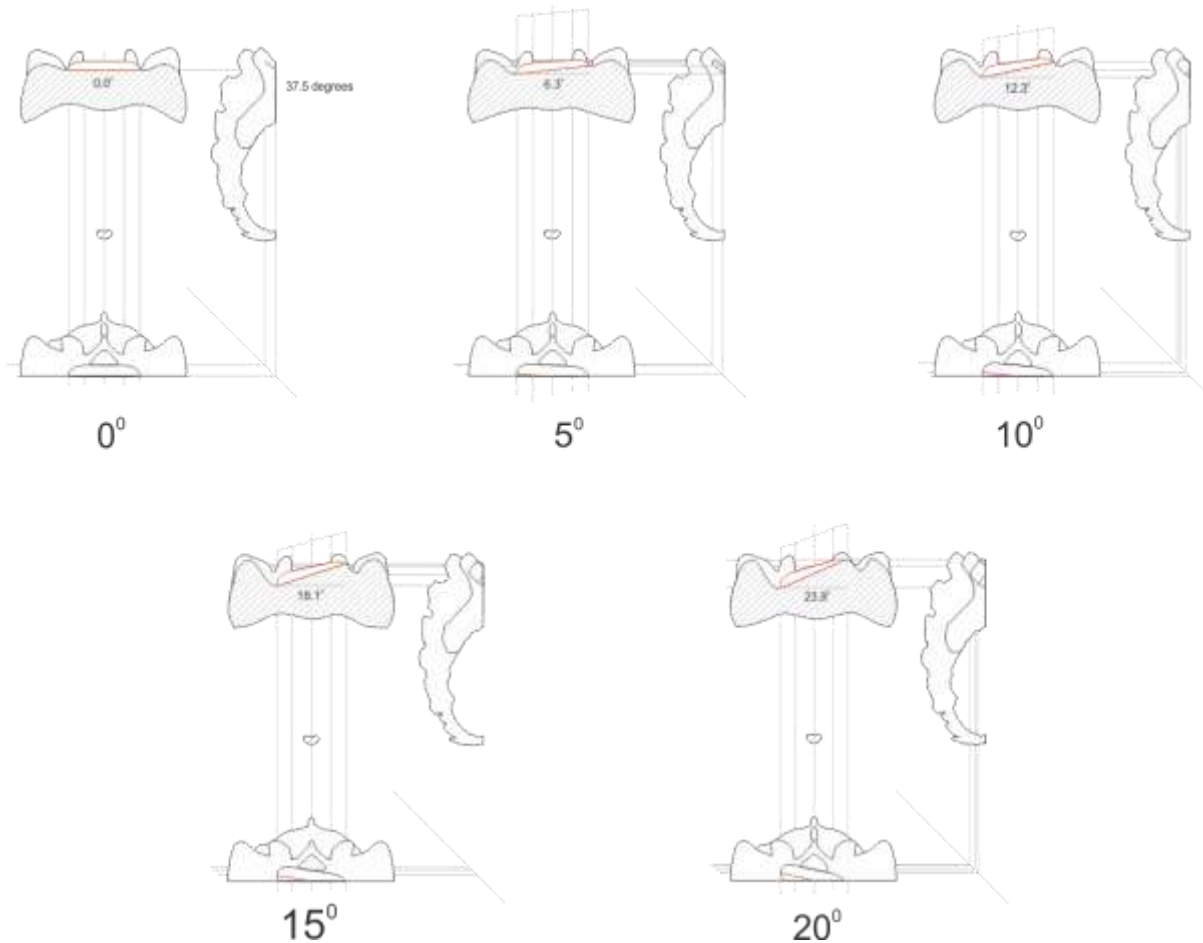
**Figure 124.** Five orthographic projections of an idealised sacrum with 0, 5, 10, 15 and 20 degrees of sacral obliquity and the sacral base angled at 37.5 degrees to the horizontal plane

### 6.1.3 Orthographic projection of pelvic MPR

Orthographic projections of an idealised graphical model of the sacrum were constructed as they would be orientated in erect posture with five different degrees of sacral obliquity (0°, 5°, 10°, 15°, and 20°). The models were drawn with a vertical cutting plane aligned with the transverse axis of the sacral base. This plane produced the same sectional view of the sacrum as would be produced by a multiplanar reconstruction of computed tomography data. The image anterior to the cutting plane was removed and the exposed section drawn in the A-P view. The slope of the cross-sectional view of the sacral base was measured and recorded as the absolute sacral obliquity angle. The sacral base angle for each



projection was  $37.5^\circ$ . This angle was chosen for the sacral projections as it was the same angle used for the plain film imaging of the pelvic phantom (Figure 125).



**Figure 125. Orthographic projection of five sacrum drawn with specified amounts of sacral obliquity (0, 5, 10, 15, 20 degrees) in the erect position (37.50 SBA) as they would appear as a multiplanar reconstruction (MPR)**

Similar orthographic projections of an idealised graphical model of the sacrum with five different degrees of sacral obliquity were constructed with the sacral base aligned to the horizontal plane. A vertical cutting plane was constructed to align with the transverse axis of the sacral base. The slope of the sacral base was measured on the projected image and recorded as the sacral obliquity angle. This view represented the sacral base view of the pelvis with the cutting plane perpendicular to the sacral base. It was the same orientation obtained from the pelvic phantom CT data using multiplanar reconstruction (Figure 126).

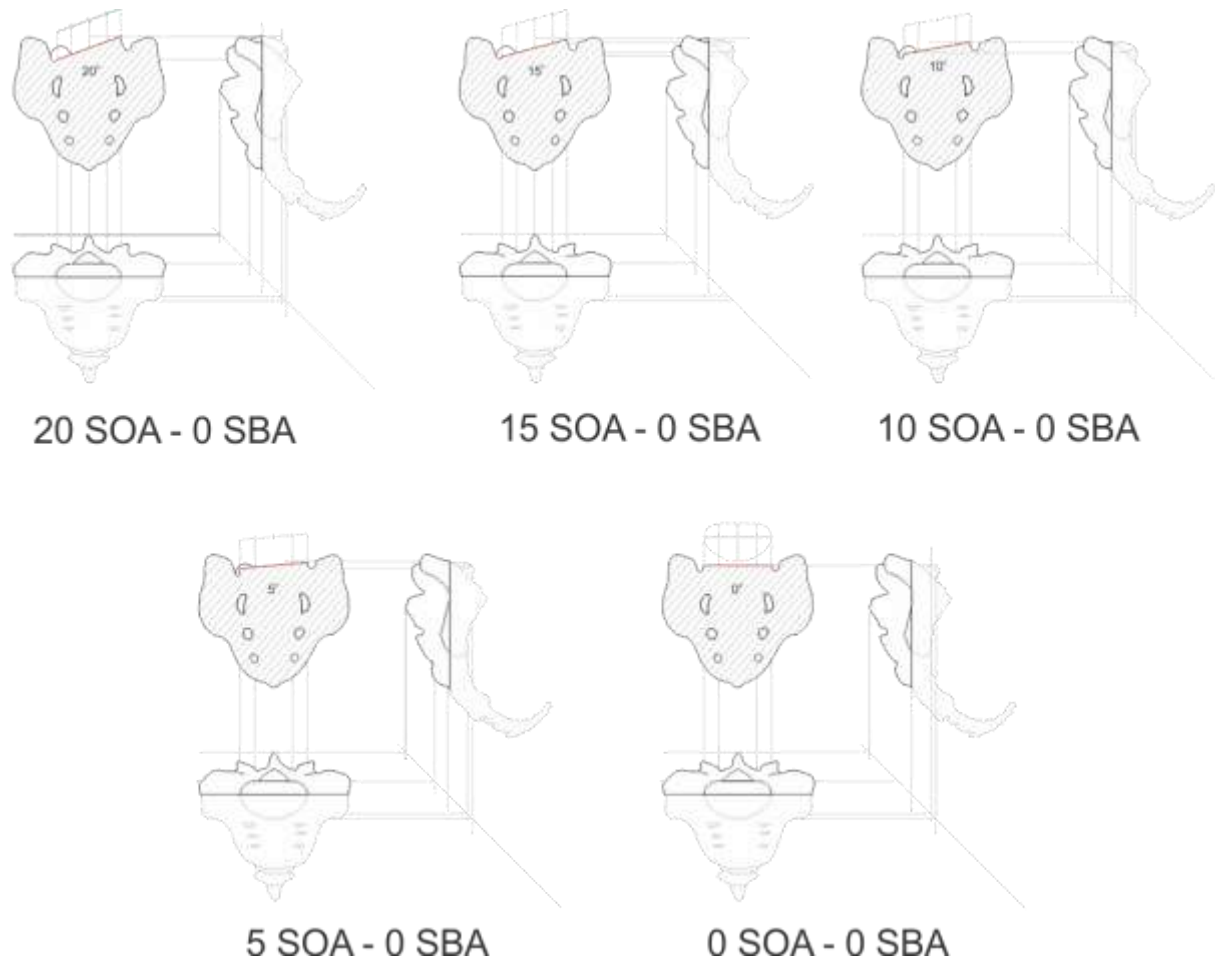
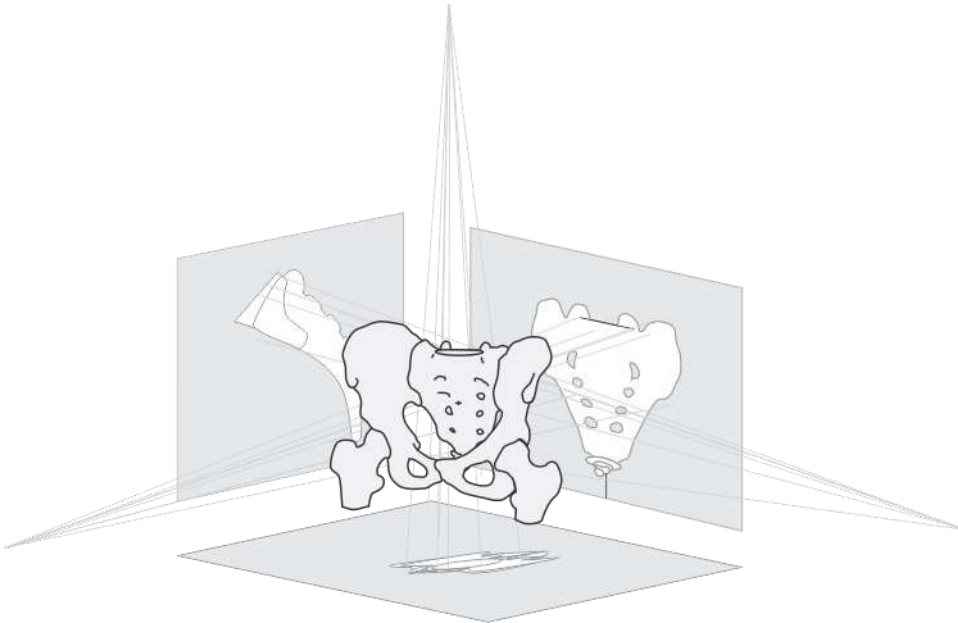


Figure 126. Orthographic projection of sacral graphic model with 00, 50, 100,150, and 200 of sacral obliquity with a vertical cutting plane passing through the transverse axis of the sacral base

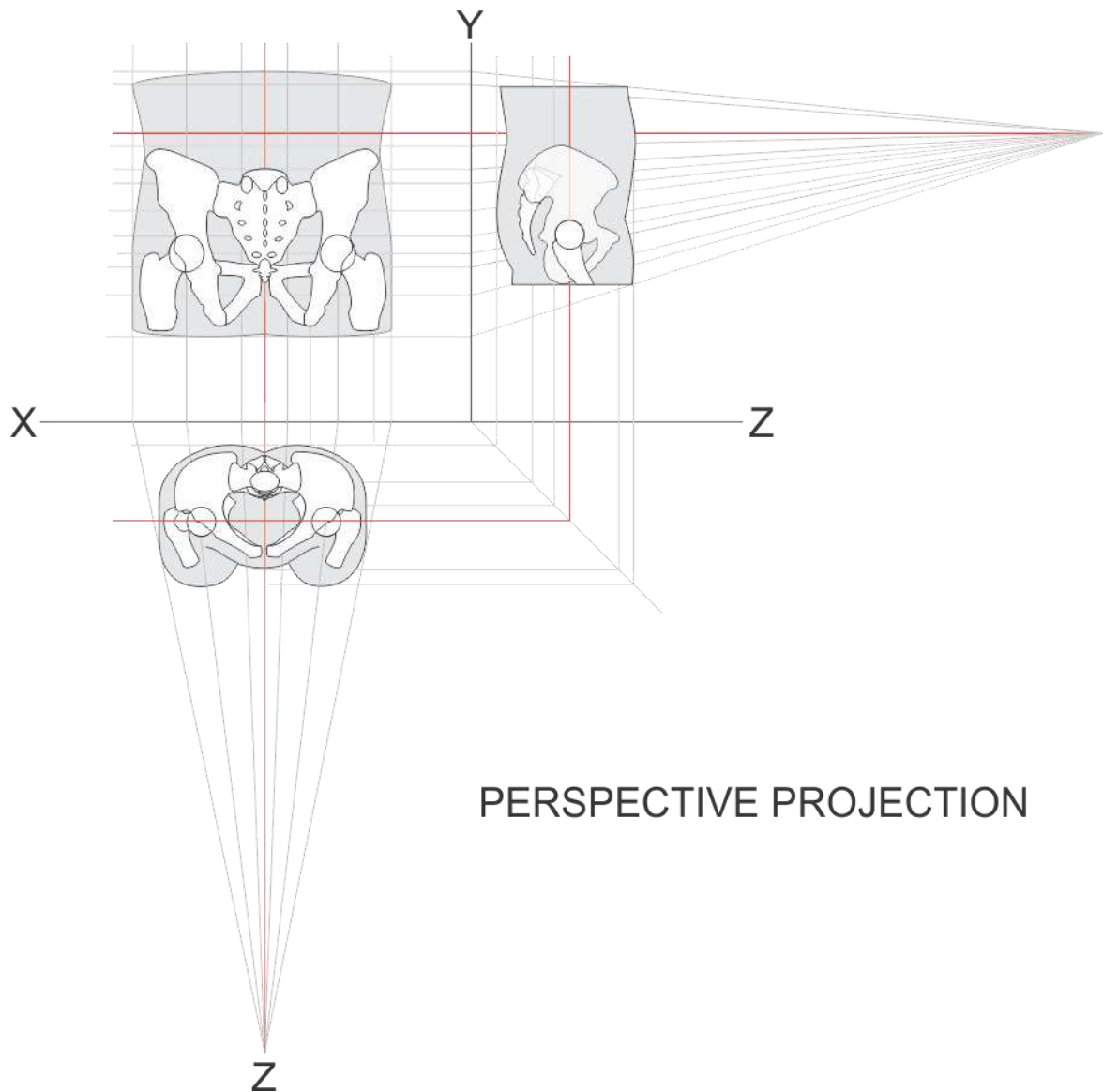
## 6.2 PERSPECTIVE PROJECTION

For perspective projections the projection lines that pass through a specified point on the object emanate from a point source as they would form the focal spot of the x-ray tube in plain film radiography. This descriptive geometry technique lends itself to the graphical analysis of radiographic projection and image formation. The same idealised pelvis and sacrum was used as the basic graphical model. Perspective projection techniques were used to visualise and measure the planes of interest as they would appear on an x-ray image under ideal circumstances (Figure 127).



**Figure 127. Projectional views of the pelvis with the projection lines originating from a point and passing through specific points on the object to form an image on the respective image plane**

Perspective projection, particularly of curved or complex surfaces, produces a realistic or, 'as it would appear', image of the object. This projection inherently causes distortion of angles and distances due to the divergent rays or beam and the position of specific structures relative to the imaging plane. Some surfaces of an object such as elliptical and curved surfaces can only be approximated as definitive points on the image under these conditions (Figure 128).



## PERSPECTIVE PROJECTION

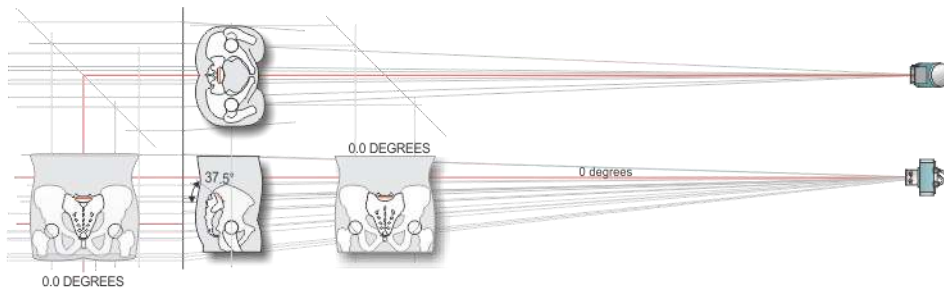
**Figure 128. A-P perspective projection of the pelvis with the side and top views used to construct the image and the origin of the projection lines**

The graphical representation of an idealised pelvis was used in four perspective projections to reproduce the angles that would be measured on different radiographic projections of the pelvis under ideal conditions. These projections involved:

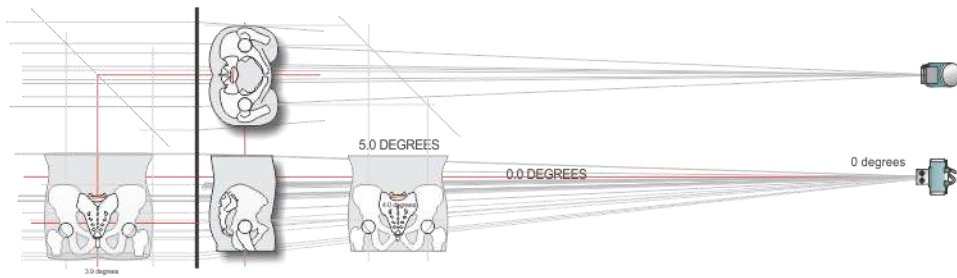
- a) Anteroposterior view (APV) of the pelvis in which the sacral base is angled downward to the front and with no rotation of the pelvis about the Y-axis. The x-ray tube is positioned in the midline of the film and perpendicular to it. The central ray was positioned above the iliac crests (Figure 129).

SOA

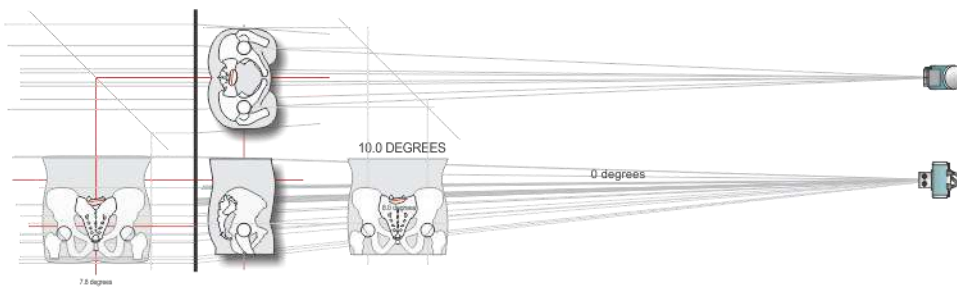
0



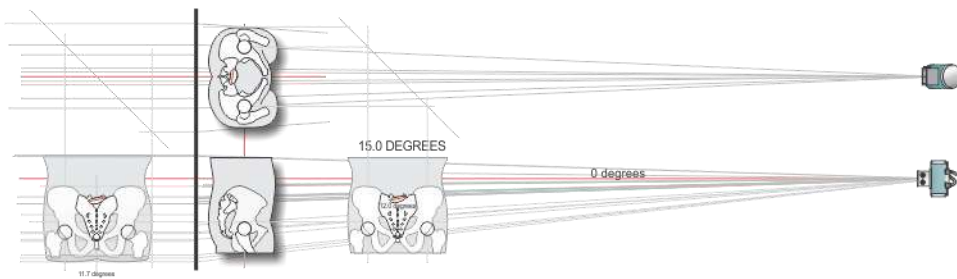
5



10



15



20

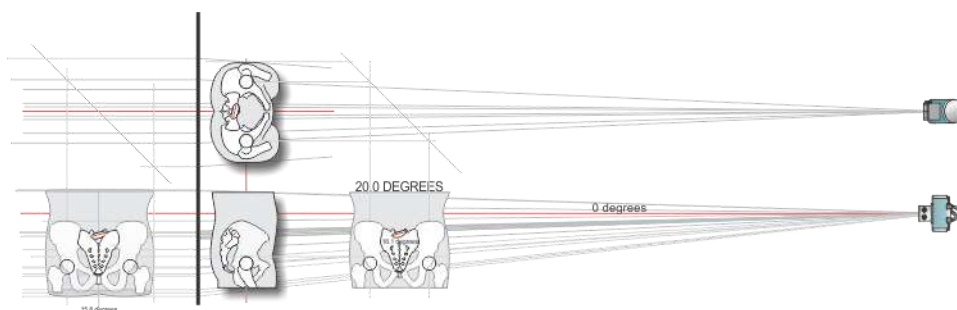


Figure 129. Perspective projection of the pelvis as it would be for an erect AP plain film radiograph. Each image represents a pelvis with varying degrees of sacral obliquity ranging from 0 - 20 degrees of tilt.

- b) For the posteroanterior view (PAV) of the pelvis the projection geometry was the same as for the anteroposterior view with the only variation being the pelvis was facing the image plane rather than facing away from it (Figure 130).

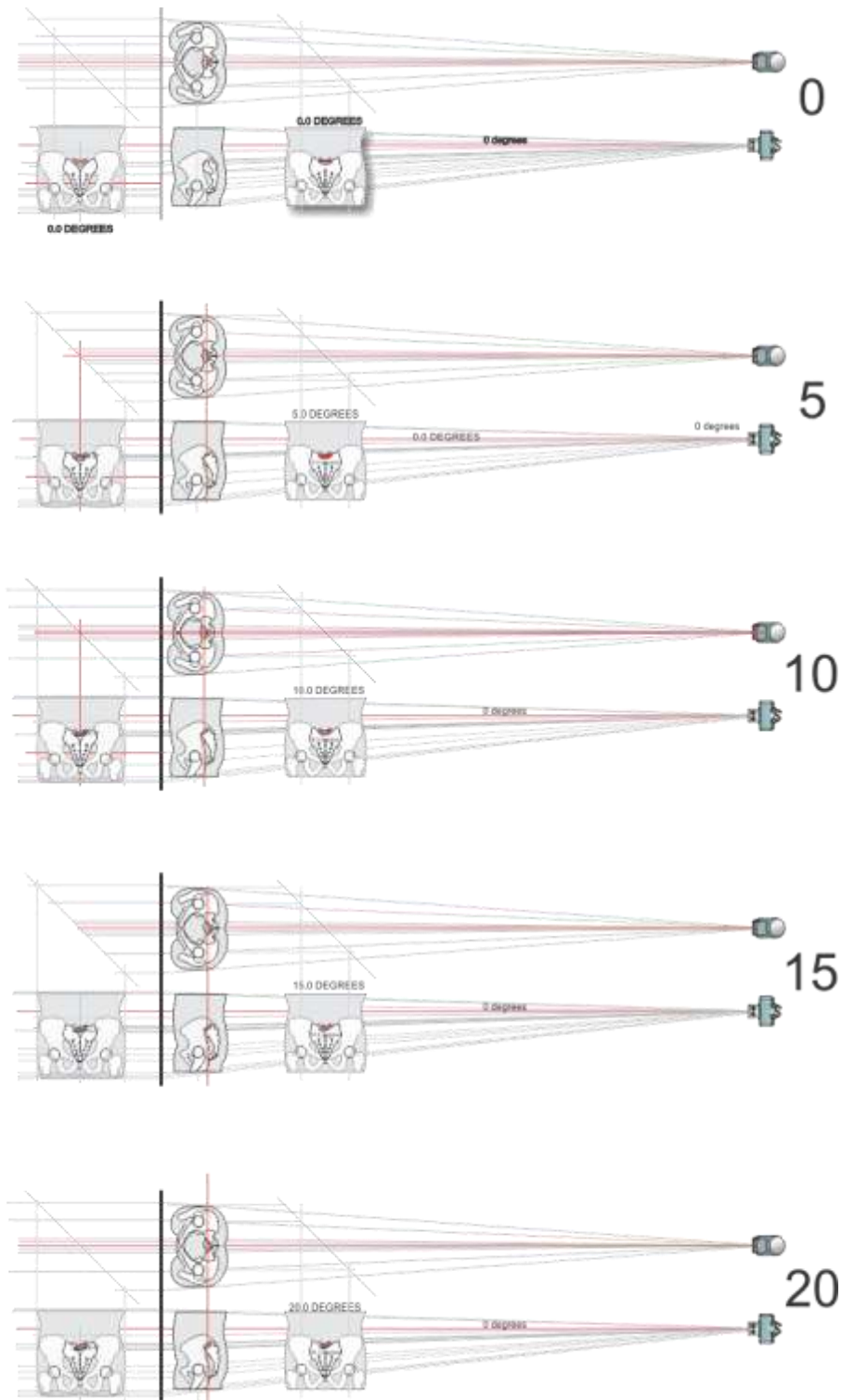


Figure 130. Perspective projection of the pelvis as it would be for an erect PA plain film radiograph. Each image represents a pelvis with varying degrees of sacral obliquity ranging from 0 - 20 degrees of tilt.

c) For the sacral base view (SBV) the pelvis was positioned in the same way as for the APV with the difference being the central ray was aligned with the plane of the sacral base while the pelvis was in the normal erect position (Figure 131).

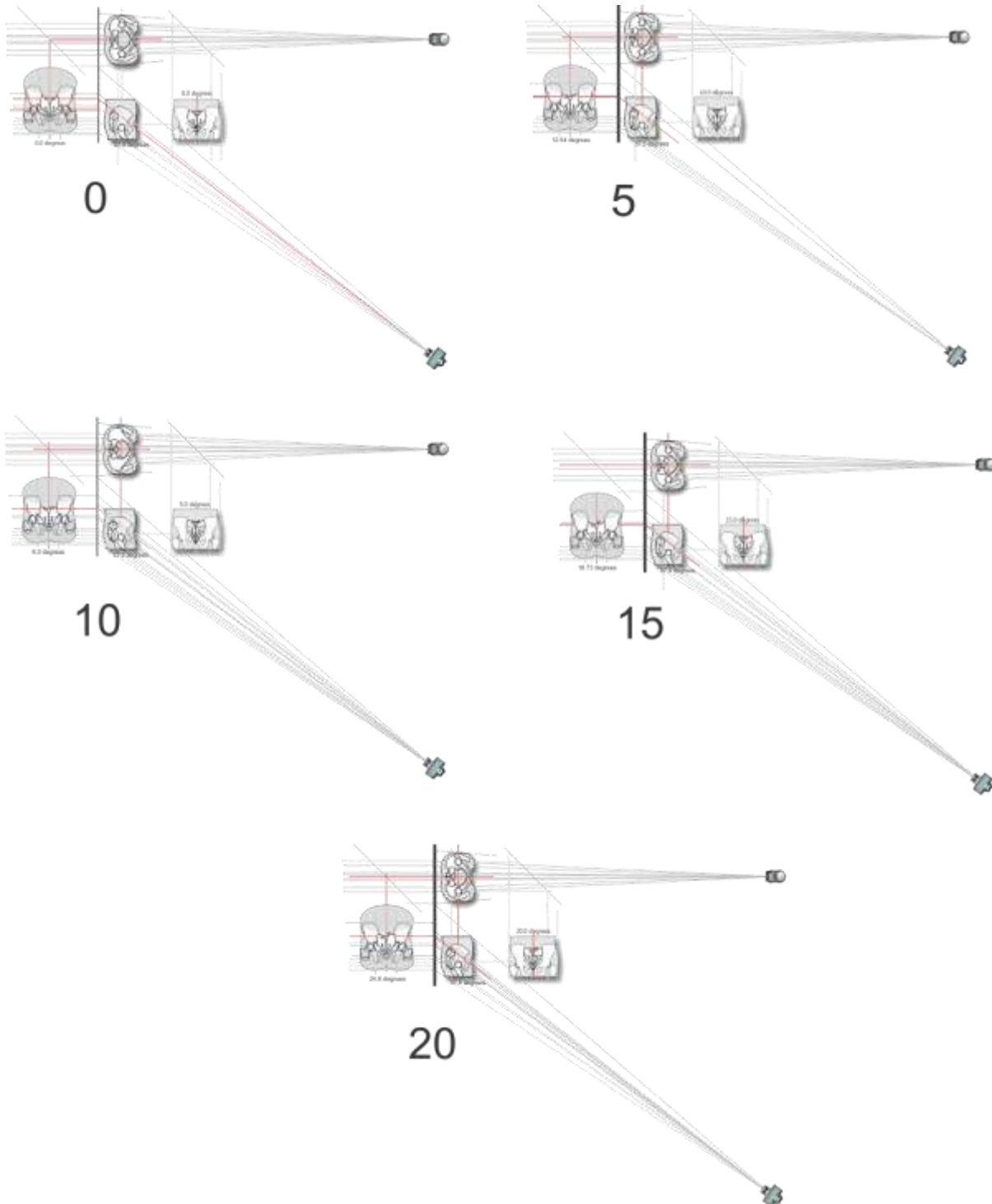


Figure 131. Perspective projection of the pelvis as it would be for an erect SBV plain film radiograph. Each image represents a pelvis with varying degrees of sacral obliquity ranging from 0 - 20 degrees of tilt.

d) The zero angled view (ZAV) was positioned the same way as the APV but with the top of the pelvis rotated backward with the plane of the sacral base horizontal. The central ray was perpendicular to the image plane and aligned to the plane of the sacral base (Figure 132).

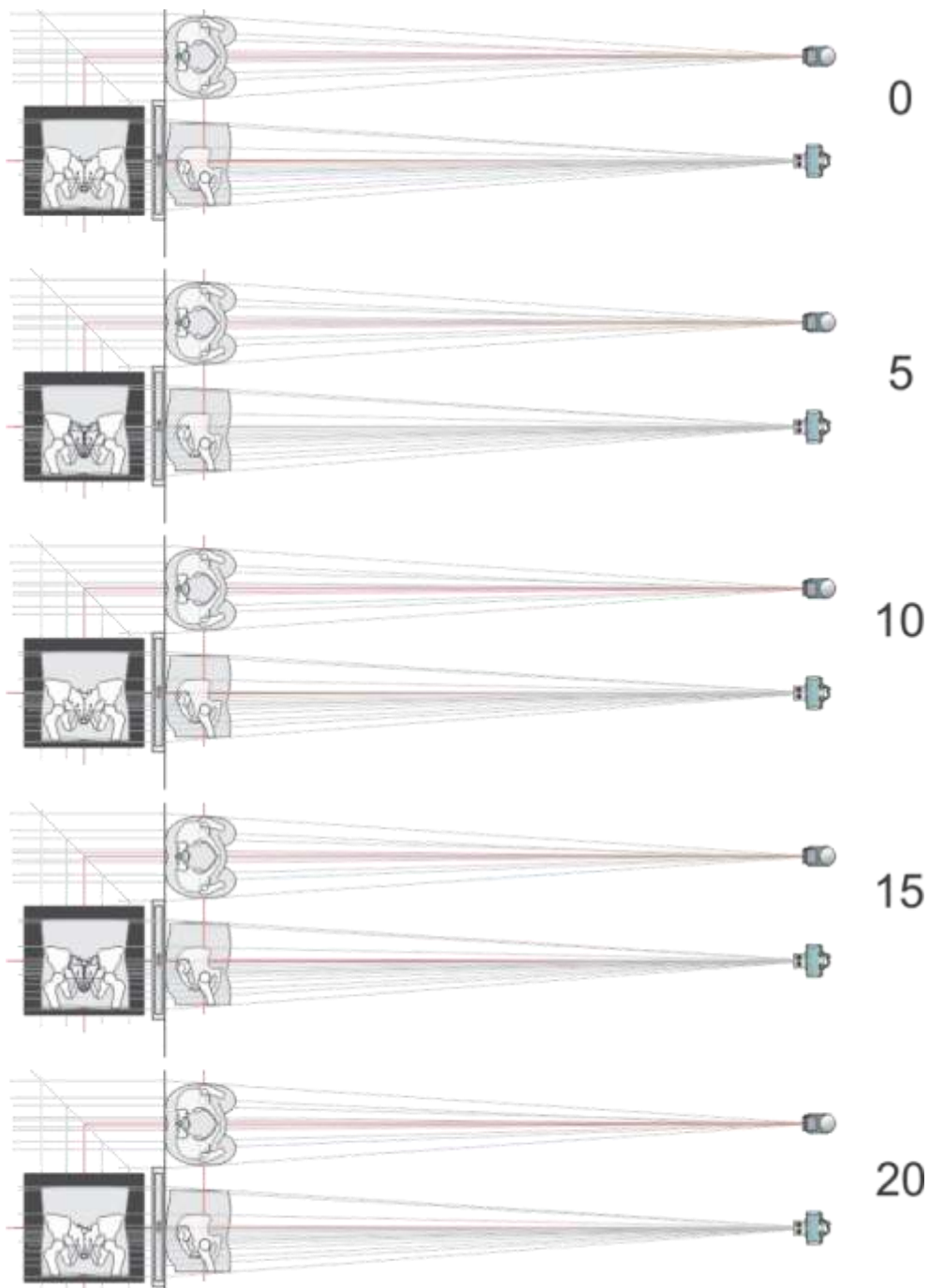


Figure 132. Perspective projection of the pelvis as it would be for a zero angle view (ZAV) plain film radiograph. Each image represents a pelvis with varying degrees of sacral obliquity ranging from 0 - 20 degrees of tilt



## 6.3 DATA ANALYSIS

### 6.3.1 Orthographic projections

Measurements obtained from the graphic model representation of CT MPR at 0, 30, 40 and 60 degree angles of the sacral base relative to the image plane (Table 9).

**Table 9. Graphic model measurements for CT MPR with the sacral base angled at 0, 30, 40 and 60 degrees relative to the image plane**

SOA		0	5	10	15	20
SBA	0	0	5	10	15	20
	30	0	5.76	11.51	17.21	22.8
	40	0	6.5	13.0	19.3	25.4
	60	0	9.92	19.43	28.19	36.05

### 6.3.2 Perspective projections

Measurements obtained from the graphic model representation of four plain film projections of the pelvis (Table 10).

**Table 10. Measurement of sacral obliquity (SOA) made on graphical models representing perspective projections of four different views of the pelvis, two A-P views with two orientations of the sacral base in the sagittal plane and a sacral base view (SBV) and P-A view. Each projection had one of five different angulations of the sacral base in the frontal plane**

Perspective Projections				
Sacral Obliquity	A-P SBA 0°	A-P SBA 37.5°	SBV 37.5°	P-A SBA 37.5°
0°	0°	0°	0°	0°
5°	5°	3.9°	6.3°	4.1°
10°	10°	7.8°	12.5°	8.2°
15°	15°	11.7°	18.7°	12.3°
20°	20°	15.8°	24.6°	16.5°

#### **6.4 SUMMARY and CONCLUSION**

The graphic model was used to provide a theoretical basis for the observed measurement discrepancies of sacral obliquity measured on radiographic images of the pelvis. Using established descriptive geometry principles and the tools of computer aided design graphic software provided an extremely accurate method of quantifying dihedral angles and their projection. The graphical model provided a link between observed radiographic measurements and the purely abstract constructs of trigonometry projection formula (Appendix 1). Projective geometry involves geometric properties that are invariant under projective transformations. They can be represented graphically to portray radiographic projection of skeletal anatomy without the errors associated with the production of radiographic images and their interpretation.

The graphical models of the pelvis in various projectional configurations confirmed the relationship between the measurement of dihedral angles and the true angle that would occur when measuring sacral obliquity on radiographic images (Appendix1).



**SACRAL OBLIQUITY MEASURED ON  
COMPUTED TOMOGRAPHY STUDIES OF  
THE *IN VIVO* PELVIS**

## CHAPTER 7

*“Variation is the hard reality, not a set of imperfect measures for a central tendency.”*

- Stephen Jay Gould

### **7.1 COMPUTED TOMOGRAPHY (CT) OF FIFTY *IN VIVO* LUMBOPELVIC SPINES**

The main objective of this chapter was to determine the distribution of sacral obliquity in a sample population comprising 50 computed tomography (CT) data sets representing computed tomography (CT) studies of the lumbopelvic region of fifty individuals were obtained from a general radiology practice. The data sets were selected by the radiographic practice as a convenient sample of consecutive radiographic studies that met the selection criteria (see below) from their computerised patient data base. They were *anonymised* and transferred to a CD disc at the radiology practice. This process removed all personally identifying information relating to each individual except for age and gender. The data sets were originally obtained on individuals who were patients referred to the radiology practice for non-specified abdominal or lumbopelvic computerised tomography examinations as a diagnostic procedure by a medical practitioner.

The specified selection criteria including requirements as approved by the ethics committee of Macquarie University included the following inclusion and exclusion criteria:

- Each patient was to be over eighteen years of age.
- The pelvic bones had to be visible, including at least part of the symphysis pubis, both femur heads, the sacral base, iliac crests and if possible the ischial tuberosities.
- The patient was not pregnant.
- No individually identifying information was to be transferred. The only data transferred was the digitised CT radiographic imaging data along with the age and gender of each individual.

- There was to be no recent history or evidence of destructive bone disease, fracture or dislocation affecting the pelvis.

A number (28) of the radiographic studies that met the ethics and other selection criteria were unable to be used for the reconstructions after they were obtained from the radiology practice because the structures of interest were not well visualised, not present or were obscured by radio-opaque contrast material as would be present with barium studies of the colon. The data set relating to each radiographic study was transferred to a computer hard drive and given a numerical file name.

#### *7.1.1 Analytical methods*

##### *(A) Multiplanar Reconstruction (MPR)*

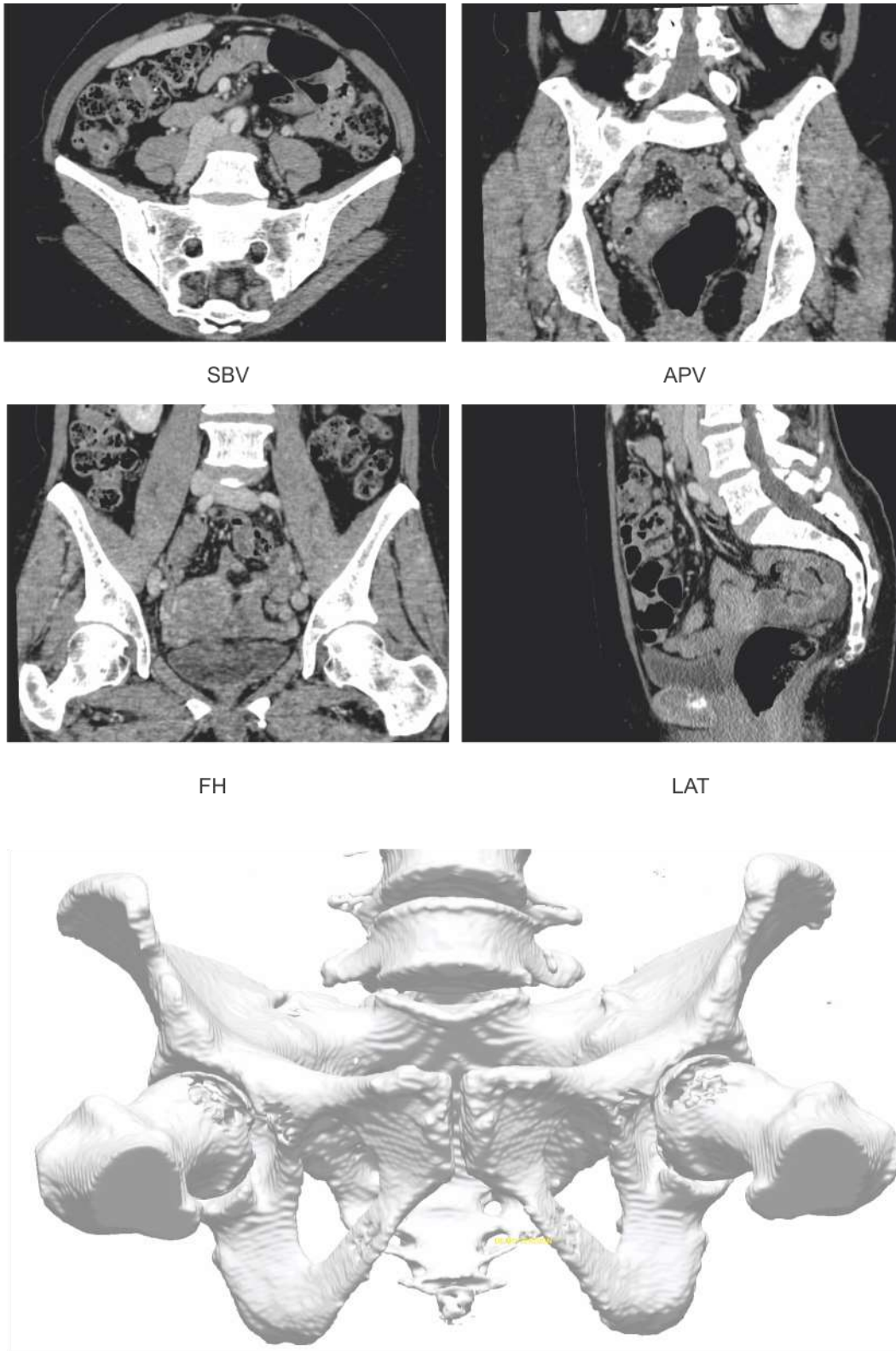
The methods used to manipulate the data and analyse the images were the same as those used for the radiographic phantom. One of the three MPR images involved the cutting plane orientated to be parallel to the bed of the CT machine and represented an A-P supine view of the lumbopelvic spine. The spine and pelvis were in the same orientation to the cutting plane as they were for the examination. Another MPR image was reconstructed from the data set with the orientation of the cutting plane rotated to be perpendicular to the plane of the sacral base and centred on the major axis of the sacral plateau.

##### *(B) 3D reconstruction*

The methods employed to generate 3D images from the pelvic phantom data sets were the same methods used to reconstruct 3D images from the fifty *in vivo* data sets obtained from the radiology practice. Imaging software (3D-DOCTOR, Able Software Corp. 5 Appletree Lane Lexington, MA 02420-2406, USA) was used to construct the 3D image and manipulate the 3D reconstruction in space and make the appropriate measurements. The

process placed the plane of the sacral base perpendicular to the imaging plane and the pubic symphysis in the vertical midline of the sacrum.

Four individual and unique images were reconstructed using predetermined protocols from each set of patient data. Repeated measurements were made with blinding of the observer to the file name that had been used to identify each data set. To ensure blinding of the observer the fifty sets were randomly presented three times for measurement over a three week period. The data sets were randomly renumbered and reordered by an independent observer with the numbering key only available to that individual. The four views were a lateral view (SBA), a multiplanar reconstruction as an A-P view of the pelvis (APV), a multiplanar reconstruction as a zero angle view of the pelvis (ZAV), and a 3D reconstruction manipulated in space to represent a sacral base view (SBV) of the pelvis (Figure 133).



### 3D RECONSTRUCTION

Figure 133. CT imaging data was reformatted as multiplanar reconstructions (MPR) and 3D volume rendering. The two MPR images for each data set represented a standard A-P plain film view and a sacral base view. The 3D image was manipulated around 3 axes of rotation so that the plane of the sacral base was viewed as a line and there was no rotation of the pelvis around the vertical axis.

The relative sacral obliquity angles measured three times on the four views of each patient data set were entered into a spreadsheet (Microsoft Excel) for organization and statistical analysis of the data. The statistical information extracted primarily related to the frequency distribution of the sacral obliquity angles in the selected population. The frequency pattern of an average of the three readings of sacral obliquity measured on the zero angle MPR view for each of the fifty individual sets would indicate if there was a normal distribution within the population possibly due to fluctuating asymmetry and random measuring errors. This pattern would be expressed as a normal Gaussian curve around a mean.

Fluctuating asymmetry has been defined as random differences between the two sides of a morphological trait such as the bilateral symmetry of the upright axial skeleton. The distribution of fluctuating asymmetry would be a normal curve around zero mean.

Bias or directional asymmetry with a right or left shift of the mean involves a significant departure from zero of the normally distributed mean of right and left differences of a morphological trait. Examples in the body would be the chambers of the heart and lobes of the lungs.

Antisymmetry has a zero mean, median and mode but with bilateral variation resulting in bimodal distribution (368) (Figure 134). Palmer and Strobeck (369) suggest that antisymmetry “presumably results from a genetic predisposition of individuals towards asymmetry but, within a given sample, some individuals develop a left bias while others develop a right bias.” The distribution pattern for an antisymmetric trait is bimodal with the frequency of individuals exhibiting right or left bias is roughly equal in the population.



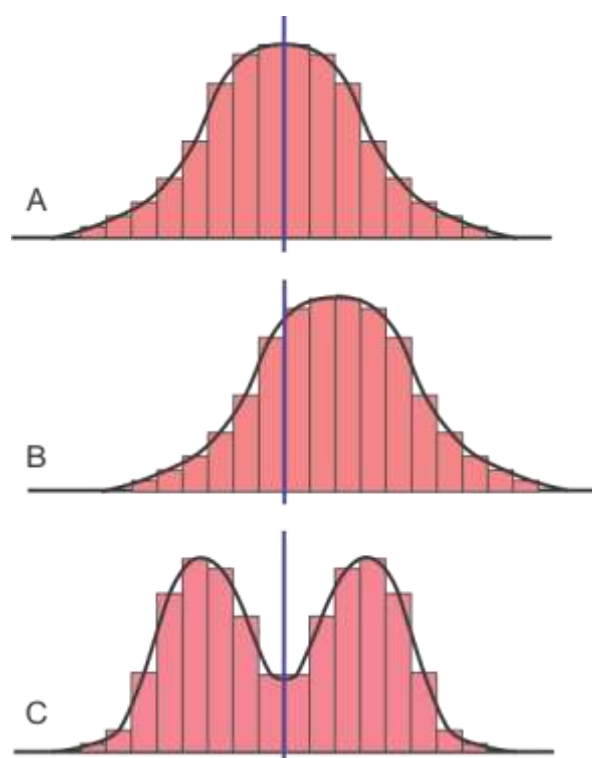


Figure 134. Representation of three different frequency distribution graphs with the zero value illustrated as a blue line that represent fluctuating asymmetry (A), directional asymmetry (B), and antisymmetry (C)

The quantitative measurements were also used to assess the intra-observer reliability of the measurements. This statistical analysis of the data was used to assess the contribution of random error to the frequency distribution pattern.

## 7.2 *IN VIVO* STUDIES OF THE PELVIS USING MPR AND VOLUME RENDERING

A sample of 50 *in vivo* computed tomography (CT) studies of patients referred to a radiographic practice were analysed using multiplanar reconstructions (MPR) and 3D volume rendering. The average age of the subjects was 48.3 years ranging from 21 years of age to 81 years of age and comprised 27 females and 23 males.

The two reconstructions represented a zero angled view (SBV) and A-P view (APV) of the sacral base. A 3D reconstruction of each data set produced a volume rendering of the pelvis with the sacral base level and aligned with the X-axis (3D View). There was no rotation of the pelvis around the Y-axis with the femur heads aligned with the X-axis in the

transverse view. The analysis was carried out three times for each view by the one observer with the mean for each set used to identify the distribution pattern of sacral obliquity (Table 11).

**Table 11.** 50 in vivo CT studies were measured to determine sacral obliquity on two MPR views representing the A-P and Sacral Base views as well as a 3D reconstruction with the sacral base level.

Age	Gender	APV (MPR)	SBV (MPR)	3D
26	M	-5.5	-4.9	-5.2
38	M	-0.9	0.0	0.1
46	F	5.4	4.4	5.3
63	M	11.4	9.5	9.4
54	M	-2.7	-1.9	-1.6
28	F	-5.0	-4.6	-4.6
35	M	-3.3	-2.2	-2.1
51	F	-5.1	-4.2	-5.0
44	M	-4.0	-3.6	-4.0
43	F	0.9	0.8	-0.2
56	M	1.0	0.9	0.5
37	M	-1.1	-1.0	-2.2
28	F	-0.9	-0.8	-1.4
70	M	2.0	1.7	1.7
55	M	-1.6	-0.9	0.7
59	F	0.9	0.3	0.4
76	F	5.4	5.1	5.1
72	M	4.2	3.8	4.1
51	M	-3.6	-2.7	-2.5
46	M	5.4	5.0	3.9
44	F	-3.7	-2.5	-2.5
50	M	1.0	0.4	0.8
58	M	-2.2	-1.9	-1.8
31	F	0.0	0.0	-0.4
34	M	0.9	0.8	0.5
23	F	4.2	3.4	3.7
37	F	-1.4	-1.3	-1.1
38	M	3.2	2.4	2.8
35	M	-5.7	-4.3	-4.4
44	M	2.0	1.2	2.1
57	F	-0.7	-0.2	-0.4
57	F	0.0	0.0	-0.3
39	M	4.7	4.0	3.6
73	F	2.2	2.1	2.4
42	F	1.9	1.1	0.9
50	F	-3.3	-3.2	-2.8
55	F	3.5	3.3	3.9
51	F	-2.6	-2.0	-1.8
22	F	-1.7	-0.9	-1.3
68	F	4.4	2.5	3.1
61	M	-2.2	-1.1	-0.8
28	F	0.0	0.0	1.1
37	F	-2.3	-2.2	-2.2
64	F	-5.4	-3.1	-3.0
65	F	1.0	0.7	0.5
21	F	2.7	1.9	2.5
36	M	2.1	1.1	2.9
66	F	-3.3	-2.5	-2.6
81	F	-4.7	-3.3	-2.6
70	M	-1.9	-1.7	-0.8

The average for SBV data set was used to create a graph with results of sacral obliquity measurements arranged in the order of magnitude (Figure 135).

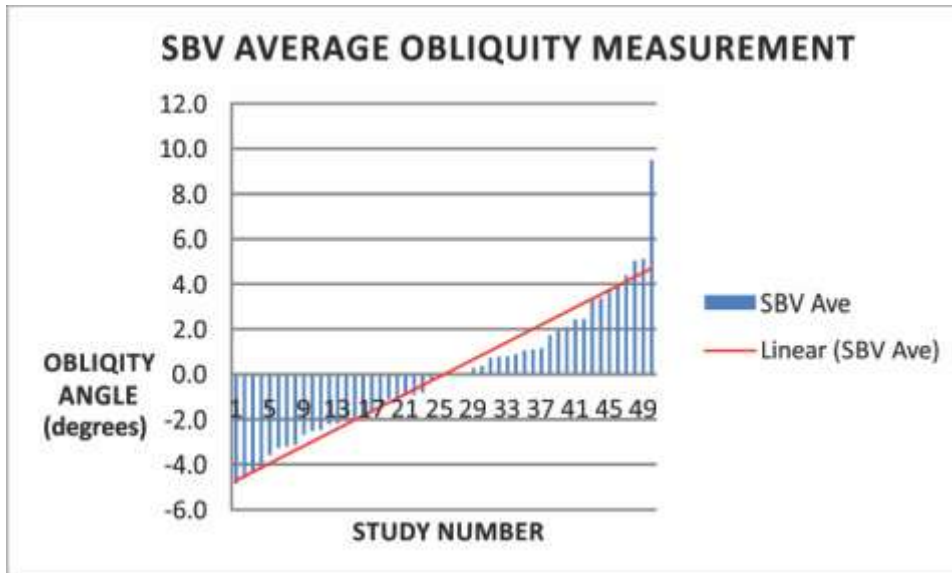


Figure 135. Average measurement of SOA (in degrees) from the analysis of 50 CT data sets on three occasions by one observer. Minus values on the left and plus values on the right arranged in order of magnitude.

Frequency distribution histogram of sacral obliquity in the study population (Figure 136).

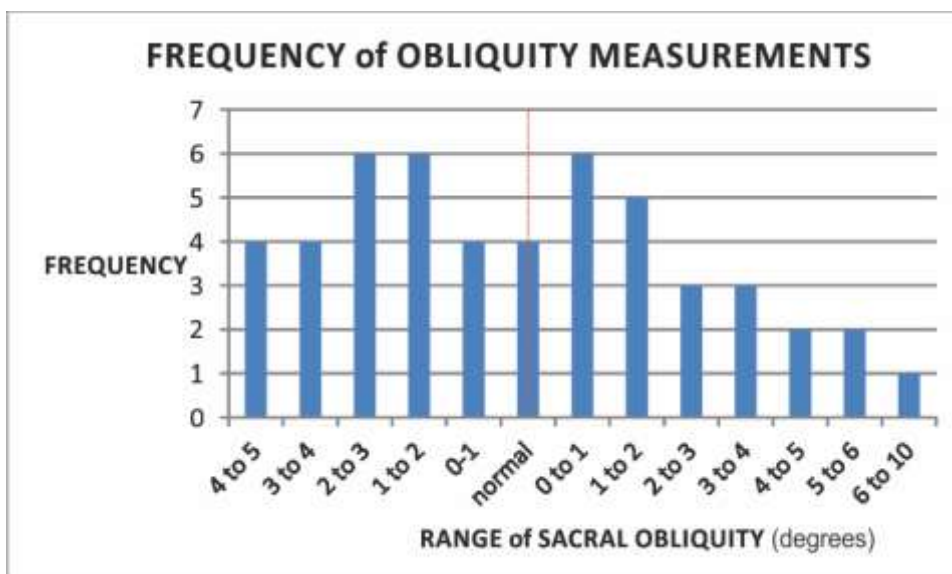


Figure 136. Frequency of CT MPR (SBV) cases (n=50) in groups representing one degree intervals with negative values on the left and positive on the right. Red dotted line represents value for mean, median and mode (zero).

### 7.3 SUMMARY and CONCLUSION

Statistical analysis of 50 computed tomography (CT) data sets to determine the frequency distribution of sacral obliquity in a sample population suggests a departure from symmetry that is a bimodal pattern of sacral obliquity that represents antisymmetry. It has been suggested by Palmer *et al* (370) that antisymmetry can range from quite conspicuous to subtle and hard to detect. Antisymmetry is characterised by a zero mean, a bimodal  $l_i - r_i$  distribution and unpredictable side of laterality.

If symmetry with a normal distribution pattern was observed in the frequency pattern of the data it could have represented fluctuating asymmetry or *developmental noise* (371), random error in the measurement of obliquity or a combination of both of these factors. A symmetrical pattern if established would imply a normal or ideal mechanical orientation for the sacral base in upright posture around which variation occur justifying clinical intervention.

Directional asymmetry of the sacral base would represent a departure of the mean of the frequencies of sacral obliquity offset to either left or the right. Examples of directional asymmetry around the sagittal plane of the body are the number of lobes of the lungs on either side and chambers of the heart. In the sample studied the mean, mode and median were all zero. The average degree of obliquity to the left was  $2.4^\circ$  and to the right was  $2.6^\circ$ . The data did not suggest that age, handedness or genders are related to the side or amount of obliquity.



**CORRECTING SACRAL OBLIQUITY IN SITTING  
AND STANDING POSTURES**

<b>CHAPTER 8</b>
------------------

*“Do not lose your knowledge that man's proper estate is an upright posture, an intransigent mind and a step that travels unlimited roads.”*

- Ayn Rand

### **8.1 CORRECTING SACRAL OBLIQUITY**

The objective of this chapter is to provide an accurate and reliable mathematical basis in the form of corrective algorithms to level the sacral base in standing and sitting posture that incorporates the three major contributing factors to sacral tilt. These factors are leg length imbalance (anisomelia) in standing posture, pelvic asymmetry in the form of ischial tilt in sitting posture and sacral asymmetry which is common to both postures. These three factors interact in various ways to produce sacral tilt and require classification according to the algorithm that needs to be applied to determine the amount of any orthotic intervention.

Sacral obliquity, whether the result of leg length imbalance (anisomelia), sacral asymmetry or structural and functional asymmetry of the pelvis, has been suggested as a cause of structural changes in the lumbar spine by Giles and Taylor (55), pain syndromes by Cailliet (52) and functional disorders of the musculoskeletal system (77). Specific treatments involving shoe inserts, foot orthotics and heel lifts have been suggested as methods to reduce leg length imbalance, pelvic obliquity and sacral obliquity in standing posture (54, 65, 372, 373). In a similar way, ischial lifts have been used to compensate for pelvic obliquity and to level the sacral base in sitting posture (78, 374, 375). These interventions have an implied outcome of levelling the sacral plateau as the sacral plateau is the superior articulation of the pelvis forming the structural base for the flexible spine above. The presumption with these interventions is that the sacral base should ideally be level in the frontal (coronal) plane.

Different clinical methods have been used, proposed or investigated to determine the need for, and to quantify the amount of compensation or correction needed to level the sacral base. Methods commonly used to assess the pelvis or more specifically, the sacral base, either directly or indirectly involve radiographic imaging (11, 14, 66, 254, 376), static and motion palpation (202, 377), goniometry (378), rasterstereography and visual assessment (141, 291), and orthopaedic tests including supine and erect leg length assessment (56, 80, 169). However, radiographic imaging is considered the '*gold standard*' for quantifying leg length imbalance and pelvic (sacral) obliquity (69). Although other clinical methods have been employed to quantify and prescribe heel lifts they are not generally considered to be as valid or reliable for quantifying heel or ischial lifts needed to level the sacral base or normalising pelvic obliquity (69). Brady *et al* (56) conclude from their review of the relevant literature that clinicians should exercise caution when undertaking intervention strategies for limb length inequality less than 5mm when the identified limb length inequality has been determined using clinical techniques rather than radiographic assessment. They cite studies that indicate structural asymmetry of the reference points, difficulty in palpating bony landmarks and inexperience on the part of the examiner as possible causes of inaccuracy. Van der Wurff *et al* (170) conclude as a result of a review of the relevant literature, that there were no demonstrable reliable outcomes and therefore no evidence on which to base acceptance of mobility tests of the sacroiliac joints (SIJ) into daily clinical practice.

Radiographic techniques for the evaluation of limb length, pelvic distortion, either functional or structural, and sacral base levelness have been widely used or advocated as assessment methods in a clinical setting by musculoskeletal practitioners and therapists (7, 11, 27, 56, 78, 254, 284, 379). As an example, an osteopathic approach to what is described as 'sacral base levelling' involves the measurement of angles between lines representing the sacral base and femur heads drawn on A-P radiographs and a line representing the horizontal plane (Figure 137). This method has been used or advocated

by osteopaths such as Tilly (189), Irvin (65), Juhl et al (83) and Kuchera and Kuchera (8) to assess *levelness* of the sacral base in upright posture. In a validity study by Fann (11), the measurement of pelvic obliquity and orientation of the sacral base, induced by a heel lift of known size, was based on similar radiographic analytical methods. Kuchera and Kuchera (8) quote an accuracy of  $\pm 0.75\text{mm}$  for the type of radiographic analysis of sacral base levelness using similar reference points and methods to those evaluated by Fann. In their text they suggest that osteopathic physicians are more interested in levelling the sacral base than making leg lengths equal and emphasise that the sacral base is of greater clinical significance than differences in leg length.

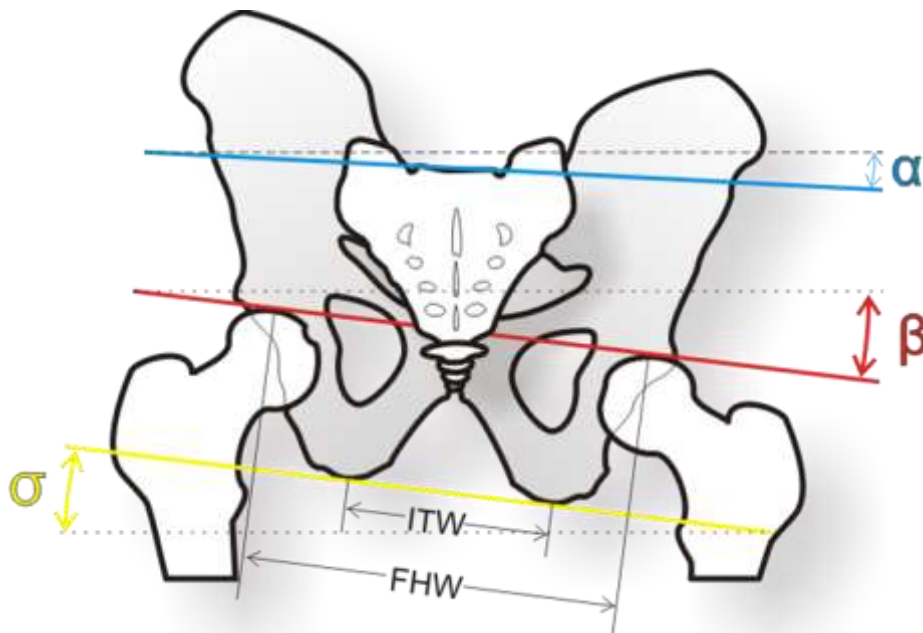


Figure 137. Angle  $\alpha$  represents sacral obliquity, angle  $\beta$  represents the angle formed between the plane of the femur heads and the horizontal plane, angle  $\sigma$  represents the angle formed between the plane of the ischial tuberosities and the horizontal plane. ITW is the width between tangent points on each ischial tuberosity. FHW is the width of the tangent points on the femur heads.

Using a very similar radiographic assessment method Irvin (65) tested the hypothesis that a mildly *unlevelled* sacral base corrected by using a heel lift would decrease an associated lateral bend of the lumbar spine. Kuchera (34) specifically addressed the use of lift therapy as a component of osteopathic clinical procedures and suggests that patterns of imbalance in the spine with accompanying pain syndromes may be due to as little as 1/16th of an inch



(1.5mm) difference in leg length. He suggests the amount of initial lift can be calculated using a formula developed by Heilig (372). The formula is expressed as:  $L < [SBU]/[D+C]$ . In this formula,  $L$  is the lift required,  $SBU$  is the amount of sacral base *unleveling*, and  $D$  is the duration that the *unleveling* has been present and is assigned a value of **1** to **3**. A value of **1** is allotted if the duration is from 0-10 years, **2** if from 10-30 years and **3** for 30 + years.  $C$  is the amount of compensation for sacral base *unleveling* that is present in the spine. If none is observed it is given a value of 0. Rotation of lumbar vertebra into the convexity of the compensatory scoliotic curve is given a value of 1. Wedging of vertebra, altered size of facet joints, and osteophytic lipping and spurring is given a value of 2.

Irvin specifically assessed the reduction of lumbar scoliosis by using a heel lift to level the sacral base. He used radiographs to measure the '*unlevelness*' of the sacral base and used this measurement as the basis for prescribing an appropriate heel lift. The sacral base ranged from 2 to 17mm (mean of 6.7mm  $\pm$ 1.0mm) of equivalent leg length imbalance using radiographic analytical methods similar to those described by Kuchera and Kuchera (8). Following the use of a prescribed heel lift the '*unlevelness*' was 2.6mm  $\pm$ 0.4mm ( $P<.001$ ).

Evaluation of relative and absolute pelvic orientation has been an integral part of many chiropractic spinal assessment techniques (9, 13, 16, 41, 78, 79, 105, 265, 284, 374). Widely used chiropractic techniques such as the Gonstead technique (380) and Chiropractic BioPhysics (CBP) (105) employ radiographic analysis of the pelvis in upright posture along with orthopaedic tests to quantify relative leg lengths, pelvic positional asymmetry and the orientation of the sacral base. Other techniques such as Activator methods (90, 381) and Thompson technique (382) use leg length inequality (LLI) as an indicator of pelvic misalignment. Knudson (72, 136) suggested that practitioners of manual medicine who derive vectors for intervention based on leg checking procedures should consider the possibility that the direction of pelvic torsion may be variable depending on

whether the LLI is of anatomical or functional origin (Figure 34). Walker (139) as well as Hestbaeck and Leboeuf (80) have independently examined the validity and clinical protocols used for assessing leg length imbalance (LLI). Both concluded from their reviews of the relevant literature that while the detection of the manipulative lesion in the lumbopelvic spine depends on valid and reliable tests, such tests have not been established. As a result the presence of the manipulative lesion associated with sacral obliquity remains hypothetical. Cooperstein and Lew (383) reviewed the literature relating to a commonly held view within the chiropractic profession and other manual therapists that leg length inequality can affect torsion of the pelvis and by implication the level of the sacral base. They were only able to retrieve nine papers, none of which directly measured pelvic torsion. Direct measurement of sacroiliac movement that would result in sacral obliquity suggests that very little angulation of the sacral base could be attributed to pelvic torsion. Anisomelia was measured in 100 young or middle-aged adults suffering from chronic low-back pain by Hoikka et al (74). The anisomelia had a good correlation with pelvic tilt assessed from the iliac crests and a moderate correlation with sacral tilt. The authors of this study concluded that radiographically demonstrable anisomelia does not correlate well with scoliosis while sacral tilt correlated well with the lumbar scoliosis when the tilt was more than 3 degrees.

Mechanical efficiency of the bipedal human body, upright in an orthogonal environment and acted upon by the ubiquitous force of gravity implies left-right structural symmetry (384). Mechanical symmetry of the body would require the balanced distribution of duplicate body parts and reflective structural symmetry around the vertical axis of the body in the frontal plane. The objective of this study was to quantify the amount of linear displacement required at the ischium, femur heads or sacroiliac joints to restore the sacral base to the horizontal plane in upright posture with all other factors being equal. The measurements were made using graphical analysis and the calculations using trigonometrically based algorithms.

Numerous therapeutic interventions used by a variety of practitioners and therapists have the objective of levelling the sacral base, leg lengths or pelvis and involve the use of heel lifts, ischial lifts and manipulation of the pelvis. Few if any of these methods have been specifically validated in relation to levelling the sacral base generally or removing sacral obliquity specifically.

Plain film radiographs taken in erect posture are commonly used to assess the positional integrity of the spine and pelvis by clinicians. Specific analytical procedures such as the Gonstead method (380) commonly used by chiropractors and the procedures described by Kutchea and Kutchea (8) used by osteopaths have been employed in a clinical setting to quantify what is hypothesised as pelvic misalignment or pelvic torsion that would have an influence on orientation of the sacral base in the frontal plane (Figure 15) and (Figure 19). However, the validity of plain film radiographs for the measurement of pelvic misalignment in the range that would be anticipated, suggested or corrected by manual therapists has been questioned (191).

A difficulty with validating such measurements on radiographic images for a given individual is in differentiating misalignments from projection distortion, structural asymmetry and the reliable identification of landmarks. A further difficulty arises when applying statistical data relating to the normal amount and type of movement found in the sacroiliac joints and the pubic symphysis to specific misalignment patterns observed clinically and patterns measured on radiographs (29). This study is designed to circumvent these issues by developing and applying mathematical and graphical models to an idealised three dimensional pelvic model in order to analyse the theoretical geometrical relationships of the pelvis and lower limbs and to quantify the effect specific relationships would have on the orientation of the sacral base in standing and sitting postures and how these patterns could be corrected in a clinical setting using orthotic devices. An orthotic device is an externally

applied device used to modify the structural and functional characteristics of the neuromuscular and skeletal system (385).

## **8.2 CALCULATING ORTHOTIC SIZE**

An idealised graphical pelvic model was developed in order to validate the trigonometrically based formulae used to calculate the degree of theoretical sacral obliquity that would result from various combinations of leg length imbalance, innominate (ischial) asymmetry and theorised pelvic misalignments involving joints of the pelvis. The formulae were based on geometrical relationships and movement patterns that have been identified, or proposed mainly by clinicians, to exist between the structural components of the pelvis and lower limbs. These patterns have been suggested as mechanisms underlying clinically observed sacral and pelvic obliquity, pain syndromes and spinal functional patterns (50, 77, 83).

The geometrical and trigonometrically based algorithms were used to determine the amount of sacral obliquity that would theoretically occur and therefore would require correction in order to level the base of the spine in relation to different standing and sitting patterns in orthogonal environments. These involve patterns associated with clinically observed pelvic torsion or misalignment and structural asymmetry of the pelvis and lower limbs.

Sacral obliquity in standing posture could result from any combination of structural and functional asymmetry involving the innominate bones, sacrum or bones and joints of the lower limbs. Structural asymmetry of the axial skeleton could be due to fluctuating asymmetry of bones of the pelvis or lower limbs, injury such as fractures, surgical interventions, diseases such as Legg-Calve-Perthes disease and Rickets (386, 387), or physiological processes such as those that underlie Wolff's and Hueter-Volkman laws (46, 289, 388). The Hueter-Volkman law proposes that growth particularly of long bones is retarded by increased mechanical compression, and accelerated by reduced loading or tension forces in comparison with normal values (46).

Functional asymmetry of the axial skeleton in erect posture can also be caused voluntarily by the adoption of specific lateralised postures and loading patterns. Pelvic torsion and misalignments of the pelvis are considered by some clinicians and authors as functional patterns that can cause functional leg length imbalance and by implication sacral obliquity (50, 77).

In sitting posture, structural asymmetry within the pelvis can result in an angulation between the plane representing the sacral base and a plane containing the tangent point on each ischial tuberosity (3). Proposed misalignments involving bones of the pelvis could theoretically have the potential to cause absolute sacral obliquity. Another cause of absolute sacral obliquity in sitting posture that could be considered a functional obliquity results from upper body muscular weakness associated particularly with quadriplegia and paraplegia. This pattern has been described in wheelchair bound patients (389, 390). Sacral obliquity of this type resulting from upper body weakness or neuropathology of the trunk was not specifically modelled in this study as it is not generally the direct result of pelvic asymmetry.

The bones of the adult pelvis include the two innominate bones and the sacrum that articulate at three individual joints, the two diarthrodial sacroiliac joints and the amphiarthrodial symphysis pubis. The predominant movement at the sacroiliac joints has been described as nutation and counter-nutation of the sacrum (100). While a number of authors and clinicians have proposed torsion of the innominate bones as a possible cause or contributing factor in sacral obliquity the validity of their assessment methods have been questioned. Only very small amounts or no rotation at all of the sacrum around the Z-axis have been demonstrated *in vivo*. For example, Stureson (155) found no Z-axis rotation (SD 0.3) of the sacrum in going from supine to standing positions.

The change in position of the innominate bones has also been related to both normal and abnormal movement at the sacroiliac joints induced by a shearing action at the symphysis pubis. A change in functional leg lengths has been suggested as a mechanism for the resulting sacral obliquity (13).

A number of techniques used by physiotherapists, medical musculoskeletal specialists, and in particular osteopaths and chiropractors involve assessment and non-invasive correction of specific pelvic misalignments (16, 50, 77, 145, 391). Some of the assessment methods involve radiographic analysis while other methods involve orthopaedic and clinical assessment of the pelvis. The validity and reliability of these methods has been questioned in their application as clinical procedures (80, 391).

This study involved the development and application of graphical and trigonometric models to test the theoretical contribution pelvic structural asymmetry, pelvic torsion or misalignment has on sacral obliquity. The study also involved the quantification of orthotic devices such as heel and ischial lifts that would be needed to level the sacral base in sitting and standing postures when absolute or relative sacral obliquity was found to be present in a clinical setting.

Appropriate trigonometric functions were selected and incorporated into equations in order to calculate the vertical distance that the femur head or ischial tuberosity would need to be elevated in order to level the sacral base in sitting or standing postures and to correct for pelvic misalignment. With pelvic misalignment or torsion, formulae were also developed to calculate the amount of vertical height change at the sacral base as a result of either one or both of the innominate bones rotating around one of three theorised axes. The axes were approximated as representing the centre of the femur heads, symphysis pubis and the sacroiliac joints.

Specific combinations and magnitudes of sacral obliquity, leg length imbalance (anisomelia) and ischial tuberosity angulations in the frontal plane required different formula to calculate the vertical distances involved. These patterns of imbalance could be grouped into seven distinct relationships each with a unique formula. The equation for each pattern or combination of factors depended on the angular relationship of the sacral base to either the ischium or femur heads. The relationships were the result of the angle of these factors to the horizontal plane in both their initial and final position after correction.



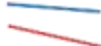




For standing posture, the calculations were based on the measurement of the absolute sacral obliquity angle (SOA), the width of the femur heads (FWH) and the femur head angle (FHA) (Figure 137). These measurements were used as they represented factors that could be obtained directly or derived as approximations from A-P or sacral base radiographic views of the lumbopelvic spine.

For the purpose of developing formulae to calculate the vertical distances involved, the angles and distances were considered the true value. The assumption was that the angles were true dihedral angles and the distances had been corrected for magnification. The ischial tuberosity angle (ITA) and the distance between the ischial tuberosities (ITW) could also be obtained from the same films provided the relative anatomical structures could be visualised (Figure 137).

#### *8.2.1 Absolute and relative sacral obliquity in standing posture*

The various configurations relating the plane of the sacral base to the plane of the femur heads in upright (erect) standing posture were divided into seven distinct categories. The seven patterns are made up of a normal (orthogonal) pattern plus six abnormal (asymmetrical) patterns that relate sacral obliquity and femur head angle to the horizontal plane (Table 12).

**Table 12. The seven configurations relating the plane of the sacral base (blue line) to the plane of the femur heads (red line) in upright (erect) posture**

Pattern No	Description of relationship between SAO and FHA	Graphic representation of variables
1	No SOA, No FHA	
2	No SOA, FHA	
3	SOA < FHA	
4	SOA = FHA	
5	SOA > FHA	
6	SOA, No FHA	
7	SOA opposite FHA	

The relative magnitude of the variables (SOA and FHA) dictates the makeup of the respective equations. The three significant angles measured on various radiographic images are the sacral obliquity angle  $\angle\alpha$ , the femur head angle  $\angle\beta$  and the ischial tuberosity angle  $\angle\sigma$ . The patterns are based on the relationships of the components of the pelvis and lower limbs relative to each other and to the horizontal plane. These patterns are illustrated schematically with the overall postural pattern, the angles involved and radiographic images demonstrating the particular pattern.

#### Standing Pattern 1

Pattern 1 represents an orthogonal relationship of the femur heads, sacral base and gravity (Figure 138). Both relative and absolute sacral obliquity are parallel and horizontal. The femur head line (FHL) and sacral base line (SBL) drawn on A-P erect radiographs have no angular measurement relative to the horizontal plane (Figure 139).



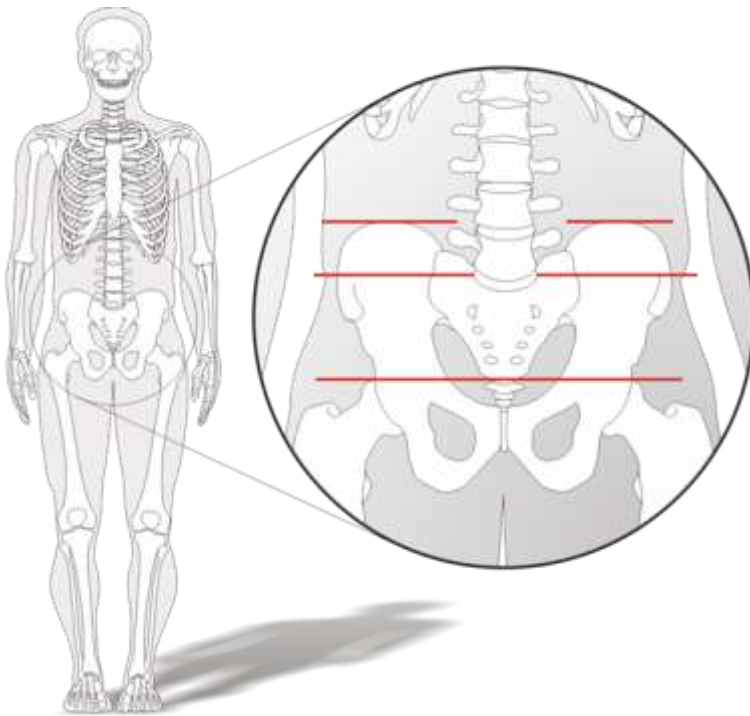


Figure 138. Pattern 1 represents the orthogonal relationship of the femur heads, sacral base and gravity erect posture with both sacral obliquity and femur heads parallel and horizontal

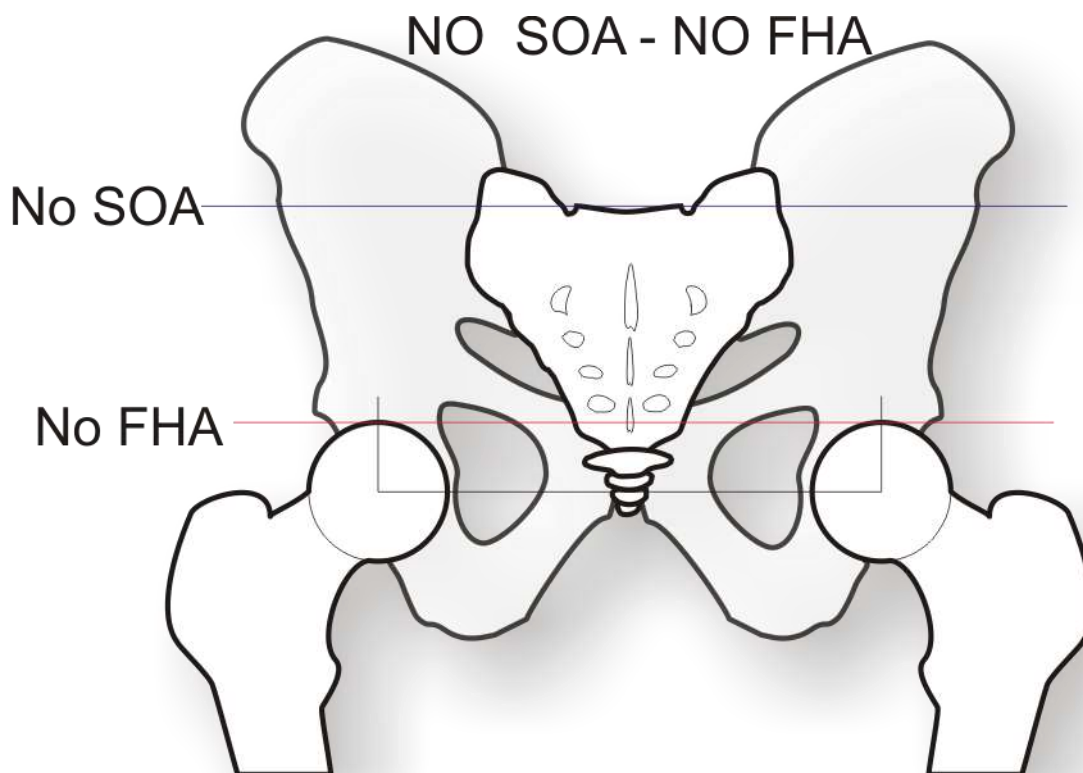


Figure 139. Standing Pattern 1 with no absolute or relative sacral obliquity and no leg length imbalance

Erect A-P lumbopelvic radiographs can be used to visualise standing pattern 1 with no sacral obliquity (blue line) and no leg length imbalance (red line). The radiographic analysis reveals no  $\angle\alpha$  (sacral obliquity) and no  $\angle\beta$  (femur head angle) (Figure 140).

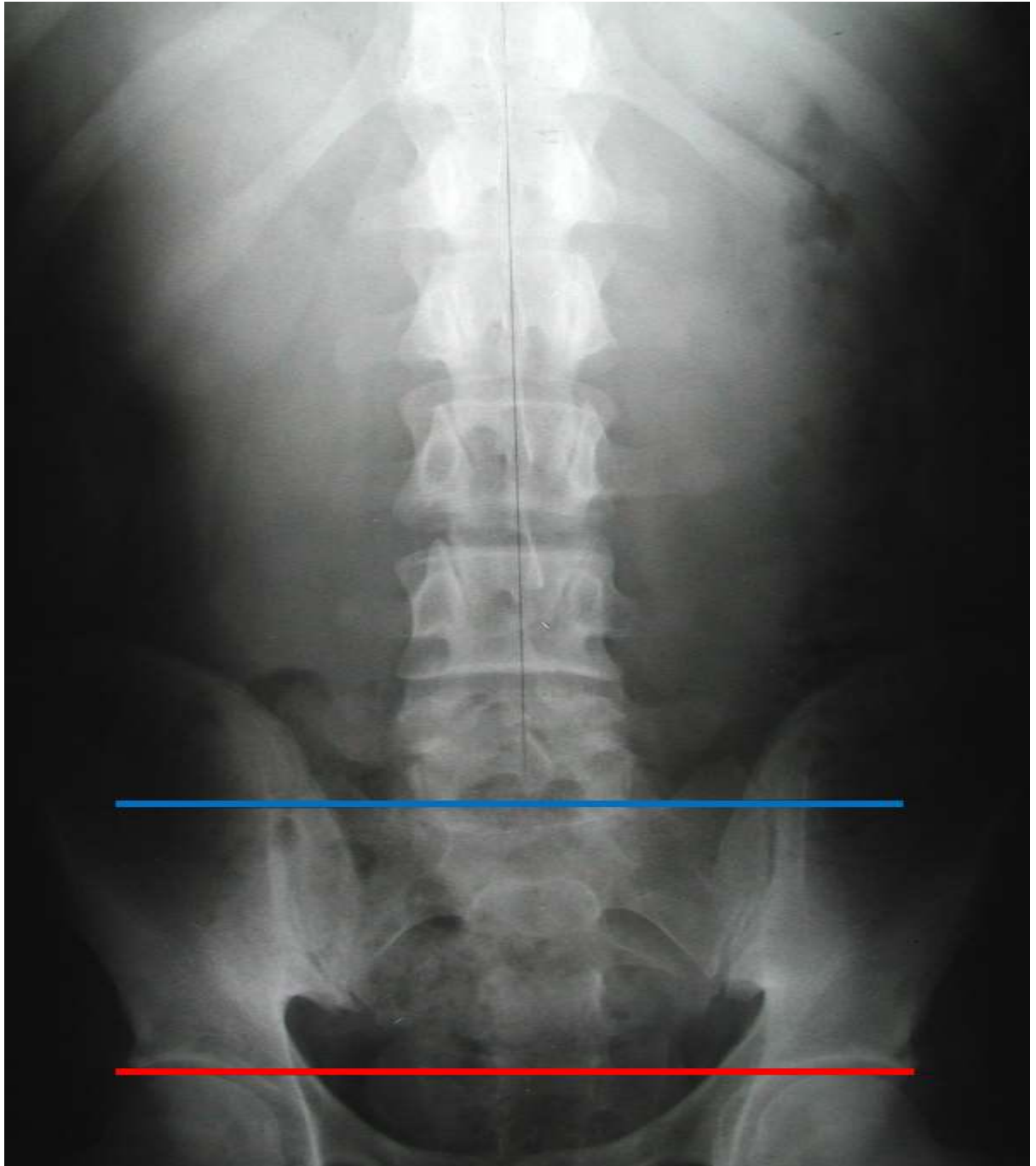
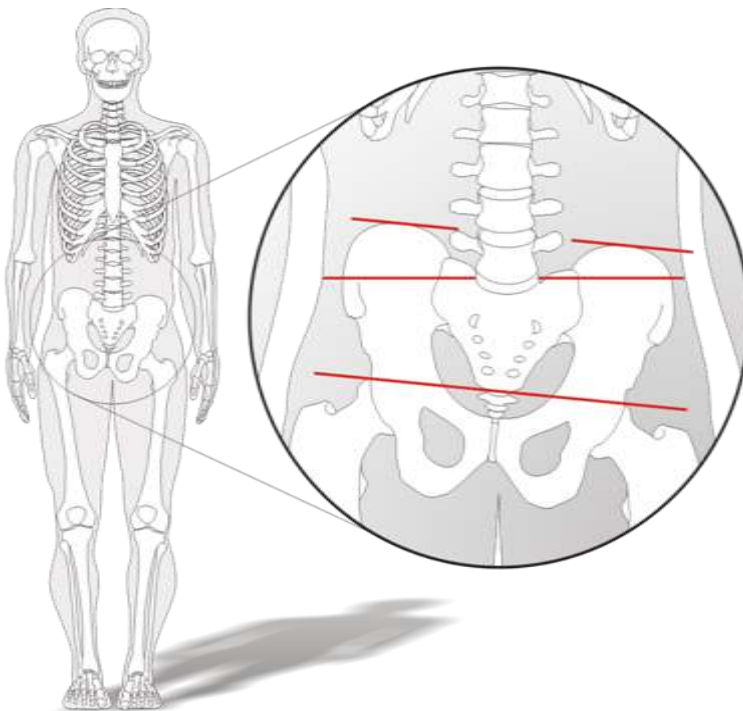


Figure 140. Erect A-P lumbopelvic radiograph representing standing pattern 1 with no sacral obliquity (blue line) and no leg length imbalance (red line). – (no angle  $\alpha$  and no angle  $\beta$ )

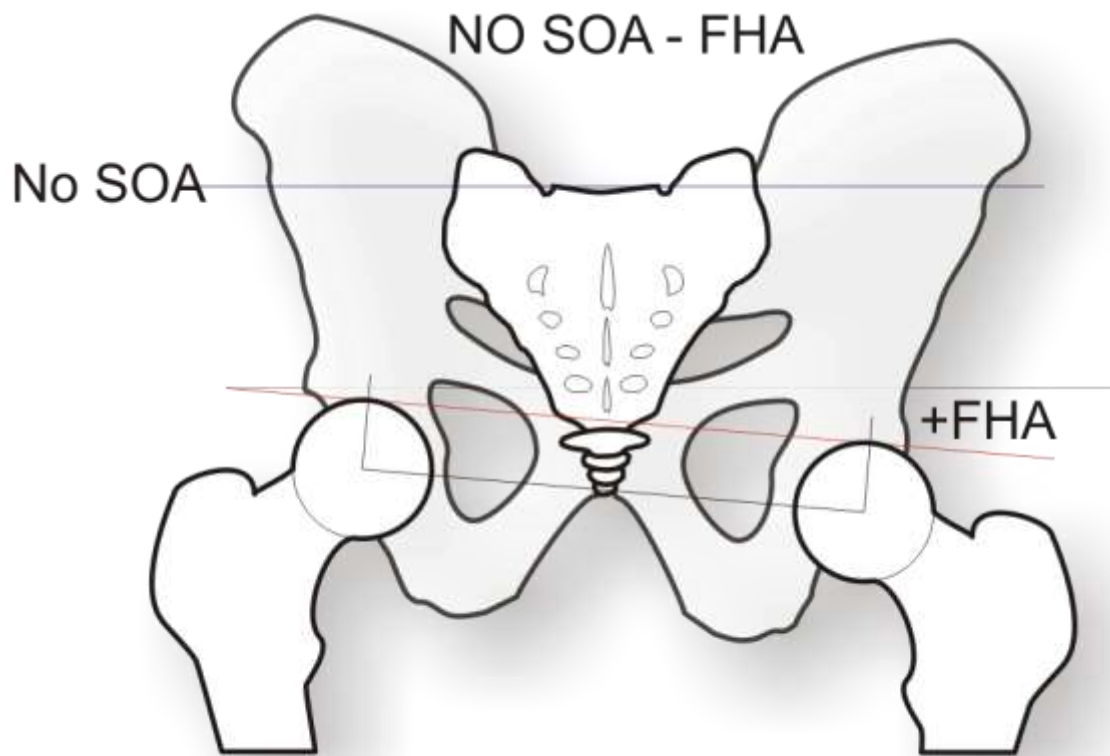
## Standing Pattern 2

With pattern 2 there is no absolute sacral obliquity in standing posture but there is relative sacral obliquity present. The relative sacral obliquity is due to a combination of anisomelia and an asymmetry of the sacrum or pelvis that compensates for the anisomelia with a resulting level sacral base in standing posture (Figure 141).



**Figure 141. Pattern 2 with no absolute sacral obliquity in standing posture but relative sacral obliquity. The relative sacral obliquity is due to a combination of anisomelia and an asymmetry of the sacrum or pelvis that results in a level sacral base in standing posture**

The positive (+) or negative (-) femur head angle is measured relative to the horizontal plane while there is no measured angulation of the sacral base in the frontal plane. The result is a positive (+) or negative (-) that is exactly opposite the femur head angle in direction and equal in magnitude (Figure 142).



**Figure 142. Standing pattern 2 with no absolute sacral obliquity angle but with leg length imbalance due to lower limb anisomelia and relative sacral obliquity**

An erect A-P lumbopelvic radiograph illustrates standing pattern 1 with no sacral obliquity (blue line) but with measureable leg length imbalance (red line) resulting in a positive (+) or negative (-) femur head angle. The radiographic analysis reveals no  $\angle\alpha$  (SOA) but there is a (+/-)  $\angle\beta$  (FHA) (Figure 143).

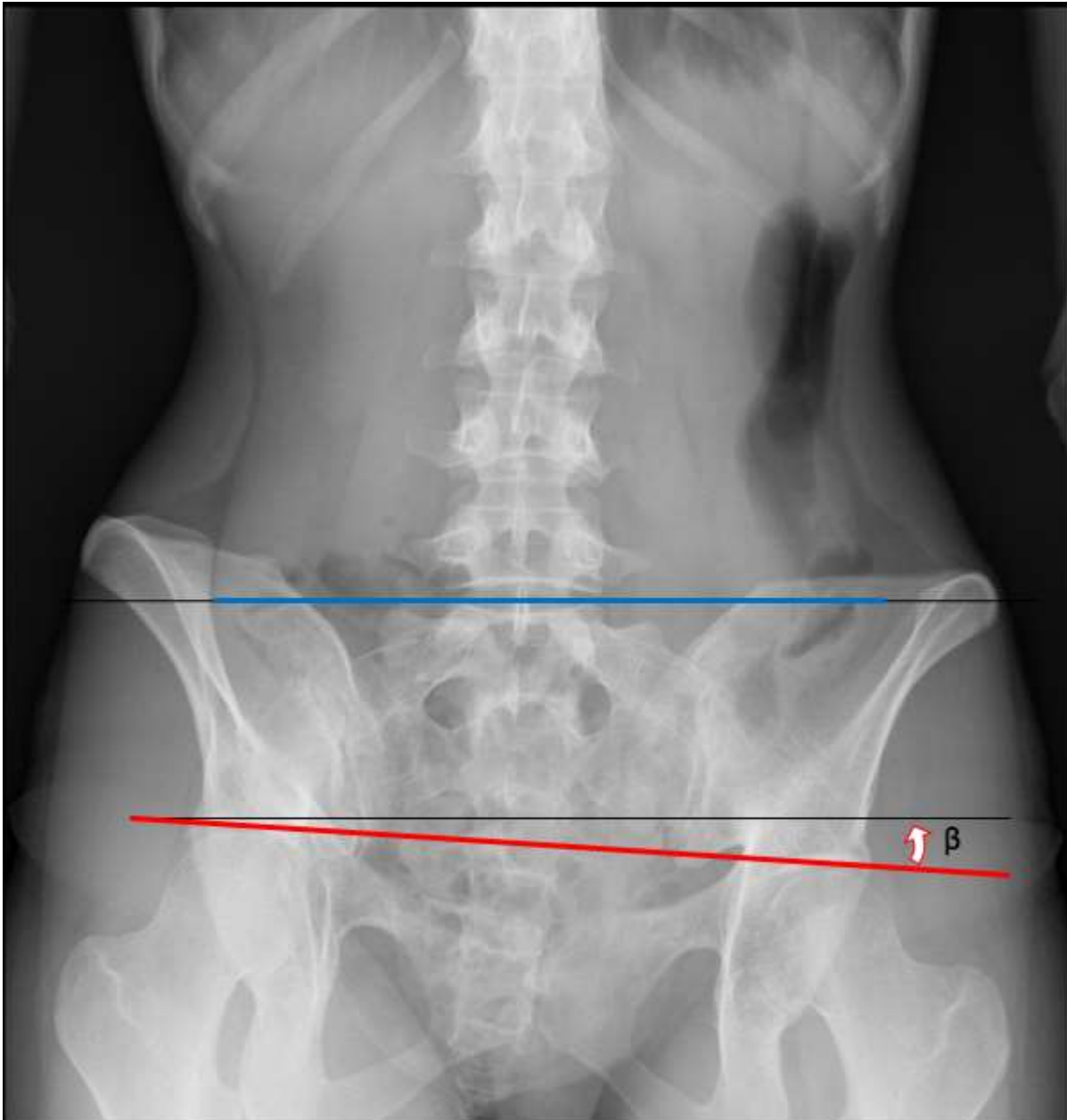
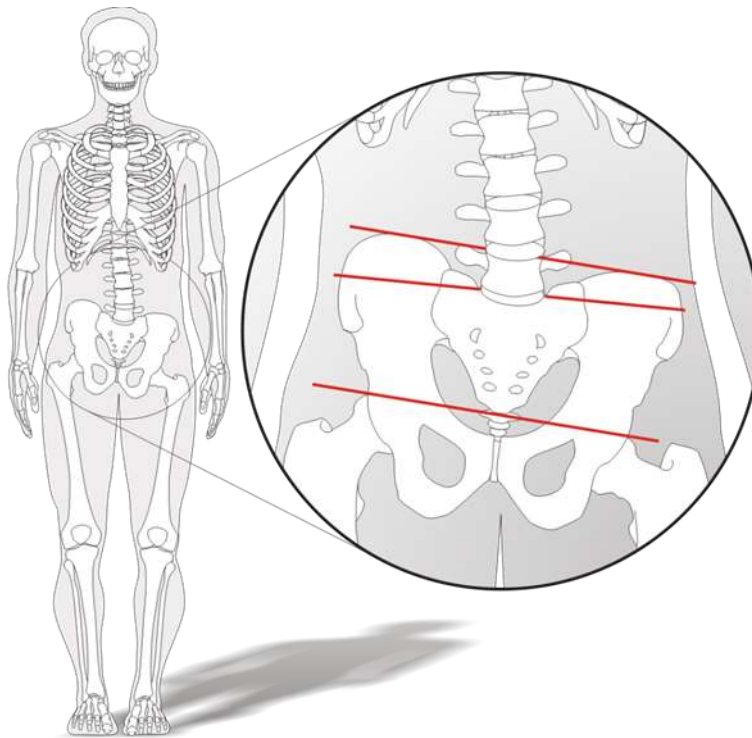


Figure 143. Erect A-P lumbopelvic radiograph (sacral base view) representing standing pattern 2 with no sacral obliquity with leg length imbalance. – (no angle  $\alpha$  with angle  $\beta$ )

### Standing Pattern 3

Pattern 3 occurs when there is ipsilateral anisomelia and absolute sacral obliquity with the leg length imbalance producing a greater angle relative to the horizontal plane. This configuration results in a contralateral relative sacral obliquity in both sitting and standing posture (Figure 144). In standing posture the base of the spine (sacral plateau) is tilted in one direction while in sitting posture the sacral base would be tilted in the opposite direction if the resting surfaces were level.



**Figure 144.** Pattern 3 has ipsilateral anisomelia and absolute sacral obliquity in standing posture. The anisomelia is greater than the sacral obliquity resulting in contralateral relative sacral obliquity

Standing pattern 3 results from absolute sacral obliquity angle that is less than the ipsilateral femur head angle due to leg length imbalance. Relative sacral obliquity is contralateral to the femur head angle (Figure 145).

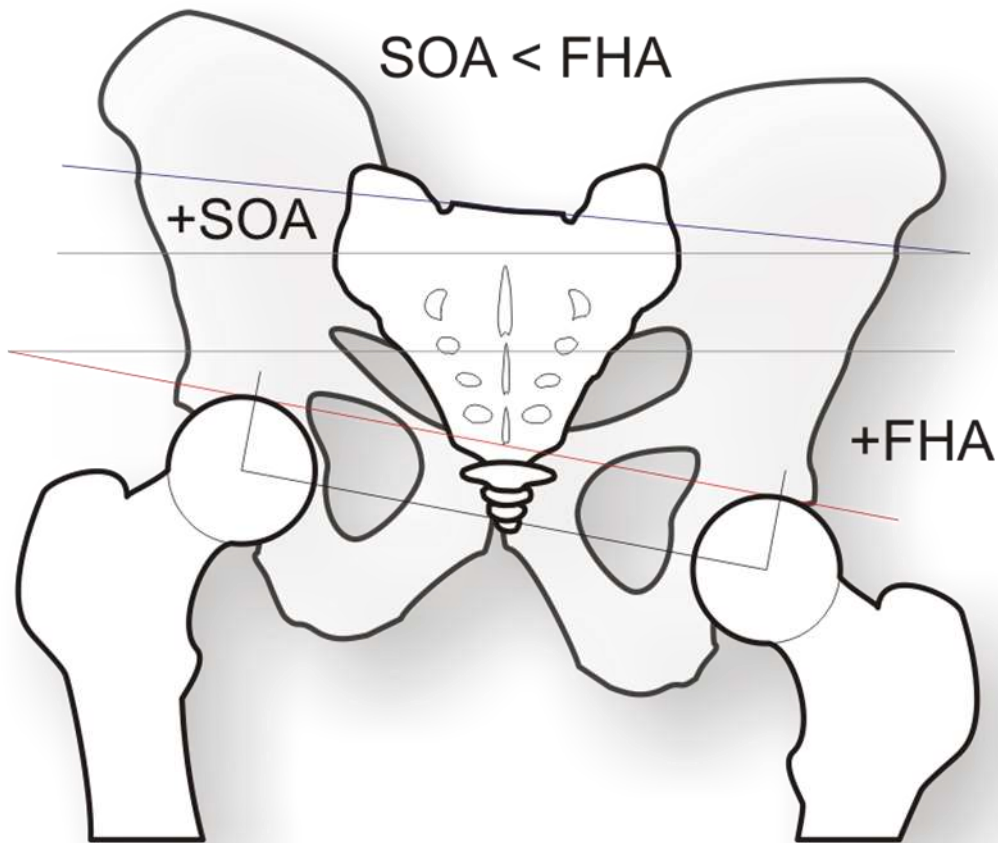


Figure 145. Standing pattern 3 with absolute sacral obliquity less than the ipsilateral leg length imbalance due to relative sacral obliquity contralateral to the femur head angle

Erect A-P lumbopelvic radiograph (sacral base view) can be taken representing standing posture with a pattern 3 configuration. This configuration involves absolute sacral obliquity and leg length imbalance on the same side with the sacral obliquity less than the femur head angle. The result is relative sacral obliquity in the opposite direction to the femur head angle ( $+\angle\alpha < +\angle\beta$ ) (Figure 146).



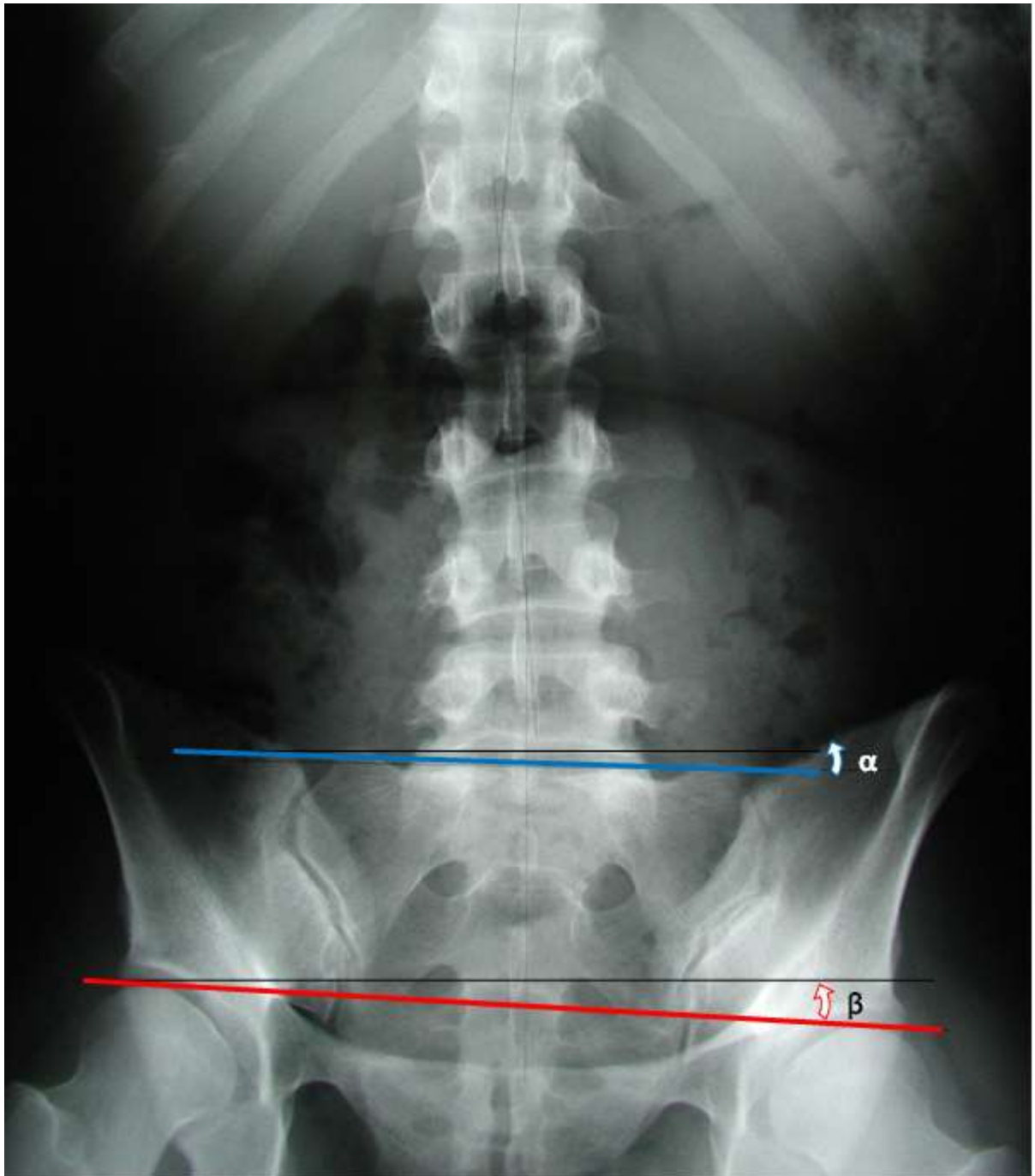
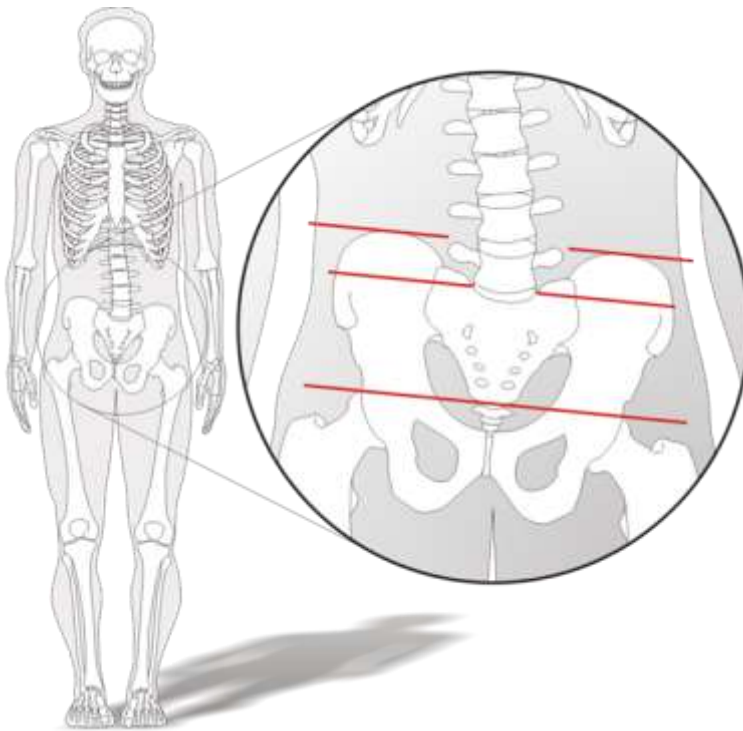


Figure 146. Erect A-P lumbopelvic radiograph (sacral base view) representing standing posture with a pattern 3 configuration. This configuration involves absolute sacral obliquity and leg length imbalance on the same side with the sacral obliquity less than the femur head angle. The result is relative sacral obliquity in the opposite direction to the femur head angle ( $\text{angle } \alpha < \text{angle } \beta$ )

#### Standing Pattern 4

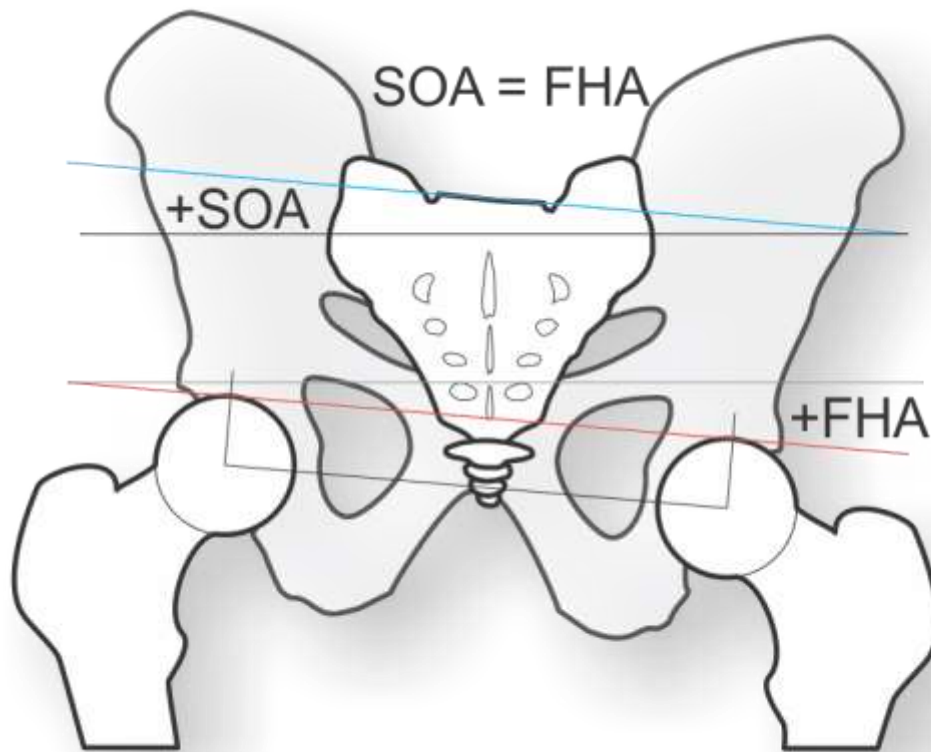
With pattern 4 there is anisomelia (FHA) but no relative sacral obliquity. This results in an absolute sacral obliquity equal to the degree of anisomelia ( $\text{SOA } \angle \alpha = \text{FHA } \angle \beta$ ) (Figure 147).





**Figure 147. Pattern 4 involves anisomelia (FHA) but no relative sacral obliquity. This results in an absolute sacral obliquity equal to the degree of anisomelia. SOA (angle  $\alpha$ ) = FHA (angle  $\beta$ )**

Standing pattern 4 results from anisomelia (FHA) causing the same degree of absolute sacral obliquity with no relative sacral obliquity. The absence of relative sacral obliquity is due to internal pelvic symmetry coupled with anisomelia (Figure 148).



**Figure 148. Standing pattern 4 with anisomelia (FHA) and the same degree of absolute sacral obliquity (SOA) with no relative sacral obliquity**

An x-ray image of standing pattern 4 shows absolute sacral obliquity (SOA) with no relative sacral obliquity. This configuration results from the combination of pelvic symmetry coupled with anisomelia. The absolute sacral obliquity angle ( $\angle\alpha$ ) and femur head angle ( $\angle\beta$ ) are measured as the same angular deviation on the radiographic image (Figure 149).

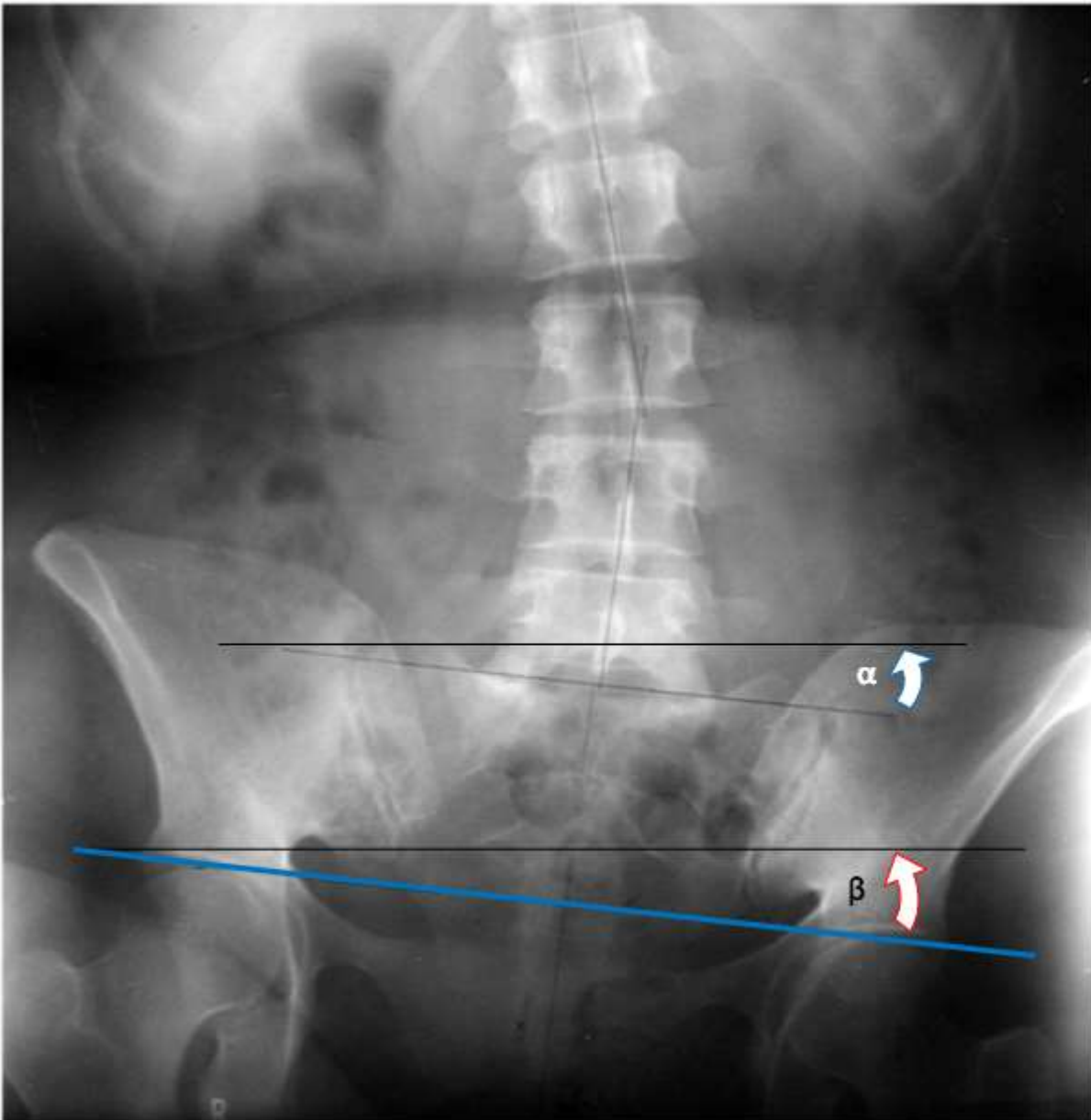
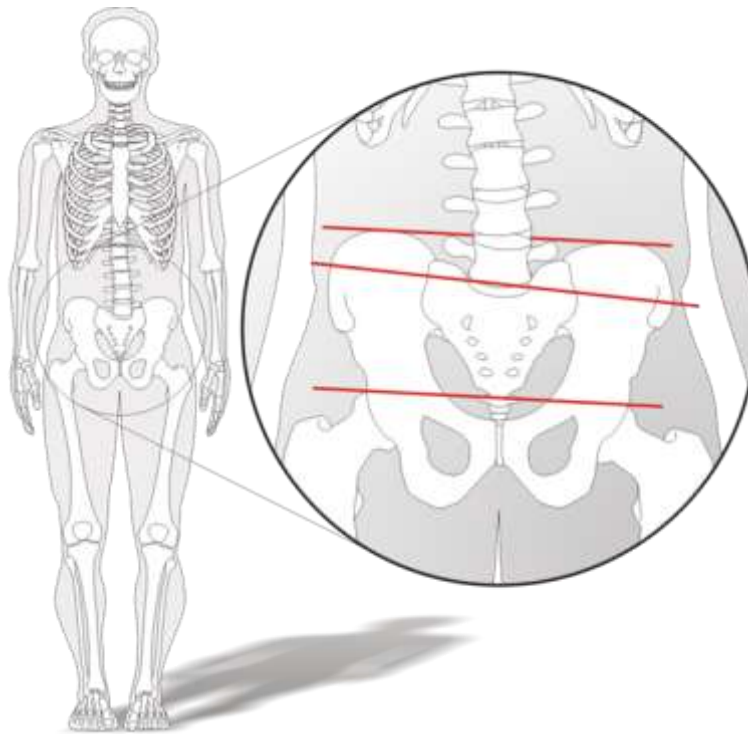


Figure 149. An x-ray image of standing pattern 4 shows absolute sacral obliquity (SOA) with no relative sacral obliquity

### Standing Pattern 5

The characteristics of standing pattern 5 are absolute sacral obliquity (SOA) with ipsilateral relative sacral obliquity and ipsilateral anisomelia. The anisomelia results in a femur head angle that is less than the measured sacral obliquity angle (SOA). This configuration is due to pelvic or sacral asymmetry with a lesser degree of anisomelia (FHA) on the same side (Figure 150)



**Figure 150. Standing pattern 5 with absolute sacral obliquity (SOA) and ipsilateral relative sacral obliquity. This configuration is due to pelvic or sacral asymmetry with a lesser degree of anisomelia (FHA) on the same side**

Standing pattern 5 involves absolute sacral obliquity (SOA) with a lesser amount of ipsilateral relative sacral obliquity. This results from pelvic or sacral asymmetry with anisomelia on the same side that creates a femur head angle (FHA) that is less than the angulation of the sacral obliquity (Figure 151).

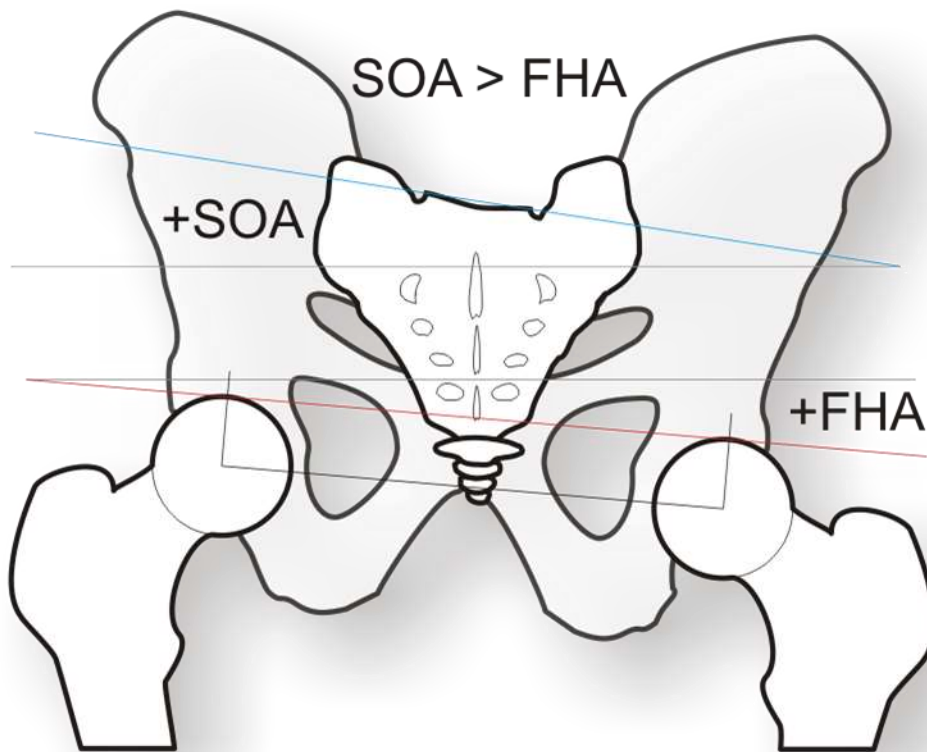


Figure 151. Standing pattern 5 involves absolute sacral obliquity (SOA) with ipsilateral relative sacral obliquity. This due to pelvic or sacral asymmetry with anisomelia on the same side

Standing pattern 5 is measured on erect A-P lumbopelvic radiographs (sacral base view) representing a standing pattern with absolute sacral obliquity (SOA) and leg length imbalance (FHA) resulting in relative sacral obliquity in the same direction SOA ( $\alpha$ ) > FHA ( $\beta$ ) (Figure 152).

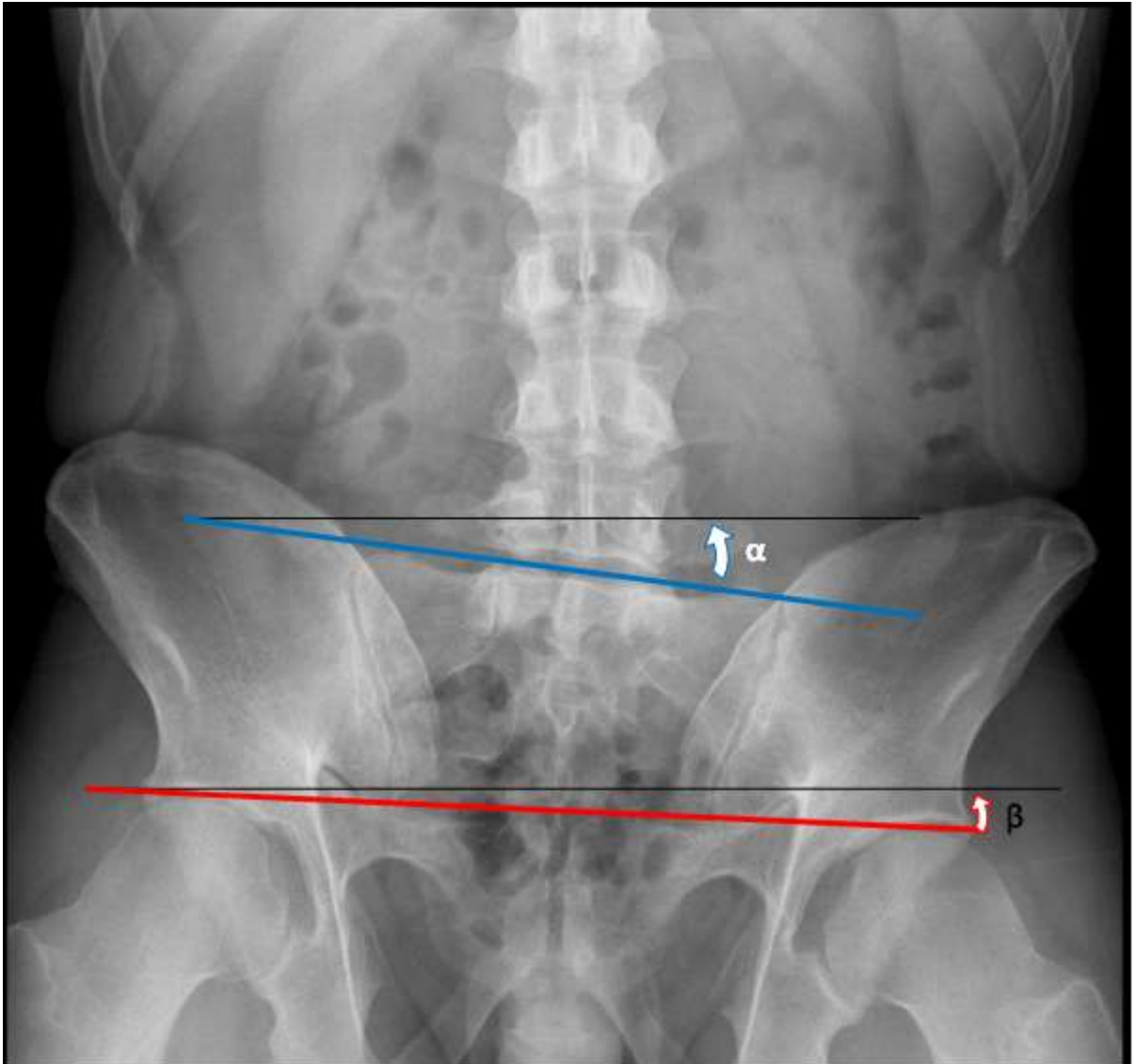
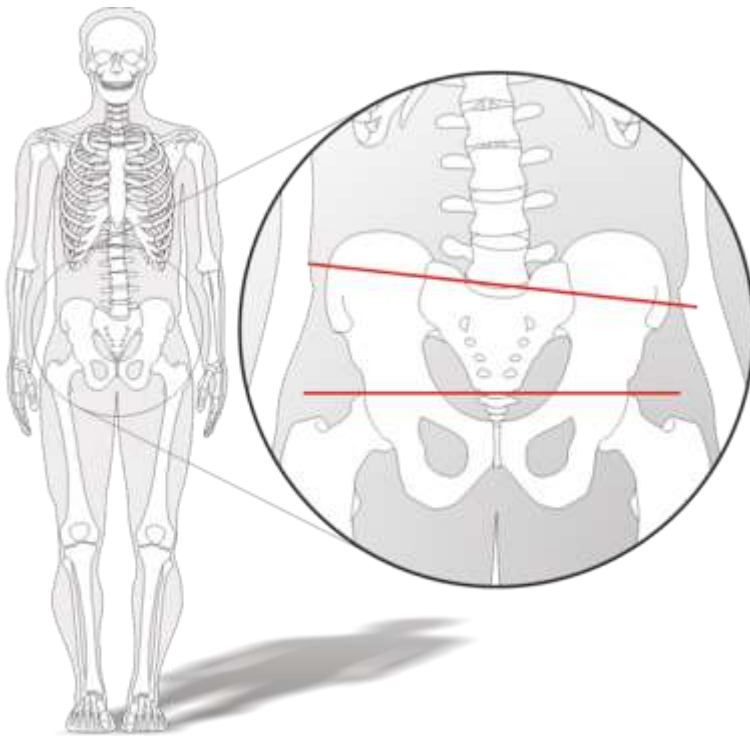


Figure 152. Erect A-P lumbopelvic radiograph (sacral base view) representing a standing pattern 5 with absolute sacral obliquity (SOA) and leg length imbalance (FHA) and an ipsilateral relative sacral obliquity

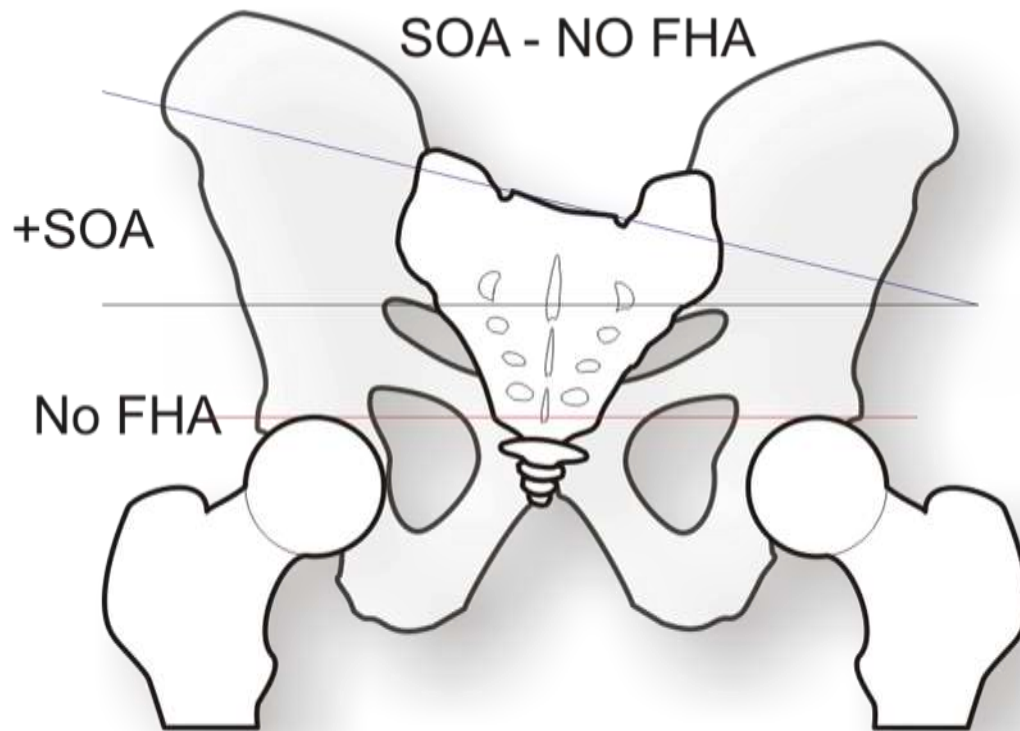
### Standing Pattern 6

Standing pattern 6 represents an absolute sacral obliquity (SOA) with the same amount of relative sacral obliquity. The relative sacral obliquity is the result of absolute sacral obliquity combined with no anisomelia ( $0^\circ$  FHA) (Figure 153).



**Figure 153. Standing pattern 6 with absolute sacral obliquity (SAO) as a result of relative sacral obliquity with no anisomelia (no FHA)**

Pattern 6 represents sacral obliquity with no other factors involved. With no femur head angle, absolute sacral obliquity and relative sacral obliquity have the same measured angle. Absolute sacral obliquity is measured as angular displacement from the horizontal plane and relative sacral obliquity is measured relative to the plane of the femur heads (Figure 154).



**Figure 154.** With pattern 6 there is no femur head angle involved, and absolute and relative sacral obliquity measure the same

Pattern 6 is represented on erect A-P lumbopelvic radiographic images (sacral base view) as a measured angular deviation of the sacral base from the horizontal plane (absolute sacral obliquity) with no leg length imbalance measured as a zero femur head angle (FHA). This results in relative sacral obliquity SOA ( $\alpha$ ) with  $0^\circ$  FHA ( $\beta$ ) (Figure 155).



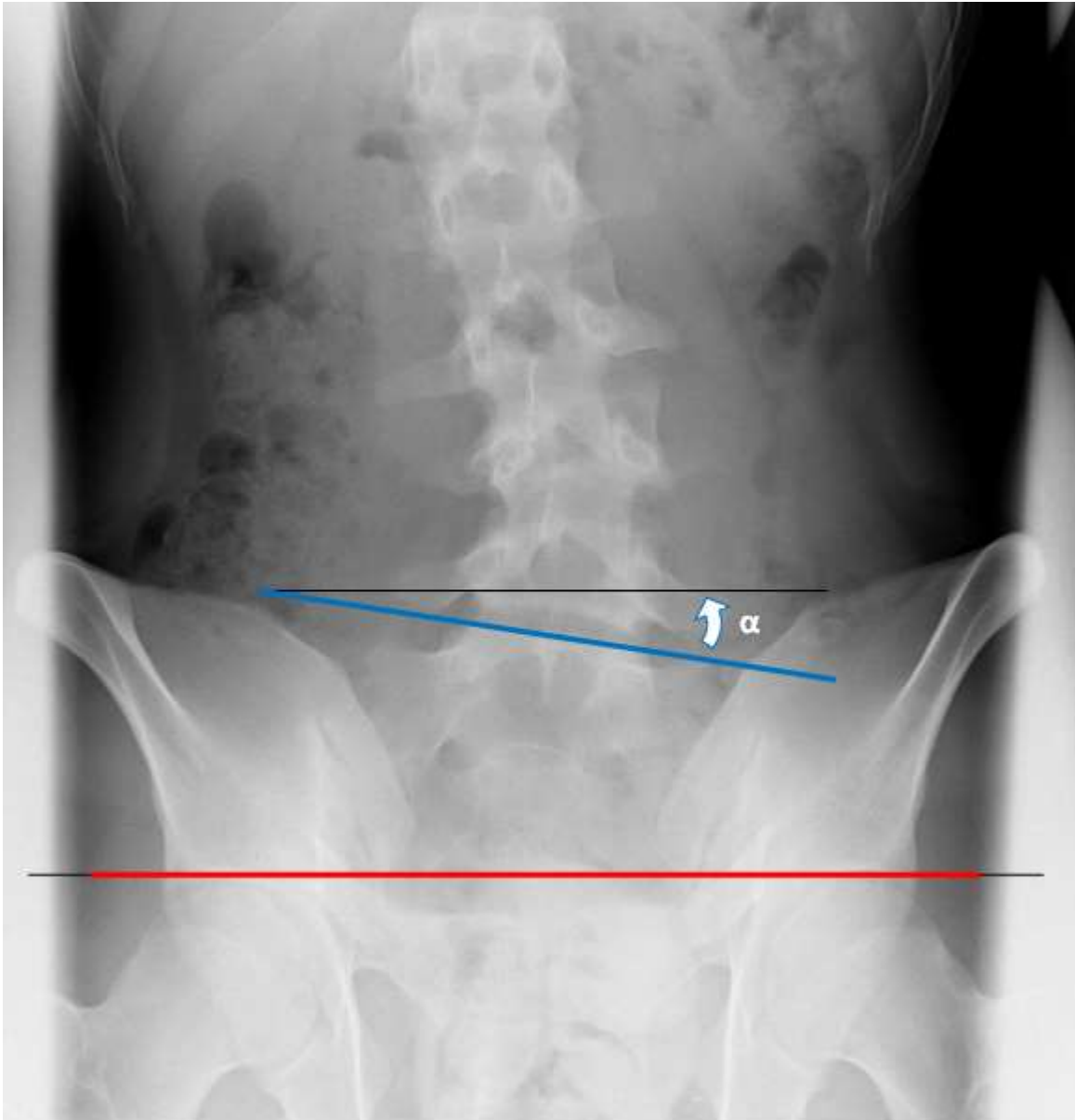
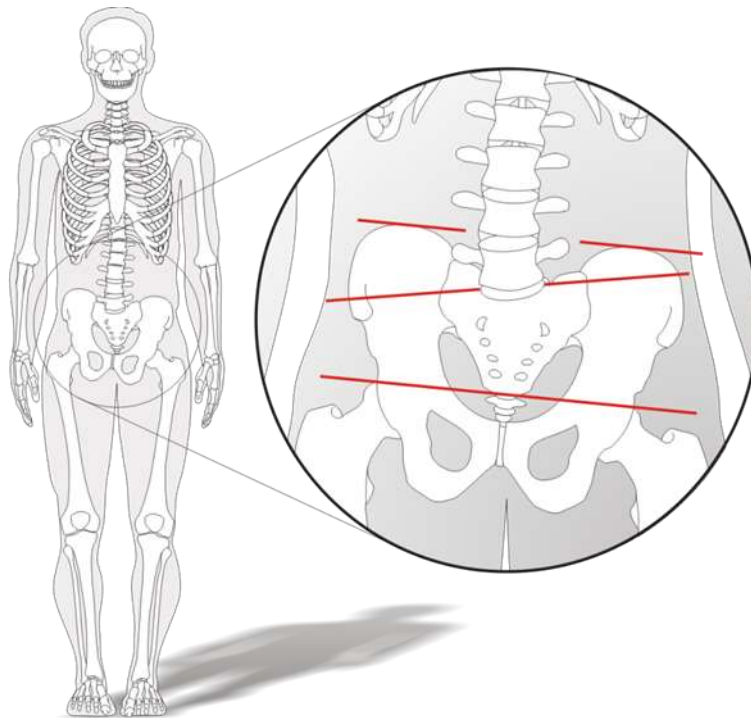


Figure 155. On an erect A-P lumbopelvic radiographic image (sacral base view) an angular deviation of the sacral base is measured from the horizontal plane (SOA) with a zero femur head angle (FHA)

### Standing Pattern 7

Standing pattern 7 involves absolute sacral obliquity (SOA) with contralateral leg length imbalance (FHA) resulting in relative sacral obliquity contralateral to the shorter leg. In erect posture the relative sacral obliquity is partially offset by the contralateral anisomelia so that the absolute sacral obliquity is less than the relative sacral obliquity (Figure 156).



**Figure 156. Standing pattern 7 involves absolute sacral obliquity (SOA) with contralateral leg length imbalance (FHA)**

Standing pattern 7 has absolute sacral obliquity (SOA) in one direction and contralateral leg length imbalance in the other direction so they have opposite signs (+/-) indicating the direction of rotation. This results in relative sacral obliquity that has a sign indicating direction of movement (+/-) the opposite of that for the femur head angle as it always represents contralateral rotation to the shorter leg (Figure 157).

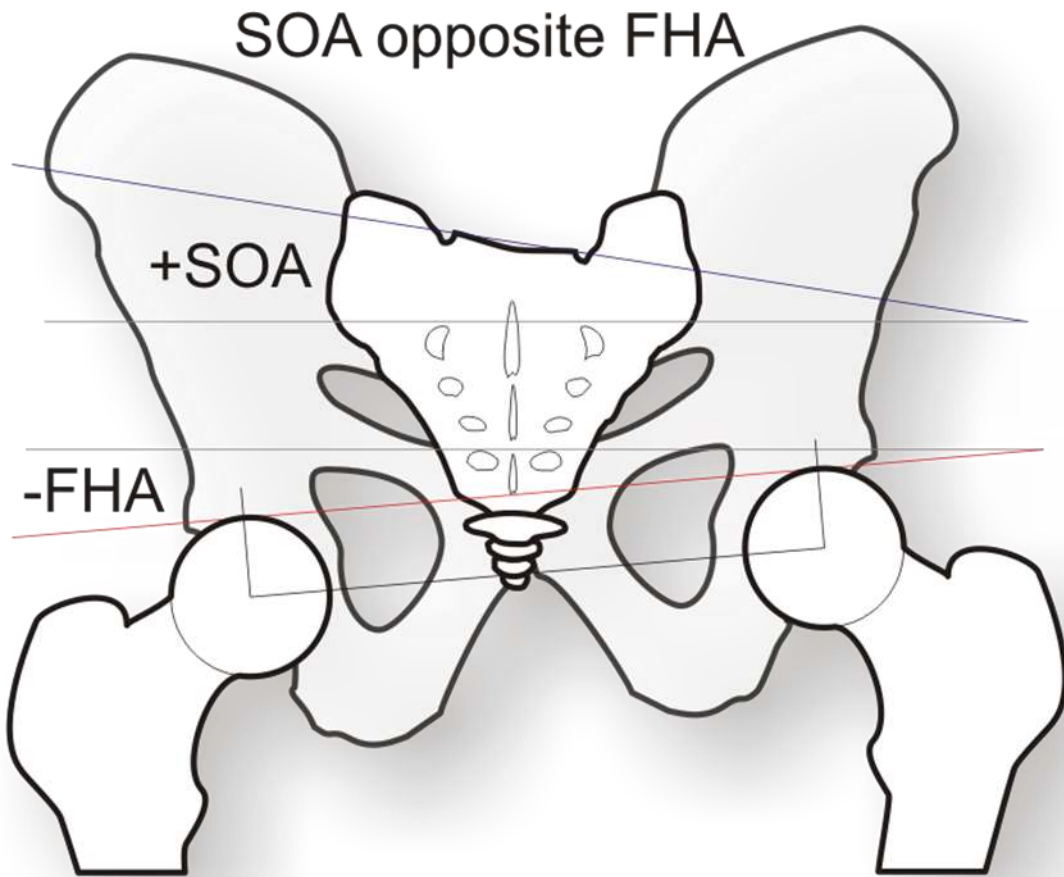
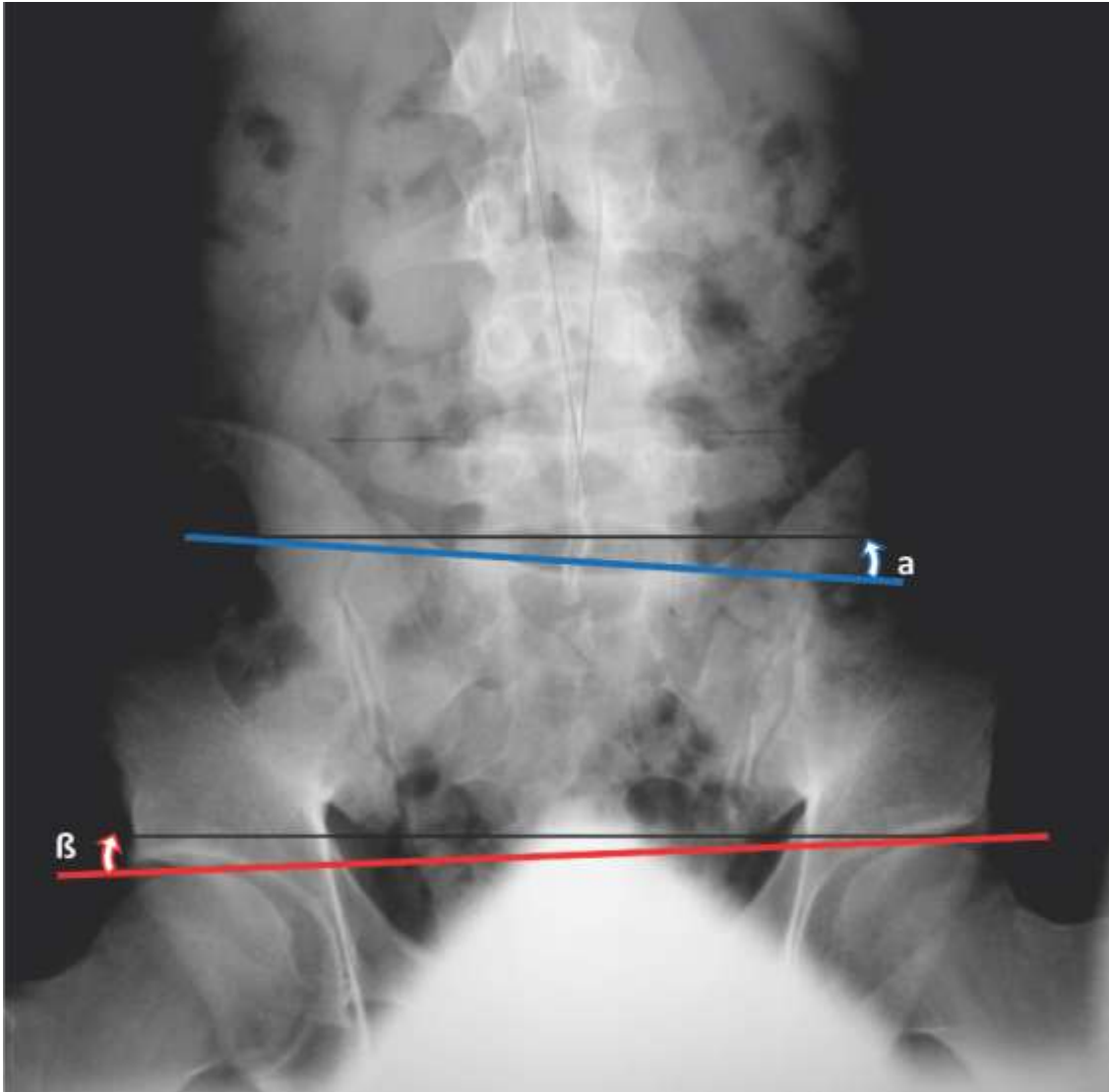


Figure 157. Standing pattern 7 has absolute sacral obliquity (SOA) in one direction and contralateral leg length imbalance in the other direction so they have opposite signs (+/-) indicating the direction of rotation


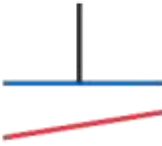
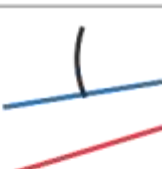

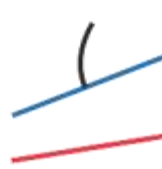
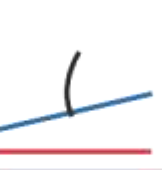
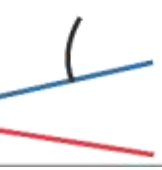
Erect A-P lumbopelvic radiograph (sacral base view) can be used to measure angles representing absolute sacral obliquity (SOA) and leg length imbalance (FHA). Standing pattern 7 involves absolute sacral obliquity (SOA) and leg length imbalance (FHA) on opposite sides resulting in relative sacral obliquity in the same direction as the absolute sacral obliquity (SOA opposite FHA) (Figure 158).



**Figure 158.** Standing pattern 7 involves absolute sacral obliquity (SOA) and leg length imbalance (FHA) on opposite sides resulting in relative sacral obliquity in the same direction as the absolute sacral obliquity (SOA opposite FHA)

The standing patterns are similar to those attributed to Lloyd and Eimerbrink by Hielig (372) and used by Juhl *et al* (83) in their study of asymmetry of the pelvis in the frontal plane (Table 13). None of the studies identified in the literature relating to sacral obliquity patterns provide information on the validity of the measurements used in the pelvic analysis. For example there is no indication if the obliquity measurements referred to in the studies relate to true dihedral angles or apparent dihedral angles measured on standard plain film pelvic radiographs.

Table 13. Seven standing patterns used by Juhl et al in their study of asymmetry of the pelvis in the frontal plane

Pattern No	Osteopathic Pattern (Juhl et al)	Pattern Description	Graphical representation
1	Normal	Normal No anisomelia No sacral obliquity	
2	II	No sacral tilt, femoral head unleveling	
3	IA	Disproportion same side, femoral head unleveling greater	
4	I	Parallel unleveling anisomelia only	
5	IB	Disproportion same side, sacral base unleveling greater	
6	III	Primary sacral tilt, sacral base unleveling only	
7	IV	Contralateral tilt, unleveling to opposite sides	

While the categorisation used by Juhl and his colleagues was primarily based on clinical or therapeutic considerations, in this study categorisation of pelvic patterns was developed to relate each of the components as a trigonometric function in order to calculate the amount needed to level the sacral base relative to the horizontal plane. The particular pattern dictated the specific formula required to calculate the vertical height that one femur head would need to be raised in order to level the sacral base in standing posture. The

calculated distance was designated the leg length equivalent (LLE). The formulae were different and specific for each of the configurations that formed the seven patterns. The formulae were developed for both standing patterns to calculate the amount one foot would need to be raised in order to level the sacral base in erect standing posture and sitting patterns to calculate the amount one ischial tuberosity would have to be raised in order to level the sacral base in erect sitting posture.

Descriptions of the seven patterns and the trigonometrical functions associated with these patterns are outlined in (Table 14). The patterns are accompanied by graphical representations of the scalene triangles on which the trigonometrical functions are based. They represent the angular relationship between the horizontal plane and both the sacral base and plane of the femur heads. The lines represent the plane of the sacral base viewed edge on (as a line) in the frontal (X-Y) plane and the plane containing the tangent points of the femur heads. The angles are designated as parallel to the horizontal plane, or positive if inferior on the right or negative if inferior on the left relative to the horizontal plane.

**Table 14. Table of the seven standing pelvic patterns, descriptions of the patterns and the amount needed to level the sacral base (LLE). The lines represent the plane of the sacral base (SOA) (blue), and the plane of the femur heads (FHA) (red)**

Pattern	Description	SBA / FHA relationship
1	Normal with no sacral obliquity angle (SOA) and no femur head angle (FHA)	No SOA, No FHA
2	Normal sacra l obliquity angle (SOA) with a + or – femur head angle (FHA)	No SOA, FHA
3	Sacral obliquity angle (SOA) and femur head angle (FHA) inclined in the same direction with the sacral base angle less than the femur head angle	SOA < FHA
4	Sacral obliquity angle (SOA) and femur head angle (FHA) inclined in the same direction and equal in magnitude	SOA = FHA
5	Sacral obliquity angle (SOA) and femur head angle (FHA) inclined in the same direction with the sacral base angle greater than the femur head angle	SOA > FHA
6	Sacral obliquity angle (SOA) with no femur head angle (FHA)	SOA, No FHA
7	Sacral obliquity angle (SOA) with femur head angle (FHA) inclined in the opposite direction	SOA opposite FHA

If both angles are in the same direction (both + or both -) the larger angle is in bold. In developing the formulae for the correction of sacral obliquity the assumption was made that the pelvis could rotate around the femur head as a unit on the side opposite sacral inferiority. A further assumption was based on investigations by Stureson (155), Fann (11) and Yochum (185) and involved the relative movement of the sacroiliac joint around the Z-axis. These studies suggest that, due to very limited movement of the sacrum around the z-axis relative to the ilium, there is a linear relationship between the height of a heel lift placed under one foot in erect posture and the resulting change in angulation of the sacral base in the frontal plane.

Others (72, 383, 392) have suggested that one or both of the innominate bones rotate relative to the sacrum as a result of either a natural short leg or induced LLI as a result of a heel lift placed under one foot. Cooperstein and Lew, in a review of the literature relating to the relationship between pelvic torsion and LLI state that the response to heel lift therapy used for the correction of scoliosis can be complicated and made variable by the impact torsion effect has overall on the pelvis.

The equations used the width between tangent points formed as the contact point on both femur heads and a plane parallel to the sacral base (FWW). The FHW represented the length of the hypotenuse of a right-angled triangle. The height of the side opposite the acute angle ( $\beta$ ) formed between the plane line of the femur heads and the horizontal plane line (FHA) was calculated using the *sine* function of that angle multiplied by the width of the femur heads ( $\beta * FHW$ ). The sacral obliquity angle ( $\alpha$ ) was multiplied by the femur head width ( $\alpha * FHW$ ) or was added or subtracted from the femur head angle (FHA) as indicated by the different patterns ( $\beta-\alpha$ ,  $\alpha-\beta$ ,  $\alpha+\beta$ ) with the *sine* of the resulting angle multiplied by the width of the femur heads.


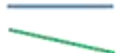

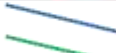





### 8.2.2 *Absolute and relative sacral obliquity in sitting posture*

Similar patterns to the standing pelvic patterns were identified based on the relationship of the ischial tuberosities to the sacral base. The patterns were created by relating the absolute sacral obliquity (SOA) with the angle formed between a plane representing the ischial tuberosities and the horizontal plane. The lines represent the plane of the sacral base viewed edge-on in the frontal (x-y) plane and the plane containing the tangent points of the ischial tuberosities.

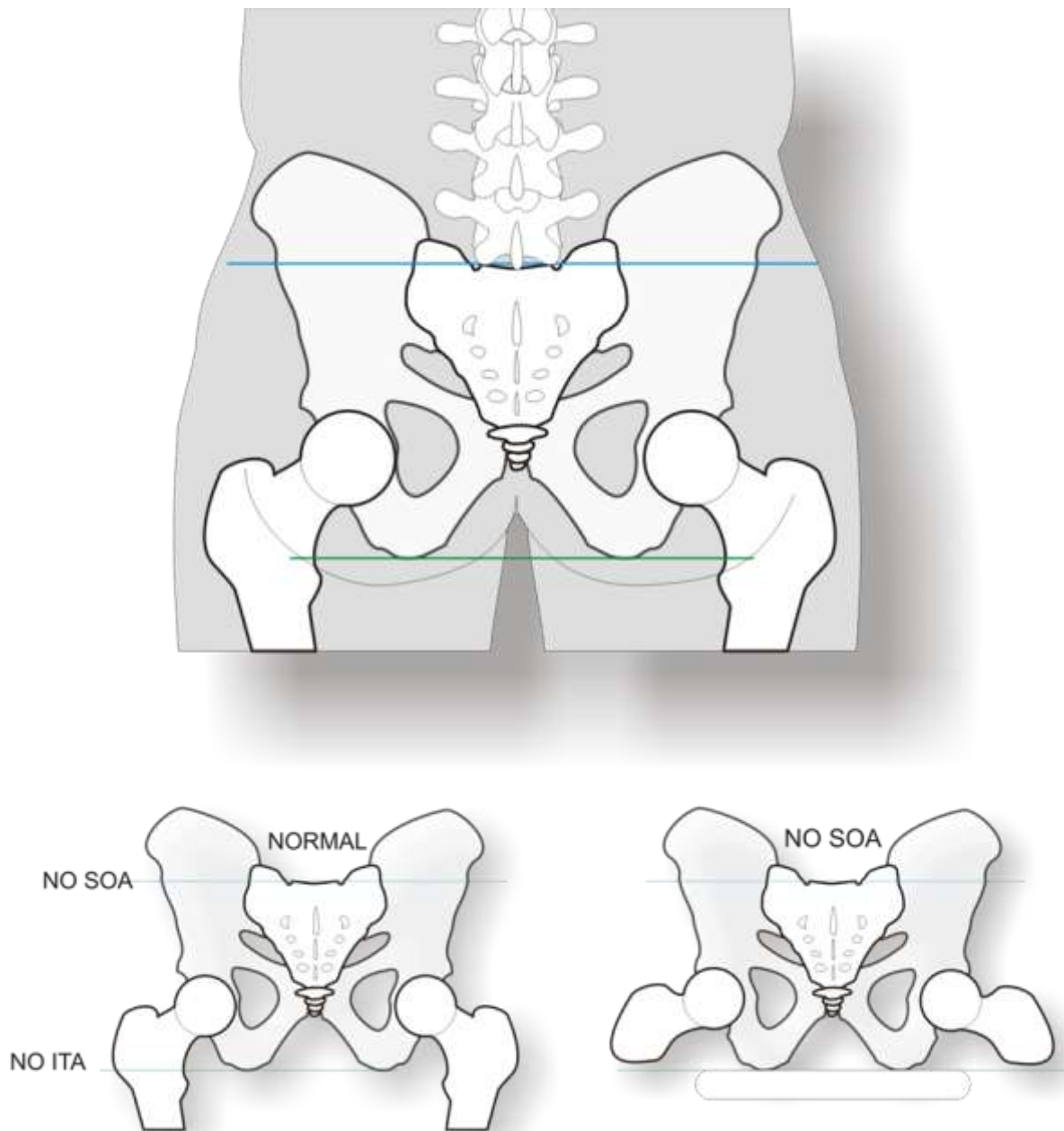
In the following diagrams and radiographic views the blue lines represent the sacral base, the green lines represent the line tangent to the ischial tuberosities and the black lines represent the horizontal plane. The angles are designated as parallel to the horizontal plane, or positive if inferior on the right or negative if inferior on the left relative to the horizontal plane. If both angles are in the same direction the greater angle is in bold. The seven patterns are comprised of normal (orthogonal) plus six abnormal patterns that relate sacral obliquity and the ischial tuberosity angle to a horizontal plane (Table 15). The relative magnitude of the variables (SOA and ITA) along with the width of the tangent points on the tuberosities dictate the makeup of the respective trigonometrical equations used to calculate the amount the indicated ischial tuberosity would need to be raised in order to level the sacral base in level sitting posture.

**Table 15. The seven sitting patterns are comprised of normal (orthogonal) plus six abnormal patterns that relate sacral obliquity and the ischial tuberosity angle to a horizontal plane in erect posture**

Pattern	Description	Variable
1	No SOA, No ITA	
2	No SOA, ITA	
3	SOA < ITA	
4	SOA = ITA	
5	SOA > ITA	
6	SOA, No ITA	
7	SOA opposite ITA	

### Sitting pattern 1

With sitting pattern 1 there is no absolute or relative sacral obliquity and no pelvic (ischial) asymmetry. The result is in sitting posture on a level base, the sacral plateau is horizontal with no absolute sacral obliquity (Figure 159).



**Figure 159. Sitting pattern 1 with no absolute or relative sacral obliquity and no pelvic (ischial) asymmetry**

The measurements indicating sitting pattern 1 made on erect A-P lumbopelvic radiograph (sacral base view) demonstrate no measurable sacral obliquity nor angulation of the ischial tuberosities relative to the horizontal plane (no angle  $\alpha$  and no angle  $\sigma$ ) (Figure 160).

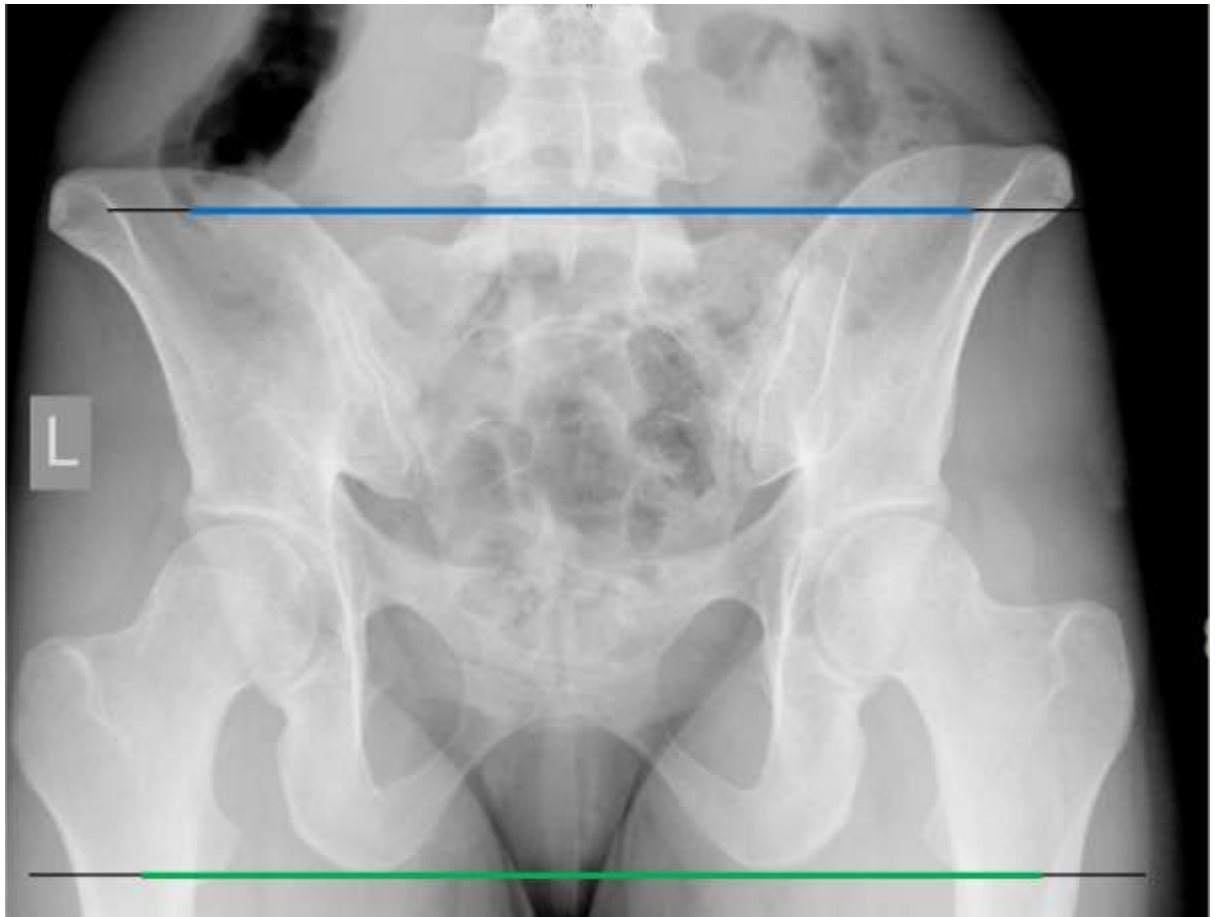
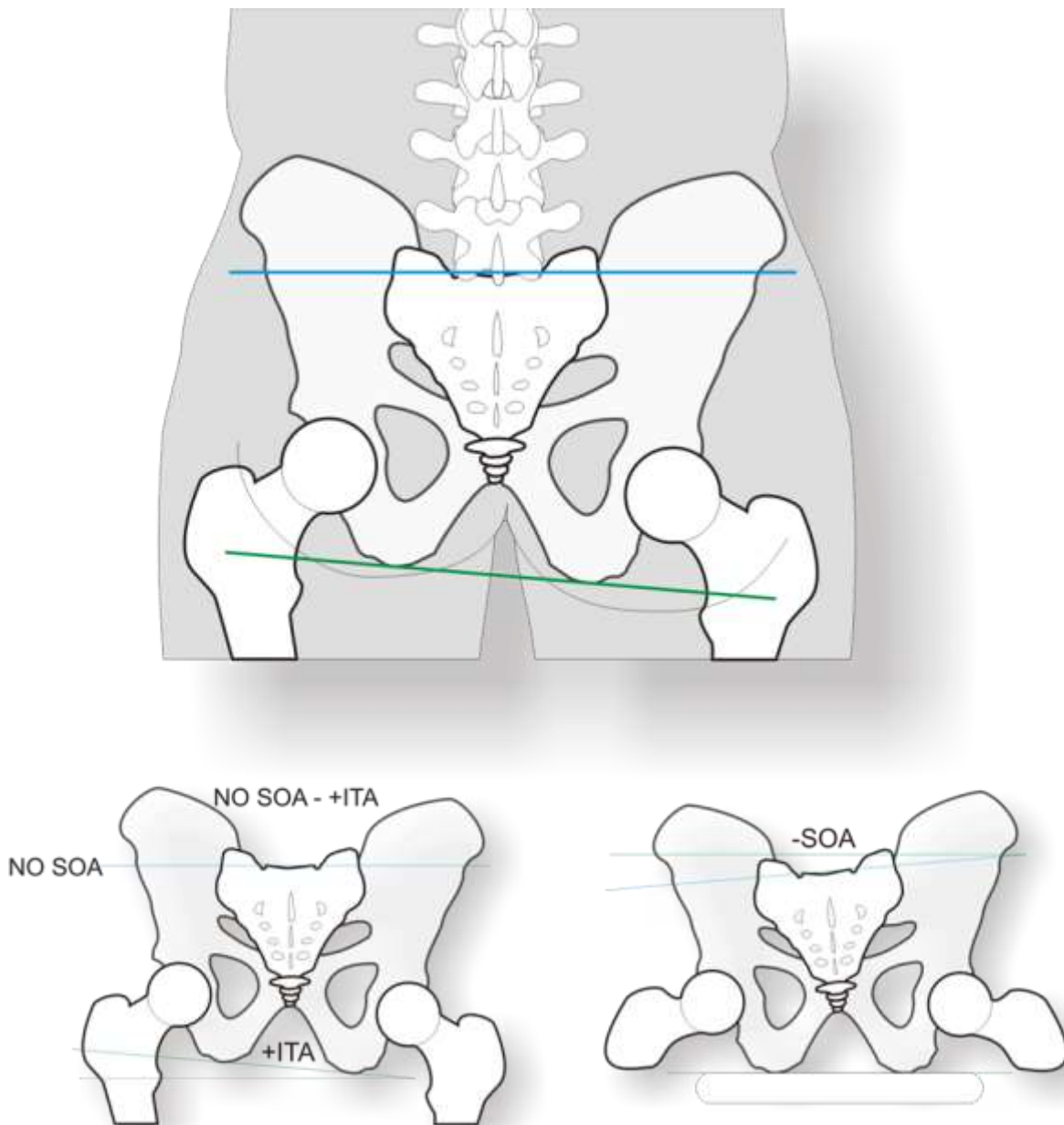


Figure 160. Erect A-P lumbopelvic radiograph (sacral base view) of sitting pattern 1 with no sacral obliquity angle (SOA) and no ischial tuberosity angle (ITA)

### Sitting pattern 2

The features of sitting pattern 2 are the absence of absolute sacral obliquity (SOA) in erect posture coupled with pelvic asymmetry resulting in a measureable ischial tuberosity angle (ITA). This configuration produces a relative sacral obliquity (SOA/ITA) that is opposite in direction and the same magnitude as the ischial tuberosity angle. The relative sacral obliquity is due to pelvic asymmetry or a combination of pelvic symmetry, anisomelia and sacral obliquity. Sitting posture on a level surface produces a sacral obliquity angle to the side opposite the ischial tuberosity angle (Figure 161).



**Figure 161. Sitting pattern 2 involves no absolute sacral obliquity (SOA) in erect posture with relative sacral obliquity resulting from pelvic asymmetry combined with contralateral anisomelia**

Measurement of erect A-P lumbopelvic radiographs (sacral base view) that demonstrate sitting pattern 2 reveal no sacral obliquity angle (SOA -  $\alpha$ ) but have a positive (+) or negative (-) ischial tuberosity angle (ITA -  $\sigma$ ) (Figure 162).

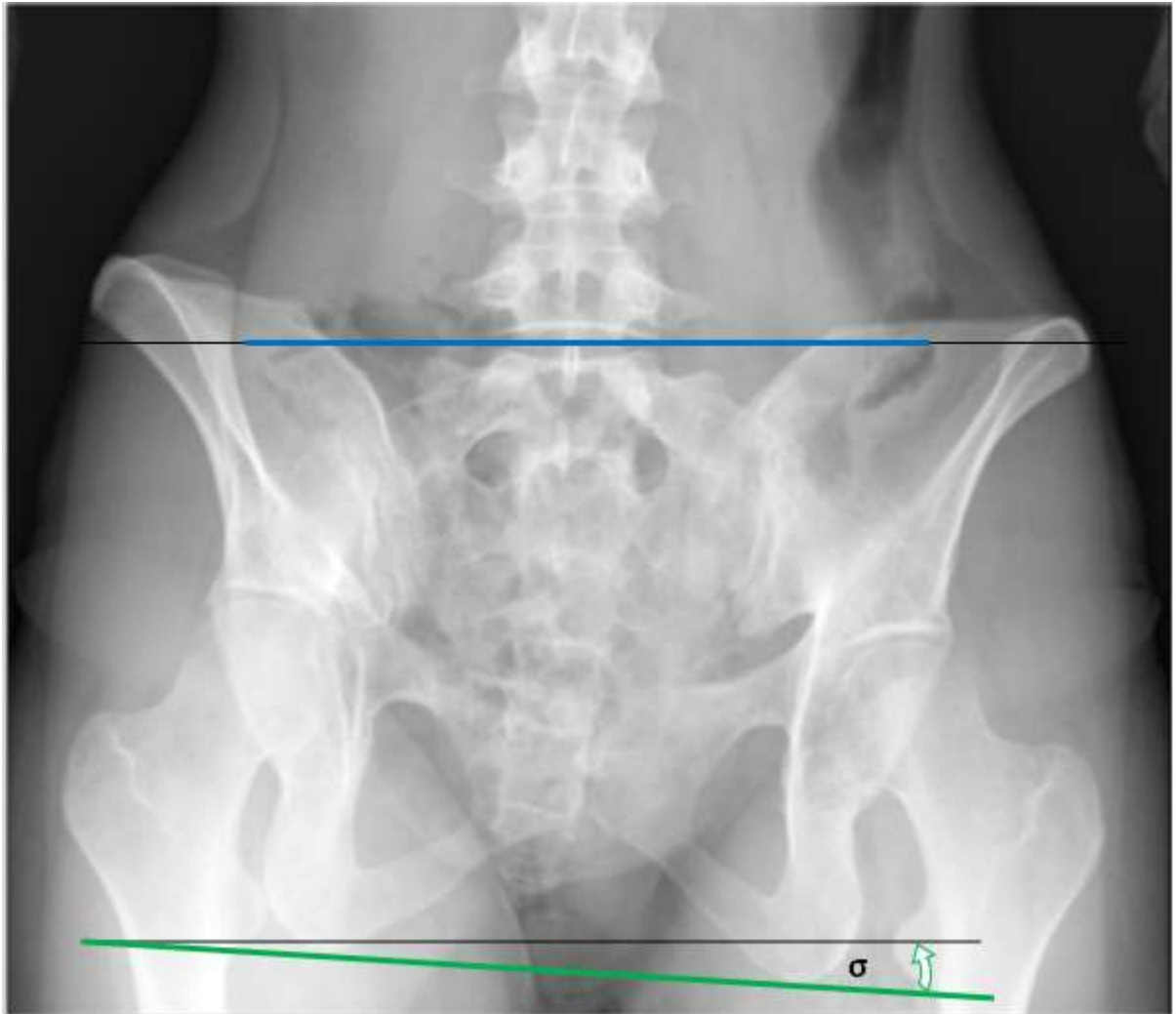
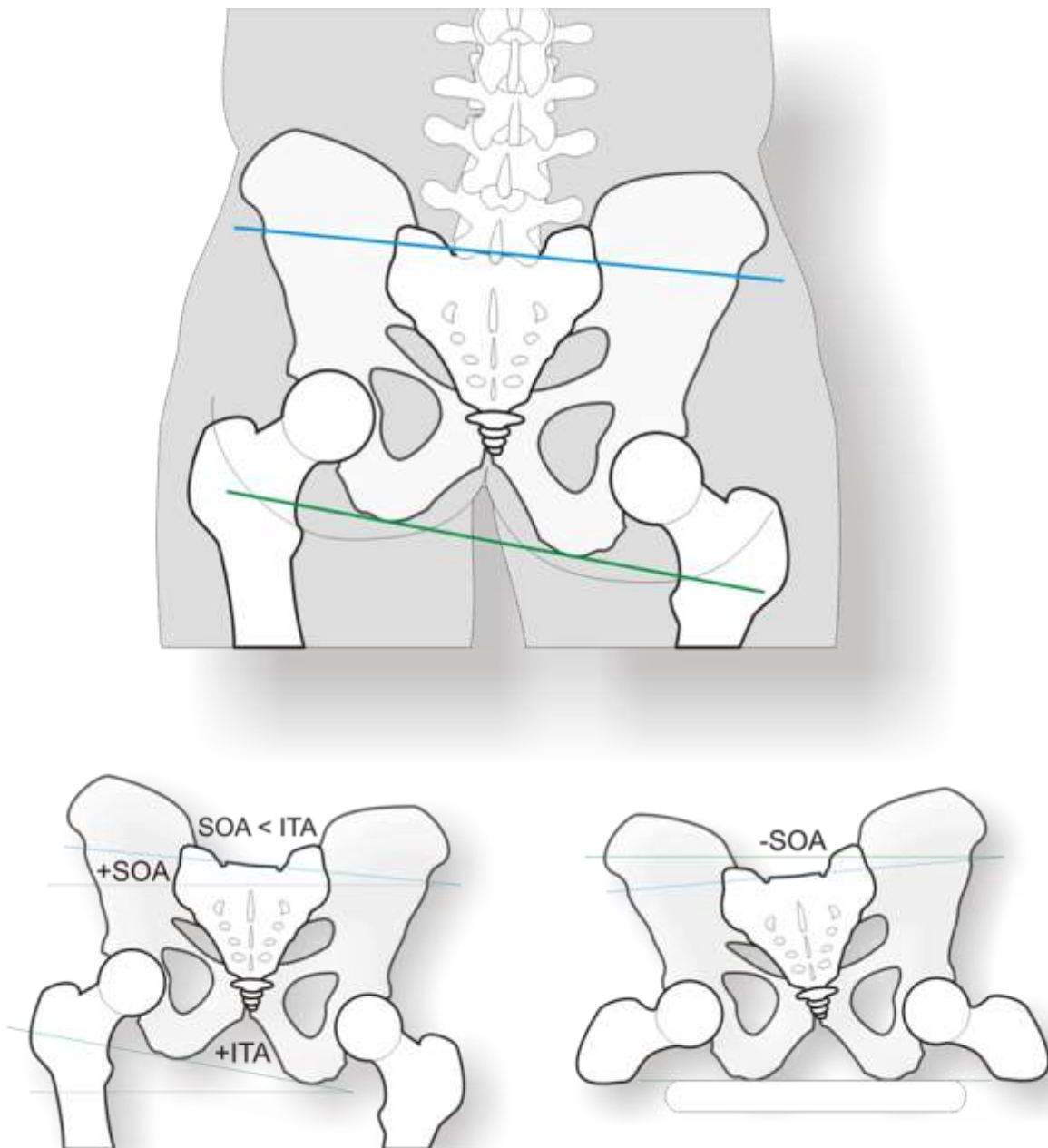


Figure 162. Erect A-P lumbopelvic radiograph that demonstrates sitting pattern 2 with no sacral obliquity angle (SOA -  $\alpha$ ) and a positive (+) ischial tuberosity angle (ITA -  $\sigma$ ). The blue line represents the sacral base, the green line the line tangent to the ischial tuberosities and the black lines represent the horizontal plane.

### Sitting Pattern 3

Sitting pattern 3 involves absolute sacral obliquity combined with contralateral relative sacral obliquity (SOA/ITA) that results from pelvic (ischial) asymmetry coupled with anisomelia or sacral base asymmetry (Figure 163). The ITA is greater than the relative sacral obliquity (SOA/ITA). In erect standing posture this configuration results in some degree of absolute sacral obliquity (SOA). In level sitting posture there is sacral obliquity (SOA) in the opposite direction because of the angle formed by the ischial tuberosities and the sacral base (relative sacral obliquity).



**Figure 163. Sitting pattern 3 with absolute and contralateral relative sacral obliquity**

Erect A-P lumbopelvic radiographs of sitting pattern 3 reveal a measured sacral obliquity (SOA) with an ischial tuberosity angle (ITA) rotated in the same direction but of greater magnitude than the sacral obliquity  $[(+/-) \alpha < (+/-) \sigma]$  (Figure 164).

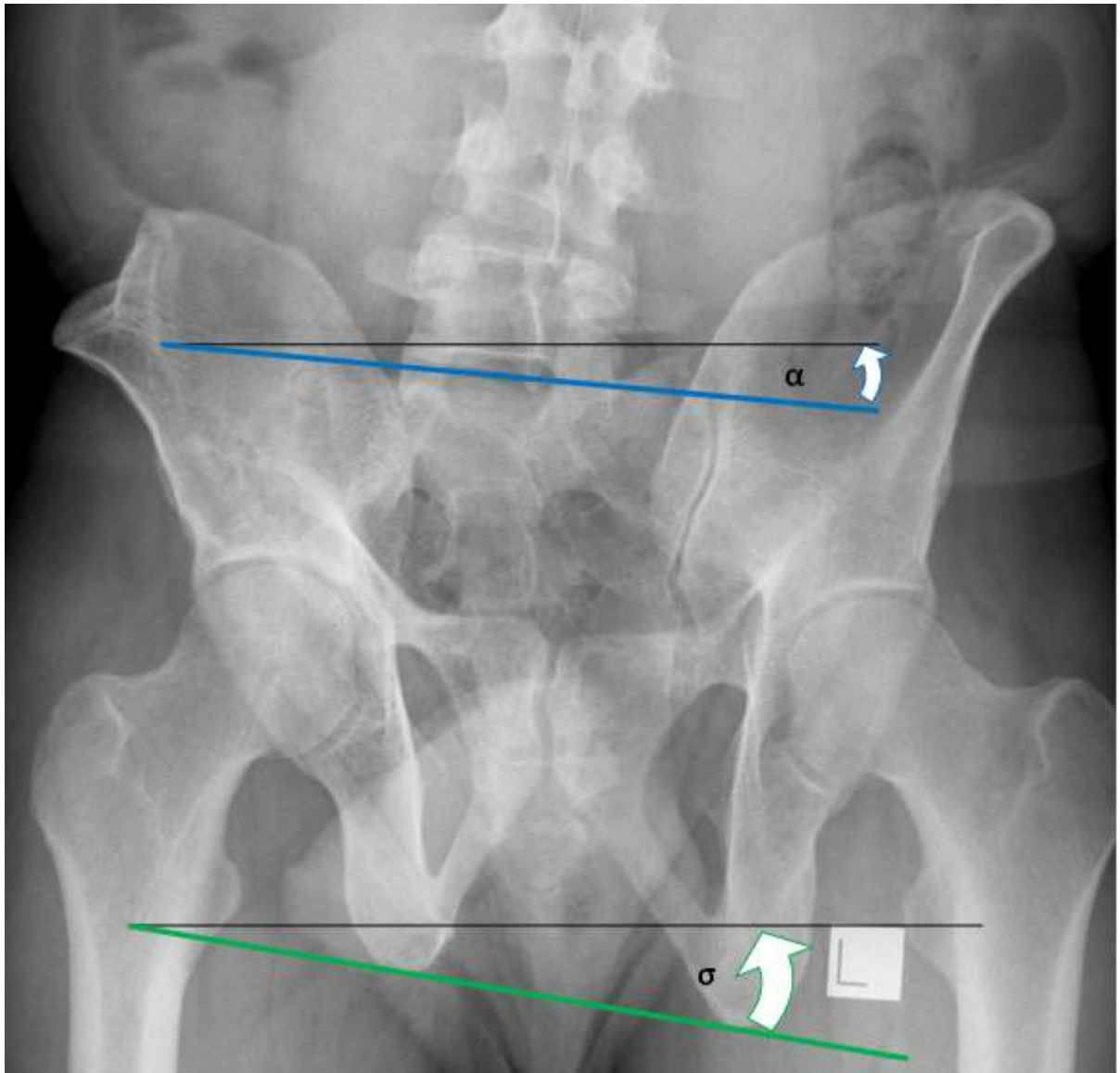


Figure 164. Erect A-P lumbopelvic radiograph (sacral base view) of sitting pattern 3 with sacral obliquity and an ischial tuberosity angle in the same direction and of greater magnitude

#### Sitting Pattern 4

Sitting pattern 4 involves absolute sacral obliquity (SOA) and with an equal ischial tuberosity angle (ITA) but no relative sacral obliquity in relation to the ischial tuberosities (SOA/ITA). This configuration is due to either contralateral sacral and ischial asymmetry coupled with no anisomelia (**A**), or a symmetrical pelvis combined with anisomelia (**B**). In level sitting posture there is no absolute sacral obliquity angle (**C**) (Figure 165).



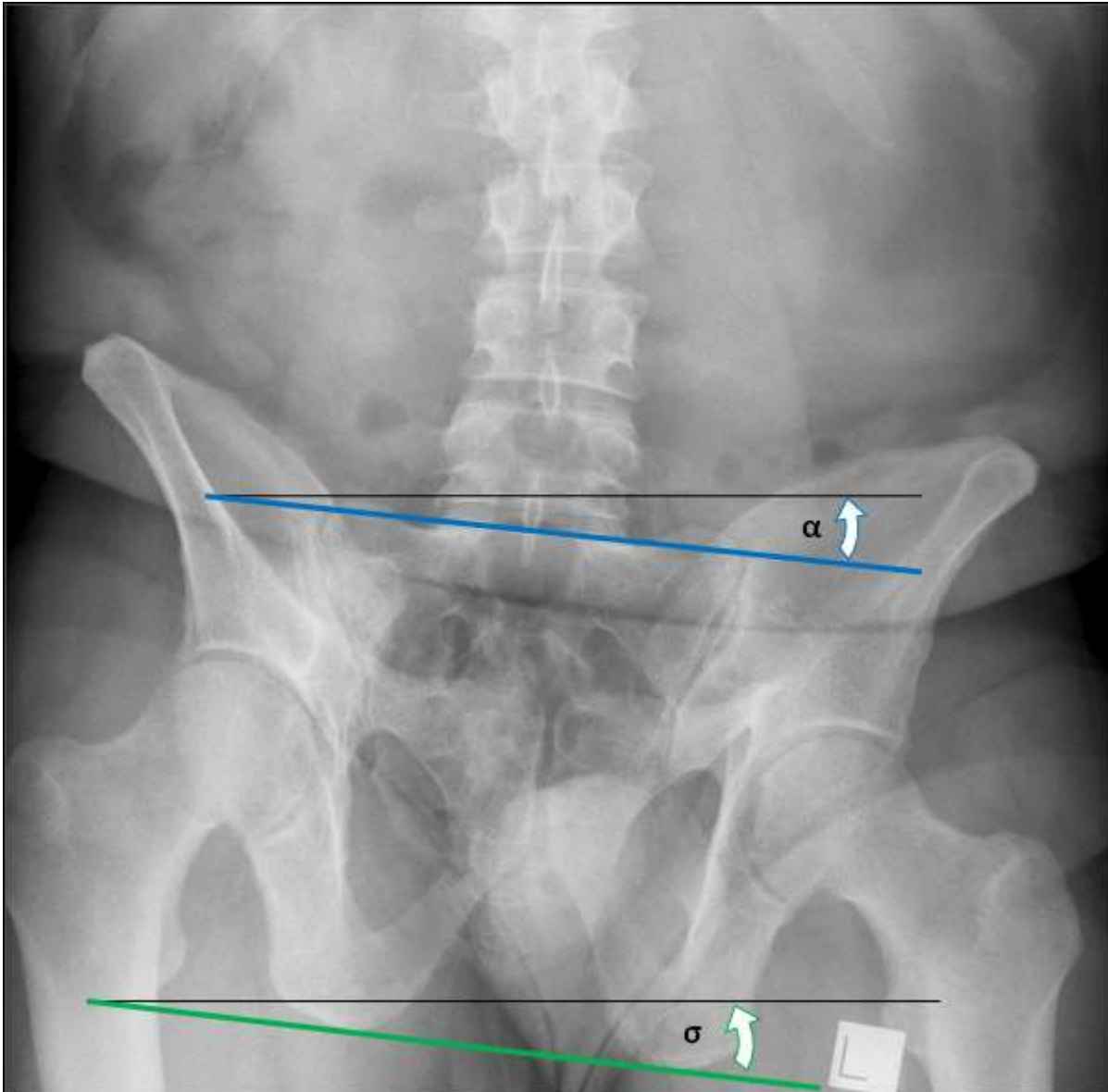


Figure 165. Erect A-P lumbopelvic radiograph (sacral base view) of sitting pattern 4 with the same amount and direction of SOA and ITA

Measurement of erect A-P lumbopelvic radiographs (sacral base view) exhibiting a sitting pattern 4 have the same measured amount of sacral obliquity and ischial tuberosity angle ( $+\alpha = +\sigma$ ) (Figure 165)

The effect anisomelia has on sacral obliquity in sitting and standing postures for pattern 4 can be illustrated with a series of radiographic images of one individual taken in the supine, erect standing and sitting positions. Structural symmetry of the pelvis is demonstrated in the supine lumbopelvic view with no SOA, FHA or ITA (Figure 166).

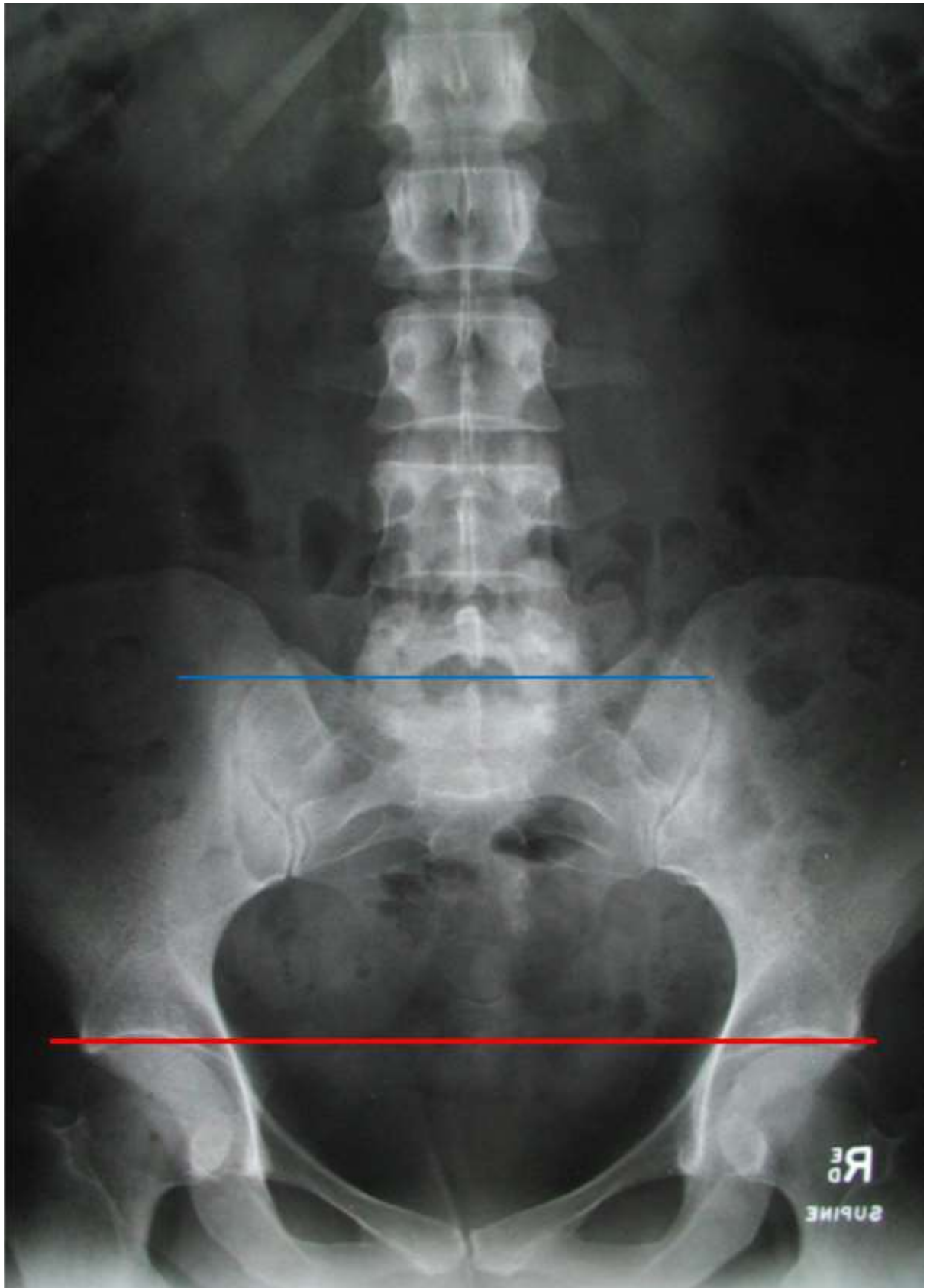


Figure 166. Plain film AP radiograph of an individual taken in the supine position with no measureable pelvic asymmetry or sacral obliquity or ischial tilt

A plain film radiographic image of the same individual in erect standing posture reveals no relative sacral obliquity (symmetrical pelvis) with anisomelia (FHA) resulting in absolute sacral obliquity (SOA) (Figure 167)

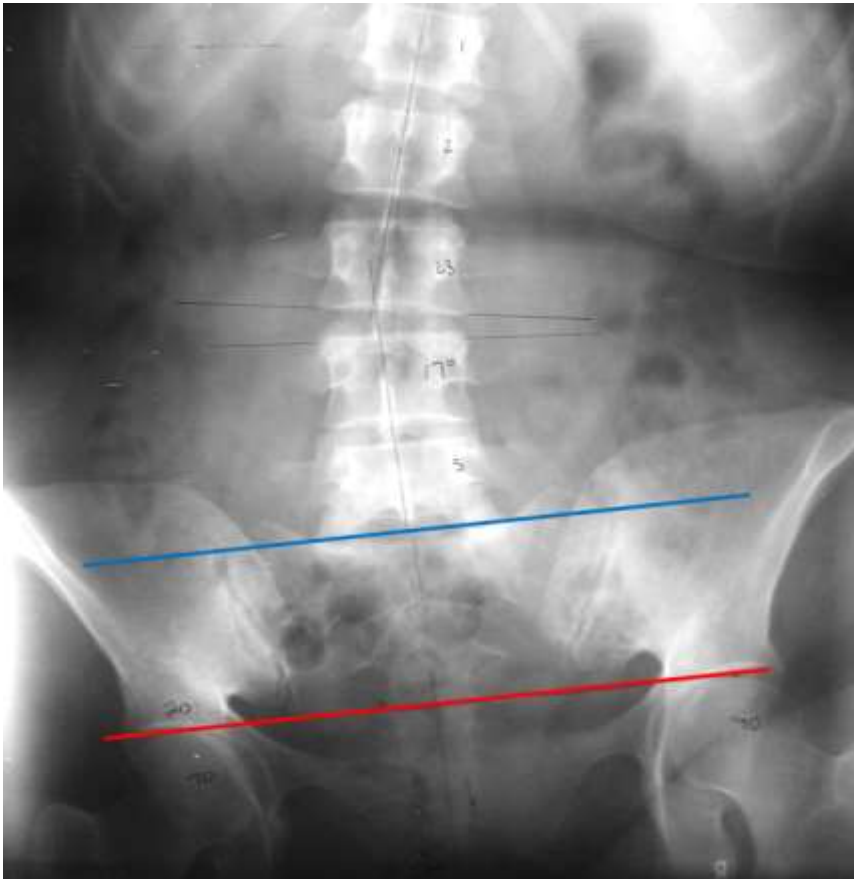


Figure 167. Erect AP radiograph of individual standing with no relative sacral obliquity (symmetrical pelvis). Anisomelia results in the same amount of absolute sacral and ischial obliquity

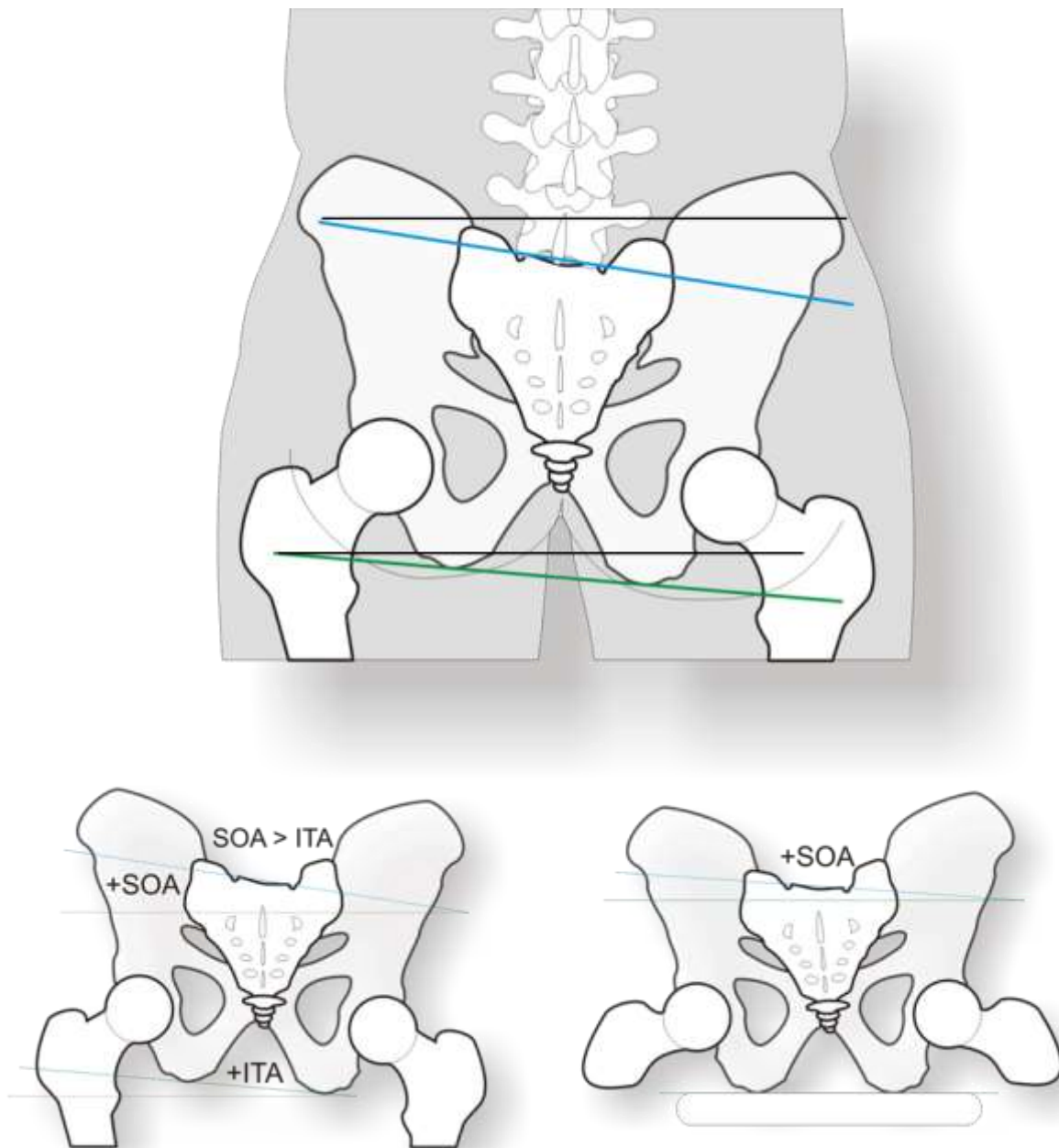
Plain film radiograph of the individual in level sitting posture reveals no measured absolute sacral obliquity (SOA). The anisomelia is removed in sitting posture with the weight transferring primarily to the ischial tuberosities (393). The result is a levelling of the sacral base in sitting posture (Figure 168).



**Figure 168.** AP radiograph of the individual sitting with sacral base view of the sacrum. There is no absolute sacral obliquity (SOA) in the sitting position on a level surface with the anisomelia removed

### Sitting Pattern 5

Sitting pattern 5 involves absolute sacral obliquity (SOA) with a lesser ischial tuberosity angle in standing posture. This combination produces an ipsilateral relative sacral obliquity (SOA/ITA). This configuration can result from a combination of pelvic (ischial) asymmetry, anisomelia and sacral obliquity (Figure 169).



**Figure 169.** Sitting pattern 5 with absolute sacral and ischial obliquity in the same direction in erect posture and with the sacral obliquity greater than the ischial obliquity. In upright sitting posture the ipsilateral relative sacral obliquity (to the ischial tuberosities) results in a residual degree of sacral obliquity (SOA)

Measurement of erect A-P lumbopelvic radiograph (sacral base view) demonstrating sitting pattern 5 reveal absolute sacral obliquity (+/- $\alpha$ ) with a greater degree of ipsilateral ischial tuberosity obliquity (+/- $\sigma$ ) (Figure 170)

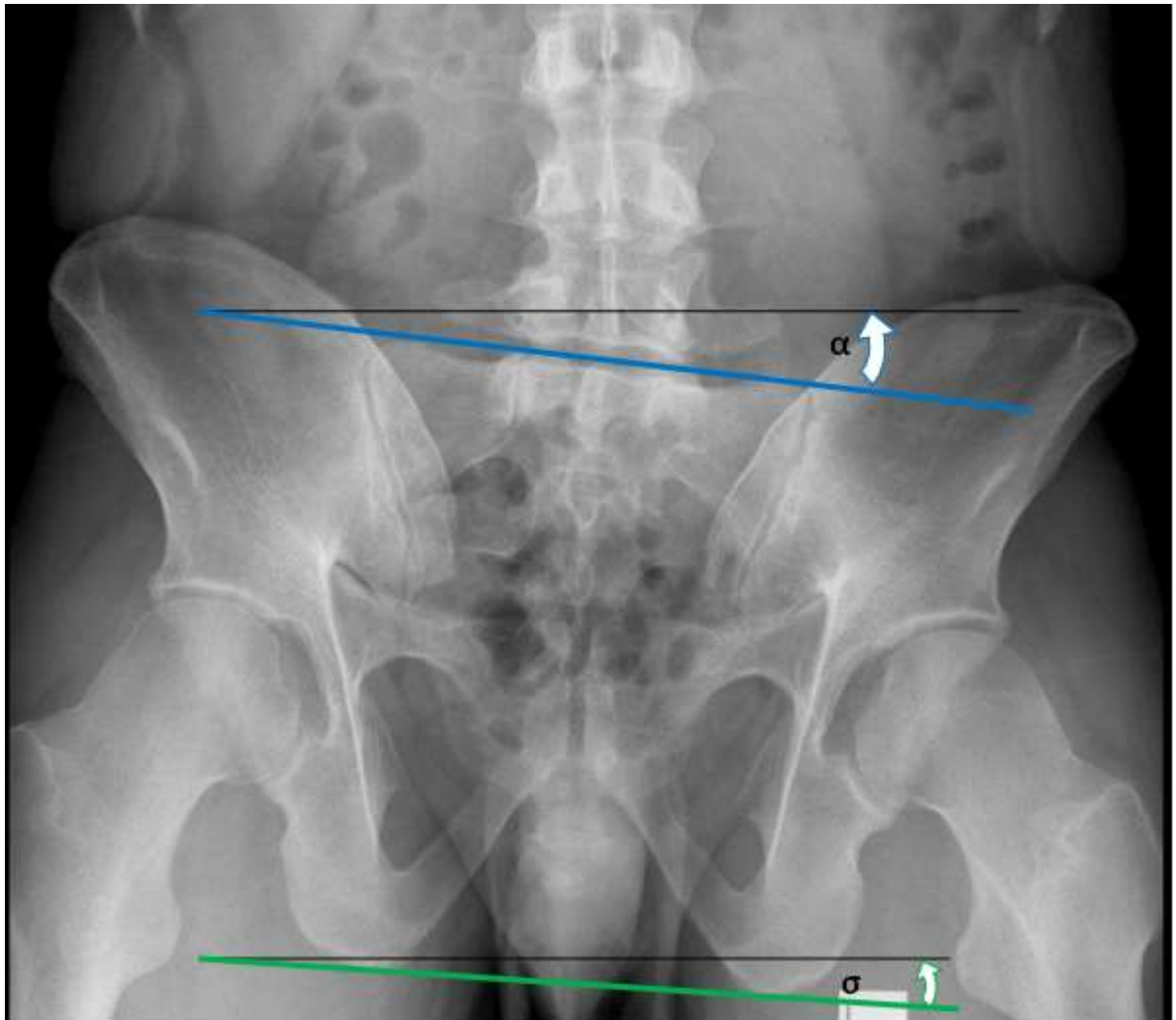
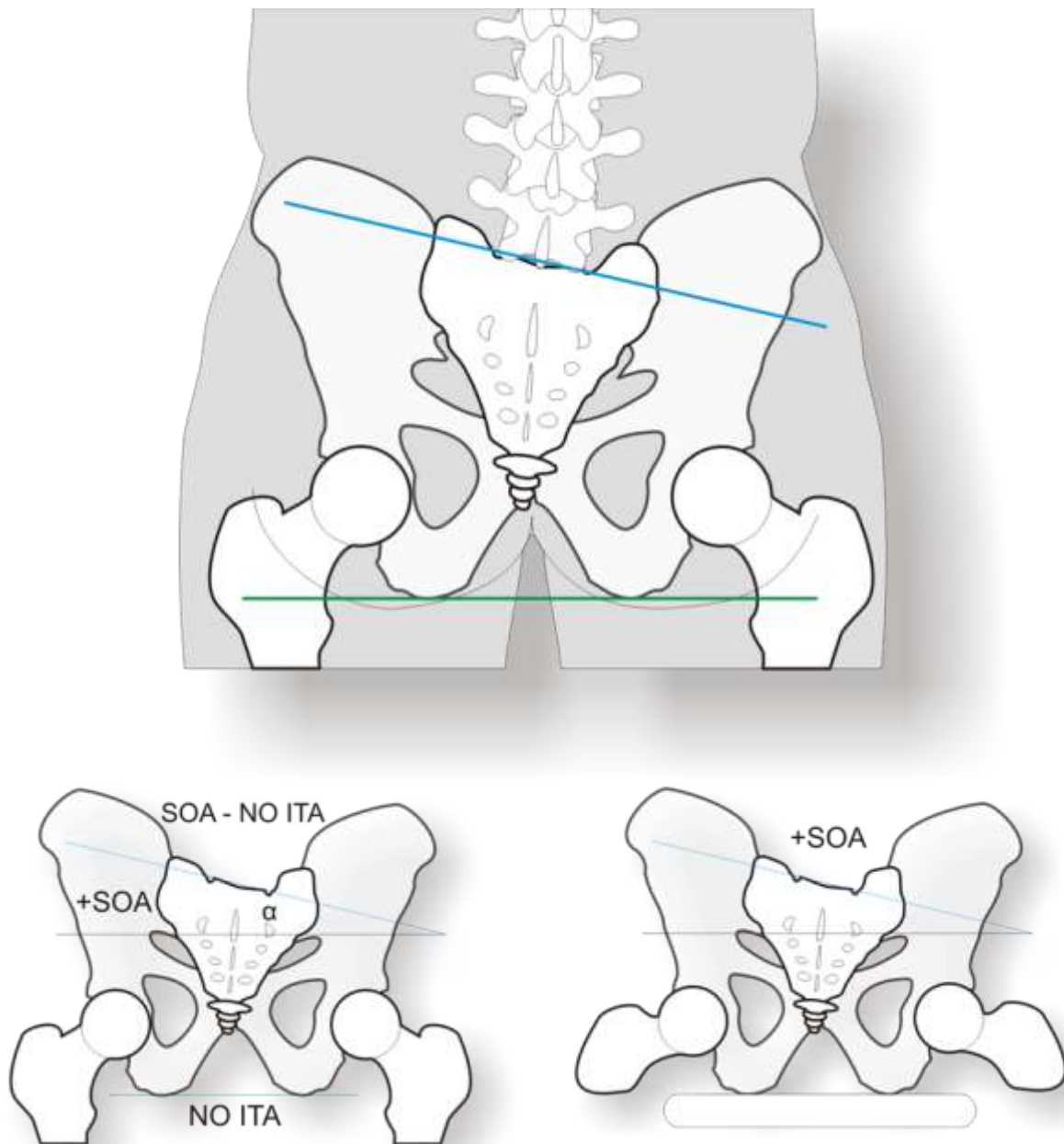


Figure 170. Erect A-P lumbopelvic radiograph (sacral base view) sitting pattern 5 with SOA and smaller ipsilateral ITA

### Sitting Pattern 6

Sitting pattern 6 involves absolute sacral obliquity (SOA) with no ischial tuberosity obliquity (ITA) in standing posture. The SOA remains the same in standing and sitting postures due to the level ischial tuberosities. The ipsilateral relative sacral obliquity (SOA/ITA) due to sacral and/or pelvic (ischial) asymmetry is always greater than the SOA in erect posture (Figure 171).





**Figure 171. Pattern 6 involves absolute sacral obliquity (SOA) with no ischial tuberosity obliquity (ITA) in standing posture. SOA remains the same in both standing and sitting postures**

Measurement of erect A-P lumbopelvic radiographs (sacral base view) demonstrating sitting pattern 6 reveal sacral obliquity ( $+\alpha$ ) with no ischial tuberosity angle ( $\sigma$ ) in upright standing posture (Figure 172). The sacral obliquity may or may not be associated with anisomelia as the SOA can be due to sacral base asymmetry or pelvic asymmetry or a combination of both coupled with anisomelia.

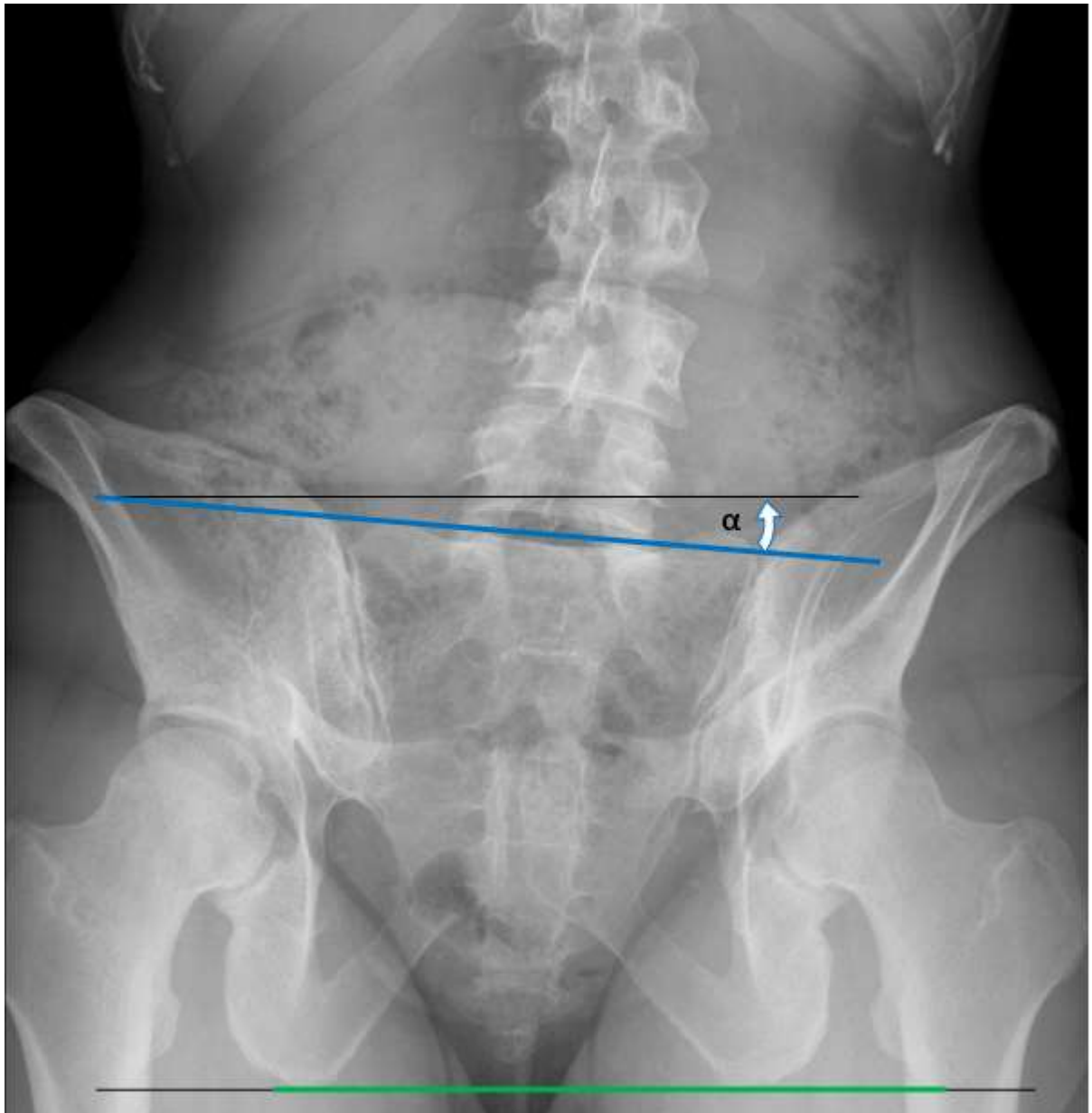
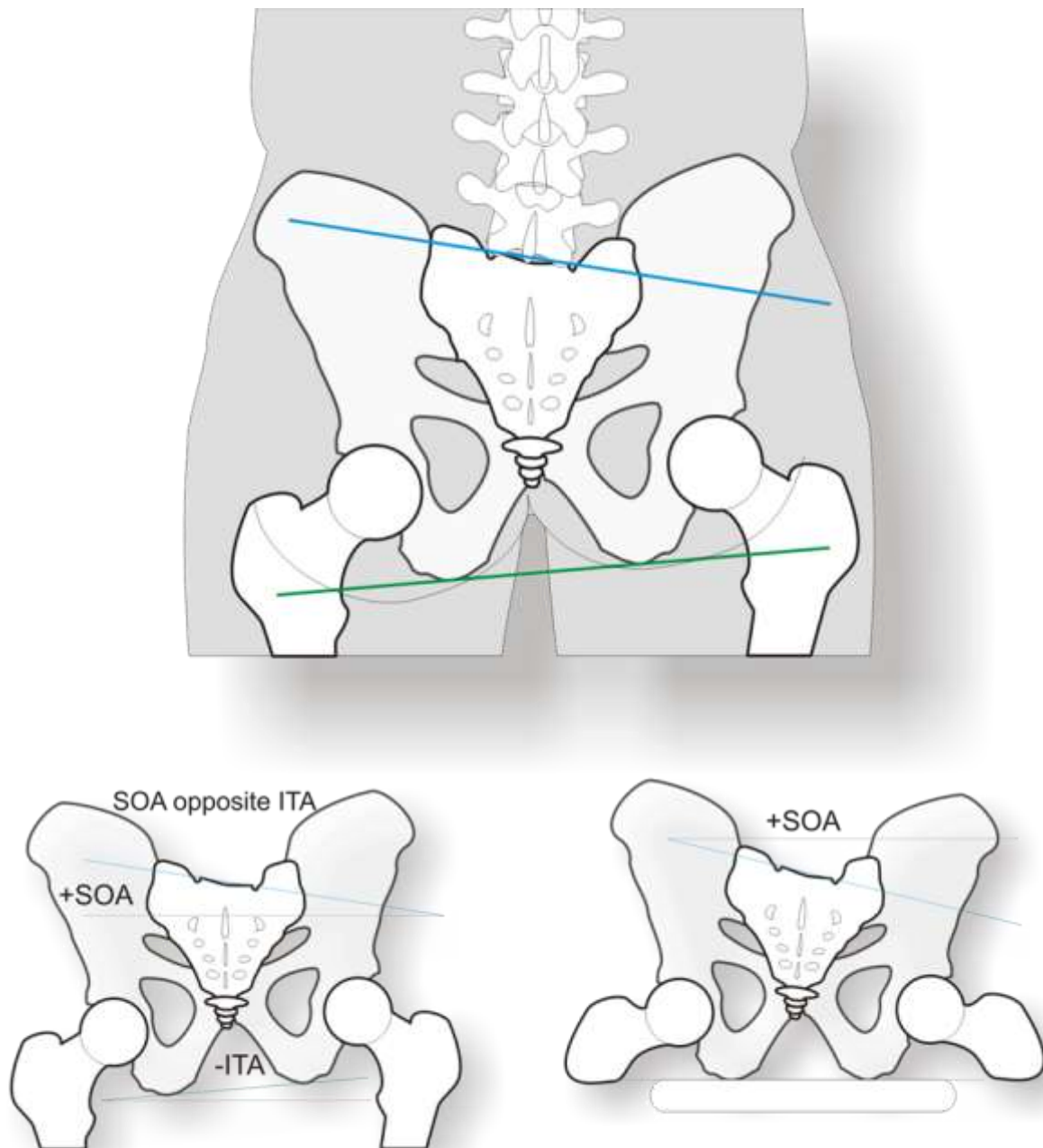


Figure 172. Erect A-P lumbopelvic radiograph (sacral base view) sitting pattern 6 with SOA (+ $\alpha$ ) but with no ITA ( $\sigma$ )

### Sitting Pattern 7

Sitting pattern 7 involves absolute sacral obliquity (SOA) and a contralateral ischial tuberosity angle measured in erect standing posture. This configuration can be due to a combination of sacral and/or pelvic (ischial) asymmetry and anisomelia (Figure 173). The effect is to create a relative sacral obliquity angle (SOA/ITA) that is greater than the standing sacral obliquity angle. This configuration produces an increase in absolute SOA in level sitting posture.





**Figure 173. Sitting pattern 7 involves absolute sacral obliquity (SOA) and contralateral ischial tuberosity angle (ITA)**

Measurement of erect A-P lumbopelvic radiograph (sacral base view) demonstrating sitting pattern 7 are characterised by absolute sacral obliquity ( $\pm\alpha$ ) with contralateral ischial tuberosity obliquity ( $\pm\sigma$ ) (Figure 174).

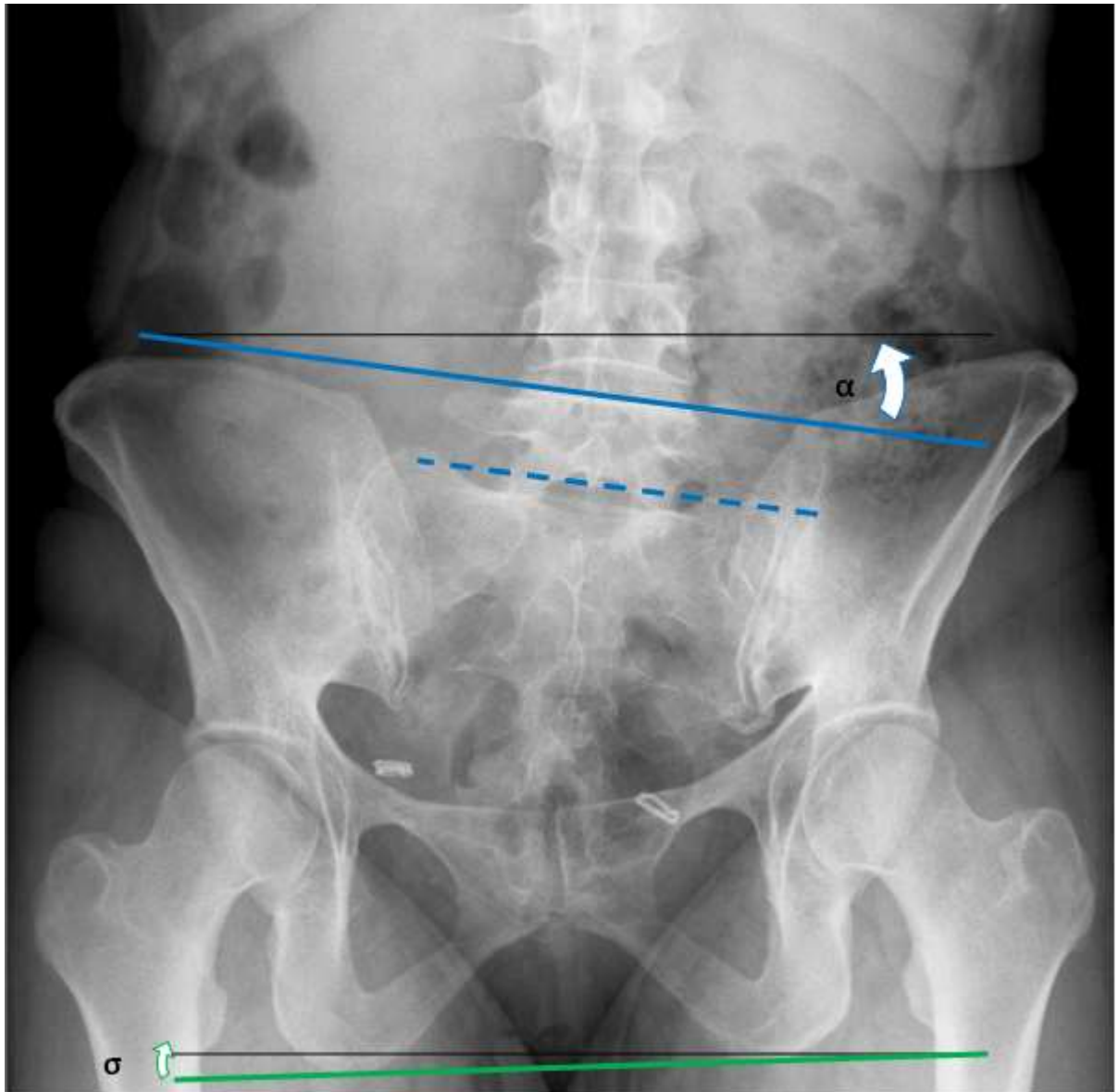








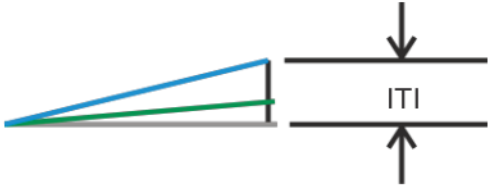
Figure 174. Erect A-P lumbopelvic radiograph (sacral base view) demonstrating sitting pattern 7 with SOA (+ $\alpha$ ) and opposite ITA (+ $\sigma$ )

The seven patterns comprising normal, plus six abnormal patterns relate ischial tuberosity angle (ITA) and sacral obliquity (SOA) to the horizontal plane. The relative magnitude of the angles dictates the makeup of the respective trigonometrical equations.

The five sitting patterns that involve sacral obliquity in sitting posture have associated algorithms that calculate the amount that the appropriate ischial tuberosity would have to be raised in order to level the sacral base in level sitting posture. These algorithms are based on the degree of absolute sacral obliquity in erect posture and the degree of ischial

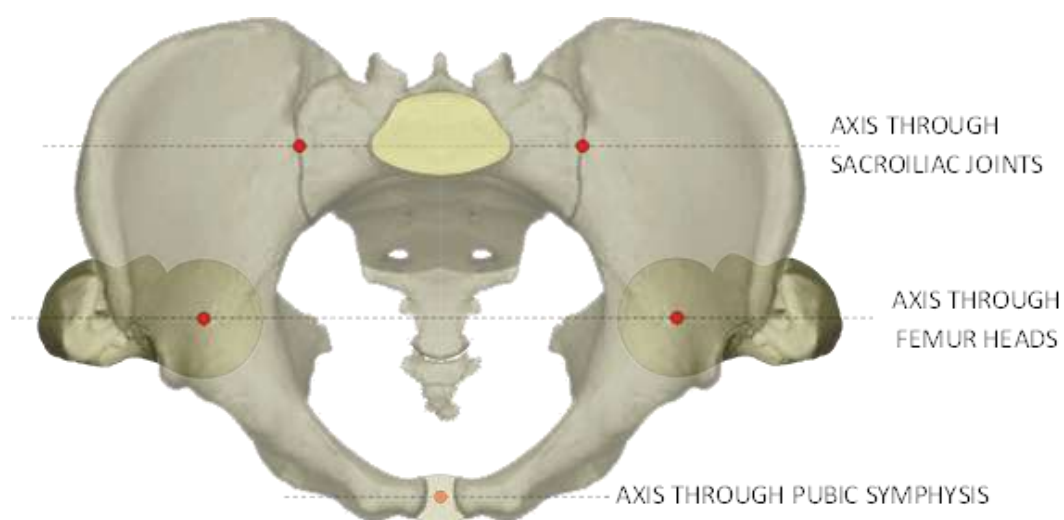
tuberosity obliquity in erect posture (Table 16). The third component is the width of the tangent points on the ischial tuberosities.

**Table 16. The five sitting patterns involving sacral obliquity in sitting posture has an associated algorithm that calculates the amount that the appropriate ischial tuberosity would have to be raised in order to level the sacral base in level sitting posture. The blue line represents the degree of sacral obliquity (SOA) while the green line represents ischial obliquity**

Pattern	Description	SBA / ITA relationship (sitting)
1	Normal with no sacral obliquity angle (SOA) and no ischial tuberosity angle (ITA)	 No SOA, No ITA
2	No sacral obliquity angle (SOA) combined with a + / - ischial tuberosity angle (ITA)	 No SOA, ITA
3	Sacral obliquity angle (SOA) and ischial tuberosity angle (ITA) inclined in the same direction with the sacral base angle less than the ischial tuberosity angle	 SOA < ITA
4	Sacral obliquity angle (SOA) and ischial tuberosity angle (ITA) inclined in the same direction and equal in magnitude	 SOA = ITA
5	Sacral obliquity angle (SOA) and ischial tuberosity angle (ITA) inclined in the same direction with the sacral base angle greater than the ischial tuberosity angle	 SOA > ITA
6	Sacral obliquity angle (SOA) with no ischial tuberosity angle (ITA)	 SOA, No ITA
7	Sacral obliquity angle (SOA) with ischial tuberosity angle (ITA) inclined in the opposite direction	 SOA opposite ITA

### 8.2.3 Pelvic misalignment / torsion

Trigonometry based formulae were also developed to calculate the proposed or theoretical effect rotation or translation of innominate bones as described by clinicians such as Gonstead and Schamberger (13, 77) would have on sacral obliquity. They independently describe sacroiliac dysfunction that involves positional dis-relationships where innominate bones misalign relative to each other or the sacrum. Rotations and translations, primarily involving the sacroiliac joints, have been proposed as the underlying mechanism of clinically observed pelvic pain and functional syndromes. The rotation and translation of an innominate bone relative to the sacrum were divided into one of three movement patterns involving two rotations and one translation at the sacroiliac joints. The rotations were designated as occurring around one of three axes. The three axes were through, or close to the sacroiliac joints, the femur heads and the pubic symphysis (Figure 175).



**Figure 175. Top view of the pelvis illustrating theoretical axes that passes through points located in the sacroiliac joints, the centre of the femur heads and the pubic symphysis**

Posterior (-) or anterior (+) rotations were designated as occurring around the theoretical axis that passes through these points. While the exact location of these axes, particularly of the sacroiliac joints, has been debated, their approximate location was assumed as being accurate enough and relevant enough for calculation of the effect they would have on sacral obliquity in erect posture (Figure 176).

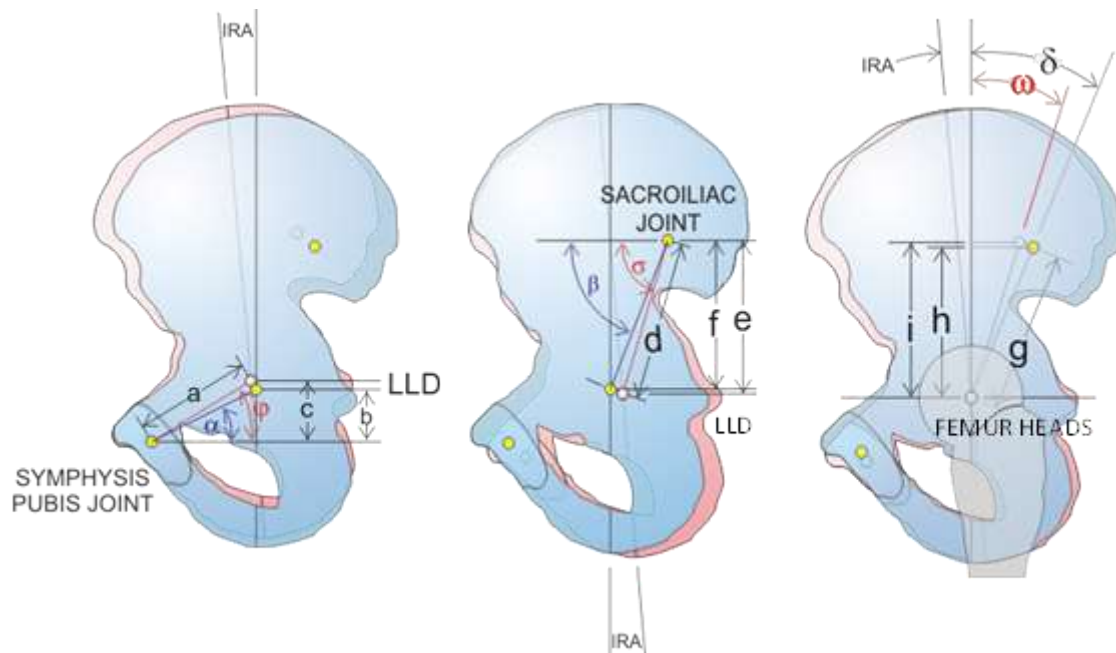


Figure 176. Three axes of rotation of an innominate bone pass through, or close to the pubic symphysis (left), sacroiliac joints (centre), or femur heads (right)

Radiographic images that would be consistent with the concept of innominate rotation with the axis of rotation located in the symphysis pubis joint would (Figure 177).

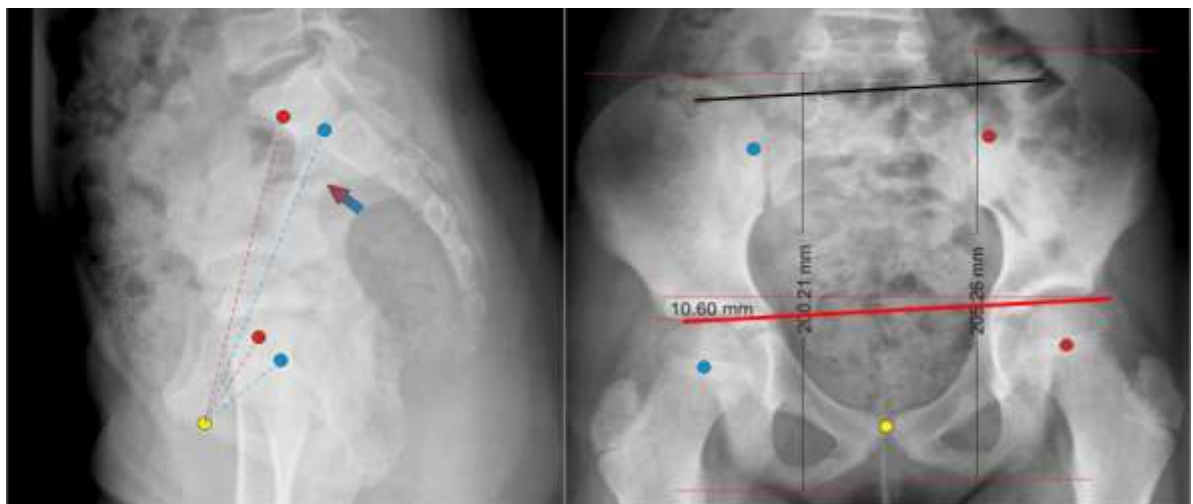
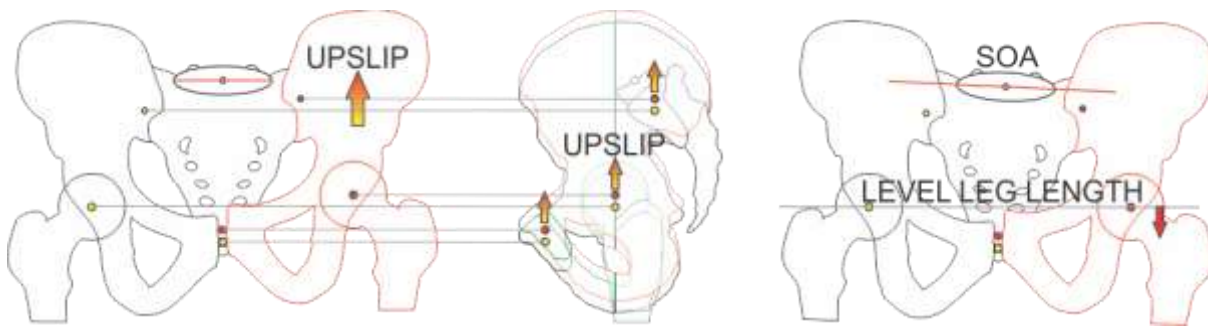


Figure 177. Radiographic images of the pelvis that would be consistent with innominate rotation with the axis of rotation located in the symphysis pubis joint

An upward translation of one innominate bone relative to the rest of the pelvis (upslip) as described by Schamberger (77) was considered to occur equally in superior direction at the sacroiliac joint, the femur heads and the pubic symphysis (Figure 178). If the 'upslip'

occurs in an otherwise symmetrical pelvis the sacral base would tilt down (SOA) on the involved side in erect standing posture with both legs level. The degree of tilt (relative sacral obliquity) would be proportional to the amount translation of the innominate and the width of the pelvis.



**Figure 178. 'Upslip' of the sacroiliac joint has been described as direct upwards translation of an innominate relative to the sacrum and symphysis pubis**

With this model of proposed pelvic misalignment, an A-P x-ray image of the pelvis with the iliac crest, symphysis ramus, ischial tuberosity and femur head higher on one side relative to the other side, could be interpreted as an *upslip* or *downslip* of one or both innominate bones relative to the sacrum. However, if the film was taken in erect standing posture the femur heads would remain in their level position (Figure 179).



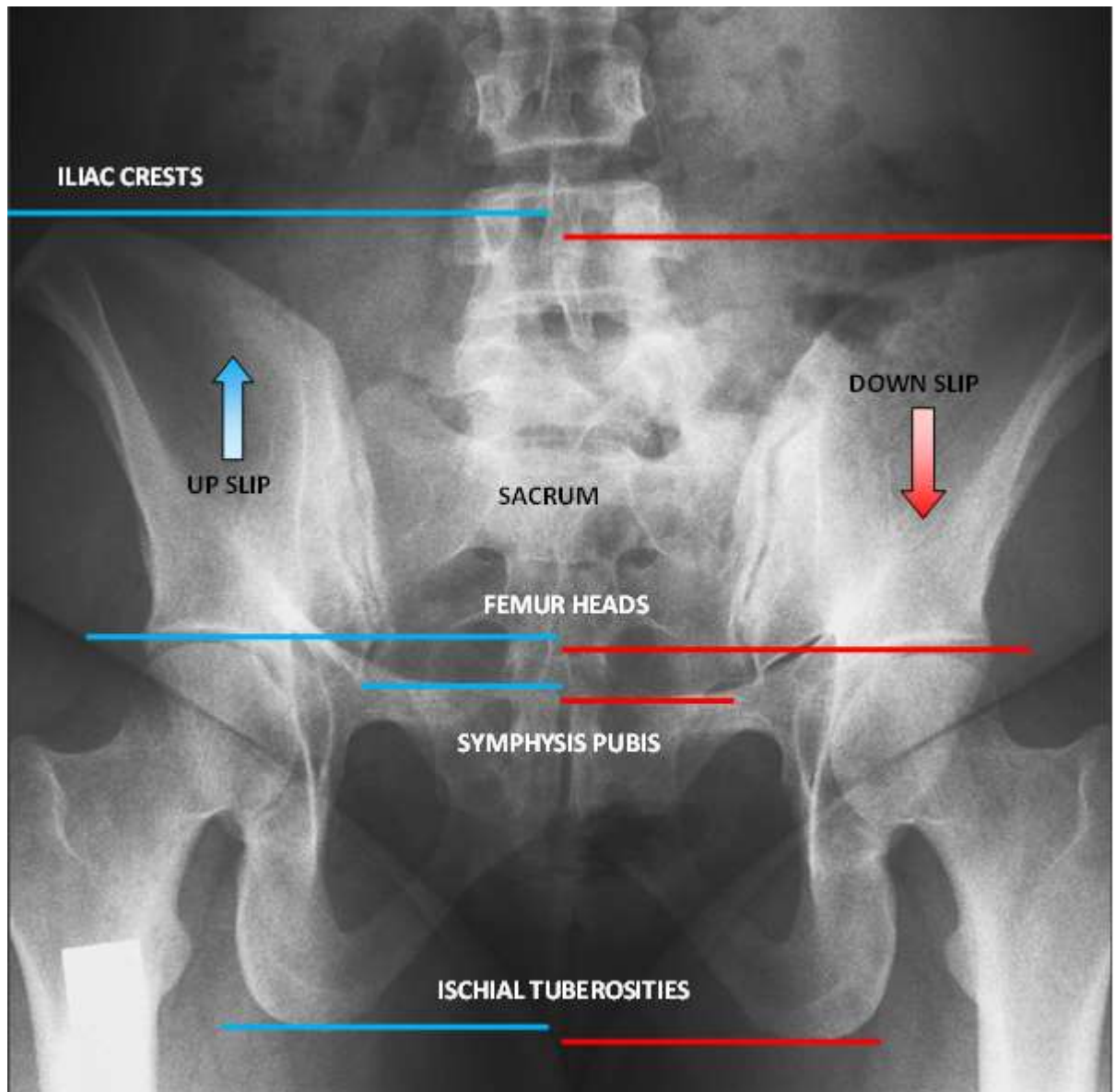


Figure 179. Radiographic image consistent with up or down slip of an innominate bone relative to the sacrum. The reference structures on one side of the pelvis are elevated compared to the same structures on the opposite side consistent with translation

### 8.3 MATHEMATICAL and GRAPHICAL MODELS

An idealised representation of the adult human pelvis was developed using the methods of descriptive geometry in order to develop and test algorithms used in calculating the size of heel and ischial lifts needed to correct sacral obliquity in sitting and standing postures. Paré *et al* (20) define descriptive geometry as the science of graphic representation and solution of space problems and is based on the principles of orthographic projection. Orthographic projection is a method of representing an object by a line drawing on a



projection plane which is perpendicular to the parallel projectors. These projections can be used to solve problems involving the spatial relationships of points and planes associated with specific structures. The projections also allow or facilitate changes in the orientation of the structure and viewing angles.

A graphical model representing the angles and linear relationships of an idealised pelvis and femur heads was modified to represent various configurations of leg length imbalance, ischial tuberosity obliquity and sacral obliquity in erect standing and sitting postures using CorelDraw® (Ottawa, Canada), a computer graphics program. Distances were drawn to scale representative of an adult human pelvis but were not necessarily the actual dimensions of a pelvis.

The graphical models were used to validate mathematical equations developed to calculate the vertical displacement of one femur head relative to the other for various configurations of the pelvis and limbs in standing posture and the effect this would have on sacral obliquity. The same model was modified to represent various configurations of the pelvis in relation to sacral obliquity and ischial tuberosity obliquity as they would influence sitting postures. These distances represent the amount, proportional to the scale of the drawing, that the lower limb or ischium would need to be raised in order to level the sacral base in the frontal plane when the pelvis was represented in a standing or sitting position respectively.

### *8.3.1 Standing posture*

The basic model was modified to produce the seven different configurations needed to represent the relationships of the plane of the sacral base and femur heads to the horizontal plane. The relationships were based on the side of each angle (if any) and which of the two angles was the greater, the sacral obliquity angle (SOA) or the femur head angle (FHA). The basic configuration (normal) had both the sacral obliquity angle and the femur

head angle aligned to the horizontal plane. For the other configurations, rotation around the Z-axis was designated positive if the direction of the slope of the sacral base or plane of the femur heads was lower on the right and negative if lower on the left. Only those seven configurations with no sacral obliquity or with a positive sacral obliquity angle were used. An additional six configurations represented mirror images of the patterns used for the graphic models and were not included for analysis.

Three measurements were made using the appropriate dimensioning tools incorporated in the graphics program. The angles and distances representing the absolute sacral obliquity angle, absolute femur head angle and the distance between the centres of the femur heads or the tangent points of the femur heads and a plane resting on them were measured in the frontal plane (Figure 180). They were recorded as angles in degrees for the two angles and millimetres for the linear distance between the tangent points on the femur heads. The measurements were arbitrarily made with three decimal places of accuracy as the drawing program was capable of measurements with accuracy to ten decimal places.

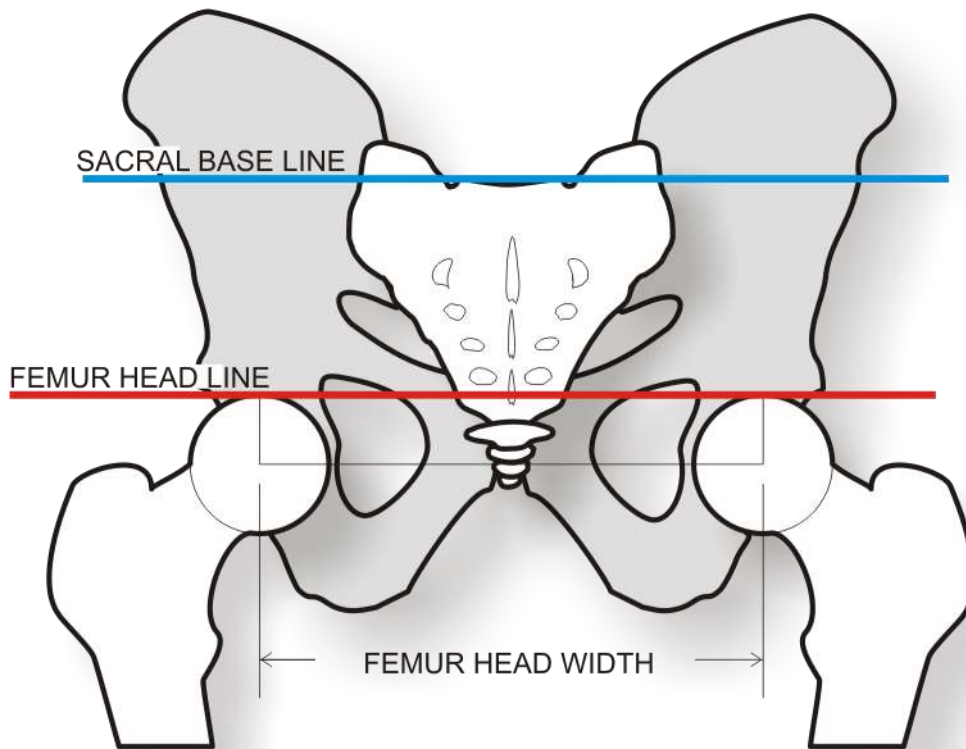
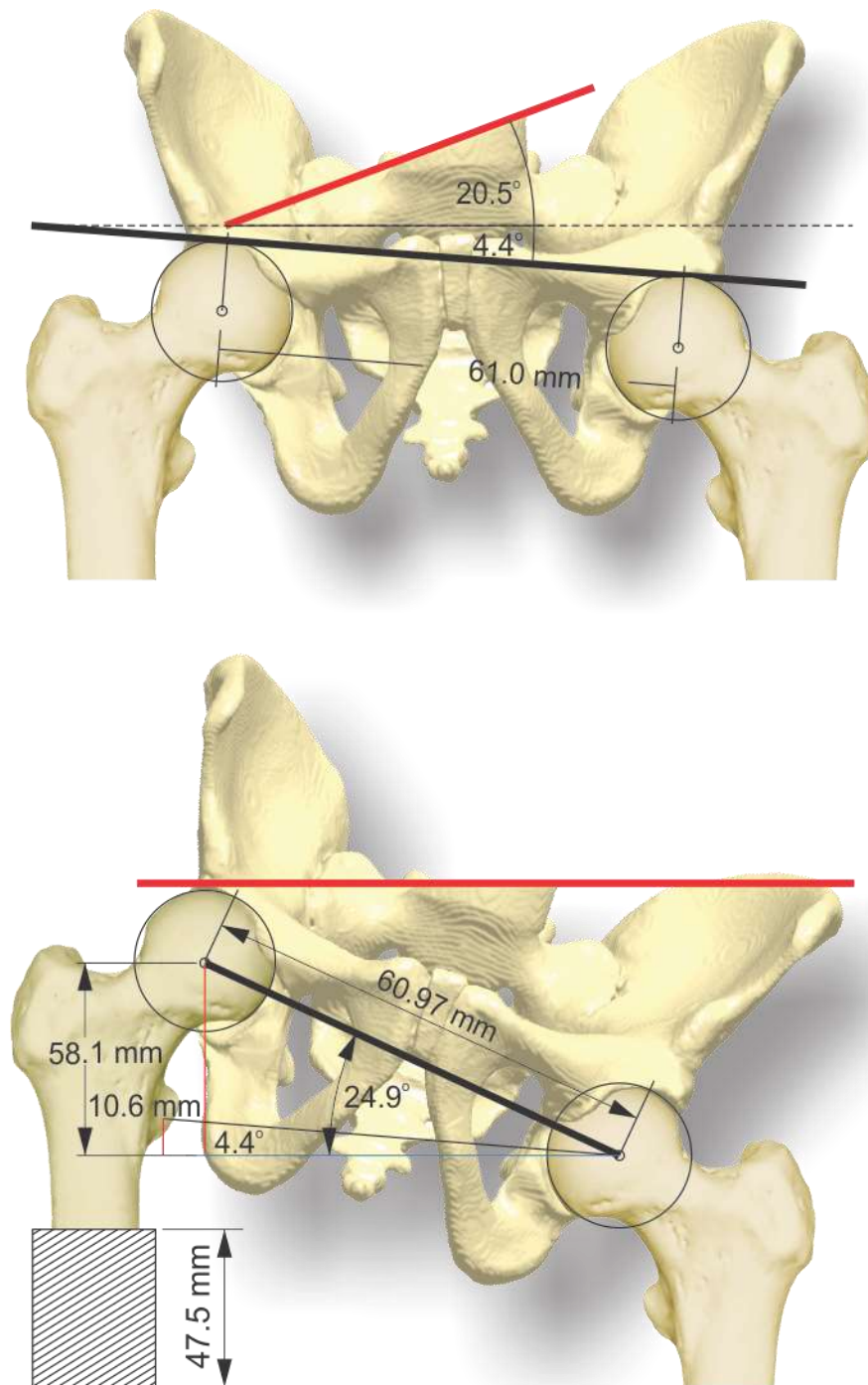


Figure 180. Reflective symmetry with lines representing the plane of the sacral base and plane of the femur heads in the frontal plane. Angulation of these lines to the horizontal plane form a sacral obliquity angle (SOA) and femur head angle (FHA) respectively. The width of the femur heads (FWH) is the distance between the tangent points on the femur heads formed by the femur head line

Most radiographic measurements relating to leg length imbalance are made to the nearest millimetre and angles to the nearest degree. The amount of angulation used to represent sacral obliquity and the angle of the femur heads were chosen for convenience rather than being representative of an actual individual pelvis. While the linear measurements and scaling of the pelvic drawings were not to actual size, dimensions and structural relationships remained consistent as the model was graphically manipulated (Figure 181).

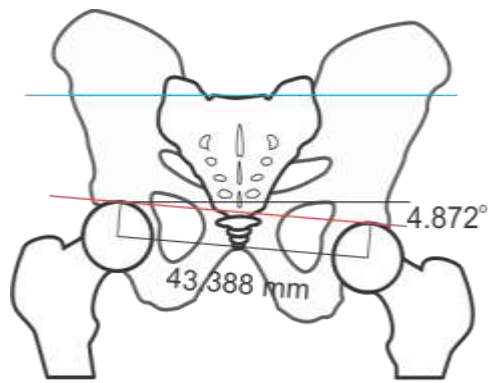


**Figure 181.** Graphic representation of the amount needed to raise one limb in order to level the sacral base in erect posture

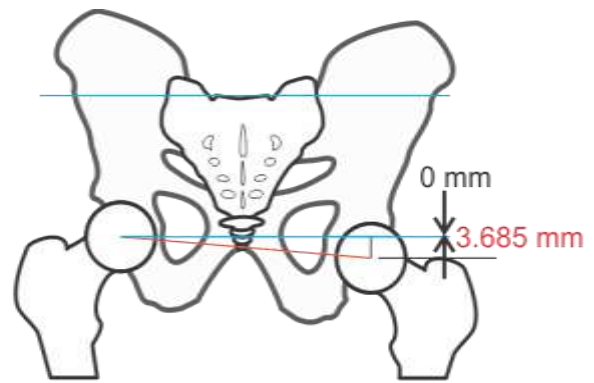
The six models representing a combination of anisomelia and sacral obliquity that result in a measured absolute sacral obliquity or femur head angle were individually manipulated as required using the '*rotation*' function in the drawing program so that the sacral base was

aligned to the horizontal plane. The axis of rotation was the centre of the femur head on the lower side of the sacral obliquity. The degree of rotation was the same degree of angulation and in the opposite direction as the measured sacral obliquity.

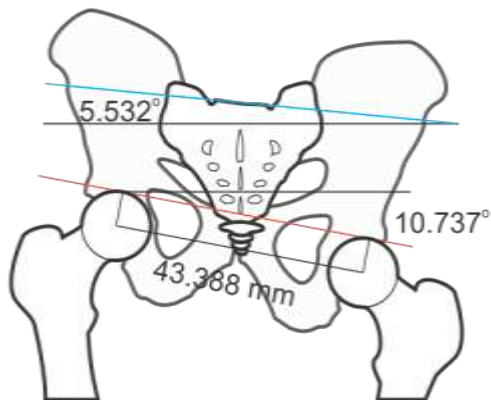
The vertical height from the upper most point on the stationary femur head to the upper most point of the opposite femur head in the rotated position with the sacral base level was measured in millimetres with an accuracy of three decimal places (Figure 182) and (Figure 183). This distance represented the theoretical vertical adjustment to the leg length needed to level the sacral base for that configuration. In a clinical setting, this distance would be the height of a heel lift, foot orthotic or shoe insert needed to compensate for obliquity of the sacrum in erect posture with all other factors being equal. It would also represent the change in limb length for surgical intervention in extreme cases.



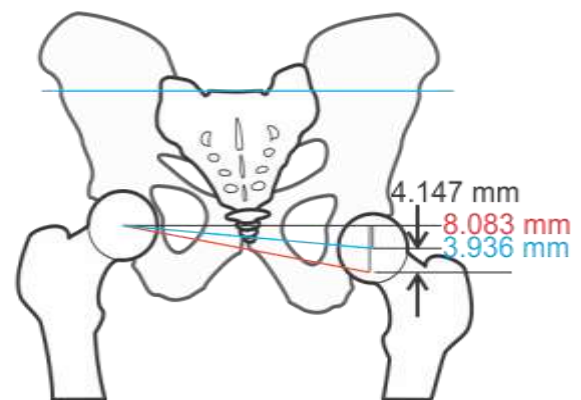
STANDING PATTERN 2



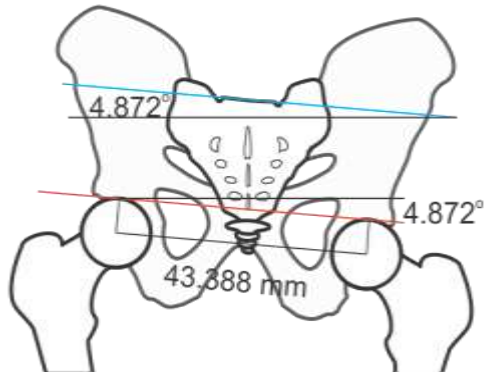
PATTERN 2 CORRECTED



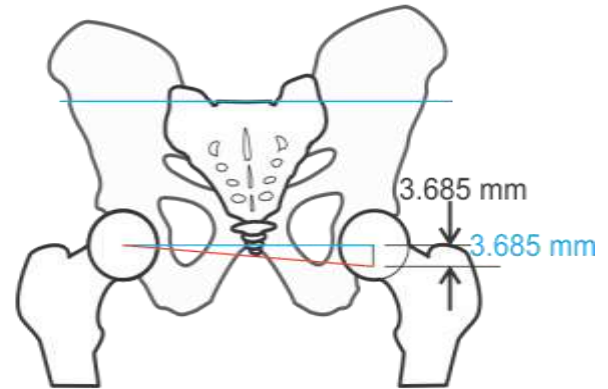
STANDING PATTERN 3



PATTERN 3 CORRECTED



STANDING PATTERN 4



PATTERN 4 CORRECTED

Figure 182. Three standing patterns (2 - 4) in erect position as they would be measured on a plain film radiograph (left) and with sacral obliquity corrected (right). On the corrected pelvis the measurement in RED is the amount of actual leg length imbalance, the measurement in BLUE is the amount of change in leg length needed to level the sacral base and the BLACK is the amount of lift needed to level the sacral base

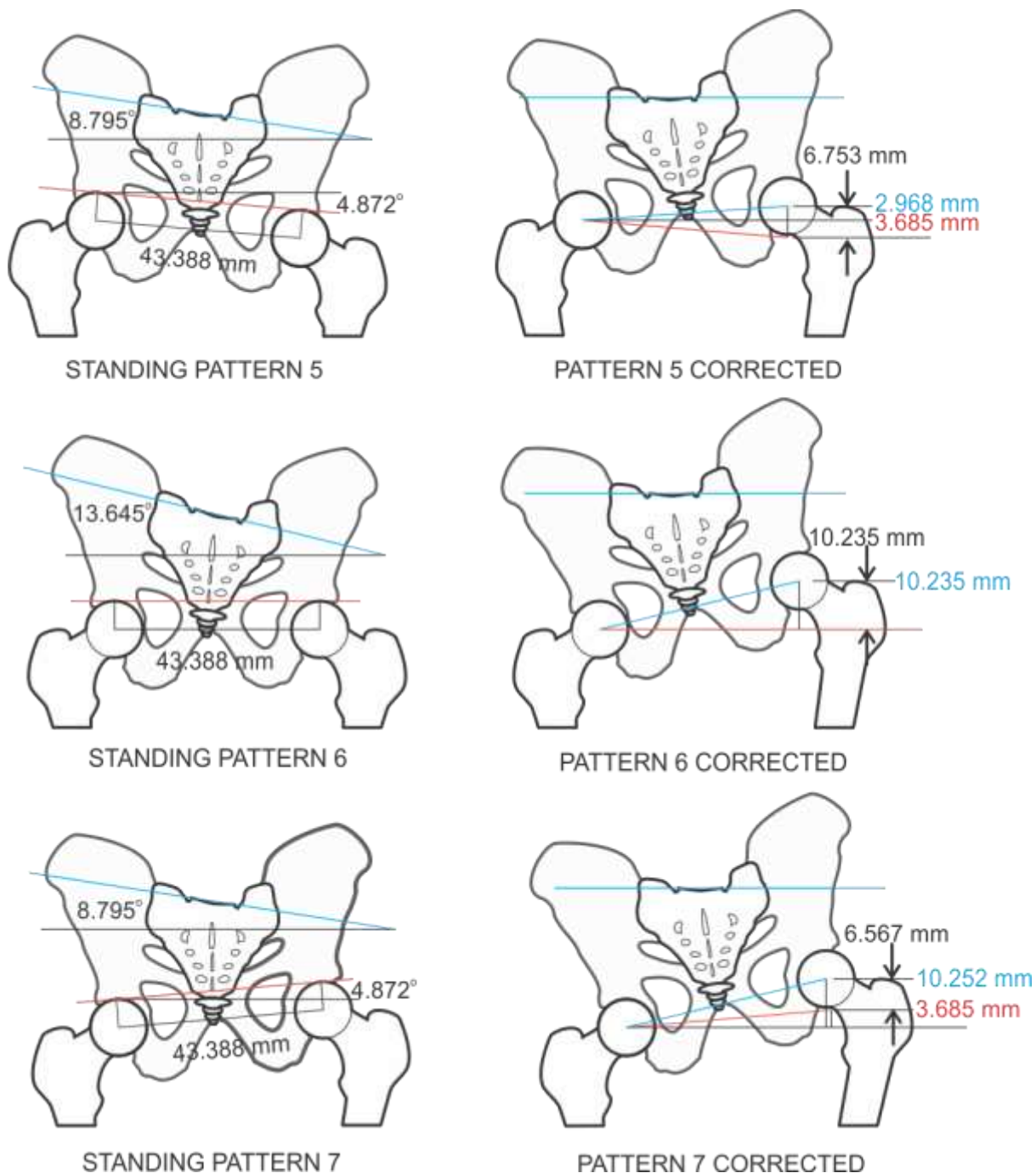


Figure 183. Three standing patterns (5 - 7) in erect position as they would be measured on a plain film radiograph (left) and with sacral obliquity corrected (right) using a shoe insert. RED is the amount of actual leg length imbalance, BLUE is the amount of change in leg length needed to level the sacral base and the BLACK is the height of the lift needed to level the sacral base

Another line drawing and measurement method has been suggested and used primarily by osteopathic educators, clinicians and researchers including Kuchea and Kuchea (8), Fann et al (58), Juhl *et al* (83), Irvin (65) and Tilly (189). The method uses a radiographic analytical protocol (or a slight variation) to quantify the vertical height of a heel lift or shoe



orthotic needed to level the sacral base in the frontal (X-Y) plane. The method involves constructing vertical lines perpendicular to the bottom edge of the film through the highest point of each femoral head. A line representing the plane of the sacral base is constructed through two points representing the convergence of the sacral ale and the articular pillars on the A-P radiographic image. The height (relative to the bottom of the film) of points where this line crosses the two vertical lines passing through the high point of the femur heads is measured. The difference in height between the two points is calculated and represents the sacral base *unleveling* (SBU) (Figure 184).

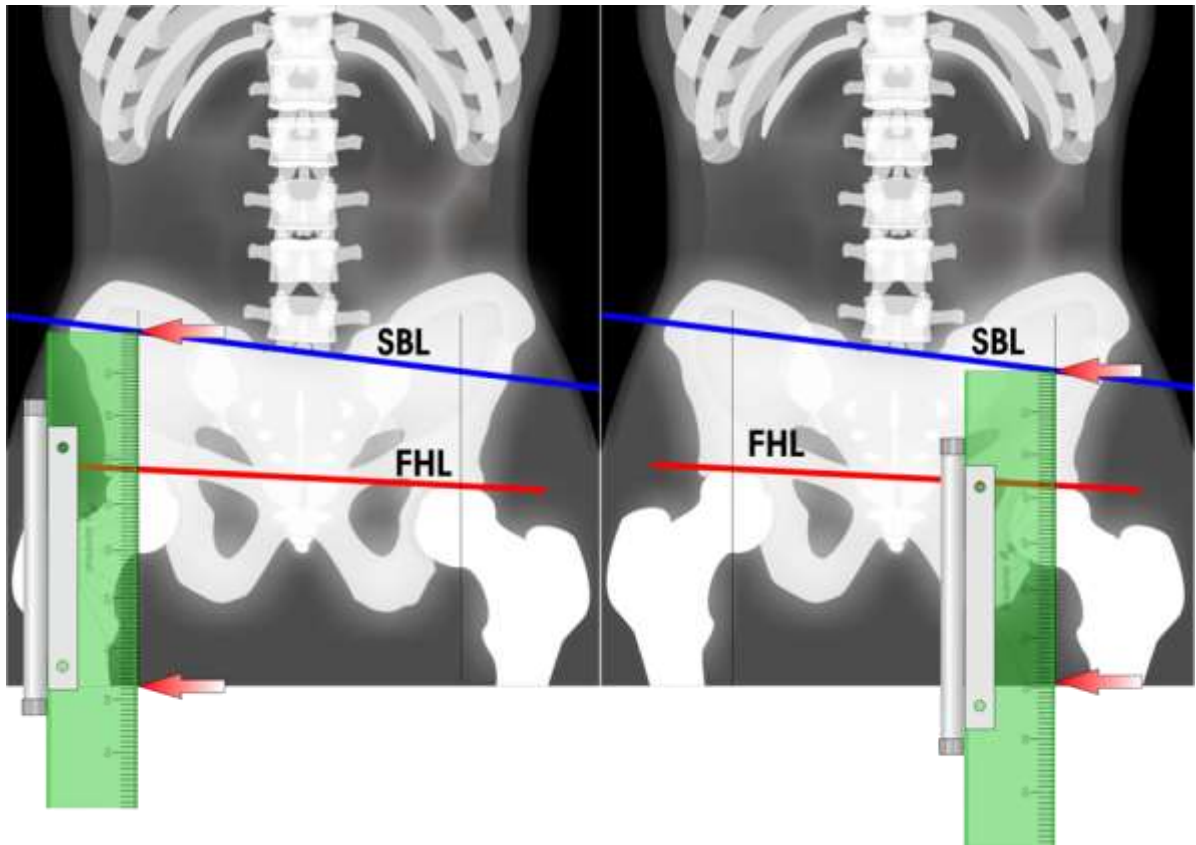


Figure 184. Some clinicians use the difference in height of points where the sacral base line crosses two vertical lines passing through the high point of the femur heads for the purpose of prescribing heel lifts is measured and the difference in height between the two points represents the amount of sacral base unleveling (SBU)

A similar process can be used to calculate the difference in height of the ischial tuberosities on an erect standing radiograph if they are visible on the film. While levelling of the sacral base is the primary objective of the analysis, femoral head unleveling (FHU), can also be



calculated using the same technique. One limitation of this method is that it does not account for the difference between pelvic obliquity (symmetrical pelvis) related to anisomelia and sacral obliquity due to sacral asymmetry (Figure 185).

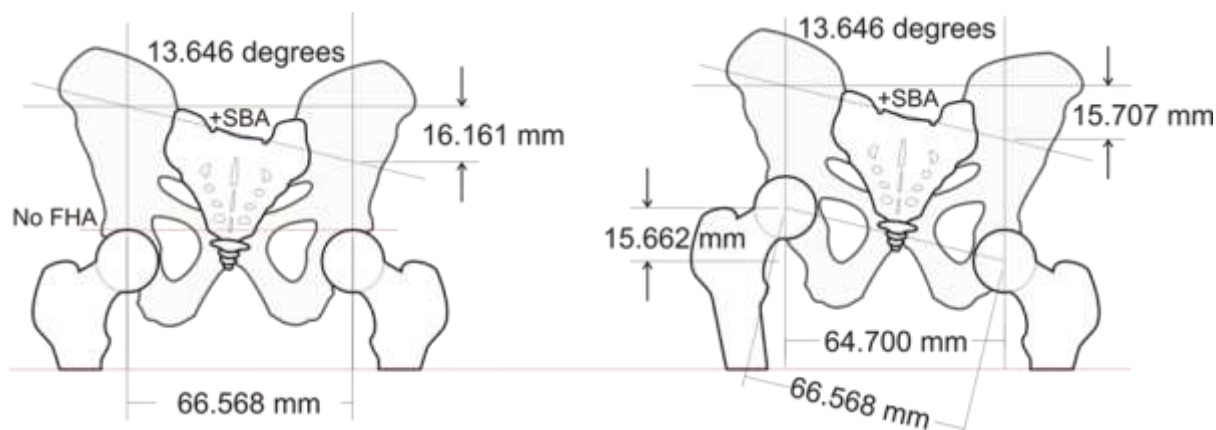
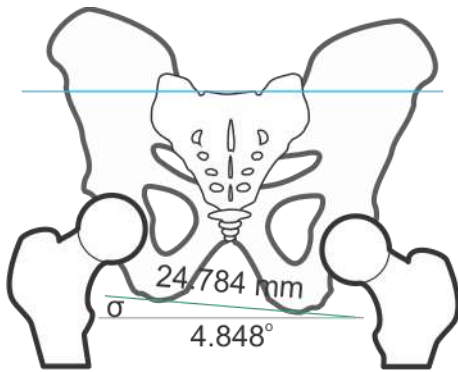


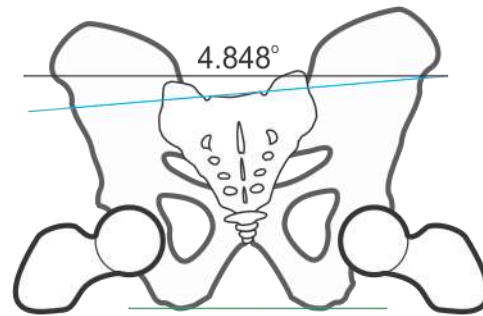
Figure 185. The pelvis on the left has the same degree of sacral obliquity and the same width between the femur heads as the pelvis on the right. Even with the same dimensions they can have different measurements for the degree of lift needed to level the sacral base because of the different femur head angles. The pelvis on the left has no anisomelia but has sacral asymmetry while the pelvis on the right has anisomelia producing an equivalent amount of sacral obliquity

### 8.3.2 Sitting posture

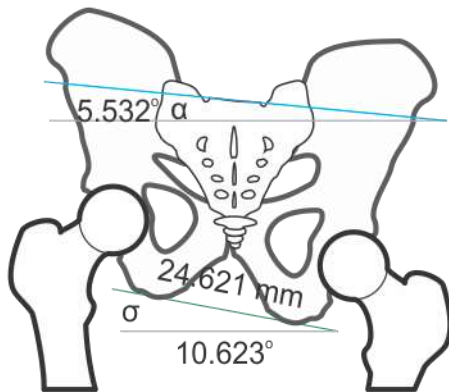
Seven pelvic graphical models were constructed to represent the same combinations of sacral obliquity and asymmetry as for leg length imbalance only with ischial tuberosity imbalance substituted for the femur head imbalance. The ischial tuberosities of each innominate bone were drawn as part of the pelvis in erect posture with analogous relationships to the sacral base as with the leg length imbalances and as they would be visualised on an erect A-P lumbopelvic radiograph. Six of the configurations (excluding normal) were rotated from the erect position to represent the orientation of the pelvis in sitting posture. In this position the lowest point of each ischial tuberosity was aligned to a horizontal plane. The angle formed between the plane of the sacral base and horizontal plane was measured as it would be with the orientation of the pelvis in the sitting posture (Figure 186) and (Figure 187).



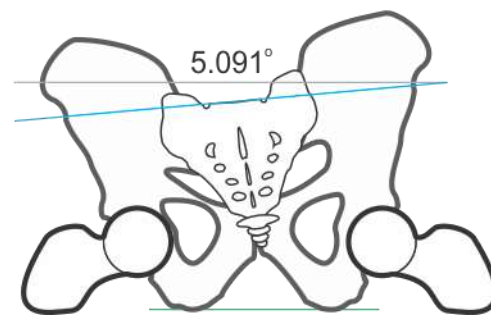
SITTING PATTERN 2 ERECT



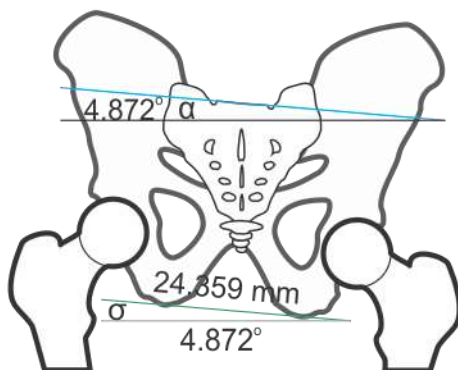
PATTERN 2 SITTING



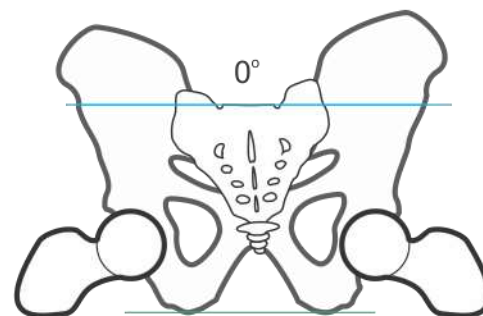
SITTING PATTERN 3 ERECT



PATTERN 3 SITTING

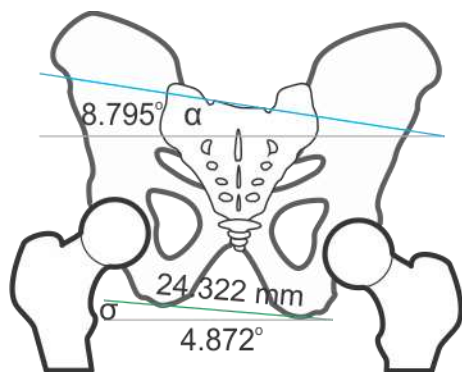


SITTING PATTERN 4 ERECT

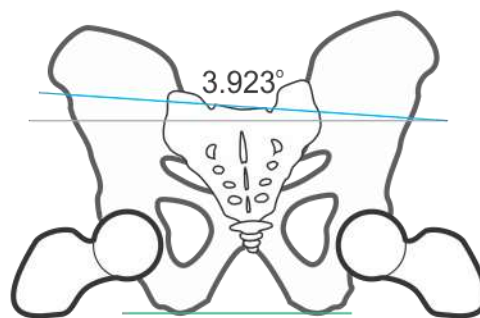


PATTERN 4 SITTING

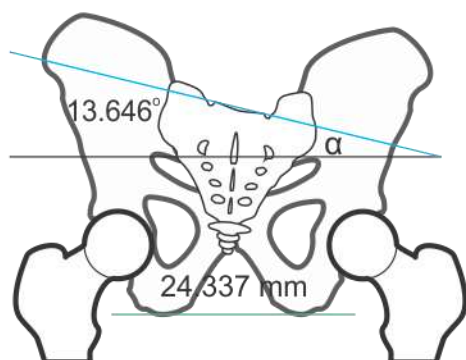
Figure 186. Three of the sitting configurations (excluding normal) 2-4, were rotated from the erect position (left) to represent the orientation of the pelvis in sitting posture (right).



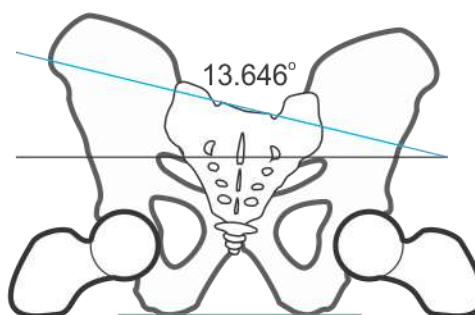
SITTING PATTERN 5 ERECT



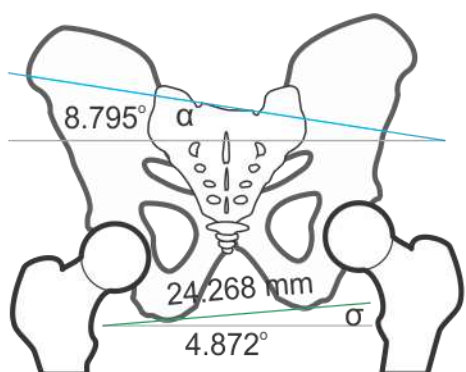
PATTERN 5 SITTING



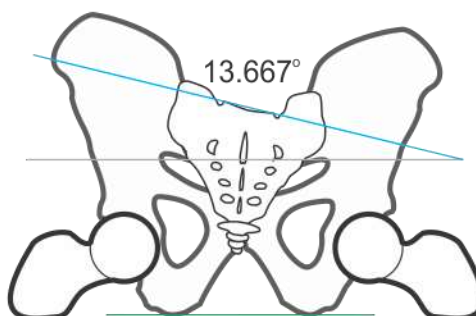
SITTING PATTERN 6 ERECT



PATTERN 6 SITTING



SITTING PATTERN 7 ERECT



PATTERN 7 SITTING

Figure 187. Three of the sitting configurations (excluding normal) 5-7, were rotated from the erect position (left) to represent the orientation of the pelvis in sitting posture (right).

### 8.3.3 Pelvic Misalignment / Torsion

Two specific types of movement of the innominate bones relative to the sacrum were identified from the literature and represented graphically as idealised orthographic projections of the pelvis. The angles and distances of a hypothetical amount of rotation or displacement were measured. The two types of movement involved anterior and posterior rotation around the X-axis ( $\pm R_x$ ) and translation along the Y-axis ( $\pm T_y$ ). Three axes of rotation were modelled and one translation. The three centres of rotation approximated a line joining the centre of the sacroiliac joints, a line joining the centre of the femur heads and the centre of the symphysis pubis joint. The translation was represented as an upward displacement of one innominate relative to the other with no associated rotation (Figure 188). In each of the graphical representations of the four pelvic misalignment patterns the leg lengths were considered to be level before the positional changes were made. The pelvis incorporating the misalignments was then rotated when necessary so that it rested on level femur heads following the internal positional changes. The pelvis was further rotated around the centre of the femur head on the side of the high sacral base to level the sacral base. The vertical distance between the ischial tuberosity in the level position and the level sacral base position was recorded as the amount of lift need to remove sacral obliquity. This amount would also represent the amount of leg length imbalance that could be expected to be corrected by restoring normal alignment to the misaligned pelvis.

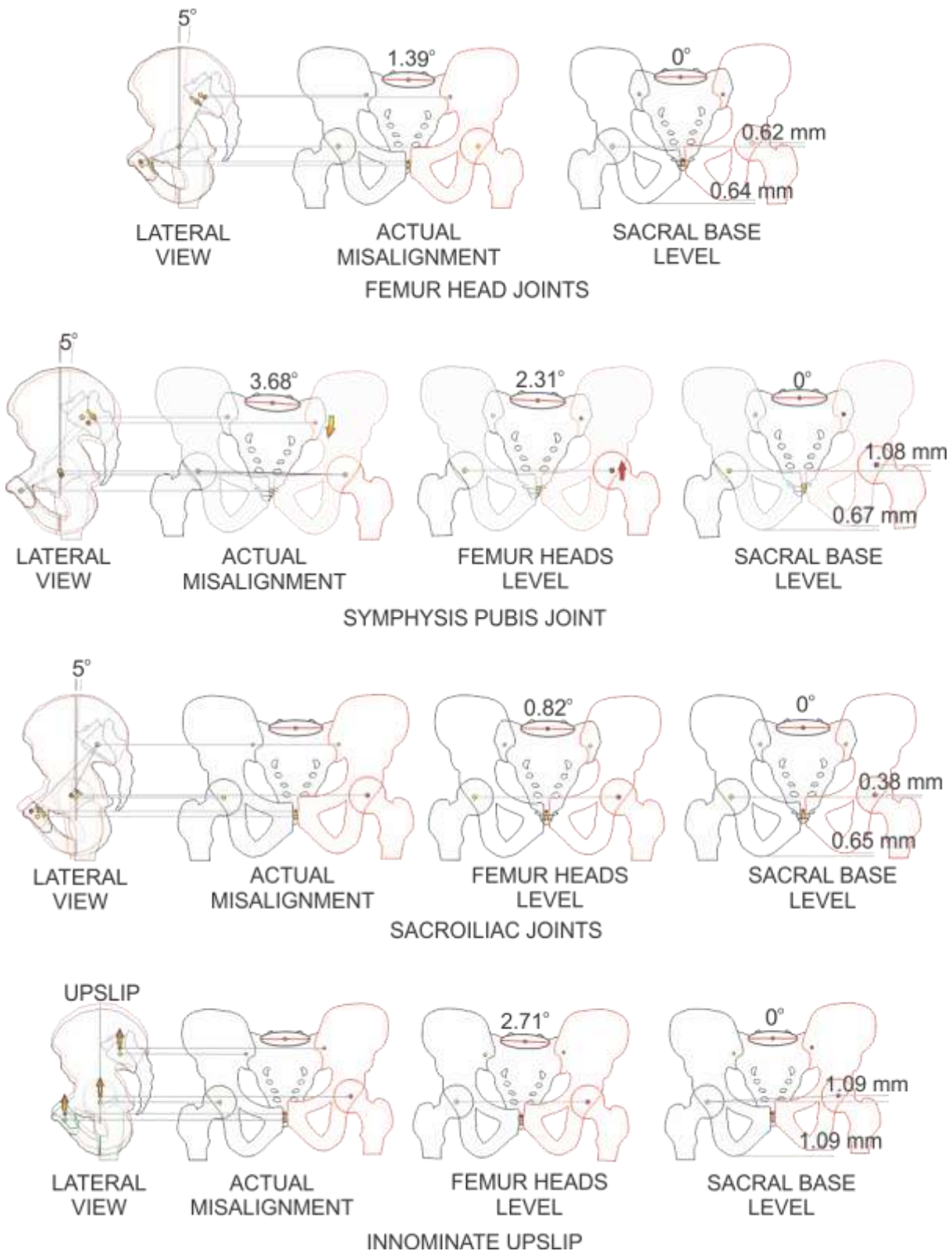


Figure 188. Graphic modelling of the three pelvic rotations and one innominate translation. The rotations were modelled with rotation in only one direction around one of the specific axes. One innominate was rotated 5 degrees relative to the other around the specified axis. The translation involved upward displacement of one innominate bone relative to the other

## 8.4 RESULTS

### 8.4.1 Trigonometric model

#### 8.4.1.1 Standing

The development of equations to calculate the leg length equivalent (LLE) based on sacral obliquity angle, femur head angle and femur head width in standing posture resulted in five different formulae for patterns 3 to 7. Patterns 1 and two needed no correction as there was no absolute sacral obliquity present. If the femur head width is measured in millimetres the height of the heel lift or foot orthotic will be in millimetres (Table 17).

**Table 17. Equations to calculate the leg length equivalent (LLE) based on sacral obliquity angle, femur head angle and femur head width in standing posture**

Pattern number	Algorithm for calculating corrective orthotic height in mm
1	normal
2	none
3	$[\sin \beta * FHW] - [\sin (\beta - \alpha) * FHW]$
4	$\sin \beta * FHW$
5	$[\sin \beta * FHW] + [\sin (\alpha - \beta) * FHW]$
6	$\sin \alpha * FHW$
7	$[\sin (\alpha + \beta) * FHW] - [\sin \beta * FHW]$

#### 8.4.1.2 Sitting

Algorithms were developed to calculate the amount needed to level the sacral base in erect sitting posture with various degrees and combinations of sacral obliquity and ischial tuberosity obliquity (Table 18).

Table 18. Algorithms used to calculate the amount needed to level the sacral base in erect sitting posture for six pelvic patterns involving sacral obliquity

Pattern number	Algorithm for calculating corrective ischial lift height in mm
1	normal
2	$\sin \sigma * ITW$
3	$\sin (\sigma - \alpha) * ITW$
4	none
5	$\sin (\alpha - \sigma) * ITW$
6	$\sin \alpha * ITW$
7	$\sin (\alpha + \sigma) * ITW$

Algorithms were developed calculate the effect various hypothetical or proposed pelvic misalignments would have on apparent sacral obliquity in erect posture (Table 19).

Table 19. Algorithms used to calculate the effect various hypothetical or proposed pelvic misalignments would have on apparent sacral obliquity in erect posture

Pelvic misalignment with axis located at:	Algorithm for calculating ASOA due to pelvic misalignment
Sacroiliac joint	$\sin \text{FHA (ASOA)} = [(d * \sin [\beta \pm \text{IRA}]) - (d * \sin \beta)] / \text{FWW}$ $\text{LLI} = \sin \text{ASOA} * \text{FWW}$ $\text{ITI} = \sin \text{ASOA} * \text{ITW}$
Symphysis pubis	$\sin \text{FHA} = [(a * \sin [\alpha \pm \text{IRA}]) - (a * \sin \alpha)] / \text{FWW}$ $\sin \text{ASOA (absolute)} = [(a^1 * \sin [\alpha^1 \pm \text{IRA}]) - (a^1 * \sin \alpha^1)] / \text{SIW}$ $\text{ASOA (relative) with femur heads level} = \text{ASOA} - \text{FHA}$ $\text{LLI} = \sin \text{ASOA} * \text{FWW}$ $\text{ITI} = \sin \text{ASOA} * \text{ITW}$
Femur heads	$\sin \text{ASOA} = [g * \cos (\omega + \text{IRA}) - (g * \cos \omega)] / \text{SIW}$ $\text{LLI} = \sin \text{ASOA} * \text{FWW}$ $\text{ITI} = \sin \text{ASOA} * \text{ITW}$
Upslip/Downslip	$\sin \text{ASOA with femur heads level} = \text{FWW} / \text{LLD (upslip)}$



### 8.4.2 Graphical model

#### 8.4.2.1 Standing patterns

The six idealised pelvic graphic models representing combinations of sacral obliquity or leg length imbalance (or both) was manipulated using a graphics program to level the sacral base. The axis of rotation was the centre of the femur head opposite the side the lift was to be placed. The change in leg length needed to compensate for sacral obliquity was measured and recorded.

Standing pelvic pattern 2 with level sacral base (Figure 189)

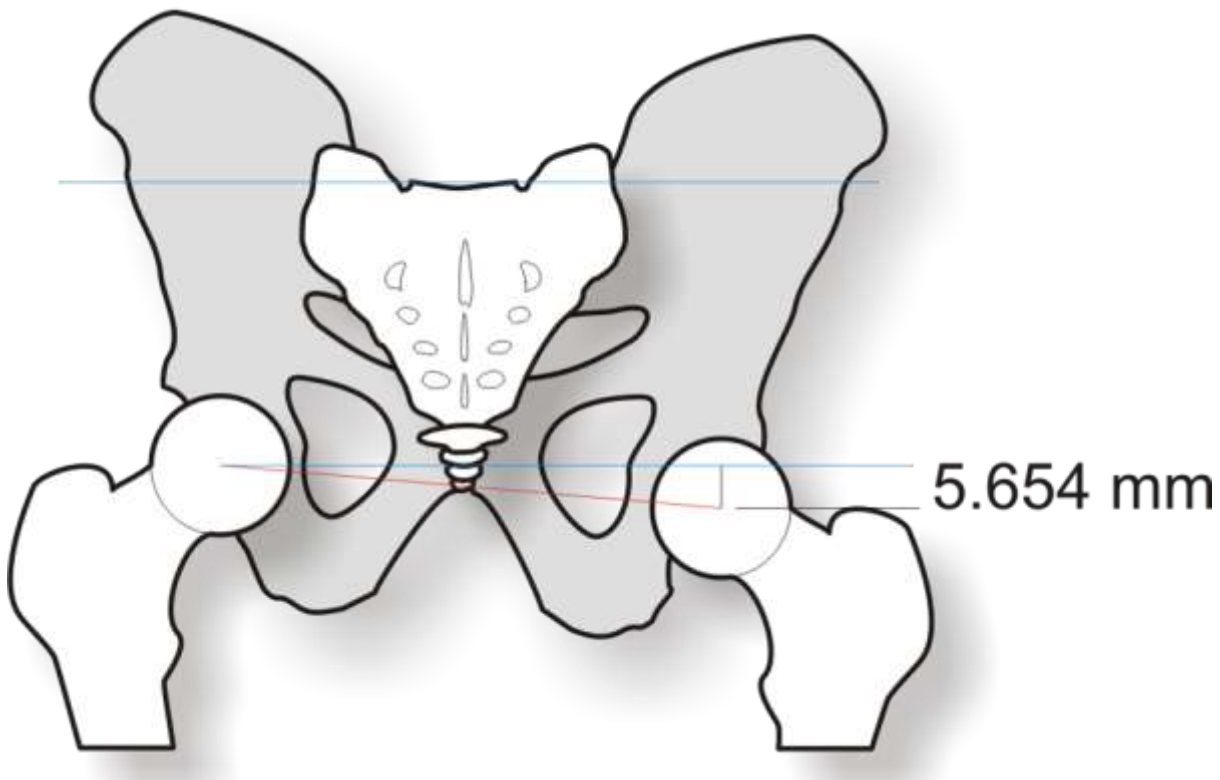


Figure 189. Standing pelvic pattern 2 with level sacral base

Standing pelvic pattern 3 rotated to level the sacral base with the vertical change in height of the femur head (Figure 190).

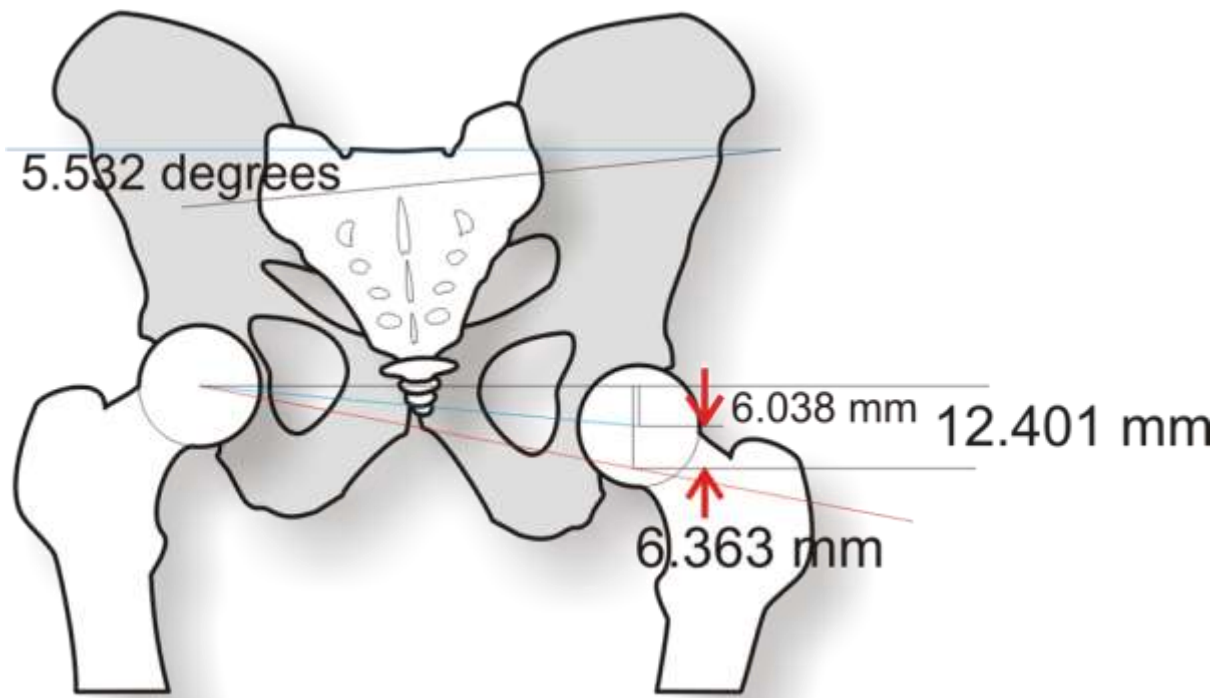


Figure 190. Standing pelvic pattern 3 rotated to level the sacral base with the vertical change in height of the femur head

Standing pelvic pattern 4 rotated to level the sacral base with the vertical change in height of the femur head (Figure 191).

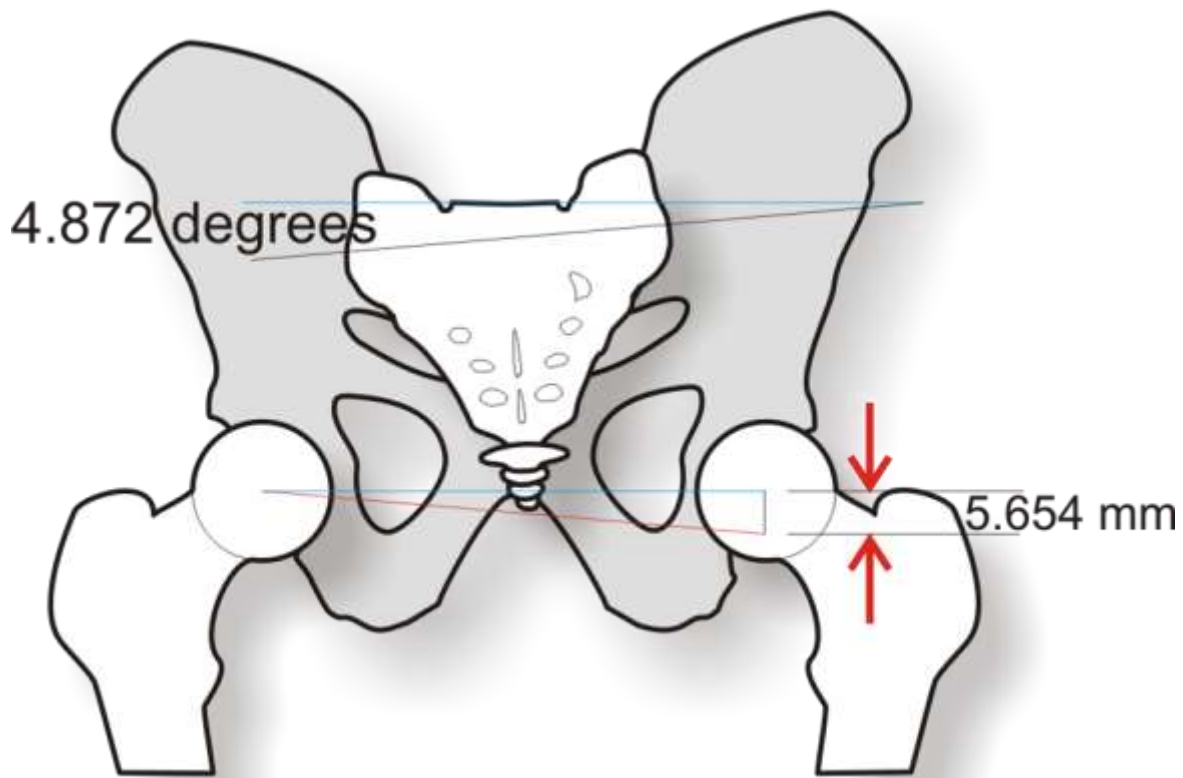


Figure 191. Standing pelvic pattern 4 rotated to level the sacral base with the vertical change in height of the femur head

Standing pelvic pattern 5 rotated to level the sacral base with the vertical change in height of the femur head (Figure 192).

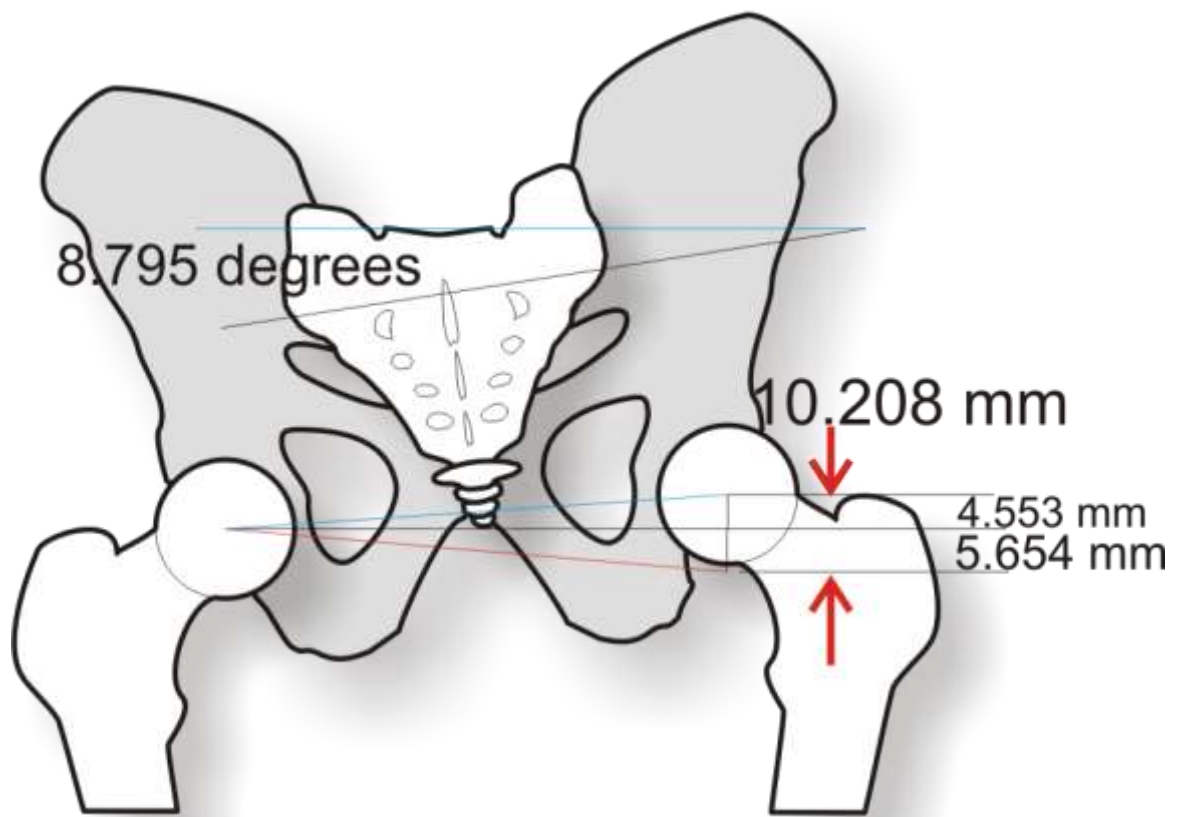


Figure 192. Standing pelvic pattern 5 rotated to level the sacral base with the vertical change in height of the femur head

Standing pelvic pattern 6 rotated to level the sacral base with the vertical change in height of the femur head (Figure 193).

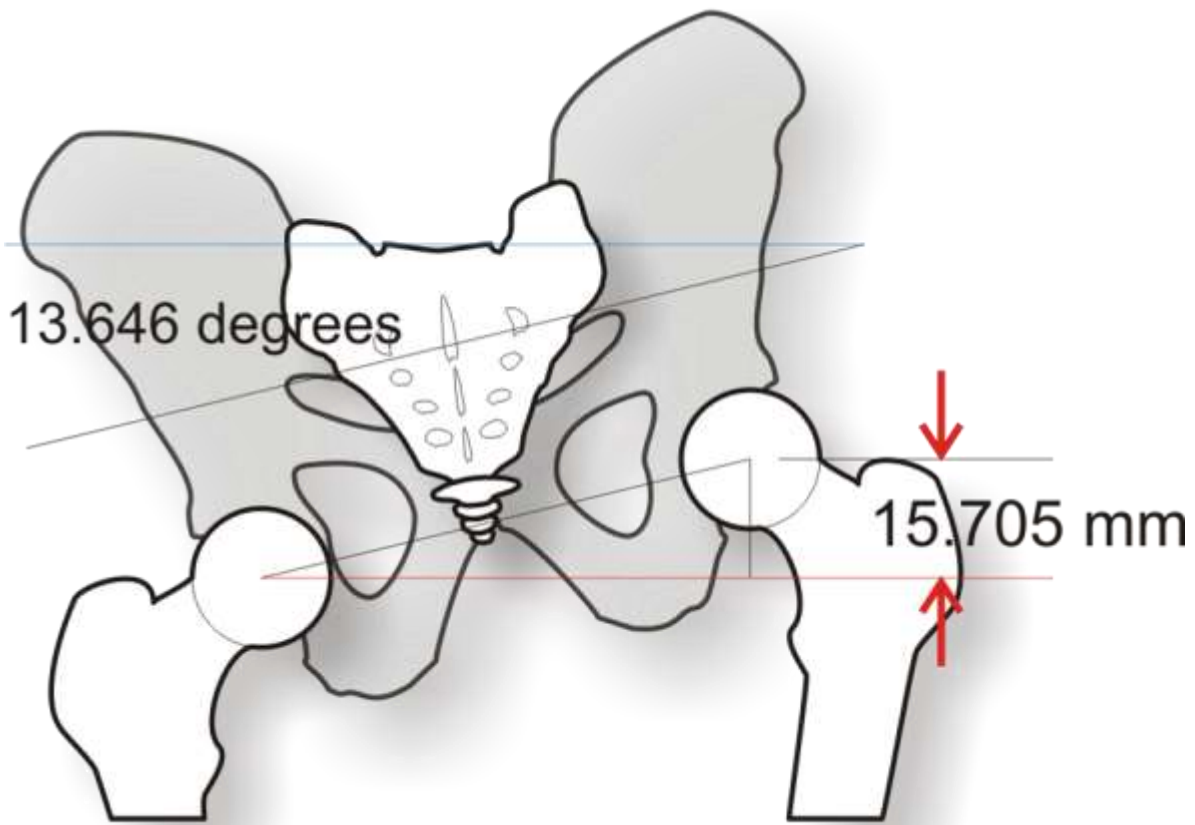


Figure 193. Standing pelvic pattern 6 rotated to level the sacral base with the vertical change in height of the femur head

Standing pelvic pattern 7 rotated to level the sacral base with the vertical change in height of the femur head (Figure 194).

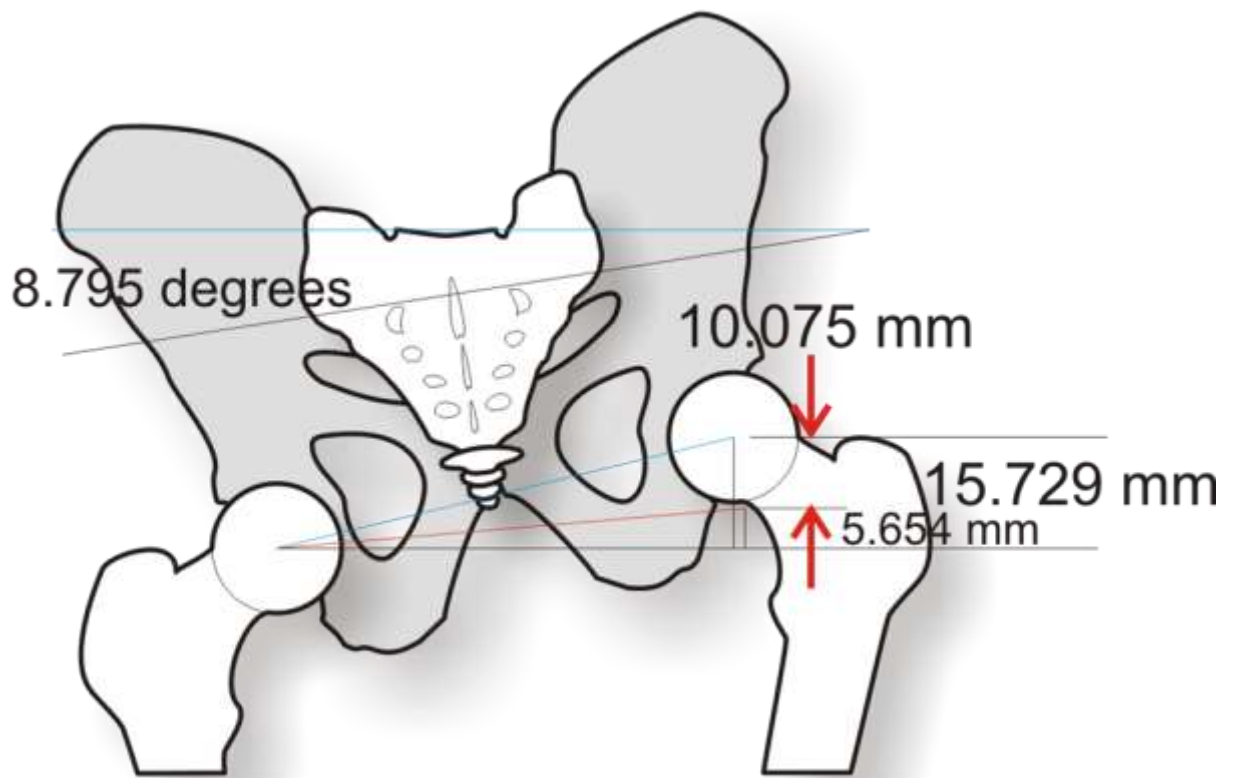


Figure 194. Standing pelvic pattern 7 rotated to level the sacral base with the vertical change in height of the femur head

Measurements were made of the amount needed to level the sacral base in erect posture based on graphical models of the pelvis and femur heads with various combinations of sacral obliquity and leg length imbalance (Table 20).

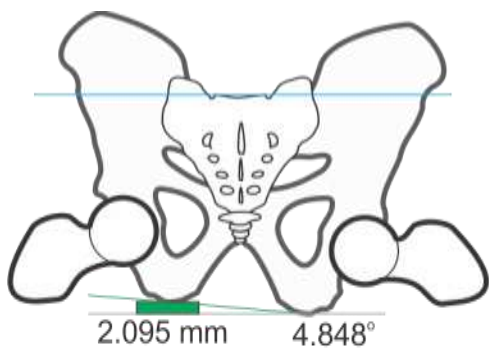
**Table 20. Measurement of the amount needed to level the sacral base in erect posture for the various combinations of sacral obliquity and leg length imbalance**

Pattern No.	Sacral Obliquity Angle (SOA)	Femur Head Angle (FHA)	Femur Head Width (FHW)	Leg length imbalance	Change in vertical height
1	0°	0°	66.569mm	0mm	0mm
2	0°	4.872°	66.569mm	5.654mm	0mm
3	5.532°	10.737°	66.569mm	6.038mm	6.363mm
4	4.872°	4.872°	66.569mm	5.654mm	5.654mm
5	8.795°	4.872°	66.569mm	(-)4.553mm	10.208mm
6	13.646°	0°	66.569mm	(-)15.705mm	15.705mm
7	8.795°	(-)4.872°	66.569mm	(-)15.729mm	10.075mm

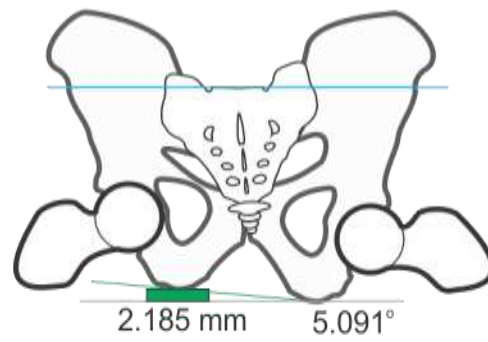
#### *8.4.2.2 Sitting patterns*

The five graphic models of the pelvis with an absolute sacral obliquity in sitting posture were then rotated around the ischial tuberosity on the elevated side of the sacral base to level the base. The angle through which each pelvis was rotated was equal to, but in the opposite direction to the absolute sacral base obliquity of the sacrum in the sitting position. For one pelvis (pattern 4), the sacral base was horizontal (no absolute sacral obliquity) in the sitting position so no further rotation was required. This configuration is due to equal but opposite obliquity of the sacral base and the ischial tuberosities resulting in the two planes being parallel to each other or a symmetrical pelvis associated with anisomelia as measured on an A-P radiograph. The vertical difference in height of the ischial tuberosities in the rotated position with the sacral base level was measured using the vertical dimensioning tool in CorelDraw graphics program (Figure 195).

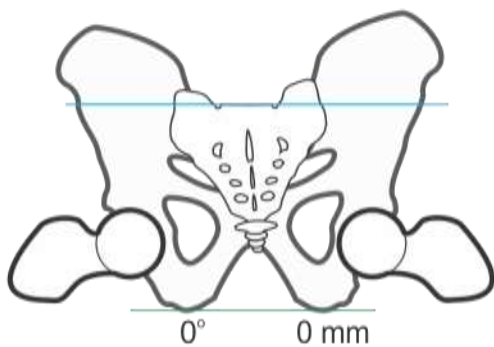




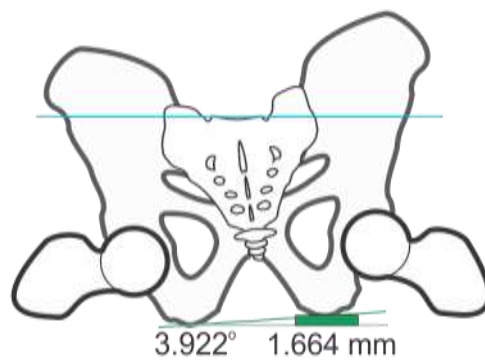
PATTERN 2 CORRECTED SITTING



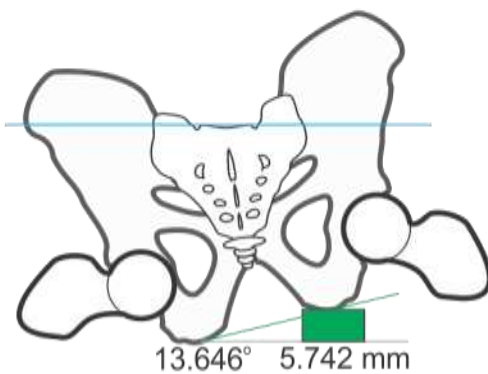
PATTERN 3 CORRECTED SITTING



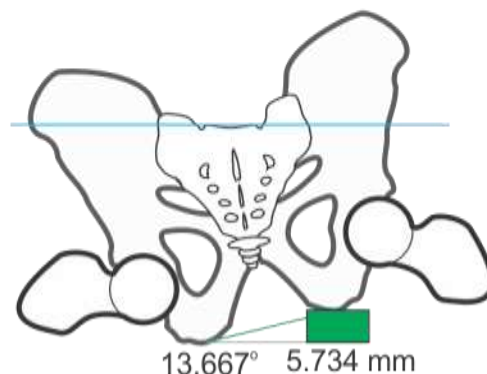
PATTERN 4 CORRECTED SITTING



PATTERN 5 CORRECTED SITTING



PATTERN 6 CORRECTED SITTING



PATTERN 7 CORRECTED SITTING

Figure 195. The amount the ischial tuberosity needs to be raised for each of the sitting patterns in order to level the sacral base is indicated under the appropriate ischial tuberosity (green block) and the dimension in millimetres

Measurements were made of the amount needed to level the sacral base in erect sitting posture based on graphical models of the pelvis and ischial tuberosities with various combinations of sacral obliquity and ischial tuberosity obliquity (Table 21).

**Table 21. Measurement of the amount needed to level the sacral base in erect sitting posture based on graphical models of the pelvis with combinations of sacral and ischial obliquity**

Pattern No.	Sacral Obliquity Angle (SOA)	Ischial Tuberosity Angle (ITA)	Width (ITW)	Sitting SOA (-ITA)	Change in vertical height
1	0°	0°	24.784mm	0°	0mm
2	0°	4.848°	24.784mm	4.848°	2.095mm
3	5.532°	10.623°	24.621mm	(-)5.091°	2.185mm
4	4.872°	4.872°	24.359mm	0°	0mm
5	8.795°	4.872°	24.322mm	3.922°	1.664mm
6	13.646°	0°	24.337mm	13.646°	5.742mm
7	8.795°	(-)4.872°	24.268mm	13.667°	5.734mm

#### 8.4.3 Pelvic Misalignment

The amount of sacral obliquity that could be expected from torsion within the pelvis due to the rotation or translation of an innominate bone relative to the sacrum and opposite innominate bone is difficult to predict and quantify as a theoretical construct. A reason for the lack of clarity is that those who often propose and describe the type and amounts of movement are clinicians or the analysis is based on clinical assessments (77, 131, 377). In this respect they do not generally specify a single location for the centre of rotation (COR) of the sacroiliac joint or the mechanical behaviour of the system. In published studies the loading and coupling patterns of the pelvis are not described in sufficient detail to allow accurate predictions of the precise location of rotation centres and how the system functions *in vivo*.

The formulae and graphical models developed to analyse the degree of sacral obliquity expected to occur as a result of pelvic misalignments are based on assumptions relating to the general location of the axis of rotation, but the amount of rotation is not representative of the amount commonly reported at the sacroiliac joints or symphysis pubis. The graphical representations act as generalised depictions of the type and amount of movement involved (Figure 176), (Figure 178) and (Figure 188).

Measurement of the amount that would needed to level the sacral base as a result of pelvic misalignments with various axes of rotation and/or directions of movement (Table 22).

**Table 22. Measurement of the amount that would needed to level the sacral base as a result of pelvic misalignments with various axes of rotation and/or directions of movement**

Axis of Rotation	Sacroiliac joints	Femur Heads	Symphysis Pubis	Up/down slip
Sacral Obliquity Angle (SOA)	0°	1.39°	3.68°	0°
Innominate rotation (-) / translation	5°	5°	5°	5mm
SOA with level femur heads	0.82°	1.39°	2.31°	2.71°
Ischial Tuberosity Width (ITW)	15.63mm	15.21mm	16.02mm	14.29mm
Femur head width (FHW)	26.03mm	25.36mm	26.69mm	23.79mm
Sacroiliac joint width (SIJW)	15.53mm	15.14mm	15.96mm	14.21mm
Level sacral base LLI	0.38mm	0.62mm	1.08mm	1.09mm
Level sacral base ITI	0.65mm	0.64mm	0.67mm	1.09mm

## 8.5. MATHEMATICAL and GRAPHICAL ANALYSIS

### 8.5.1 Standing patterns (Table 23)

**Table 23. Comparison of measurements obtained from the graphical pelvic model and calculations based on the appropriate algorithm for standing postures**

Pattern No.	Formula to calculate change in vertical height of femur head using dimensions from graphical model	Graphical model measurement
1	None	0.000
2	None	0.000
3	$\begin{aligned} & [\sin \beta * FHW] - [\sin (\beta - \alpha) * FHW] \\ & [\sin 10.737 * 66.569] - [\sin (10.737 - 5.532) * 66.569] \\ & 12.402 - 6.039 = \mathbf{6.363mm} \end{aligned}$	6.363mm
4	$\begin{aligned} & \sin \beta * FHW \\ & \sin 4.872 * 66.569 = \mathbf{5.654mm} \end{aligned}$	5.654mm
5	$\begin{aligned} & [\sin \beta * FHW] + [\sin (\alpha - \beta) * FHW] \\ & [\sin 4.872 * 66.569] + [\sin (8.795 - 4.872) * 66.569] \\ & 5.654 + 4.554 = \mathbf{10.208mm} \end{aligned}$	10.208mm
6	$\begin{aligned} & \sin \alpha * FHW \\ & \sin 13.646 * 66.569 = \mathbf{15.705mm} \end{aligned}$	15.705mm
7	$\begin{aligned} & [\sin (\alpha + \beta) * FHW] - [\sin \beta * FHW] \\ & [\sin 13.667 * 66.569] - [\sin 4.872 * 66.569] \\ & 15.729 - 5.654 = \mathbf{10.075mm} \end{aligned}$	10.075mm

### 8.5.2 Sitting patterns (Table 24)

**Table 24. Comparison of measurements obtained from the graphical pelvic model and calculations based on the appropriate algorithm for sitting postures**

Pattern No.	Formula to calculate change in vertical height of ischial tuberosity using dimensions from graphical model	Graphical model measurement
1	None	<b>0.000</b>
2	$\sin(\sigma - \alpha) * ITW$ $\sin(4.848 - 0) * 24.784 = \mathbf{2.099mm}$	<b>2.095mm</b>
3	$\sin(\sigma - \alpha) * ITW$ $\sin(10.623 - 5.532) * 18.372$ $\sin 5.091 * 24.621 = \mathbf{2.185mm}$	<b>2.185mm</b>
4	None	<b>0.000</b>
5	$\sin(\alpha - \sigma) * ITW$ $\sin(8.795 - 4.872) * 18.150$ $\sin 3.923 * 24.322 = \mathbf{1.664mm}$	<b>1.664mm</b>
6	$\sin(\alpha - \sigma) * ITW$ $\sin(13.646 - 0) * 24.337 = \mathbf{5.742mm}$	<b>5.742mm</b>
7	$\sin(\alpha + \sigma) * ITW$ $\sin(8.795 + 4.872) * 18.109$ $\sin 13.667 * 24.268 = \mathbf{5.734mm}$	<b>5.734mm</b>

### 8.5.3 Pelvic misalignments (Table 25)

**Table 25. Table comparing calculated ASOA using algorithms with measurements made on graphical models. The input measurements used for the algorithms were obtained from the graphical models**

axis located at:	Algorithm for calculating ASOA due to pelvic misalignment	Graphic measurement
Sacroiliac joint	$\sin \text{ASOA} = [(a * \sin [\alpha \pm \text{IRA}]) - (a * \sin \alpha)] / \text{FWH}$ $= (10.33 * \sin [62.68 + 5]) - (10.33 * \sin 62.68)$ $26.03$ $= 0.832^\circ$ $\text{LLI} = \sin 0.832 * 26.03$ $= 0.378\text{mm}$	<b>0.83°</b>  <b>0.38mm</b>
Symphysis pubis	$\sin \text{ASOA} = [(d * \sin [\beta \pm \text{IRA}]) - (d * \sin \beta)] / \text{FWH}$ $= (17.41 * \sin [50.11]) - (17.41 * \sin 45.11)$ $15.96$ $= 3.678^\circ$ $\text{ASOA (relative)} = 3.678 - 1.365$ $= 2.313^\circ$ $\text{LLI} = \sin 2.31 * 26.69$ $= 1.075\text{mm}$	<b>3.678°</b>  <b>2.313°</b>  <b>1.076mm</b>
Femur heads	$\sin \text{ASOA} = [g * \cos (\omega + \text{IRA}) - (g * \cos \omega)] / \text{SIW}$ $= [10.062 * \cos (27.318 + 5)] - (10.062 * \cos 27.318)$ $15.14$ $= 1.392^\circ$ $\text{LLI} = \sin 1.392 * 25.36\text{mm}$ $= 0.616\text{mm}$	<b>1.394°</b>  <b>0.62mm</b>
Upslip / Downslip	$\sin \text{ASOA with femur heads level} = \text{LLD} / \text{FWH (upslip)}$ $\sin (1.095 / 23.79) = 2.638^\circ$ $\text{LLI} = \sin 2.638 * 23.79$ $= 1.094\text{mm}$	<b>2.638°</b>  <b>1.09mm</b>

## 8.6 DISCUSSION

An objective of many musculoskeletal practitioners and therapists is to establish or maintain a level foundation for the spinal column. Numerous studies have investigated the validity, reliability and clinical significance of leg length imbalance (LLI) and its effect on spinal balance. However, there have been very few studies that have specifically investigated the relationship between pelvic asymmetry and lower limb anisomelia and the effect this relationship has on sitting and standing posture. In one study that specifically investigated

the prevalence of frontal plane pelvic postural asymmetry (sacral obliquity) combined with leg length imbalance, Juhl *et al* (83) classified pelvic asymmetry into six (seven including normal or symmetrical) types of pelvic postural asymmetry. They suggest that this classification system is based on unpublished osteopathic teaching material that they attribute to Lloyd and Eimerbrink and later published in 1978 as a practical system of heel lift intervention by Heilig (372). For their study they used a slightly modified osteopathic radiographic analytical procedure for assessing pelvic asymmetry and leg length imbalance as described by William *et al* (394). The basis of their classification system was the absolute obliquity rated to the amount of leg length imbalance as measured on erect radiographs.

The numbering of the various patterns used by Juhl *et al* would seem arbitrary and they offer no reason of their numbering system or the order or relationship of the various configurations other than it is based on the system used by Lloyd and Eimerbrink and Heilig. Ebrall (16) illustrates and describes six distinct lumbopelvic patterns or phases of misalignment that he credits to the earlier work of Schafer (103). These patterns involve the relative position of the femur heads, iliac crests and the sacrum. Schafer describes six postural patterns (seven including orthogonal) that he attributes to functional and structural problems. The developer of the Logan Basic Methods (374) describes the sacrum as a platform upon which the spine rests and determines the '*subluxation*' patterns in the spine above. Logan directed much attention to corrections that would level the sacral base in the frontal plane. He outlines body framework abnormalities that he divides into ten typical distortion patterns. Six of the distortion patterns involve an inferiority of the sacral base in the frontal plane. Logan explores the effect the patterns have on both sitting and standing postures.

Esposito and Philipson (395) in their text on chiropractic technique illustrate sacral obliquity secondary to rotation of one ilium relative to the sacrum around the sacroiliac joint. They

describe an anterior superior rotation of the involve ilium resulting in an elevated sacral base on the side of the involved joint. The opposite misalignment is described as a posterior inferior rotation of the ilium resulting in inferiority of the sacral base on the involved side. From these illustrations and descriptions of the correction of the rotation of the ilia at the sacroiliac joint there is a presumed change to the level of the sacral base.

While radiographic analysis is considered the *gold standard* for measuring leg length differences and pelvic asymmetry (69) there are very few studies specifically designed to establish the validity of erect A-P lumbopelvic radiographs to measure sacral obliquity.

Numerous chiropractic techniques have been used clinically to assess the absolute and relative positional relationships of the bony segments of the pelvis and lower limbs (136). However, very few have attempted to validate the prescription of heel and ischial lifts with correction of specific structural asymmetry of the sacrum. There are no commonly used chiropractic techniques that have been shown to be valid for quantifying sacral obliquity in a clinical setting (139).

The Gonstead method is a commonly used chiropractic technique that involves the analysis of radiographs of the lumbopelvic spine as a clinical assessment method for quantifying positional integrity of individual segments of the axial skeleton. The method involves the measurement of femur head height on erect A-P radiographs of the lumbopevic spine. The measured leg length difference is designated as either a measured difference or actual difference. The actual difference is the measured difference plus or minus a theoretical correction of a misalignment of the pelvis. The Gonstead technique provides a method for calculating the effect pelvic distortion will have on the amount of measured leg length difference. The technique also provides a formula for determining the degree of change expected as a result of correcting pelvic misalignments measured on radiographs (13).



Based on the Gonstead technique protocols a heel lift may be suggested to correct an actual leg length difference. The protocol makes no direct reference to the inferiority of the sacral base although the sacral notch is measured as a deviation from the horizontal. There are two contraindications to the use of a heel lift that Gonstead states are important. The first is a recommendation to never prescribe a lift for a patient when the lumbar scoliosis is on the opposite side of the low femur head. The second states that a lift is never to be prescribed for a patient when the lumbar bodies have rotated to the side opposite the low femur head. Neither of these contraindications allows for, or takes into consideration the possibility that relative sacral obliquity could be a confounding factor influencing the spinal structures above.

The validity of the Gonstead radiographic analysis methods has been questioned in respect to errors associated with both radiographic projection and the analytical processes (line drawing) used in the radiographic analysis. The similar graphic modeling and trigonometric processes have been used to investigate systematic errors associated with the Gonstead radiographic analytical method (237, 396, 397).

## **8.7 SUMMARY and CONCLUSION**

This chapter involved analysing the combination of factors that produce sacral obliquity from a mathematical and geometrical perspective. The result was the development of categories from which corrective algorithms can be produced for each unique combination of factors. Each category required its own algorithm to determine the amount of correction required in either standing or sitting posture. The corrective algorithms were verified using geometrical, mathematical and graphical simulations.



## **SUMMARY AND CONCLUSIONS**

## CHAPTER 9

*"We shall not cease from exploration  
And the end of all our exploring  
Will be to arrive where we started  
And know the place for the first time."*

T.S.Eliot - The Gidding

### 9.1 INTRODUCTION

It is difficult to quantify the difference between measured angles on radiographs and the true dihedral angles that form the functional *in vivo* spine without invasive or complex imaging techniques. The pelvic model and analytical methods developed for this study were used to identify the presence of systematic errors that may be associated with the quantification of dihedral angles such as sacral obliquity on plane film and computed tomography images. Random error could be expected with any angular measurements made on radiographic images. These types of error can generally be identified with statistical analysis of the data. However, because systematic error is not a random variation around a mean it is more difficult to identify and correct unless it is assessed against a known 'gold standard' or 'yardstick'.

The quantification of sacral obliquity undertaken in this study using different radiographic views and different imaging modalities suggests that unless specific imaging and analysis protocols are used the resulting angular measurements will intrinsically contain systematic errors. This conclusion is supported by the consistent variation in the measurement of sacral obliquity in different views of the same segment or in the quantification of known amounts of sacral obliquity. This variation in the measurement of sacral and vertebral obliquity could significantly influence the analysis and clinical interpretation of spinal radiographic images.

The scoliosis research society has specifically defined ‘*sacral obliquity*’ as “angular deviation of the sacrum from the line drawn parallel to a line across the femoral heads on a supine A-P view of the sacrum.” They differentiate sacral obliquity from pelvic obliquity by defining the latter as “*angulation of the pelvis from the horizontal in the frontal plane, possibly secondary to a contraction below the pelvis, e.g. of the hip joint. If this angulation is due to a leg length inequality, then the leg lengths should be equalized to create a level pelvis for measurement purposes.*” Pelvic obliquity under this definition may or may not result in absolute sacral obliquity, which would be an inclination of the sacral base relative to the horizontal plane. Relative sacral obliquity may be present according to these definitions with or without pelvic obliquity. This can come about because the relationship between the femur heads and sacral base is defined as sacral obliquity, not the position of the sacral base relative to the horizontal plane. A limitation of these definitions is that they do not make clear how either pelvic or sacral obliquity is measured and what landmarks or reference points are to be used to assess the obliquity.

## 9.2 LIMITATIONS OF STUDY

The use of dry bone specimens and a radiographic phantom for this study allowed a direct comparison of radiographic methods and analytical procedures involving plain film radiographs and digital imaging. This was done to detect and quantify potential systematic errors associated with the measurement of sacral obliquity on radiographic images. The study did not address questions of *clinical validity* or *clinical utility* of the measurements made on the images.

There was a significant limitation associated with the use of the particular dry bone specimens that was common to other cadaveric specimens and in vivo studies. Unless the obliquity measured on the images could be verified post examination using potentially destructive techniques there was no reliable method to establish a direct relationship between the radiographic image and the actual degree of obliquity inherent in the

specimen. However, this limitation did not affect the objective of this aspect of the study of identifying the presence of systematic error.

The radiographic phantom overcame the problem of validating the radiographic procedures and analytical methods through the use of predetermined degrees of sacral obliquity. However, with this method there was no technique employed to verify that the degree of sacral obliquity and the type of asymmetry it represented was consistent with sacral obliquity reported to have been measured on radiographic images by various clinicians. The pelvic model was not calibrated to ensure reflective symmetry or that the sacral base on which the sacral wedges were attached was parallel to the plane of the structures representing the femur heads. These limitations did not detract from the primary objective of this aspect of the study to identify and quantify systematic error associated with the radiographic measurement of sacral obliquity as measured on different views of the same bone or model.

Because it was not possible in this study to confirm the amount of sacral and vertebral obliquity measured on radiographic images with actual *in vivo* degree of obliquity, idealised graphical models and the use of projective geometry were used. These images provided a basis for developing and validating algorithms and protocols to determine true sacral and vertebral obliquity.

### **9.3 CLINICAL IMPLICATIONS OF THE STUDY**

Even though the sample sizes in this study were limited to sixteen individual sacrum, fifty CT data sets and five variations of the pelvic model, the data obtained from radiographic images of the specimens and the radiographic phantom supports the concept that when taking spinal radiographs or acquiring digital images, the angle of the central ray relative to the segment, orientation of the segment and image plane (film) along with reference points used in the analysis can significantly influence the validity of the measurement of obliquity

in specific cases. Based on this finding, the measurement of sacral obliquity on plain film A-P lumbopelvic radiographs and CT imaging cannot be assumed to be independent of the projection angle and positioning of the segment.

Seven radiographic imaging techniques for quantifying sacral obliquity were assessed using data from this study. Four (4) of the views involve plain film radiography, two (2) involve CT imaging and three (3) involve slot scan imaging. Each of these techniques has advantages and disadvantages in the clinical measurement of sacral obliquity. The advantages and disadvantages have been generally characterised for each of the views relative to the amount of ionising radiation needed, accuracy and ease of analysis as well as the cost and availability of the particular radiographic study.

### ***Plain film***

The four erect A-P views of the lumbopelvic spine and hips include:

1. A-P standing view with the central ray positioned to the centre of the film.
2. Angled (Ferguson's) view of the sacral base taken in erect standing posture with the x-ray tube tilted and the central ray positioned to align with the sacral base.
3. Zero angle view of the sacral base central ray aligned with the sacral base and perpendicular to the image plane (film).
4. Sitting erect sacral base view with the central ray aligned and angled to align with the sacral base (Figure 196).

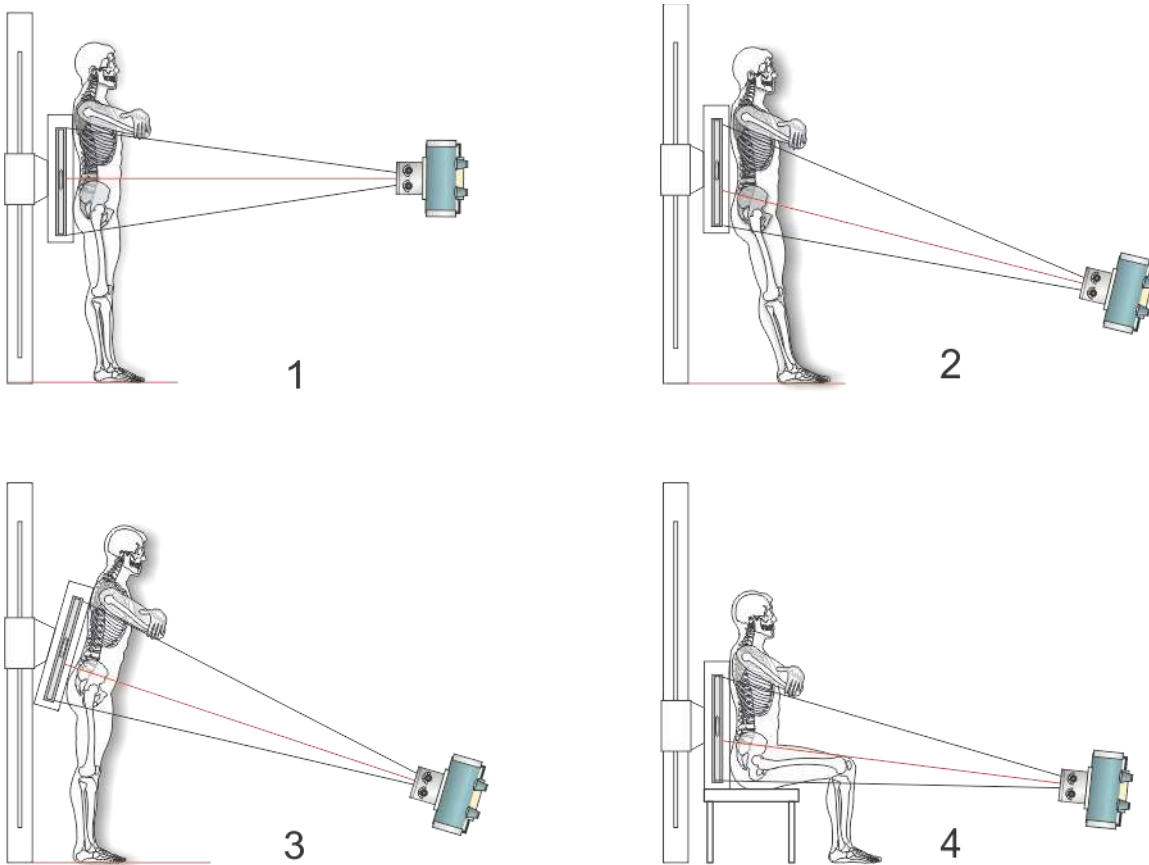
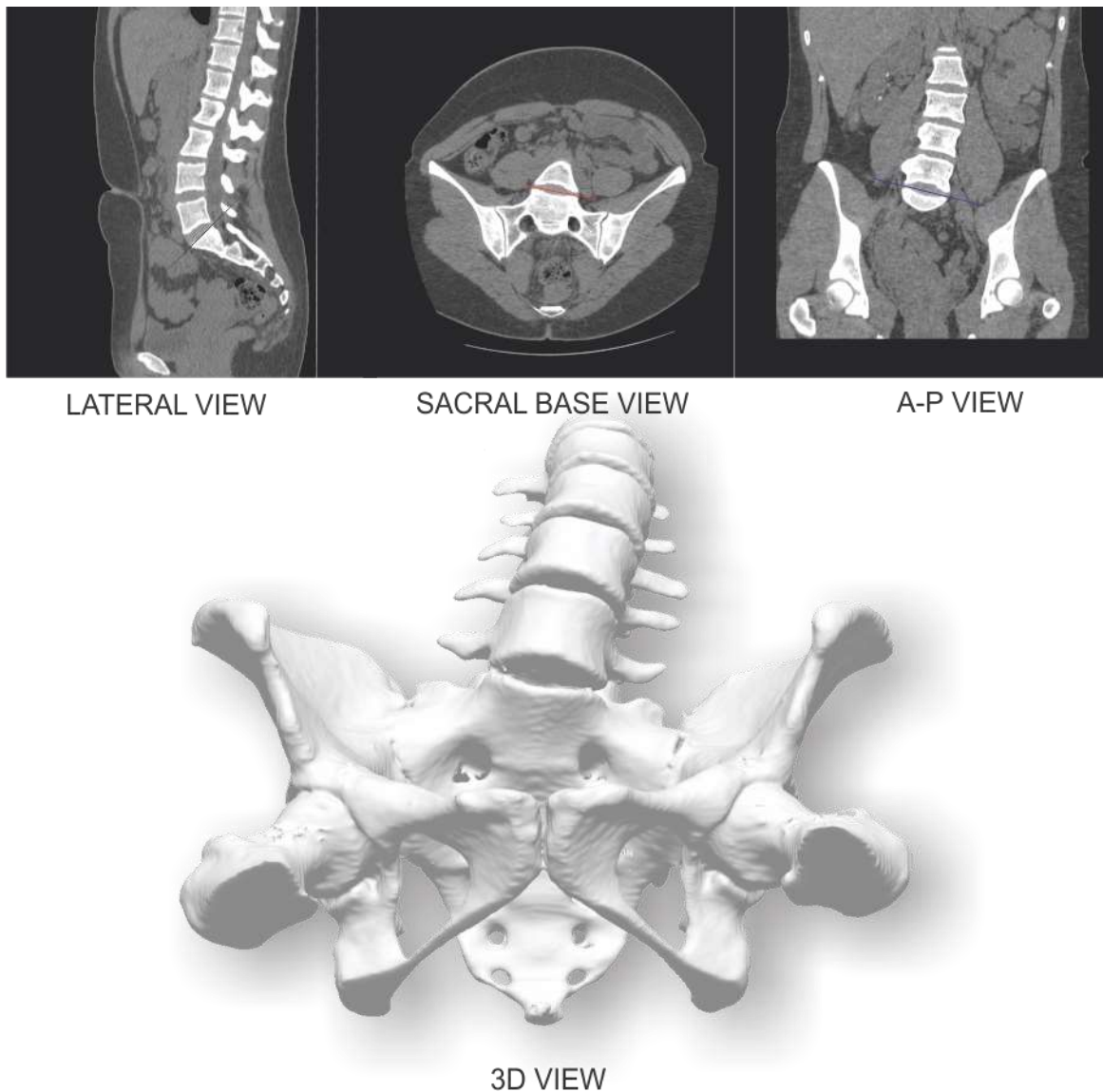


Figure 196. Four erect A-P views of the lumbopelvic spine and hips. 1. A-P standing view 2. Sacral base (Ferguson's) view 3. Zero angle view 4. Sitting sacral base view

### **Computed Tomography**

The two computed tomography (CT) views include:

1. Multiplanar reconstructions (MPR)
  - a. Parallel to the table top and centred on the sacral base.
  - b. Perpendicular to, and centred on the sacral base.
2. Volume rendered (3D) images (Figure 197).



**Figure 197.** Three MPR views and volume rendered 3D image of the radiographic phantom with 15 degrees of simulated sacral obliquity. The first multiplanar reconstruction is a mid-sagittal plane through the pelvis and shows the orientation of the sacral base relative to the table top. In the second view the reconstructed plane is perpendicular to the sacral base and for the third view the image plane is parallel to the table top. The 3D image is a volume rendered reconstruction of the same data set. The 3D image has been manipulated to remove pelvic rotation and orientate the pelvis so that the plane of the sacral base is horizontal.

### ***Slot Scan (CT Imaging)***

The three slot scan views are:

1. CT scout view (Figure 198).
2. Linear slit scanning radiography / Planar slot scan digital radiography (SSDR).
3. Biplane slot scan radiography (Figure 199) and (Figure 200).





LATERAL

A-P VIEW

Figure 198. Lateral and A-P computed tomography scout views of the lumbopelvic spine



Figure 199. Simultaneously acquired biplanar slot scan radiographic images of patient in erect standing posture, lateral view on the left and A-P view on the right. Image used with permission EOS imaging.



Figure 200. Slot scan image taken in erect sitting posture. Image used with permission EOS imaging.

## Advantages And Disadvantages Of Each Radiographic View

### *Plain film views* (Table 26)

- i. A-P view
- ii. Sacral base view
- iii. Zero angle view
- iv. Sitting sacral base view

Table 26. Advantages and disadvantages of plain film imaging of the pelvis

View	Advantages	Disadvantages
A-PV	Routine series for lumbopelvic spine	<p>Difficult to visualise sacral base</p> <p>Sacral obliquity measured as apparent dihedral angel</p> <p>No measuring or positioning constant</p>
SBV	<p>Sacral base visualised as the end view of a plane</p> <p>Reduces influence of pelvic rotation on the measurement of sacral obliquity</p>	<p>Some exaggeration of sacral obliquity angle</p> <p>Difficulty in estimating sacral base angle for tube angle</p>
ZAV	<p>Sacral base projected as true dihedral angle</p> <p>flattened lumbar curve</p>	Abnormal posture
SITTING	<p>Similar advantages as SBV</p> <p>Minimises variables associated with radiographing the spine in standing posture</p>	<p>Unable to measure and assess the impact of leg length imbalance on standing posture</p>

**CT imaging** (Table 27)

- i. MPR
- ii. Volume rendered 3D

Table 27. Advantages and disadvantages of computed tomography (CT) imaging of the pelvis

View	Advantages	Disadvantages
MPR	Cutting plane can be positioned at any angle and depth through the data set	<p>Generally images are only obtained in non-weight bearing decubitus posture</p> <p>Only structures lying in the same plane can be directly compared</p> <p>High exposure to ionising radiation</p>
3D	3D image can be manipulated by rotating and tilting the reconstructed image to provide a true dihedral angle of the planes being measured	<p>Generally images are only obtained in non-weight bearing decubitus posture</p> <p>Reference points may be obscured by overlying structure</p>

**Slot scan imaging** (Table 28)

- i. Scout views
- ii. Planar slot scan
- iii. Biplane slot scan

Table 28. Advantages and disadvantages of slot scan imaging of the pelvis

View	Advantages	Disadvantages
Scout View	Generally routine part of CT examination	Generally images are only obtained in non-weight bearing decubitus posture  Comparatively expensive
Planar Slot Scan	Lower exposure to ionising radiation  No vertical distortion	Requires two views taken independently of each other
Biplane Slot Scan	Lower exposure to ionising radiation  Synchronisation of reference points	Computer generated made to points, planes and angles on reference model  Poor availability

#### 9.4 FUTURE RESEARCH RELATED TO THE MEASUREMENT OF SACRAL OBLIQUITY

Based on the findings of this study that relate to the measurement and correction of sacral obliquity, future research could explore the clinical application of the information. Epidemiological studies could expand the *in vivo* findings of this study using specific CT imaging involving a larger sample size of randomly selected subjects. Epidemiological studies could also be used to identify the distribution, incidence, prevalence and characteristics of sacral obliquity in the general population or in relation to specific groups such as low back pain sufferers. These studies could be helpful in the development of preventative strategies and better clinical management of patients with these conditions. Without epidemiological data it is not possible to speculate on the clinical implications of sacral obliquity or its association with any particular pain syndrome or musculoskeletal condition.

Further studies could involve validating the amount of heel and ischial lift needed to level the sacral base in both sitting and standing posture. Evidence based guidelines could then be applied in a clinical setting to determine the efficacy of correcting sacral obliquity with heel and ischial lifts.

Another area of research involves assessing the reliability and clinical utility of specific radiographic modalities (CT, PF, Slot Scan) and radiographic views (erect A-P, sacral base) in measuring sacral obliquity. This could help remove underestimation or overestimation of sacral obliquity by standardising radiographic imaging and analytical techniques. This would help to develop a greater understanding and management of back problems and pain syndromes.

Future research could explore the impact sacral obliquity has on the musculoskeletal areas above the pelvis. Theoretically a tilt of the sacral base could result in bilateral asymmetry of the spinal muscles, presence of minor scoliosis throughout the spine and joint tropism. Many clinical assessments such as range of movement and posture are based on the assumption of normal being represented by symmetry around a vertical axis.

## **9.5 CONCLUSION**

The first question to be explored when looking at the measurement of sacral obliquity on radiographic images, was the possibility of systematic errors effecting the measurement of the sacral obliquity and hence the validity of the measurements. Measurements derived from two specific radiographic views employing plain film radiography of dry bone sacral specimens indicated the presence of systematic error with particular views, reference points and analytical methods in the measurement of dihedral angles such as sacral obliquity. This was supported by graphic analysis of images employing the principles of projective geometry.

It was found that the nature and magnitude of the error is specific to both the view and imaging modality used to visualise the structures of interest and the analytical methods employed to obtain the angles representing the structures involved. Algorithms were developed using the information obtained from plain film and CT imaging of the radiographic phantom to compensate for the inherent systematic errors in measuring dihedral angles such as sacral obliquity on two dimensional radiographic images.

Sacral obliquity was examined for fifty in vivo sacrums based on CT studies. It showed an antisymmetric pattern for sacral obliquity in the population study. The clinical application of this information resulted in a classification system of sacral obliquity with accompanying corrective algorithms for orthotic intervention.

These results have implications for clinicians and researchers interested in quantifying the positional and anatomical relationships between segments of the spine and pelvis using radiographic techniques.

Clinicians and researchers who take and use radiographs to assess positional integrity of the spine and pelvis generally believe that doing so has clinical significance. It is therefore important to know that the radiographic and analytical methods they employ are not only reliable but also provide valid information in relation to the structures being evaluated.

This study suggests that there are potentially significant systematic errors associated with the measurement of dihedral angles such as sacral obliquity and Cobbs angles made on standard radiographic and CT images due to projection angles or viewing planes and the analytical methods employed. The specific radiographic methods and analytical procedures commonly used in clinical practice or recommended as a method for measuring sacral obliquity and investigated in this study each had associated systematic errors. Only



by following strict protocols for generating and analysing images can the systematic errors be eliminated or minimised.

With more time spent in an orthogonal environment skeletal asymmetry increases in importance. Sacral obliquity could be an important contributor to skeletal asymmetry that has gone relatively unnoticed. As sitting time and standing on hard flat surfaces increases the importance of having a level sacral base is becoming more significant. The information gained from this study can be used to calculate the size of orthotic intervention required to level the base of the spine in either standing or sitting posture.

<b>REFERENCES</b>
-------------------

1. Broome DR, Hayman LA, Herrick RC, Braverman RM, Glass RB, Fahr LM. Postnatal maturation of the sacrum and coccyx: MR imaging, helical CT, and conventional radiography. *American Journal of Roentgenology*. 1998 1998/04/01;170(4):1061-6.
2. Sugar O. How the sacrum got its name. *Journal of the American Medical Association*. 1987;257(15):2061-3.
3. Al-Eisa E, Egan D, Deluzio K, Wassersug R. Effects of pelvic asymmetry and low back pain on trunk kinematics during sitting: a comparison with standing. *Spine (Phila Pa 1976)*. 2006 Mar 1;31(5):E135-43. PubMed PMID: 16508537. Epub 2006/03/02. eng.
4. Al-Eisa E, Egan D, Wassersug R. Fluctuating asymmetry and low back pain. *Evolution and human behavior*. 2004;25:31-7.
5. Brown WM, Price ME, Kang J, Pound N, Zhao Y, Yu H. Fluctuating asymmetry and preferences for sex-typical bodily characteristics. *Proceedings of the National Academy of Sciences*. 2008 September 2, 2008;105(35):12938-43.
6. Stokes IA, Aronsson DD. Computer-assisted algorithms improve reliability of King classification and Cobb angle measurement of scoliosis. *Spine (Phila Pa 1976)*. 2006 Mar 15;31(6):665-70. PubMed PMID: 16540871. Epub 2006/03/17. eng.
7. Cassar-Pullicino VN, Eisenstein SM. Imaging in scoliosis: what, why and how? *Clin Radiol*. 2002 Jul;57(7):543-62. PubMed PMID: 12096851. Epub 2002/07/05. eng.
8. Kuchera ML, Kuchera WA. Radiographic aspects of the postural study. In: Ward RC, editor. *Foundations for Osteopathic Medicine*. 2 ed. Philadelphia: Lippincott Williams and Wilkins; 2003. p. 591-602.
9. Plaughner G. The role of plain film radiography in chiropractic clinical practice. *Chiropr J Aust*. 1992;22(4):153-61.

10. Katz DE, Durrani AA. Factors that influence outcome in bracing large curves in patients with adolescent idiopathic scoliosis. *Spine (Phila Pa 1976)*. 2001 Nov 1;26(21):2354-61. PubMed PMID: 11679821. Epub 2001/10/27. eng.
11. Fann AV. Validation of postural radiographs as a way to measure change in pelvic obliquity. *Arch Phys Med Rehabil*. 2003 Jan;84(1):75-8. PubMed PMID: 12589624. Epub 2003/02/18. eng.
12. Cremata EE, Plaughner G, Cox WA. Technique system application: the Gonstead approach. *Chiropr Tech*. 1991;3(1):19-25.
13. Herbst RW. The A-P ilium misalignment. *Gonstead chiropractic science and art*. Mount Horeb, WI: Sci-Chi Publications; 1968.
14. Fann AV, Lee R, Verbois GM. The reliability of postural x-rays in measuring pelvic obliquity. *Arch Phys Med Rehabil*. 1999 Apr;80(4):458-61. PubMed PMID: 10206611. Epub 1999/04/17. eng.
15. Harrison DE, Harrison DD, Troyanovich SJ. Reliability of spinal displacement analysis of plain X-rays: a review of commonly accepted facts and fallacies with implications for chiropractic education and technique. *Journal of manipulative and physiological therapeutics*. 1998 May;21(4):252-66. PubMed PMID: 9608381. Epub 1998/06/03. eng.
16. Ebrall PS. *Assessment of the spine*. Edinburgh: Churchill Livingstone; 2004.
17. Verbois GM, Fann AV. Idiopathic scoliosis and sacral base unlevelness: a case report. *Am J Phys Med Rehabil*. 1997;76(2):164.
18. Schiller JR, P. EC. Spinal deformity and athletics. *Sports Med Arthrosc Rev*. 2008;16(1):26-31.
19. Micheli LJ, Trepman E. Spinal deformities. In: Torg JSS, R. J., editor. *Current Therapy in Sports Medicine*. 3rd edition ed. St. Louis: Mosby-Year Book; 1995. p. 91-6.
20. Paré EG, Loving RO, Hill IL. *Descriptive Geometry*. 3 ed. New York: Macmillian; 1968.

21. Holliday-Darr K, Stewart SA. *Applied Descriptive Geometry*. 2 ed. Albany: Delmar; 1998.
22. Gashler M, Martinez T, editors. Tangent space guided intelligent neighbor finding. *The 2011 International Joint Conference on Neural Networks*; 2011; San Jose, CA: IEEE.
23. Morrissy RT, Goldsmith GS, Hall EC, Kehl D, Cowie GH. Measurement of the Cobb angle on radiographs of patients who have scoliosis. Evaluation of intrinsic error. *J Bone Joint Surg Am*. 1990 Mar;72(3):320-7. PubMed PMID: 2312527. Epub 1990/03/01. eng.
24. Mior SA, Kopansky-Giles DR, Crowther ER, Wright JG. A comparison of radiographic and electrogoniometric angles in adolescent idiopathic scoliosis. *Spine (Phila Pa 1976)*. 1996 Jul 1;21(13):1549-55. PubMed PMID: 8817783. Epub 1996/07/01. eng.
25. Goldberg CJ, Kaliszer M, Moore DP, Fogarty EE, Dowling FE. Surface topography, Cobb angles, and cosmetic change in scoliosis. *Spine (Phila Pa 1976)*. 2001 Feb 15;26(4):E55-63. PubMed PMID: 11224901. Epub 2001/02/27. eng.
26. Langensiepen S, Semler O, Sobottke R, Fricke O, Franklin J, Schönauf E, et al. Measuring procedures to determine the Cobb angle in idiopathic scoliosis: a systematic review. *European Spine Journal*. 2013;22(11):2360-71.
27. Sacral obliquity, a poorly understood congenital anomaly, (2002).
28. Schwender JD, Denis F. Coronal plane imbalance in adolescent idiopathic scoliosis with left lumbar curves exceeding 40 degrees: the role of the lumbosacral hemicurve. *Spine (Phila Pa 1976)*. 2000 Sep 15;25(18):2358-63. PubMed PMID: 10984789. Epub 2000/09/14. eng.
29. Harrison DD, Harrison DE, Troyanovich SJ, Hansen DJ. The anterior-posterior full-spine view: the worst radiographic view for determination of mechanics of the spine. *Chiropractic Technique*. 1996;8(4):163-70.

30. Adams MA, Bogduk N, Burton K, Dolan P. The biomechanics of back pain. Edinburgh: Churchill Livingstone; 2002.
31. Schiowitz S. Pelvic and sacral anatomic considerations. In: DiGiovanna EL, Schiowitz S, Dowling DJ, editors. An osteopathic approach to diagnosis and treatment. 3 ed. Philadelphia: Lippincott Williams & Wilkins 2005. p. 285-92.
32. Kuchera ML, Kappler RE. Considerations of posture and group curves. In: DiGiovanna EL, Schiowitz S, Dowling DJ, editors. An osteopathic approach to diagnosis and treatment. 3 ed. Philadelphia: Lippincott Williams & Wilkins; 2005. p. 300-590.
33. Cailliet R. Scoliosis diagnosis and management. Philadelphia: F. A. Davis Company; 1986.
34. Kuchera M. Postural considerations in coronal, horizontal, and sagittal planes. In: Ward RC, editor. Foundations for Osteopathic Medicine. 2 ed. Philadelphia: Lippincott Williams and Wilkins; 2003. p. 614-32.
35. Tawfik B. Symmetry and linearity of trunk function in subjects with non-specific low back pain. Clin Biomech (Bristol, Avon). 2001 Feb;16(2):114-20. PubMed PMID: 11222929. Epub 2001/02/27. eng.
36. McGill S. Low back disorders evidence- based prevention and rehabilitation. Champaign (IL): Human Kinetics; 2002.
37. Cheng JS, Song JK. Anatomy of the sacrum. Neurosurg Focus. 2003 Aug 15;15(2):E3. PubMed PMID: 15350034. Epub 2004/09/08. eng.
38. Hoek van Dijke GA, Snijders CJ, Stoeckart R, Stam HJ. A biomechanical model on muscle forces in the transfer of spinal load to the pelvis and legs. J Biomech. 1999 Sep;32(9):927-33. PubMed PMID: 10460129. Epub 1999/08/25. eng.
39. Plochocki JH. Directional bilateral asymmetry in human sacral morphology. Int J Osteoarchaeol 2002;12:349-55.
40. Carstens C. Congenital tilt of the sacral plateau and the fate of the spine. Z Orthop Ihre Grenzgeb. 1988 Sep-Oct;126(5):532-8. PubMed PMID: 3239175. Epub

1988/09/01. Der kongenitale Schiefstand des Sakralplateaus und das Schicksal der Wirbelsäule. ger.

41. Illi FW. The vertebral column: lifeline of the body. Chicago Illinois: National College of Chiropractic; 1951.
42. Al-Eisa E, Egan D, Deluzio K, Wassersug R. Effects of pelvic skeletal asymmetry on trunk movement: three-dimensional analysis in healthy individuals versus patients with mechanical low back pain. *Spine (Phila Pa 1976)*. 2006 Feb 1;31(3):E71-9. PubMed PMID: 16449891. Epub 2006/02/02. eng.
43. Legaye J, Duval-Beaupere G. Sagittal plane alignment of the spine and gravity: a radiological and clinical evaluation. *Acta Orthop Belg*. 2005 Apr;71(2):213-20. PubMed PMID: 16152857. Epub 2005/09/13. eng.
44. Richardson C, Hodges PW, Hides J. Therapeutic exercise for lumbopelvic stabilization. Edinburgh: Churchill Livingstone; 2004.
45. Schijvens AWM, Snijders CJ, Serroo JM, Snyder JGN. Mechanics of the spine: analysis of its flexibility and rigidity, postural control, and correction of the pathological spine. In: Ghista DN, editor. *Osteoarthromechanics*. New York: McGraw-Hill Book Company; 1982.
46. Stokes IAF. Hueter-Volkmann law and pathomechanism: one theory fits all diagnoses. In: Sevastik JA, Diab KM, editors. *Research into spinal deformities 1*: IOS Press; 1997. p. 455-6.
47. Stokes IAF, Spence H, Aronsson DD, Kilmer D, Gupta D. Mechanical modulation of vertebral and disc growth rate. In: Sevastik JA, Diab KM, editors. *Research into spinal deformities 1*: IOS Press; 1997. p. 67-71.
48. Mente PL, Spence H, Stokes IAF, Aronsson DD. Vertebral wedging due to asymmetric loading. In: Sevastik JA, Diab KM, editors. *Research into spinal deformities 1*: IOS Press; 1997. p. 103-5.
49. Lenke L. SRS terminology committee and working group on spinal classification, revised glossary of terms. 2000.

50. Timgren J, Soinila S. Reversible pelvic asymmetry: an overlooked syndrome manifesting as scoliosis, apparent leg-length difference, and neurologic symptoms. *Journal of manipulative and physiological therapeutics*. 2006 Sep;29(7):561-5. PubMed PMID: 16949945. Epub 2006/09/05. eng.
51. Baker R. Pelvic angles: a mathematically rigorous definition which is consistent with a conventional clinical understanding of the terms. *Gait Posture*. 2001 Feb;13(1):1-6. PubMed PMID: 11166548. Epub 2001/02/13. eng.
52. Cailliet R. Low back pain syndrome. 2 ed. Philadelphia: F. A. Davis Company; 1979.
53. Hoffman KS, Hoffman LL. Effects of adding sacral base leveling to osteopathic manipulative treatment of back pain: a pilot study. *J Am Osteopath Assoc*. 1994 Mar;94(3):217-20, 23-6. PubMed PMID: 8200825. Epub 1994/03/01. eng.
54. Fann AV. In-shoe interventions ease back pain through postural correction. *BioMechanics*. 2001;805:39-44.
55. Giles LG, Taylor JR. Lumbar spine structural changes associated with leg length inequality. *Spine (Phila Pa 1976)*. 1982 Mar-Apr;7(2):159-62. PubMed PMID: 7089692. Epub 1982/03/01. eng.
56. Brady RJ, Dean JB, Skinner TM, Gross MT. Limb length inequality: clinical implications for assessment and intervention. *J Orthop Sports Phys Ther*. 2003 May;33(5):221-34. PubMed PMID: 12774997. Epub 2003/05/31. eng.
57. Knutson GA. Incidence of foot rotation, pelvic crest unleveling, and supine leg length alignment asymmetry and their relationship to self-reported back pain. *Journal of manipulative and physiological therapeutics*. 2002 Feb;25(2):110E. PubMed PMID: 11896379. Epub 2002/03/16. eng.
58. Fann AV, Hammaker AF, Spencer HJ, Kligman S, Gray RP. The impact of structural therapy on functioning and pain in chronic pain patients: a pilot study. *Journal of Back and Musculoskeletal Rehabilitation*. 2007;20(1):1-9.

59. Fann AV. The prevalence of postural asymmetry in people with and without chronic low back pain. *Arch Phys Med Rehabil.* 2002 Dec;83(12):1736-8. PubMed PMID: 12474179. Epub 2002/12/11. eng.
60. Friberg O. Clinical symptoms and biomechanics of lumbar spine and hip joint in leg length inequality. *Spine (Phila Pa 1976).* 1983 Sep;8(6):643-51. PubMed PMID: 6228021. Epub 1983/09/01. eng.
61. Defrin R, Ben Benyamin S, Aldubi RD, Pick CG. Conservative correction of leg-length discrepancies of 10mm or less for the relief of chronic low back pain. *Arch Phys Med Rehabil.* 2005 Nov;86(11):2075-80. PubMed PMID: 16271551. Epub 2005/11/08. eng.
62. Anderson RG, Hayak R, Foggerty MP. Leg length inequality and the side of low back pain a pilot study. *COMSIG Review* 1995;4(2):33-6.
63. Zabjek KF, Leroux MA, Coillard C, Martinez X, Griffet J, Simard G, et al. Acute postural adaptations induced by a shoe lift in idiopathic scoliosis patients. *European spine journal : official publication of the European Spine Society, the European Spinal Deformity Society, and the European Section of the Cervical Spine Research Society.* 2001 Apr;10(2):107-13. PubMed PMID: 11345630. Epub 2001/05/11. eng.
64. Beaudoin L, Zabjek KF, Leroux MA, Coillard C, Rivard CH. Acute systematic and variable postural adaptations induced by an orthopaedic shoe lift in control subjects. *European spine journal : official publication of the European Spine Society, the European Spinal Deformity Society, and the European Section of the Cervical Spine Research Society.* 1999;8(1):40-5. PubMed PMID: 10190853. Epub 1999/04/06. eng.
65. Irvin RE. Reduction of lumbar scoliosis by use of a heel lift to level the sacral base. *J Am Osteopath Assoc.* 1991 Jan;91(1):34, 7-44. PubMed PMID: 1997458. Epub 1991/01/01. eng.



66. Papaioannou T, Stokes I, Kenwright J. Scoliosis associated with limb-length inequality. *J Bone Joint Surg Am*. 1982 Jan;64(1):59-62. PubMed PMID: 7054204. Epub 1982/01/01. eng.
67. Childs JD, Piva SR, Erhard RE. Immediate improvements in side-to-side weight bearing and iliac crest symmetry after manipulation in patients with low back pain. *Journal of manipulative and physiological therapeutics*. 2004 Jun;27(5):306-13. PubMed PMID: 15195038. Epub 2004/06/15. eng.
68. Mahar RK, Kirby RL, MacLeod DA. Simulated leg-length discrepancy: its effect on mean center-of-pressure position and postural sway. *Arch Phys Med Rehabil*. 1985 Dec;66(12):822-4. PubMed PMID: 4074116. Epub 1985/12/01. eng.
69. Gurney B. Leg length discrepancy. *Gait Posture*. 2002 Apr;15(2):195-206. PubMed PMID: 11869914. Epub 2002/03/01. eng.
70. Kakushima M, Miyamoto K, Shimizu K. The effect of leg length discrepancy on spinal motion during gait: three-dimensional analysis in healthy volunteers. *Spine (Phila Pa 1976)*. 2003 Nov 1;28(21):2472-6. PubMed PMID: 14595166. Epub 2003/11/05. eng.
71. ten Brinke A, van der Aa HE, van der Palen J, Oosterveld F. Is leg length discrepancy associated with the side of radiating pain in patients with a lumbar herniated disc? *Spine (Phila Pa 1976)*. 1999 Apr 1;24(7):684-6. PubMed PMID: 10209798. Epub 1999/04/21. eng.
72. Knutson GA. Anatomic and functional leg-length inequality: a review and recommendation for clinical decision-making. Part I, anatomic leg-length inequality: prevalence, magnitude, effects and clinical significance. *Chiropr Osteopat*. 2005 Jul 20;13:11. PubMed PMID: 16026625. Pubmed Central PMCID: 1232860. Epub 2005/07/20. eng.
73. Levangie PK. The association between static pelvic asymmetry and low back pain. *Spine (Phila Pa 1976)*. 1999 Jun 15;24(12):1234-42. PubMed PMID: 10382251. Epub 1999/06/26. eng.

74. Hoikka V, Ylikoski M, Tallroth K. Leg-length inequality has poor correlation with lumbar scoliosis. A radiological study of 100 patients with chronic low-back pain. *Arch Orthop Trauma Surg.* 1989;108(3):173-5. PubMed PMID: 2525016. Epub 1989/01/01. eng.
75. Nourbakhsh MR, Arab AM. Relationship between mechanical factors and incidence of low back pain. *J Orthop Sports Phys Ther.* 2002 Sep;32(9):447-60. PubMed PMID: 12322811. Epub 2002/09/27. eng.
76. Dieck GS, Kelsey JL, Goel VK, Panjabi MM, Walter SD, Laprade MH. An epidemiologic study of the relationship between postural asymmetry in the teen years and subsequent back and neck pain. *Spine (Phila Pa 1976).* 1985 Dec;10(10):872-7. PubMed PMID: 2938272. Epub 1985/12/01. eng.
77. Schamberger W. The malalignment syndrome. Implications for medicine and sport. London: Churchill Livingstone; 2002.
78. Barge FH. Chiropractic technic Scoliosis Vol III. Davenport (IA): Bawdin Printing Inc; 1982.
79. Liebensohn C. Rehabilitation of the spine. A practitioner's manual. Philadelphia: Lippincott Williams & Wilkins; 1996.
80. Hestbaek L, Leboeuf-Yde C. Are chiropractic tests for the lumbo-pelvic spine reliable and valid? A systematic critical literature review. *Journal of manipulative and physiological therapeutics.* 2000 May;23(4):258-75. PubMed PMID: 10820299. Epub 2000/05/23. eng.
81. Piva SR, Erhard RE, Childs JD, Hicks G, Al-Abdulmohsin H. Reliability of measuring iliac crest level in the standing and sitting position using a new measurement device. *Journal of manipulative and physiological therapeutics.* 2003 Sep;26(7):437-41. PubMed PMID: 12975630. Epub 2003/09/17. eng.
82. Boulay C, Tardieu C, Benaim C, Hecquet J, Marty C, Prat-Pradal D, et al. Three-dimensional study of pelvic asymmetry on anatomical specimens and its clinical

- perspectives. *J Anat.* 2006 Jan;208(1):21-33. PubMed PMID: 16420376. Pubmed Central PMCID: 2100175. Epub 2006/01/20. eng.
83. Juhl JH, Ippolito Cremin TM, Russell G. Prevalence of frontal plane pelvic postural asymmetry--part 1. *J Am Osteopath Assoc.* 2004 Oct;104(10):411-21. PubMed PMID: 15537798. Epub 2004/11/13. eng.
  84. Tullberg T, Blomberg S, Branth B, Johnsson R. Manipulation does not alter the position of the sacroiliac joint. A roentgen stereophotogrammetric analysis. *Spine (Phila Pa 1976).* 1998 May 15;23(10):1124-8; discussion 9. PubMed PMID: 9615363. Epub 1998/06/06. eng.
  85. Badii M, Shin S, Torreggiani WC, Jankovic B, Gustafson P, Munk PL, et al. Pelvic bone asymmetry in 323 study participants receiving abdominal CT scans. *Spine (Phila Pa 1976).* 2003 Jun 15;28(12):1335-9. PubMed PMID: 12811280. Epub 2003/06/18. eng.
  86. Dott GA, Hart CL, McKay C. Predictability of sacral base levelness based on iliac crest measurements. *J Am Osteopath Assoc.* 1994 May;94(5):383-90. PubMed PMID: 8056627. Epub 1994/05/01. eng.
  87. Hawes MC, O'Brien JP. The transformation of spinal curvature into spinal deformity: pathological processes and implications for treatment. *Scoliosis.* 2006;1(1):3. PubMed PMID: 16759413. Pubmed Central PMCID: 1459276. Epub 2006/06/09. eng.
  88. Danbert RJ. Clinical assessment and treatment of leg length inequalities. *Journal of manipulative and physiological therapeutics.* 1988 Aug;11(4):290-5. PubMed PMID: 3049890. Epub 1988/08/01. eng.
  89. Rothenberg RJ. Rheumatic disease aspects of leg length inequality. *Semin Arthritis Rheum.* 1988 Feb;17(3):196-205. PubMed PMID: 2977450. Epub 1988/02/01. eng.
  90. Colloca CJ. Leg length inequality: An assessment of asymmetry. In: Fuhr AW, Colloca CJ, Green JR, Keller TS, editors. *Activator Methods.* St. Louis: Mosby; 2000. p. 65-88.

91. Krawiec CJ, Denegar CR, Hertel J, Salvaterra GF, Buckley WE. Static innominate asymmetry and leg length discrepancy in asymptomatic collegiate athletes. *Manual therapy*. 2003 Nov;8(4):207-13. PubMed PMID: 14559043. Epub 2003/10/16. eng.
92. Al-Eisa E, Egan D, Fenety A. The association between lateral pelvic tilt and asymmetry in sitting pressure distribution. *J Manual Manipulative Ther*. 2004;12(3):133-42.
93. Fredericks TK, Butts SE. Objectively determining comfortable lumbar support in task seating 2005. Available from: URL: <http://www.haworth.com/en-us/Knowledge/Workplace-Library/Documents/Objectively-Determining-Comfortable-Lumbar-Support-in-Task-Seating.pdf>.
94. Albin T. Every back is different 2009 [22.1.12]. Available from: URL: [http://www.haworth.com/en-us/Knowledge/Workplace-Library/Documents/Every\\_Back\\_is\\_Different.pdf](http://www.haworth.com/en-us/Knowledge/Workplace-Library/Documents/Every_Back_is_Different.pdf).
95. Nag PK, Hsiang S. Ergonomics in manual materials handling tasks. *ICMR Bulletin*. 2000;30(8).
96. Nordqvist C. Don't Sit Up Straight, It's Bad For Your Back 2006 [21 Jan. 2012]. Available from: <http://www.medicalnewstoday.com/articles/57654.php>.
97. Manganiello A. Lower Extremity dysmetria, scoliosis, low back pain and spondylosis. In: Sevastic JA, Diab KM, editors. *Research into Spinal Deformities 1*. Amsterdam: IOS Press; 1997. p. 111-3.
98. Bialy M, Klapotocz P, Gnat R. Functional asymmetry of the spine in standing and sitting positions. *Acta Univ PalackiOlomuc, Gymn*. 2010;40(1):53-60.
99. Hildebrandt RW. *Chiropractic spinigraphy a manual of technology and interpretation*. Revised ed. Wheaton (IL): MS Hilmark Publications; 1980.
100. Kapandji IA. *The physiology of the joints Volume 3. The trunk and the vertebral column*. 2 ed. Edinburgh: Churchill Livingstone; 1974.
101. Normand MC, Descarreaux M, Harrison DD, Harrison DE, Perron DL, Ferrantelli JR, et al. Three dimensional evaluation of posture in standing with the PosturePrint: an

- intra- and inter-examiner reliability study. *Chiropr Osteopat.* 2007;15:15. PubMed PMID: 17892559. Pubmed Central PMCID: 2077332. Epub 2007/09/26. eng.
102. Fehrsen-Du Toit R. *The Good Back Book*. London: New Holland Publishers; 2002.
  103. Scafer RC. *Clinical Biomechanics musculoskeletal Actions and reactions*. Baltimore: Williams & Wilkins; 1987.
  104. Carlson JM. Clinical biomechanics of orthotic treatment of idiopathic scoliosis. *JPO.* 2003;15(4S):17-30.
  105. Harrison DD, Janik TJ, Harrison GR, Troyanovich S, Harrison DE, Harrison SO. Chiropractic biophysics technique: a linear algebra approach to posture in chiropractic. *Journal of manipulative and physiological therapeutics.* 1996 Oct;19(8):525-35. PubMed PMID: 8902664. Epub 1996/10/01. eng.
  106. Cranz G. *The Chair - Rethinking Culture, Body and Design*. New York: W. W. Norton and Company; 1998.
  107. Cranz G. The Alexander Technique in the world of design: posture and the common chair. *Journal of bodywork and movement therapies.* 2000;4(2):90-8.
  108. Wilson A. *The Complete Guide to Good Posture at Work*. London: Vermilion; 1996.
  109. Mandal AC. The seated man (Homo Sedens) the seated work position. Theory and practice. *Applied ergonomics.* 1981 Mar;12(1):19-26. PubMed PMID: 15676394. Epub 1981/03/01. eng.
  110. Fine J. *The Ultimate Back Book: understand, manage, and conquer your back pain.* 2 ed. Toronto: Stoddart Publishing; 2000.
  111. Yanker G. *Exercise Rx: The lifetime prescriptions for reducing medical risks and sports injuries*. New York: Oxford University Press; 2002.
  112. D. HD, Yanik TJ, Troyanovich SJ, Harrison DE, Colloca CJ. Evaluation of the assumptions used to derive an ideal normal cervical spine model. *J Manipulative Physiol Ther.* 1997;20(4):246-56.
  113. Bettany-Saltikov JA, van Schaik P, Warren J. Straight spines in young adults: the exception or the rule? Poster presentations. *Eur Spine J.* 2000;9:314-64.

114. Ross JK, Bereznick DE, McGill SM. Atlas-axis facet asymmetry. Implications in manual palpation. *Spine (Phila Pa 1976)*. 1999 Jun 15;24(12):1203-9. PubMed PMID: 10382246. Epub 1999/06/26. eng.
115. Jacob G, McKenzie R. Spinal therapeutics based on responses to loading. In: Liebenson C, editor. *Rehabilitation of the Spine: A Practitioner's Manual*. Baltimore: Williams and Wilkins; 1996. p. 225.
116. Asher MA, Burton DC. Adolescent idiopathic scoliosis: natural history and long term treatment effects. *Scoliosis*. 2006;1(1):2. PubMed PMID: 16759428. Pubmed Central PMCID: 1475645. Epub 2006/06/09. eng.
117. Horton SJ, Franz A. Mechanical Diagnosis and Therapy approach to assessment and treatment of derangement of the sacro-iliac joint. *Manual therapy*. 2007 May;12(2):126-32. PubMed PMID: 16891145. Epub 2006/08/08. eng.
118. Little P, Lewith G, Webley F, Evans M, Beattie A, Middleton K, et al. Randomised controlled trial of Alexander technique lessons, exercise, and massage (ATEAM) for chronic and recurrent back pain. *Bmj*. 2008;337:a884. PubMed PMID: 18713809. Epub 2008/08/21. eng.
119. Weiss HR. Conservative treatment of idiopathic scoliosis with physical therapy and orthoses. *Orthopade*. 2003 Feb;32(2):146-56. PubMed PMID: 12607080. Epub 2003/02/28. Die konservative Behandlung der idiopathischen Skoliose durch Krankengymnastik und Orthesen. ger.
120. Brooks PM, March LM, Bogduk N, Bellamy N. Australian Acute Musculoskeletal Pain Guidelines Group. Evidence-based Management of Acute Musculoskeletal Pain. In: NHMRC, editor. *Brisbane: Australian Academic Press*; 2004.
121. Canavese F, Kaelin A. Adolescent idiopathic scoliosis: Indications and efficacy of nonoperative treatment. *Indian journal of orthopaedics*. 2011 Jan;45(1):7-14. PubMed PMID: 21221217. Pubmed Central PMCID: 3004085. Epub 2011/01/12. eng.

122. Schiller JR, Thakur NA, Eberson CP. Brace management in adolescent idiopathic scoliosis. *Clinical orthopaedics and related research*. 2010 Mar;468(3):670-8.  
PubMed PMID: 19484317. Pubmed Central PMCID: 2816747. Epub 2009/06/02.  
eng.
123. Weiss HR, Negrini S, Hawes MC, Rigo M, Kotwicki T, Grivas TB, et al. Physical exercises in the treatment of idiopathic scoliosis at risk of brace treatment -- SOSORT consensus paper 2005. *Scoliosis*. 2006;1:6. PubMed PMID: 16759360.  
Pubmed Central PMCID: 1481573. Epub 2006/06/09. eng.
124. Weiss HR, Goodall D. The treatment of adolescent idiopathic scoliosis (AIS) according to present evidence. A systematic review. *European journal of physical and rehabilitation medicine*. 2008;44(2):177-93.
125. Lehnert-Schroth C. Introduction to the three-dimensional scoliosis treatment according to Schroth. *Physiotherapy*. 1992;78(11):810-15.
126. Hawes MC. The use of exercises in the treatment of scoliosis: an evidence-based critical review of the literature. *Pediatric rehabilitation*. 2003 Jul-Dec;6(3-4):171-82.  
PubMed PMID: 14713583. Epub 2004/01/10. eng.
127. Negrini S, Antonini G, Carabalona R, Minozzi S. Physical exercises as a treatment for adolescent idiopathic scoliosis. A systematic review. *Pediatric rehabilitation*. 2003 Jul-Dec;6(3-4):227-35. PubMed PMID: 14713590. Epub 2004/01/10. eng.
128. Cassella MC, Hall JE. Current treatment approaches in the nonoperative and operative management of adolescent idiopathic scoliosis. *Phys Ther*. 1991 Dec;71(12):897-909. PubMed PMID: 1946624. Epub 1991/12/01. eng.
129. Timm KE. Sacroiliac joint dysfunction in elite rowers. *Orthop Sports Phys Ther*. 1999;29(5):288-93.
130. Cibulka MT, Delitto A. A comparison of two different methods to treat hip pain in runners. *J Orthop Sports Phys Ther*. 1993;17(4):172-6.
131. DonTigny RL. Function and pathomechanics of the sacroiliac joint: A review. *Phys Ther*. 1985;65(1):35-44.

132. Nicholas NS. Atlas of Osteopathic techniques. Philadelphia N S Nicholas and Philadelphia College of Osteopathic Medicine; 1974.
133. Gatterman MI, Cooperstein R, Lantz C, Perle SM, Schneider MJ. Rating specific chiropractic technique procedures for common low back conditions. Journal of manipulative and physiological therapeutics. 2001;24(7):449-56.
134. Christensen MG. Job Analysis of Chiropractic in Australia and New Zealand. Greeley, Colorado: National Board of Chiropractic Examiners; 1994.
135. Mannello DM. Leg length inequality. Journal of manipulative and physiological therapeutics. 1992 Nov-Dec;15(9):576-90. PubMed PMID: 1469342. Epub 1992/11/01. eng.
136. Knutson GA. Anatomic and functional leg-length inequality: a review and recommendation for clinical decision-making. Part II. The functional or unloaded leg-length asymmetry. Chiropr Osteopat. 2005 Jul 20;13:12. PubMed PMID: 16080787. Pubmed Central PMCID: 1198238. Epub 2005/08/06. eng.
137. McGrath MC. Palpation of the sacroiliac joint: An anatomical and sensory challenge. International Journal of Osteopathic Medicine. 2006;9(3):103-7.
138. Lesho EP. An overview of osteopathic medicine. Arch Fam Med. 1999 Nov-Dec;8(6):477-84. PubMed PMID: 10575385. Epub 1999/11/27. eng.
139. Walker BF. The reliability of chiropractic methods used for the detection of spinal subluxation. An overview of the literature. Australas Chiropr Osteopathy. 1996 Mar;5(1):12-22. PubMed PMID: 17987135. Pubmed Central PMCID: 2050611. Epub 1996/03/01. eng.
140. Reinert OC. Post-conference Impressions and Conclusions. In: Campbell JR, Serfatin R, Laufenberg P, Shrader TL, editors. A collection of monographs on the biomechanics of the pelvis from the Denver conference of the ACA Council on Technic held June 17-20. Denver Colorado: Des Moines Iowa; 1980. p. 136-8.
141. Drerup B, Hierholzer E. Movement of the human pelvis and displacement of related anatomical landmarks on the body surface. J Biomech. 1987;20(10):971-7.



142. Harrison DE, Harrison DD, Troyanovich SJ. The sacroiliac joint: a review of anatomy and biomechanics with clinical implications. *Journal of manipulative and physiological therapeutics*. 1997 Nov-Dec;20(9):607-17. PubMed PMID: 9436146. Epub 1998/01/22. eng.
143. Kuklo TR, Potter BK, Polly Jr DW, O'Brien MF, Schroeder TM, Lenke LG. Reliability analysis for manual adolescent idiopathic scoliosis measurements. *Spine (Phila Pa 1976)*. 2005 Feb 15;30(4):444-54. PubMed PMID: 15706343. Epub 2005/02/12. eng.
144. Basaloglu H, Turgut M, Taser FA, Ceylan T, Basaloglu HK, Ceylan AA. Morphometry of the sacrum for clinical use. *Surg Radiol Anat*. 2005 Dec;27(6):467-71. PubMed PMID: 16211321. Epub 2005/10/08. eng.
145. Lee D, Hodges P. *The Pelvic Girdle*. 3 ed. Edinburgh: Churchill Livingstone; 2004.
146. Delport EG, Cucuzzella TR, Kim N, Marley J, Pruitt C, Delport AG. Lumbosacral transitional vertebrae: incidence in a consecutive patient series. *Pain Physician*. 2006 Jan;9(1):53-6. PubMed PMID: 16700281. Epub 2006/05/17. eng.
147. Konin GP, Wallz DM. Lumbosacral transitional vertebrae: classification, imaging findings, and clinical relevance. *American Journal of Neuroradiology*. 2010;31(10):1778-86.
148. Hu N, Cunningham BW, Sponsler PD, Kikkawa J, Mcfee PC. Kinematic analysis of the sacroiliac junction: A comprehensive investigation using human cadaveric spines. *The Spine Journal*. 2009;9(10 Supplement):47S.
149. McGrath MC. Clinical considerations of sacroiliac joint anatomy: a review of function, motion and pain. *J Osteopath Med*. 2004;7(1):16-24.
150. DonTigny RL. Mechanics and treatment of the sacroiliac joint. *J Man Manip Ther*. 1993;1(1):3-12.
151. Goode A, Hegedus EJ, Sizer P, Brismee JM, Linberg A, Cook CE. Three-dimensional movements of the sacroiliac joint: a systematic review of the literature and assessment of clinical utility. *The Journal of manual & manipulative therapy*.

- 2008;16(1):25-38. PubMed PMID: 19119382. Pubmed Central PMCID: 2565072.  
Epub 2009/01/03. eng.
152. Walker JM. The sacroiliac joint: a critical review. *Phys Ther.* 1992 Dec;72(12):903-16. PubMed PMID: 1454866. Epub 1992/12/01. eng.
  153. Cohen SP. Sacroiliac joint pain: a comprehensive review of anatomy, diagnosis, and treatment. *Anesth Analg.* 2005 Nov;101(5):1440-53. PubMed PMID: 16244008.  
Epub 2005/10/26. eng.
  154. Sturesson B, Uden A, Vleeming A. A radiostereometric analysis of movements of the sacroiliac joints during the standing hip flexion test. *Spine (Phila Pa 1976).* 2000 Feb 1;25(3):364-8. PubMed PMID: 10703111. Epub 2000/03/07. eng.
  155. Sturesson B, Selvik G, Uden A. Movements of the sacroiliac joints. A roentgen stereophotogrammetric analysis. *Spine (Phila Pa 1976).* 1989 Feb;14(2):162-5.  
PubMed PMID: 2922636. Epub 1989/02/01. eng.
  156. Sturesson B, Uden A, Vleeming A. A radiostereometric analysis of the movements of the sacroiliac joints in the reciprocal straddle position. *Spine (Phila Pa 1976).* 2000 Jan 15;25(2):214-7. PubMed PMID: 10685486. Epub 2000/02/24. eng.
  157. Richardson CA, Snijders CJ, Hides JA, Damen L, Pas MS, Storm J. The relation between the transversus abdominis muscles, sacroiliac joint mechanics, and low back pain. *Spine (Phila Pa 1976).* 2002 Feb 15;27(4):399-405. PubMed PMID: 11840107. Epub 2002/02/13. eng.
  158. van Wingerden JP, Vleeming A, Buyruk HM, Raissadat K. Stabilization of the sacroiliac joint in vivo: verification of muscular contribution to force closure of the pelvis. *Eur Spine J.* 2004 May;13(3):199-205. PubMed PMID: 14986072. Epub 2004/02/27. eng.
  159. Sproule JA, Kumar S, Larkin J, O'Rourke SK. Odontoid-lateral mass asymmetry in minimally symptomatic patients: a normal variant. *Eur J Orthop Surg Traumatol.* 2003;13:63-6.

160. Burwell RG, Aujla RK, Freeman BJC, Cole AA, Kirby AS, Pratt RK, et al. Patterns of extra-spinal left-right skeletal asymmetries in adolescent girls with lower spine scoliosis: 1. Relative lengthening of the ilium on the curve concavity – real increase or innominate rotation/ torsion effect? . J Bone Joint Surg Br. 2008;90-B:445.
161. Kanchan T, Mohan Kumar TS, Pradeep Kumar G, Yoganarasimha K. Skeletal asymmetry. J Forensic Leg Med. 2008 Apr;15(3):177-9. PubMed PMID: 18313014. Epub 2008/03/04. eng.
162. Čuk T, Leben-Seljak P, Štefančič M. Lateral asymmetry of human long bones. Variability and Evolution. 2001;9:19-32.
163. Auerbach BM, Ruff CB. Limb bone bilateral asymmetry: variability and commonality among modern humans. Journal of Human Evolution. 2006;50(2):203-18.
164. Giles LG. Lumbosacral facet "joint angles" associated with leg length inequality. Rheumatol Rehabil. 1981 Nov;20(4):233-8. PubMed PMID: 6458081. Epub 1981/11/01. eng.
165. Peck S, Peck L, Kataja M. Skeletal asymmetry in esthetically pleasing faces. Angle Orthod. 1991 Spring;61(1):43-8. PubMed PMID: 2012321. Epub 1991/01/01. eng.
166. Steel J. Skeletal Indicators of Handedness. In: Cox M, Mays S, editors. Human Osteology in Archaeology and Forensic Science. London: Greenwich Medical Media; 2002. p. 381-402.
167. Kmita A, Lucas NP. Reliability of physical examination to assess asymmetry of anatomical landmarks indicative of pelvic somatic dysfunction in subjects with and without low back pain. Int J Osteopath Med. 2008;11:16-25.
168. Huijbregts P. Sacroiliac joint dysfunction; evidence-base diagnosis. Orthopaedic Division Review. 2004;May/June:18-32, 41-4.
169. Bowman C, Gribble R. The value of the forward flexion test and three tests of leg length changes in the clinical assessment of movement of the sacroiliac joint. J Orthop Med. 1995;17(2):66-7.

170. van der Wurff P, Meyne W, Hagmeijer RHM. Clinical tests of the sacroiliac joint, A systematic methodological review. Part 2: Validity. . *Manual Therapy*. 2000;5(2):89-96.
171. Schiowitz S, DiGiovanna EL, DiGiovanna JA. Gait and postural considerations. In: DiGiovanna EL, Schiowitz S, Dowling DJ, editors. *An Osteopathic Approach to Diagnosis and Treatment*. 3 ed. Philadelphia: Lippincott Williams & Wilkins; 2005. p. 293-303.
172. Montgomery DM, Egan IF, Pollard HP. Palpable unilateral sacral prominence as a clinical sign of lower limb anisomelia: a pilot study. *Journal of manipulative and physiological therapeutics*. 1995 Jul-Aug;18(6):353-6. PubMed PMID: 7595109. Epub 1995/07/01. eng.
173. Simpson R, Gemmell H. Accuracy of spinal orthopaedic tests: a systematic review. *Chiropr Osteopat*. 2006;14:26. PubMed PMID: 17076888. Pubmed Central PMCID: 1635718. Epub 2006/11/02. eng.
174. Plaughner G, Hendricks AH, Doble Jr RW, Bachman TR, Araghi HJ, Hoffart VM. The reliability of patient positioning for evaluating static radiologic parameters of the human pelvis. *Journal of manipulative and physiological therapeutics*. 1993 Oct;16(8):517-22. PubMed PMID: 8263430. Epub 1993/10/01. eng.
175. Holmgren U, Waling K. Inter-examiner reliability of four static palpation tests used for assessing pelvic dysfunction. *Manual therapy*. 2008 Feb;13(1):50-6. PubMed PMID: 17210266. Epub 2007/01/11. eng.
176. Mayer TG, Kondraske G, Beals SB, Gatchel RJ. Spinal range of motion. Accuracy and sources of error with inclinometric measurement. *Spine (Phila Pa 1976)*. 1997 Sep 1;22(17):1976-84. PubMed PMID: 9306526. Epub 1997/10/27. eng.
177. Stovall BA, Kumar S. Reliability of bony anatomic landmark asymmetry assessment in the lumbopelvic region: application to osteopathic medical education. *J Am Osteopath Assoc*. 2010 Nov;110(11):667-74. PubMed PMID: 21135198. Pubmed Central PMCID: 3124075. Epub 2010/12/08. eng.

178. Tong HC, Heyman OG, Lado DA, Isser MM. Interexaminer reliability of three methods of combining test results to determine side of sacral restriction, sacral base position, and innominate bone position. *J Am Osteopath Assoc.* 2006 Aug;106(8):464-8. PubMed PMID: 16943516. Epub 2006/09/01. eng.
179. Vernon H, Bureau J. A radiographic study of the incidence of low sacral base and lumbar lateral curvature related to the presence of an apparent short leg. *J Can Chiro Assoc.* 1983;27(1):11-5.
180. Rhodes DW, Mansfield ER, Bishop PA, Smith JF. The validity of the prone leg check as an estimate of standing leg length inequality measured by X-ray. *Journal of manipulative and physiological therapeutics.* 1995 Jul-Aug;18(6):343-6. PubMed PMID: 7595107. Epub 1995/07/01. eng.
181. Dowling DJ. Evaluation of the pelvis. In: DiGiovanna EL, Schiowitz S, Dowling DJ, editors. *An Osteopathic Approach to Diagnosis and Treatment.* 3 ed. Philadelphia: Lippincott Williams & Wilkins; 2005. p. 304-12.
182. Pearsall DJ, Reid JG, Hedden DM. Comparison of three noninvasive methods for measuring scoliosis. *Phys Ther.* 1992 Sep;72(9):648-57. PubMed PMID: 1508972. Epub 1992/09/01. eng.
183. Gross MT, Burns CB, Chapman SW, Hudson CJ, Curtis HS, Lehmann JR, et al. Reliability and validity of rigid lift and pelvic leveling device method in assessing functional leg length inequality. *J Orthop Sports Phys Ther.* 1998 Apr;27(4):285-94. PubMed PMID: 9549712. Epub 1998/04/29. eng.
184. Maigne J-Y, Aivaliklis A, Pfefer F. Results of sacroiliac joint double block and value of sacroiliac pain provocation tests in 54 patients with low back pain. *Spine (Phila Pa 1976).* 1996;21(16):1889-92.
185. Yochum TR, Barry MS. Examination and treatment of the short leg. *J Chiropr* 1994;31(12):28-32.

186. Ruch WJ, Ruch BM. An analysis of pubis symphysis misalignment using plain film radiography. *Journal of manipulative and physiological therapeutics*. 2005 Jun;28(5):330-5. PubMed PMID: 15965407. Epub 2005/06/21. eng.
187. Yochum TR, Rowe LJ. *Essentials of Skeletal Radiology*. 2 ed. Baltimore: Williams & Wilkins; 1996.
188. Tilley P. Cephalic angle film for sacral base visualization. *J Am Osteopath Assoc*. 1968 Jun;67(10):1153-6. PubMed PMID: 5187139. Epub 1968/06/01. eng.
189. Tilley P. Radiographic identification of the sacral base. *J Am Osteopath Assoc*. 1966 Jul;65(11):1177-83. PubMed PMID: 5178347. Epub 1966/07/01. eng.
190. Perdriolle R, Le Borgne P, Dansereau J, de Guise J, Labelle H. Idiopathic scoliosis in three dimensions: a succession of two-dimensional deformities? *Spine (Phila Pa 1976)*. 2001 Dec 15;26(24):2719-26. PubMed PMID: 11740362. Epub 2001/12/12. eng.
191. Weinert DJ. Influence of axial rotation on chiropractic pelvic radiographic analysis. *Journal of manipulative and physiological therapeutics*. 2005 Feb;28(2):117-21. PubMed PMID: 15800511. Epub 2005/04/01. eng.
192. Geijer H, Beckman K, Jonsson B, Andersson T, Persliden J. Digital radiography of scoliosis with a scanning method: initial evaluation. *Radiology*. 2001 Feb;218(2):402-10. PubMed PMID: 11161153. Epub 2001/02/13. eng.
193. Cargill SC, Pearcy M, Barry MD. Three-dimensional lumbar spine postures measured by magnetic resonance imaging reconstruction. *Spine (Phila Pa 1976)*. 2007 May 15;32(11):1242-8. PubMed PMID: 17495783. Epub 2007/05/15. eng.
194. Rajwani T, Bagnall KM, Lambert R, Videman T, Kautz J, Moreau M, et al. Using magnetic resonance imaging to characterize pedicle asymmetry in both normal patients and patients with adolescent idiopathic scoliosis. *Spine (Phila Pa 1976)*. 2004 Apr 1;29(7):E145-52. PubMed PMID: 15087811. Epub 2004/04/17. eng.

195. Jinkins JR, Dworkin JS, Damadian RV. Upright, weight-bearing, dynamic-kinetic MRI of the spine: initial results. *Eur Radiol.* 2005 Sep;15(9):1815-25. PubMed PMID: 15906040. Epub 2005/05/21. eng.
196. Birchall D, Hughes DG, Hindle J, Robinson L, Williamson JB. Measurement of vertebral rotation in adolescent idiopathic scoliosis using three-dimensional magnetic resonance imaging. *Spine (Phila Pa 1976).* 1997 Oct 15;22(20):2403-7. PubMed PMID: 9355222. Epub 1997/11/14. eng.
197. Schmitz A, Jaeger UE, Koenig R, Kandyba J, Wagner UA, Giesecke J, et al. A new MRI technique for imaging scoliosis in the sagittal plane. *European Spine Journal.* 2001 Apr;10(2):114-7. PubMed PMID: 11345631. Epub 2001/05/11. eng.
198. Oestreich AE, Young LW, Young Poussaint T. Scoliosis circa 2000: radiologic imaging perspective. I. Diagnosis and pretreatment evaluation. *Skeletal Radiol.* 1998 Nov;27(11):591-605. PubMed PMID: 9867177. Epub 1998/12/29. eng.
199. Alyas F, Connell D, Saifuddin A. Upright positional MRI of the lumbar spine. *Clin Radiol.* 2008 Sep;63(9):1035-48. PubMed PMID: 18718234. Epub 2008/08/23. eng.
200. McKenzie RA. *The Lumbar Spine Mechanical Diagnosis and Therapy.* Wellington (NZ): Spinal Publications; 1981.
201. Winter RB, Pinto WC. Pelvic obliquity. Its causes and its treatment. *Spine (Phila Pa 1976).* 1986 Apr;11(3):225-34. PubMed PMID: 3715623. Epub 1986/04/01. eng.
202. Riddle DL, Freburger JK. Evaluation of the presence of sacroiliac joint region dysfunction using a combination of tests: A multicenter intertester reliability study. *Phys Ther.* 2002 August 2002;82(8):772-81.
203. Grieve GP. *Common Vertebral Joint Problems.* New York: Churchill Livingstone; 1981.
204. Gibbons P, Dumper C, Gosling C. Inter-examiner and intra-examiner agreement for assessing simulated leg length inequality using palpation and observation during a standing assessment. *J Osteopath Med.* 2002;5(2):53-8.

205. Ingelmark BE, Lindstrom J. Asymmetries of the lower extremities and pelvis and their relations to lumbar scoliosis. A radiographic study. *Acta Morphol Neerl Scand*. 1963;5:221-34. PubMed PMID: 13956495. Epub 1963/01/01. eng.
206. Song KM, Halliday SE, Little DG. The effect of limb-length discrepancy on gait. *J Bone Joint Surg Am*. 1997 Nov;79(11):1690-8. PubMed PMID: 9384429. Epub 1997/12/31. eng.
207. Friberg O, Nurminen M, Korhonen K, Soininen E, Manttari T. Accuracy and precision of clinical estimation of leg length inequality and lumbar scoliosis: comparison of clinical and radiological measurements. *Int Disabil Stud*. 1988;10(2):49-53. PubMed PMID: 3403498. Epub 1988/01/01. eng.
208. McCaw ST, Bates BT. Biomechanical implications of mild leg length inequality. *Br J Sports Med*. 1991 Mar;25(1):10-3. PubMed PMID: 1913023. Pubmed Central PMCID: 1478813. Epub 1991/03/01. eng.
209. McCaw ST. Leg length inequality. Implications for running injury prevention. *Sports Med*. 1992 Dec;14(6):422-9. PubMed PMID: 1470794. Epub 1992/12/01. eng.
210. Steen H, Terjesen T, Bjerkreim I. Anisomelia. Clinical consequences and treatment. *Tidsskr Nor Laegeforen*. 1997 Apr 30;117(11):1595-600. PubMed PMID: 9198942. Epub 1997/04/30. Anisomeli. Kliniske konsekvenser og behandling. nor.
211. Soukka A, Alaranta H, Tallroth K, Heliovaara M. Leg-length inequality in people of working age. The association between mild inequality and low-back pain is questionable. *Spine (Phila Pa 1976)*. 1991 Apr;16(4):429-31. PubMed PMID: 1828627. Epub 1991/04/01. eng.
212. Edelmann P. Equal pelvic crest or horizontal upper sacral line? *Z Orthop Ihre Grenzgeb*. 1981 Feb;119(1):111-4. PubMed PMID: 7281905. Epub 1981/02/01. Beckengeradstand oder Sakrumgeradstand? ger.
213. Gemmell HA, Jacobson BH. Incidence of sacroiliac joint dysfunction and low back pain in fit college students. *Journal of manipulative and physiological therapeutics*. 1990 Feb;13(2):63-7. PubMed PMID: 2137851. Epub 1990/02/01. eng.



214. Egund N, Olsson TH, Schmid H, Selvik G. Movements in the sacroiliac joints demonstrated with roentgen stereophotogrammetry. *Acta Radiol Diagn (Stockh)*. 1978;19(5):833-46. PubMed PMID: 717034. Epub 1978/01/01. eng.
215. Jacob HA, Kissling RO. The mobility of the sacroiliac joints in healthy volunteers between 20 and 50 years of age. *Clin Biomech (Bristol, Avon)*. 1995 Oct;10(7):352-61. PubMed PMID: 11415579. Epub 1995/10/01. Eng.
216. Smidt GL, Wei SH, McQuade K, Barakatt E, Sun T, Stanford W. Sacroiliac motion for extreme hip positions. A fresh cadaver study. *Spine (Phila Pa 1976)*. 1997 Sep 15;22(18):2073-82. PubMed PMID: 9322317. Epub 1997/10/10. eng.
217. Colachis SCJ, Worden RE, Bechtol CO, Strohm BR. Movement of the sacroiliac joint in the adult male: A preliminary report. *Arch Phys Med Rehabil*. 1963 Sep;44:490-8. PubMed PMID: 14050722. Epub 1963/09/01. eng.
218. Weisl H. The movements of the sacroiliac joint. *Acta Anat (Basel)*. 1955;23(1):80-91. PubMed PMID: 14349535. Epub 1955/01/01. eng.
219. Potter NA, Rothstein JM. Intertester reliability for selected clinical tests of the sacroiliac joint. *Phys Ther*. 1985 Nov;65(11):1671-5. PubMed PMID: 2932746. Epub 1985/11/01. eng.
220. Cattley P, Winyard J, Trevaskis J, Eaton S. Validity and reliability of clinical tests for the sacroiliac joint. A review of literature. *Australas Chiropr Osteopathy*. 2002 Nov;10(2):73-80. PubMed PMID: 17987177. Pubmed Central PMCID: 2051080. Epub 2007/11/08. eng.
221. Brismée JM, Atwood K, Fain M, Hodges J, Sperle A, Swaney M, et al. Interrater reliability of palpation of three-dimensional segmental motion of the lumbar spine. *J Man Manip Ther*. 2005;13(4):216-21.
222. Freburger JK, Riddle DL. Measurement of sacroiliac joint dysfunction: a multicenter intertester reliability study. *Phys Ther*. 1999 Dec;79(12):1134-41. PubMed PMID: 10630282. Epub 2000/01/12. eng.

223. Slipman CW, Patel RK, Whyte WS, Lenrow DA, Ellen MI, Chou LH, et al.  
Diagnosing and managing sacroiliac pain. *J Musculoskel Med*. 2001;18(6):325-32.
224. Freburger JK, Riddle DL. Using published evidence to guide the examination of the sacroiliac joint region. *Phys Ther*. 2001 May;81(5):1135-43. PubMed PMID: 11319939. Epub 2001/04/26. eng.
225. Leitzes AH, Potter HG, Amaral T, Marx RG, Lyman S, Widmann RF. Reliability and accuracy of MRI scanogram in the evaluation of limb length discrepancy. *J Pediatr Orthop*. 2005 Nov-Dec;25(6):747-9. PubMed PMID: 16294130. Epub 2005/11/19. eng.
226. Adam CJ, Izatt MT, Harvey JR, Askin GN. Variability in Cobb angle measurements using reformatted computerized tomography scans. *Spine (Phila Pa 1976)*. 2005 Jul 15;30(14):1664-9. PubMed PMID: 16025038. Epub 2005/07/19. eng.
227. Anderson NG, Fenwick JL, Wells JE. Intrinsic measurement bias on computed tomography scout view is unpredictable: Computed tomography pelvimetry using a phantom. *Australas Radiol*. 2006 Apr;50(2):127-31. PubMed PMID: 16635030. Epub 2006/04/26. eng.
228. Vrtovec T, Pernus F, Likar B. A review of methods for quantitative evaluation of spinal curvature. *European spine journal*. 2009 May;18(5):593-607. PubMed PMID: 19247697. Pubmed Central PMCID: 3233998. Epub 2009/02/28. eng.
229. Vrtovec T, Ourselin S, Gomes L, Likar B, Pernus F. Automated generation of curved planar reformations from MR images of the spine. *Phys Med Biol*. 2007 May 21;52(10):2865-78. PubMed PMID: 17473356. Epub 2007/05/03. eng.
230. Greiner KA. Adolescent idiopathic scoliosis: radiologic decision-making. *Am Fam Physician*. 2002 May 1;65(9):1817-22. PubMed PMID: 12018804. Epub 2002/05/23. eng.
231. Richards PJ, Pattison JM, Belcher J, Decann RW, Anderson S, Wynn-Jones C. A new tilt on pelvic radiographs: a pilot study. *Skeletal Radiol*. 2009 Feb;38(2):113-22. PubMed PMID: 18566814. Epub 2008/06/21. eng.

232. Ernst E. Chiropractors' use of X-rays. *Br J Radiol.* 1998 Mar;71(843):249-51.  
PubMed PMID: 9616232. Epub 1998/06/09. eng.
233. Slane PR, Bull PW. Femur head height error on AP pelvic x-rays with alterations of source-to-image distance, central ray position, and object-to-film distance. *Chiropr J Aust.* 2006;36(2):46-50.
234. Foss OA, Klaksvik J, Benum P, Anda S. Pelvic rotations: a pelvic phantom study. *Acta Radiol.* 2007 Jul;48(6):650-7. PubMed PMID: 17611873. Epub 2007/07/06.  
eng.
235. Ravi B, Rampersaud R. Clinical magnification error in lateral spinal digital radiographs. *Spine (Phila Pa 1976).* 2008 May 1;33(10):E311-6. PubMed PMID: 18449031. Epub 2008/05/02. eng.
236. Phillips RB, Frymoyer JW, Mac Pherson BV, Newburg AH. Low back pain: a radiographic enigma. *Journal of manipulative and physiological therapeutics.* 1986 Sep;9(3):183-7. PubMed PMID: 2945887. Epub 1986/09/01. eng.
237. Schram SB, Hosek RS, Silverman HL. Spinographic positioning errors in gonstead pelvic x-ray analysis. *J Manipulative Physiol Ther.* 1981;4(4):179-81.
238. Haas M, Taylor JA, Gillette RG. The routine use of radiographic spinal displacement analysis: a dissent. *Journal of manipulative and physiological therapeutics.* 1999 May;22(4):254-9. PubMed PMID: 10367763. Epub 1999/06/15. eng.
239. Harrison DE, Harrison DD, Colloca CJ, Betz J, Janik TJ, Holland B. Repeatability over time of posture, radiograph positioning, and radiograph line drawing: an analysis of six control groups. *Journal of manipulative and physiological therapeutics.* 2003 Feb;26(2):87-98. PubMed PMID: 12584507. Epub 2003/02/14.  
eng.
240. Harrison DE, Holland B, Harrison DD, Janik TJ. Further reliability analysis of the Harrison radiographic line-drawing methods: crossed ICCs for lateral posterior tangents and modified Risser-Ferguson method on AP views. *Journal of*

- manipulative and physiological therapeutics. 2002 Feb;25(2):93-8. PubMed PMID: 11896376. Epub 2002/03/16. eng.
241. Coleman R, Harrison D, Fischer T, Harrison SO. Correlation and quantification of relative 2-dimensional projected vertebral endplate z-axis rotations with 3-dimensional y-axis vertebral rotations and focal spot elevations. *Journal of manipulative and physiological therapeutics*. 2000 Jul-Aug;23(6):414-9. PubMed PMID: 10951312. Epub 2000/08/22. eng.
  242. Troyanovich SJ, Harrison SO, Harrison DD, Harrison DE, Payne MR, Janik TJ, et al. Chiropractic biophysics digitized radiographic mensuration analysis of the anteroposterior lumbopelvic view: a reliability study. *Journal of manipulative and physiological therapeutics*. 1999 Jun;22(5):309-15. PubMed PMID: 10395433. Epub 1999/07/08. eng.
  243. Plaugher G, Hendricks AH. The inter- and intraexaminer reliability of the Gonstead pelvic marking system. *Journal of manipulative and physiological therapeutics*. 1991 Nov-Dec;14(9):503-8. PubMed PMID: 1761961. Epub 1991/11/01. eng.
  244. Zengel F, Davis BP. Biomechanical analysis by chiropractic radiography: Part II. Effects of X-ray projectional distortion on apparent vertebral rotation. *Journal of manipulative and physiological therapeutics*. 1988 Oct;11(5):380-9. PubMed PMID: 3235925. Epub 1988/10/01. eng.
  245. Zengel F, Davis BP. Biomechanical analysis by chiropractic radiography: Part III. Lack of effect of projectional distortion on Gonstead vertebral endplate lines. *Journal of manipulative and physiological therapeutics*. 1988 Dec;11(6):469-73. PubMed PMID: 3075648. Epub 1988/12/01. eng.
  246. Bayliss C, Maugham L. Cushion selection and prescription for clients with spinal cord injury. In: Team SO, editor. 2001.
  247. Alman BA, Kim HK. Pelvic obliquity after fusion of the spine in Duchenne muscular dystrophy. *The Journal of bone and joint surgery British volume*. 1999 Sep;81(5):821-4. PubMed PMID: 10530843. Epub 1999/10/26. eng.

248. Kanlayanaphotporn R, Trott P, Williams M, Fulton I. Contribution of soft tissue deformation below the sacrum to the measurement of total height loss in sitting. *Ergonomics*. 2001 Jun 10;44(7):685-95. PubMed PMID: 11437203. Epub 2001/07/05. eng.
249. Shoham Y, Meyer S, Katz-Leurer M, Tamar Weiss PL. The influence of seat adjustment and a thoraco-lumbar-sacral orthosis on the distribution of body-seat pressure in children with scoliosis and pelvic obliquity. *Disabil Rehabil*. 2004 Jan 7;26(1):21-6. PubMed PMID: 14660195. Epub 2003/12/09. eng.
250. Alm M, Gutierrez E, Hultling C, Saraste H. Clinical evaluation of seating in persons with complete thoracic spinal cord injury. *Spinal Cord*. 2003 Oct;41(10):563-71. PubMed PMID: 14504614. Epub 2003/09/25. eng.
251. Snijders CJ, Hermans PF, Kleinrensink GJ. Functional aspects of cross-legged sitting with special attention to piriformis muscles and sacroiliac joints. *Clin Biomech (Bristol, Avon)*. 2006 Feb;21(2):116-21. PubMed PMID: 16260074. Epub 2005/11/02. eng.
252. Privacy Act 1988 2012 [updated 5 April 2012; cited 2012 4th June]. Commonwealth Act - C2012C00414]. Available from:  
<http://www.comlaw.gov.au/Details/C2012C00414>.
253. Michaud SB, Gard SA, Childress DS. A preliminary investigation of pelvic obliquity patterns during gait in persons with transtibial and transfemoral amputation. *J Rehabil Res Dev*. 2000 Jan-Feb;37(1):1-10. PubMed PMID: 10847567. Epub 2000/06/10. eng.
254. Ammendolia C, Bombardier C, Hogg-Johnson S, Glazier R. Views on radiography use for patients with acute low back pain among chiropractors in an Ontario community. *Journal of manipulative and physiological therapeutics*. 2002 Oct;25(8):511-20. PubMed PMID: 12381973. Epub 2002/10/17. eng.
255. Wilson RL. *Chiropractic Radiography and Quality Assurance Handbook*. Boca Raton: Informa Health Care; 1999.

256. Aubin CE, Dansereau J, Petit Y, Parent F, de Guise JA, Labelle H. Three-dimensional measurement of wedged scoliotic vertebrae and intervertebral disks. *European spine journal : official publication of the European Spine Society, the European Spinal Deformity Society, and the European Section of the Cervical Spine Research Society*. 1998;7(1):59-65. PubMed PMID: 9548361. Epub 1998/04/21. eng.
257. Lundh C, Lindmark G, Wilbrand H. Reliability of radiographic pelvimetry. A methodological study. *Acta Obstet Gynecol Scand*. 1986;65(5):411-6. PubMed PMID: 3776483. Epub 1986/01/01. eng.
258. Kuklo TR, Potter BK, O'Brien MF, Schroeder TM, Lenke LG, Polly Jr DW. Reliability analysis for digital adolescent idiopathic scoliosis measurements. *J Spinal Disord Tech*. 2005 Apr;18(2):152-9. PubMed PMID: 15800433. Epub 2005/04/01. eng.
259. Jackson BL, Barker WF, Pettibon BR, Woggon D, Bentz J, Hamilton D, et al. Reliability of the Pettibon patient positioning system for radiographic production. *J Vertebral Subluxation Res*. 2000;4(1):3-11.
260. Gavin TM. Research forum – Methodology – measurements part 1: principles and theory. *J Prosthetics and Orthotics*. 1996;8(2):45-51.
261. Brickman P, Frobin W, Leivseth G. *Musculoskeletal Biomechanics*. New York Thieme; 2002.
262. Chernukha KV, Daffner RH, Reigel DH. Lumbar lordosis measurement. A new method versus Cobb technique. *Spine (Phila Pa 1976)*. 1998 Jan 1;23(1):74-9; discussion 9-80. PubMed PMID: 9460156. Epub 1998/02/14. eng.
263. Haenle M, Heitner A, Mittelmeier W, Barbano R, Scholz R, Steinhauser E, et al. Assessment of cup position from plain radiographs: impact of pelvic tilting. *Surg Radiol Anat*. 2007 Feb;29(1):29-35. PubMed PMID: 17216294. Epub 2007/01/12. eng.
264. Dieck RH. *Measurement uncertainty : methods and applications*. Research Triangle Park, NC: ISA; 2006.

265. Phillips RB. An evaluation of the graphic analysis of the pelvis on the A-P full spine radiograph. *ACA J Chiropr* 1975;9:s139-s48.
266. Harrison DD. X-ray: equipment alignment and patient positioning. In: Harrison DD, editor. *CHIROPRACTIC: The physics of spinal correction CBP technique*. Evanston, Wyo: CBP Nonprofit, Inc.; 1994. p. 1-17.
267. Bould M, Barnard S, Learmonth ID, Cunningham JL, Hardy JR. Digital image analysis: improving accuracy and reproducibility of radiographic measurement. *Clin Biomech (Bristol, Avon)*. 1999 Jul;14(6):434-7. PubMed PMID: 10521626. Epub 1999/10/16. eng.
268. Dybkaer R. Result, error and uncertainty *Scandinavian Journal of Clinical & Laboratory Investigation*. 1995;55(2):97-118.
269. Burke S. Missing values, outliers, robust statistics & non-parametric methods. *LC-GC Europe Online Supplement, Statistics & Data Analysis*. 2001;2:19-24.
270. de Quiros ACB, Lopez R, Aranda-Mena G, Edwards P, editors. Human reliability as a source of error in research. *Proceedings of the 24th Annual ARCOM Conference*, 1-3 September; 2008: Association of Researchers in Construction Management.
271. Banerjee A, Chitnis UB, Jadhav SL, Bhawalkar JS, Chaudhury S. Hypothesis testing, type I and type II errors. *Industrial Psychiatry Journal*. 2009;18(2):127-31.
272. Anderson N, Humphries N, Wells JE. Measurement error in computed tomography pelvimetry. *Australas Radiol*. 2005;49:104-7.
273. Rosenfeldt MP, Harding IJ, Hauptfleisch JT, Fairbank JT. A comparison of traditional protractor versus Oxford Cobbometer radiographic measurement: intraobserver measurement variability for Cobb angles. *Spine (Phila Pa 1976)*. 2005 Feb 15;30(4):440-3. PubMed PMID: 15706342. Epub 2005/02/12. eng.
274. Facanha-Filho FAM, Winter RB, Lonstein JE, Koop S, Novacheck T, L'Heureux Jr EA, et al. Measurement accuracy in congenital scoliosis. *J Bone Joint Surg Am*. 2001;83-A(1):42-5.

275. Sheaffer JC, Eleazer PD, Scheetz JP, Clark SJ, Farman AG. Endodontic measurement accuracy and perceived radiograph quality: effects of film speed and density. *Oral surgery, oral medicine, oral pathology, oral radiology, and endodontics*. 2003;96(4):441-8.
276. Baksı B. Measurement accuracy and perceived quality of imaging systems for the evaluation of periodontal structures. *Odontology*. 2008;96(1):55-60.
277. Kuklo TR, Potter BK, Schroeder TM, F. OBM. Comparison of manual and digital measurements in adolescent idiopathic scoliosis. *Spine (Phila Pa 1976)*. 2006;31(11):1240-6.
278. Wills BPD, Auerbach JD, Zhu X, Caird MS, Horn BD, Flynn JM, et al. Comparison of Cobb angle measurement of scoliosis radiographs with preselected end vertebrae. *Spine (Phila Pa 1976)*. 2007;32(1):98-105.
279. Kawchuk G, McArthur R. Scoliosis quantification: an overview. *J Can Chiropr Assoc*. 1997;41(3):137-44.
280. Carman DL, Browne RH, Birch JG. Measurement of scoliosis and kyphosis radiographs. Intraobserver and interobserver variation. *The Journal of Bone and Joint Surgery*. 1990;72(3):328-33.
281. Gstoettner M, Sekyra K, Walochnik N, Winter P, Wachter R, Bach CM. Inter- and intraobserver reliability assessment of the Cobb angle: manual versus digital measurement tools. *Eur Spine J*. 2007 Oct;16(10):1587-92. PubMed PMID: 17549526. Pubmed Central PMCID: 2078306. Epub 2007/06/06. eng.
282. Park J-H, Baasantseren G, Kim N, Park G, Kang J-M, Lee B. View image generation in perspective and orthographic projection geometry based on integral imaging. *Optics Express*. 2008;16(12):8800-13.
283. Berthonnaud E, Hilmi R, Dimnet J. Accessing 3D location of standing Pelvis: relative position of sacral plateau and acetabular cavities versus pelvis. *Radiology Research and Practice*. 2012;2012:1-10.



284. Pettibon BR, Harrison DD. Pettibon spinal bio-mechanics theory and implications. 2 ed. Vancouver Washington: Pettibon Bio-Mechanics Institute; 1981.
285. Harrison DD, Cailliet R, Janik TJ, Troyanovich SJ, Harrison DE, Holland B. Elliptical modeling of the sagittal lumbar lordosis and segmental rotation angles as a method to discriminate between normal and low back pain subjects. *J Spinal Disord*. 1998 Oct;11(5):430-9. PubMed PMID: 9811104. Epub 1998/11/12. eng.
286. Harrison DE, Harrison DD, Cailliet R, Janik TJ, Holland B. Radiographic analysis of lumbar lordosis: centroid, Cobb, TRALL, and Harrison posterior tangent methods. *Spine (Phila Pa 1976)*. 2001 Jun 1;26(11):E235-42. PubMed PMID: 11389407. Epub 2001/06/05. eng.
287. Zengel F, Davis BP. Biomechanical analysis by chiropractic radiography: Part I. A simple method for determining X-ray projectional distortion. *Journal of manipulative and physiological therapeutics*. 1988 Aug;11(4):273-80. PubMed PMID: 3049888. Epub 1988/08/01. eng.
288. Ahn A, Grodzinsky AJ. Relevance of collagen piezoelectricity to "Wolff's Law": a critical review. *Medical Engineering and Physics*. 2009;31(7):733-41.
289. Pearson OM, Lieberman DE. The aging of Wolff's "Law": ontogeny and responses to mechanical loading in cortical bone. *YEARBOOK OF PHYSICAL ANTHROPOLOGY*. 2004;74:63-99.
290. Miullender MG, Huiskes R. Proposal for the regulatory mechanism of Wolff's law. *Journal of Orthopaedic research*. 1995;13(4):503-12.
291. Hierholzer E, Drerup B, zu Bentrup M. Influence of leg length discrepancy on rasterstereographic back shape parameters. In: Sevastic JA, Diab KM, editors. *Research into Spinal Deformities 1*. Amsterdam: IOS press; 1997. p. 265.
292. Merolli A. Definitions and terminology for assessment of spinal shape. In: Sevastic JA, Diab KM, editors. *Research into Spinal Deformities 1*. Amsterdam: IOS Press; 1997. p. 3.

293. Our Mission: Gonstead chiropractic society (Australia); [cited 2012 22.1.12].  
Available from: <http://www.gonstead.com.au/>.
294. Harrison DE, Harrison DD, Troyanovich SJ. Three-dimensional spinal coupling mechanics: Part I. A review of the literature. *J Manipulative Physiol Ther.* 1998;21(2):101-13.
295. Harrison DE, Harrison DD, Troyanovich SJ. Three-dimensional spinal coupling mechanics: Part II. Implications for chiropractic theories and practice. *J Manipulative Physiol Ther.* 1998;21(3):177-86.
296. Panjabi M, Yamamoto I, Oxland T, Crisco J. How does posture affect coupling in the lumbar spine? *Spine (Phila Pa 1976).* 1989;14(9):1002-11.
297. Lund T, Nydegger T, Schlenzka D, Oxland TR. Three-dimensional motion patterns during active bending in patients with chronic low back pain. *Spine (Phila Pa 1976).* 2002;27(17):1865-74.
298. Peterson MJ, Adkins HV. Measurement and redistribution of excessive pressures during wheelchair sitting: A clinical report. *Phys Ther.* 1982;62(7):990-4.
299. Wright N. Imaging in scoliosis. *Archives of disease in childhood.* 2000;82(1):38-40.
300. Schultz G, Phillips RB, Cooley J, Hall T, Hoyt T, Gendreau D, et al. Diagnostic imaging of the spine in chiropractic practice: recommendations for utilisation. *Chiropr J Aust.* 1992;22:141-52.
301. Kricun ME. *Imaging Modalities in Spinal Disorders.* Philadelphia: W.B. Saunders Company; 1988.
302. Coleman RR, Harrison DE, Bernard BB. The effects of combined x-axis translations and y-axis rotations on projected lamina junction offset. *Journal of manipulative and physiological therapeutics.* 2001 Oct;24(8):509-13. PubMed PMID: 11677550. Epub 2001/10/26. eng.
303. Lembeck B, Mueller O, Reize P, Wuelker N. Pelvic tilt makes acetabular cup navigation inaccurate. *Acta Orthop.* 2005 Aug;76(4):517-23. PubMed PMID: 16195068. Epub 2005/10/01. eng.

304. Chi WM, Cheng CW, Yeh WC, Chuang SC, Chang TS, Chen JH. Vertebral axial rotation measurement method. *Comput Methods Programs Biomed.* 2006 Jan;81(1):8-17. PubMed PMID: 16303206. Epub 2005/11/24. eng.
305. Carlson JM. Clinical biomechanics of orthotic treatment of thoracic hyperkyphosis. *JPO.* 2003;15(4):S31-5.
306. Howe JW. Imaging the Low Back. In: Hutcheson CJ, Howe JW, editors. *The Low Back and Pelvis.* Maryland: Jones & Bartlet; 1997. p. 63.
307. Oakley PA, Grice KS, Harrison DE. A study of the effects of central ray vertical (y-axis) positioning, pelvis (y-axis) rotation and pelvis (x-axis) translation on measurement of the anatomical short leg from the anteroposterior (AP) Ferguson radiograph. *Clinical Chiropractic.* 2011;14(4):155.
308. Nnadi C, Fairbank J. Scoliosis: a review. *Paediatrics and Child Health.* 2010 5//;20(5):215-20.
309. East M. Imaging the L5-S1 joint space. *Radiologic Technology.* 2007;79(1):75-7.
310. Sungita YY, Mdoe SSL, Msaki P. Diagnostic X-ray facilities as per quality control performances in Tanzania. *Journal of Applied Clinical Medical Physics.* 2006;7(4):66-73.
311. Toennies KD, Oishi S, Koster D, Schroth G. Accuracy of distance measurements in biplane angiography. In: Kim Y, editor. *Proceedings of Medical Imaging: Image Display;* San Diego: SPIE; 1997. p. 19-30.
312. Gray JE, Winkler NT, Stears J, Frank ED. *Quality control in diagnostic imaging.* Gaithersburg, Maryland: Aspen Publishers, Inc.; 1983.
313. Fox JL. The central x-ray beam in stereotaxis. *Am J Roentgenol Radium Ther Nucl Med.* 1970 Sep;110(1):166-9. PubMed PMID: 4918286. Epub 1970/09/01. eng.
314. Mitulescu AM, Skalli WS, Mitton DM, De Guise JDG. Three-dimensional surface rendering reconstruction of scoliotic vertebrae using a non stereo-corresponding points technique. *European Spine Journal.* 2002;11(4):344-52.

315. Kawakami N, Tsuji T, Imagama S, Lenke LG, Puno RM, Kuklo TR. Classification of congenital scoliosis and kyphosis: A new approach to the three-dimensional classification for progressive vertebral anomalies requiring operative treatment. *Spine (Phila Pa 1976)*. 2009;34(17).
316. Willén J, Danielson B, Gaulitz A, Niklason T, Schönström N, Hansson T. Dynamic effects on the lumbar spinal canal: axially loaded CT-myelography and MRI in patients with sciatica and/or neurogenic claudication. *Spine (Phila Pa 1976)*. 1997;22(24):2968-76.
317. Hioki A, Miyamoto K, Sakai H, Shimizu K. Lumbar axial loading device alters lumbar sagittal alignment differently from upright standing position a computed tomography study. *Spine (Phila Pa 1976)*. 2010;35(9):995-1001.
318. Irving BJ, Maree GJ, Hering ER, Douglas TS. Radiation dose from a linear slit scanning x-ray machine with full-body imaging capabilities. *Radiation Protection Dosimetry*. 2008;130(4):482-9.
319. Kroft LJM, Veldkamp WJH, Mertens BJA, Van Delft J-PA, Geleijns J. Dose reduction in digital chest radiography and perceived image quality. *Br J Radiol*. 2007;80(960):984-8.
320. Körner M, Weber CH, Wirth S, Pfeifer KJ, Reiser MF, Treitl M. Advances in digital radiography: physical principles and system overview. *Radiographics*. 2007;27(3):675-86.
321. Deschênes S, Charron G, Beaudoin G, Labelle H, Dubois J, Miron M-C, et al. Diagnostic imaging of spinal disorders. *Spine (Phila Pa 1976)*. 2010;35(9):989-94.
322. Chidiac JJ, Shofer FS, Al-Kutoubi A, Laster LL, Ghafari J. Comparison of CT scanograms and cephalometric radiographs in craniofacial imaging. *Orthod Craniofac Res*. 2002;5:104-13.
323. Sabharwal S, Zhao C, McKeon JJ, McClemens E, Edgar M, Behrens F. Computed radiographic measurement of limb-length discrepancy. *The Journal of Bone and Joint Surgery*. 2006;88-A(10):2243-51.

324. Samei E, Lo JY, Yoshizumi TT, Jesneck JL, Dobbins JT, Floyd CE, et al. Comparative scatter and dose performance of slot-scan and full-field digital chest radiography systems. *Radiology*. 2005 June 1, 2005;235(3):940-9.
325. Illés T, Tunyogi-Csapó M, Somoskeöy S. Breakthrough in three-dimensional scoliosis diagnosis: significance of horizontal plane view and vertebra vectors. *European Spine Journal*. 2011;20(1):135-43.
326. Després P, Beaudoin G, Gravel P, de Guise JA. Evaluation of a full scale gas microstrip detector for low-dose X-ray imaging. *Nuclear Instruments and Methods in Physics Research*. 2005;A 536:52-60.
327. Despres P, Beaudoin G, Gravel P, de Guise JA. Physical characteristics of a low-dose gas microstrip detector for orthopedic x-ray imaging. *Medical physics*. 2005 Apr;32(4):1193-204. PubMed PMID: 15895603. Epub 2005/05/18. eng.
328. Glaser DA, Doan J, Newton PO. Comparison of 3D Spinal Reconstruction Accuracy: Biplanar Radiographs with EOS Versus Computed Tomography. *Spine (Phila Pa 1976)*. 2012 Mar 13. PubMed PMID: 22415001. Epub 2012/03/15. Eng.
329. Ilharreborde B, Steffen JS, Nectoux E, Vital JM, Mazda K, Skalli W, et al. Angle measurement reproducibility using EOS three-dimensional reconstructions in adolescent idiopathic scoliosis treated by posterior instrumentation. *Spine (Phila Pa 1976)*. 2011;36(20):E1306-13.
330. Gille O, Champain N, Benchikh-El-Fegoun A, Vital J-M, Skalli W. Reliability of 3D reconstruction of the spine of mild scoliotic patients. *Spine (Phila Pa 1976)*. 2007;32(5):568-73.
331. Wessberg P, Danielson BI, Willen J. Comparison of Cobb angles in idiopathic scoliosis on standing radiographs and supine axially loaded MRI. *Spine (Phila Pa 1976)*. 2006 Dec 15;31(26):3039-44. PubMed PMID: 17173001. Epub 2006/12/19. eng.

332. Tilson ER, Strickland GD, Gibson SG. An overview of radiography, computed tomography, and magnetic resonance imaging in the diagnosis of lumbar spine pathology. *Orthopaedic Nursing*. 2006;25(6):415-20.
333. Murphey MD, Quale JL, Martin NL, Bramble JM, Cook LT, Dwyer III SJ. Computed radiography in musculoskeletal imaging: state of the art. *American Journal of Roentgenology* 1992;158(1):19-27.
334. Issler SL, Torardi CC. Solid state chemistry and luminescence of X-ray phosphors. *Journal of Alloys and Compounds*. 1995;229(1):54-65.
335. Fung KK, Gilboy WB. "Anode heel effect" on patient dose in lumbar spine radiography. *Br J Radiol*. 2000 May;73(869):531-6. PubMed PMID: 10884750. Epub 2000/07/08. eng.
336. Schueler BA. Clinical applications of basic x-ray physics principles. *Radiographics*. 1998 May-Jun;18(3):731-44; quiz 29. PubMed PMID: 9599394. Epub 1998/05/26. eng.
337. Seibert JA. X-Ray imaging physics for nuclear medicine technologists. Part 1: basic principles of X-ray production. *Journal of Nuclear Medicine Technology*. 2004 September 1, 2004;32(3):139-47.
338. Bull S. *Skeletal Radiography. A concise introduction to projection radiography*. 2 ed. Stanley UK: Toolkit Publications; 2005.
339. Derbyshire B. Correction of acetabular cup orientation measurements for X-ray beam offset. *Med Eng Phys*. 2008;30(9):1119-25.
340. Hahn PY, Strobel JJ, Hahn FJ. Verification of lumbosacral segments on MR images: identification of transitional vertebrae. *Radiology*. 1992 Feb;182(2):580-1. PubMed PMID: 1732988. Epub 1992/02/01. eng.
341. Hsieh CY, Vanderford JD, Moreau SR, Prong T. Lumbosacral transitional segments: classification, prevalence, and effect on disk height. *Journal of manipulative and physiological therapeutics*. 2000 Sep;23(7):483-9. PubMed PMID: 11004653. Epub 2000/09/27. eng.

342. Mahato NK. Pedicular anatomy of the first sacral segment in transitional variations of the lumbo-sacral junction. *Spine (Phila Pa 1976)*. 2011;36(18):E1187-92.
343. Stokes IAF, Iatridis JC. Mechanical conditions that accelerate intervertebral disc degeneration: overload versus immobilization. *Spine (Phila Pa 1976)*. 2004;29(23):2724-32.
344. Hadi AS. Identifying multiple outliers in multivariate data. *Journal of the Royal Statistical Society Series B (Methodological)*. 1992;54(3):761-71.
345. Walfish S. A review of statistical outlier methods. *Pharmaceutical Technology*. 2006;30(11):82-8.
346. Stokes IA, Aronsson DD, Ronchetti PJ, Labelle H, Dansereau J. Reexamination of the Cobb and Ferguson angles: bigger is not always better. *J Spinal Disord*. 1993 Aug;6(4):333-8. PubMed PMID: 8219547. Epub 1993/08/01. eng.
347. Goris BC, Kuipers M, De Vries J, Wever DJ, Verkerke GJ, Veldhuizen AG. On the determination of the angular orientation of a vertebra. *J Biomech Eng*. 2002 Feb;124(1):134-6. PubMed PMID: 11873772. Epub 2002/03/05. eng.
348. Deacon P, Flood BM, Dickson RA. Idiopathic scoliosis in three dimensions. A radiographic and morphometric analysis. *The Journal of bone and joint surgery British volume*. 1984 Aug;66(4):509-12. PubMed PMID: 6746683. Epub 1984/08/01. eng.
349. Crawford NR, Yamaguchi GT, Dickman CA. A new technique for determining 3-D joint angles: the tilt/twist method. *Clin Biomech (Bristol, Avon)*. 1999 Mar;14(3):153-65. PubMed PMID: 10619103. Epub 2000/01/05. eng.
350. Uysal T, Baysal A, Yagci A. Evaluation of speed, repeatability, and reproducibility of digital radiography with manual versus computer-assisted cephalometric analyses. *The European Journal of Orthodontics*. 2009 October 1, 2009;31(5):523-8.
351. Greenman PE. Lift therapy: use and abuse. *J Am Osteopath Assoc*. 1979 Dec;79(4):238-50. PubMed PMID: 159883. Epub 1979/12/01. eng.

352. Loder RT, Urquhart A, Steen H, Graziano G, Hensinger RN, Schlesinger A, et al. Variability in Cobb angle measurements in children with congenital scoliosis. The Journal of bone and joint surgery British volume. 1995 Sep;77(5):768-70. PubMed PMID: 7559707. Epub 1995/09/01. eng.
353. Goh S, Price RI, Leedman PJ, Singer KP. A comparison of three methods for measuring thoracic kyphosis: implications for clinical studies. Rheumatology (Oxford). 2000 Mar;39(3):310-5. PubMed PMID: 10788541. Epub 2000/05/02. eng.
354. Tannast M, Mistry S, Steppacher SD, Reichenbach S, Langlotz F, Siebenrock KA, et al. Radiographic analysis of femoroacetabular impingement with Hip2Norm - reliable and validated. Journal of Orthopaedic Research. 2008;26(9):1199-205.
355. Kakaty DK, Fischer AF, Hosalkar HS, Siebenrock KA, Tannast M. The ischial spine sign. Clinical orthopaedics and related research. 2010;468(3):769-74.
356. Goldman LW. Principles of CT and CT technology. Journal of Nuclear Medicine Technology. 2007;35(3):115-28.
357. Romans L. CT image quality  
[www.cewebsource.com/coursePDFs/CTimageQuality.pdf](http://www.cewebsource.com/coursePDFs/CTimageQuality.pdf); ECEI; 2012 [cited 2012 10th April].
358. Mathematics and Physics of Emerging Biomedical Imaging: The National Academies Press; 1996.
359. Mahesh M. The AAPM/RSNA physics tutorial for residents search for isotropic resolution in CT from conventional through multiple-row detector. Radiographics. 2002;22(4):949-62.
360. Brink JA, Heiken JP, Wang G, McEnery KW, Schlueter FJ, Vannier MW. Helical CT: Principles and technical considerations. Radiographics. 1994;14(4):887-93.
361. Barton C, Salineros M, Rakhra K, Beaulé P. Validity of the alpha angle measurement on plain radiographs in the evaluation of cam-type femoroacetabular impingement. Clinical orthopaedics and related research. 2011  
2011/02/01;469(2):464-9. English.



362. Lin F, Lim D, Wixson RL, Milos S, Hendrix RW, Makhsous M. Validation of a computer navigation system and a CT method for determination of the orientation of implanted acetabular cup in total hip arthroplasty: a cadaver study. *Clin Biomech (Bristol, Avon)*. 2008;23(8):1004-11.
363. Yu S-H, Nahm D-S, Baek S-H. Reliability of landmark identification on monitor-displayed lateral cephalometric images. *American journal of orthodontics and dentofacial orthopedics : official publication of the American Association of Orthodontists, its constituent societies, and the American Board of Orthodontics*. 2008;133(6):790.e1-.e6.
364. Delamare EL, Liedke GS, Vizzotto MB, da Silveira HLD, Ribeiro JLD, Silveira HED. Influence of a programme of professional calibration in the variability of landmark identification using cone beam computed tomography-synthesized and conventional radiographic cephalograms. *Dentomaxillofacial Radiology*. 2010 October 1, 2010;39(7):414-23.
365. Couceiro CP, Vilella OdV. Imagens em 2D e 3D geradas pela TC Cone-Beam e radiografias convencionais: qual a mais confiável? *Dental Press Journal of Orthodontics*. 2010;15:40-1.
366. Calhoun PS, Kuszyk BS, Heath DG, Carley JC, Fishman EK. Three-dimensional Volume Rendering of Spiral CT Data: Theory and Method1. *Radiographics*. 1999 May 1, 1999;19(3):745-64.
367. Chen DM. Application of 3D CAD for basic geometric elements in descriptive geometry. *Engineering Design Graphics Journal*. 2000;64(1):10-7.
368. Troyanovich S, Miller KJ. A clinical study of fluctuating asymmetry and leg length inequality. *Annals of vertebral subluxation research*. 2011;2011(Sept 12):92-8.
369. Palmer AR, Strobeck C. Fluctuating asymmetry as a measure of developmental stability: Implications of non-normal distributions and power of statistical tests. *Acta Zoologica Fennica*. 191:57-72.

370. Palmer AR, Strobeck C, Chippindale AK. Bilateral variation and the evolutionary origin of macroscopic asymmetries. *Genetica*. 1993;89:201-18.
371. Graham JH, Freeman DC, Emlen JM. Antisymmetry, directional asymmetry, and dynamic morphogenesis. *Genetica*. 1993;89:121-37.
372. Heilig D. Principles of lift therapy. *Journal of the American Osteopathic Association*. 1978;77:466-72.
373. Hill JSF. Heel lift protocols, their assessment and application in the chiropractic practice [Literature review]. Chesterfield, MO Logan University; 2010.
374. Logan HB. Textbook of Logan Basic Methods. St. Louis: Logan Basic College of Chiropractic; 1950.
375. Christensen K. Pelvic unleveling. *Dynamic Chiropractic*. 2000;18(9):1-4.
376. Anderson R. Misalignments in the human pelvis measured on radiographs. *J Hum Evol*. 1948;13:593-600.
377. Liebenson C. The relationship of the sacroiliac joint, stabilization musculature, and lumbo-pelvic instability. *Journal of Bodywork and Movement Therapies*. 2004;8:43-5.
378. Burdett RG, Brown KE, Fall MP. Reliability and validity of four instruments for measuring lumbar spine and pelvic positions. *Phys Ther*. 1986;66(5):677-84.
379. Ashman BC, Gray AJ, McPhee IB, Slinger BS, D. SA, F. TTK, et al. The role of the radiologist in the diagnosis of scoliosis - a new perspective2009. Available from: <http://www.srf-india.org/pubfiles/18.pdf>.
380. Cooperstein R. Gonstead Chiropractic Technique (GCT). *Journal of chiropractic medicine*. 2003;2(1):16-24.
381. Fuhr AW, Menke M. Status of activator methods chiropractic technique, theory, and practice. *Journal of manipulative and physiological therapeutics*. 2005;28(2):135.e1-20.

382. Schneider M, Homonai R, Moreland B, Delitto A. Interexaminer reliability of the prone leg length analysis procedure. *Journal of manipulative and physiological therapeutics*. 2007;30(7):514-21.
383. Cooperstein R, Lew M. The relationship between pelvic torsion and anatomical leg length inequality: a review of the literature. *Journal of chiropractic medicine*. 2009 Sep;8(3):107-18. PubMed PMID: 19703666. Pubmed Central PMCID: 2732247. Epub 2009/08/26. eng.
384. Winter DA. Human balance and posture control during standing and walking *Gait and Posture*. 1995;3(4):193-214.
385. Bowers R, Ross K. Best practice statement: use of ankle-foot orthoses following stroke. *NHS Quality Improvement Scotland [Internet]*. 2009.
386. Grzegorzewski A, Synder M, Kozlowski P, Szymczak W, Bowen RJ. Leg length discrepancy in Legg-Calve-Perthes disease. *Journal of Pediatric Orthopaedics*. 2005;25(2):206-9.
387. Raczkowski JW, Daniszewska B, Zolynski K. Functional scoliosis caused by leg length discrepancy. *Archives of Medical Science*. 2010;6(3):393-8.
388. Frost HM. A 2003 update of bone physiology and Wolff's Law for clinicians. *Angle Orthod*. 2004 2004/02/01;74(1):3-15.
389. House MJ. Wheelchair seat angle and lumbar support are critical factors for resolution of flexible spinal deformity and decubitus ulcer in persons with spinal cord injury. *Journal of Neurologic Physical Therapy*. 2006;30(4):216  
10.1097/01.NPT.0000281322.93071.4c.
390. Mayfield JK, Erkkila JC, Winter RB. Spine deformity subsequent to acquired childhood spinal cord injury. *The Journal of Bone and Joint Surgery*. 1981;63-A(9):1401-11.
391. Cooperstein R, Lisi A. Pelvic torsion: anatomic considerations, construct validity, and chiropractic examination procedures. *Top Clin Chiropr*. 2000;7(3):38-49.

392. Cummings G, Scholz JP, Barnes K. The effect of imposed leg length difference on pelvic bone symmetry. *Spine (Phila Pa 1976)*. 1993 Mar 1;18(3):368-73. PubMed PMID: 8475440. Epub 1993/03/01. eng.
393. Makhsous M, Lin F, Bankard J, Hendrix R, Hepler M, Press J. Biomechanical effects of sitting with adjustable ischial and lumbar support on occupational low back pain: evaluation of sitting load and back muscle activity. *BMC Musculoskelet Disord*. 2009;10(1):17. PubMed PMID: doi:10.1186/1471-2474-10-17.
394. William MK, Kuchera ML, Kuchera WA. Radiographic technical aspects of the postural study. In: Ward RC, editor. *Foundations for Osteopathic Medicine*. Baltimore, MD: Williams and Wilkins; 1997.
395. Esposito S, Philipson S. *Spinal adjustment technique: the chiropractic art* First ed. St. Ives, N.S.W: Well Adjusted Publishing; 2005.
396. Dulhunty JA. A mechanical and graphical evaluation of the Gonstead pelvic radiographic analysis. *Chiropractic Journal of Australia*. 1997;27(3):98-110.
397. Dulhunty JA. Geometrical considerations in assessing the validity of the gonstead method for measuring PI and AS ilium misalignments on pelvic radiographs. *Chiropractic Journal of Australia*. 2005;35(1):21-8.
398. Stokes IA, Bigalow LC, Moreland MS. Measurement of axial rotation of vertebrae in scoliosis. *Spine (Phila Pa 1976)*. 1986;11(3):213-8.
399. van der Bom MJ, Groote ME, Vincken KL, Beek FJ, Bartels LW. Pelvic rotation and tilt can cause misinterpretation of the acetabular index measured on radiographs. *Clinical orthopaedics and related research*. 2011;469(6):1743-9.

**APPENDIX 1**  
**CORRECTIVE ALGORITHMS TO DETERMINE TRUE SACRAL OBLIQUITY**

*“The relation between what we see and what we know is never settled.....*

*the knowledge, the explanation, never quite fits the sight.”*

— John Berger

Trigonometric functions can be used to calculate theoretical values for various specified angles associated with the measurement of sacral obliquity such as sacral base and pelvic rotation angles as well as angles associated with the measurement of vertebral alignment such as Cobb angles. The formulae are based on specific input angles that related to both orthographic projections, viewing angles and the orientation of the object. The output values represented the actual dihedral angles as opposed to the angles that would be measured on radiographic images. The formulae can also be used to calculate what measured angles would be expected on an image for a specified object orientation and projection method. For this purpose the calculations were based on the true dihedral values representing rotations of various structures. The process involved developing formulae that relate actual or true dihedral angles to the apparent angles that would be measured on the various images or projections.

The objective was to develop algorithms that could be used to calculate true dihedral angles ( $\theta_x$ ) from the apparent dihedral angle ( $\alpha_x$ ) and projected angles ( $\phi_x$ ) as they would be measured on orthographic projections, conventional plain film radiographs, CT multiplanar reconstructions (MPR) or 3D reconstructions. Algorithms were also developed to calculate the apparent dihedral angles ( $\alpha_x$ ) that would be measured when a plane representing an object was viewed from different perspectives. Similar algorithms were developed to calculate the anticipated apparent dihedral angle ( $\alpha_x$ ) based on the true dihedral angle ( $\theta_x$ ) with and without accompanying rotation in the horizontal ( $\theta_3$ ) and vertical planes ( $\theta_2$ ). The

initial given factors (angles) were sacral and vertebral obliquity angles ( $\theta_1$ ,  $\theta_5$ ), sacral and vertebral base angles ( $\theta_2$ ,  $\theta_6$ ) and the pelvic and vertebral rotation angles ( $\theta_3$ ,  $\theta_7$ ). These values represented the true rotation angle of the sacral plateau and vertebral endplate around the global  $Z_g$ ,  $X_g$ , and  $Y_g$  axes respectively.

### **ALGORITHMS USED TO CALCULATE ROTATION ANGLES**

Pelvic and vertebral rotations were calculated from measurements that could be obtained from orthographic projections, plain film radiographs, or CT images. All measurements were recorded and calculations made using Microsoft Excel (2010). Calculation of the influence rotation has on the measurement of sacral and vertebral obliquity as they would be measured on orthographic projections, plain film radiographs and CT images was based on an estimation of horizontal pelvic and vertebral rotation angles in degrees ( $\theta_3$ ,  $\theta_7$ ) from linear measurements made on projected images, plain film radiographs and CT images using trigonometric formula similar to the one developed by Stokes *et al* (398) and a method reported on by Illés *et al* (325). They employ trigonometric functions to calculate the degree of rotation based on measurements made on radiographic images. The calculation of pelvic rotation using these formulae represents an approximation of the actual rotation around the Y-axis for plain film radiographs as the calculations are based on orthographic projection principles rather than perspective projection as would be the case for measurements made on radiographic images of the spine (Figure 201). The factors primarily associated with plane film magnification are the source imaged distance (SID) and object image distance (OID). Short source to image distances (SID) may introduce errors due to unequal magnification of the involved structures but at longer distances the effect of magnification is generally minimised (237, 244, 399).

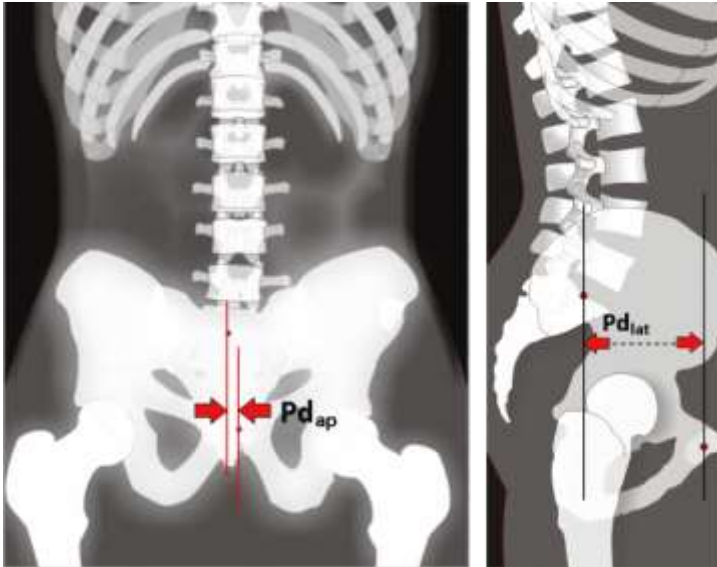


Figure 201. Rotation of the pelvis measured as horizontal displacement ( $Pd_{ap}$ ) of the symphysis pubis relative to the sacral tubercle on an AP radiograph (left). Horizontal distance ( $Pd_{lat}$ ) measured between the symphysis pubis and the sacral tubercle needed to calculate pelvic rotation on an AP radiographic image measured on the lateral radiograph.

Similar measurements were made on orthographic projection images representing pelvic rotation angle ( $PRA \theta_3$ ) and vertebral rotation angle ( $VRA - \theta_7$ ) (Figure 202)

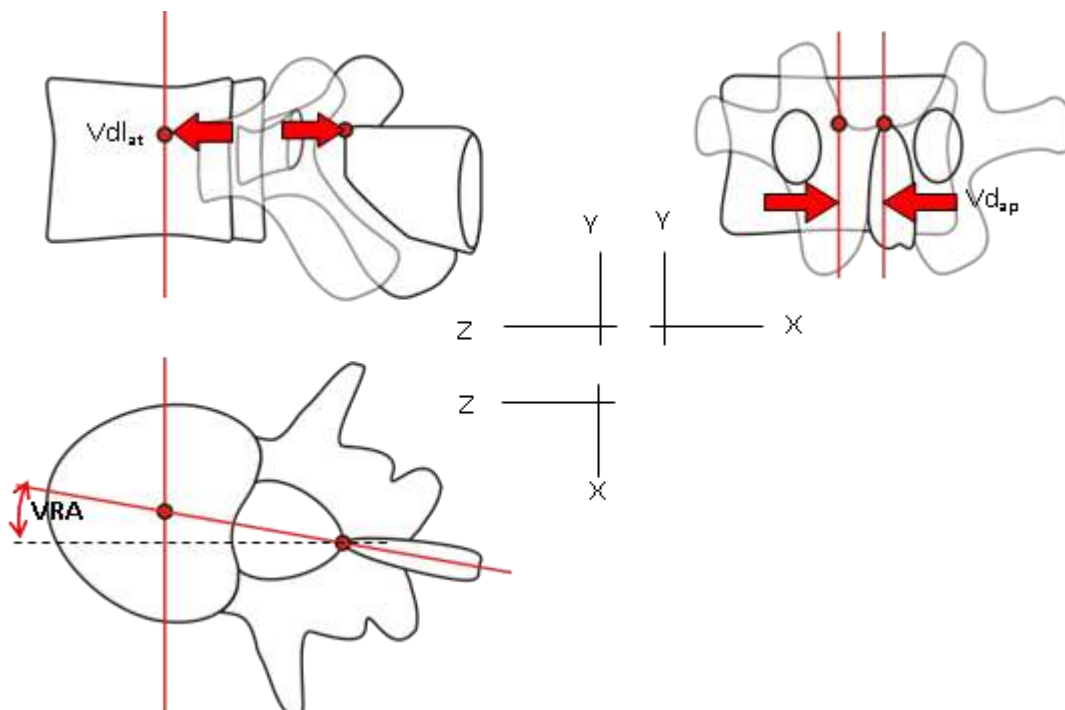


Figure 202. Rotation of a vertebra can be calculated by measuring horizontal displacement ( $Vd_{ap}$ ) of the vertebral body relative to the spinous process on an AP radiograph (right). Horizontal distance ( $Vd_{lat}$ ) needed to calculate vertebral rotation on an AP radiographic image is measured as the distance between the vertebral body and the lamina junction on the lateral radiograph (left).

Algorithms used to calculate pelvic rotation angles (PRA -  $\theta_3$ ) and vertebral rotation angles (VRA -  $\theta_7$ ) on orthographic projections were:

$$\tan PRA (\theta_3) = Pd_{ap} / Pd_{lat} \quad [1]$$

$$\tan VRA (\theta_7) = Vd_{ap} / Vd_{lat} \quad [2]$$

### ALGORITHMS TO CALCULATE BASE ANGLES ON ORTHOGRAPHIC PROJECTIONS

The sacral base angle ( $\theta_2$ ) and vertebral base angle ( $\theta_6$ ) were calculated using algorithms with data derived from measurements that represented the apparent sacral base ( $\alpha_2$ ) and vertebral base ( $\alpha_6$ ) angles, along with the pelvic rotation ( $\theta_3$ ) and vertebral rotation ( $\theta_7$ ) angles (Figure 203).

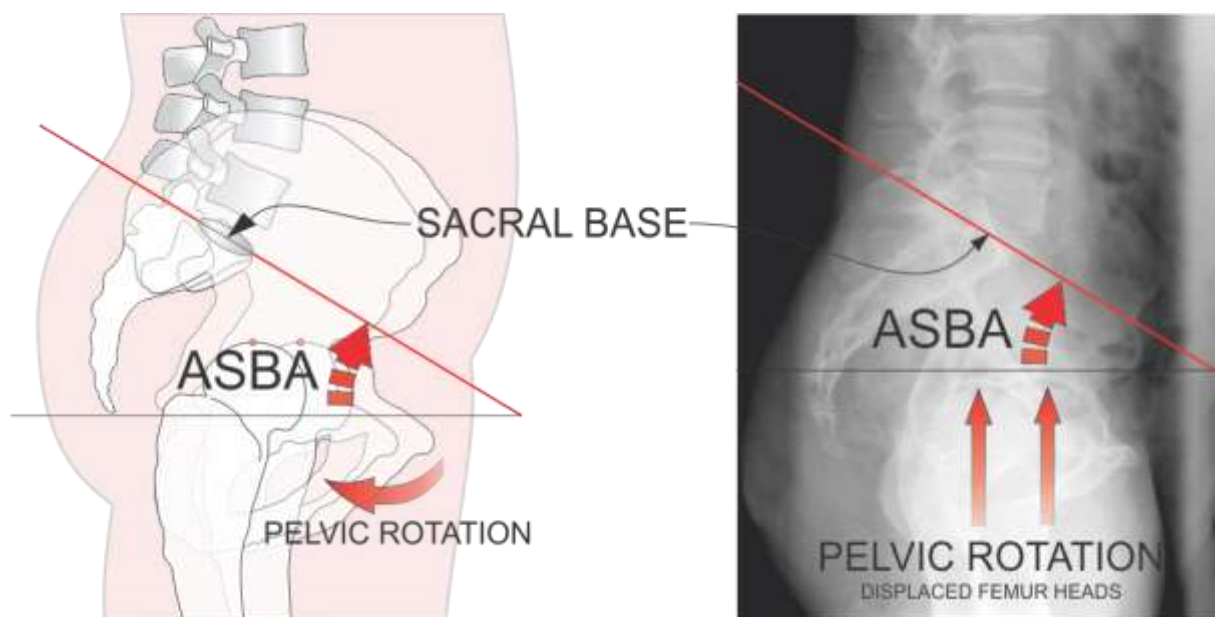


Figure 203. The apparent sacral base angle (ASBA) is a measurement on an orthographic projected image of the sacral base in the sagittal plane when the sacrum is rotated around Z-axes in addition to the X-axis rotation being measured. The resulting measurement is an apparent dihedral angle (left)

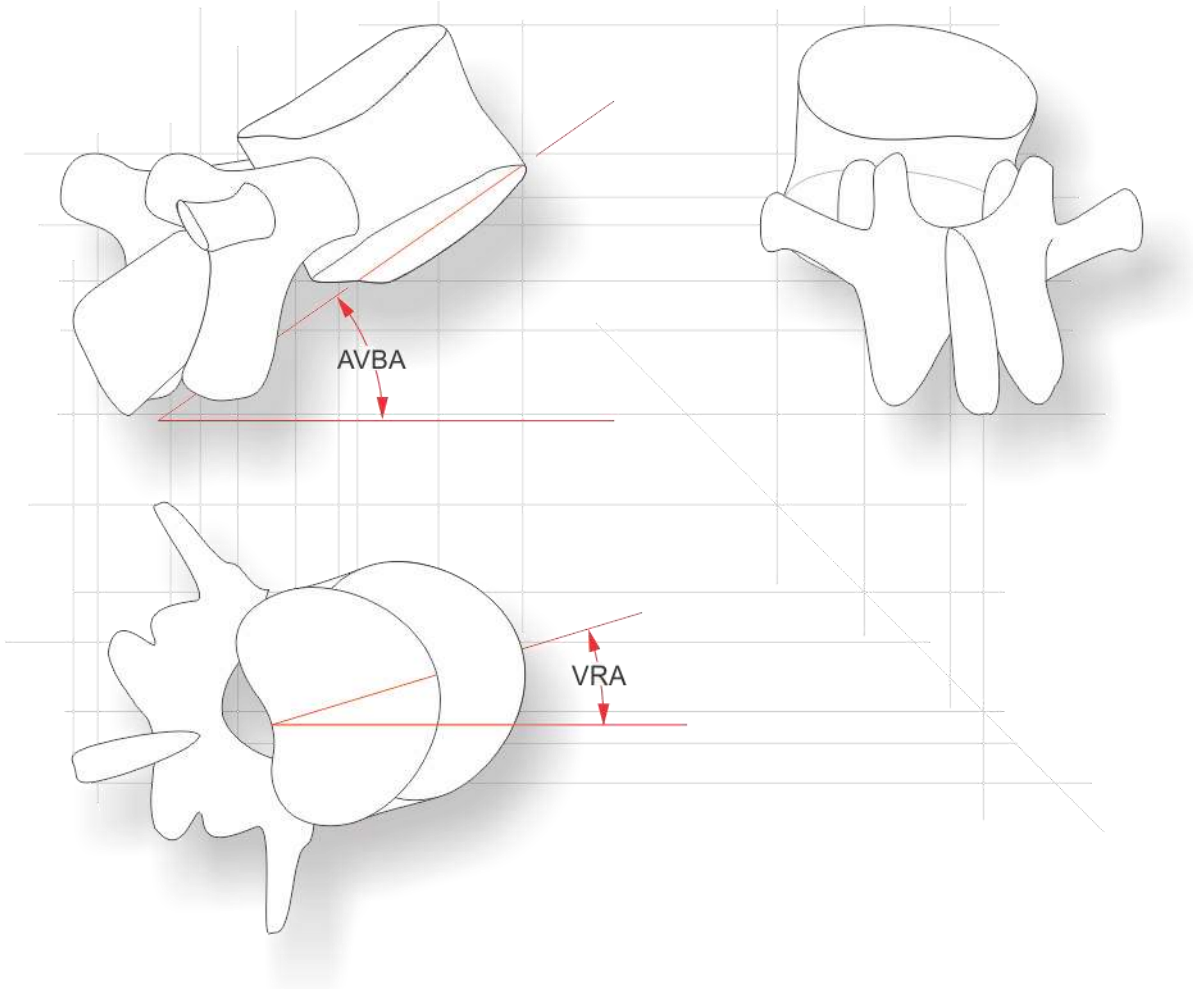
Algorithms used to calculate sacral base angle (SBA -  $\theta_2$ ) and vertebral base angle (VBA -  $\theta_6$ ) on orthographic projections were:

$$\tan SBA (\theta_2) = \tan ASOA (\alpha_2) * \cos PRA (\theta_3) \quad [3]$$

$$\tan VBA (\theta_6) = \tan AVOA (\alpha_6) * \cos VRA (\theta_7) \quad [4]$$



The apparent sacral base angle ( $\alpha_2$ ) and apparent vertebral base angle ( $\alpha_6$ ) were calculated using algorithms based on data derived from measurements that represented the true sacral base angle ( $\theta_2$ ) and vertebral base angle ( $\theta_6$ ) along with the pelvic and vertebral rotation angles ( $\theta_3$ ,  $\theta_7$ ) (Figure 204).



**Figure 204.** The apparent vertebral base angle (AVBA) is the angle formed by a line drawn along the centre of the image representing the base of the vertebra and a line representing the horizontal plane. The vertebral rotation angle (VRA) represents the degree of rotation of the vertebra around the Y-axis.

Algorithms used to calculate apparent sacral base angle (ASBA -  $\alpha_2$ ) and apparent vertebral base angle (AVBA  $\alpha_6$ ) on orthographic projections were:

$$\tan ASBA (\alpha_2) = \frac{\tan SBA (\theta_2)}{\cos PRA (\theta_3)} \quad [5]$$

$$\tan AVBA (\alpha_6) = \frac{\tan VBA (\theta_6)}{\cos VRA (\theta_7)} \quad [6]$$

### ALGORITHMS TO CALCULATE OBLIQUITY ANGLES

True dihedral angles (TDA) representing true sacral obliquity angle (SOA -  $\theta_1$ ) and true vertebral obliquity angle (VOA -  $\theta_5$ ) were calculated using algorithms with measurements derived from orthographic projections of the sacrum and lumbar vertebra. The algorithms were based on the measurement of graphical representations of a sacral or vertebral base angle ( $\alpha_1$ ,  $\alpha_5$ ), and apparent sacral and vertebral obliquity angles ( $\alpha_{1.3}$ ,  $\alpha_{5.3}$ ) without any accompanying pelvic or vertebral rotation ( $\theta_3$ ,  $\theta_7$ ) respectively (Figure 205).

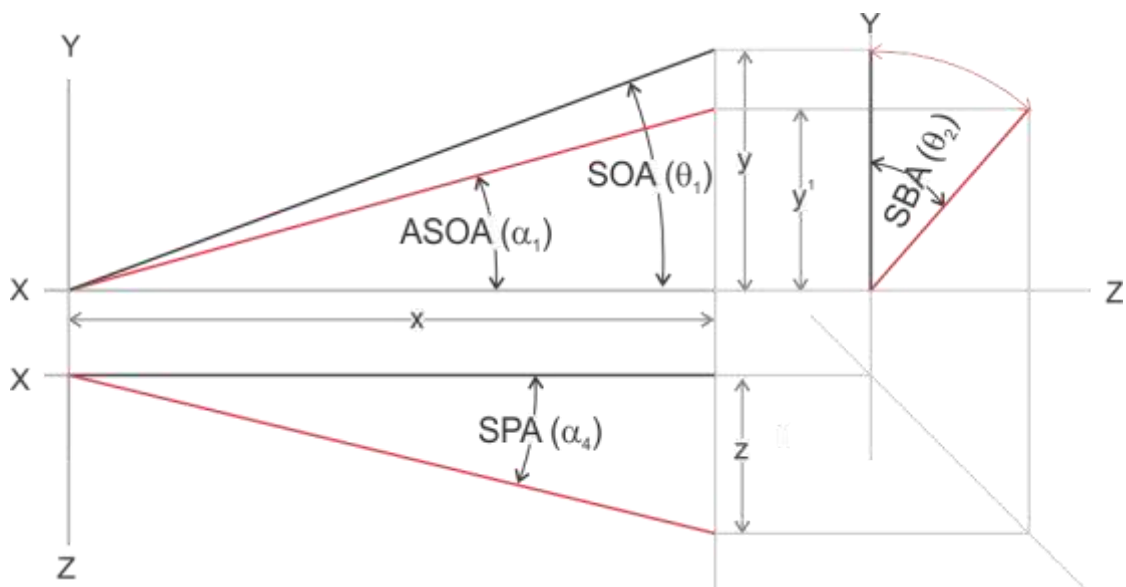


Figure 205. Orthographic projection of the relationship between a graphical representation of the sacral obliquity angle (SOA) and the apparent sacral obliquity angle (ASOA) due to the influence of the sacral base angle (SBA)

Algorithms used to calculate sacral obliquity angle (SOA -  $\theta_1$ ) and vertebral obliquity angle (VOA -  $\theta_5$ ) using factors as they would be measured on orthographic projection images with no pelvic or vertebral rotation ( $\theta_3$  and  $\theta_7$ ) were:

$$\tan SOA (\theta_1) = \frac{\tan ASOA (\alpha_{1.3})}{\cos SBA (\theta_2)} \quad [7]$$

$$\tan VOA (\theta_5) = \frac{\tan AVOA (\alpha_{5.3})}{\cos VBA (\theta_6)} \quad [8]$$

Apparent sacral obliquity angle (ASOA -  $\alpha_{1.4}$ ) and apparent vertebral obliquity angle (AVOA -  $\alpha_{5.4}$ ) are representations of apparent dihedral angles (ADA) as they would be seen on conventional radiographic images (DR, CR and PF radiographic images) of the sacrum or vertebra receptively (Figure 206).

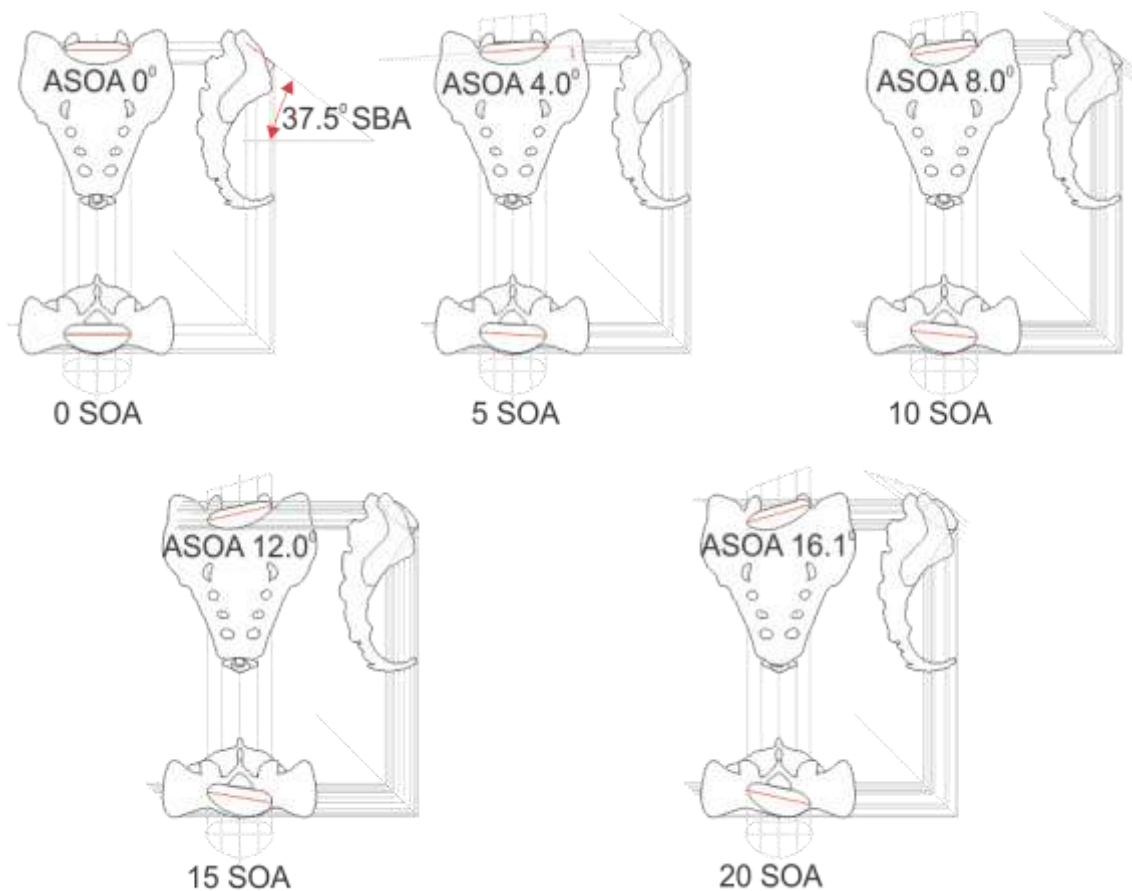
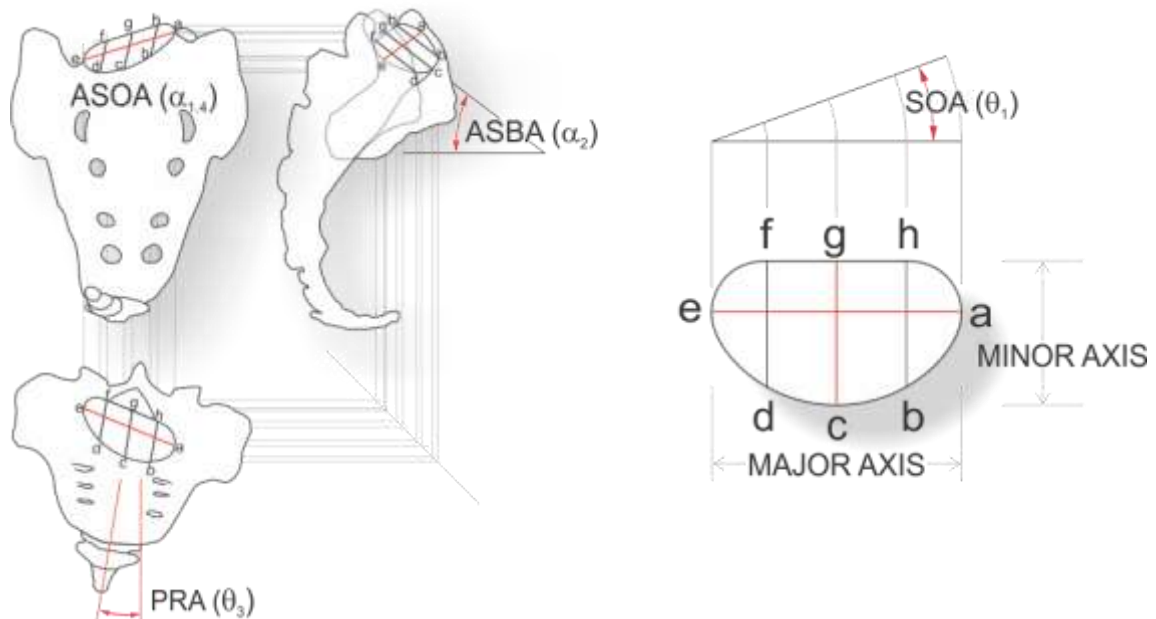


Figure 206. Orthographic projection of a sacrum with 0, 5, 10, 15, and 20 degrees of sacral obliquity (SOA) and a sacral base angle (SBA) of 37.5 degrees. The apparent sacral obliquity angle is measured as the angle of the major axis of the sacral base relative to the horizontal plane on the AP image

The same angular measurements of apparent sacral obliquity and apparent vertebral obliquity were made on orthographic projections of graphical representations of an idealised sacrum and vertebra with additional Y-axis rotation ( $\theta_3$ ,  $\theta_7$ ) accompanying the base and obliquity angles. Algorithms were used to calculate the true sacral and vertebral obliquity angles using these measurements (Figure 207).



**Figure 207.** Orthographic projection of an image representing an ideal sacral segment with a known amount of sacral obliquity (SOA), sacral base angle (SBA) and pelvic rotation (PRA). This results in an apparent sacral obliquity angle (ASOA) measured on the AP orthographic projection.

Algorithms used to calculate sacral obliquity angle ( $\theta_1$ ) and vertebral obliquity angle ( $\theta_5$ ) as they would be measured on orthographic projections used to represent plain film images with Y-axis pelvic or vertebral rotation ( $\theta_3$  and  $\theta_7$ ) were:

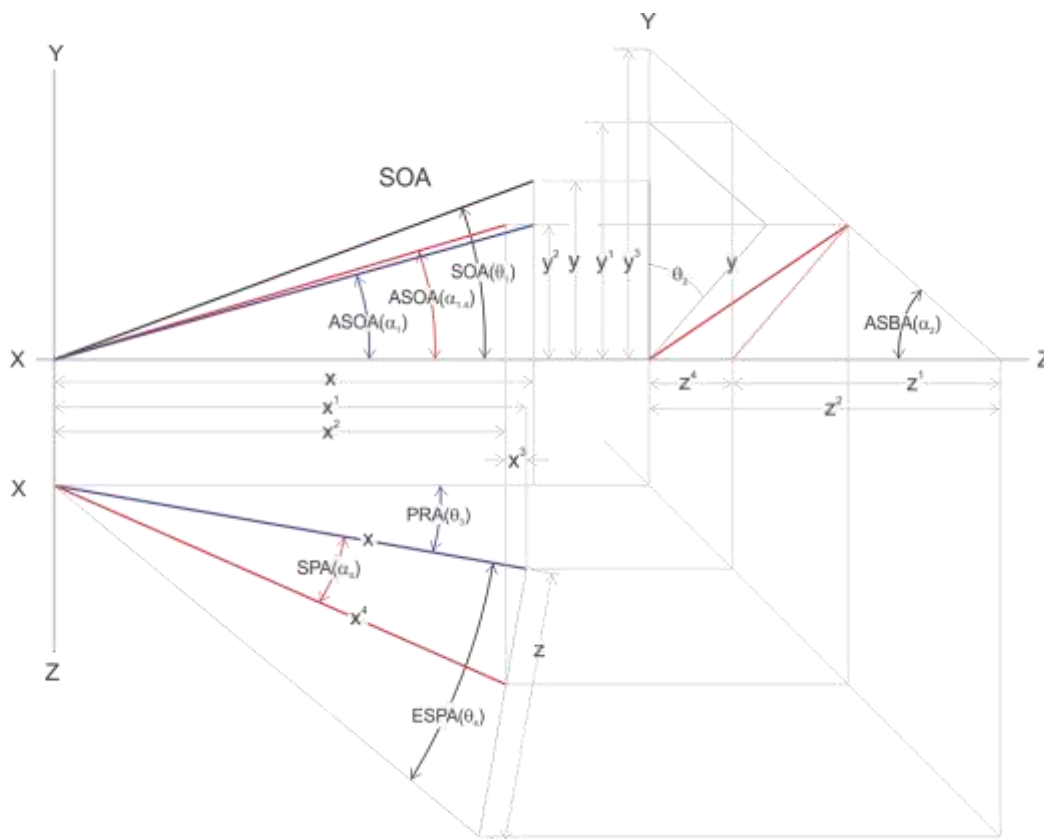
$$\tan SOA(\theta_1) = \frac{\tan ASOA(\alpha_{1.4}) * \cos [PRA(\theta_3) + SPA(\alpha_3)]}{\cos SBA(\theta_2) * \cos SPA(\alpha_3)} \quad [9]$$

$$\tan VOA(\theta_5) = \frac{\tan AVOA(\alpha_{5.4}) * \cos [VRA(\theta_7) + VPA(\alpha_7)]}{\cos VBA(\theta_6) * \cos VPA(\alpha_7)} \quad [10]$$

### ALGORITHMS TO CALCULATE APPARENT OBLIQUITY ANGLES

Algorithms were also developed to calculate the apparent sacral obliquity angle (ASOA -  $\alpha_{1.3}$ ) and apparent vertebral obliquity angle (AVOA -  $\alpha_{5.3}$ ) that would be measured on

orthographic images representing AP plain film radiographs. The algorithms were based on given true dihedral angles representing the sacral and vertebral base angles ( $\theta_2$ ,  $\theta_6$ ) and the sacral and vertebral obliquity angles ( $\theta_1$ ,  $\theta_5$ ). The apparent sacral and vertebral obliquity angles ( $\alpha_{1.4}$ ,  $\alpha_{5.4}$ ) that would be expected on conventional radiographic (PF) images with pelvic or vertebral rotation were calculated using the developed algorithms. The algorithms were based on the true dihedral angles (TDA) representing the sacral and vertebral obliquity angles ( $\theta_1$ ,  $\theta_5$ ), sacral and vertebral base angles ( $\theta_2$ ,  $\theta_6$ ) with an accompanying pelvic or vertebral rotation angle ( $\theta_3$ ,  $\theta_7$ ) respectively (Figure 206) (Figure 208).



**Figure 208. The apparent dihedral angle ( $\alpha_{1.4}$ ) representing sacral obliquity angle (SOA) measured as an orthographic projection with both X-axis and Y-axis rotation of the oblique sacral base**

Algorithms used to calculate apparent sacral obliquity angle ( $\alpha_{1.3}$ ) and apparent vertebral obliquity angle ( $\alpha_{5.3}$ ) as would be measured on an orthographic projection representing plain film (PF) with no pelvic or vertebral rotation were:

$$\tan ASOA(\alpha_{1.3}) = \cos SBA(\theta_2) * \tan SOA(\theta_1) \quad [11]$$

$$\tan AVOA(\alpha_{5.3}) = \cos VOA(\theta_5) * \tan VBA(\theta_6) \quad [13]$$

Algorithms used to calculate apparent sacral obliquity angle ( $\alpha_{1.4}$ ) and apparent vertebral obliquity angle ( $\alpha_{5.3}$ ) as they would be measured on orthographic projection images representing plain film images with Y-axis pelvic or vertebral rotation ( $\theta_3$  and  $\theta_7$ ) were:

$$\tan ASOA(\alpha_{1.4}) = \frac{\tan SOA(\theta_1) * \cos SBA(\theta_2) * \cos PRA(\alpha_3)}{\cos [PRA(\theta_3) + SPA(\alpha_3)]} \quad [12]$$

$$\tan AVOA(\alpha_{5.4}) = \frac{\tan VOA(\theta_5) * \cos VBA(\theta_6) * \cos VRA(\alpha_7)}{\cos [VRA(\theta_7) + VPA(\alpha_7)]} \quad [14]$$

#### ALGORITHMS TO CALCULATE OBLIQUITY ANGLES ON CT IMAGES

The true dihedral angles (TDA) of sacral and vertebral obliquity angles ( $\theta_1$ ,  $\theta_5$ ) were calculated from measurements that represent the sacral and vertebral base angles ( $\theta_2$ ,  $\theta_6$ ), along with the apparent sacral and vertebral angles ( $\alpha_{1.1}$ ,  $\alpha_{5.1}$ ) obtained from multiplanar reconstructions (MPR) of the A-P (coronal), transverse (axial) and lateral (sagittal) planes of specific spinal structures visualised on computerised tomography (CT) data sets. The MPR views represent an orthographic projection of structures that would be seen when three mutually perpendicular cutting planes pass through a computed tomographic data set at various orientations relative to the structure or plane involved (Figure 209).

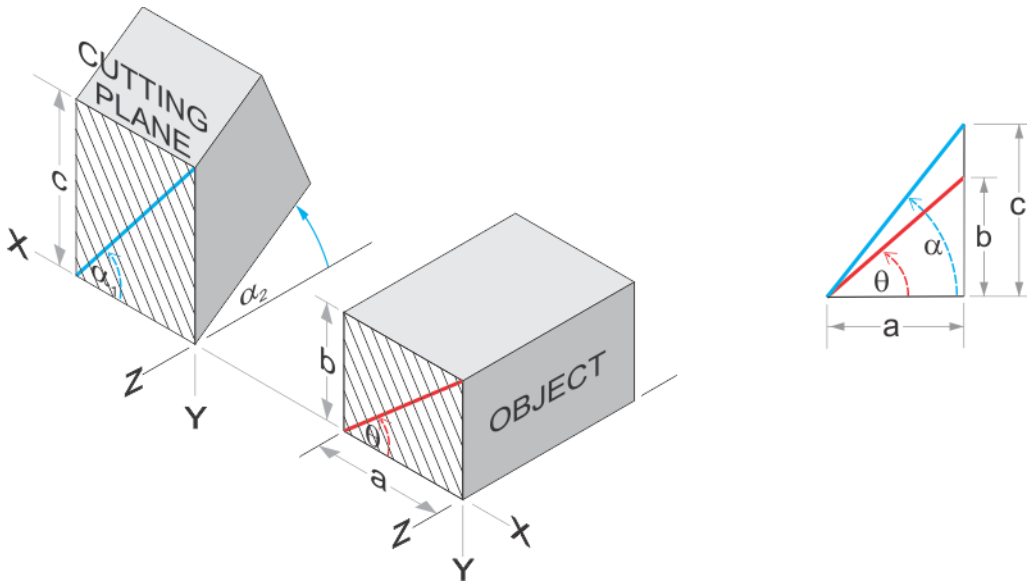


Figure 209. A cutting plane passing through and object positioned in two different orientations to the x-axis in a similar way to an MPR image plane. A diagonal line was constructed to represent the measurement of a dihedral angle on an MPR image in each orientation

Algorithms were used to calculate true sacral and vertebral obliquity ( $\theta_1$ ,  $\theta_5$ ) using the sacral vertebral base angles ( $\theta_2$ ,  $\theta_6$ ) and apparent sacral and vertebral obliquity angles ( $\alpha_{1.1}$ ,  $\alpha_{5.1}$ ) with no accompanying pelvic or vertebral rotation ( $\theta_3$ ,  $\theta_7$ ) around the vertical axis (Yg) based on orthographic projections were:.

$$\tan SOA(\theta_1) = \tan ASOA-CT(\alpha_{1.1}) * \cos SBA(\theta_2) \quad [15]$$

$$\tan VOA(\theta_5) = \tan AVOA-CT(\alpha_{5.1}) * \cos VBA(\theta_6) \quad [16]$$

The true dihedral angles (TDA) representing relative sacral and vertebral obliquity angles ( $\theta_1$ ,  $\theta_5$ ) were also calculated from measurements made of the apparent sacral obliquity angle ( $\alpha_{1.2}$ ) and apparent vertebral obliquity angle ( $\alpha_{5.2}$ ), apparent sacral base angle ( $\alpha_2$ ) and pelvic rotation angle ( $\theta_3$ ) and vertebral rotation angle ( $\theta_7$ ) on computerised tomography (CT) multiplanar (MPR) images.

Algorithms for calculating the sacral obliquity angle ( $\theta_1$ ) and vertebral obliquity angle ( $\theta_5$ ) with Y-axis rotation were:

$$\tan SOA(\theta_1) = \frac{[\tan ASOA(\alpha_{1.2}) / (\cos PRA(\theta_3) * \tan ASBA(\alpha_2))] - \sin (PRA(\theta_3))}{\cos PRA(\theta_3) * \sin SBA(\theta_2)} \quad [17]$$

$$\tan VOA(\theta_5) = \frac{[\tan AVBA(\alpha_{5.2}) / (\cos VRA(\theta_7) * \tan AVBA(\alpha_6))] - \sin VRA(\theta_7)}{\cos VRA(\theta_7) * \sin VBA(\theta_6)} \quad [18]$$

Algorithms were used to calculate the apparent sacral and apparent vertebral obliquity angles ( $\alpha_{1.1}$ ,  $\alpha_{5.1}$ ) that would be measured on MPR images derived from computed tomography (CT) data sets. The calculations were based on given values such as the true dihedral angles representing the angle between the image plane and the plane of the sacral or vertebral base ( $\theta_2$ ,  $\theta_6$ ) and the sacral and vertebral obliquity angles ( $\theta_1$ ,  $\theta_5$ ).

Algorithms for calculating apparent sacral and vertebral obliquity angles ( $\alpha_{1.1}$ ,  $\alpha_{5.1}$ ) with no Y-axis rotation were:

$$\tan ASOA(\alpha_{1.1}) = \frac{\tan \theta_1}{\cos \theta_2} \quad [19]$$

$$\tan AVOA (\alpha_{5.1}) = \frac{\tan \theta_5}{\cos \theta_6} \quad [21]$$

The apparent sacral and apparent vertebral obliquity angles ( $\alpha_{1.4}$ ,  $\alpha_{5.4}$ ) that would be expected on an MPR image with Y-axis rotation were calculated given the true dihedral angles (TDA) representing the sacral and vertebral obliquity angle ( $\theta_1$ ,  $\theta_5$ ), sacral and vertebral base angles ( $\theta_2$ ,  $\theta_6$ ) and pelvic rotation and vertebral angles ( $\theta_3$ ,  $\theta_7$ ).

Algorithms for calculating apparent sacral and vertebral obliquity angles ( $\alpha_{1.2}$ ,  $\alpha_{5.2}$ ) with Y-axis rotation were:

$$\tan \alpha_{1.2} = \frac{\cos \theta_3 * \tan \alpha_2 * \sin (\theta_4 + \theta_3)}{\cos \theta_4} \quad [20]$$

$$\tan \alpha_{5.2} = \frac{\cos \theta_7 * \tan \alpha_6 * \sin (\theta_9 + \theta_7)}{\cos \theta_9} \quad (22)$$



### CALCULATING SACRAL BASE ANGLE (SBA)

Because A-P lateral images of the involved structures are not necessarily bi-planar in the routine radiographic examination of the spine and pelvis measurements of distances such as the object to image distance (OID) and angles such as the sacral base angle (SBA) made on one image cannot be directly transferred to the other.

To overcome this lack of congruency between the two images a method was developed to determine what the sacral base angle (SBA) would have been when it was projected on the A-P image. On the A-P image two arbitrary points were chosen (A,B) representing superimposed structures or two points lying on the same horizontal plane. Ideally these two structures would be close to the midline of the body with as much anteroposterior separation as possible. Another requirement is that both structures should be visible and identifiable on a lateral image of the same region. To calculate the vertical angle of the divergent beam that passes through the superimposed points relative to the central ray, the distance from the superimposed structures to the central ray measured is measured on the A-P image and divided by the SID (Figure 210).

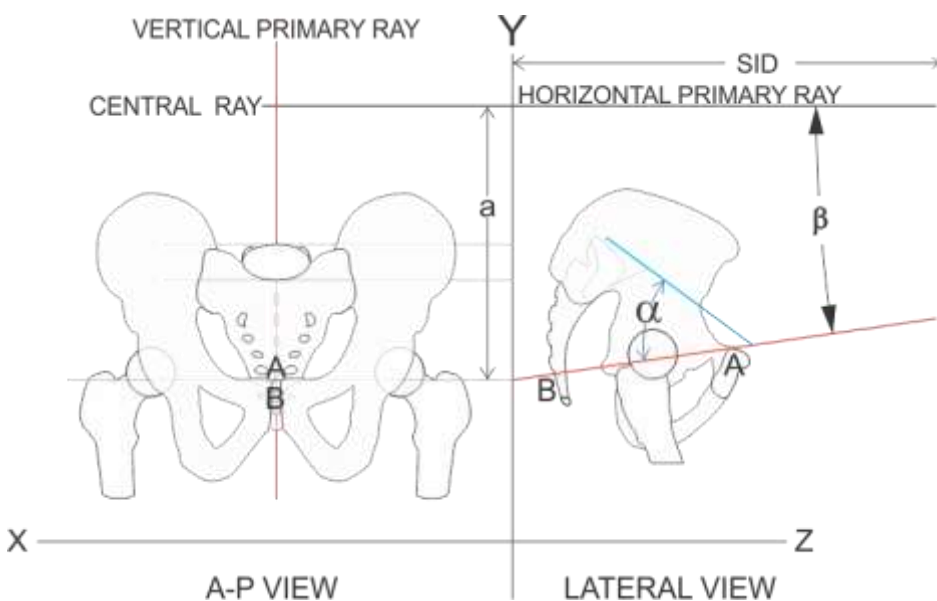


Figure 210. A drawing representing the factors used to calculate the orientation of the sacral base as seen on the A-P image of the pelvis

The result is calculated as the tan of the divergent beam that passes through the superimposed points (A) and (B):

$$\tan \beta = a/SID$$

[24]

The sacral base angle projected on the A-P radiographic image can be calculated by adding or subtracting angle ( $\beta$ ) from angle ( $\alpha$ ) (Figure 211):

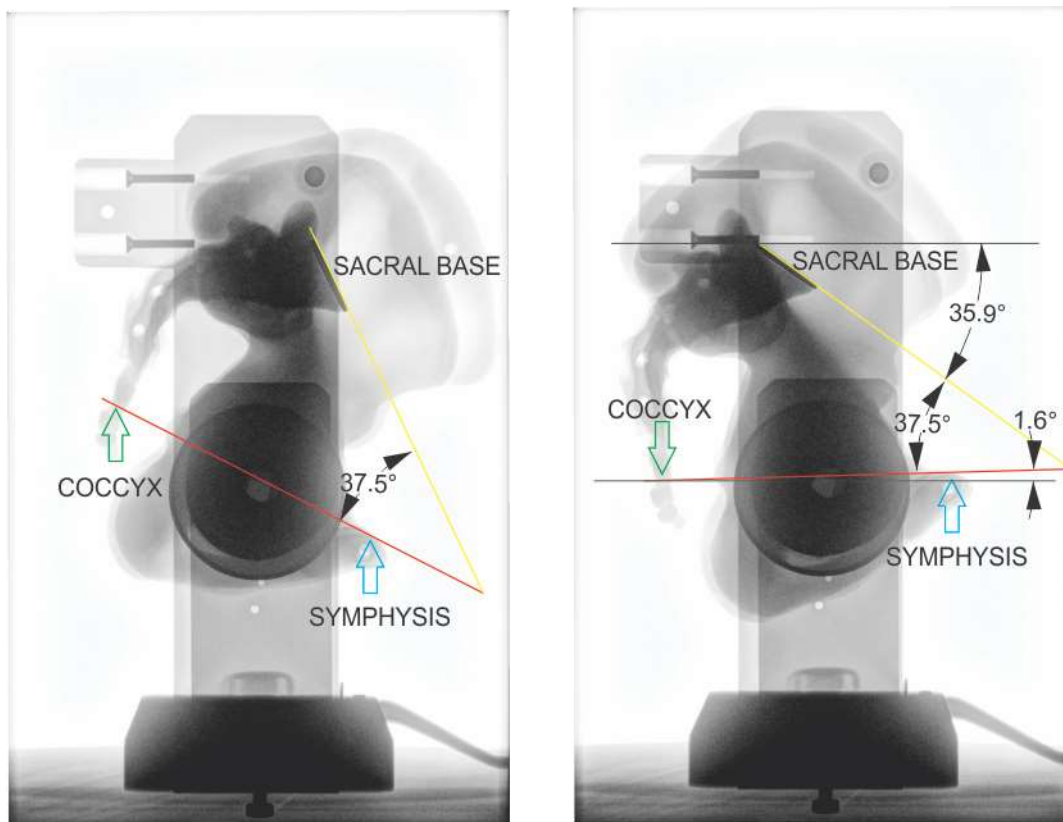


Figure 211. Lateral view of the pelvic phantom with the sacral base orientated as it was for the A-P view (right image) and at a non-specified angle (left image). The angle between the line joining the two points superimposed on the A-P image and the sacral base was measured on the lateral pelvic image.

$$SBA = \alpha \pm \beta$$

[25]

Angle ( $\beta$ ) is subtracted from angle ( $\alpha$ ) when the central ray (CR) is located above the sacral base on the A-P pelvic image and is added when the central ray is located below the sacral base on the A-P image (Figure 212).

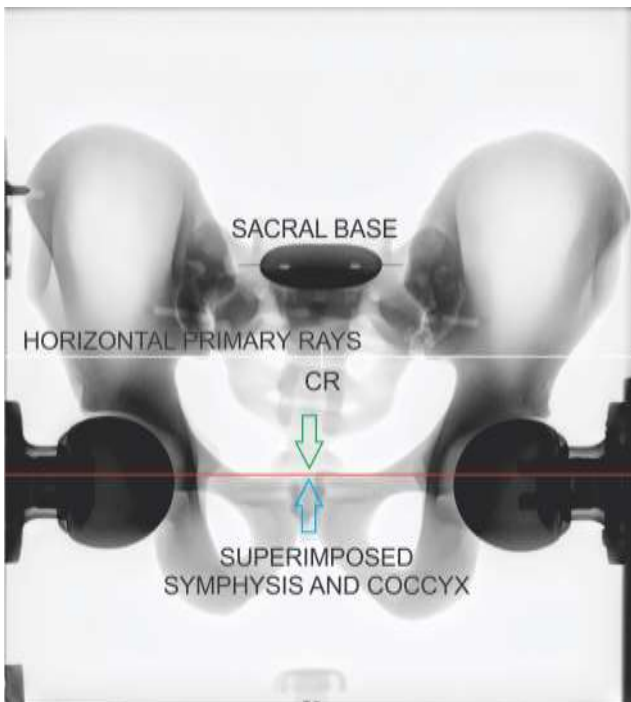


Figure 212. An erect A-P plain film view of a pelvic phantom illustrating the superimposition of an identifiable point on the sacrum or coccyx and the upper border of the symphysis pubis and the location of the central ray in the centre of the image. The vertical distance from the central ray to the superimposed points is measured on the DICOM image.

Calculating Plan Rotation Angle (PRA) from radiographic images.

$$\tan PRA = \frac{\tan (90 - LPA)}{(\tan (90 - PFHA)) - (\tan (90 - LPA) * \tan PPA)} \quad [26]$$

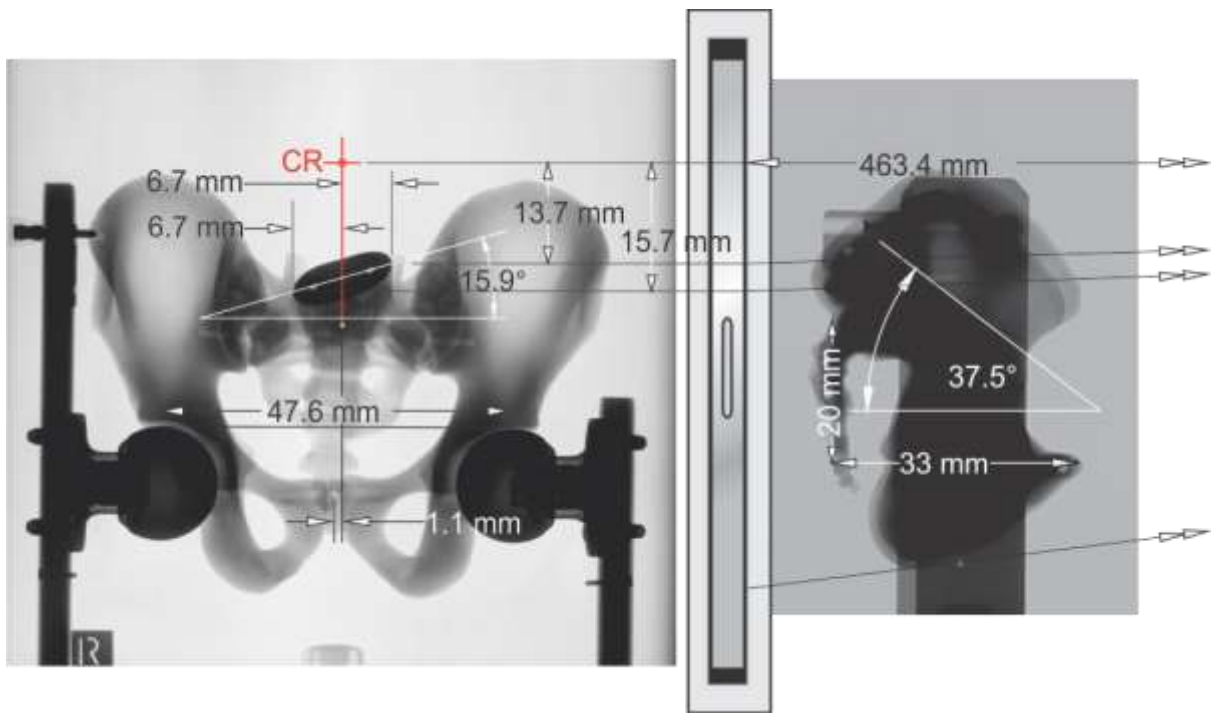
## SUMMARY and CONCLUSIONS

*Protocols to obtain true dihedral angles on radiographic images*

1. Central ray has to be perpendicular to the image plane
2. The plane of the structure being measured on the radiographic image such as the sacral base or vertebral endplate must be projected as a line on the image.
3. The two planes forming the angle being measured must be parallel to the image plane.

Algorithm to calculate true dihedral angles from radiographic images

The true sacral obliquity angle can be calculated from measurements obtained from plain film radiographs and source to image distance using the general formula (Figure 213):



**Figure 213.** Plain film radiographic images (AP and LAT) of the pelvic phantom with 20 degrees of sacral obliquity with measurements needed to calculate true sacral obliquity from the image

The simple question asked as the basis for this study was “can sacral obliquity be measured accurately on radiographic images.” The simple answer to that question as a result of this study is “no”. The more comprehensive answer is that the degree of sacral obliquity can be determined by applying algorithms to compensate for inherent systematic errors associated with the measurement of dihedral angles on radiographic images. Alternately, radiographic protocols have been developed that if adhered to would ensure or enhance the validity of sacral obliquity measurements *in vivo*.

Those clinicians who now use radiographic images to assess the positional integrity of the spine in erect posture may be under or over estimating the degree of obliquity of the sacral base and other segments of the spine. Lack of valid information in this respect could have clinical implications in the treatment and management of patients with musculoskeletal conditions as suggested by Brown *et al* (27).

<p style="text-align: center;"><b><i>Appendix 2</i></b> <b>Abbreviations and Glossary of Terms</b></p>
--

Abbreviations and description of terms used in the document have been tabulated as follows:

Radiographic terms (Table A)

True and apparent vertebral obliquity angles (Table B).

True and apparent sacral obliquity angles (Table C).

Angles associated with projected structures and planes (Table D).

Linear measurements made on radiographic images (Table E).

These Tables are followed by an alphabetical list of definitions of important terms used in the thesis.

<i>Abbreviations</i>			
2D	Two-dimensional	PF (PFR)	Plain Film Radiography
3D	Three-dimensional	PPA	Plan Projection Angle
APA	Anteroposterior Angle	PSIS	Posterior Superior Iliac Spine
APV	Anteroposterior View	CPA	Compound Projection Angle
ASIS	Anterior Superior Iliac Spine	SBA	Sacral Base Angle
CR	Computed Radiology	SBV	Sacral Base View
CT	Computed Tomography	SID	Source to Image Distance
DICOM	Digital Imaging Communication for Medicine	SOD	Source to Object Distance
DR	Digital Radiology	SPDR	Scan Projection Digital Radiography
FBA	Ferguson's Base Angle	SPL	Sacral Plane Line
FHL	Femur Head Line	SSDR	Slot Scan Digital Radiology
HPR	Horizontal Primary Rays	TPA	True Plane Angle
ICL	Intercrestal Line	VPR	Vertical Primary Rays
LLI/LLD	Leg Length Imbalance / Deficiency	X-Y plane	Coronal (frontal) plane
LPA	Lateral Projection Angle	X-Z plane	Transverse (axial) plane
MPR	Multipanar reconstruction	Y-Z plane	Sagittal plane
OID	Object to Image Distance	ZAV	Zero Angle View

Table A Abbreviations of radiographic terms

True Dihedral Vertebral Obliquity Angles		
True Angle	Abbreviation	Description
$\theta_5$	VOA	Vertebral Obliquity Angle
$\theta_6$	VBA	Vertebral Base Angle
$\theta_7$	VRA	Vertebral Rotation Angle
$\theta_8$	TCA	Cobb's Angle
$\theta_9$	EVPA	Extended Vertebral Plan Angle
Apparent Dihedral Vertebral Obliquity Angles		
Measured Angle	Abbreviation	Description
$\alpha_{5,1}$	AVO-CT	Apparent Vertebral Obliquity Angle
$\alpha_{5,2}$	AVO-CT+R	Apparent Vertebral Obliquity Angle
$\alpha_{5,3}$	AVO-PF	Apparent Vertebral Obliquity Angle
$\alpha_{5,4}$	AVO-PF+R	Apparent Vertebral Obliquity Angle
$\alpha_6$	AVBA	Apparent Vertebral Base Angle
$\alpha_7$	AVRA	Apparent Vertebral Rotation Angle
$\alpha_8$	ACA	Apparent Cobb's Angle
$\alpha_9$	VPA	Vertebral Plan Angle

Table B Symbols and abbreviations associated with the measurement of true and apparent vertebral obliquity angles

True Dihedral Sacral Obliquity Angles		
True Angle	Abbreviation	Description
$\theta_1$	SOA	Sacral Obliquity Angle
$\theta_2$	SBA	Sacral Base Angle
$\theta_3$	PRA	Pelvic Rotation Angle
$\theta_4$	ESPA	Extended Sacral Plan Angle
Apparent Dihedral Sacral Obliquity Angles		
Measured Angle	Abbreviation	Description
$\alpha_{1,1}$	ASO-CT	Apparent Sacral Obliquity Angle
$\alpha_{1,2}$	ASO-CT+R	Apparent Sacral Obliquity Angle
$\alpha_{1,3}$	ASO-PF	Apparent Sacral Obliquity Angle
$\alpha_{1,4}$	ASO-PF+R	Apparent Sacral Obliquity Angle
$\alpha_2$	ASBA	Apparent Sacral Base Angle
$\alpha_3$	APRA	Apparent Pelvic Rotation Angle
$\alpha_4$	SPA	Sacral Plan Angle

Table C Symbols and abbreviations associated with the measurement of true and apparent sacral obliquity angles



Projected angles		
Measured Angle	Abbreviation	Description
$\varphi_1$	PSBA	Projected Sacral Base Angle
$\varphi_2$	PPRA	Projected Pelvic Rotation Angle
$\varphi_3$	PSOA	Projected Sacral Obliquity Angle
$\varphi_4$	PVOA	Projected Vertebral Obliquity Angle
$\varphi_5$	PVBA	Projected Vertebral Base Angle
$\varphi_6$	PVRA	Projected Vertebral Rotation Angle
$\varphi_7$	PCA	Projected Cobb Angle
$\varphi_8$	LPA	Lateral Projection Angle
$\varphi_9$	PPA	Plan Projection Angle

Table D Symbols and abbreviations for projected angles

Linear measurements	
Measured Distance	Description
$x$	True measurement along x axis
$y$	True measurement along y axis
$z$	True measurement along z axis
$x_x$	Apparent distance along x axis
$y_x$	Apparent distance along y axis
$z_x$	Apparent distance along z axis
$D_v$	Vertical distance from central ray to reference point in the frontal plane
$D_h$	Horizontal distance from central ray to reference point in the frontal plane

Table E Symbols and abbreviations for linear measurements

## Definitions

### Descriptive geometry

Descriptive geometry is the branch of geometry that uses the representation of three-dimensional objects such as skeletal structures in two dimensions using a specific set of procedures and protocols. The protocol used allows spinal and pelvic structures to be drawn in such a way that the drawing represents the dimensions and angles of an actual or theorised three-dimensional spine. In the resulting drawing, all geometric aspects of the spine and pelvis are accounted for as representing their true size and shape. The protocols allow the object to be represented on a two-dimensional drawing surface as if seen from any position in space.

### Displacement

#### *Absolute displacement*

Absolute displacement is the measured degree of angular or linear displacement of an object, or the degree of rotation and linear displacement of a local reference frame, in relation to the global (Newtonian or inertial) frame of reference.

#### *Relative displacement*

Relative displacement is the measured degree of angular or linear displacement of an object or structure within a reference frame. Relative displacement can also occur between two or more structures within a reference frame. The reference frame itself can be moveable or arbitrarily assigned to a specified structure. The reference frame generally consists of three axes (X, Y, Z) formed at the junction or origin (0) of three mutually perpendicular planes. The pelvic reference frame was chosen for the analysis of relative sacral obliquity.

### *Right hand thumb rule*

The direction of translations and rotations within the reference plane or movement of the reference plane is designated as positive (+) or negative (-) arbitrarily based on the right hand thumb rule. The right hand thumb rule states that with the thumb of the right hand aligned to the axis of rotation and pointing in the direction designated as positive, the fingers of the right hand point in the direction of positive rotation. The positive (+) X-axis was designated as being to the left, the positive (+) Y-axis upwards and the positive (+) Z-axis to the front.

### Measured and calculated distances

#### *Femur Head Width (FWW)*

The horizontal distance representing the width of the femur heads in the X-Y plane measured on AP pelvic radiographs and CT images. The distance is measured between the tangent point on the head of the femur where it touches the line representing the plane of the femurs (femur head line).

#### *Ischial Tuberosity Width (ITW)*

The horizontal distance representing the width between the ischial tuberosity of each innominate bone in the X-Y plane as measured on AP pelvic radiographs and CT images. The distance is measured between the tangent points on the lower most curve of the visible ischial tuberosity (ischial tuberosity line).

#### *Equivalent Leg length Imbalance (ELLI)*

$L_Y$  - Equivalent leg length imbalance (ELLI) is the calculated change in leg length in upright posture that would result in a levelling of the sacral base in the coronal (X-Y) plane.

#### *Equivalent Ischial Tuberosity Imbalance (EITI)*

$L_Y$  - Equivalent ischial tuberosity imbalance (EITI) is the calculated change in ischial tuberosity height in upright sitting posture that would result in a levelling of the sacral base in the coronal (X-Y) plane.

*Horizontal pelvic and vertebral displacement ( $Pd_{ap}$ ) ( $Pd_{lat}$ ) ( $Vd_{ap}$ ) ( $Vd_{lat}$ )*

( $Pd_{ap}$ ) horizontal distance of the projected image of the symphysis pubis from the projected image of the second sacral spinous process measured on an AP radiograph.

( $Pd_{lat}$ ) the horizontal distance from the projected image of the symphysis pubis to the projected image of the second sacral spinous process measured on a lateral radiograph.

( $Vd_{ap}$ ) horizontal distance of the projected image of the vertebral body from the projected image of the luminal junction of the same vertebral measured on an AP radiograph.

( $Vd_{lat}$ ) the horizontal distance from the projected image of the centre of the vertebral body to the projected image of the luminal junction of the same vertebra measured on a lateral radiograph.

Projection methods

*Orthographic projection*

Orthographic projection produces an image of a specified, imaginary object, such as an idealised or specified sacrum or vertebra, as viewed from any direction of space. It is distinguished by parallel projectors from the imaged object that intersects a plane of projection at right angles. In linear algebra and functional analysis, a projection is a linear transformation  $P$  from a vector space to itself such that  $p^2 = p$ . Projections map the whole vector space to a subspace and leave the points in that subspace unchanged. This definition of "projection" formalises and generalises the idea of graphical projection. Given a plane in 3D space, the projection area of the *orthographic projection function* is considered the half space on one side of (and including) the plane. Given a point  $p^2$  in the

projection area, if  $p^2$  is not in the plane, there is one line that both passes through  $p^2$  and is perpendicular to the plane. If  $p$  is the point at the intersection of that line with the plane, the projection  $P$  assigns the value  $p$  to  $p^2$ . That is  $P(p^2) = p$ . If the point  $p^2$  lies in the plane,  $P(p^2) = p^2$  so that points in the plane are fixed points of the projection. In the case that the plane is the XY-plane,  $P(x, y, z) = (x^1, y^1, 0)$ . Orthographic projection differs from other projection methods in that it allows measurement of true dihedral angles due to the ability to view the object from any angle. Specific orthographic projections show true angular relationships between objects or surfaces.

### *Perspective projection*

Perspective projection allows definition or analysis of the magnification and distortion inherent in plain film radiography. Perspective projection distorts the angular relationship between objects or structures due to the relationship of an object to the point source of the projection lines. The projection of a point associated with the object is not unique, as all points on a specific projection line will have the same value in reference to the image plane. Radiographic imaging is a specific form of perspective or point projection that generally involves positioning the object being studied between the x-ray source (focal spot) and the image plane or film. For any given image this results in a single point projection (focal spot) creating a specific source image distance (SID) and a specific object image distance (OID). The relationship of a point on an object  $(x, y, z)$  to the corresponding point on the image  $(x^1, y^1, 0)$  is inversely proportional to the source to image distance (SID) and proportional to the object to image distance (OID). This relationship can be expressed as:

$$x/(SID) = x^1/(SID) + (OID).$$

## Reference frames

### *Global reference frame*

A fixed and unmoveable reference frame relative to the ground with the vertical axes aligned to the vector representing the earth's gravitational force. The three axes ( $X_G$ ,  $Y_G$ ,  $Z_G$ ) represent the junction of three mutually perpendicular planes,  $X_G$ - $Y_G$ ,  $X_G$ - $Z_G$ ,  $Y_G$ - $Z_G$ . The  $Y$ -axis is aligned to the gravitational force vector.

### *Pelvic reference frame*

A local rectangular coordinate system with the origin ( $O$ ) centred on the sacral base. The  $X$ -axis is aligned with the transverse (major) axis of the sacral base. The  $Y$ -axis is perpendicular to the sacral base. The  $Z$ -axis is aligned to the mid sagittal plane (minor axis) of the sacral base and orientated to the end plate of the segment. The direction of the positive (+)  $X$ -axis is to the left, the positive (+)  $Y$ -axis is upward or superior and the positive (+)  $Z$ -axis is to the front or anterior. The three axes ( $X_P$ ,  $Y_P$ ,  $Z_P$ ) represent the junction of three mutually perpendicular planes,  $X_P$ - $Y_P$ ,  $X_P$ - $Z_P$ ,  $Y_P$ - $Z_P$  representing the frontal or coronal, axial or transverse and sagittal planes of the body respectively.

## Reference planes

### *Plane of the sacral base*

The sacral base or plateau is the relatively flat upper surface of the sacrum that forms the structural foundation for the superimposed flexible spine above. Viewed from above it is roughly oval shaped but is 'bean' shaped as a normal variant. The upper surface is slightly concave with a rounded outer rim. The plane representing the sacral base can be considered the flat surface that would rest on the outer rim with at least three points of contact. The major axis of the sacral base is aligned to the  $X_P$ - $Y_P$  (frontal) plane and lies along the  $X$ -

axis. The Y-axis of the pelvic reference frame is perpendicular to the surface of the sacral base plane and located at the junction of the X and Z-axes.

#### *Plane of the femur heads*

The femur heads are approximately spherical in shape. The plane of the femur heads is specified and constructed as either a tangent to the upper surface of both femur heads or a plane that passes through the centre of the femur head (axis of rotation). An infinite number of theoretical planes can be constructed as tangents to both femur heads or through the centres of both femur heads. The angulation of the femur head plane relative to the plane of the sacral base can vary depending on the individual plane chosen and rotation of elements of the pelvis around axes other than the axis of interest. The plane of the femur heads is arbitrarily aligned with the X and Z-axes of the plane of the sacral base. With no relative sacral obliquity, the two planes (sacral base and femur head) are parallel in the three orthogonal planes.

#### *Plane of reflective symmetry*

Symmetry is an attribute of a shape or structure with exact reflection of form on opposite sides of a dividing line or plane. Symmetry in biological structures can involve the balanced distribution of duplicate body parts or shapes creating bilateral symmetry around in a specified plane. Vertical reflective symmetry of the human body exists when the body as a whole or specific structure can be divided into mirror images by a vertical plane passing through the middle (sagittal plane) of the body or structure. This is known as line or reflective symmetry. In two dimensions, a bilaterally equal structure or object would have an axis of symmetry.

In 3D space, the same structure would have a plane of symmetry. The axis or plane of symmetry of a two or three -dimensional figure is a line or plane that is constructed bisecting the structure so that any number of perpendicular lines



can be constructed and extended in both directions from the line or plane of symmetry. Any two points lying on the perpendicular lines at equal distances from the presumed axis of symmetry must be identical in shape and transposed in position and orientation around the axis of symmetry. Vertical structural asymmetry exists when the body or specific structure cannot be divided into symmetrical halves by a vertical plane passing through the middle (sagittal plane) of the body or structure.

#### *Viewing or image plane*

A viewing or image plane is the surface, either real or virtual, on which a three-dimensional object is projected or viewed. It can be either a real image such as a radiographic photosensitive film or a virtual computer-generated image. The relationship between the lines of projection and the angle of the object relative to the viewing or image plane will influence the resulting two-dimensional representation. Two inherent characteristics of a viewing or image plane that can alter the appearance of the three-dimensional object being viewed are magnification and distortion.

#### *Cutting plane*

A cutting plane indicates a plane or planes exposed by cutting and removing an imaginary section of the object. The exposed plane is called the sectional view and the line representing the end view of the plane that is used to cut the object is referred to as the cutting plane line. This process is used to form graphical reconstructions of various planes generated from CT data and to view planes passing through three-dimensional reconstructions obtained from CT data sets. Cutting planes are used as a descriptive geometry technique to view internal structures within an object and to view the true positional relationship of points or surfaces within the object.

## Radiographic views

### *A-P view*

For a standard erect anteroposterior (A-P) view of the lumbopelvic spine the central ray is positioned so that it is centred on the film and perpendicular to it. The result is the central ray positioned approximately at the level of the third lumbar vertebra and in line with the vertical mid-line of the film and perpendicular to the image plane.

### *Sacral base (Ferguson's) view*

For the sacral base view the central ray is aligned with, and angled to the same degree as the plane of the sacral base. Vertical alignment is to the mid line of the film. Unless the plane of the sacral base is horizontal the central ray is angled relative to the image plane (film).

### *P-A view*

The posteroanterior (P-A) view is the same as the anteroposterior (A-P) film except that the lumbopelvic spine is facing in the opposite direction with the front of the pelvis facing the film instead of facing the tube as in the A-P view.

### *Zero Angle View*

For the zero angle view the central ray is aligned with, and angled to the same degree as the plane of the sacral base. Vertical alignment is to the mid line of the film. The plane of the sacral base is horizontal with the central ray perpendicular to the image plane (film).

## Reference lines

Specific lines were drawn or constructed on conventional radiographs, digital images or CT images and graphical representations of the pelvis to assess the relative or absolute angulation and linear displacement of the various skeletal structures involved. The lines are constructed and measured in the same way

for the analysis of graphical representations of the same structures seen on the radiographic images. Where applicable the lines and angles were incorporated into trigonometrically based equations used to calculate the theoretical relationships of the same structures.

#### *Femur head line (FHL)*

The femur head line is constructed on conventional radiographs or images from CT studies of the lumbopelvic spine. The line represents the plane of the femur heads. It can be used to measure the angle of the plane of the femur heads relative to the X-axis in the X-Y plane of the reference frame or absolute horizontal plane when measured on erect films or images.

#### *Sacral plane line (SPL)*

The sacral plane line is drawn in the frontal (X-Y) plane to represent the horizontal plane of the sacral base or sacral plateau. The sacral plane line is drawn on the superior lateral margins of the sacral base as they appear on the radiographic or digital image. The line can be used to measure an angle relative to other pelvic and spinal structures or the absolute angle formed to the horizontal plane when measured on erect films or images.

#### *Horizontal plane line (HPL)*

The horizontal plane line represents a plane perpendicular to the vector representing the force of gravity. The horizontal plane line is consistent in all erect views (front and side) even though its vertical location along the  $Y_g$ -axis may vary.

#### *Intersulcate line (ISL)*

The intersulcate line is constructed on the standard erect AP views of the pelvis and is used as an alternate reference line to the sacral plane line (SPL). The line is constructed to measure the orientation of the sacrum around the Z-axis in the coronal plane. The line is constructed by joining reference points located at

the junction of the boarder of the sacral ala and the lateral aspects of the superior articular processes.

*Apparent sacral plane line (ASPL)*

The apparent sacral plane line is drawn in the frontal (X-Y) plane to represent the apparent horizontal plane of the sacral base or sacral plateau. The apparent sacral plane line is drawn on any visible symmetrical structures to represent the plane of the sacral base as they appear on the radiographic or digital image. The line can be used to measure an angle relative to other pelvic and spinal structures or the absolute angle formed to the horizontal plane when measured on erect films or images.

*Sacral base line (SBL)*

The sacral base line represents the plane of the sacral base or sacral plateau in the sagittal (Y-Z) plane and is perpendicular to the sacral base line. It can be used to measure an angle relative to other pelvic and spinal structures or the absolute angle formed to the horizontal plane when measured on erect films or images. When the sacral base line is used to measure absolute position it forms an angle in relation to the horizontal plane line and is known as Ferguson's base angle.

*Vertebral plane line (VPL)*

The vertebral plane line (VPL) is drawn in the frontal (X-Y) plane to represent end view of the horizontal plane of the vertebral body or vertebral end plate. The vertebral plane line is drawn on the superior or inferior lateral margins of the vertebral body as they appear on the radiographic or digital image. The line represents the x-axis of the plane of the vertebral end plate. The line can be used to measure the angle of the vertebra relative to other vertebra or spinal structures or the absolute angle formed to the horizontal plane when measured on erect films or images. A vertebral plane line (VPL) can be constructed in the frontal (X-Y) plane to represent the major axis of the elliptical image of the

projected horizontal plane of the base of the vertebral body or vertebral end plate when the plane is not projected edge on as a line. The vertebral plane line can be drawn on either the superior or the inferior lateral margins of the vertebral body as they appear on radiographic or digital images.

#### *Vertebral base line (VBL)*

The vertebral base line represents the plane of the vertebral body in the sagittal (Y-Z) plane. It can be used to measure an angle relative to other vertebra and spinal structures or the absolute angle formed to the horizontal plane when measured on erect films or images.

#### *Ischial tuberosity line (ITL)*

The ischial tuberosity line is constructed as a tangent to the inferior margin of the ischial tuberosity in the frontal (X-Y) plane on conventional radiographs, digital images and CT reconstructions.

#### *Intercristal or Iliac crest line (ICL)*

The intercristal line represents the edge of an imaginary horizontal plane drawn as a tangent to the superior margin of the iliac crests. The intercristal line is used in a clinical setting as a palpated reference plane for assessing pelvic orientation or tilt. It is also used to quantify pelvic obliquity in the frontal plane on AP radiographs or CT images by constructing a line on plain film radiographs and computer generated radiographic images.

### Specified angles

The specified angles used in the graphical and trigonometrical analysis corresponded with angles measured on radiographic images. In order to quantify vertebral and sacral obliquity and Cobb angles on radiographic images, the angles measured or calculated were divided into one of three groups.

A true dihedral angle (TDA) is the degree of angulation between two planes. The dihedral angle is measured in a plane perpendicular to the line of intersection of the two planes forming the angle. The dihedral angle can also be measured as the angle formed by the intersection of vectors that are perpendicular to the planes. The dihedral angle  $\theta_{AB}$  between two planes denoted  $A$  and  $B$  is the angle between their two normal unit vectors  $\mathbf{n}_A$  and  $\mathbf{n}_B$  where  $\cos \theta_{AB} = \mathbf{n}_A \cdot \mathbf{n}_B$ .

The lines drawn perpendicular to the endplates of the vertebra forming a scoliosis to measure Cobb's angle on conventional radiographs are representations of these vectors. A true dihedral angle can only be measured when viewing the object or on images such as radiographs and digital reconstructions of CT data, if the planes forming the dihedral angle are projected or seen as a line and the line representing the junction of the planes is projected or seen as a point.

The apparent dihedral angle (ADA) is the measured degree of angulation between two planes when the image or viewing plane on which the angle is measured or viewed is not perpendicular to the line of intersection of the two planes forming the dihedral angle or when the image or viewing plane is not perpendicular to the planes involved.

Perspective projection is a type of projection where three-dimensional objects are not projected along parallel lines, but along lines emerging from a single (small) point as is the case with an x-ray beam with the rays emanating from the focal spot within the x-ray tube. This has the effect that distant objects appear smaller than nearer objects of the same size.

### True Dihedral Angles (TDA) $\theta_x$

True dihedral angles are represented in the line drawing analysis of radiographic images of the pelvis and spine. The lines, representing planes, and the angles defining the angular relationship of the planes involved, were recreated as graphical representations of both plain film radiographic and computed tomographic images. In the orthographic projections and radiographic analysis, lines represented the end view of planes and the junction of the planes were visualised as a point in one of the other views.

### *Sacral obliquity angle (SOA) $\theta_1$*

Sacral obliquity is measured as the true dihedral angle of the sacral base relative to the vertical line of symmetry of the sacrum, the femur heads or horizontal plane. It is measured as angular displacement around the  $Z_p$ -axis in the  $X_p$ - $Y_p$  plane. The angle is measured by extending the sacral base line (SBL) to meet the femur head line (FHL) for relative sacral obliquity within the local reference plane or a horizontal plane line (HPL) for absolute sacral obliquity in the global reference plane. The angle measured between the sacral base line (SBL) and the femur head line (FHL) in the  $X_p$ - $Y_p$  plane is referred to as relative sacral obliquity. The measured angle between the sacral plane line (SPL) and the horizontal plane line (HPL) in the  $X_g$ - $Y_g$  plane is referred to as absolute sacral obliquity.

### *Sacral base angle (SBA) $\theta_2$*

The sacral base angle is measured on lateral radiographs with no Y-axis rotation and is a true dihedral angle measurement of the degree of absolute slope of the sacral base in the sagittal plane. It represents the tilt of the plane of the sacral plateau around the  $X_g$  axis. It is measured as the acute angle formed between the plane of the sacrum and the horizontal ( $X_g$ - $Z_g$ ) plane. The sacral

base angle is measured by projecting the sacral plane line (SPL) to meet an arbitrary horizontal plane line (HPL) in the lateral or sagittal (Y-Z) plane.

*Pelvic rotation angle (PRA)  $\theta_3$*

The pelvic rotation angle (PRA) is the measurement of the absolute degree of rotation of the structures that make up the pelvis and their associated local orthogonal reference frame in relation to the vertical (Y) axis of the global reference system or viewing plane. The pelvic rotation angle (PRA) is measured as degrees of rotation of the local reference frame representing the plane of vertical symmetry around a centre of rotation perpendicular to the viewing plane. The pelvic rotation angle is measured in the horizontal ( $X_G$ - $Y_G$ ) plane from the junction of the pelvic rotation line (PRL) and the Z-axis of the global reference frame. Relative pelvic rotation angle would involve rotation of specific pelvic structures such as the ilia around the Y-axis within the local orthogonal reference frame centred on and aligned to the sacral base.

*Extended sacral plan angle (ESPA)  $\theta_4$*

The extended sacral angle (ESA) is the angle measured on the plan (X-Z) view of an orthographic projection when one plane is tilted around an axis perpendicular to the line of intersection of the plane and the reference frame that form a dihedral angle. The angle is measured between the X-axis of the reference frame and the line representing the intersection of the tilted plane and the X-Z plane in the plan view.

*Vertebral obliquity angle (VOA)  $\theta_5$*

Vertebral obliquity angle (VOA) is the measured dihedral angle of the vertebral body relative to horizontal plane. It is measured as angular displacement around the  $Z_g$ -axis in the X-Y plane. The angle is measured by extending the vertebral plane line (VPL) to meet the horizontal plane line (HPL). The measured angle between the vertebral plane line (VPL) and the horizontal plane



line (HPL) in the  $X_g$ - $Y_g$  plane is referred to as apparent vertebral obliquity angle (AVOA).

*Vertebral base angle (VBA)  $\theta_6$*

The vertebral base angle is the true dihedral angle measured in the  $Y_g$ - $Z_g$  plane and is formed by rotation of the plane of the end plate of a vertebra around the  $X_g$ -axis and is measured relative to the horizontal ( $X_g$ - $Z_g$ ) plane on plane films and CT images.

*Vertebral rotation angle (VRA)  $\theta_7$*

The vertebral rotation angle (VRA) is the measurement of the absolute degree of rotation of a vertebra and its associated local orthogonal reference frame in relation to the vertical (Y) axis of the global reference system or viewing plane. The vertebral rotation angle (VRA) is measured as degrees of rotation of the local reference frame around a centre of rotation perpendicular to the viewing plane. The vertebral rotation angle is measured in the horizontal (X-Y) plane from the junction of the vertebral rotation line (VRL) and the Z-axis of the global reference frame. Relative vertebral rotation is the angular displacement of the vertical plane of symmetry of a specific vertebra around the Y-axis within the local orthogonal reference frame centred on and aligned to the sacral base or relative to other segments.

*True Cobb angle (TCA)  $\theta_8$*

The true Cobb angle (TCA) is constructed from the vertebral obliquity angle (VOA) of the segments that are at either end of the curve being measured. When assessing a curve the apical vertebra is first identified as this segment generally has the greatest linear displacement in the horizontal plane, rotation around the vertical axis and the vertebra with the least tilted end plate. The end vertebra is then identified as the vertebra forming a tangent point between the curve above and below. The end vertebra is generally the most superior and inferior vertebra of the curve being studied. They are also generally the least

displaced and rotated and have the maximally tilted end plate. A vertebral plane line (VPL) is drawn along the superior end plate of the superior end vertebra and a second line (VPL) drawn along the inferior end plate of the inferior end vertebra. If the end plates are indistinct, the line may be drawn through the pedicles. The angle between these two lines, or lines drawn perpendicular to them is measured as the apparent Cobb angle (ACA), represents a compound angle, and is measured as an apparent dihedral angle.

*Extended vertebral plan angle (EVPA)  $\theta_9$*

The angle measured on the plan (X-Z) view of an orthographic projection when one plane is tilted around an axis perpendicular to the line of intersection of the plane and the reference frame that form a dihedral angle. The angle is measured between the X-axis of the reference frame and the line representing the intersection of the tilted plane and the X-Z plane in the plan view.

*Apparent Dihedral Angles (ADA)  $\alpha_x$*

Apparent dihedral angles are formed on two-dimensional orthographic images when the object is projected onto the viewing plane so that the line formed at the junction of the two planes being measured is not viewed as a point in one view or the edge of the planes are not projected as lines in a perpendicular view.

*Apparent sacral obliquity angle (ASOA)  $\alpha_1$*

The apparent sacral obliquity (ASOA) angle is a measurement generally used for the quantification of lateral sacral tilt as measured on an orthographic projection of the pelvis. A line (ASBL) is drawn on an image representing the pelvis along the superior end plate of the sacral base. Another line (FHL) is drawn as a tangent to the upper surface of both femur heads. Apparent sacral obliquity measured as an absolute value is the measured angle between an extension of the apparent sacral plane line (ASPL) and a horizontal plane line

(HPL) in the global reference frame. The angle measured between the apparent sacral plane line (ASBL) and the femur head line (FHL) in the  $X_p$ - $Y_p$  plane is referred to as relative apparent sacral obliquity. The measured angle between the sacral plane line (SPL) and the horizontal plane line (HPL) in the  $X_g$ - $Y_g$  plane is referred to as absolute apparent sacral obliquity.

#### *ASOA (CT) $\alpha_{1.1}$*

The angle measured on a computed tomographic (CT) image with no rotation around the Y-axis is an apparent dihedral angle representing sacral obliquity. The angle is measured on a cutting plane through an image stack generated from a computerised tomography (CT) study. The resulting image is not perpendicular to the line of intersection of the two planes forming the angle or the reference plane.

#### *ASOA (CT +R) (as measured on computed tomographic images with rotation) $\alpha_{1.2}$*

The apparent dihedral angle representing sacral obliquity measured on a cutting plane through an image stack from a computerised tomography (CT) study that was not perpendicular and was rotated relative to the line of intersection of the two planes forming the dihedral angle. The planes forming the dihedral angle do not project as a line and the line formed by the junction of the two planes is not projected as a point.

#### *ASOA (orthographic projection with no Y-axis rotation) $\alpha_{1.3}$*

The apparent dihedral angle representing sacral obliquity measured as an orthographic projection with X-axis rotation and no Y-axis rotation.

#### *ASOA (+R) (orthographic projection with Y-axis rotation) $\alpha_{1.4}$*

The apparent dihedral angle representing sacral obliquity measured as an orthographic projection with X-axis rotation and Y-axis rotation.

#### *Apparent sacral base angle (ASBA) $\alpha_2$*

The apparent sacral base angle (ASBA) is a measurement on an orthographic projected image of the sacral base in the sagittal plane when the sacrum is rotated around either the X, or Z-axes in addition to the X-axis rotation being measured. The resulting measurement is an apparent dihedral angle.

*Apparent pelvic rotation angle (APRA)  $\alpha_3$*

Apparent pelvic rotation is the horizontal displacement of two pelvic reference points seen on an A-P radiographic image such as the second sacral spinous process and the centre of the symphysis pubis that are in the same vertical plane perpendicular to the image plane with no actual Y-axis rotation present. The apparent horizontal displacement can be due to projection distortion or rotation of the structures involved around axes other than the Y-axis.

*Sacral plan angle (SPA)  $\alpha_4$*

The angle measured on the plan (X-Z) view of an orthographic projection or horizontal plane through the object when the plane forming the dihedral angle is rotated around the horizontal (X) axis that is perpendicular to the line of intersection of the two planes forming the dihedral angle.

*Apparent vertebral obliquity angle (AVOA)  $\alpha_5$*

The apparent vertebral obliquity angle (AVOA) is a measurement generally used for the quantification of curves in a scoliotic spine as measured on an orthographic projection or CT image of the spine. A line (VPL) is drawn representing the superior or inferior end plate of the vertebra of interest as seen on the radiographic image. If the end plates are indistinct, the line may be drawn through the pedicles of the vertebral. The apparent vertebral obliquity angle is formed at the junction of the vertebral plane line (VPL) and the horizontal plane line (HPL). The acute angle formed between lines drawn perpendicular to the vertebral plane lines constructed on two vertebrae can be measured as the combined angulation of the two lines.

*AVOA (CT) (as measured on CT images)  $\alpha_{5.1}$*

The apparent dihedral angle representing vertebral obliquity measured on a cutting plane through an image stack from a computerised tomography (CT) study that is not perpendicular to one of the two planes forming the angle.

*AVOA (CT +R) (as measured on CT images with X or Y-axis rotation)  $\alpha_{5.2}$*

The apparent dihedral angle representing vertebral obliquity measured on a cutting plane through an image stack from a computerised tomography (CT) study that was not perpendicular and was rotated relative to the line of intersection of the two planes forming the dihedral angle. The planes forming the dihedral angle do not project as a line and the line formed by the junction of the two planes is not projected as a point.

*AVOA (orthographic projection images with no Y-axis rotation)  $\alpha_{5.3}$*

The apparent dihedral angle representing sacral obliquity measured on an orthographic projection with X-axis rotation and no Y-axis rotation.

*AVOA (+R) (measured on orthographic projection images with X or Y-axis rotation)  $\alpha_{5.4}$*

The apparent dihedral angle representing vertebral obliquity measured on conventional radiographs or digital images when the plane (film or image) on to which a true dihedral angle has been projected or viewed was not perpendicular and was also rotated relative to the line of intersection of the two planes forming the dihedral angle.

*Apparent vertebral base angle (AVBA)  $\alpha_6$*

An apparent vertebral base angle (AVBA) is the angle measured on a lateral ( $Y_g$ - $Z_g$  plane) image of the spine between an extension of the vertebral base line (VBL) representing the lateral profile of the end plate of a vertebra and a horizontal plane line (HPL).

*Apparent Vertebral Rotation Angle (AVRA)  $\alpha_7$*

Apparent vertebral rotation is the horizontal displacement of two vertebral reference points seen on an A-P radiographic image such as the spinous

process and the centre of the vertebral body that are in the same vertical plane perpendicular to the image plane with no actual Y-axis rotation present. The apparent horizontal displacement can be due to projection distortion or rotation of the structures involved around axes other than the Y-axis.

*Apparent Cobb angle (ACA)  $\alpha_8$*

( $\alpha_8$ ) In an S-shaped scoliosis where there are two contiguous curves, the lower end vertebra of the upper curve will be the same as the upper end vertebra of the lower curve. The true dihedral angle would be the angulation between the planes representing the end plates of the vertebra at either end of the curve viewed along the junction of the planes. An apparent Cobb angle is the apparent dihedral angle formed when the viewing direction or image plane does not align with the junction of the two planes forming the angle or the end view of the planes is not a line.

*Vertebral plan angle (VPA)  $\alpha_9$*

The angle measured on the plan (X-Z) view of an orthographic projection or horizontal plane through the object when the plane forming the dihedral angle is tilted around a horizontal (X) axis perpendicular to the line of intersection of the two planes forming the dihedral angle.

*Projected compound angles (PCA)  $\phi_x$*

Plain film radiographic images are used primarily by clinicians to measure specified angles such as sacral base angle (SBA) and Cobb angle. These images are produced from rays emanating from a point source (focal spot) with compound rotations around all three axes.

*Projected sacral base angle (PSBA)  $\phi_1$*

The projected sacral base angle (PSBA) is a measurement on a projected image of the sacral base in the sagittal plane when the sacrum is rotated

around either the X, or Z-axes in addition to the X-axis rotation being measured.

The resulting measurement is an apparent dihedral angle.

*Projected pelvic rotation angle (PPRA) (measured on plain film radiographs)  $\varphi_2$*

The projected pelvic angle is the angle calculated from measurements obtained directly from A-P or P-A plain film radiographic images of the pelvis.

*Projected sacral obliquity angle (PSOA)  $\varphi_3$*

The projected sacral obliquity angle is the angle measured directly on A-P or P-A plain film radiographic image of the pelvis.

*Projected vertebral obliquity angle (PVOA)  $\varphi_4$*

The projected vertebral obliquity angle (PVOA) is a measurement generally used for the quantification of curves in a scoliotic spine as measured on an A-P or P-A plain film radiographic projection or CT image of the spine. A line (VPL) is drawn representing the superior or inferior end plate of the vertebra of interest as seen on the radiographic image. If the end plates are indistinct, the line may be drawn through the pedicles of the vertebral. The apparent vertebral obliquity angle is formed at the junction of the vertebral plane line (VPL) and the horizontal plane line (HPL). The acute angle formed between lines drawn perpendicular to the vertebral plane lines constructed on two vertebra can be measured as the combined angulation of the two lines.

*Projected vertebral base angle  $\varphi_5$*

The projected vertebral base angle (PVBA) is a measurement on a projected image of the vertebral endplate in the sagittal plane when the vertebra is rotated around either or both the X -, or Z-axes in addition to the X-axis rotation being measured. The resulting measurement is an apparent dihedral angle.

*Projected vertebral rotation angle (PVRA)  $\varphi_6$*

The projected vertebral rotation angle (PVRA) is the amount specified reference points are displaced around a vertical axis on an A-P radiographic image.

*Projected Cobb angle (PCA)  $\varphi_7$*

Because the Cobb angle projects as a curvature and is measured in a single plane only, it fails to account for other rotations. A measured Cobb angle on a radiographic image may not accurately demonstrate the severity of three-dimensional spinal deformities. The projection of a compound angle produces an apparent dihedral angle based on the projected vertebral obliquity angle (AVO) as measured on AP radiographic and CT images. The projected Cobb angle is the combination of the true Cobb angle with systematic error relating to the measurement of apparent dihedral angles plus the inherent errors associated with projection distortion.

*Lateral projection angle (LPA)  $\phi_8$*

Angle formed between the central ray and a specified reference point in the lateral (Y-Z) plane. The angle is calculated from source image distance (SID) and the distance measured on the radiographic image from the central ray to the reference point.

*Plan projection angle (PPA)  $\phi_9$*

Angle formed between the central ray and a specified reference point in the frontal (Y-X) plane. The angle is calculated from source image distance (SID) and the distance measured on the radiographic image from the central ray to the reference point.



### APPENDIX 3 FINAL ETHICS APPROVAL LETTER



Mr John Dulhunty  
Department of Health and Chiropractic  
Division of Environmental and Life Sciences  
College of Science and Technology

30 June 2006

Dear Mr Dulhunty

#### FINAL APPROVAL LETTER

**Title of Project: A retrospective analysis of sacral obliquity as measured on routine lumbo-pelvic CT images**  
**Reference Number: HE26MAY2006-D04706**

Thank you for your recent correspondence. Your responses have satisfactorily addressed the outstanding issues raised by the Committee. You may now proceed with your research. This approval is subject to the following condition:

1. With reference to your response to item 3, Appendix D, please forward a copy of the formal letter that you will be sending to the radiologist and a copy of the correspondence from the radiologist in reply to this letter, indicating their agreement to participate in this study.

Please note the following standard requirements of approval:

1. Approval will be for a period of twelve months. At the end of this period, if the project has been completed, abandoned, discontinued or not commenced for any reason, you are required to submit a Final Report on the project. If you complete the work earlier than you had planned you must submit a Final Report as soon as the work is completed. The Final Report is available at <http://www.ro.mq.edu.au/ethics/human/forms>.
2. However, at the end of the 12 month period if the project is still current you should instead submit an application for renewal of the approval if the project has run for less than five (5) years. This form is available at <http://www.ro.mq.edu.au/ethics/human/forms>. If the project has run for more than five (5) years you cannot renew approval for the project. You will need to complete and submit a Final Report (see Point 1 above) and submit a new application for the project. (The five year limit on renewal of approvals allows the Committee to fully re-review research in an environment where legislation, guidelines and requirements are continually changing, for example, new child protection and privacy laws).
3. Please remember the Committee must be notified of any alteration to the project.
4. You must notify the Committee immediately in the event of any adverse effects on participants or of any unforeseen events that might affect continued ethical acceptability of the project.
5. At all times you are responsible for the ethical conduct of your research in accordance with the guidelines established by the University (<http://www.ro.mq.edu.au/ethics/human>).
6. If you will be applying for or have applied for internal or external funding for the above project it is your responsibility to provide Macquarie University's Grants Officer with a copy of this letter as soon as possible. The Grants Officer will not inform external funding agencies that you have final approval for your project and funds will not be released until the Grants Officer has received a copy of this final approval letter.

Yours sincerely

CRO File: 06/742

ETHICS REVIEW COMMITTEE (HUMAN RESEARCH)  
MACQUARIE UNIVERSITY (E11A)  
SYDNEY, NSW, 2109 AUSTRALIA

Secretary: Ph: (02) 9850 7854 Fax: (02) 9850 8799 E-mail: [kdesilva@vc.mq.edu.au](mailto:kdesilva@vc.mq.edu.au)  
[http://www.ro.mq.edu.au/eth\\_hum.htm](http://www.ro.mq.edu.au/eth_hum.htm)

Portrait (85)